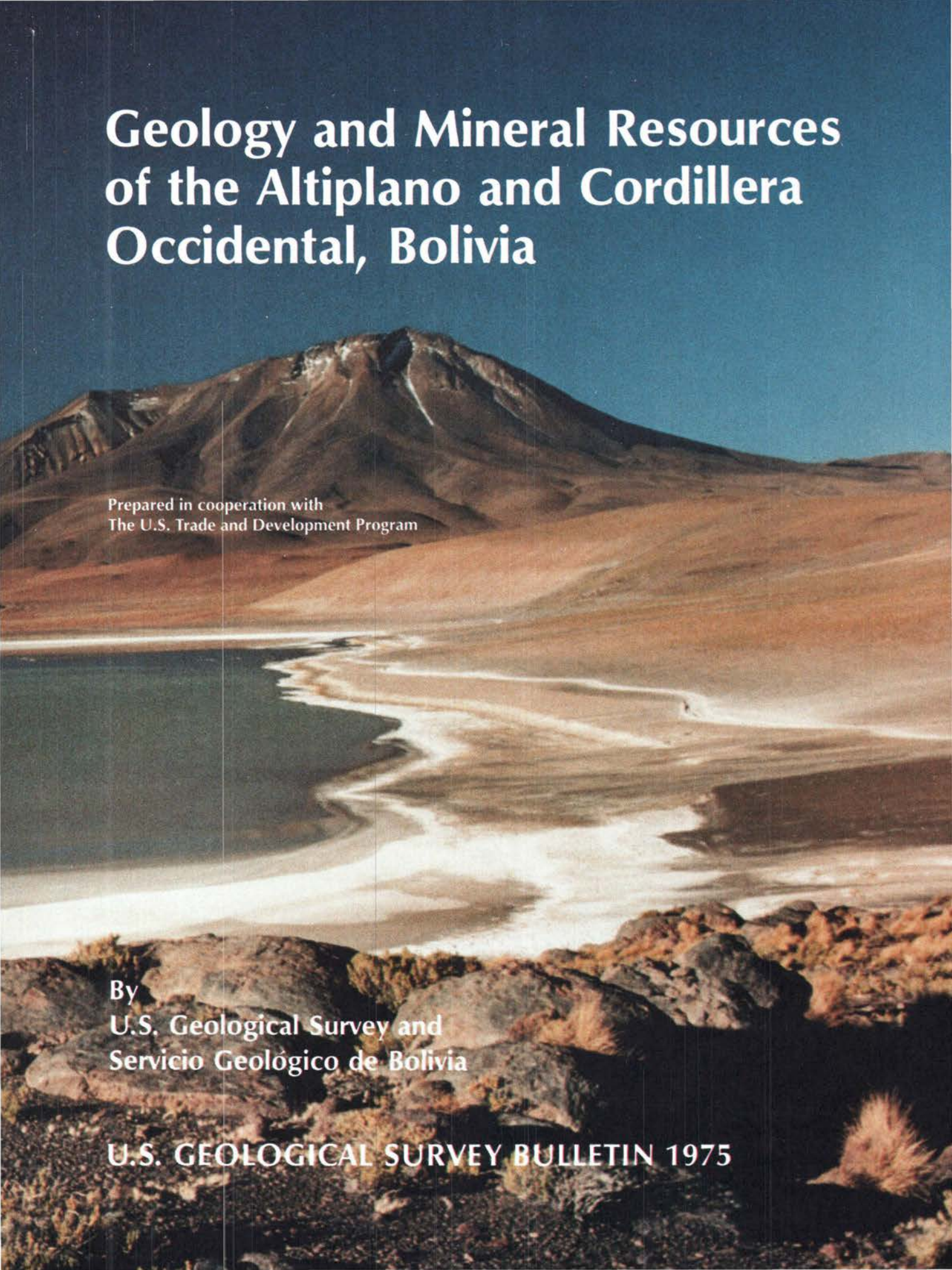
Geology and Mineral Resources of the Altiplano and Cordillera Occidental, Bolivia



Prepared in cooperation with
The U.S. Trade and Development Program

By
U.S. Geological Survey and
Servicio Geológico de Bolivia

U.S. GEOLOGICAL SURVEY BULLETIN 1975

Geology and Mineral Resources of the Altiplano and Cordillera Occidental, Bolivia

By U.S. GEOLOGICAL SURVEY and
SERVICIO GEOLOGICO DE BOLIVIA

With a section on Application of economic evaluations to deposit models
By DONALD I. BLEIWAS and ROBERT G. CHRISTIANSEN,
U.S. Bureau of Mines

Prepared in cooperation with
The U.S. Trade and Development Program

U.S. GEOLOGICAL SURVEY BULLETIN 1975

U.S. DEPARTMENT OF THE INTERIOR
MANUEL LUJAN, JR., Secretary

U.S. GEOLOGICAL SURVEY
Dallas L. Peck, Director

Any use of trade, product, or firm names in this publication is for descriptive purposes only and does not imply endorsement by the U.S. Government.

UNITED STATES GOVERNMENT PRINTING OFFICE: 1992

For sale by the
Books and Open-File Reports Section
U.S. Geological Survey
Federal Center
Box 25425
Denver, CO 80225

Library of Congress Cataloging-in-Publication Data

Geology and mineral resources of the Altiplano and Cordillera Occidental, Bolivia / by U.S. Geological Survey and Servicio Geológico de Bolivia ; with a section on Application of economic evaluations to deposit models, by Donald I. Bleiwas / and Robert G. Christiansen.
p. cm. — (U.S. Geological Survey bulletin ; 1975)
"Prepared in cooperation with the U.S. Trade and Development Program."
Includes bibliographical references.
1. Mines and mineral resources—Altiplano. 2. Mines and mineral resources—Bolivia—Cordillera Occidental. 3. Geology—Altiplano. 4. Geology—Bolivia—Cordillera Occidental. I. Geological Survey (U.S.) II. Servicio Geológico de Bolivia. III. Series.
QE75.B9 no. 1975
[TN39.A4]
557.3 s—dc20 91-30115
[553'.0984] CIP

FOREWORD

It is a genuine pleasure to introduce this important volume on Bolivian mineral resources. The work that led to this publication is a significant new chapter in a long and productive history of cooperation between the Servicio Geológico de Bolivia and the U.S. Geological Survey. The geologic research described herein, funded by the U.S. Trade and Development Program, is an outstanding example of the type of cooperative effort that can be used to assist national decisions regarding wise use of mineral resources. One of the specific features of this project is the application of mineral deposit models to classic mining areas in Bolivia. The data that result from these studies enrich our knowledge of mineral deposits worldwide.

I applaud the exceptional cooperative spirit and professional talents of all of the people in the Servicio Geológico de Bolivia, the U.S. Trade and Development Program, and the U.S. Geological Survey who have worked so successfully to make this project and this publication possible.

Dallas Peck
Director, U.S. Geological Survey

FOREWORD

This bulletin contains some of the most important information about Bolivian economic geology that has been produced in recent years. Its importance exceeds mere scientific knowledge and it represents a product of the joint international effort between the geological surveys of Bolivia and the United States. Bolivia has a long and important mining history, and mineral resources will probably continue to be the basis of our economy for many years to come. We hope this Bulletin will help, at a higher level, to design national policies related to mineral resources. At a basic level, it can be considered as a guide for the development of future exploration and investment of the mining industry in nontraditional areas of the Andean region of Bolivia.

Bolivia has long been known for the rich polymetallic vein deposits located in the Cordillera Oriental, Cerro Rico de Potosí being the best example. After hundreds of years of mining, these deposits are still productive and the Cordillera Oriental has been our most traditional domain for mineral exploration. However, their richness also limited our perspectives for investigating other geological domains of our large territory. Therefore, when the Project for the Mineral-Resource Assessment of the Altiplano and the Cordillera Occidental was funded by a generous grant ($1,350,000) from the U.S. Trade and Development Program (TDP) and the counterpart support from Dirección de Financiamiento y Ajilazación de Desembolsos–U.S. Agency for International Development (DIFAD–USAID) through their Economic Compensation Fund ($600,000), the door was open for exploration of these two large, important and almost unknown areas. In the future, we expect this Bulletin will help investors in exploration to convert the Altiplano and the Cordillera Occidental into what the Cordillera Oriental was in the past.

The area of the project covered 150,000 km^2 of the Western Andean region of Bolivia, a region between 3,500 to 6,000 m in elevation. This difficult terrain includes some of the most remote areas in Bolivia, and close cooperation between United States and Bolivian geologists, as well as strong logistical support, were very important to carry out the field coverage needed for the assessment. In addition to the compilation and reprocessing of existing information, the latest techniques in remote sensing, geochemistry, and geophysics were used. The already existing aeromagnetic data, that covered almost 60 percent of the area, were reprocessed and TDP contributed funding that will be used to cover areas not previously surveyed. Even though Bolivia has the Salar de Uyuni, the largest salar and lithium reserves of the world, this is the first time that we have assessed the potential of industrial minerals in the region.

This important publication will not be the only product of the project; future publications will provide additional knowledge about topics not fully covered by this Bulletin. Furthermore, the transfer of knowledge has already yielded results, and we expect that Bolivian geologists will continue with this work in a constructive and long-lasting relationship with the USGS. I am happy and proud to introduce you to the pages of this document, and I would like to acknowledge the effort of all the authorities and professionals that made it possible to produce it, especially to the Minister of Mines and Metallurgy of Bolivia, the American Ambassador to Bolivia, and the Director of DIFAD–Ministry of Planning Affairs.

Marcelo Claure Zapata
Director, Servicio Geológico de Bolivia

FOREWORD

The U.S. Trade and Development Program (TDP) is an independent U.S. Government agency with an exclusive mandate to promote U.S. exports for major development projects in middle-income and developing countries. TDP facilitates the access of these countries to U.S. technology by funding U.S. technical assistance in the planning stages of high-priority developmental projects that also represent U.S. export and investment opportunities.

Most of TDP's program involves feasibility studies on specific investment projects. Occasionally, however, a broader sector approach is more appropriate. Thus, in July 1989, as part of an overall effort to promote the development of the Bolivian mining sector, TDP provided a grant of $2 million to the Ministry of Mines and Metallurgy. The grant was earmarked for a series of related activities, including the preparation of this important bulletin, an aeromagnetic survey, and the preparation of a compendium of the economic geology of Bolivia.

We are confident that the information presented herein by the U.S. Geological Survey and the Geological Survey of Bolivia will provide the groundwork for the further development of the Bolivian mining sector, which is so important to that country, while at the same time introducing the U.S. Industry to business opportunities there. Because of its specialized function and small size, TDP has a great deal of flexibility in achieving its objectives. The evaluation of Bolivia's Altiplano and Cordillera Occidental mineral resources which follows is an excellent example of how TDP can effectively utilize its resources to achieve substantial gains for the both the host country and potential U.S. suppliers and investors.

Worldwide, TDP's mining activities over the past several years total more than $6 million. Furthermore, the recognized need to foster closer relationships between the U.S. and the countries of Latin America, and the economic restructuring now under way in many Latin American countries, including Bolivia, has led TDP to dramatically increase its involvement in the region over the past three years.

As economic and commercial relations between the United States and Latin America continue to advance, the time has come for the mining sectors of the region to expand their cooperation. It is TDP's sincere hope that this bulletin will encourage U.S. firms to provide the equipment, technology, and capital needed to assist Bolivia in further developing its mining sector.

Priscilla Rabb Ayres
U.S. Trade and Development Program

CONTENTS

Background notes on U.S. Geological Survey-Bolivia cooperative activities *by* Thor H. Kiilsgaard, Harry A. Tourtelot, Norman J Page, *and* S.J. Kropschot **1**

Summary **4**

Resumen **7**

Introduction **10**

Acknowledgments **12**

Geologic setting *by* Donald H. Richter, Steve Ludington, *and* Eduardo Soria-Escalante **14**

A geochemical study of the La Joya district *by* Robert Learned, Michael S. Allen, Orlando André-Ramos, *and* René Enriquez-Romero **25**

Remote sensing *by* Daniel H. Knepper, Jr. *and* Shirley L. Simpson **47**

Gravity and magnetic studies *by* John W. Cady *and* Richard A. Wise **56**

Mineral deposit models *by* Steve Ludington, G.J. Orris, Dennis P. Cox, Keith R. Long, *and* Sigrid Asher-Bolinder **63**

Geology of known mineral deposits **90**

Application of economic evaluations to deposit models *by* Donald I. Bleiwas *and* Robert G. Christiansen **210**

Methods of resource assessment *by* Steve Ludington, G.J. Orris, *and* Dennis P. Cox **218**

Undiscovered metallic deposits *by* Steve Ludington, Dennis P. Cox, Orlando André-Ramos, Angel Escobar-Diaz, Eduardo Soria-Escalante, W. Earl Brooks, B.M. Gamble, Keith R. Long, John W. Cady, *and* Daniel H. Knepper **220**

Undiscovered nonmetallic deposits *by* G.J. Orris, Sigrid Asher-Bolinder, Orlando André-Ramos, Angel Escobar-Diaz, Eduardo Soria-Escalante, John W. Cady, Daniel H. Knepper, Dennis P. Cox, Keith R. Long, *and* Steve Ludington **225**

References **230**

Appendices

A. Mines, prospects, and mineral occurrences, Altiplano and Cordillera Occidental, Bolivia *by* Keith R. Long **243**

B. Locations, descriptions, and analyses of samples collected as part of the study of the Altiplano and Cordillera Occidental, Bolivia **273**

C. Data for geochronology samples collected as part of the study of the Altiplano and Cordillera Occidental, Bolivia **363**

PLATES

[Plates are in pocket]

1. Geologic map of the Altiplano and Cordillera Occidental, Bolivia *by* Sherman P. Marsh, Donald H. Richter, Steve Ludington, Eduardo Soria-Escalante, *and* Angel Escobar-Diaz
2. Map of potentially hydrothermally altered rocks interpreted from LANDSAT Thematic Mapper images, Altiplano and Cordillera Occidental, Bolivia *by* Daniel H. Knepper Jr. *and* Shirley L. Simpson
3. Selected Thematic Mapper images of the Altiplano and Cordillera Occidental, Bolivia
4. Simple Bouguer gravity anomaly map of the Altiplano and Cordillera Occidental, Bolivia *by* John W. Cady
5. Residual total field aeromagnetic map of the Altiplano and Cordillera Occidental, Bolivia *by* Richard A. Wise
6. Map showing mines, prospects, and mineral occurrences, Altiplano and Cordillera Occidental, Bolivia *by* Keith R. Long
7. Map showing areas designated permissive and favorable for selected mineral deposit types, Altiplano and Cordillera Occidental, Bolivia *by* Steve Ludington *and* Dennis P. Cox
8. Map showing areas designated permissive for selected nonmetallic mineral deposit types, Altiplano and Cordillera Occidental, Bolivia *by* G.J. Orris

Background Notes on U.S. Geological Survey-Bolivia Cooperative Activities

By Thor H. Kiilsgaard, Harry A. Tourtelot, Norman J Page, *and* S.J. Kropschot

The U.S. Geological Survey (USGS) has been privileged to have assisted Bolivian earth science agencies in a succession of cooperative projects for more than 50 years. These notes, while far from comprehensive, attempt to document some of the important milestones of this historic cooperation.

The first formal involvement of the USGS in Bolivia resulted from the creation of an Interdepartmental Committee on Scientific and Cultural Cooperation (ICSCC) by President F.D. Roosevelt in 1938. The ICSCC, under the direction of the U.S. Department of State, was authorized to coordinate the overseas programs of 26 departmental and independent Federal agencies. Strategic-mineral studies in the Western Hemisphere were discussed at the Eighth Pan-American Scientific Congress held in Washington, D.C. in May 1940. Within this framework, and with $25,000 from the U.S. Department of State, the USGS began geologic investigations of strategic and critical minerals in Latin America. Eugene Callahan and James F. McAllister of the USGS went to Bolivia to work with Friedrich Ahlfeld and Jorge Muñoz Reyes during December to May 1940–41; they evaluated tin, tungsten, and antimony mines and deposits.

Allotments for Latin American studies from the U.S. Department of State were increased and supplemented by funds from the U.S. Board of Economic Warfare, and later by the U.S. Foreign Economics Administration. Studies of mineral commodities in 16 Latin American countries were coordinated between 1940 and 1946. During this period, Quentin Dreyer Singewald led a mineral resource-assessment mission to Colombia, which also included special short-term studies of mineral deposits in, among other places, Bolivia.

As part of President Roosevelt's Good Neighbor Policy, the ICSCC programs were administered by the Office of the Coordinator for Inter-American Affairs, which during World War II became recognized as the Institute of Inter-American Affairs. In 1944, the U.S. Office of Inter-American Affairs published a compilation of information entitled, "Bolivia Storehouse of Metals."

After the formation of the United Nations in 1945 and the 1949 enunciation of President Truman's Point IV Doctrine, the United States involvement as a source of technical assistance expanded considerably. The Point IV Doctrine Mission to Bolivia requested that the USGS send a geologist to make a preliminary investigation of some occurrences of phosphate rock that had been reported to the Agricultural Section. The occurrence of phosphate rock was of interest to the Agricultural Section of the Point IV Mission because of its potential use as a fertilizer, which would not only increase agricultural production, but would decrease foreign exchange expenditures on imported fertilizer.

Harry A. Tourtelot (USGS) reported to the Point IV Mission in the American Embassy in La Paz in late January 1952 and discussions about the purposes of the geological cooperative program were initiated. Tourtelot visited several reported phosphate occurrences, but all proved to be too small to be significant.

Results of the field work were reported to the Point IV Ambassador, the Director of the Agriculture Section of the Point IV Mission, and the Corporación Boliviana de Fomento of the Bolivan Government, and no additional field studies on phosphate rock were approved. The Corporación, however, expressed interest in limestone that could be used for making cement and funded additional field work by Tourtelot.

About the same time, city engineers in La Paz, a city that was plagued with landslides because the valley in which it lies is underlain by soft sedimentary rocks, requested assistance. They asked if geologic studies could identify areas where landslides had occurred, areas in which landslides were likely to occur, how landslides might be

Manuscript approved for publication September 24, 1991.

prevented, and how the ground could be stabilized after sliding. Earnest Dobrovolny, an engineering geologist from the USGS, arrived to assist the city engineers in 1954.

In 1953, the U.S. Government entered into an agreement with the Bolivian Government aimed at assisting the Bolivian mining industry. In 1958, a second agreement between the Bolivian Ministerio de Economía and the U.S. Operation Mission to Bolivia (USOM), International Cooperation Administration was negotiated. The second agreement resulted in the formation of the Bolivian Department of Supervised Mining Credit, a program under which USOM participated in the loan of funds to Bolivian mining operators for exploration and development.

In August 1959, another agreement between the Ministerio de Economía and the Ministerio de Minas (later the Ministerio de Minas y Petróleo), was negotiated, creating the Desarrollo de Yacimientos Minerales (DYM) under the Ministerio de Minas. The DYM program was a modification of a plan proposed by a firm of mining consultants engaged by USOM to advise on the minerals situation in Bolivia (Ford, Bacon, and Davis, unpub. manuscript, 1956), and was developed to help the Ministerio de Minas provide technical assistance to private mine operators about mineral exploration, mine development and operation, and mineral benefaction. Personnel were to be trained to provide technical assistance to private mine operators, as well as to conduct reconnaissance studies near mineral deposits and more detailed investigations at selected localities that might contain large low-grade mineral deposits. In addition, DYM personnel were to supply guidance to small private mine operators on management and bookkeeping, service loan contracts previously subscribed under the Department of Supervised Mining Credit, collect outstanding payment on loans, and supervise assistance projects associated with the loans.

The DYM was staffed with the same individuals that formerly had cooperated with Ford, Bacon, and Davis on the supervised Mining Credit program. In July 1959, when the program ceased to grant loans to mine operators, the small staff consisted of one geologist, Gustavo Donoso, who directed the technical work, two engineers, and several technicians who had mining and ore-milling experience, but little formal education.

The Ford, Bacon, and Davis consultants recommended that USOM contact the USGS for assistance in meeting their objectives, and, at the request of USOM, the USGS entered into an agreement with the U.S. International Cooperation Administration to provide technical assistance in mineral resource investigations to the Ministerio de Minas in October 1959.

The USGS assigned Thor H. Kiilsgaard to help build a permanent central government geological and economic mineral advisory service within the Ministerio de Minas and to assist in training young Bolivian geologists. Kiilsgaard arrived in Bolivia in November 1959, and was promptly detailed to DYM, where he served as Director of DYM operations until he departed in February 1960. Much of his time was spent in the field with DYM staff members examining areas and recommending two reconnaissance mapping projects. The two projects were chosen because they exhibited potential for mineral deposits, and although suitable base maps were not available, aerial photography was. The first project mapped the principal copper-producing region of Bolivia that extends from the Corocoro mine southeast to the Chacarilla mine. The second project mapped a belt-like area 15-km wide that contained several lead-zinc mines and prospects along the northeastern shore of Lake Titicaca.

The Corocoro-Chacarilla geologic mapping study, begun in the spring of 1960, was completed in January 1962; the resulting geologic map was published as Boletín 1 of the Departamento Nacional de Geología (Meyer and Murillo, 1961), the first technical report published under the jointly sponsored Ministerio de Minas-USOM/Bolivia program. Boletín 2, published in 1968, covered work done during the second project (Rivas, 1968).

Kiilsgaard also recommended preparation of a photogeologic base map of an area east of Oruro; suggested changes in the technical assistance given to private mine operators; urged publication of technical assistance reports; and proposed publication of an annual report consisting of mineral production statistics, generalized information on the DYM program, and mine and mill reports.

In September 1960, the DYM was reorganized and became known as the Departamento Nacional de Geología (DENAGEO); Gustavo Donoso became the first Director. In June 1965, the department was given its present name, Servicio Geológico de Bolivia (GEOBOL).

USGS geologists were detailed by USOM to work with GEOBOL as technical advisers; Charles M. Tschanz arrived in November 1960, and remained until January 1965, and James F. Seitz arrived in 1961 and remained until 1966. They helped guide the Bolivian staff in carrying out objectives of the GEOBOL program. In addition, Reed J. Anderson and Sam Rosenblum of the USGS worked in Bolivia during the period 1960–67.

During a visit in April 1965, Kiilsgaard was gratified to find that 118,000 km^2 of Bolivia had been mapped geologically and maps covering 34,000 km^2 had been published. Significant among these published reports were those of Meyer and Murillo (1961), Drobrovony (1962), Reyes and others (1962), Ahlfeld and Schneider-Scherbina (1964), and Branisa (1965). More than 50 young Bolivian geologists and engineers had undergone or were undergoing technical training, and technical assistance was being provided to 420 private mine operators.

During 1967, Fernando Urquidi (GEOBOL) participated in training at the chemical laboratories in the USGS. This was to prove to be the last activity of the

USOM/Bolivia program; U.S. aid to this program ended in June 1967, and participation by the USGS with GEOBOL ceased, not to be renewed for 8 years.

Between 1975 and 1980, the Ministerio de Minas y Metalurgía and the USGS had a memorandum of understanding for technical assistance in mineral exploration and development. One of the objectives of the project was to apply computer technology to mineral resources and Allen L. Clark and James A. Calkins of the USGS visited Bolivia to discuss the Computerized Resource Information Bank (CRIB). As a result of these discussions, Fernando Urquidi made many entries and updates on mines and prospects in Bolivia using information from published literature and Corporación Minera de Bolivia (COMIBOL) internal reports. Harold Kirkemo and John DeYoung provided advice on the initiation of a revolving mineral exploration fund. The CRIB data file has evolved into the Mineral Resource Data System (MRDS) and data from this pre-1980 activity is included in appendix A.

The USGS–GEOBOL cooperative investigation of the mineral resources on the Altiplano and in the Cordillera Occidental, the project reported on here, resulted from Bolivian requests for USGS technical assistance in the revitalization and redirection of Bolivia's national mining industry, which, because of falling tin and petroleum prices, had fallen into sharp decline by 1987. The Ministerio de Minas y Metalurgía subsequently embarked on an ambitious program with the world banking community to revitalize and strengthen the nation's mining industry.

At the encouragement of Robert S. Gelbard, the American Ambassador to Bolivia, visiting U.S. Secretary of State George Schultz suggested in August 1988 that the USGS might assist in the international program to aid the mining industry of Bolivia by assessing the mineral resources. Later that month, Jaime Villalobos, Bolivian Minister of Mines and Metallurgy, called at USGS headquarters in Reston, Vir., to convey Bolivia's interest in USGS participation. Minister Villalobos asked the USGS to prepare a cooperative program of geologic investigation and mapping to assess the mineral resources of Bolivia. By October 1988, the USGS had prepared a proposal for a USGS–GEOBOL cooperative "Bolivia Mineral Resource Assessment Program." The ambitious 5-year program proved difficult to realize, and in early 1989, the two parties agreed to attempt to accomplish the national mineral resource assessment in successive projects beginning with the mineral-rich Altiplano and Cordillera Occidental.

In May 1989, the Regional Director of the U.S. Trade and Development Program (TDP), Daniel D. Stein, visited La Paz and met with Ambassador Gelbard and Minister Villalobos to discuss the possibility of TDP support to begin a USGS–GEOBOL assessment of the mineral resources of Bolivia. On July 13, 1989, TDP Director Priscilla Rabb Ayres signed a $2,000,000 agreement with the Ministerio de Minas y Metalurgía to help revitalize and strengthen the mining industry of Bolivia. That agreement provided for a 2-year USGS–GEOBOL cooperative assessment of the known and undiscovered mineral resources of the Bolivian Altiplano and the adjoining Cordillera Occidental. By August 1989, USGS and GEOBOL scientists, working with American Embassy representatives Leslie Sternberg and Fernando Urquidi, had agreed upon a program to assess the high Andean plateau's mineral wealth. The joint assessment began on January 17, 1990, and concluded two years later with the publication of this volume.

Summary

GEOLOGY

In southwestern Bolivia, the Andes Mountains consist of three contiguous morphotectonic provinces, which are, from west to east, the Cordillera Occidental, the Altiplano, and the Cordillera Oriental. Only the two western provinces are the subject of this report. The basement beneath the study area, which is as thick as 70 km, is believed to be similar to the rocks exposed immediately to the east, in the Cordillera Oriental, where a polygenic Phanerozoic fold and thrust belt consists largely of Paleozoic and Mesozoic marine shales and sandstones. Deposited mostly on Precambrian basement, the rocks of the Cordillera Oriental were deformed during at least three tectonic-orogenic cycles, the Caledonian (Ordovician), the Hercynian (Devonian to Triassic), and the Andean (Cretaceous to Cenozoic).

The Altiplano is a series of high, intermontane basins that formed primarily during the Andean cycle, apparently in response to folding and thrusting. Its formation involved the eastward underthrusting of the Proterozoic and Paleozoic basement of the Cordillera Occidental, concurrent with the westward overthrusting of the Paleozoic miogeosynclinal rocks of the Cordillera Oriental. These thrusts resulted in continental foreland basins that received as much as 15,000 m of sediment and interlayered volcanic rocks during the Cenozoic. Igneous activity accompanying early Andean deformation was primarily focused further west, in Chile. During the main (Incan) pulse of Andean deformation, beginning in the Oligocene and continuing at least until the middle Miocene, a number of volcano-plutonic complexes were emplaced at several localities on the Altiplano, particularly along its eastern margin with the Cordillera Oriental, and to the south, in the Sud Lípez area. In Pleistocene time, most of the Altiplano was covered by large glacial lakes. The great salars of Uyuni and Coipasa are Holocene remnants of these lakes.

The Cordillera Occidental consists of late Miocene to Recent volcanic rocks, both lava flows and ash-flow tuffs, primarily of andesitic to dacitic composition, that have been erupted in response to the subduction of the Nazca plate beneath the continent of South America. This underthrusting continues, and many of the volcanoes that form the crest of the Andes and mark the international border with Chile are presently active.

The 1:500,000-scale geologic map that is part of this report (pl. 1) was compiled largely from unpublished 1:250,000-scale geologic maps prepared by Servicio Geológico de Bolivia geologists during the last 20 years. Changes resulting from fieldwork conducted as part of this project were incorporated into the map. Modifications were also made to the map on the basis of additional information from other published and unpublished maps, including theses from the Universidad Mayor de San Andres and maps supplied by Yacimientos Petrolíferos Fiscales Bolivianos. The geologic formations used in the 1:250,000-scale compilations were grouped into 15 map units for the 1:500,000-scale map, and were chosen specifically to support the delineation of permissive areas for the occurrence of mineral deposits. Twelve newly determined potassium-argon ages were used to help group the map units (app. C).

GEOCHEMISTRY

A geochemical study was designed for the La Joya polymetallic district to test the effectiveness of traditional geochemical exploration techniques in the high, arid environment of the Altiplano. The study demonstrates that the pathfinder elements, arsenic, antimony, and bismuth are clearly associated with precious metals, and that their distribution in surficial deposits adequately delineates areas where known mineralized rocks crop out.

REMOTE SENSING

Analysis of Thematic Mapper satellite images resulted in the identification of more than 130 areas where hydrothermal alteration has visibly affected rocks in the study area (pl. 2). The detailed interpretation was made possible because the high elevation and clear weather in the study area combined to produce very high quality imagery (pl. 3). Many of the identified altered areas are clearly related to known mining districts, but others are in remote and poorly mapped locations, and may indicate undiscovered hydrothermal mineral deposits.

GEOPHYSICS

Analysis of the gravity of the study area shows that the area of the Altiplano underlying the great salars, Uyuni

and Coipasa, is distinguished by northnortheast-trending gravity anomalies, whereas, to the northeast, the Altiplano is distinguished by northnorthwest-trending gravity anomalies (pl. 4).

The aeromagnetic map shows that the great salars and Cordillera Occidental are distinguished by high magnetic relief caused by known and inferred Quaternary and Tertiary volcanic rocks, with possible contributions by hypabyssal intrusions that feed these rocks (pl. 5). To the northeast, the rest of the Altiplano shows low magnetic relief and no long-wavelength magnetic anomalies.

There are two possible explanations for the contrasting trends in the gravity and magnetic data for the salars and Cordillera Occidental. It is most likely that the apparent east-west magnetic anomalies in the salars are the result of the low magnetic latitude. However, it is possible that the gravity map reflects Tertiary or older structural trends, whereas the magnetic map reflects crosscutting Quaternary volcanism.

MINERAL DEPOSITS

Mineral deposits were classified according to deposit type, using, wherever possible, guidelines established by the U.S. Geological Survey in earlier resource assessments. Because of the unique geologic character of the central Andes in Bolivia, some new deposit types were developed. Twenty-eight specific mineral deposit types are discussed, and the geologic factors that control their occurrence and distribution are outlined. All identified mineral occurrences are plotted on a map (pl. 6), and areas permissive for many of the deposit types are delineated (pls. 7, 8).

Sediment-hosted copper deposits are the most widespread deposit type in the study area, although, compared to worldwide deposits of this type, the size of Bolivian deposits is limited by the small size of reductant traps in the sedimentary sequence.

Although it is not yet known to occur in important amounts, gold may occur in the study area in pre-Tertiary rocks, in sediment-hosted gold deposits, syntectonic antimony deposits, or low-sulfide gold-quartz vein deposits.

Bolivian polymetallic vein deposits have been the source of the most important mineral resources of the study area in the past. Silver and tin were the principal mined commodities, but quantities of copper, lead, zinc, antimony, bismuth, and tungsten were also mined. We show that these deposits, known primarily for tin and silver, belong to the same general class of deposits, and that they are related to dacitic igneous centers emplaced between about 25 Ma and 10 Ma. In the future, gold may be an increasingly important product of these deposits, as exemplified by the Kori Kollo deposit in the La Joya district, which contains about 65,000,000 t at grades of 2.3 g/t Au and 15 g/t Ag.

The study area contains large areas that exhibit geologic characteristics associated with porphyry and epithermal precious-metal deposits. The present level of exploration, however, is insufficient to differentiate the environments specifically permissive for the various deposit types within this group, such as porphyry gold, quartz-alunite veins, quartz-adularia veins, and hot-spring deposits, but the remote-sensing study revealed many areas that may represent the upper parts of any of these deposits.

Other metallic mineral deposit types that were evaluated include basaltic copper, sandstone uranium, placer gold, polymetallic replacement, distal disseminated silver, epithermal manganese, volcanogenic uranium, and rhyolite-hosted tin deposits.

The study area contains an environment that is permissive for evaporite deposits of lithium and boron that may be of worldwide importance. Two great salars on the Altiplano, Uyuni and Coipasa, and many smaller ones, may contain large resources of these materials, as well as sodium carbonate, sodium sulfate, and potash. Zeolites, diatomite, and other materials may also be important.

Other industrial mineral deposit types that were evaluated include barite, dimension stone, and fumarolic sulfur deposits.

The largest portion of this report consists of descriptions of individual mineral sites that were the subject of field studies. These descriptions are organized by deposit type, and include reports on sediment-hosted copper and related deposits, deposits related to young volcanic rocks, Bolivian polymetallic vein deposits, metal deposits of other types, and industrial mineral deposits. Basic descriptions and locations for all known mineral deposits and occurrences in the study area are presented in tabular form (app. A). Important results of the field studies include (1) new descriptions of the sediment-hosted copper deposits in the Corocoro and other areas, (2) a detailed description of the La Joya gold-bearing polymetallic district, (3) descriptions of the poorly known polymetallic deposits in the southernmost part of the Altiplano, in Sud Lípez province, and (4) first descriptions of many saline, alkaline lakes on the southern Altiplano that may contain undiscovered resources of lithium, potassium, boron, zeolites, diatomite, and other materials.

ECONOMIC FEASIBILITY

The U.S. Bureau of Mines prepared an economic sensitivity analysis for three different mineral deposit types in the study area. Detailed cost and price estimates were tailored to specific hypothetical cases, to identify the factors to which mining operations are most sensitive in Bolivia. Infrastructure and transportation, especially in more remote regions of the study area, were found to have a dramatic effect on the economics of a potential mining operation; metal price and ore grade are the next most important factors.

UNDISCOVERED DEPOSITS

In an attempt to quantify our knowledge about the mineral resources of the study area, we made probabilistic estimates of numbers of deposits for selected deposit types. There is a 50 percent chance for the occurrence of 40 or more sediment-hosted copper deposits in the study area. These will be relatively small, but could provide local sources of employment. The likelihood for important resources in basaltic copper or sandstone-hosted uranium deposits is low. The undiscovered gold resource in sediment-hosted gold and syntectonic antimony deposits is indeterminate, however, because of their typical large size, the resource that might exist in these deposit types would be significant. Precious-metal placers may occur in the study area, but there is insufficient information to delineate a permissive area. The resources of silver, lead, zinc, tin, tungsten, bismuth, antimony, and gold in polymetallic vein deposits may be significant; large resources remain to be discovered in 20 known districts in the study area; in addition to these known areas, we estimate there is a 50 percent chance for the occurrence of an additional 6 or more undiscovered deposits. Epithermal precious-metal deposits are similar to sediment-hosted gold deposits in that the value of individual deposits is high, but the undiscovered resource is indeterminate. We have identified more than 130 altered areas in young volcanic rocks, some of which may be related to epithermal precious-metal deposits of various kinds. The number of expected rhyolite-hosted tin and volcanogenic uranium deposits is very low, and any resource contained in them would probably be negligible.

We estimate there is a 50 percent chance for the occurrence of 20 or more lacustrine borate deposits in Cenozoic lacustrine sediments related to the evaporation of lakes in closed basins on the Altiplano. In addition, there is a 50 percent chance for the occurrence of 5 or more lacustrine diatomite deposits in the same permissive area; this area also may contain significant resources of bedded halite and potash, gypsum, sodium sulfate and carbonate, hectorite, and sedimentary zeolites which we are unable to quantify, because of insufficient information. The same area may have resources of lithium, boron, sodium, and potash in interstitial brines trapped in evaporitic sediments, as well as in saline, alkaline lake waters. Barite veins related to polymetallic or other hydrothermal metal deposits, could be a source of barite. Dimension stone for local use is produced at several localities in the study area, and there may be additional resources. Sulfur, in fumarolic sulfur deposits related to Quaternary volcanoes, is currently produced from several mines, and there may be additional resources.

Resumen

GEOLOGIA

En el suroeste de Bolivia, la Cordillera de Los Andes está constituida por tres provincias morfotectónicas contiguas que son, de oeste a este, la Cordillera Occidental, el Altiplano y la Cordillera Oriental. Este informe se refiere solamente a las dos provincias occidentales. Se cree que el basamento por debajo del área de estudio, el cual tiene un espesor de hasta 70 km y es similar a las rocas expuestas inmediatamente al este, en la Cordillera Oriental, donde el cinturón de pliegues y escurrimientos consiste principalmente de lutitas marinas y areniscas paleozoicas y mesozoicas. Las rocas de la Cordillera Oriental, depositadas principalmente sobre zócalo precámbrico, fueron deformadas durante, al menos, tres ciclos orogénicos-tectónicos; el Caledónico (Ordovícico), el Hercínico (Devónico a Triásico) y el Andino (Cretácico a Cenozoico).

El Altiplano es una serie de cuencas intermontañas que se formaron principalmente durante el ciclo andino, aparentemente en respuesta a plegamientos y escurrimientos. Su formación incluye el subescurrimiento hacia el este, del zócalo proterozoico y paleozoico de la Cordillera Occidental, junto con el sobrescurrimiento hacia el oeste de rocas miogeosinclinal paleozoico de la Cordillera Oriental. Estos escurrimientos originaron cuencas continentales de antepaís que recibieron durante el Cenozoico hasta 15.000 m de sedimentos y rocas volcánicas interestratificadas. La actividad ígnea que acompañó a la deformación andina temprana estuvo principalmente centrada más al oeste, en Chile. Durante el pulso principal (Incaica) de la deformación andina, que empezó en el Oligoceno y continuó al menos hasta el Mioceno Medio, varios complejos plutónico-volcánicos se emplazaron en varias localidades del Altiplano, particularmente a lo largo del borde oriental con la Cordillera Oriental y al sur, en el área de Sud Lípez. Durante el Pleistoceno, la mayor parte del Altiplano estaba cubierta por grandes lagos glaciales. Los grandes salares de Uyuni y Coipasa son remanentes de estos lagos.

La Cordillera Occidental está constituida por rocas volcánicas miocenas tardías a recientes consistentes de flujos de lava y tobas de flujo de cenizas, de composición esencialmente andesítica a dacítica, que han sido eruptadas como consecuencias de la subducción de la placa de Nazca, debajo del continente sudamericano. Este subcorrimiento continúa en el presente y muchos de los volcanes que forman la cresta de los Andes y que marcan la frontera internacional con Chile están actualmente activos.

El mapa geológico a escala 1:500.000 que es parte del presente informe (lámina 1) fue compilado principalmente a partir de mapas geológicos inéditos a escala 1:250.000, preparados por geólogos del Servicio Geológico de Bolivia durante los últimos 20 años. Se ha incorporado en este mapa cambios surgidos como producto del trabajo de campo realizado durante este proyecto. También se hicieron modificaniones basadas en información adicional de otros mapas publicados y no publicados, incluyendo tesis de la Universidad Mayor de San Andrés y mapas suministrados por Yacimientos Petrolíferos Fiscales Bolivianos. Las formaciones geológicas usadas en las compilaciones a escala 1:250.000 fueron agrupadas en 15 unidades para el mapa a escala 1:500.000 y fueron escogidas especificamente para apoyar la delineación de áreas permisivas para la ocurrencia de depósitos minerales. Para ayudar a agrupar las unidades del mapa se utilizaron doce edades potasio-argón recientemente realizadas (apendice C).

GEOQUIMICA

Se ha diseñado un estudio geoquímico para la zona polimetálica de La Joya con el objeto de probar la eficacia de las técnicas tradicionales de exploración geoquímica en el ambiente alto y árido del Altiplano. El estudio demuestra que los elementos guías arsénico, antimonio y bismuto están claramente asociados con los metales preciosos y que su distribución en depósitos superficiales delinea adecuadamente las áreas donde afloran rocas mineralizadas conocidas.

SENSORES REMOTOS

El análisis de los imágenes de satélite Thematic Mapper permitió la identificación de más de 130 localidades en el área de estudio donde la alteración hidrotermal ha afectado visiblemente a las rocas (lámina 2). La interpretación detallada fue posible gracias a que la gran altura y el tiempo despejado se combinaron para producir imágenes de alta calidad (lámina 3). Muchas de las áreas alteradas que fueron identificadas están claramente relacionadas a distri-

tos mineros conocidos, pero otras se ubican en regiones remotas y escasamente mapeadas y podrían indicar depósitos hidrotermales aún no descubiertos.

GEOFISICA

El análisis gravimétrico del área de estudio, muestra que el área del Altiplano por debajo de los grandes salares de Uyuni y Coipasa, se distingue por la presencia de anomalías gravimétricas con rumbo norte-noroeste (lámina 4), mientras que hacia el sureste, el Altiplano está caracterizado por anomalías gravimétricas con rumbo norte-noreste.

El mapa aeromagnético muestra que los grandes salares y la Cordillera Occidental poseen un alto relieve magnético causado por rocas volcánicas, cuaternarias y terciarias, conocidas e inferidas, con posibles contribuciones de intrusiones hipoabisales que alimentaron estas rocas (lámina 5). Hacia el noreste, el resto del Altiplano muestra un bajo relieve magnético sin anomalías magnéticas de onda larga.

Hay dos posibles explicaciones para las tendencias contrastantes en los datos de gravedad y magnetismo de los salares y la Cordillera Occidental. Es más probable que las aparentes anomalías magnéticas este-oeste en los salares sean resultado de la baja latitud magnética. Sin embargo, es también posible que el mapa gravimétrico refleje tendencias estructurales terciarias o aún más antiguas, mientras que el mapa magnético refleje volcanismo cuaternario discordante.

DEPOSITOS MINERALES

Los depósitos minerales se clasificaron según tipos de depósitos, usando, cuando era posible, las normas establecidas por el U.S. Geological Survey en previas evaluaciones de recursos. Debido al carácter geológico peculiar de la región de los Andes centrales en Bolivia, se han desarrollado algunos nuevos tipos de depósitos. Se discuten veintiocho tipos específicos de depósitos minerales y se han esquematizado factores geológicos que controlan su presencia y distribución. Todas las ocurrencias minerales identificadas están ubicadas en un mapa (lámina 6) y se han delineado las áreas permisivas para muchos de los tipos de depósitos (láminas 7, 8).

El cobre en roca sedimentaria es el tipo de depósito más común en el área del estudio, aunque comparado con los depósitos mundiales de esta clase, el tamaño de los depósitos bolivianos está limitado por las pequeñas dimensiones de las trampas reductoras en la secuencia sedimentaria.

Aunque no se conoce aún la presencia de oro en cantidades importantes, este puede ocurrir en el área de estudio en las rocas pre-terciarias, en depósitos de oro en roca sedimentaria, en depósitos de antimonio sintectónico o en depósitos de vetas de oro-cuarzo pobres en súlfuros.

En el pasado, los depósitos de vetas polimetálicas bolivianas han sido la fuente de recursos minerales más importantes en el área de estudio. Los principales productos explotados eran plata y estaño, pero tambien se extraían cantidades importantes de cobre, plomo, zinc, antimonio, bismuto y tungsteno. Nosotros mostramos que estos depósitos, conocidos principalmente por estaño y plata, pertenecen a la misma clase general de depósitos y que ellos están relacionados a centros ígneos dacíticos emplazados entre aproximadamente 25 Ma y 10 Ma. En el futuro, el oro de estos depósitos puede ser un producto cada vez más importante, como está demostrado por el depósito Kori Kollo del distrito minero de La Joya, que contiene aproximadamente 65.000.000 t con contenidos de 2,3 g/t Au y 15 g/t Ag.

El área de estudio contiene extensas zonas con características geológicas asociadas a depósitos porfiríticos y epitermales de metales preciosos. Sin embargo, el nivel actual de exploración es insuficiente para diferenciar los ambientes específicamente permisivos para los varios tipos de depósitos dentro de este grupo, tales como pórfido de oro, vetas de cuarzo-alunita, vetas de cuarzo-adularia y depósitos de aguas termales. Sin embargo, el estudio de sensores remotos reveló muchas áreas que pueden representar las partes superiores de cualquiera de estos depósitos.

Otros tipos de depósitos minerales metálicos que fueron evaluados incluyen cobre basáltico, uranio en areniscas, placeres de oro, reemplazamiento polimetálico, diseminación distal de plata, manganeso epitermal, uranio volcanogénico y depósitos de estaño en riolitas.

El área de estudio posee un ambiente que es permisivo para depósitos evaporíticos de litio y boro que pueden ser de importancia mundial. Dos grandes salares en el Altiplano, Uyuni y Coipasa y muchos otros más pequeños, pueden contener grandes recursos de estos elementos, así como carbonato de sodio, sulfato de sodio y potasa. También pueden ser importantes las ceolitas, diatomitas y otros.

Otros tipos de depósitos de minerales industriales que fueron evaluados incluyen barita, roca para uso arquitectónico y depósitos de azufre fumarólico.

La mayor parte de este informe consiste de descripciones de localidades mineralizadas que fueron objeto de estudios de campo. Estas descripciones están organizadas según el tipo de depósito e incluyen informes sobre cobre en roca sedimentaria y depósitos relacionados, a rocas volcánicas jóvenes, depósitos de vetas polimetálicas bolivianas, depósitos metálicos de otros tipos y depósitos de minerales industriales. Las descripciones básicas y localización de todos los depósitos y ocurridos conocidos en el área de estudio está presentada en forma tabular (apendice A). Los resultados más importantes de las investigaciones en el campo incluyen (1) nuevas descripciones de los depósitos

de cobre en roca sedimentaria de Corocoro y otras áreas, (2) una descripción detallada del distrito polimetálico aurífero de La Joya, (3) descripciones de los depósitos polimetálicos poco conocidos de la región más sureña del Altiplano, en la provincia de Sud Lípez y (4) las primeras descripciones de muchos lagos salinos y alcalinos del Altiplano Sur que pueden contener recursos aún no descubiertos de litio, potasio, boro, ceolitas, diatomitas y otros materiales.

FACTIBILIDAD ECONOMICA

El U.S. Bureau of Mines ha preparado un análisis de sensitividad económica para tres tipos diferentes de depósitosde minerales en el área de estudio. Las estimaciones detalladas de costos y precios fueron adecuadas a casos hipotéticos específicos con la finalidad de identificar los factores a los cuales son más sensitivos las operaciones mineras en Bolivia. Se encontró que la infraestructura y el transporte, especialmente en las regiones más remotas del área de estudio, tienen un efecto dramático en la rentabilidad de una operación minera en potencia. El precio del metal y la ley del mineral son los factores más importantes después de los mencionados.

DEPOSITOS NO DESCUBIERTOS

En un esfuerzo para cuantificar nuestro conocimiento sobre los recursos minerales del área de estudio, hicimos estimaciones probabilísticas de números de depósitos para tipos seleccionados de depósitos. Existe una probabilidad de 50 porciento para la ocurrencia de 40 o más depósitos de cobre en roca sedimentaria en el área de estudio. Estos depósitos serían relativamente pequeños, pero podrían proveer fuentes locales de empleo. Existe una baja probabilidad de recursos importantes de cobre basáltico o depósitos de uranio en arenisca. Los recursos aún no descubiertos de oro en sedimentos y en los depósitos de antimonio sintectónico están indeterminados. Sin embargo, debido a su típico gran tamaño los recursos que podrían existir en estos tipos de depósitos serían significativos. Aunque los placeres de metales preciosos pueden ocurrir en el área de estudio, no existe información suficiente para delinear un área permisiva. Los recursos de plata, plomo, zinc, estaño, tungsteno, bismuto, antimonio y oro en depósitos de vetas polimetálicas bolivianas pueden ser significativos; grandes recursos restan por ser descubiertos en 20 distritos conocidos en el área de estudio. Además de estas áreas conocidas, estimamos que existe una probabilidad del 50 porciento de que ocurran al menos otros 6 depósitos no descubiertos. Los depósitos epitermales de metales preciosos se asemejan a los depósitos de oro en roca sedimentaria en el alto valor de los depósitos individuales, pero los recursos aún no descubiertos son indeterminados. Hemos identificado más de 130 áreas alteradas en rocas volcánicas jóvenes, algunas de las cuales están probablemente relacionadas a los depósitos epitermales de metales preciosos de varias clases. Se esperan muy pocos depósitos de estaño en riolita y de uranio volcanogénico y cualquier recurso contenido en ellos probablemente sería insignificante.

Estimamos que hay una posibilidad del 50 porciento para la ocurrencia de 20 o más depósitos lacustres de boratos en sedimentos lacustres cenozoicos relacionados a la evaporación de lagos en cuencas cerradas en el Altiplano. Además, existe una probabilidad de 50 porciento para la ocurrencia de 5 o más depósitos de diatomita lacustre en la misma área permisiva. Esta área también puede contener recursos significativos de halita estratificada, potasa, yeso, sulfato y carbonato de sodio, hectorita y ceolitas sedimentarias que no pudimos cuantificar por la falta de suficiente información. La misma área puede tener recursos de litio, boro, sodio y potasa en salmueras intersticiales atrapadas en sedimentos evaporíticos, así como en lagos salinos y alcalinos. Vetas de barita relacionadas a depósitos polimetálicos y otros depósitos metálicos hidrotermales pueden ser fuentes de barita. Roca para uso arquitectónico para uso local es producida en varias localidades en el área de estudio y pueden haber recursos adicionales. Azufre, en depósitos de azufre fumarólico relacionados a volcanes cuaternarios, es actualmente producido en varias minas y podrían existir recursos adicionales.

Introduction

FIGURE

1. Map showing geographic features and named 1:250,000-scale quadrangles **11**

Since prehistoric times, the area we know as Bolivia has been famous for its mineral wealth. When the Spanish began to explore what was known to them as Upper Perú in the 16th century, they discovered that the Quechua, Aymara, and other Native American peoples had been mining precious metals for hundreds of years. Unparalleled production of precious metals from the New World, including the silver mines of Bolivia, supported the Spanish Empire for the next 200 years. Native uprisings, followed by the wars for independence which culminated in the founding of Bolivia in 1825, interrupted production of silver in the area. After independence, interest in mining was renewed and tin began to gain importance on world markets. Today, despite the reversals of the 1980's, mining continues to be a mainstay of the Bolivian economy.

The focus of this study consists of two physiographic provinces in the westernmost part of Bolivia, the Altiplano, a flat plain at an elevation of about 3,800 m, and the Cordillera Occidental, a volcanic mountain chain that helps define the borders with Peru and Chile and reaches altitudes of higher than 6,000 m. The study area includes all or parts of 16 1:250,000-scale quadrangles (fig. 1). It is bounded on the east by the Cordillera Oriental, the main structural manifestation of the Andes Mountains in Bolivia.

The current study is a cooperative venture between the U.S. Geological Survey (USGS), the U.S. Bureau of Mines (USBM), and the Servicio Geológico de Bolivia (GEOBOL). As a preliminary phase, a search of the existing published and unpublished literature was undertaken from February 1990 to April 1991. This phase was followed by combined USGS and GEOBOL field parties that visited selected sites in the study area between April and November 1990. The U.S. Bureau of Mines study uses USGS and GEOBOL data and was designed to evaluate economic factors that may control development of several different mineral deposit types. Yacimientos Petrolíferas Fiscales de Bolivia (YPFB), the state-owned oil company in Bolivia, provided extensive geophysical data that complemented our studies.

Although the past few years have witnessed major strides in understanding the geologic processes that have shaped the central Andes, there is still a general lack of detailed knowledge for most of the region. The Altiplano and Cordillera Occidental study area is an excellent example; geologic information ranges from extensive for a few of the better known mining areas to virtually nonexistent for much of the area.

Because the quality of a mineral-resource analysis depends almost entirely on the quality of the available geologic information base, we have attempted to counter deficiencies in field geologic data, by including new chemical and isotopic data, satellite imagery, and geophysical data in our study. Although these new data are invaluable in helping provide a better understanding of geologic processes and in developing deposit models, they are no substitute for detailed geologic field investigations.

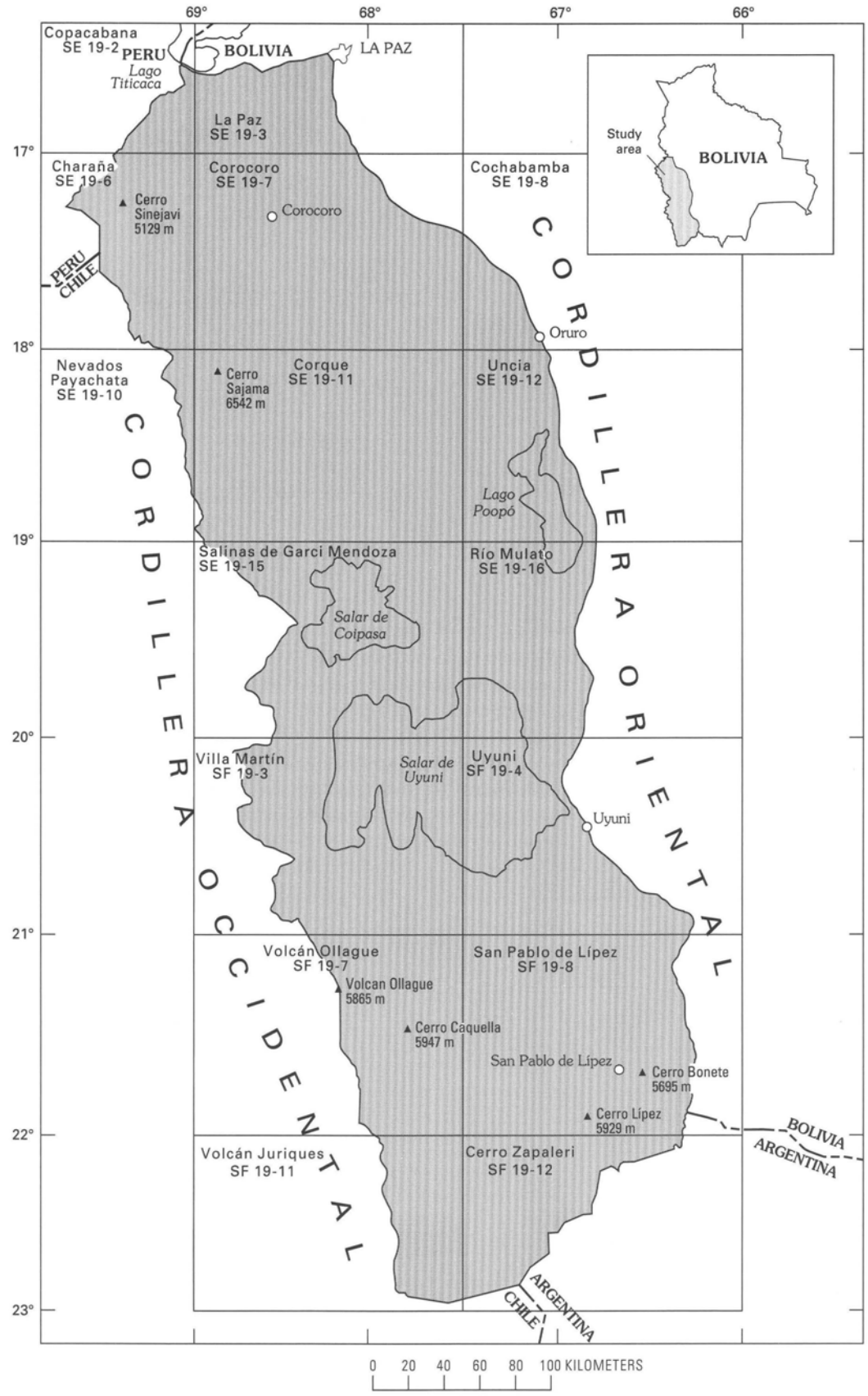


Figure 1. Map showing some geographic features on the Altiplano and in the Cordilleras Occidental and Oriental, Bolivia. Named 1:250,000-scale quadrangles and outline of study area (shaded) are shown.

Acknowledgments

This volume reflects the contributions of a great many individuals, without whose help completion of this project would not have been possible.

Initial planning by Norman J Page and Darrell Herd (USGS), Jaime Villalobos and Lorgio Ruíz (Ministerio de Minería y Metalurgía), Milton Suárez (GEOBOL), and Leslie Sternberg and Fernando Urquidi (American Embassy, La Paz) resulted in a proposal to assess the mineral resources of the Bolivian Altiplano and Cordillera Occidental. Three agencies provided financial support to the project, and we would like to specifically thank Daniel Stein, of the U.S. Trade and Development Program, Robert Kramer, of the U.S. Agency for International Development program in Bolivia, and Fernando Méndez and Peter Fozzard, of the World Bank. The design of the project benefited greatly from input from the North American mining community, in particular, from Robert Cinq-Mars and Richard Law (LITHCO), Douglas Smith (ASARCO), A.L. Lawrence (Phelps Dodge), Luís Vega (Battle Mountian Gold), David Holmes (Meridian Minerals), Hans Schreiber (Behre Dolbear), John Gustavson and Leland Cress (Gustavson Associates), Charles Melbye (consultant to Aurífera Altiplanica), and Craig Bow (consulting geologist). Additional input was received from Orlando Martino and Harold Bennett of the U.S. Bureau of Mines, and A.T. Ovenshine and John DeYoung, Jr. of the USGS. Special thanks are due to the American Ambassador to Bolivia, Robert Gelbard, for his enthusiastic support of this project. Robert Learned acted as in-country coordinator. Gregory E. McKelvey coordinated the project in the United States.

We wish to thank numerous people in Bolivia who were instrumental to this project, especially exploration geologists, mine owners, and government officials: Alberto Oño (COMIBOL, Corocoro Mine), Jaime Quiroga, Carlos Murillo, Saveno Mamani and Hernán Camacho (Cía Minera Yana Mallcu), Jaime Villalobos and Carlos Zamora (EXPROMIN), Gonzalo Rico (Empresa Nacional de Electrificación, Sol de Mañana Geothermal Project), Charles Bruce, Johnny Delgado, Rodolfo Aguirre, Stewart Redwood and Craig McEwan (MINTEC), John Hertel and John Waghorn (EMICRUZ), Gonzalo Sánchez, Abdón Flores and Oscar Bonifaz (COMSUR), Guido Arce, Oscar Anzoleaga, Kirk Schmidt, Marwin Columba, Mario Mercado and Alvaro Ugalde (Cía. Minera Inti Raymi/Battle Mountain Gold Co.), Douglas Smith and Lawson Entwistle (ASARCO), Jeffrey Abbott (Homestake International), Peter Matthews and Hugh Stuart (Pan Andean S.A.), David DeWitt and Glenn Melosh (UNOCAL), Walter Huarachai (Mina Candelaria), Victor Chambi (EMICLA), Gonzalo Garrón (Horsu S.A.), and the staff at the San José de Berque mine. Consulting geologists who contributed information include Jim MacNamee, Fred Barnard, Oscar Ballivian, and H.G. Freydanck. Hugo Alarcón and the staff at the Instituto de Geología Económica and the Facultad de Ciencias Geológicas of the Universidad Mayor de San Andrés were very helpful. Hernán Uribe, Hernán Murillo, and William Blacutt assisted in some of the field work and in other matters. Geophysical data were provided by Rafael Arias, José Careaga, and Eloy Martínez (YPFB), and Francis Renschen (DMA). Base and topographic maps were kindly provided by Hamlet Kelly (DMA) and Charles Klimicek and Frank Avila (Instituto Geográfico Militar). Advice, information, and assistance was obtained in all stages of the project from Enrique Arteaga and José Pinto (United Nations Development Project), Gotthard Walser, Claude Ginet, Tom Ekström, Krister Lundquist, Fred Witschard and Hans Zweifel (Swedish Geological Co.), Gérard Hérail (Office de la Recherche Scientifique et Technique de Outre-Mer), Lothar Lahuer, Christoph Grissemann and Albrecht Schneider (Bundesanstalt für Geowissenschaften und Rohstoffe), and Simon Lamb, Logan Kennan and Leonora Hoke (Oxford University). Claudio Alejo, Corregidor of San Pablo de Lípez, the people of Comunidad Todos Santos and Guadalupe, and personnel of the Fuerzas Armadas de Bolivia in Alota and San Pablo de Lípez provided valuable assistance in the field. Logistical and administrative support were provided by Michael Shelton, Robert Goldberg, Vandoster Tabb, Mercedes Viscarra, and Tom Barnes of the American Embassy in La Paz.

Numerous colleagues in GEOBOL contributed their efforts to the project. Oscar Siles and Mauricio Hurtado managed administrative and logistic support. Herberto Pérez (Regional Geology) and Edgar Ruíz (Economic Geology) provided staff and technical assistance. Martha Fernández provided access to the library and GEOBOL files. Computer, secretarial, and messenger support was provided by Wilson Carranza, Virginia Argote, María Inés Zambrana, and Ema Tusco. Angel Yucra drafted many of the maps generated by the project and electrician Ponciano

Laura solved many problems related to radios and power for computers. Rogelio Tapia, Máximo Aliaga, Eustaquio Nina, and Wilfredo Mallea drove the field vehicles and managed accomodations in the field.

We also wish to thank many USGS colleagues who contributed in a variety of ways to ensure the success of this project.

Preparation of the digital geologic map was greatly assisted by Carl L. Rich and Carol Mladnich. Esther Castellanos digitized aeromagnetic maps provided by YPFB and Mark Webring provided programming assistance for the processing of geophysical data. Cathy Ager processed LANDSAT imagery and Eric Livo provided computer support for the image processing and analysis. Robert Hershiser, Don Huber, and Barry Moring provided technical support. Deborah Colley, Susan García, Diana Brown, Bonnie East, Patricia Tuholski, Cheryl Smith, Patricia Covarrubias, Ronnie Andreani, Robert Barrick, Mona Chin, Sandye Cole, GiGi Collins, Nancy Crossley, Carolyn Didonato, Kimianne Lee, Dottie Kubitschek, Bobbi Ann Ruddy, Linda Shook and Frances Siegal provided administrative support.

George Ericksen contributed unpublished data. Mary Rabbitt, Clifford Nelson, James McAllister, Ward Smith, and Lincoln Page kindly searched their files and memories for information relating to the history of USGS activities in Bolivia.

The manuscript was reviewed by Miles Silberman, David John, Sherman Marsh, Larry Rowan, David Ponce, Jim Case, Dan Mosier, Hal Morris, Norm Page, and Donald Singer. The volume was edited by Susan Kropschot. Pat Wilber coordinated preparation of the illustrations by Hank Williams, Joe Springfield, and Michael Kirtley. The cover was designed by Art Isom using a photograph by Sigrid Asher-Bolinder of Laguna Hedionda Norte. Additional support was provided by Denny Welp, Rob Wells, Gayle Dumonceaux, Wayne Hawkins, Tom Loesch, Norma Maes, John Preisendorf, Ginger Scott, Loretta Ulibarri, Gene Ellis, Alex Donatich, Lorna Carter, Judy Stoeser, Julia Taylor, Joan Nadeau, Shelly Fields, and Debbie Sokol.

Geologic Setting

By Donald H. Richter, Steve Ludington, *and* Eduardo Soria-Escalante

Regional overview **14**
Altiplano **16**
Cordillera Occidental **19**
Volcanic geology **19**
Older volcanic rocks **22**
Ignimbrites **22**
Stratovolcanoes **23**
Chemistry **24**
Discussion **24**

FIGURES

2. Map showing the location of the Altiplano and the Cordilleras Oriental and Occidental **15**
3. Cross section through the central Andes showing present-day crustal thickness **17**
4. Map showing some of the major structural elements and distribution of eruptive stratovolcanic centers **18**
5. Time-stratigraphic correlation chart **20**
6. Map showing some volcanic features associated with the ignimbrites and older volcanic centers **21**
7. Variation diagram showing K_2O vs. SiO_2 for Cenozoic volcanic and plutonic rocks **22**
8. Variation diagram showing total alkalies vs. SiO_2 for Cenozoic volcanic and plutonic rocks **23**

REGIONAL OVERVIEW

The Andean Cordillera of western South America is commonly referred to as the classic example of a convergent continental plate margin (Dewey and Bird, 1970; Mitchell and Reading, 1969). The cordillera consists of three segments, northern, central, and southern Andes, each with similar but distinct Mesozoic and Cenozoic histories. The area of this report, southwestern Bolivia, lies in the central Andes, astride a major oroclinal bend in the cordillera. This part of the cordillera consists of three contiguous morphotectonic provinces, which are, from west to east, the Cordillera Occidental, Altiplano, and Cordillera Oriental (fig. 2). Built across these provinces is the Central Volcanic Zone (Thorpe and others, 1982), the largest of the three active volcanic chains in the Andean Cordillera.

The Cordillera Oriental is a polygenic Phanerozoic fold and thrust belt consisting largely of Paleozoic deep marine and platform facies rocks, and Mesozoic marine, carbonaceous platform, and delta facies rocks. These rocks were deposited mostly on Precambrian basement in a deep miogeoclinal basin and were subsequently deformed during at least three tectonic-orogenic cycles: Caledonian (Ordovician), Hercynian (Devonian to Triassic), and Andean (Cretaceous to Cenozoic) (Sempéré, 1990). Source regions for the Paleozoic sediments in the miogeocline were the Precambrian Brazilian shield to the northeast, which is composed of granulitic, gneissic, and metasedimentary rocks (Litherland and others, 1989), and the 2–Ga-old Proterozoic Arequipa massif of Peru-Chile to the west and southwest (Cobbing, 1985). No volcanic arcs or major suture zones are known in the central Andes suggesting that the fold and thrust belt and its basement are an integral part of the old Pangean passive continental margin (Cobbing, 1985). Following latest Hercynian deformation, extensional tectonism accompanied by peralkaline volcanism and the emplacement of granitoid plutons during the Permo-Triassic, may have heralded the beginning of an active subduction regime (Pitcher and Cobbing, 1985). Subduction and generation of calc-alkaline magma were well established by Jurassic time and have continued in an uninterrupted fashion since then. In the Tertiary, probably primarily

during the Incaic phase of the Andean orogeny, the Cordillera Oriental fold and thrust belt formed, and was thrust westward over foreland basins of the Altiplano.

The Cordillera Occidental, composed of a western eugeosyncline-volcanic arc and an eastern miogeosyncline, developed in response to subduction (Andean orogeny) following cessation of the Hercynian orogeny (Cobbing, 1985). Shales and sandstones of the miogeosyncline were deposited in disconnected back-arc basins during a period of extensional tectonism from Late Jurassic through Early Cretaceous time. During this same period, lava flows and volcaniclastic rocks were accumulating in the outboard eugeosyncline. By Late Cretaceous time, most of the area of the Cordillera Occidental was emergent; continental

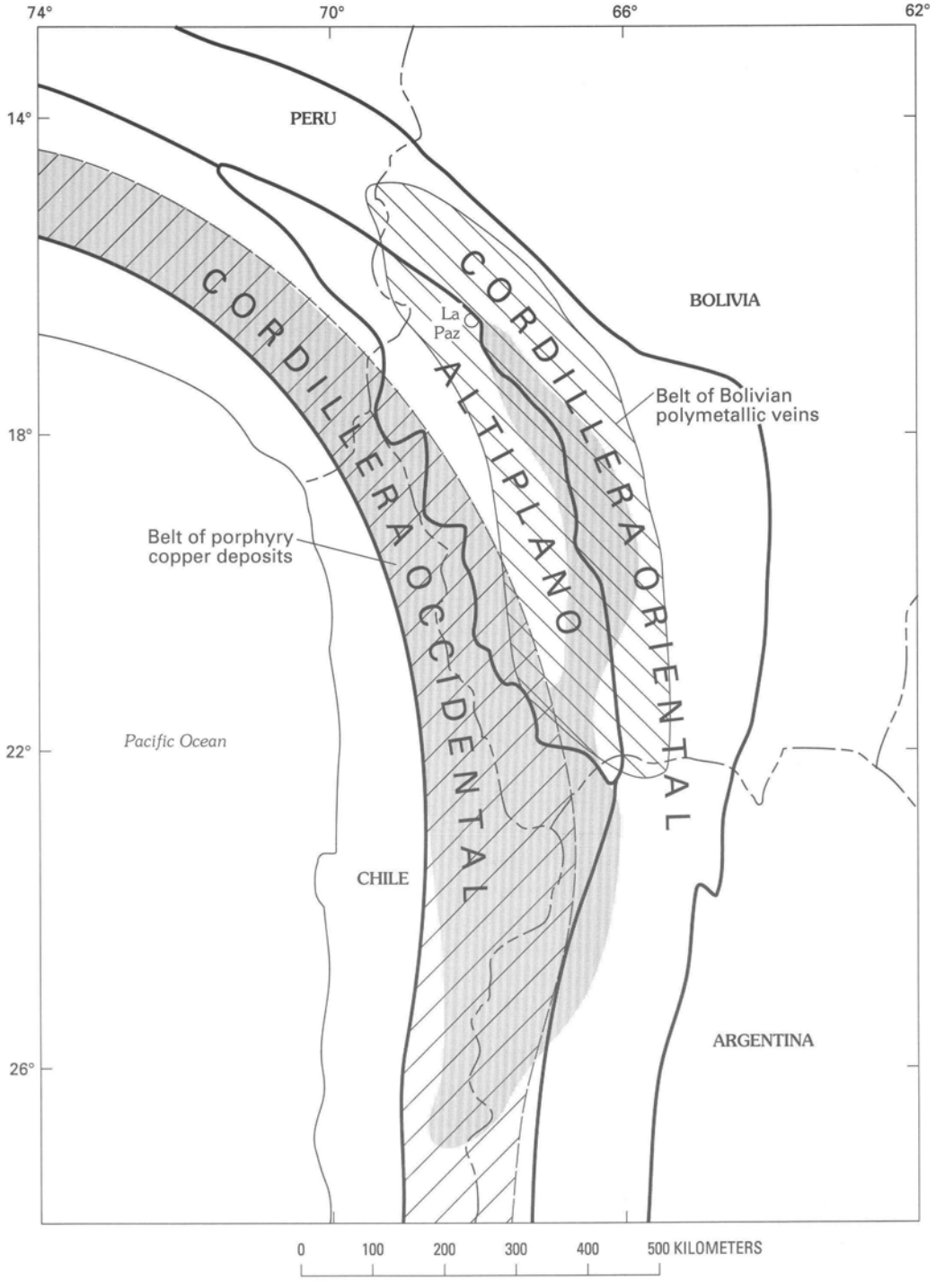


Figure 2. Map showing the location of the Altiplano and the Cordilleras Oriental and Occidental, Bolivia, Peru, Chile, and Argentina. Shaded area denotes the Central Volcanic Zone.

sediments were being deposited across the miogeosyncline and large granitoid plutons, that constitute the Coastal Batholith of Peru and Chile, were being emplaced in the eugeosyncline.

Since the beginning of the Andean orogeny, the central Andes, including the Altiplano have been predominantly a positive tectonic element along the continental margin. Continental sedimentation, which began in the Late Cretaceous, continued throughout most of the Cenozoic. In Pleistocene time most of the Altiplano was covered by large glacial lakes, the remnants of which are the present great salars.

The Altiplano and most of the Cordillera Occidental overlie an exceptionally thick (as much as 70 km) section of continental crust (James, 1971). This thick crustal root, which characterizes the central Andes, formed largely during the Miocene more or less concomitant with the uplift of the cordillera (Isacks, 1988). Pre-Mesozoic basement rocks under the eastern edge of the Altiplano, and perhaps under much of the southern part as well, apparently consist chiefly of lower Paleozoic marine shales and sandstones similar to the rocks of the Cordillera Oriental. Under much of the western part of the Altiplano the basement probably consists largely of Proterozoic crystalline rocks (Lehman, 1978; Cobbing, 1985), although Pb-isotope signatures (Worner and others, 1990) suggest that, south of about lat 20° S. beneath the Cordillera Occidental, a Paleozoic basement is present.

The Central Volcanic Zone (CVZ), of late Oligocene to Holocene age, is a broad arcuate zone (fig. 2), as wide as 400 km, that extends from southern Peru (lat 14° S.), through Bolivia and Chile, to northern Argentina (lat 28° S.) (Thorpe and others, 1982). It covers large areas of the Cordillera Occidental and developed in response to subduction of the Nazca plate beneath the continental crust of the South American plate. In Bolivia, the CVZ consists of two calc-alkaline volcanic arcs that converge at the southern end of the Altiplano. The western and best developed arc, which forms the high crest of the Cordillera Occidental, is characterized chiefly by numerous Miocene to Holocene, andesitic to dacitic stratovolcanoes. The eastern volcanic arc of the CVZ, which occurs along the western margin of the Cordillera Oriental fold and thrust belt, contains a few, and locally, very large, Miocene to Pliocene, dacitic to rhyolitic ignimbrite fields and some scattered Miocene domes, remnant stratovolcanoes, and shallow intrusives.

Two principal volcanogenic mineral belts, each containing world-class deposits, occur in the central Andes region of Bolivia and Chile. Copper (Mo, Au) porphyry deposits, associated primarily with plutonic rocks in the Late Cretaceous-Early Tertiary miogeosyncline/eugeosyncline (Sillitoe, 1973), occur in a belt west of the CVZ in Chile and Peru. Bolivian polymetallic vein deposits occur in a belt to the east, coincident with the eastern volcanic arc of the CVZ (fig. 2). The western volcanic arc of the CVZ, where Quaternary volcanoes may conceal a variety of mineral deposit types, and the Altiplano occur between the two mineral belts. On the Altiplano, Cenozoic continental sedimentary rocks host a number of stratiform copper deposits.

ALTIPLANO

The Altiplano is a series of high, contiguous intermontane basins located between the Cordillera Oriental on the east and the high volcanoes of the Cordillera Occidental on the west. Its structure and origin are still not adequately known and only recently has there been a concerted geological-geophysical effort to understand this enigmatic tectonic feature. In the following summary of the major structural features of the Altiplano we have relied heavily on the results of recent investigations by a number of geoscientists who are proposing new models for central Andean Tertiary tectonics, based largely on crustal shortening (Isacks, 1988; Sheffels, 1988, 1990; Sempéré, Hérail, Oller, Baby, and others, 1990; Sempéré, Hérail, Oller, and Bonhomme, 1990; Baby and others, 1990; Aranibar and Martinez, 1990).

Traditional theories about the origin of the Altiplano propose long periods of extension interspersed with short compressional pulses, which is expressed primarily by high-angle faulting and the formation of basins (see for example, Martinez, 1980; Sébriér and others, 1988). These traditional theories are being challenged by new concepts and hypotheses that, on the basis largely of new subsurface data, propose long periods of shortening and a model of thin-skinned tectonics that includes fold and thrust belts, wrench fault zones, and intermontane foreland basins (fig. 3).

Two extended periods of crustal shortening at 27–19 Ma and 11–5 Ma may be responsible for most of the region-wide structural deformation on the Altiplano (Sheffels, 1988; Sempéré, Hérail, Oller, Baby, and others, 1990). Other recognized Cenozoic deformational events at 42 Ma, 17–15 Ma, and 2 Ma (Sébriér and others, 1988) were of much shorter duration and possibly not of regional significance. The 27–19 Ma late Oligocene-early Miocene episode is now considered to mark the beginning of the main Andean orogeny (Incaic tectonic phase) in Bolivia (Sempéré, Hérail, Oller, and Bonhomme, 1990). Onset of this episode apparently coincided with the initiation of Tertiary volcanic activity in the central Andes and the displacement of the deformation front eastward leading to development of the Cordillera Oriental and isolation of the Altiplano from further marine incursion (Sempéré, Hérail, Oller, Baby, and others, 1990). Both the tectonism and volcanism may have been the result of a period (26–6 Ma) of fast plate convergence (Pilger, 1984) and possibly plate reorganization.

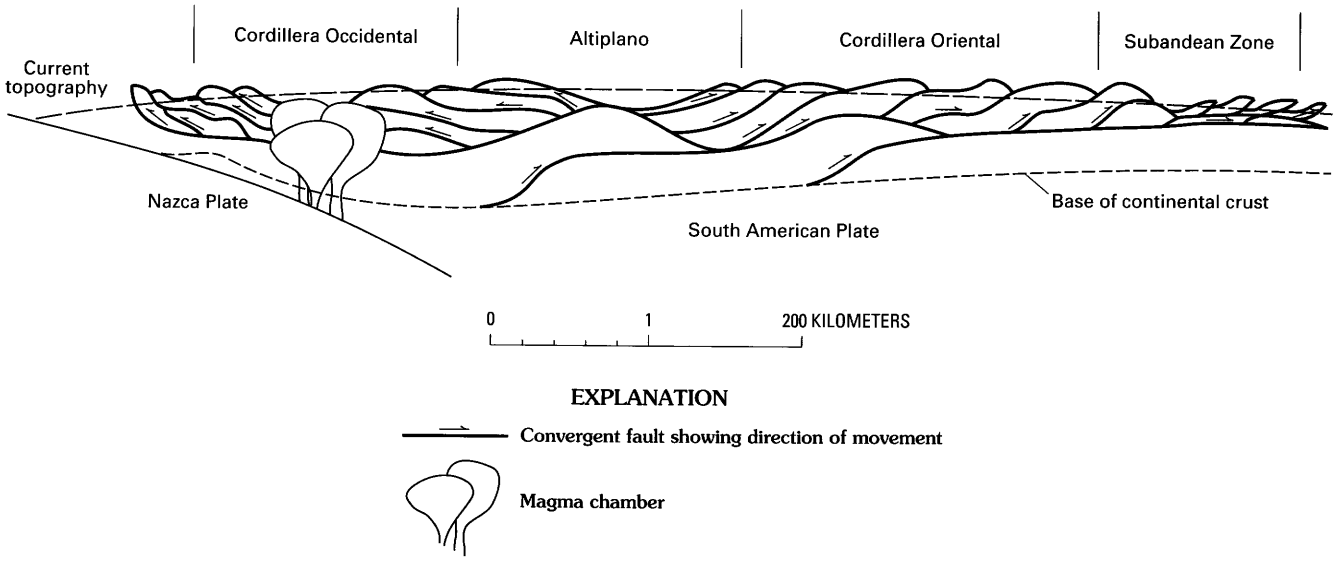


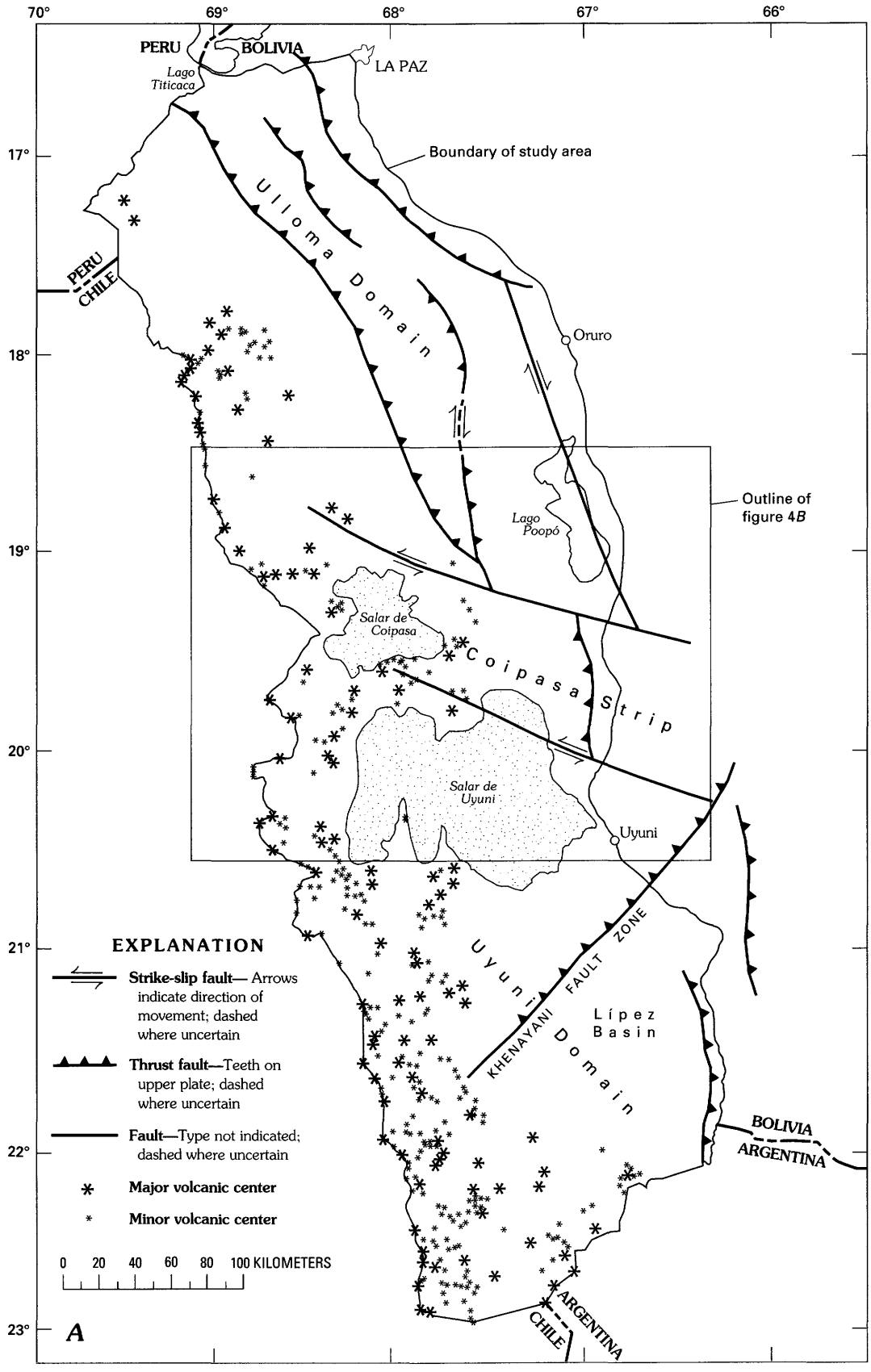
Figure 3. Diagrammatic cross section through the central Andes, at about 18° S., showing present-day crustal thickness. Crustal shortening, schematically indicated by east- and west-vergent fault systems, is considered the dominant mechanism in crustal thickening (modified from Sheffels, 1990).

In brief, the Altiplano can be characterized as a series of intermontane foreland basins that received sediments from convergent fold and thrust belts, associated with crustal shortening and thickening. Its evolution involves the eastward underthrusting of a wedge of the Cordillera Occidental and its Proterozoic basement, forming the Bolivian orocline, and the westward thrusting of the Paleozoic miogeoclinal rocks of the Cordillera Oriental (Sempéré and others, 1989). Sempéré, Hérail, Oller, Baby, and others (1990) separate the Altiplano into two structural domains separated by the Coipasa strip, an elongate block bounded by westnorthwest-trending left-lateral wrench faults (fig. 4). The Ulloma domain, north of the Coipasa strip, is primarily a northnorthwest-trending basin along a southwest-vergent fold and thrust belt. The Uyuni domain, to the south, is a northnortheast-trending fold and thrust belt containing upper Ordovician and younger rocks that is thrust eastward over its foreland (Lípez) basin by the Khenayani thrust fault system (Baby and others, 1990). To the east the Uyuni domain is bounded by a west-verging thrust fault system that places Ordovician sedimentary rocks of the Cordillera Oriental, that were deformed in late Ordovician time (Caledonian orogeny), over Cenozoic rocks of the Altiplano. Two large outliers of Ordovician rocks in the southern part of the Lípez basin, similar to those found in the Cordillera Oriental, may be large flower structures thrust at high angles by their boundary faults against Eocene to early Miocene sedimentary rocks (Baby and others, 1990) (pl. 1).

The structural interpretation of the Altiplano by Aranibar and Martinez (1990) differs somewhat in detail from that of Baby and others (1990) and Sempéré, Hérail, Oller, Baby, and others (1990), especially on the central and southern Altiplano. Although Aranibar and Martinez (1990) mention westnorthwest-trending lateral displacements in the area of the Coipasa strip (fig. 4), they do not show such faulting on their structural map. Instead, they extend the San Andres-Tambillo fault system south, across the Coipasa strip, to the Khenayani fault system, an interpretation that appears to be supported by the aeromagnetic data. A more significant difference, however, between these two structural interpretations, is in the nature of the Khenayani fault system on the southern Altiplano. Aranibar and Martinez (1990) show the Khenayani as a left-lateral wrench fault system, whereas Baby and others (1990) show it as a relatively high-angle thrust fault. We prefer the latter, as the fault juxtaposes post-Caledonian, Silurian sedimentary rocks against Tertiary formations in the Lípez basin.

During the Tertiary as much as 15,000 m of continental sedimentary rocks were deposited in rapidly subsiding basins on the Altiplano (Martinez, 1980). Deposition of these sediments began in the Paleocene and Eocene; in the Oligocene and Miocene, coincident with deformation in the region, sedimentation rates were as much as 1 mm/yr (Lavenu, 1986). In general, the Tertiary Altiplano rocks overlie unconformably a basement of folded Paleozoic sedimentary rocks that is locally covered by thin, marine to continental sedimentary rocks of Cretaceous age. A time-stratigraphic correlation chart for some of the major Tertiary formations of the Altiplano is shown in figure 5.

The thickest Tertiary sedimentary rocks are apparently in the northern and central Altiplano. Deposition of the Eocene-Oligocene Tiahuanacu Formation (fig. 5) initiated filling of a foreland basin east of the Andean orogenic front. The Tiahuanacu Formation consists of about 2,500 m of continental redbeds that thicken and coarsen upwards (Sempéré, Hérail, Oller, and Bonhomme, 1990).


70°
69°
68°
67°
66°
17°
18°
19°
20°
21°
22°
23°
PERU
BOLIVIA
Lago Titicaca
LA PAZ
Boundary of study area
Ulloma Domain
PERU
CHILE
Oruro
Outline of figure 4B
Lago Poopó
Salar de Coipasa
Coipasa Strip
Salar de Uyuni
Uyuni
Uyuni-Khenayani FAULT ZONE
López Basin
Domain
BOLIVIA
ARGENTINA
ARGENTINA
CHILE
EXPLANATION
Strike-slip fault— Arrows indicate direction of movement; dashed where uncertain
Thrust fault—Teeth on upper plate; dashed where uncertain
Fault—Type not indicated; dashed where uncertain
Major volcanic center
Minor volcanic center
0 20 40 60 80 100 KILOMETERS
A

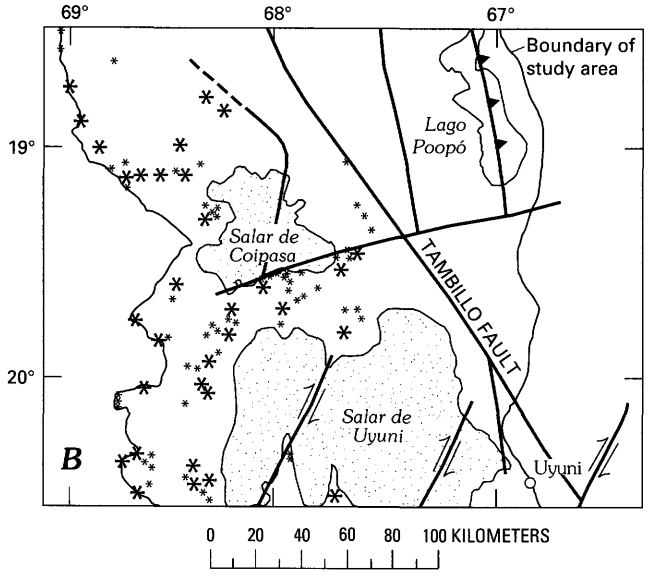


Figure 4 (above and facing page). Map of the Altiplano and Cordillera Occidental, Bolivia, showing some of the major structural elements and distribution of eruptive centers of the late Miocene to Holocene stratovolcanoes (pl. 1, unit QTev). *A*, Structure from Sempéré (1990); *B*, alternative structural interpretation of the central Altiplano from Aranibar and Martinez (1990), as discussed in text.

Another very thick section is found in the Serranía de Huayllamarca, west of Oruro. Following the major eastward jump of the Andean deformation front, during the 27–19 Ma shortening episode, coarse sandstones and conglomerates of the Coniri Formation were deposited unconformably on Tiahuanacu beds in a foreland basin, southwest of a southwest-vergent fold and thrust belt (Sempéré, 1990b). Younger sedimentary rocks consisting chiefly of sandstone, shale, and conglomerate of the Kollo-kollu and Caquiaviri Formations and parts of the Abaroa Formation, and volcanic flows and tuffs of the Mauri Formation continued to fill the subsiding basin until about Pliocene time when a second major deformational episode occurred that affected the depositional environment. Fluvial and lacustrine sand, silt, clay, and locally gravel (Charaña, Ulloma, and Umala Formations) intercalated with regional tuff units (Perez Formation, Toba 76 tuff) characterize the younger deposits of the northern Altiplano.

To the south in the central and southern parts of the Altiplano, the basal Tertiary rocks consist of a series of dark-red to purplish-red sandstone, siltstone, shale, and conglomeratic sandstone (Potoco Formation) about 1,300 m thick. These rocks conformably overlie a relatively thin Cretaceous section (Kussmaul and others, 1977).

The Potoco progrades westerly suggesting that it was a foreland deposit associated with the westerly thrusting of the Ordovician strata in the Cordillera Oriental (Baby and others, 1990). Unconformably overlying the Potoco in the south are as much as 2,600 m (Meave, 1972) of sandstone and conglomerate of the Lower Quehua and San Vicente Formations and in the central part, sandstone, shale, silt, and gypsum of the Corocoro Group. These strata, deposited after the eastward shift of the Andean deformation front, formed in a foreland basin apparently associated with eastward-directed thrusting (Baby and others, 1990). Following this sedimentary cycle, volcanic activity, beginning in late Oligocene-early Miocene time, deposited as much as 2,900 m (Meave, 1972) of volcanic and volcaniclastic rocks (Upper Quehua Formation) from a number of very large eruptive centers, especially in the southern Altiplano. By Pliocene time, most eruptive activity had shifted westward, where it presently is restricted to the Cordillera Occidental.

CORDILLERA OCCIDENTAL

The Cordillera Occidental includes the present volcanic crest of the Andes. Its boundary with the contiguous Altiplano is vague and subjective, but for the purpose of this report is arbitrarily placed at the eastern and northern limit of the Holocene-late Miocene stratovolcanoes (pl. 1, unit QTev). In the southern Altiplano, along the fringe of the Lípez basin, the distinction between the Altiplano and either the Cordillera Occidental or the Cordillera Oriental becomes even less defined because of the presence of older (late Oligocene-Miocene) volcanic centers and their proximal and distal deposits. These older volcanic rocks, which may also underlie much of the Cordillera Occidental, crop out on the northern Altiplano (Mauri Formation), central Altiplano (Carangas Volcanic Field), and north and west of the Salar de Uyuni (fig. 6).

VOLCANIC GEOLOGY

Volcanic activity on the Altiplano and in the Cordillera Occidental, Bolivia, began in late Oligocene-early Miocene time, broadly coincident with the beginning of the Incaic phase of the Andean orogeny and has continued with few interruptions to the present. Earliest activity, in the Oligocene and Miocene, resulted in the development of large eruptive complexes and concomitant intrusive activity in the southern Altiplano and along both margins of the Altiplano (fig. 2). Beginning in late Miocene time and continuing throughout the Pliocene, large volumes of ignimbrite were erupted from caldera-shield complexes (Baker, 1981; Francis and others, 1983), mostly in the southern Altiplano. Stratovolcanoes of the modern Andean arc, which form most of the Cordillera Occidental, began to build as early as late Miocene time (ca. 7 Ma) concurrent with the late stages of ignimbrite activity. Although there are no reports of historic eruptive activity, seven of the stratovolcanoes contain active fumaroles and more than a dozen show well-preserved vent structures, lava flows, and domes (Soria-Escalante and others, 1991).

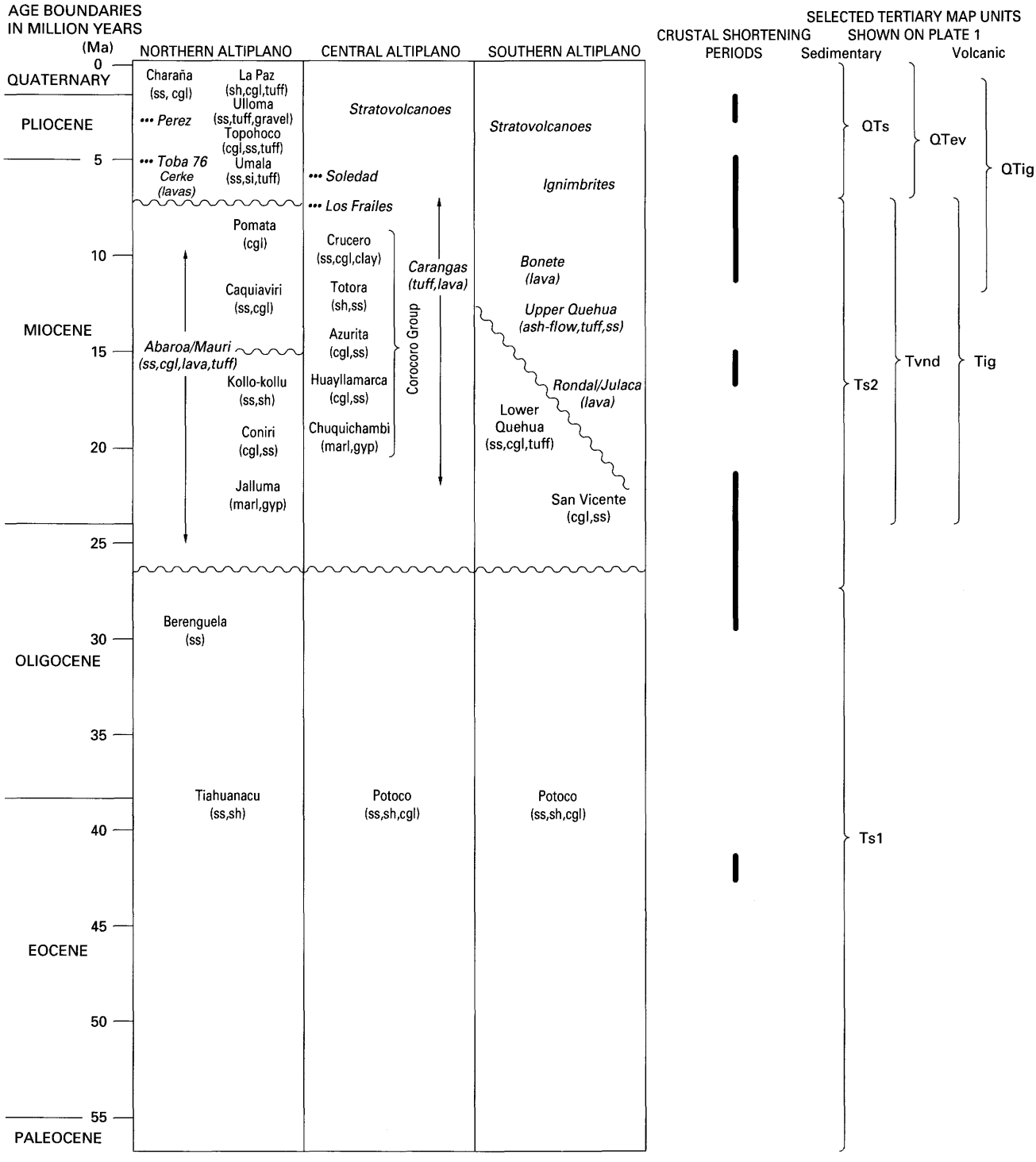


Figure 5. Time-stratigraphic correlation chart for selected Cenozoic formations and other rock units of the Altiplano and Cordillera Occidental, Bolivia, and their relationship to map units on the 1:500,000-scale geologic map (pl. 1). Formations and rock units that are primarily volcanic, shown in italics; dotted lines denote dated regional tuffs. Not all recognized formations are shown. Tertiary compressional (shortening) events from Sébrier and others (1988) and Sempéré, Hérail, Oller, Baby, and others (1990). Wavy lines denote unconformities; ss, sandstone; sh, shale; si, siltstone; cgl, conglomerate; gyp, gypsum.

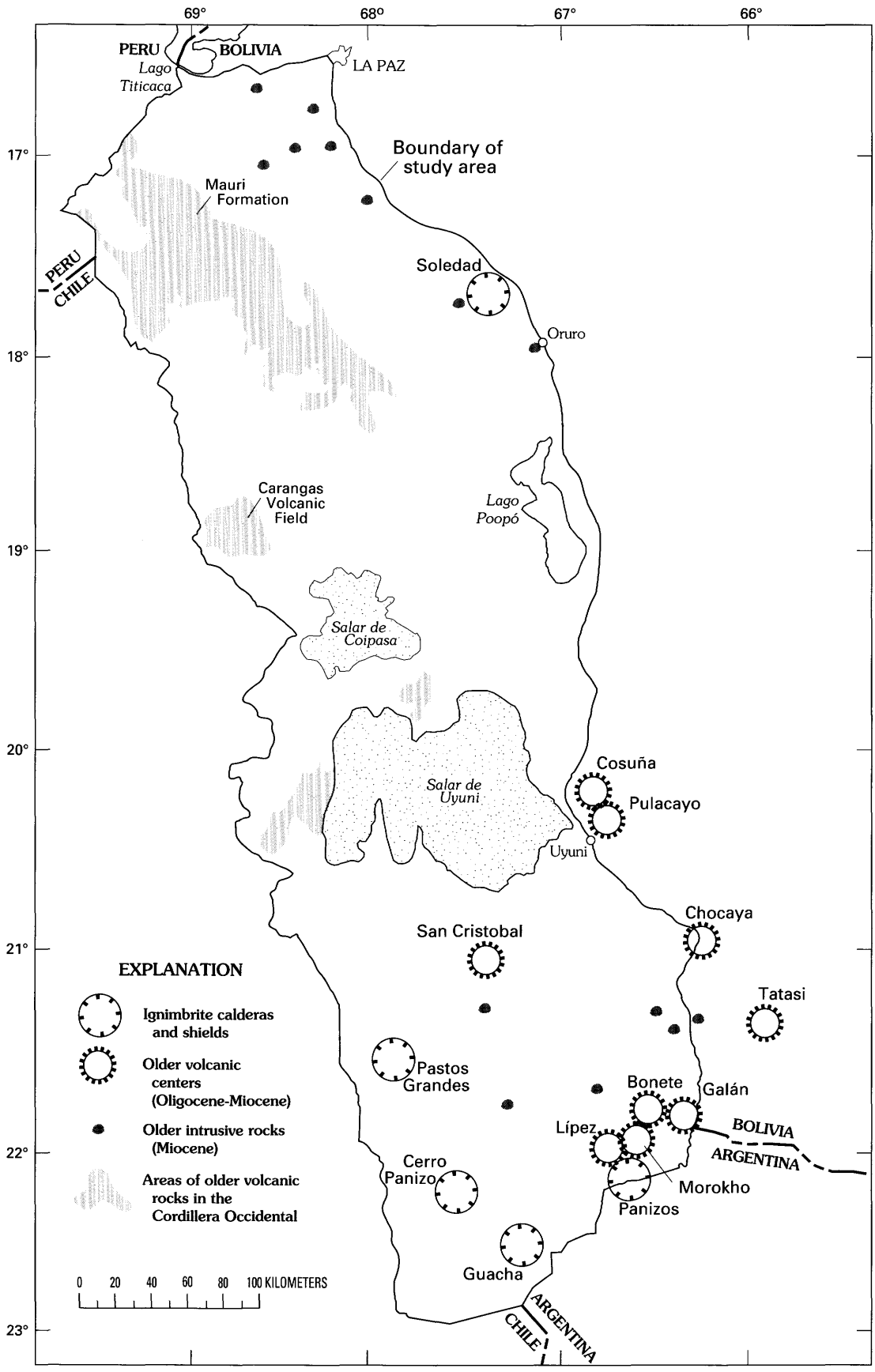


Figure 6. Map of the Altiplano and Cordillera Occidental, Bolivia, showing some volcanic features associated with the ignimbrites (pl. 1, unit QTig) and older volcanic centers (pl. 1, units Tvnd, Tig, Ti).

OLDER VOLCANIC ROCKS

The volcanic rocks associated with the large Oligocene-Miocene eruptive complexes consist of lava flows, flow breccias, lahars, pyroclastic rocks, domes, and shallow intrusive rocks chiefly of intermediate composition (pl. 1, units Tvnd, Tig, Ti). At least nine of these complexes have been identified (fig. 6). In addition, older lavas occur throughout much of the Cordillera Occidental, such as near Carangas and east and south of Berenguela, where they are part of stratigraphic sequences underlying lavas of the younger stratovolcanoes. Subvolcanic dacitic to rhyolitic intrusive rocks, that do not appear to be obviously associated with extrusive rocks, occur chiefly along the Altiplano-Cordillera Oriental border (fig. 6).

Evidence from examination of satellite imagery and from reconnaissance geologic mapping suggests that large collapse calderas may be associated with at least four of these older eruptive centers (Cosuña, Lípez, Bonete, and Morokho, fig. 6). At Cerro Cosuña, a 13-km-diameter circular topographic feature occurs in the center of a large Miocene volcanic field. Paleozoic sedimentary rocks are exposed along the western margin of the circular feature and late lavas and domes(?) fill most of the floor of the postulated caldera. At Lípez, satellite imagery discloses an oval-shaped, 13 km by 16 km, possible caldera filled with dark volcanic rocks. Cerro Lípez (el. 5,929 m), highest peak in the Lípez complex, may be a dome erupted from the structural margin. A 19-km-diameter circular drainage system in the Cerro Bonete area suggests the presence of an old, deeply eroded caldera. All known polymetallic veins in the Cerro Bonete area occur in dacitic domes in this circular feature. An apparent ring dike, coupled with another subtle circular feature, 15 km in diameter, that encircles Cerro Morokho, suggests that a large caldera, or possibly a group of calderas, may be present in the volcanic highlands extending from Cerro Bonete southwest to, and beyond, Cerro Morokho. Extensive ignimbrite units in the Upper Quehua Formation (pl. 1, unit Tig) are likely outflow sheets of these postulated calderas.

IGNIMBRITES

Ignimbrites, chiefly of dacite composition (pl. 1, unit QTig), are exposed over large areas mostly on the southern

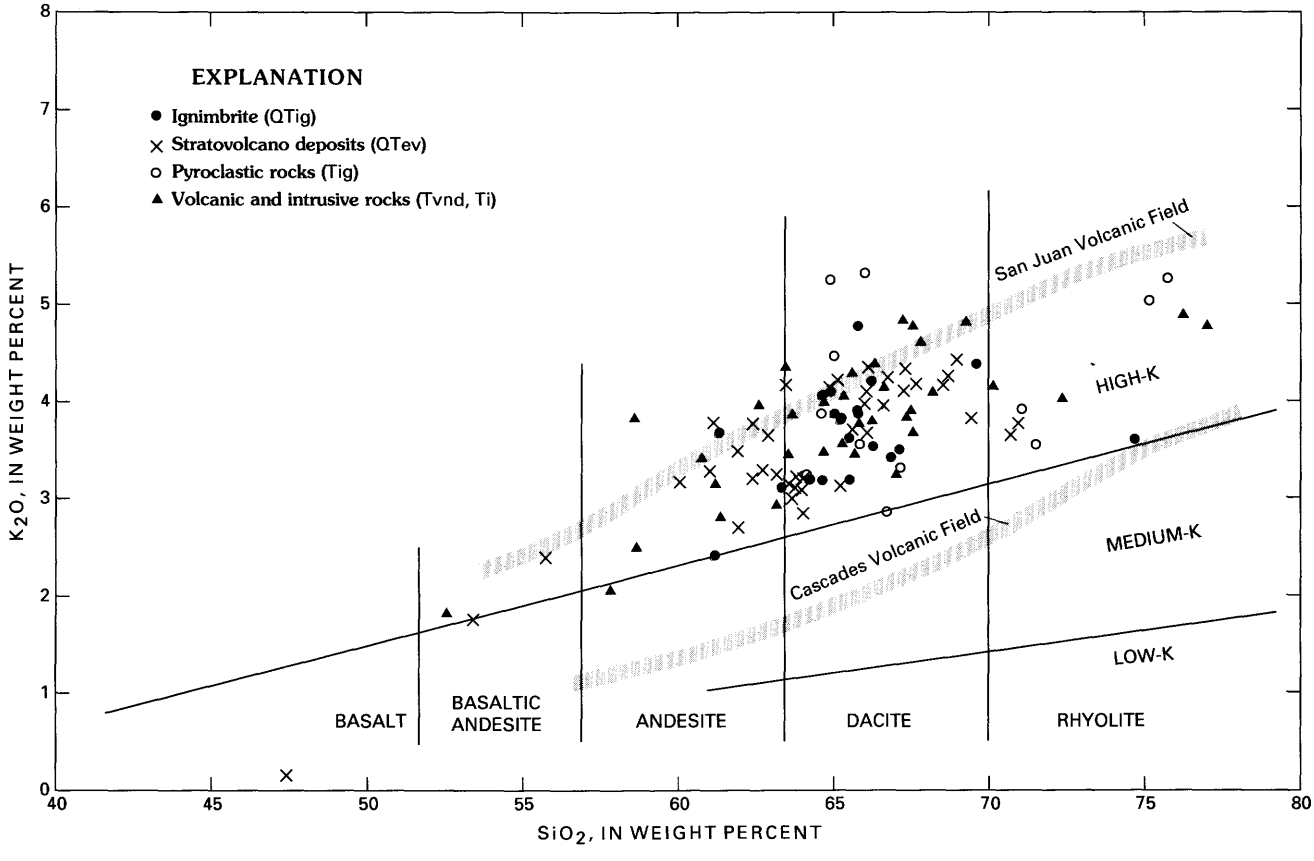


Figure 7. Variation diagram showing K_2O vs. SiO_2 for Cenozoic volcanic and plutonic rocks from the Altiplano and Cordillera Occidental, Bolivia. Discriminant lines from Peccerillo and Taylor (1976). Average trend lines for San Juan and Cascades volcanic fields from Ludington (1986).

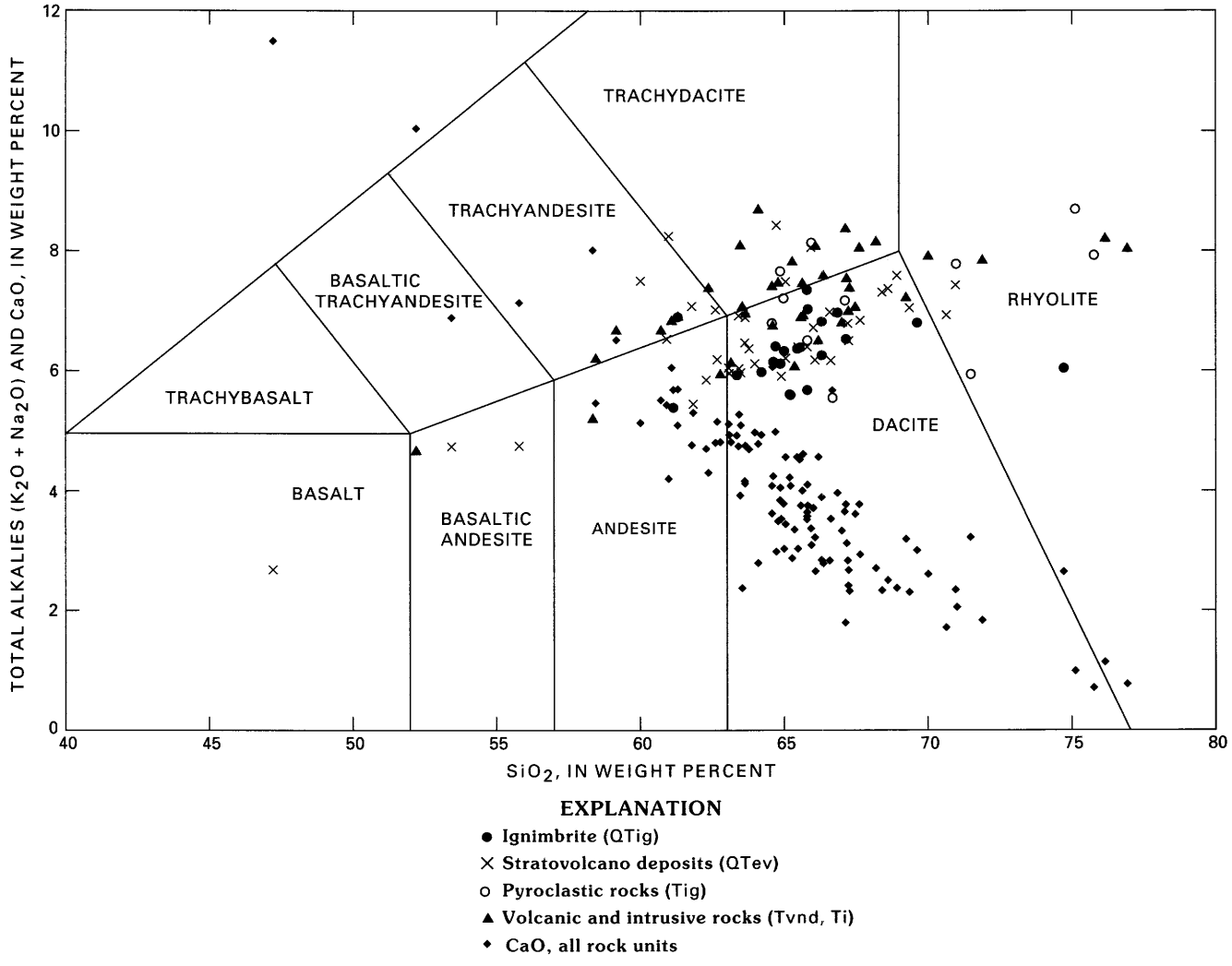


Figure 8. Variation diagram showing total alkalies vs. SiO_2 for Cenozoic volcanic and plutonic rocks from the Altiplano and Cordillera Occidental, Bolivia. Discriminant lines from Le Bas and others (1986) utilize total alkali data only. CaO values are used to determine Peacock alkalinity index.

Altiplano where they underlie, and are interlayered with, lavas of the late Miocene-Holocene stratovolcanoes (pl. 1, unit QTev). De Silva (1989) estimates that more than 10,000 km^3 of ignimbrites were erupted in the central Andes (mostly southwestern Bolivia and northern Chile) during this period of volcanic activity. On the southern Altiplano at least four source areas, mostly broad volcanic shields with shallow summit calderas, as much as 30 km in diameter, have been recognized (Baker, 1981) (fig. 6). To the north, the Soledad caldera at La Joya (Redwood, 1987b) is the northernmost recognized center for ignimbrites of map unit QTig on the Altiplano. The western part of the large Los Frailes ignimbrite field (pl. 1, unit Tmf) is exposed along the eastern margin of the central Altiplano. Its source lies in the main part of the field to the east in the Cordillera Oriental.

STRATOVOLCANOES

Stratovolcanoes of late Miocene (about 7 Ma) to Holocene age cover more than 24,000 km^2 in that part of the Cordillera Occidental and southern Altiplano encompassed by this study (pl. 1, unit QTev). In these two contiguous provinces, 109 major eruptive centers and as many as 236 minor eruptive centers have been identified (fig. 4), chiefly from satellite imagery. As used here, the distinction between major and minor eruptive centers is arbitrary. Stratovolcanoes with volumes exceeding about 10 km^3 (or with basal diameters larger than about 6 km) are considered to be major eruptive centers. Smaller composite cones, cinder cones, and dome-flow complexes, many of which occur on the flanks of the larger stratovolcanoes, are considered to be minor eruptive centers. Average volume of

the major eruptive centers is about 20–40 km^3; the largest centers in the region, such as the stratovolcanoes Sajama and Tunupa (fig. 4), may have volumes of about 90 km^3.

The larger stratovolcanoes are composed chiefly of andesitic to dacitic lava flows, flow breccias, lahars, and minor pyroclastic rocks. Domes occupy many of the vent centers of the volcanoes and sector collapse has played an important role in stratocone growth and destruction (Francis and Wells, 1988). Conspicuous hydrothermal and solfataric alteration effects are common and generally confined to areas within the immediate vent area.

CHEMISTRY

Chemical data on unaltered volcanic rocks of southwestern Bolivia are limited. The 113 new analyses performed as part of this investigation (app. B) form an important addition to the chemical database for this extremely voluminous and widespread group of lavas. Combined with the analyses of 33 samples from Fernández and others (1973) and 10 from Redwood (1987b), these data are sufficient to classify the volcanic rocks and to examine for major-element trends with relation to time, geologic setting, and type of eruptive activity. Figure 7 is a K_2O/SiO_2 variation diagram that shows the compositions of unaltered samples divided into four groups on the basis of the geologic map units shown on plate 1. Figure 8 is a total alkalies/SiO_2 variation diagram, a classification scheme recommended by the IUGS (Le Bas and others, 1986). The samples plotted on both diagrams do not include obviously altered samples (K_2O or Na_2O >6 percent; SiO_2 >80 percent). All the samples exhibit high-K, calc-alkaline affinities, similar to rocks in the eastern part of the Cordillera in North America, also emplaced over thick continental crust. Although most samples are andesites and dacites, some of the more alkalic varieties extend into the trachydacite and trachyandesite fields on figure 8. Silica contents, on a normalized anhydrous basis, range from about 47 to 76 percent, with most rocks in the 60–68 percent SiO_2 range.

Samples from all four geologic map units show a positive correlation between alkalis and SiO_2; the lavas show a higher correlation between K_2O and SiO_2 than the ignimbrites (fig. 7). Although ignimbrites of both age groups are slightly more silicic, with minimum SiO_2 contents of about 62 percent, this apparent difference may be entirely a function of inadequate sampling. Of the four most mafic samples (3 basaltic andesites and 1 basalt), three are from Recent volcanoes; the one older mafic lava is from the Escala mine area (sample no. 90BDR054), and is a single lava flow or plug, far removed from any known major extrusive center. It is atypical of the lavas erupted from the large volcanic complexes, but may be typical of a few isolated mafic lavas interlayered in the Lower Quehua Formation (pl. 1, unit Ts2).

The data points that represent CaO on figure 8 show that the Peacock alkalinity index (Peacock, 1931) is about 59 percent SiO_2, at about 5.6 percent total alkalies, well within the calc-alkalic field. Again, this characteristic is similar to rocks in the eastern part of the North American Cordillera.

DISCUSSION

In the preceding part of this section, the regional geology, supported by local geology where data are available, is briefly reviewed and discussed. Although new structural concepts are contributing to the understanding of the tectonic evolution of the Altiplano and Cordillera Occidental, the principal focus of this section is on the igneous geology. Much of the mineral wealth of Bolivia is associated with igneous rocks that were emplaced during the tectonic activity that formed the Central Andes. These igneous rocks, and the accompanying tectonism, are the result of plate margin interactions between oceanic and continental plates at the western edge of South America.

We have attempted to use geochemistry and geochronology to contribute to a better understanding of igneous processes in this region, where limited field data are available. However, we cannot overemphasize the need for detailed geologic investigations to support future resource studies.

A Geochemical Study of the La Joya District

By Robert Learned, Michael S. Allen, Orlando André-Ramos, *and* René Enriquez-Romero

Introduction **26**
Historical background **26**
Geographic setting **26**
Geologic setting **26**
Geology of the deposits **26**
- Cerro La Joya **27**
- Cerro Quiviri **27**
- Cerro Llallagua **27**
- Cerro Kori Kollo **27**
- Hills adjacent to the La Joya district **28**

Sampling and analytical procedures **28**
- Sample collection **28**
- Sample preparation **28**
- Chemical analyses **28**

Results and interpretation of geochemical data **28**
- Distribution of indicator elements in rock samples **33**
- Distribution of indicator elements in soils and sediment samples **40**

Conclusions **46**

FIGURES

9. Index map showing the location of the La Joya district **27**
10. Map showing the distribution of gold in rock samples **34**
11. Map showing the distribution of silver in rock samples **34**
12. Map showing the distribution of antimony in rock samples **35**
13. Map showing the distribution of arsenic in rock samples **35**
14. Map showing the distribution of lead in rock samples **36**
15. Map showing the distribution of zinc in rock samples **36**
16. Map showing the distribution of cadmium in rock samples **37**
17. Map showing the distribution of bismuth in rock samples **37**
18. Map showing the distribution of tin in rock samples **38**
19. Map showing the location of sample sites with factor scores >0.5 standard deviations above the mean indicated for rock factor 2 and rock factor 5 **39**
20. Map showing the location of sample sites with factor scores >0.5 standard deviations above the mean indicated for soil factor 3 , sediment factor 3, and rock factor 3 **39**
21. Map showing the location of sample sites with factor scores >0.5 standard deviations above the mean indicated for soil factor 2, sediment factor 1, and rock factor 5 **40**
22. Map showing the distribution of gold in soil samples **41**
23. Map showing the distribution of silver in soil and sediment samples **42**
24. Map showing the distribution of antimony in soil and sediment samples **42**
25. Map showing the distribution of arsenic in soil and sediment samples **43**
26. Map showing the distribution of lead in soil and sediment samples **43**
27. Map showing the distribution of zinc in soil and sediment samples **44**

28. Map showing the distribution of cadmium in soil and sediment samples 44
29. Map showing the distribution of bismuth in soil and sediment samples 45
30. Map showing the distribution of tin in soil and sediment samples 45

TABLES

1. List of chemical elements determined 29
2. Element associations determined by R-mode factor analyses on rock samples 38
3. Element associations determined by R-mode factor analyses on soil samples 46
4. Element associations determined by R-mode factor analyses on fine-fraction sediment samples 46

INTRODUCTION

A pilot geochemical study of the La Joya district was undertaken in order to assess the feasibility of geochemical exploration for this type of deposit on the Altiplano, Bolivia. This district was selected because it is representative of an economically important deposit type, its geology has been well studied, and because its geologic environment is widespread on the Altiplano. The study was undertaken to determine the elemental indicators of mineralization, their geographical distribution with respect to the known mineralization, and the most effective sample media. We anticipate that the results obtained during this study will be applicable to the evaluation of areas of comparable geology, topography, and climate throughout much of the Altiplano and elsewhere.

Sampling design and collection for this study was carried out by Learned with the assistance of André-Ramos and Enriquez-Romero. Analytical work was performed by chemists in the U.S. Geological Survey (USGS) in Denver. Data compilation, statistical analysis, and interpretation were done by Allen. Preparation of data tables and plotting of maps was done by Learned, Allen, and Ludington and the final report was prepared by Allen.

HISTORICAL BACKGROUND

Underground mining of gold- and silver-bearing veins has occurred intermittently in the La Joya district since the sixteenth century. Mining of copper- and lead-bearing veins began during the nineteenth century and has continued intermittently until recent years (Ahlfeld and Schneider-Scherbina, 1964). In the 1970's, low-grade, large-tonnage, gold and silver deposits were discovered in the district. Those deposits are presently being mined by open-pit methods, and the metals are recovered using heap-leach technology. Inti Raymi S.A., which is a joint venture between Battle Mountain Gold Corporation and Empresa Unificada, is the current operator.

GEOGRAPHIC SETTING

The La Joya district is located in the east-central part of the Bolivian Altiplano, approximately 45 km northwest of the city of Oruro (fig. 9). The region consists of a series of low, isolated hills projecting above the level of the surrounding plain. The district is within the political province of Cercado, department of Oruro. The area investigated, which is more extensive than the district itself, lies within the coordinates lat 17° 43′ to 17° 53′ S. and long 67° 17′ to 67° 40′ W.

GEOLOGIC SETTING

The Bolivian Altiplano is a series of intermontane basins of late Cretaceous to Tertiary age which lie between the Mesozoic-Cenozoic volcanic arc of the Cordillera Occidental and the Paleozoic rocks of the Cordillera Oriental (Redwood and Macintyre, 1989). In the La Joya region, a thick sequence of Pleistocene lake beds covers most of the older rocks of the basin, but ridges of Paleozoic sedimentary rocks, and discrete hills of Cenozoic plutonic and volcanic rocks project above the level of the lake beds. Dacite stocks, which are part of an inner Miocene volcanic arc present within the Altiplano and Cordillera Oriental (Redwood and Macintyre, 1989), host the mineral deposits of the La Joya district.

GEOLOGY OF THE DEPOSITS

Ahlfeld and Schneider-Scherbina (1964) have classified the deposits of the La Joya district as auriferous-pyrite subvolcanic deposits. However, in this report, we classify the deposits as Bolivian polymetallic vein deposits. Typical zoning in polymetallic vein systems related to intrusions often shows base-metals higher than and peripheral to a "higher-temperature" precious-metal suite which may correspond to a pyrite-rich deep (core) zone (Rose and others, 1979, p. 117–118). At Cornwall, England, polymetallic vein deposits display mineralogic zoning from a sulfosalt-rich upper zone, through a base metal and

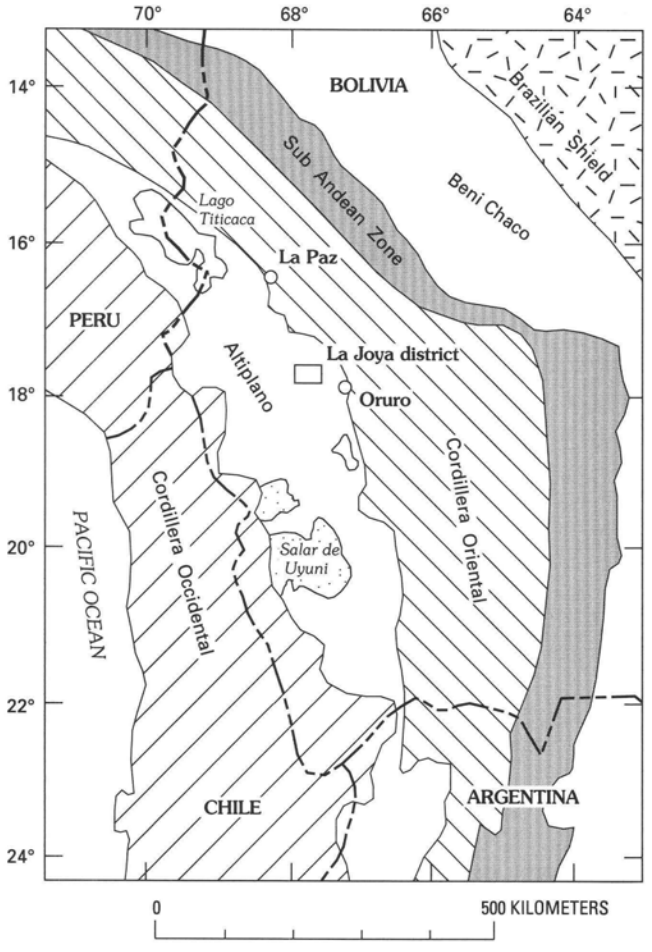


Figure 9. Index showing the location of the La Joya district, Bolivia, in relation to the physiographic regions of the central Andes (modified from Redwood, 1987).

silver-rich middle zone, to a lower zone rich in arsenic and tin sulfides and oxides (Guilbert and Park, 1986, p. 229–241). At Catavi, Bolivia, base-metal veins of zinc, lead, and silver are peripheral to tin-silver veins (Guilbert and Park, 1986, p. 434). The following descriptions of the deposits at Cerros La Joya, Quiviri, Llallagua, and Kori Kollo in the La Joya district are summarized from Ahlfeld and Schneider-Scherbina (1964), Anzoleaga and others (1990), and the description by Long and others in the section on Geology of known mineral deposits. Descriptions of several areas peripheral to the La Joya district are also included in this section.

CERRO LA JOYA

At Cerro La Joya, a dacite stock intrudes arenaceous lutites of Devonian age (Catavi Formation). Both rock units show intense sericitization and propylitization. This hill is the site of the old Carmen and San Pablo mines. The vein deposits here cut both rock units, and the principal ore minerals in the hypogene zone are pyrite, enargite, tennantite, arsenopyrite, and minor bismuthinite. A breccia zone with a tourmaline-bearing matrix that is cut by sulfide veins is present on the upper part of the hill. In the zone of supergene enrichment, the principal ore minerals are chalcocite, covellite, chalcopyrite, and residual tennantite. In the zone of oxidation, silver and copper minerals have been leached out and only gold remains.

CERRO QUIVIRI

Cerro Quiviri is the northernmost of three hills (Quiviri, Llallagua, and Kori Kollo) which are aligned along a northwest-trend east of Cerro La Joya. At Cerro Quiviri, altered dacite supports a roof pendant of altered Catavi Formation sedimentary rocks. Mineralization is concentrated in northeast-trending fracture in both units. Alteration of rocks on this hill is erratic, with fresh rock abundant.

CERRO LLALLAGUA

At Cerro Llallagua an altered dacite stock intrudes lutites of the Catavi Formation. The dacite here and at Cerro Kori Kollo appear identical and are believed to be continuous at depth. Cerro Llallagua is the site of the old San Andres mine. Large (1–2-m wide) northeast-trending sulfide veins cut both igneous and sedimentary rocks to depths of at least 200 m. In addition, closely spaced veinlet mineralization similar to that found at Cerro Kori Kollo is present in dacite. Veins contain quartz, pyrite, marcasite, pyrrhotite, arsenopyrite, sphalerite, chalcopyrite, galena, boulangerite, jamesonite, stibnite, and wolframite. Relative abundances of the minerals vary within and between veins. Gold is associated with pyrite, and occurs as grains 2–5 microns in diameter.

CERRO KORI KOLLO

Cerro Kori Kollo is the site of the only current mining activity in the La Joya district. The dacite porphyry stock that constitutes the hill is intensely altered, principally sericitized and silicified. Alunite and jarosite occur as post-mineralization fracture fillings. Mineralization is present as northeast-trending veins and veinlets that in places become so frequent that they appear to form breccia zones. Hypogene vein minerals include pyrite, arsenopyrite, tetrahedrite, chalcopyrite, stibnite, sphalerite, galena, and electrum. Gold occurs in grains 5–14 microns in diameter, between crystals of tetrahedrite and stibnite, and with disseminated pyrite. In the lower and outer parts of the deposit marcasite replaces pyrite. In the zone of oxidation, gold occurs in grains 2–15 microns in diameter, and is associated with quartz, pyrite, limonite, and jarosite.

HILLS ADJACENT TO THE LA JOYA DISTRICT

To the west of the La Joya district are several low hills that are described by Redwood (1987b) as rhyolitic lava domes. These rhyolites (about 9 Ma) postdate the dacite of the La Joya stock (about 15 Ma), but predate the volcanic rocks of the Esquentaque Massif (about 5 Ma), to the southeast of the district. At Kiska, southsouthwest of the La Joya district (see the description by Ludington and others in the section on Geology of known mineral deposits), Paleozoic sedimentary rocks are intruded by intensely silicified and sericitized dacite, comparable to the rocks of the upper zone of Cerro Kori Kollo. The volcanic rocks of the Esquentaque Massif are composed principally of dacitic lava flows (Esquentaque Lavas) that overlie a relatively thin section of pyroclastic rocks (Soledad Tuffs). A zone of argillic and silicic alteration on the eastern side of the massif has been interpreted as the subsurface part of a fossil hot spring (Redwood, 1987b).

SAMPLING AND ANALYTICAL PROCEDURES

Geochemical sampling was undertaken to determine elemental indicators of mineralization and their dispersion around mineralized rock, in order to assess the feasibility of geochemical exploration for this type of mineral deposit on the Altiplano. Rock samples were collected to assess the combinations of elements that were indicative of alteration, mineralization, and mineralization types. Soil samples were collected to determine the effects of weathering on the dispersion of indicator elements in the surficial environment. Because drainage sediment is a composite of eroded materials of a large drainage basin, its chemical analysis has proven to be highly effective as a means of identifying basins within large study areas that contain exposed mineralized rock. Analysis of these sediments is therefore widely used in reconnaissance exploration, particularly in mountainous terrains characterized by active erosion. However, on the arid Altiplano, a combination of slow erosion rates coupled with a topography of isolated hills on large flats has resulted in poorly developed drainage systems. For these reasons, drainage-sediment sampling was used where possible, but was supplemented by collection of base-of-slope (colluvial soil) samples. We refer to samples of drainage sediment as sediment samples in this section.

SAMPLE COLLECTION

Geochemical sampling for this study included detailed surveys of rocks and soils in areas of known mineralization (for example, Cerro Kori Kollo), and a more regional survey of sediment and rock surrounding the La Joya district. Soil samples were collected at Cerro Kori Kollo, Cerro Llallagua, Cerro Quiviri, and in the hills west of the district (Cerros Kiska, Quimsa Chata, Nueva Llallagua, and Chanka). Sediment samples were taken at Cerro La Joya, from the hills to the east of Cerro La Joya in which Paleozoic rocks are exposed, and from the Esquentaque Massif to the southeast of the district. Sediment-sample sites were located around the base of each hill, but above the highest level of Pleistocene lake sedimentation. The spacing between sediment-sample sites around the base of each hill ranges from approximately 200 to 500 m. Rock samples were also taken at all soil- and sediment-sample sites where outcrops occurred within 30 m of the collection site. Each sediment, soil, and rock sample was a composite of 4–6 subsamples collected in an area no larger than 20 m in longest dimension, and is composed of approximately 0.5 kg of material.

SAMPLE PREPARATION

Rock samples were crushed and then pulverized preceding chemical analysis. Sediment samples were air dried at ambient temperature and then sieved to -0.25 mm and +0.25 mm fractions. Both fractions were subsequently pulverized to <0.06 mm prior to chemical analysis. Soil samples were oven-dried at 110 °C, and then pulverized before chemical analysis.

CHEMICAL ANALYSES

The samples were analyzed for 35 elements utilizing the six-step semiquantitative emission spectrographic method of Grimes and Marranzino (1968). Ten elements (Ag, As, Au, Bi, Cd, Cu, Mo, Pb, Sb, Zn) were determined by inductively coupled-plasma atomic emission spectrometry (ICP) (Motooka, 1988). Gold was also determined by atomic-absorption spectrophotometry (AAS), using a graphite furnace (O'Leary and Meier, 1984). Emission spectrography provides total chemical determinations, whereas the ICP and AAS procedures require acid dissolution of samples which result in partial determinations. For example, copper held in refractory iron oxides and silicate minerals in a sample would be detected by emission spectrography but may not be detected in the ICP analysis because of the insolubility of these minerals.

RESULTS AND INTERPRETATION OF GEOCHEMICAL DATA

The geochemical data obtained in this study are presented in appendix B. Summary statistics (minimum,

Table 1. *List of chemical elements determined, La Joya district, Bolivia*

[Units of concentration in parts per million (ppm) or percent (%). Data are expressed in terms of minimum, maximum, mean, and standard deviation. Leaders (--) indicate no data; <, less than; N.D., not determined]

Element	Units of concentration	No. of valid determinations	Minimum concentration	Maximum concentration	Mean concentration	Standard deviation
			Rock samples			
Emission spectrography						
Ba	ppm	118	70	1,000	500	300
Fe	%	118	.1	15	3	2
Mg	%	112	.02	1.5	.5	.5
Ca	%	93	.05	1.5	.7	.5
Ti	%	116	.1	1	.5	.2
Mn	ppm	117	10	3,000	200	500
Ag	ppm	29	.5	30	5	7
As	ppm	4	200	1,500	500	700
Au	ppm	0	<10	<10	--	--
B	ppm	113	10	1,000	70	150
Ni	ppm	91	5	70	20	15
Be	ppm	68	1	2	1	.3
Bi	ppm	5	10	30	20	7
Cd	ppm	0	<20	<20	--	--
Co	ppm	64	10	30	10	3
Cr	ppm	118	10	300	100	50
Cu	ppm	111	5	300	20	30
La	ppm	84	50	100	70	15
Mo	ppm	34	5	30	10	7
Nb	ppm	0	<20	<20	--	--
V	ppm	117	15	200	50	30
Pb	ppm	104	10	7,000	150	700
Sb	ppm	6	100	500	200	150
Sc	ppm	44	5	7	5	.7
Sn	ppm	10	10	50	30	20
Sr	ppm	98	100	700	200	100
W	ppm	2	20	20	20	--
Y	ppm	62	10	70	15	7
Zn	ppm	9	300	2,000	1,000	500
Zr	ppm	118	30	700	200	100
Na	%	94	.2	2	1	.5
P	%	1	.2	.2	.2	--
Ga	ppm	113	5	70	30	15
Ge	ppm	0	<10	<10	--	--
Th	ppm	0	<100	<100	--	--
Atomic-absorption spectrophotometry						
Au	ppm	57	0.002	4.3	0.15	0.60
Inductively coupled-plasma spectrometry						
As	ppm	104	0.69	1,000	65	190
Bi	ppm	52	.62	34	3.2	6.1
Cd	ppm	97	.031	25	.69	2.9
Sb	ppm	93	.65	270	18	45
Zn	ppm	118	1.7	1,400	99	240

Table 1. *List of chemical elements determined, La Joya district, Bolivia*--Continued

Element	Units of concentration	No. of Valid determinations	Minimum concentration	Maximum concentration	Mean concentration	Standard deviation
Cu	ppm	118	2.8	280	19	28
Pb	ppm	115	.71	4,000	170	540
Ag	ppm	80	.045	29	2.0	4.9
Mo	ppm	118	1.2	18	5.0	3.1
Au	ppm	8	.18	5	1.3	1.6
			Soil samples			
Emission spectrography						
Ba	ppm	50	200	1,000	500	150
Fe	%	50	1	7	2	1
Mg	%	50	.15	1	.5	.2
Ca	%	50	.15	10	1	2
Ti	%	50	.2	.7	.3	.1
Mn	ppm	50	70	3,000	300	500
Ag	ppm	22	.5	30	3	7
As	ppm	2	500	700	700	150
Au	ppm	0	<10	<10	--	--
B	ppm	50	20	100	70	20
Ni	ppm	47	7	30	15	5
Be	ppm	41	1	2	1	0.3
B	ppm	5	15	70	50	30
Cd	ppm	0	<20	<20	--	--
Co	ppm	37	10	15	10	1
Cr	ppm	50	10	70	20	10
Cu	ppm	50	10	300	30	50
La	ppm	21	50	70	50	10
Mo	ppm	0	<5	<5	--	--
Nb	ppm	0	<20	<20	--	--
V	ppm	50	20	100	50	20
Pb	ppm	47	10	700	100	150
Sb	ppm	5	100	300	200	70
Sc	ppm	18	5	10	7	2
Sn	ppm	4	15	30	30	7
Sr	ppm	49	100	500	200	70
W	ppm	0	<20	<20	--	--
Y	ppm	39	10	30	15	5
Zn	ppm	5	200	1,000	500	300
Zr	ppm	49	70	1,000	300	200
Na	%	50	.3	1.5	1	.3
P	%	8	.2	.7	.3	.15
Ga	ppm	49	7	50	20	7
Ge	ppm	0	<10	<10	--	--
Th	ppm	0	<100	<100	--	--
Atomic-absorption spectrophotometry						
Au	ppm	24	0.002	1.4	0.14	0.34
Inductively coupled-plasma spectrometry						
As	ppm	49	8.10	1,200	74	170
Bi	ppm	14	.77	22	5.8	7.8
Cd	ppm	49	.042	3.3	.38	.56
Sb	ppm	44	.75	140	15	29
Zn	ppm	49	11	650	90	130

Table 1. *List of chemical elements determined, La Joya district, Bolivia*--Continued

Element	Units of concentration	No. of Valid determinations	Minimum concentration	Maximum concentration	Mean concentration	Standard deviation
Cu	ppm	49	7.1	70	18	12
Pb	ppm	49	4.7	710	120	190
Ag	ppm	37	.047	13	1.1	2.3
Mo	ppm	49	.11	1.9	.74	.35
Au	ppm	2	.27	1.0	.64	.51
			Coarse-fraction sediment samples (+0.25 mm)			
Emission spectrography						
Ba	ppm	92	200	1,000	500	150
Fe	%	92	1.5	5	3	.7
Mg	%	92	.15	1	.7	.2
Ca	%	92	.15	1.5	1	.7
Ti	%	92	.2	.7	.5	.1
Mn	ppm	92	100	2,000	300	300
Ag	ppm	24	.3	50	.5	10
As	ppm	1	<200	200	--	--
Au	ppm	0	<10	<10	--	--
B	ppm	92	10	2,000	70	200
Ni	ppm	92	5	70	30	15
Be	ppm	78	1	1.5	1	.2
Bi	ppm	3	10	150	70	70
Cd	ppm	0	<20	<20	--	--
Co	ppm	76	10	20	10	3
Cr	ppm	92	10	70	30	15
Cu	ppm	92	10	500	30	70
La	ppm	70	30	500	70	50
Mo	ppm	0	<5	<5	--	--
Nb	ppm	1	<20	150	--	--
V	ppm	92	20	100	70	15
Pb	ppm	92	10	700	50	100
Sb	ppm	0	<100	<100	--	--
Sc	ppm	41	5	10	7	1
Sn	ppm	3	15	150	50	70
Sr	ppm	92	100	500	300	100
W	ppm	2	30	100	70	50
Y	ppm	68	10	30	15	10
Zn	ppm	3	200	500	300	150
Zr	ppm	92	50	100	150	100
Na	%	92	.5	2	1.5	.5
P	%	0	<.2	<.2	--	--
Ga	ppm	92	10	50	30	10
Ge	ppm	0	<10	<10	--	--
Th	ppm	0	<100	<100	--	--
Atomic-absorption spectrophotometry						
Au	ppm	0	N.D.	N.D.	N.D.	N.D.
Inductively coupled-plasma spectrometry						
As	ppm	88	4.1	570	32	67
Bi	ppm	28	<.6	190	9.5	36
Cd	ppm	84	<.3	4.5	.24	.58
Sb	ppm	69	<.6	650	15	78
Zn	ppm	89	11	670	65	86

Table 1. *List of chemical elements determined, La Joya district, Bolivia*--Continued

Element	Units of concentration	No. of Valid determinations	Minimum concentration	Maximum concentration	Mean concentration	Standard deviation
Cu	ppm	88	7.1	330	24	39
Pb	ppm	88	4.7	1300	59	170
Ag	ppm	46	<.45	67	2.1	10
Mo	ppm	87	.11	2.3	.80	.44
Au	ppm	1	<.15	2.0	--	--
			Fine-fraction sediment samples (-0.25 mm)			
Emission spectrography						
Ba	ppm	94	200	700	300	100
Fe	ppm	91	1.5	5	2	.5
Mg	ppm	91	.15	1	.5	.2
Ca	%	91	.3	3	.7	.3
Ti	%	91	.3	.7	.5	.1
Mn	ppm	91	100	1,000	200	100
Ag	ppm	24	0.5	20	2	5
As	ppm	0	<200	<200	--	--
Au	ppm	0	<10	<10	--	--
B	ppm	91	20	500	70	50
Ni	ppm	91	5	30	10	5
Be	ppm	84	1	2	1	.3
Bi	ppm	2	10	150	70	100
Cd	ppm	0	<20	<20	--	--
Co	ppm	60	10	15	10	2
Cr	ppm	90	10	100	20	10
Cu	ppm	91	10	300	20	30
La	ppm	61	50	200	70	30
Mo	ppm	0	<5	<5	--	--
Nb	ppm	1	20	20	20	--
V	ppm	91	30	100	70	15
Pb	ppm	86	10	200	20	30
Sb	ppm	1	500	500	500	--
Sc	ppm	56	5	15	5	2
Sn	ppm	3	15	50	30	20
Sr	ppm	91	150	300	200	50
W	ppm	1	100	100	100	--
Y	ppm	80	10	30	10	5
Zn	ppm	1	300	300	300	--
Zr	ppm	91	70	1,000	500	200
Na	%	91	.5	.2	1	.3
P	%	1	.2	.2	.2	--
Ga	ppm	91	5	50	20	10
Ge	ppm	0	<10	<10	--	--
Th	ppm	0	<100	<100	--	--
Atomic-absorption spectrophotometry						
Au	ppm	0	N.D.	N.D.	N.D.	N.D.
Inductively coupled-plasma spectrometry						
As	ppm	94	6.1	190	18	23
B	ppm	48	.61	93	3.0	13
Cd	ppm	94	.054	1.8	.15	.23
Sb	ppm	94	.71	310	5.9	32
Zn	ppm	94	20	300	43	35

Table 1. *List of chemical elements determined, La Joya district, Bolivia*--Continued

Element	Units of concentration	No. of Valid determinations	Minimum concentration	Maximum concentration	Mean concentration	Standard deviation
Cu	ppm	94	7.6	180	15	18
Pb	ppm	94	8.5	330	27	47
Ag	ppm	67	.046	39	.81	4.8
Mo	ppm	94	.33	1.1	.53	.16
Au	ppm	1	2.5	2.5	2.5	--

maximum, mean, and standard deviation) were calculated for each element in each data set to assess their distributions. These are presented in table 1. Most elements display truncated distributions, because of the relatively high limits of determination for the methods employed. Additionally, some distributions are distinctly bimodal. Therefore, to assess the spatial distribution of the elements in the samples, maps were constructed after a nonrigorous grouping of the data (figs. 10–18, 22–30). Four classes were generally used which correspond roughly to (1) > X + 2 × S.D., (2) between X + S.D. and X + 2 × S.D., (3) between X and X + S.D., and (4) < X, where X is the mean and S.D. the standard deviation. The elemental distributions of figures 10–18 and 22–30 are those of the La Joya district, whereas the concentration intervals accompanying these figures are based upon the data of the entire study area, including the hills west of the La Joya district and the Esquentaque Massif. With few exceptions, the concentrations of the indicator elements in samples taken outside the La Joya district were below the median concentration or marginally above it. For some elements, the lower concentration intervals include censored values (concentrations below the limit of analytical detection for the method employed). The statistical parameters shown in table 1, however, include only uncensored values.

In an effort to determine the element associations indicative of mineralization and alteration, R-mode factor analysis was employed. This method is a multivariate statistical method which relies on the mutual correlation of variables to define statistically meaningful associations of variables, in this case, elements. The method has the effect of reducing a data set which contains a large number of variables to a simplified factor model of the data set that has a smaller number of variables (factors) that are combinations of the original variables. A factor model is chosen such that it contains a majority of the essential information present in that original data set. The goal of creating factors is to demonstrate the inherent element associations in the data which have geologic meaning, for example, an association that reflects a geologic feature or process, such as mineralization. For additional information about factor analysis see Davis (1986) or Howarth and Sinding-Larsen (1983).

Before treatment of data in each set, elements with greater than 50 percent qualified values (not detected [N] or detected below detection limit [L]) were removed and not included in the factor analysis. Qualified values remaining in the data were replaced with values based on the following scheme: L value = 0.7 × (L value); N value = 0.5 × (N value). Data derived from emission spectrography were log-transformed, because of the geometric reporting interval. No transformations were applied to AAS or ICP data.

DISTRIBUTION OF INDICATOR ELEMENTS IN ROCK SAMPLES

Examination of the distribution of elements in rock samples reveals that multielement anomalies are spatially related to mineralized areas. High-level anomalies of Au, Ag, Sb, As, Pb, Zn, Cd, Bi, and Sn are present in samples from Cerro Kori Kollo, Cerro Llallagua, Cerro Quiviri, and Cerro La Joya (figs. 10–18). At each locality differences in contents of metal and associations of metal are observed. For example Zn and Cd values are highest at Cerro Llallagua and Cerro Quiviri, whereas Au, Ag, Sb, and As are highest at Cerro Kori Kollo. Additionally, Sn contents are anomalously high in samples from Cerro Kori Kollo (fig. 18). Differences in metal contents of samples from each locality may reflect district zoning, level of erosion within vertically zoned systems, differences in mineralization type, or supergene effects.

In order to determine element associations in rock samples, analyses for 30 elements and 118 rock samples were entered into the R-mode factor analysis program. A seven-factor model was chosen for this data set because it explains more than 76 percent of the overall variance in the original data, and more than 70 percent of the variation for each element, except Fe, V, B, La, Y, Bi, and Cd, most of which are related to lithology. Element associations were derived by including the elements with significant (>0.4) loadings (correlation coefficients) on the factors. The element associations for rocks are shown in table 2.

Three rock factors with the following elemental associations, rock factor 2, Pb-Sb-As-Ag-Cu; rock factor 3, Zn-Cd-Mn-Co; and rock factor 5, Au-Bi-As-Ag; are specifically related to mineralization. The other element associations obtained from factor analysis were lithologically related and are not discussed here. Factor analysis clarifies the elemental associations indicated by inspection

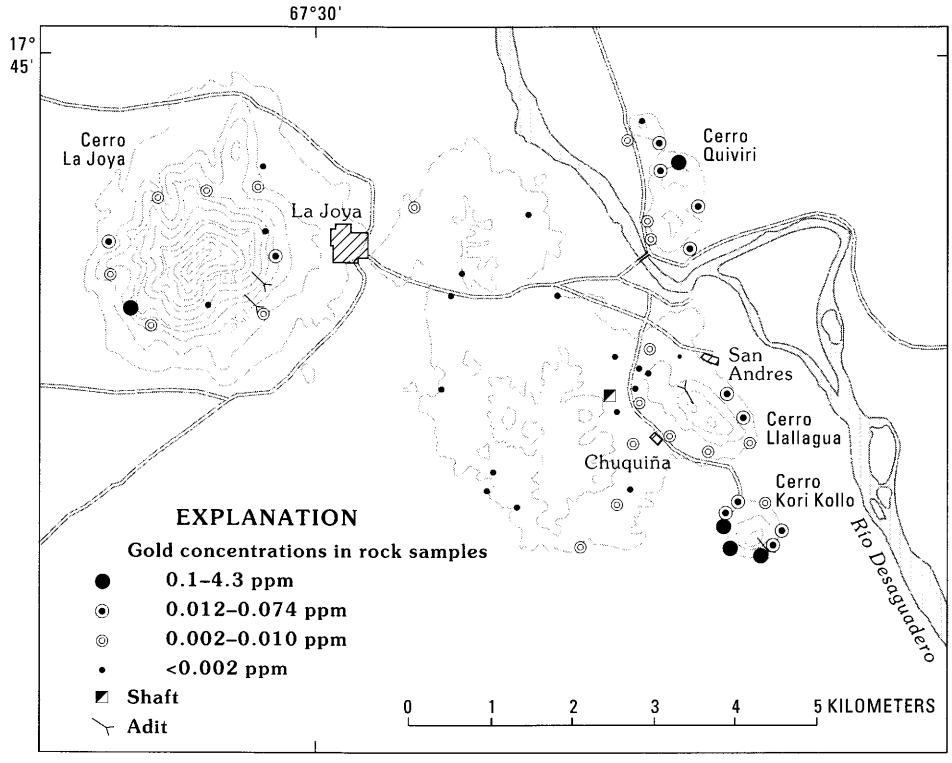


Figure 10. Map showing the distribution of gold concentrations in rock samples, La Joya district, Bolivia. Base modified from Cerro La Joya (6041 I) and Soledad (6140 IV) topographic quadrangles; contour interval, 40 m.

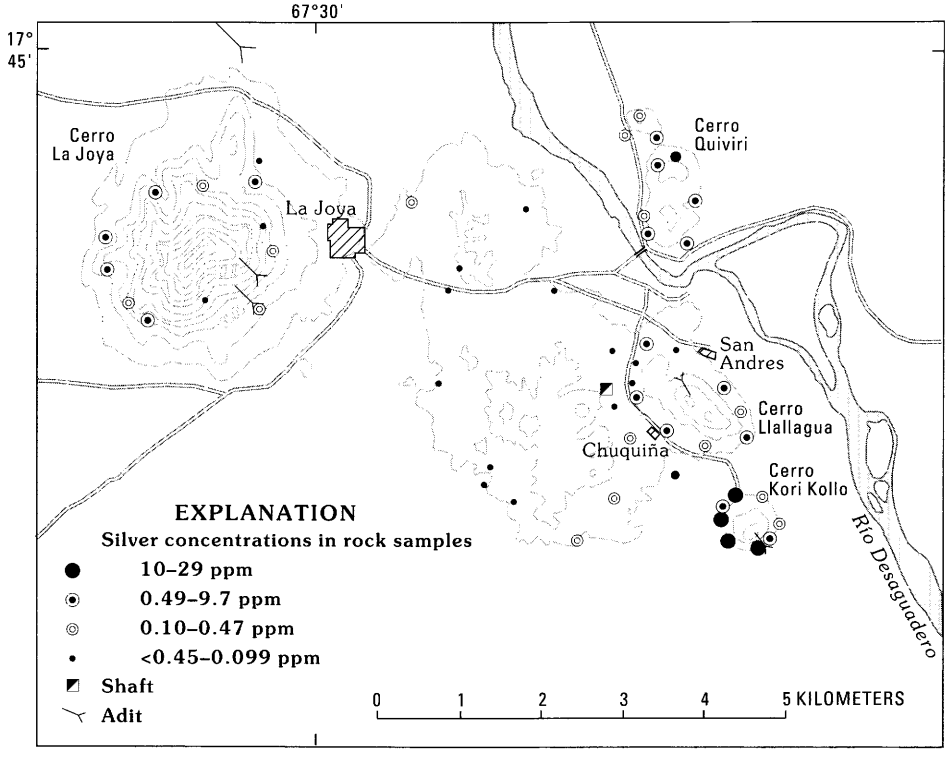


Figure 11. Map showing the distribution of silver concentrations in rock samples, La Joya district, Bolivia. Base modified from Cerro La Joya (6041 I) and Soledad (6140 IV) topographic quadrangles; contour interval, 40 m.

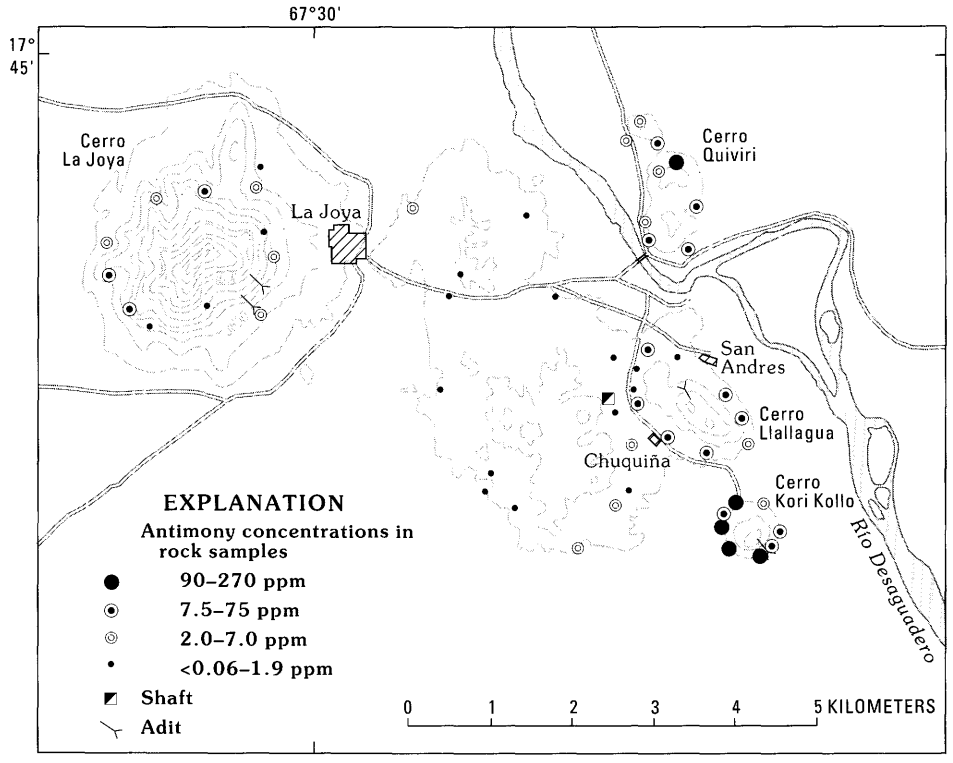


Figure 12. Map showing the distribution of antimony concentrations in rock samples, La Joya district, Bolivia. Base modified from Cerro La Joya (6041 I) and Soledad (6140 IV) topographic quadrangles; contour interval, 40 m.

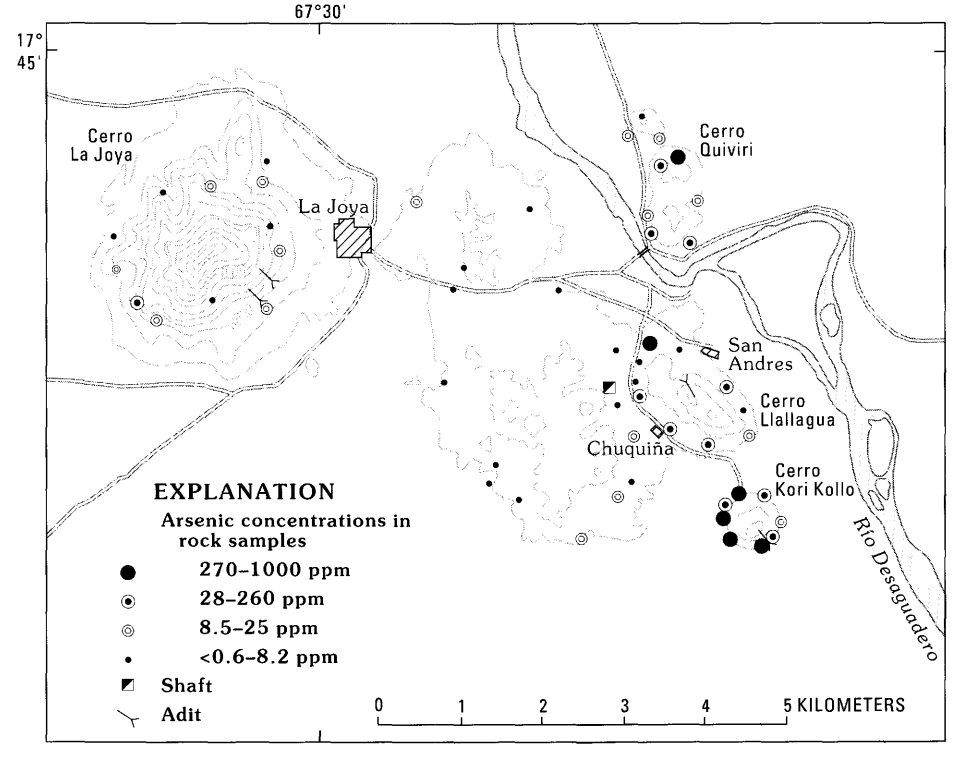


Figure 13. Map showing the distribution of arsenic concentrations in rock samples, La Joya district, Bolivia. Base modified from Cerro La Joya (6041 I) and Soledad (6140 IV) topographic quadrangles; contour interval, 40 m.

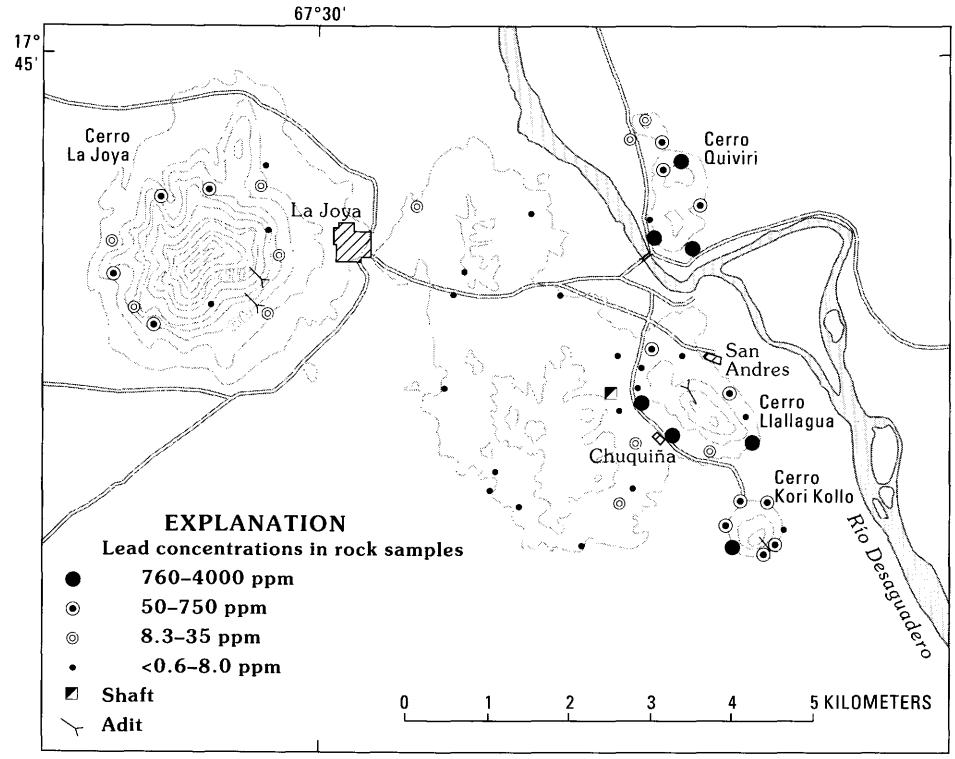


Figure 14. Map showing the distribution of lead concentrations in rock samples, La Joya district, Bolivia. Base modified from Cerro La Joya (6041 I) and Soledad (6140 IV) topographic quadrangles; contour interval, 40 m.

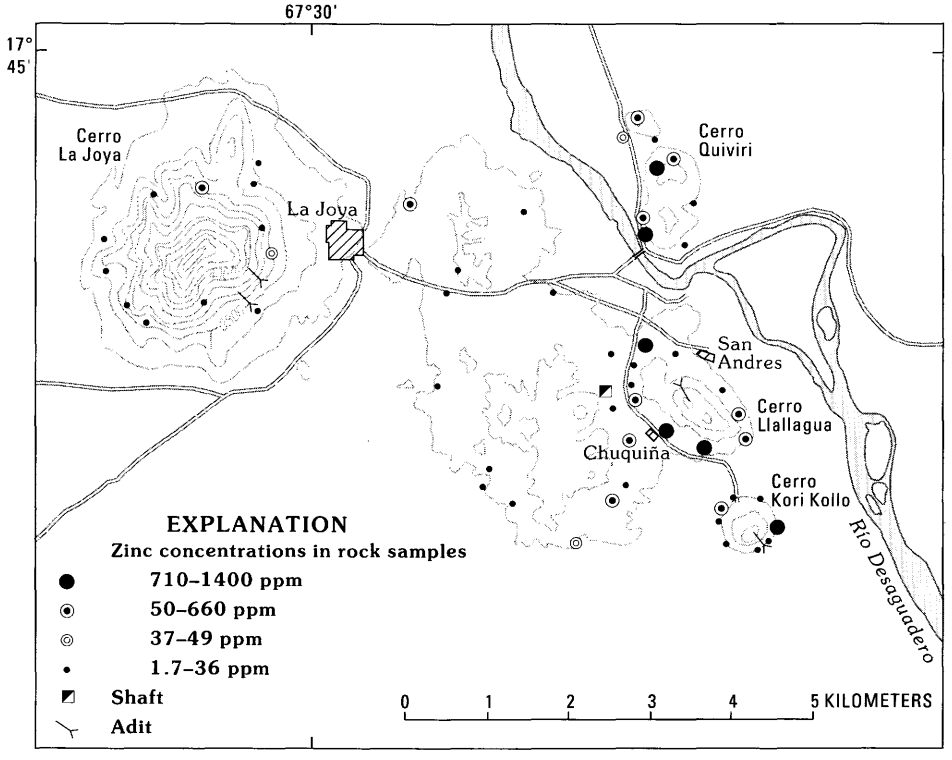


Figure 15. Map showing the distribution of zinc concentrations in rock samples, La Joya district, Bolivia. Base modified from Cerro La Joya (6041 I) and Soledad (6140 IV) topographic quadrangles; contour interval, 40 m.

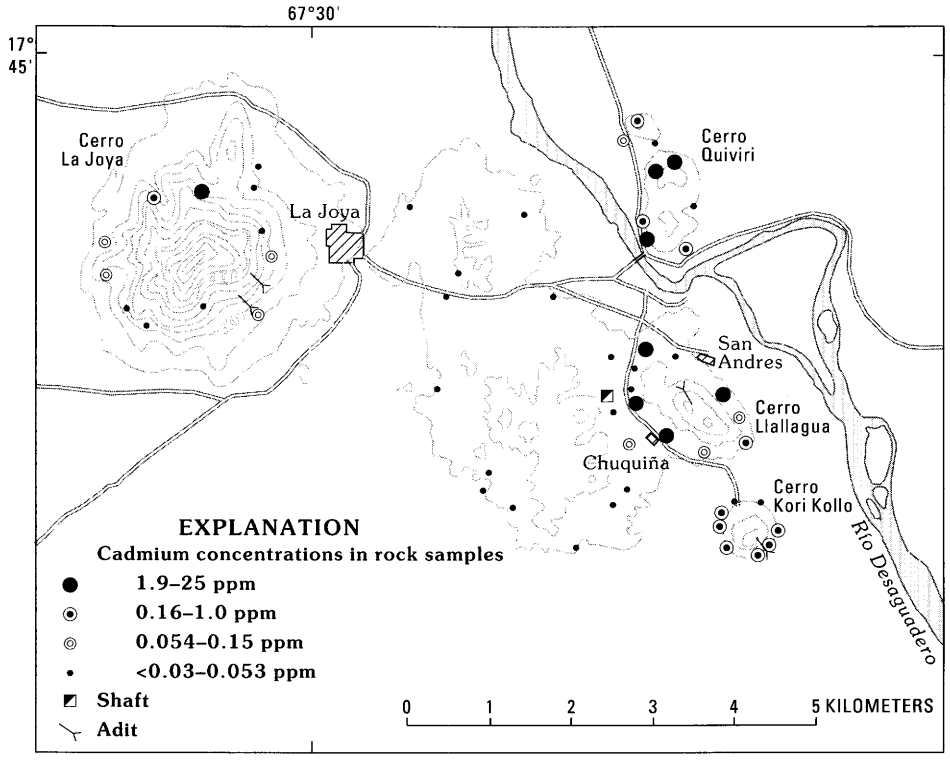


Figure 16. Map showing the distribution of cadmium concentrations in rock samples, La Joya district, Bolivia. Base modified from Cerro La Joya (6041 I) and Soledad (6140 IV) topographic quadrangles; contour interval, 40 m.

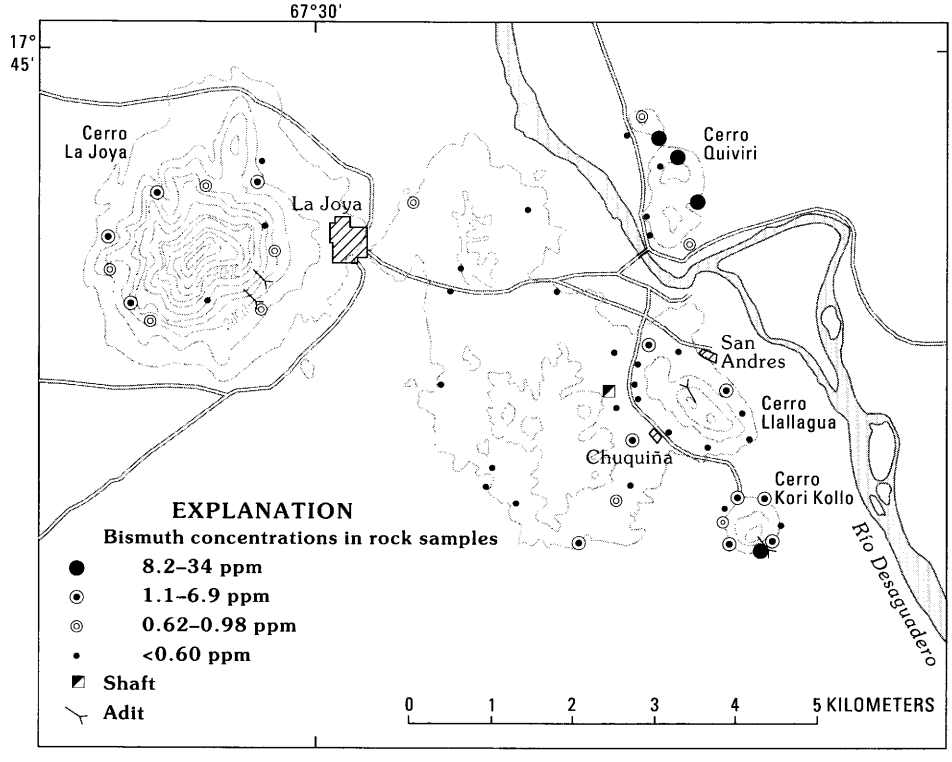


Figure 17. Map showing the distribution of bismuth concentrations in rock samples, La Joya district, Bolivia. Base modified from Cerro La Joya (6041 I) and Soledad (6140 IV) topographic quadrangles; contour interval, 40 m.

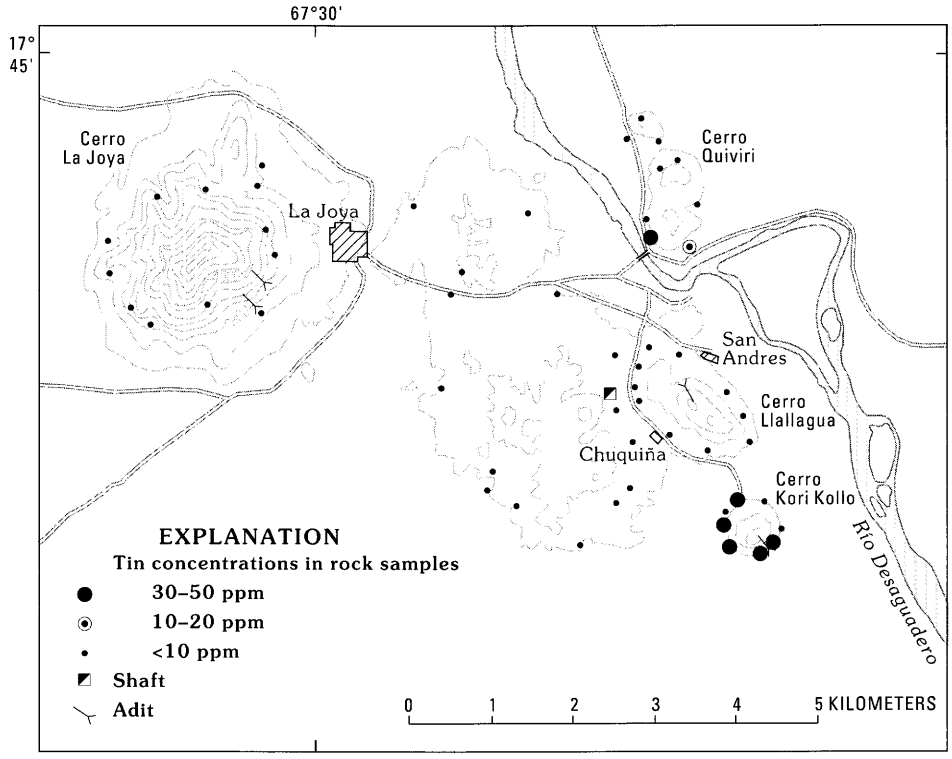


Figure 18. Map showing the distribution of tin concentrations in rock samples, La Joya district, Bolivia. Base modified from Cerro La Joya (6041 I) and Soledad (6140 IV) topographic quadrangles; contour interval, 40 m.

Table 2. *Element associations determined by R-mode factor analyses on 118 rock samples from La Joya district, Bolivia*

[Parentheses denote elements with loadings below 0.4, but statistically significant. Leaders (--) indicate none identified]

Rock factor	Element associations with positive loading	Element associations with negative loading
1	Ca-Na-Ba-Ga-Mg-Sr-Co-Be-La-Mn-Fe-Ni-Cr	--
2	Pb-Sb-As-Ag-Cu-(Au)	Ni
3	Zn-Cd-Mn-Co-(Ni)-(Pb)	--
4	Ti-Zr-Y-B-La-V	--
5	Au-Bi-As-Ag-(Fe)-(Sb)	--
6	Cr-Mo	--
7	Cu-V-Ni	--

of single-element plots. High values for the association Pb-Sb-As-Ag-Cu occur at each of the four localities (fig. 19) found to have anomalous metal contents from single element plots. However, high values for the association Zn-Cd-Mn-Co are uniquely coincident with Cerro Quiviri and Cerro Llallagua (fig. 20). The latter elements in most acid hydrothermal systems (and surficial environments) have high mobility and display the greatest dispersion from the center of the mineralizing system (Rose and others, 1979). In contrast, high values for the gold-rich association Au-Bi-As-Ag are coincident with samples from Cerro Kori Kollo (fig. 21). The association of Au and Ag with Bi, As, and Sn (fig. 18), which have generally low mobility in hydrothermal systems and are characteristic of the central or higher-temperature parts of polymetallic vein systems, suggests that the precious-metal deposit at Kori Kollo may be a deeper-level manifestation of the Bolivian polymetallic vein deposit type. The spatial relationship of these metal associations to each other suggest to us that although a variety of metals (Pb-Sb-As-Ag-Co) indicate, in general, the presence of polymetallic mineralization, the other metal associations (Zn-Cd-Mn-Co and Au-Bi-As-Ag) may be useful in defining level of exposure within these mineralized systems.

The uncertainty as to whether the mineralization at each of the four localities is related to one large hydrothermal system or to distinct individual systems related to small intrusive bodies, as well as the lack of understanding of how oxidation and weathering have affected metal dispersion are both questions that must be addressed. Cupolas of altered dacite have been identified at each locality, which would appear to support the argument that the four hills may represent separate hydrothermal systems which are probably related to the same igneous event. Oxidation of sulfide minerals is observed at each locality, although of variable extent, but because of their proximity, the localities

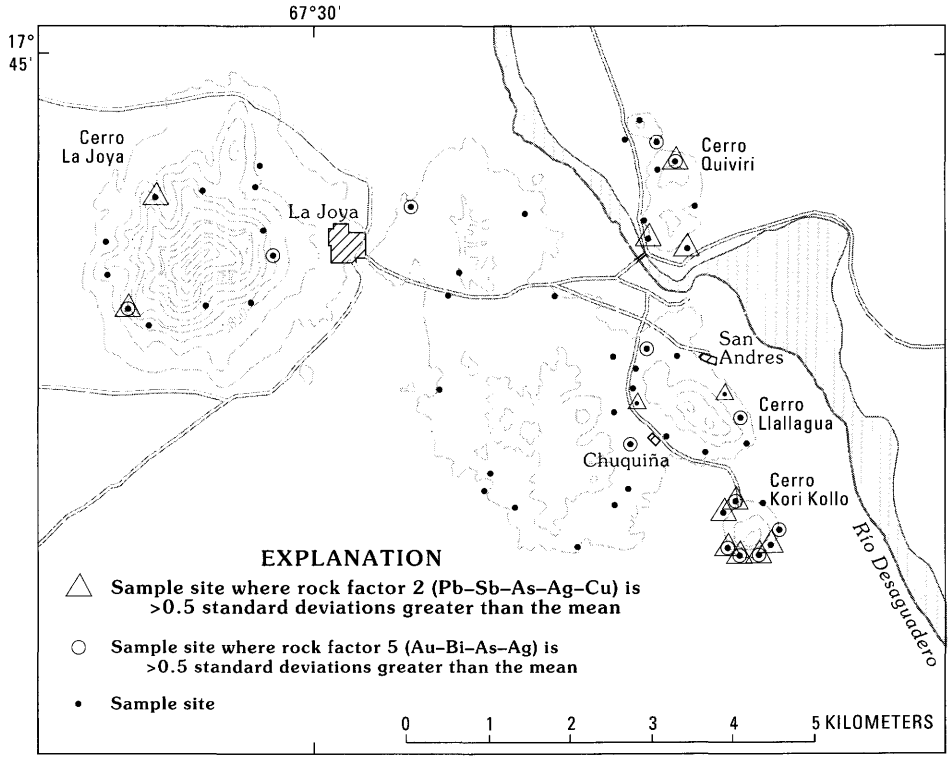


Figure 19. Map showing the location of sample sites with factor scores >0.5 standard deviations above the mean indicated for rock factor 2 (Pb-Sb-As-Ag-Cu) and rock factor 5 (Au-Bi-As-Ag), La Joya district, Boliva. Base modified from Cerro La Joya (6041 I) and Soledad (6140 IV) topographic quadrangles; contour interval, 40 m.

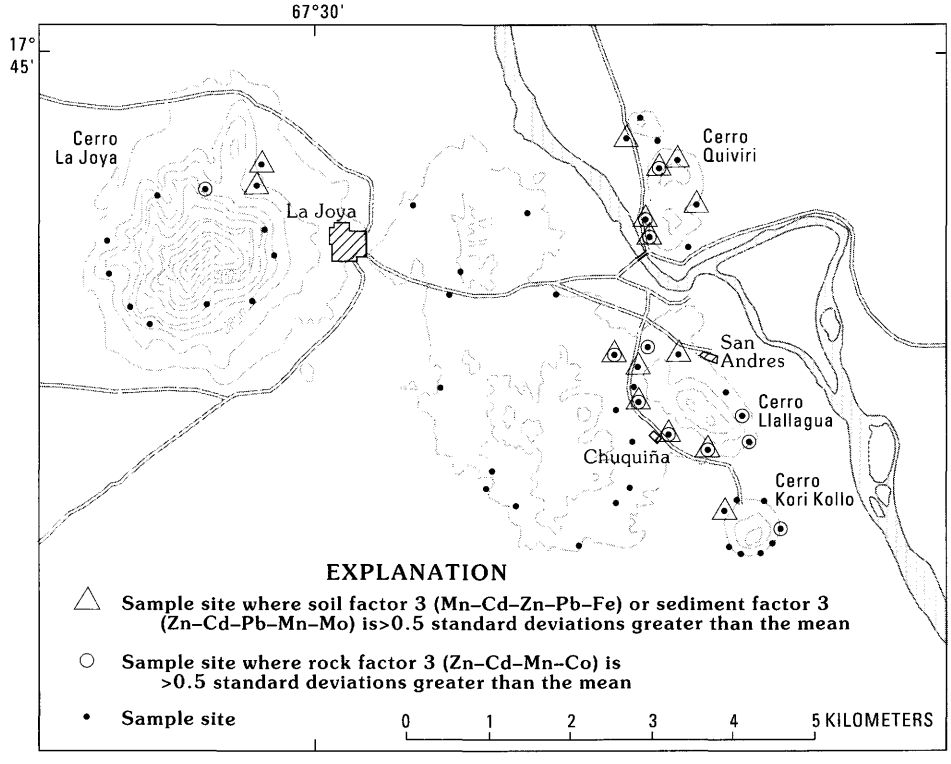


Figure 20. Map showing the location of sample sites with factor scores >0.5 standard deviations above the mean indicated for soil factor 3 (Mn-Cd-Zn-Pb-Fe), sediment factor 3 (Zn-Cd-Pb-Mn-Mo), and rock factor 3 (Zn-Cd-Mn-Co). Base modified from Cerro La Joya (6041 I) and Soledad (6140 IV) topographic quadrangles; contour interval, 40 m.

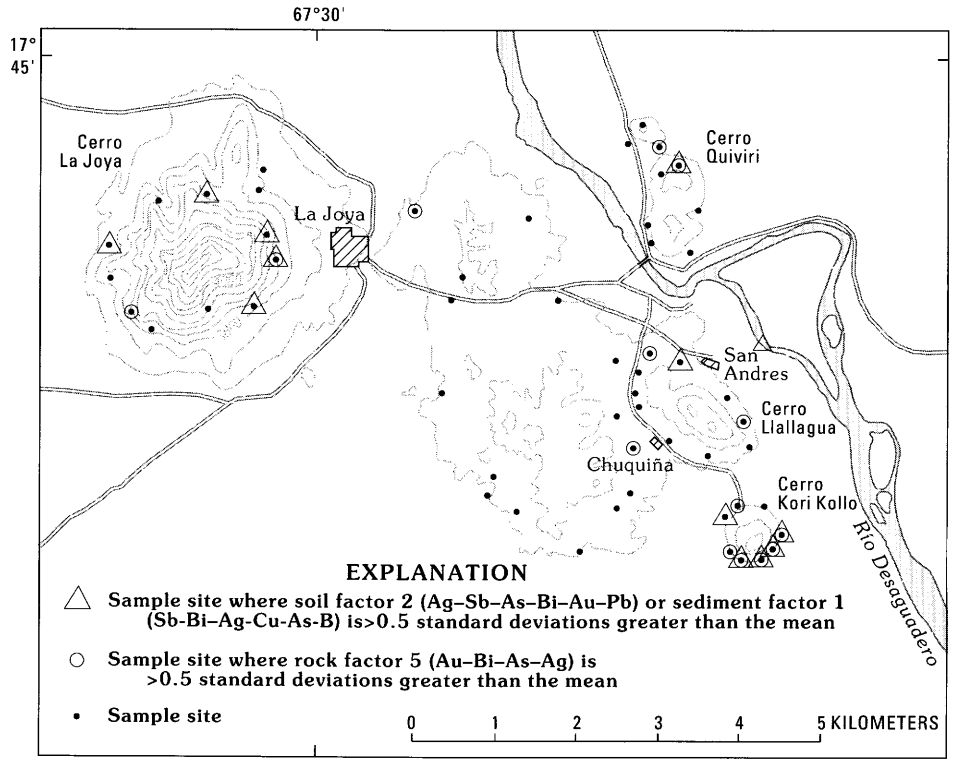


Figure 21. Map showing the location of sample sites with factor scores >0.5 standard deviations above the mean indicated for soil factor 2 (Ag-Sb-As-Bi-Au-Pb), sediment factor 1 (Sb-Bi-Ag-Cu-As-B) and rock factor 5 (Au-Bi-As-Ag), La Joya district, Bolivia. Base modified from Cerro La Joya (6041 I) and Soledad (6140 IV) topographic quadrangles; contour interval, 40 m.

have probably been exposed to similar conditions of oxidation and weathering; the variability of oxidation is probably influenced by the degree of hypogene alteration and fracturing.

If mineralization at each of the localities (La Joya, Quiviri, Llallagua, Kori Kollo) is due to distinct cupolas and separate hydrothermal systems, and our interpretation of base-metal (higher) to precious-metal (lower) zoning is valid, then geochemical anomalies at Cerro Quiviri and Cerro Llallagua may indicate precious-metal deposits at depth. The fluid-inclusion data presented in the discussion in the section on Geology of known mineral deposits indicates that vein temperatures at Cerros Llallagua and Quiviri may have been less than at Cerro Kori Kollo; the temperatures from Cerros Llallagua and Quiviri are consistent with shallower (or more distal) deposition of metals. The highest temperatures and most saline inclusions measured in the La Joya district are at Cerro La Joya. Detailed mapping, sampling, and drilling will probably be necessary to assess the presence and mineralogic nature of zoning at these localities.

DISTRIBUTION OF INDICATOR ELEMENTS IN SOILS AND SEDIMENT SAMPLES

Data for soil and coarse-fraction (+0.25 mm) sediment samples were combined because (1) soil samples were taken to supplement the drainage survey where drainage systems were poorly developed; (2) these sample media were collected in roughly similar settings of high relief and low rainfall where sediment transport distance is short; and (3) similar statistics for elements in each medium warrant combination (table 1). The summary statistics presented in table 1 indicate that element concentrations are lower in fine-fraction than in coarse-fraction sediment. Anomaly-to-background contrast is also slightly lower for the fine-fraction sediment data. This indicates that metals are being dispersed from mineralized rock predominantly by mechanical rather than chemical processes, something that could be expected on the arid Altiplano. Thus, coarse-fraction sediment and (or) heavy-mineral-concentrate samples may be of greatest value in reconnaissance-scale geochemical exploration.

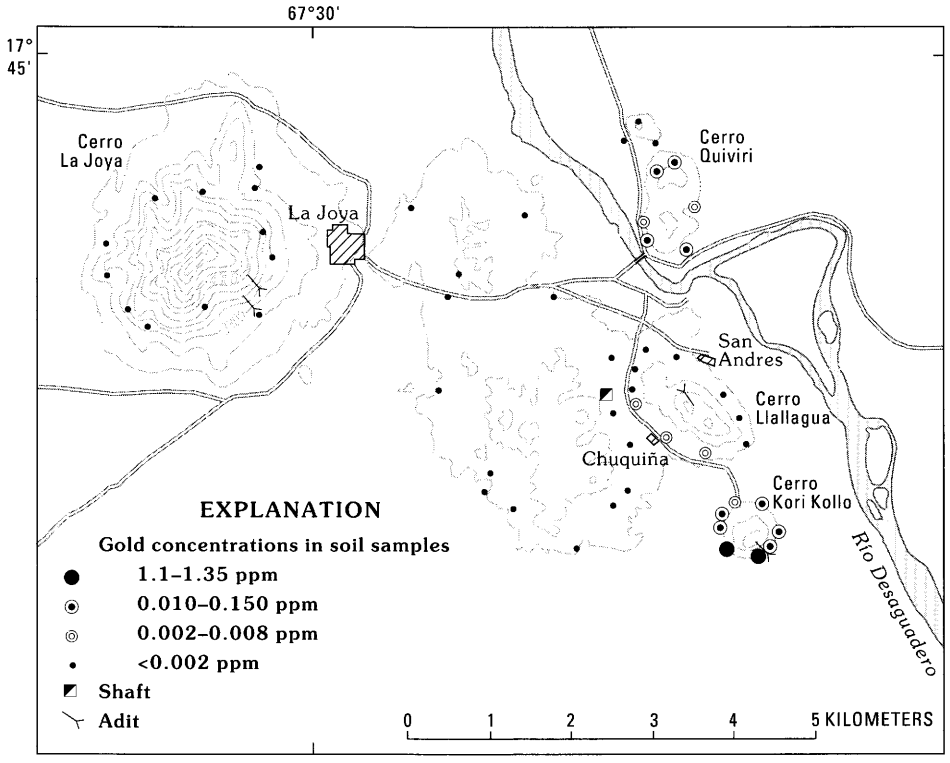


Figure 22. Map showing the distribution of gold concentrations in soil samples, La Joya district, Bolivia. Base modified from Cerro La Joya (6041 I) and Soledad (6140 IV) topographic quadrangles; contour interval, 40 m.

The distributions of the indicator elements in soils and coarse sediments (figs. 22–30) are similar to the distribution of the respective elements in rocks (figs. 10–18). For example, high values for Ag, Sb, As, and Pb can be seen at Cerro La Joya, Cerro Quiviri, Cerro Llallagua, and Cerro Kori Kollo. High contents of Au in soils at Cerro Kori Kollo and Cerro Quiviri are coincident with results from rock samples; there are also a few soil and coarse-sediment samples with elevated Au values from Cerro Llallagua. No soil and coarse sediment samples anomalous in Au were collected from Cerro La Joya (fig. 22). Soils and coarse sediments collected from Cerro Quiviri and Cerro Llallagua contain high values for Zn and Cd; lower, but elevated, values for these elements can be seen in samples from Cerro La Joya and Cerro Kori Kollo (figs. 27, 28). High values of Bi and Sn occur in soils and coarse sediment samples collected from Cerro La Joya and Cerro Kori Kollo (figs. 29, 30). Two samples with anomalous copper concentrations were collected from the southern slope of Cerro La Joya but are not shown.

In order to determine the element associations of metals in soil samples, analyses for 31 elements and 50 soil samples were entered into the R-mode factor analysis program. A five-factor model was chosen for this data set because it explains more than 70 percent of the overall variance in the original data, and explains more than 60 percent of the variation for each element except Ti, Na, Ni, Zr, Y, Be, La, and Mo, which are related principally to lithology. Element associations were derived by including elements with significant (>0.4) loadings (correlation coefficients) on the factors. The element associations for soil samples are shown in table 3.

R-mode factor analysis was also used to determine the element associations in fine-fraction (–0.25 mm) sediment data. Data from analyses of 31 elements and 94 samples were entered into the R-mode factor analysis program. A seven-factor model was selected for this data set because it explains more than 77 percent of the variance in the original data set and more than 70 percent of the variance for each element except Ba, Cr, La, Na, Y, and Zr, which are principally related to igneous rocks. The element associations for fine-fraction sediment data are shown in table 4.

To some degree, the R-mode factor analysis results of the soil and sediment data corroborate the base-metal and precious-metal associations described above for single element plots. The two soil factors reflecting mineralization are soil factor 2, Ag-Sb-As-Bi-Au-Pb and soil factor 3, Mn-Cd-Zn-Pb-Fe. The two sediment factors reflecting mineralization are sediment factor 1, Sb-Bi-Ag-Cu-As-B and sediment factor 3, Zn-Cd-Pb-Mn-Mo. Although gold

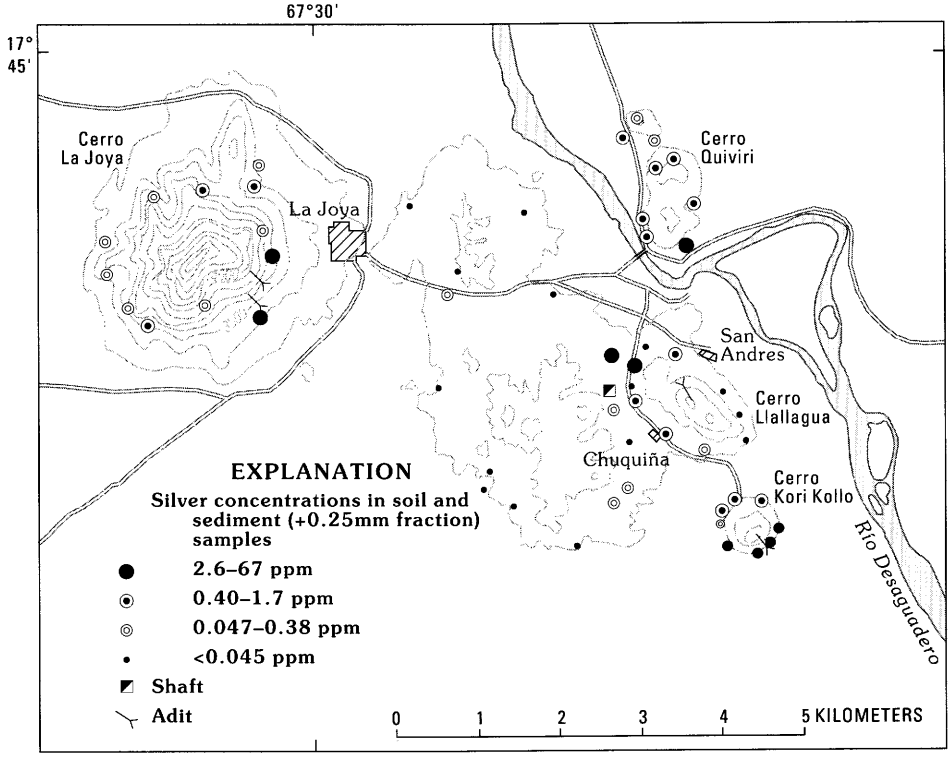


Figure 23. Map showing the distribution of silver concentrations in soil and sediment (+0.25 mm fraction) samples, La Joya district, Bolivia. Base modified from Cerro La Joya (6041 I) and Soledad (6140 IV) topographic quadrangles; contour interval, 40 m.

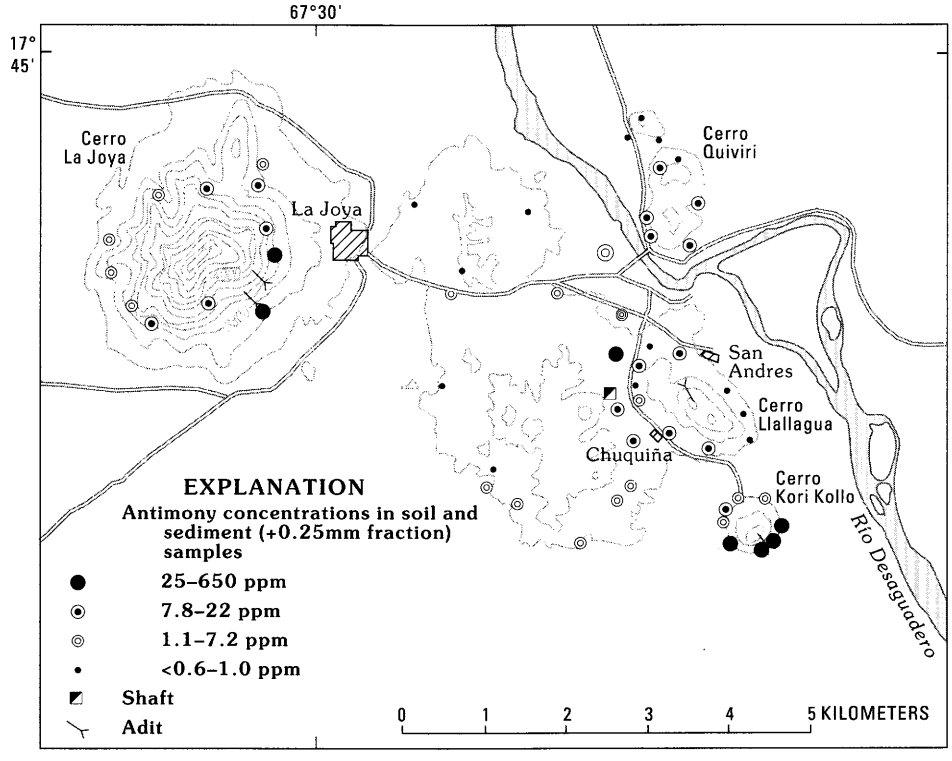


Figure 24. Map showing the distribution of antimony concentrations in soil and sediment (+0.25 mm fraction) samples, La Joya district, Bolivia. Base modified from Cerro La Joya (6041 I) and Soledad (6140 IV) topographic quadrangles; contour interval, 40 m.

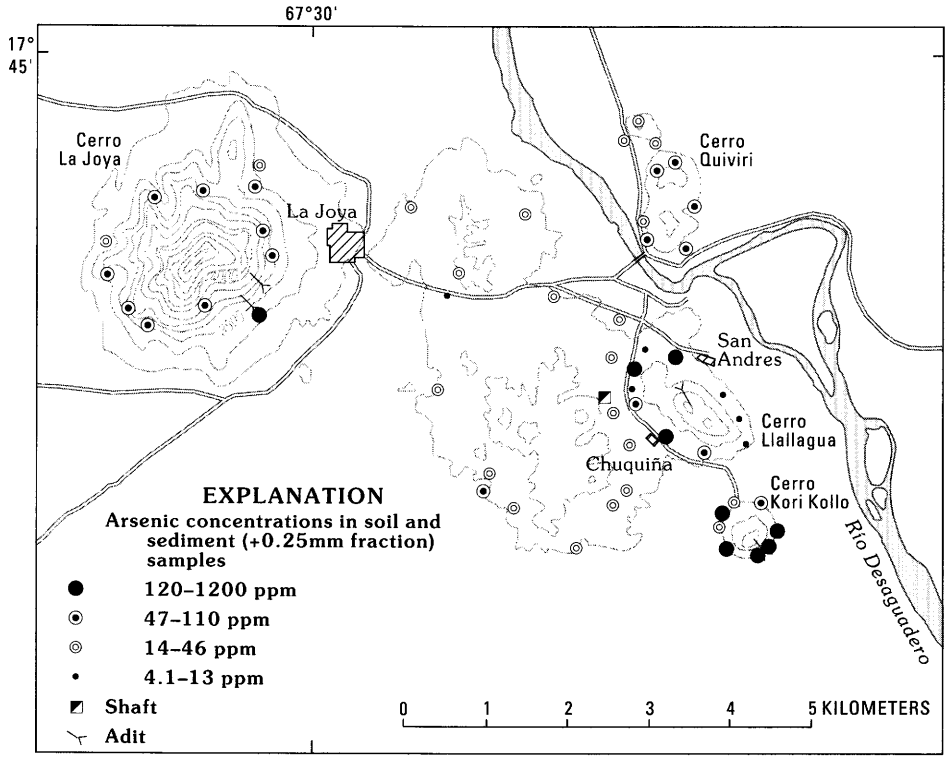


Figure 25. Map showing the distribution of arsenic concentrations in soil and sediment (+0.25 mm fraction) samples, La Joya district, Bolivia. Base modified from Cerro La Joya (6041 I) and Soledad (6140 IV) topographic quadrangles; contour interval, 40 m.

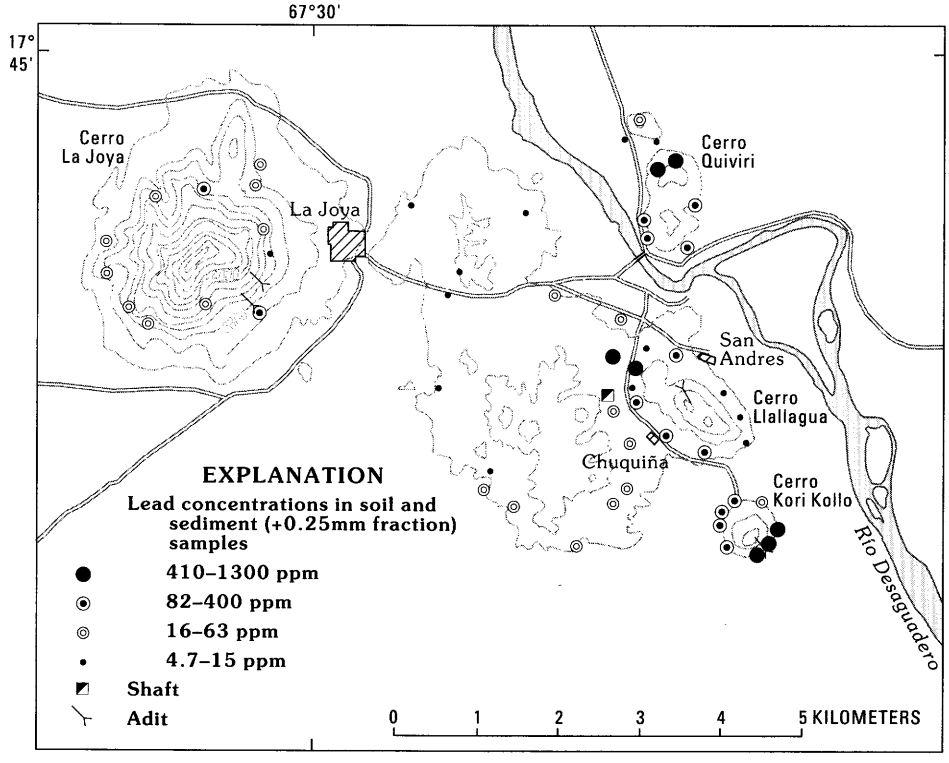


Figure 26. Map showing the distribution of lead concentrations in soil and sediment (+0.25 mm fraction) samples, La Joya district, Bolivia. Base modified from Cerro La Joya (6041 I) and Soledad (6140 IV) topographic quadrangles; contour interval, 40 m.

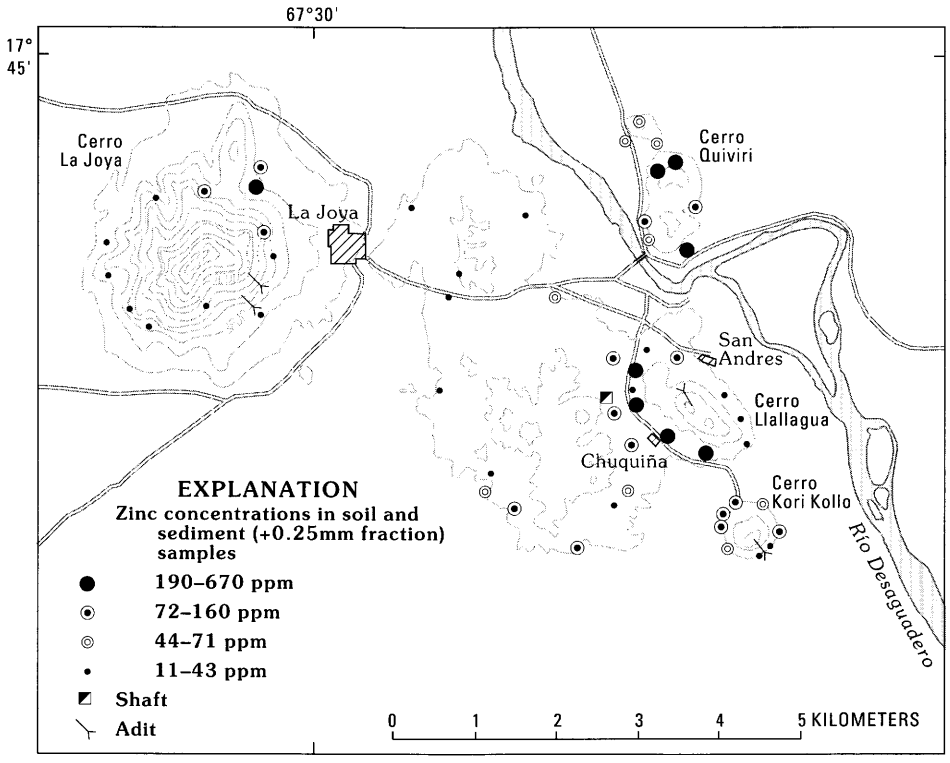


Figure 27. Map showing the distribution of zinc concentrations in soil and sediment (+0.25 mm fraction) samples, La Joya district, Bolivia. Base modified from Cerro La Joya (6041 I) and Soledad (6140 IV) topographic quadrangles; contour interval, 40 m.

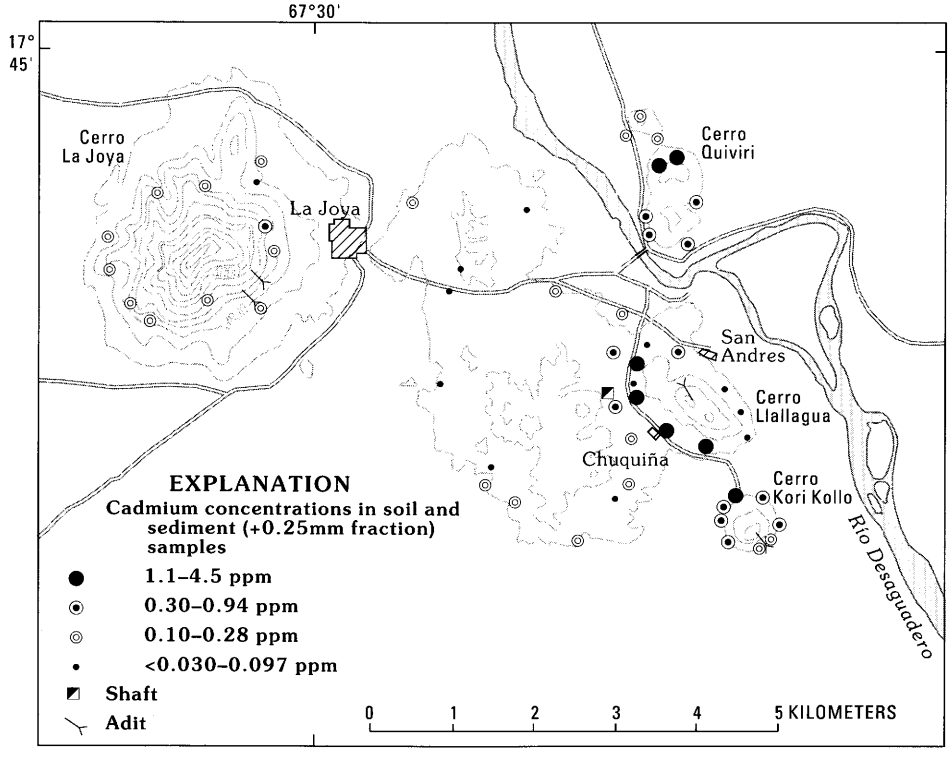


Figure 28. Map showing the distribution of cadmium concentrations in soil and sediment (+0.25 mm fraction) samples, La Joya district, Bolivia. Base modified from Cerro La Joya (6041 I) and Soledad (6140 IV) topographic quadrangles; contour interval, 40 m.

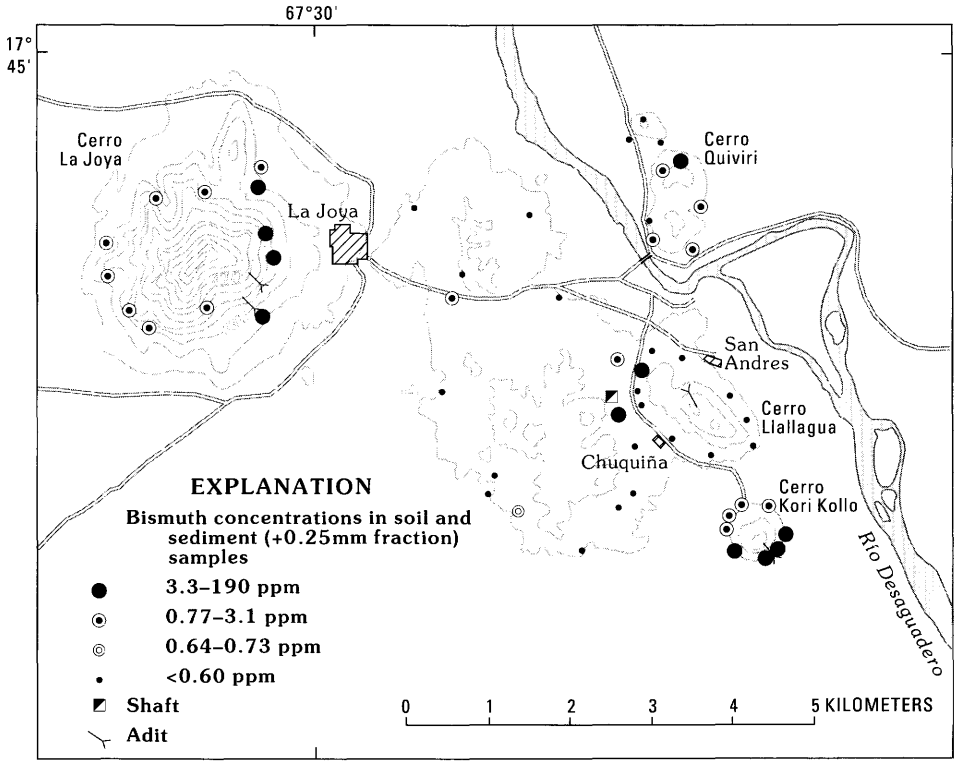


Figure 29. Map showing the distribution of bismuth concentrations in soil and sediment (+0.25 mm fraction) samples, La Joya district, Bolivia. Base modified from Cerro La Joya (6041 I) and Soledad (6140 IV) topographic quadrangles; contour interval, 40 m.

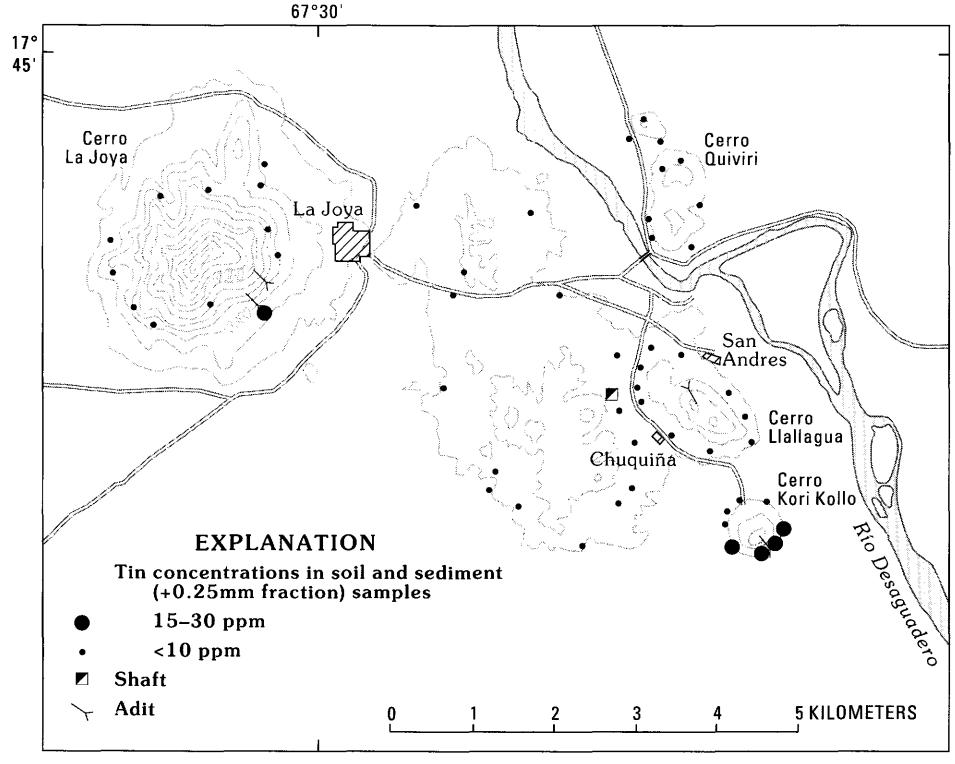


Figure 30. Map showing the distribution of tin concentrations in soil and sediment (+0.25 mm fraction) samples, La Joya district, Bolivia. Base modified from Cerro La Joya (6041 I) and Soledad (6140 IV) topographic quadrangles; contour interval, 40 m.

Table 3. *Element associations determined by R-mode factor analysis on 50 soil samples from the La Joya district, Bolivia*

[Parentheses denote elements with loadings below 0.4, but statistically significant. Leaders (--) indicate none identified]

Soil factor	Element associations with positive loading	Element associations with negative loading
1	Ga-Cr-Be-Sc-Cu-Mg	--
2	Ag-Sb-As-Bi-Au-Pb-(Mo)	Co-Na-Ni-Ti
3	Mn-Cd-Zn-Pb-Fe	B
4	Zr-V-Y-B-Sc-Fe-Ti-Pb	Ca-Sr-Na
5	Mg-Cu-Co-Sc-Cr	--

Table 4. *Element associations determined by R-mode factor analysis on 94 fine-fraction sediment samples from the La Joya district, Bolivia*

[Parentheses denote elements with loadings below 0.4, but statistically significant]

Sediment factor	Element associations with positive loading
1	Sb-Bi-Ag-Cu-As-B
2	Ga-Mg-La-Ba-Na-Fe-Sr
3	Zn-Cd-Pb-Mn-Mo
4	V-Ti-Cr-Zr-(Fe)
5	Be-B-(Zr)
6	Ca-Sr
7	Co-Sc-Ni-Fe-(Mn)

was not analyzed for in sediments, it would likely fall into sediment factor 1. The coincidence of base-metal anomalies in the soil and sediment samples at Cerro Quiviri and Cerro Llallagua is seen on figure 20. Anomalies for the precious-metal suites in the soil and sediment samples are coincident at Cerro Kori Kollo and Cerro La Joya (fig. 21).

CONCLUSIONS

Our geochemical study of the La Joya district has (1) determined a suite of metals that are characteristic of polymetallic veins, (2) provided information on the effectiveness of different sample media in the detection of mineralization, and (3) revealed through interpretation of multi-element geochemical data using factor analysis that element associations may be indicative of zoning within a polymetallic vein deposit type. The study of the La Joya district has demonstrated that rock geochemistry on the Altiplano is particularly useful in defining the suite of metals generally indicative of polymetallic vein mineralization (Sb, As, Ag, Au, Bi, Pb, Zn, Sn); factor analysis of the data provides information concerning possible zoning of these systems. Variations in associations of elements between specific localities (igneous centers?), together with geologic and fluid-inclusion data from other work lead us to conclude that the polymetallic vein deposits may be vertically zoned, with upper or peripheral zones rich in base metals and sulfosalts, and lower or central parts rich in precious metals, Sn, and B. Element associations indicative of the base-metal and precious-metal zones are Zn-Cd-Mn-Co-(Ni)-(Pb) and Au-Bi-As-Ag-Sn-(Fe)-(Sb), respectively. If these interpretations are correct, potential exists for discovery of precious-metal deposits at depth beneath Cerro Quiviri and Cerro Llallagua similar to those at Cerro Kori Kollo because deeper parts of the vein systems may already be exposed at Cerro Kori Kollo and Cerro La Joya.

Sampling and multi-element factor analysis of sediment provide geochemical information that is essentially the same as that provided by rock samples in the high-relief and arid environment of the Altiplano and is a more rapid method of reconnaissance exploration. Analyses of coarse-fraction (+0.25 mm) sediment provides data with higher metal values and anomaly-to-background contrast than does fine-fraction (–0.25 mm) sediment, and therefore may be more useful as a sampling medium. However, to obtain equally representative samples of coarse or fine materials, a larger sample must be collected of coarse material than of fine material. The higher concentrations of metals in coarse-fraction sediment relative to fine-fraction sediment indicates that mechanical erosion is probably the dominant method of dispersion of metals in the region of the La Joya district. This being true, heavy-mineral-concentrates from sediment samples could be useful in detecting gold, which is difficult to detect accurately in coarse sediment. In addition, in regions where drainage systems are longer than 5 km, heavy-mineral concentrates could prove useful because of longer detectable dispersion trains.

Remote Sensing

By Daniel H. Knepper, Jr. *and* Shirley L. Simpson

Introduction **47**
Thematic Mapper data characteristics and coverage **47**
Digital image processing **48**
Computer facilities and software **48**
Common digital processing functions **48**
Contrast stretching **48**
Edge enhancement **50**
Data calibration **50**
Masking **51**
Thematic Mapper images **51**
Black-and-white, single-band **51**
Simulated natural color composite **52**
Color-infrared composite **53**
Color-ratio composite **53**
Masked color-ratio composite **53**
Interpretation of potentially hydrothermally altered rocks **54**

FIGURES

31. Map showing centers of Landsat Thematic Mapper images **49**
32. Nondirectional edge enhancement algorithm **51**
33. Landsat Thematic Mapper image of southern end of the Altiplano and Cordillera Occidental **52**

TABLES

5. Landsat Thematic Mapper spectral bands **48**
6. Landsat Thematic Mapper data **50**
7. Ratios, minerals, and color-ratio composite image color **53**

INTRODUCTION

The primary objective of the remote-sensing studies conducted as part of the mineral-resource evaluation of the Altiplano and Cordillera Occidental, Bolivia, was to prepare a map showing the distribution of potentially hydrothermally altered rocks as determined by spectral-reflectance characteristics of the surface derived from measurements made by the Thematic Mapper (TM) systems on Landsats 4 and 5 (pl. 2). The 30-m ground resolution and the 6 spectral bands in the visible and near-infrared wavelength region make Landsat TM data ideal for many regional and local geologic studies. However, to obtain the maximum use of the data, different types of images must be prepared for specific analysis. For this study, 5 types of images were prepared: simulated natural color, color-infrared composite, color-ratio composite, masked color-ratio composite, and black-and-white single-band images. The digitally processed images were also used in this study to identify volcanic features and geologic structures, discriminate between lithologic units, and as the basis of photoreconnaissance to identify potentially mineralized areas for later field evaluation.

THEMATIC MAPPER DATA CHARACTERISTICS AND COVERAGE

Digital TM data are contained in 6 spectral bands (table 5) in the visible and near-infrared portions of the

Table 5. *Landsat Thematic Mapper Spectral Bands*

[IR, infared]

Band	Range
1	0.45-0.52 μm (blue)
2	.52-0.60 μm (green)
3	.63-0.69 μm (red)
4	.76-0.90 μm (IR)
5	1.55-1.75 μm (IR)
6	10.4-12.5 μm (IR)
7	2.08-2.35 μm (IR)

spectrum, and a measurement representing the radiance received by the sensors (DN or data number) for every 30 m by 30 m area is obtained for each of the spectral bands. One of the spectral bands in the thermal infrared, band 6 (10.4–12.5 μm) was not used in this study.

Nine full TM scenes and portions of 4 other TM scenes are needed for complete coverage of the Altiplano and Cordillera Occidental (table 6); a full TM scene covers an area of approximately 185 km^2. The center of each TM scene is located in relation to a path and row designated in the Landsat Worldwide Reference System (U.S. Geological Survey and National Oceanic and Atmospheric Administration, 1982). Figure 31 shows the centers of the TM scenes used in this study.

Overall, the quality of the TM image data is good to excellent. High, thin clouds and some small, dense clouds are present in some of the data and some of the higher peaks are covered with snow, particularly in the southern part of the Altiplano; path 001/row 071 is mostly covered by clouds. However, clouds and snow do not appreciably detract from the use of most of the data. The digital data for path 233/row 076 contain clusters of bad lines caused by problems in producing the original data tapes; this problem was corrected with an averaging technique using data from an adjacent line.

DIGITAL IMAGE PROCESSING

The extraction of geologic information from digital multispectral image data requires that the nature of the digital data, as well as, the spectral characteristics of the materials exposed at the Earth's surface be understood. Different processing schemes can be applied to the digital data to identify, enhance, and display information that can then be used in different aspects of the geologic interpretations.

COMPUTER FACILITIES AND SOFTWARE

Digital processing of Landsat TM data requires a large amount of on-line disk storage because of the large size of the data sets and the number of intermediate files that must be maintained through the processing procedure. In addition, a moderately fast computer with efficient input and output is necessary to reduce the time required to process these large data sets. All of the digital image processing for this investigation was conducted at the U.S. Geological Survey (USGS), Denver, Colo. Most of the processing was done on a Perkin Elmer 3240 minicomputer with a Floating Point Systems AP–120B array processor and 1.5 gigabytes of external disk storage on-line; additional processing was done on a Sun 3/470 workstation. Digital images were displayed and analyzed at intermediate steps on a Comtal Vision 1/10 image display device. Film transparencies of the processed images (10 in. by 10 in.) were prepared from digital data tapes using an Optronics International Colorwrite C–4300 film writing system.

The image-processing software used was a USGS package developed over more than 15 years for the processing and analysis of digital satellite and aircraft remote-sensing data. This package, called REMAPP (REMote sensing Array Processing Procedures) provides a wide range of image-processing functions (Sawatzky, 1985) and has been adapted for use on an IBM-compatible personal computer with a VGA display (Livo, 1990).

COMMON DIGITAL PROCESSING FUNCTIONS

It is beyond the scope of this report to fully discuss all aspects of the digital image processing used in this study; introductory texts on remote sensing, such as Gillespie (1980) or Sabins (1987), provide background information and detailed discussions of the many aspects of digital image processing. An understanding of some of the fundamental procedures is required, however, to be able to evaluate the information content of the 5 types of images prepared during the course of this study.

CONTRAST STRETCHING

Contrast stretching is required to produce useful video or hardcopy displays of processed-image data. There are numerous stretching functions that can be applied, but the most common is a linear stretch. A linear stretch is applied by assigning new lower and upper limits to a range of data numbers (DN) and letting the DN within the range

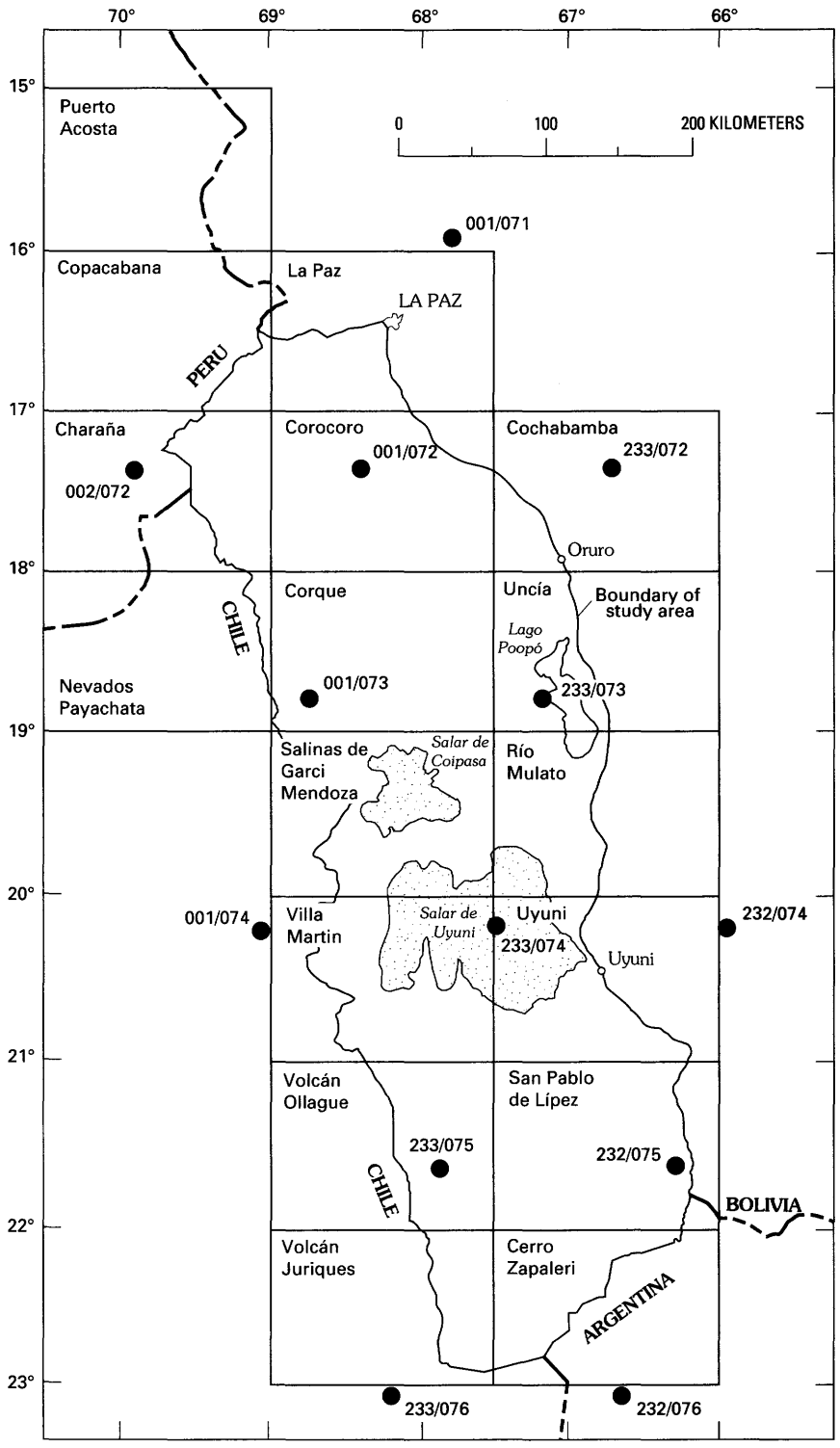


Figure 31. Map showing the centers of the Landsat Thematic Mapper images and locations of 1:250,000-scale quadrangles, Altiplano and Cordillera Occidental, Bolivia.

assume new values in a linear fashion. A linear contrast stretch can be applied to all or some part of the data, and is usually the final step in processing an image for visual interpretation. Two types of linear contrast stretching techniques were selectively applied to the processed TM images of the Altiplano and Cordillera Occidental: (1) a 2 percent linear stretch about the median; and (2) a linear shadow stretch.

Table 6. *Landsat Thematic Mapper data of the Altiplano and Cordillera Occidental, Bolivia*

Path	Row	Scene I.D.	Quads	Date	Comments
001	071	5001114001	1-4	03/12/1984	Extensive cloud cover
001	072	5012914040	1-4	07/08/1984	Good
001	073	5012914042	1-4	07/08/1984	Good
001	074	4252314093	1-4	06/12/1989	Excellent
002	072	5044014114	1-4	05/15/1985	Excellent
232	074	5086713463	3	07/16/1986	Excellent
232	075	4258913574	1-4	08/17/1989	Excellent
232	076	4258913580	1	08/17/1989	Excellent
233	072	5047413592	3	06/18/1985	Excellent
233	073	4256414031	1-4	07/23/1989	Excellent
233	074	4258014033	1-4	08/08/1989	Excellent
233	075	4258014035	1-4	08/08/1989	Good
233	076	4254814042	2	07/07/1989	Partial snow; bad lines

A 2 percent linear stretch about the median is a 2-part linear stretch that requires a knowledge of the cumulative frequency distribution of the image DN. Using the cumulative frequency distribution histogram, the DN corresponding to the lower and upper 2 percent of the data (2 percent and 98 percent) and the median point (50 percent) are identified. The DN at and below the 2nd percentile are set equal to 0, the median is set equal to an intermediate value of 127 (half way along the possible 0–255 range of 8-bit data), and the DN equal to and greater than the 98th percentile are set equal to 255. The remaining DN are assigned new DN values proportionally along the 2 segments of the stretch: 0–126 and 128–255, accordingly. The 2 percent linear contrast stretch about the median results in an increase of overall scene brightness and increased range of DN between once adjacent numbers produces greater tonal contrast on the stretched image. A 2 percent linear stretch about the median results in a loss of information contained in the lower and upper 2 percent of the original data, but the amount of useful geologic information in these parts of the data is negligible. This type of linear contrast stretch was applied to all of the processed TM data prior to the preparation of film transparencies.

For black-and-white single band images, simulated natural color images, and color-infrared composite images, a second linear stretch was superimposed on the 2 percent linear stretch about the median to increase the brightness in shadowed areas so that some of the morphological features could be seen better. To achieve this slight brightening of the darker pixels (lower DN), the DN equal to 1 were reassigned to a value greater than 1 (commonly near 16), which was determined by trial-and-error and was a function of the specific data set. The DN equal to 127 were the upper level of the stretch. The DN between 1 and 127 were then linearly stretched to produce the desired brightening of the darker pixels; the effect of this second linear stretch is greater for the lower DN and less for those DN near 127.

EDGE ENHANCEMENT

Edge enhancement is a technique used to increase the tonal contrast at the boundaries between groups of dissimilar pixels. The effect of edge enhancement is to increase the display of the high-frequency variations in an image, which results in images that appear to be in sharper focus. Figure 32 illustrates the nondirectional algorithm used for edge enhancement (Knepper, 1982).

DATA CALIBRATION

The DN of unprocessed TM data ideally represent the radiance received at the sensor as a function of the spectral reflectance of each pixel on the ground. However, the amount of radiance recorded in the data is not just from the reflected light from the Earth's surface; it includes scattered light that reaches the sensor from outside the pixel field, as well as, reduction in the radiance from the pixel because of absorption by atmospheric gasses and particulates. Spectral-reflectance measurements of several large, homogeneous features made during the acquisition of the TM data could be used to calibrate the data to percent reflectance; however, these measurements are usually impractical or impossible to make. Markham and Barker (1985) used repetitive field-spectral measurements during TM data acquisitions over White Sands, New Mex., to devise a means for deriving empirical correction factors for each band of data on the basis of (1) the satellite (Landsat 4 or 5), (2) the date of the preprocessing at the U.S. National Aeronautics and Space Administration (NASA) Goddard, and (3) the sun elevation at the time the satellite data were acquired. Applying the derived empirical multiplicative and additive factors for each band of data gives an approximation of the percent reflectance of every pixel in each band.

Although this calibration is only approximate, it provides a means for directly comparing similarly processed

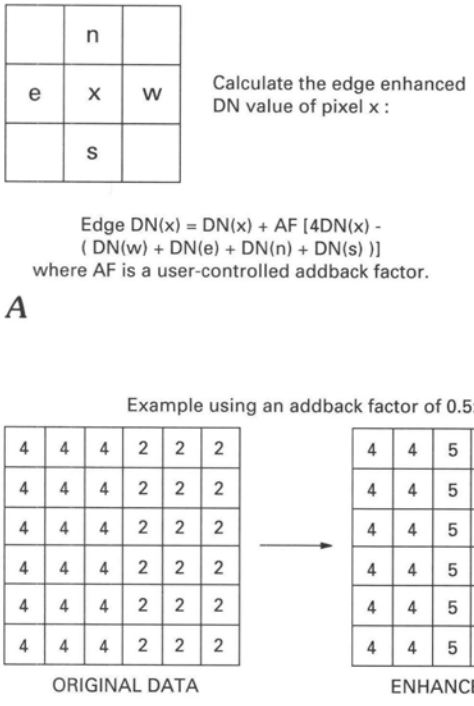


Figure 32. Nondirectional edge enhancement algorithm used to increase tonal contrast at the boundary between groups of dissimilar pixels (modified from Knepper, 1982). *A*, Algorithm shown graphically; DN, data numbers; the addback factor controls the degree of the enhancement and is user controlled. *B*, Example of nondirectional edge enhancement algorithm using an addback factor of 0.5 applied to original data and resulting enhanced data.

data acquired at widely different times and by different satellites. The Markham and Barker (1985) calibration technique was applied to the single-band data prior to the preparation of the ratio images used to detect and map possible hydrothermally altered rocks in the Altiplano and Cordillera Occidental.

MASKING

In some instances it is desirable to eliminate selected information from a processed image to increase the ability to make specific interpretations. On ratioed TM images of the Altiplano, for example, clouds, snow, water, shadows, and vegetation produce unreliable, ambiguous, or geologically meaningless ratio values. Consequently, a masking technique was designed to identify pixels containing any of these phenomenon and generate a binary (DN of 0 or 255) image mask.

The masking technique is based on the unique colors of clouds and snow (white), water and shadows (black to dark blue), and vegetation (red) on standard band 4 (red), band 3 (green), and band 2 (blue) TM color-infrared (CIR) composite images. To apply the technique, each of the 3 TM bands were contrast stretched with a 2 percent stretch about the median and entered into a computer program that calculates the hue, saturation, and value (HSV Munsell color coordinates) for each pixel in the color composite image (Raines, 1977). Based on empirical observations of HSV for numerous TM scenes transformed using this method of the western United States, the following limits were determined to provide the desired results: shadows and water, hues of 75 (blue) or neutral hues and values of 0–60 (dark); clouds and snow, values greater than 436 (bright); vegetation, hues between 209 and 307 (red to magenta). Binary digital masks were prepared for each quarter scene (quad) of TM data in the Altiplano and Cordillera Occidental and used in the preparation of the masked color-ratio composite images.

THEMATIC MAPPER IMAGES

No single digitally processed TM image can display all of the information contained in the data. Digital-image-processing methods and techniques used with TM data are different depending on how the images will be used. Consequently, determining which kinds of images best illustrate specific types of information is a very important part of the planning phase of any project. For this investigation, 5 types of images were prepared; the methods used in their preparation and the useability of each of these types of images are discussed in the following sections.

Each of the TM scenes was processed in quarter-scenes, or quads. A film of each quad was prepared at a scale of approximately 1:600,000; the film images were used to prepare enlarged prints at a scale of 1:250,000 for use in the field, laboratory analysis, and interpretation. An enlargement factor of 2.29 (229 percent) produced enlarged prints that fit the 1:250,000-scale topographic maps of the Altiplano and Cordillera Occidental very well.

BLACK-AND-WHITE, SINGLE-BAND

Black-and-white images (B/W) of selected single bands of TM data generally depict surface textures, including topography, better than color-composite images (fig. 33). Consequently, for use in identifying and mapping volcanic vents and other geologic structures, B/W images were prepared for each TM quad. The near-infrared TM bands (bands 4, 5, and 7) best display topography expressed by shadowing because of the low levels of near-infrared radiation scattered in shadows. Band 4 (0.76–0.90 μm) was chosen for this study because it has the best overall image characteristics for textural and topographic interpretations on the Altiplano and in the Cordillera Occidental.

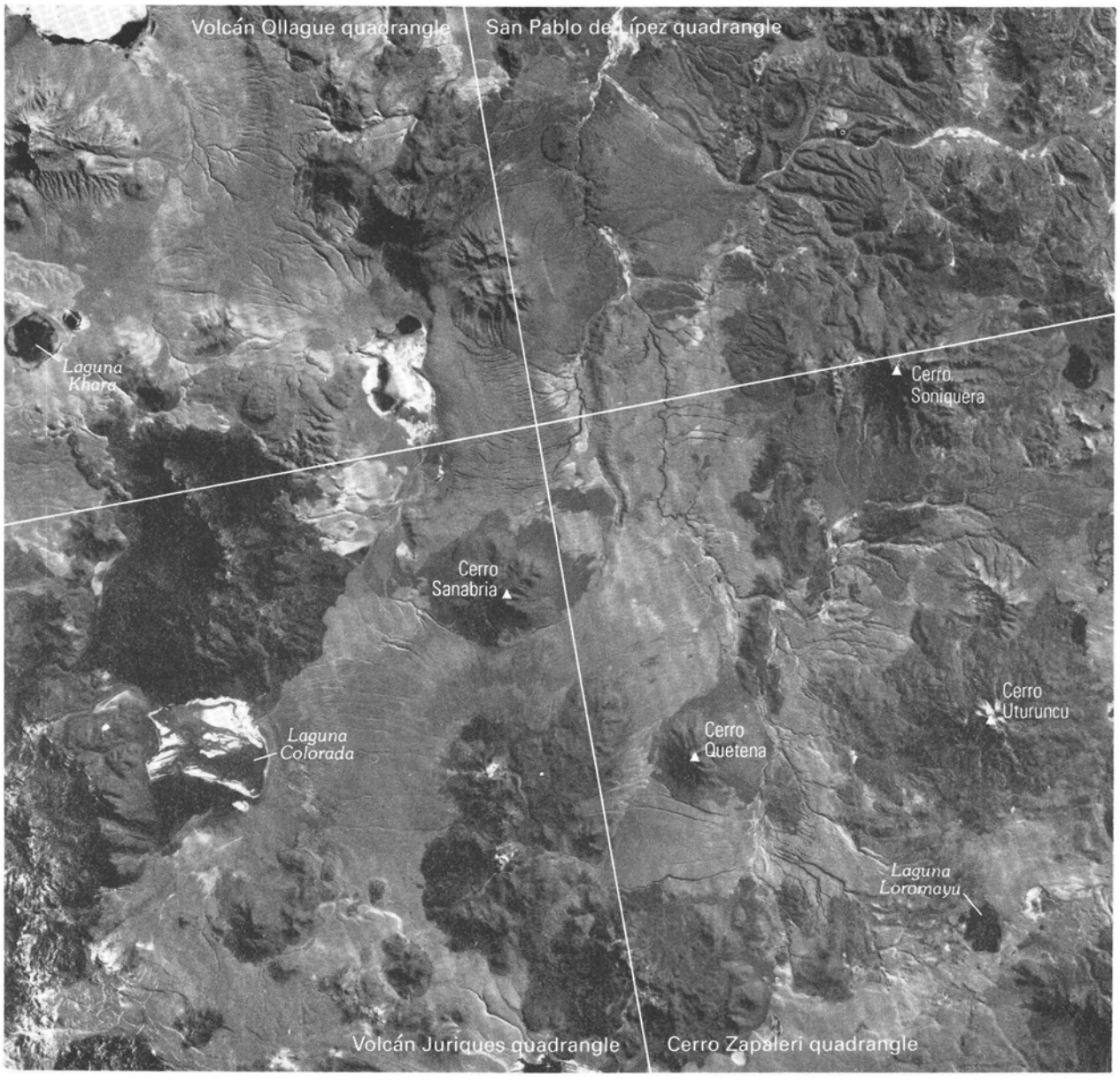


Figure 33. Black-and-white Landsat Thematic Mapper (TM) image of band 4 for path 233/row 075 at the southern end of the Altiplano and Cordillera Occidental, Bolivia. The image is centered approximately at the intersection of 4 1:250,000-scale quadrangles: Volcán Ollague, San Pablo de Lípez, Volcán Juriques, and Cerro Zapaleri. Selected prominent volcanoes and lakes are labeled for reference. Dark colors primarily represent lavas; light colors primarily represent ignimbrites.

Histograms of the frequency distribution of TM band 4 DN's for each quad were used to determine a 2 percent contrast stretch about the median DN for each quad. For these data, a 2 percent contrast stretch produces a good quality image for the high and mid-range DN values, but details in light to moderate shadows are too dark to be displayed. Consequently, a shadow stretch designed to slightly raise the brightness of only these pixels was applied.

The final digital processing of the B/W images was the application of a nondirectional edge enhancement. Edge enhancements, which increase the contrast at tonal boundaries (edges), result in the enhancement of the high-frequency components of the image data. In visual terms, such features as drainage lines, topography expressed by shadows, lithologic contacts, and interfaces between vegetation and rock appear sharper on the images with edge enhancement than on images without edge enhancement.

SIMULATED NATURAL COLOR COMPOSITE

The simulated natural color composite images (SNC) are designed to appear like small-scale color aerial

Table 7. *Ratios, minerals, and color-ratio composite image colors*

Ratio	Detects	Color on image
5/7	Detects mineral groups including clays, micas, carbonates, sulfates (alunite, gypsum, jarosite). Many alteration minerals. Also detects vegetation. Shown as group 1 on plate 2.	Red
3/1	Detects iron oxides (hematite, goethite, jarosite); red rocks. Shown as group 2 on plate 2.	Green
5/7 + 3/1	Combination of minerals/vegetation from 5/7 ratio *and* iron oxides from 3/1 ratio. Shown as group 3 on plate 2.	Yellow
3/4	Not diagnostic of any mineral or mineral group by itself. Is low for vegetation.	Blue
3/1 + 3/4	3/4 ratio, in combination with 3/1 ratio, sometimes separates jarosite from other iron oxides. Shown as group 2 on plate 2.	Cyan

photographs, simulating the true color of surface materials as seen by the human eye (pl. 3). These images are an ideal introduction to Landsat color composite images for anyone inexperienced in working with satellite images. The SNC images are formed from contrast-stretched, edge-enhanced TM bands 1 (blue), 2 (green), and 3 (red), color-coded blue, green, and red, respectively. Each of the bands was contrast-stretched using a 2 percent linear stretch about the median, as well as an additional shadow stretch to raise the brightness levels of the lowest DN's to better display subtle details in shadowed areas.

COLOR–INFRARED COMPOSITE

Color-infrared composite images (CIR) are the most common Landsat color composite images (pl. 3). The CIR images are formed from TM bands 2 (green), 3 (red), and 4 (near-infrared) color coded blue, green, and red, respectively. Like the SNC images, each band of digital data was contrast stretched using a 2 percent stretch about the median DN value, shadow stretched, and edge enhanced. In addition, a procedure to increase the saturation of the colors on the composite images was applied (Kruse and Raines, 1984). This procedure involves the digital transformation of the three bands of TM data into three digital images representing the Munsell color coordinates hue, saturation, and value. A linear contrast stretch was applied to the saturation image to increase the overall color saturation levels, and the Munsell coordinate images were transformed back into red-green-blue space and color composited. The overall visual effect of color saturation enhancement is to produce a color composite image with the same color hues as the original image, but the colors appear brighter and more vibrant. By not altering the hues of the original image, physical properties of surface materials can be interpreted by their colors, but subtle color differences on the original image are greatly enhanced and more easily delineated.

COLOR–RATIO COMPOSITE

Color-ratio composite (CRC) (pl. 3) are designed to detect the presence of specific minerals or mineral groups and display this information as colors on the images. Table 7 shows the ratios used in this study, the minerals they detect, and the color assignments on the color-ratio composite images.

On the color-ratio composite images of the Altiplano and Cordillera Occidental, red colors indicate either vegetation or one or more of the minerals or mineral groups listed above. Because of this ambiguity, the masked color-ratio composite image (MCRC) which masks vegetation was prepared. Green colors identify areas where iron oxide-bearing rocks and soils are exposed. Where both alteration minerals and (or) vegetation and iron oxides are exposed, the image colors are yellow, orange, or white. Blue colors are not diagnostic of any specific materials and only serve to discriminate materials of compositions not detected by the 3/1 and 5/7 ratios.

Interpretation of color-ratio composite images must combine recognition of the important colors and the geometric patterns in which these colors occur. For example, many large areas of green on the color-ratio composite images of the Altiplano and Cordillera Occidental are clearly related to iron oxide-bearing sedimentary strata and the erosional products derived from these rocks and, consequently, are of little interest in terms of hydrothermal alteration. Smaller, isolated patches of green and yellow-green in the sedimentary terrain, however, are reasonable targets for more study.

MASKED COLOR–RATIO COMPOSITE

Masked color-ratio composite images (MCRC) are simply color-ratio composite images with vegetation, clouds, water, and shadows masked out by replacing the

appropriate pixels in the color-ratio composite image with pixels from TM band 4 (pl. 3). Masking is done for two reasons: (1) to differentiate vegetation from minerals having high absorption in TM band 7 relative to band 5 (table 7); and (2) to restore some of the topographic information that is lost or subdued by the ratioing process. The areas depicted in shades of gray on the masked color-ratio composite images are the masked areas; the colored areas on the color-ratio composite images represent unmasked color-ratio composite pixels dominated by rocks and soils and provide information about the composition of the rocks and soils (table 7).

INTERPRETATION OF POTENTIALLY HYDROTHERMALLY ALTERED ROCKS

Landsat TM data provide a means for detecting and mapping the regional distribution of minerals or mineral groups that are often associated with hydrothermally altered rocks and weathered material derived from these rocks. The design and preparation of color-ratio composite and masked color-ratio composite images to detect the broad spectral characteristics of these minerals and display them for visual interpretation (Knepper, 1988) was previously discussed; however, several aspects of the application of TM ratio images to the mapping of potentially hydrothermally altered rocks need to be emphasized.

The TM data can be used to detect the presence of minerals in two broad groups: (1) mainly hydroxyl-bearing minerals (clays, micas, sulfates) and carbonates, and (2) iron oxides (table 7). Many of the minerals in these two groups occur in hydrothermally altered rocks or form during the weathering of hydrothermally altered rocks. However, it is not possible to determine which mineral species within the mineral groups are present because the TM spectral bands are too broad to resolve the details of the spectral differences that can be measured in the laboratory. Consequently, mapped anomalies shown on plate 2 indicate only that one or more minerals in a mineral group are present, but not which of the minerals in that group.

Although many of the minerals in the two detectable mineral groups are often associated with hydrothermally altered rocks, most are not diagnostic of hydrothermally altered rocks; only alunite and jarosite may be diagnostic but they cannot be distinguished from the other minerals in their respective groups. Most of the same minerals in these two mineral groups are also found in rocks and sediments formed in common geologic settings unrelated to mineralization and mineral deposits. Consequently, recognizing the presence of these two mineral groups by their colors on the TM ratio images is only the first step in interpreting areas of possible hydrothermally altered rocks.

The pattern formed by one or both of the mineral groups on the images and the geologic setting in which they occur are integral parts of identifying potentially hydrothermally altered rocks that may be associated with mineral deposits. For example, iron oxide minerals are present in most of the sedimentary rocks and alluvial deposits, as well as some volcanic flow units, on the Altiplano; masking does not separate iron oxides associated with hydrothermally altered rocks from iron oxide that occurs as the natural consequence of weathering of iron-bearing minerals in unaltered rocks. To identify anomalies most likely associated with hydrothermally altered rocks, two additional factors were evaluated: (1) the degree to which the occurrence is localized and apparently not a general characteristic of a lithologic unit, and (2) the proximity of the occurrence to volcanic or igneous features as interpreted on the images. These criteria were subjectively evaluated for each possible color anomaly on the color-ratio composite images and those judged most likely to be associated with a hydrothermal system are shown on plate 2. No other attempt was made to prioritize or rank the mapped anomalies.

Interpretations were made on enlarged color prints (1:250,000) of the color-ratio and masked color-ratio composite images for each TM quad. Mapping was done on overlays of the 1:250,000-scale topographic quadrangle maps physically registered to each of the enlarged images. Three catagories of potentially hydrothermally altered rocks were identified and mapped (table 7): (1) group 1, occurrences of hydroxyl-bearing minerals and (or) carbonates, (2) group 2, iron oxides, and (3) group 3, minerals from both groups 1 and 2. The anomalous areas on each topographic base map were digitized and replotted at a scale of 1:500,000 and then manually compiled on the 1:500,000-scale base map (pl. 2). Snow on the high peaks along the western border of Bolivia in the Volcán Juriques and Nevados Payachata 1:250,000-scale quadrangles and cloud cover in the northern half of the La Paz 1:250,000-scale quadrangle obscured the surface and prevented evaluation of these areas.

Plate 2 shows the distribution of potentially hydrothermally altered rocks in the study area as interpreted from the reflectance characteristics of exposed materials expressed on digitally processed Landsat TM images. The mapped anomalies are not unique to any of the various mineral deposit types on the Altiplano and in the Cordillera Occidental and only depict occurrence of minerals in broad mineral groups, many of which are often associated with hydrothermally altered rocks. In addition, shadows and, locally, vegetation obscure some of the ground surface such that some areas of potentially hydrothermally altered rocks on plate 2 probably represent the minimal extent of these

rocks. It is important to understand that plate 2 does not show the location of minerals deposits, but is only a guide for future mineral-resource assessment and exploration investigations.

Most of the mapped anomalies occur in the southern and western parts of the Altiplano and Cordillera Occidental and are associated with Tertiary eruptive or subvolcanic rocks (pl. 2). The summit areas and flanks of many, but not all, of the Tertiary volcanoes display some kind of possible alteration; many of these anomalies are spatially related to areas of known mineralization and past mining (compare pl. 2 with the map of mines and prospects, pl. 6). Many other anomalies occur in close proximity to the Tertiary volcanoes. Elsewhere, small but distinct anomalies occur in volcanic and sedimentary rocks without clear associations with igneous centers. These anomalies, along with those with clear igneous associations that are not known to be mineralized, are primary targets for future investigations.

Gravity and Magnetic Studies

By John W. Cady *and* Richard A. Wise

Introduction **56**
Gravity map **56**
DMA gravity data **56**
Detailed YPFB gravity data **58**
Processing of gravity data **58**
Aeromagnetic map **58**
YPFB–Aero Service aeromagnetic data **58**
YPFB–Prakla aeromagnetic data **58**
GEOBOL–Swedish General Consulting AB aeromagnetic data **58**
Processing of aeromagnetic data **58**
Preliminary Interpretations of gravity and aeromagnetic maps **60**
YPFB interpretation **60**
Regional interpretation of gravity map **60**
Regional interpretation of magnetic map **61**
Magnetic regions **61**
Magnetic boundary B_I–B_0 **61**
Geophysical summary **62**

FIGURES

34. Map showing location of gravity stations **57**
35. Map showing approximate location of aeromagnetic surveys **59**

INTRODUCTION

Gravity and aeromagnetic data are primary sources of information for geologic mapping, mineral exploration, and mineral-resource assessment. Gravity data are used to distinguish hidden boundaries between lithologic units with differing densities, and to estimate the depth to bedrock in sediment-filled basins. Aeromagnetic data are used to distinguish hidden boundaries between lithologic units with differing magnetic susceptibilities, such as between volcanic and sedimentary rocks, or between fresh and hydrothermally altered rocks.

Extensive gravity and aeromagnetic data sets that cover parts of the Altiplano, Cordillera Occidental, and Cordillera Oriental, were digitally processed and merged to produce a simple Bouguer gravity anomaly map (pl. 4) and a residual total field aeromagnetic map (pl. 5). A provisional interpretation has delineated areas with similar gravimetric and magnetic properties that are useful in synthesizing the geology and in determining the boundaries of areas permissive for specific types of mineral deposits.

GRAVITY MAP

DMA GRAVITY DATA

The most extensive geophysical data set available for this study is that contained in the files of the U.S. Defense Mapping Agency (DMA) Gravity Library, 3200 South Second Street, St. Louis, MO, USA 63118–3399. Principal facts from about 4,000 gravity stations provided by DMA were used in compiling plate 4. Locations of stations are shown on figure 34.

The DMA data were compiled from many different sources. Information about most of the surveys is contained in the files of the DMA Gravity Library. We did not obtain the original publications, so we cannot report information concerning base stations, types of gravity meters used, or other technical details of the surveys.

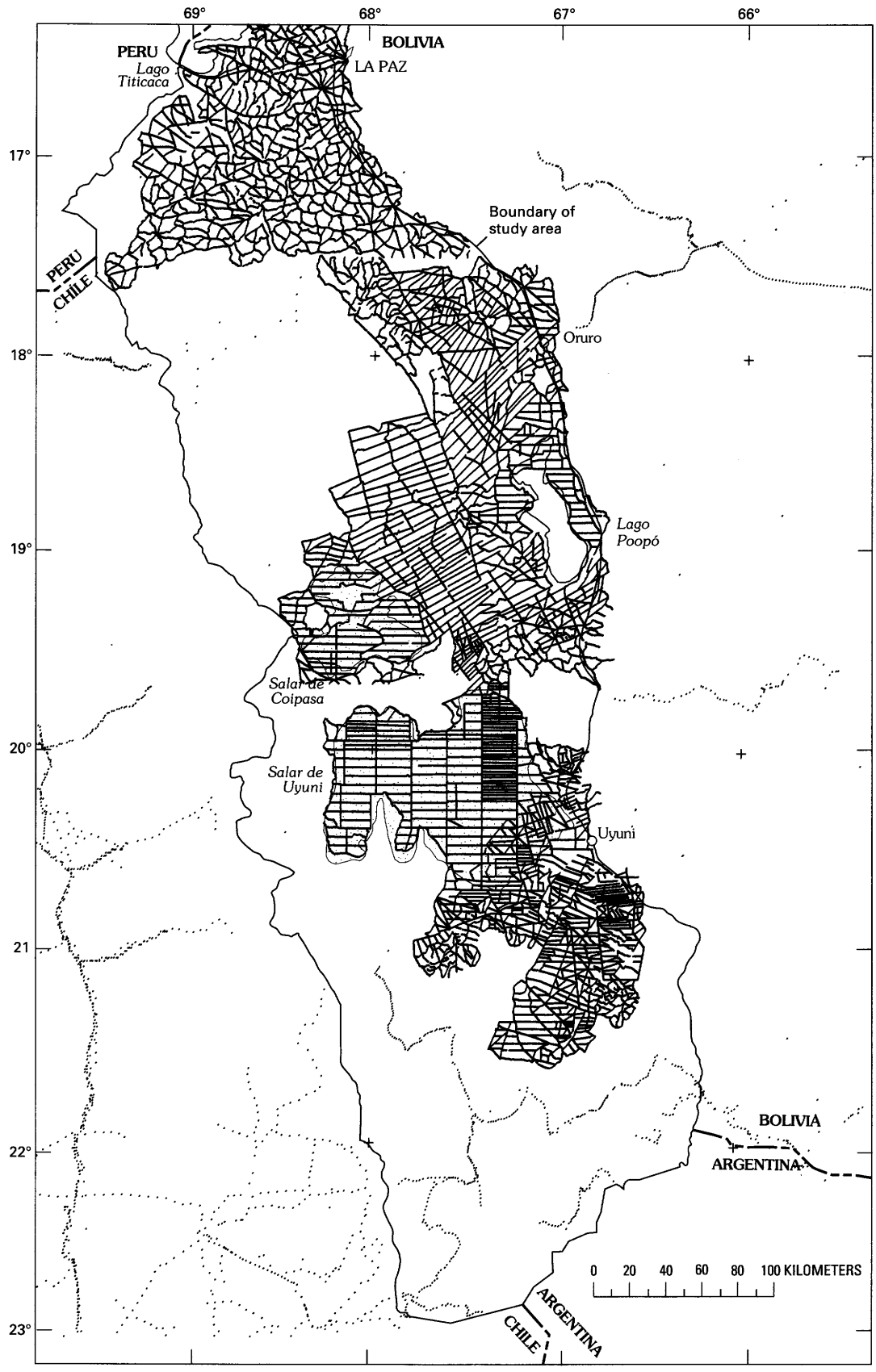


Figure 34. Location of gravity stations, Altiplano and Cordilleras Oriental and Occidental, Bolivia. Closely spaced profiles are from a survey by Yacimientos Petrolíferos Fiscales Bolivianos (YPFB). Widely spaced profiles are from multiple surveys archived in the U.S. Defense Mapping Agency (DMA) gravity library. DMA stations deleted in areas containing YPFB stations.

DMA stations are closely spaced (1–5 km) along widely separated roads (50–250 km apart, fig. 34). DMA stations from the central part of the study area were not used in favor of more detailed data described below.

DETAILED YPFB GRAVITY DATA

Through the kind cooperation of the exploration department of Yacimientos Petrolíferos Fiscales Bolivianos (YPFB), we obtained a detailed gravity survey of parts of the Altiplano (Yacimientos Petrolíferos Fiscales Bolivianos, Gerencia de Exploracion, Casilla 1659, Santa Cruz, Bolivia). Typically, stations are closely spaced (<1 km) along closely spaced lines (1–5 km, fig. 34); in places, lines are 5–20 km apart. We obtained only the digital data, not the original report, so we cannot provide information concerning base stations, type(s) of gravity meters used, or other technical details of the survey.

PROCESSING OF GRAVITY DATA

Station identification, latitude, longitude, elevation, and observed gravity were compiled for each gravity station using the principal facts provided by DMA and YPFB. Simple Bouguer anomalies were calculated using formulas published by the International Association of Geodesy (1967) and a Bouguer reduction of 2.67 g/cm^3. This density may be too high; YPFB used Bouguer reduction densities of 2.24 and 1.93 g/cm^3 when they studied the basins of the Altiplano. Stations with Bouguer anomalies much different from neighboring points were considered in error, and were eliminated from both data sets.

The YPFB data were referenced to the old Potsdam datum, which is 14.0 mGal higher than the new Potsdam datum (International Association of Geodesy, 1967) to which the DMA data were originally referenced. Therefore, 14.0 mGal was subtracted from the YPFB data to adjust them to the new Potsdam datum.

After the datum of the DMA data was adjusted to that of the YPFB data, discrepancies of as much as 20 mGal still existed in parts of the study area. Data from one major source of the DMA data set, containing 3,248 stations, includes many questionable stations that differ by as much as 20 mGal from the YPFB data set (Michael Dunnigan, DMA Gravity Library, oral commun., 1991). Therefore, all stations from source 3920 were eliminated before DMA data were merged with the YPFB data; because most of these stations are located in the area covered by the detailed YPFB data set, little additional information would be gained by correcting and adding them to the data set.

AEROMAGNETIC MAP

YPFB–AERO SERVICE AEROMAGNETIC DATA

An aeromagnetic survey was flown by Aero Service Corporation for YPFB in 1988 and 1989. Through the kind cooperation of their exploration department in Santa Cruz, we were provided with a tape of digital data for this survey as well as maps of the Prakla survey described below. The Aero Service Corporation survey was designed to determine basement depth and crustal structure for oil exploration in lower parts of the Altiplano. Flightlines were flown north-south with a spacing of 2 km and a barometric flight elevation of 5,200 m. Data were obtained on digital tape from Aero Service, Houston, Tex. The International Geomagnetic Reference field (IGRF) of the time of survey was removed from the data by the contractor. For location of the aeromagnetic surveys, see figure 35.

YPFB–PRAKLA AEROMAGNETIC DATA

An aeromagnetic survey was flown for YPFB by Prakla, Hannover, Germany, in 1967–68. The survey was designed to determine basement depth and basement structure for oil exploration in lower parts of the Altiplano. Flightlines were flown east-west with a spacing of 5 km in most areas; a few areas were flown with 2.5 or 2 km spacing. The Prakla survey was flown in segments with elevations of 4,900 m, 5,200 m, and 5,300 m barometric (fig. 35). Prakla did not remove the IGRF, but removed a planar regional surface from the data.

GEOBOL–SWEDISH GENERAL CONSULTING AB AEROMAGNETIC DATA

An aeromagnetic and electromagnetic survey was flown for the Servicio Geolíogico de Bolivia (GEOBOL) by Swedish General Consulting AB (SGCAB) in 1962 and 1963. The purpose of the survey was mineral exploration. Flightlines were flown east-west, spaced 1,000 m or 500 m, and draped 150 m above the ground. The contractor removed a regional magnetic field from the data using a filtering process, rather than the IGRF. The contoured data were digitized by Patterson, Grant, and Watson Limited of Toronto.

PROCESSING OF AEROMAGNETIC DATA

The SGCAB data, flown at only 150 m above a magnetic volcanic terrane, contain short-wavelength magnetic variations that are difficult to contour and interpret

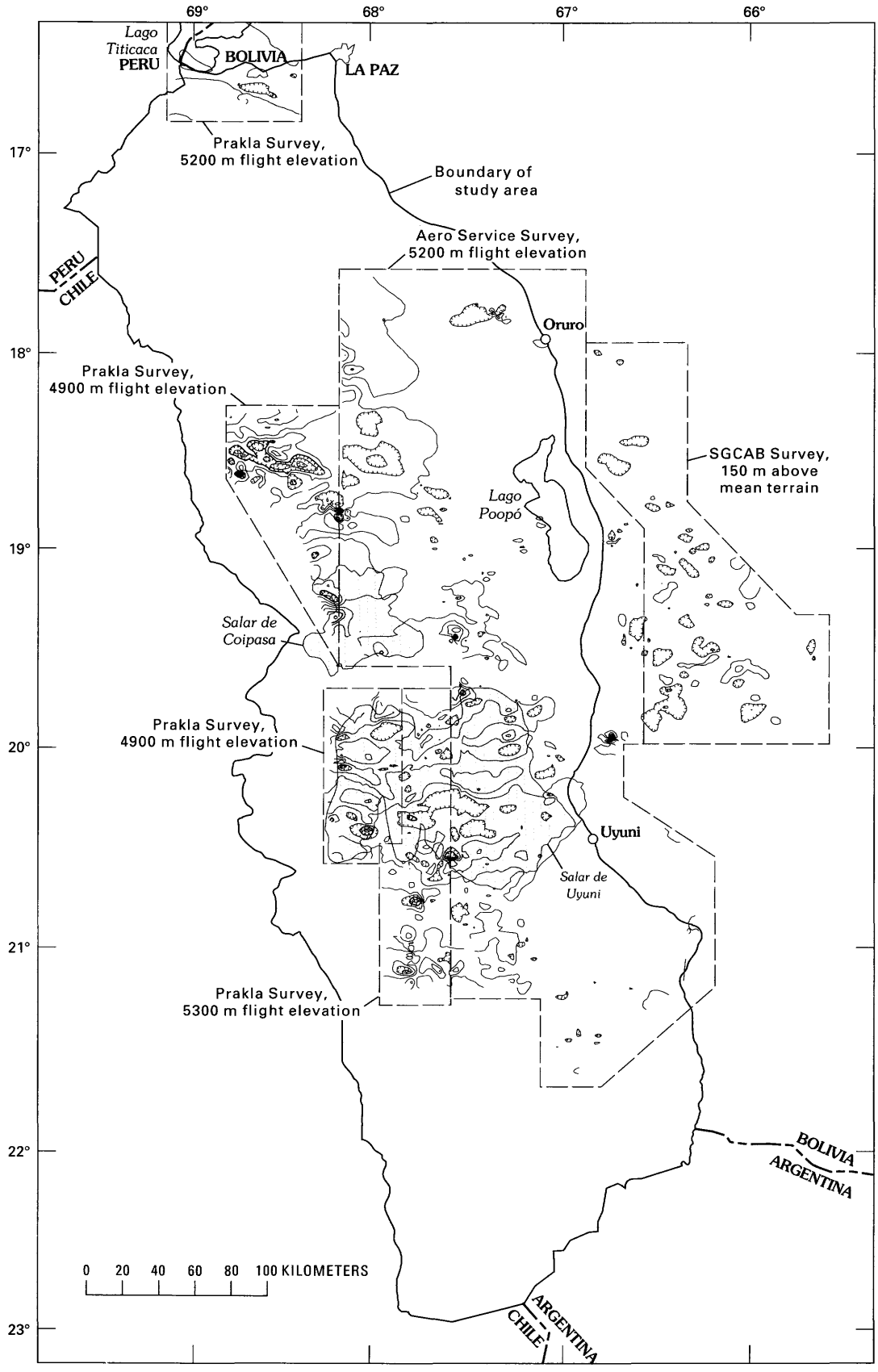


Figure 35. Map showing approximate location of aeromagnetic surveys, Altiplano and Cordillera Occidental, Bolivia. Magnetic contours are diagrammatic, with a contour interval of 10 nT.

at a scale of 1:500,000, therefore the SGCAB data were continued upward 1 km. The upward continuation is approximate, however, because the data were not obtained at constant elevation.

Comparison of the average values of each survey in their areas of overlap showed that datum adjustments were required in order to merge the surveys. The Aero Service survey was used as a reference because it was flown most recently and is contiguous with both of the other surveys. The Aero Service data represent the observed magnetic field (about 24,000 nT), minus the IGRF, plus 450 nT (added to avoid negative anomalies). The Prakla residual total field was adjusted upward 446 nT to make it match the level of the Aero Service survey. The upward-continued grid of the SGCAB aeromagnetic data was adjusted downward 636 nT. The completed contour map (pl. 5) is entitled a residual total magnetic field map; it represents the scalar value of the total magnetic field less a regional field (IGRF or filtered surface) plus or minus a constant. The gridded data sets from the three surveys were merged without interpolation, at the outer boundary of the Aero Service survey. Jagged contours mark the imperfectly leveled boundary between the various surveys.

The gravity and magnetic maps are interim products. The publication deadline of this report precluded final acquisition and processing of aeromagnetic data (especially reduction to the pole) and final processing of gravity data (especially calculation of terrain corrections and isostatic anomalies).

PRELIMINARY INTERPRETATIONS OF GRAVITY AND AEROMAGNETIC MAPS

YPFB INTERPRETATION

A preliminary interpretation of YPFB gravity and aeromagnetic data (the latter reduced to the pole), geologic, seismic-reflection, and well data are presented in an abstract by Aranibar and Martinez (1990). Their interpretation is based upon data not evaluated during the course of this project and thus may be the most authoritative interpretation of geophysical data to date. Figure 4 illustrates their ideas, and selected faults from their interpretation are included in the interpretive overprint on plates 4 and 5.

In the section discussing the Geologic setting, the structural interpretation of the Altiplano by Arinabar and Martinez (1990) is contrasted with interpretations by Baby and others (1990) and Sempéré, Hérail, Oller, Baby, and others (1990). The two interpretations differ as to the existence and location of many faults, and the type of fault, strike-slip or thrust. Without studying the seismic sections and reduced-to-the-pole aeromagnetic data used by Arinabar and Martinez (1990), we cannot resolve the discrepancies between interpretations. However, the following observations of regional scope can be made on the gravity and magnetic maps.

REGIONAL INTERPRETATION OF GRAVITY MAP

The DMA data adequately define the regional simple Bouguer gravity anomaly (pl. 4). There is a complex central gravity low (–320 to –460 mGal) over the Cordillera Occidental, Altiplano, and Cordillera Oriental. The Bouguer anomaly increases with decreasing elevation on the west slope of the Cordillera Occidental and the east slope of the Cordillera Oriental.

The Bouguer anomaly low over the Altiplano and adjacent cordilleras reaches a minimum value of –460 mGal at the Bolivia-Argentina border, where 6,000 m peaks occur. On the northern Altiplano, a local gravity minimum of –460 mGal occurs in the vicinity of peaks with elevations as high as 7,000 m near lat 69° N., long 18° W.

Within the complex central gravity low, the YPFB data show that gravity highs and lows with wavelengths of 25–50 km and peak to trough amplitudes of 20–40 mGal parallel the strike of Paleozoic through Tertiary strata. Anomaly trends are continuous from areas of exposed bedrock into areas of Quaternary cover, suggesting that basement beneath the great salars Uyuni and Coipasa is gravimetrically similar to the exposed bedrock to the north and east.

From the available gravity data we conclude that the Bolivian portion of the map area (pl. 4) can be divided into three regions characterized by differing gravity anomaly texture:

(1) Southwest of line A_1–A_0, in the area containing the Salars de Uyuni and Coipasa (the great salars) and identified as the Uyuni domain on fig. 4, gravity highs and lows trend N. 15° E. to N. 30° E. (northnortheast). Gravity anomalies in the great salars have peak to trough amplitudes of 20–40 mGal. Southeast of the great salars anomaly amplitudes drop to 10–20 mGal. Exposed Paleozoic through Tertiary strata strike parallel to the gravity anomalies, and we infer that the gravity anomalies are caused by folded and faulted Paleozoic through Tertiary strata. Gravity station coverage in the Cordillera Occidental is very sparse, and we cannot infer structures related to the Quaternary volcanic field or determine whether there is gravimetric evidence for connecting the San Andres to the Tambillo fault of Aranibar and Martinez (1990).

(2) Northeast of line A_1–A_0, in the area identified as the Ulloma domain on fig. 4, gravity highs and lows trend N. 10° W. to N. 40° W. (northnorthwest), parallel to the exposed Tertiary sedimentary and volcanic section. Following Aranibar and Martinez (1990), we infer that the

high amplitude gravity anomalies (30–50 mGal) are caused by structures involving thick Tertiary clastic deposits and possibly crystalline basement.

(3) Northeast of the Coniri and Chuquichambi faults and southeast of the Khenayani fault, gravity anomalies are subdued and irregular, trending roughly parallel to geologic strike. The subdued anomalies probably reflect thin-skinned thrusting cited by Aranibar and Martinez (1990).

REGIONAL INTERPRETATION OF MAGNETIC MAP

Magnetic Regions

The magnetic map has two regions of high magnetic relief (amplitude 450 nT peak to trough) and one region of low magnetic relief (amplitude 25–75 nT in most places):

(1) A region marked by high magnetic relief and both long- and short-wavelength magnetic anomalies is the Cordillera Occidental and that part of the Altiplano containing the great salars Uyuni and Coipasa. Much of the high magnetic relief (peak to peak amplitude 450 nT) occurs over the great salars and Quaternary volcanoes. The sharpest magnetic highs commonly occur over volcanoes. Magnetic ridges can be traced from volcanoes over the salars, indicating that volcanic rocks and possibly volcanic feeder systems are present at depth. Many volcanoes cause magnetic highs, but some cause magnetic lows. Some of the observed patterns may be caused by rocks with reverse remanent magnetization.

Within this region there are alternating magnetic highs and lows with wavelengths of 15–35 km and peak to trough amplitudes of 100–200 nT. Most of these magnetic anomalies trend east-west, contrary to the trend of gravity anomalies in the same region. One reason for the strong east-west alignment is the low magnetic latitude of about 10° S. Examination of proprietary YPFB aeromagnetic data which had been reduced to the pole showed attenuation of east-west trending anomalies and emergence of other anomaly trends. Detailed interpretation of the complex magnetic fields of this region could be improved by reduction to the pole.

(2) The area of low magnetic relief is most of the Altiplano exclusive of the great salars. The low magnetic relief is probably caused by Tertiary and Quaternary sedimentary rocks. Patches of small magnetic anomalies probably indicate Tertiary hypabyssal rocks or small volcanic centers.

(3) In the Cordillera Oriental, high magnetic relief is caused by Tertiary igneous rocks that include the Las Frailes volcanic field. The boundary of the area of high magnetic relief is irregular and probably reflects the irregular boundary of volcanic rocks exposed at the surface. The boundary is not shown on plate 4 because it is very complicated and outside the study area.

Magnetic Boundary B_1–B_0

There are lingering questions about the interpretation of the magnetic data. For example, where is the boundary between the region of high magnetic relief over the great salars and Cordillera Occidental and the region of low magnetic relief over the rest of the Altiplano? Does it coincide with the gravimetrically determined boundary A_1–A_0? Is the boundary a straight line, or curved?

Line B_1–B_0 was arbitrarily drawn almost straight, as if it represented a strike-slip fault. It marks the northeastern limit of mixed long-and-short-wavelength magnetic anomalies caused by Tertiary volcanic rocks (pl. 1, Tvnd). Short wavelength magnetic anomalies northeast of B_1–B_0 are caused by isolated volcanic cones and hypabyssal intrusive rocks and to volcanic rocks of the Cordillera Oriental. The southeastern end of B_1–B_0 coincides approximately with point A_0 at the southeastern end of gravimetrically determined line A_1–A_0. However, to the northwest, line B_1–B_0 clearly diverges from the gravity line. Line A_1–A_0 cuts across large regions of high magnetic relief. Hence there is no single northwest-trending geophysical boundary.

The magnetic relief is highly variable within the high-amplitude magnetic terrane. Some areas are relatively free of short-wavelength magnetic anomalies, suggesting that magnetic rocks are deep. In most places, however, there are both short- and long-wavelength magnetic anomalies, indicating that magnetic rocks extend from near the surface to great depth.

In the area southwest of line B_1–B_0 there are two areas of highest magnetic relief, one roughly coincident with the Salar de Uyuni and one roughly coincident with the Salar de Coipasa. Between the areas of highest magnetic relief are areas of lower relief and a relative absence of long-wavelength magnetic anomalies. An alternate, serrated boundary of the area of highest magnetic relief can be composed of many short straight and curved segments. Line B_1–B_2–B_3–B_4–B_5–B_6–B_7 (with alternate ending B_6–B_8) marks the northeastern boundary of volcano-plutonic complexes containing abundant magnetic rocks that extend from the surface to great depth.

Put more simply, the basement of the great salars is magnetically similar to, and possibly more magnetic than, the Quaternary volcanic rocks exposed outside the salars. The curving boundaries separating areas of different magnetic relief may delineate centers of igneous activity coincident with the salars.

These centers of igneous activity are 100 km or more in diameter, bigger than known calderas; however, volcanic rocks are not known to have been ejected from the great salars. Batholithic plutons are commonly 100 km in

diameter, but the magnetic field over the great salars is much more complicated than that usually found over batholiths. It is possible that the great salars coincide with plutons at depth and that swarms of feeder dikes above each pluton are the sources for the complicated magnetic anomalies.

GEOPHYSICAL SUMMARY

Gravimetrically, the area of the Altiplano underlying the great salars is distinguished by northnortheast-trending gravity anomalies. To the northeast, the remainder of the Altiplano is a terrane containing northnorthwest-trending gravity anomalies.

Magnetically, the great salars and Cordillera Occidental are distinguished by high magnetic relief caused by known and inferred Quaternary and Tertiary volcanic rocks. Hypabyssal feeder rocks at depth beneath both the volcanoes and the salars may be related to the magnetic anomalies. To the northeast, the remainder of the Altiplano is free of long-wavelength magnetic anomalies.

There are two possible explanations for the contrasting trends in the gravity and magnetic data for the great salars and Cordillera Occidental: (1) The east-west magnetic anomalies in the salars are due to the low magnetic latitude (most likely); and (2) the gravity map reflects Tertiary or older structural trends, whereas the magnetic map reflects crosscutting Quaternary volcanism. The magnetic data should be reduced to the pole to help resolve this question.

The division of the Altiplano derived from gravity interpretation is different from the division derived from magnetic interpretation: (1) Line A_1–A_0, derived from interpretation of gravity data, separates structurally discordant terranes of Paleozoic through Tertiary strata. (2) Line B_1–B_0, derived from interpretation of magnetic data, separates magnetic rocks, mainly Quaternary volcanics, from nonmagnetic rocks. Line B_1–B_0 could be replaced or supplemented by a curving boundary suggestive of the outlines of centers of igneous activity. (3) Lines A_1–A_0 and B_1–B_0 converge with the extension of the Tambillo fault of Aranibar and Martinez (1990) near Uyuni. Both lines may be part of a system of northwest-trending faults that separates a domain of northnortheast-trending structures and magnetic volcanic rocks (Uyuni domain) from a domain of northnorthwest-trending structures which is largely free of magnetic volcanic rocks (Ulloma domain).

Our interpretation of the geophysical data suggests that the Coipasa strip (Sempéré, Hérail, Oller, Baby, and others, 1990) shown on figure 4, does not exist. The Coipasa strip serves a similar function as our gravity line A_1–A_0; it separates the Ulloma domain, characterized by northnorthwest-trending folds, from the Uyuni domain, characterized by a northnortheast-trending fold and thrust belt. The gravity data provide evidence not seen in the mapped geology that the southern Salar de Coipasa is underlain by a northnortheast-trending structure marked by gravity anomaly Q, and hence belongs to the Uyuni domain.

The Coipasa strip is defined by Sempéré, Hérail, Oller, Baby, and others (1990) as the northern boundary of the northnortheast-trending Uyuni domain, a boundary that must lie north of anomaly Q. Instead, the Coipasa strip contains anomaly Q. We believe that a better choice for the northern boundary of the Uyuni domain is line A_1–A_0, which separates northnorthwest-trending gravity anomalies from northnortheast-trending gravity anomalies.

There is no evidence to support the existence of the Coipasa strip in the magnetic data. The Coipasa strip cuts across a regional boundary between magnetic and nonmagnetic rocks (line B_1–B_0 on pl. 5) without offsetting the boundary. In contrast, there is some support in the magnetic data for line A_1–A_0. Near its northwest end, line A_1–A_0 separates a zone of high amplitude magnetic anomalies to the southwest from lower amplitude magnetic anomalies to the northeast. In contrast to the Coipasa strip, line A_1–A_0 does not cross line B_1–B_0. At its east end, the Coipasa strip shown on figure 4 cuts across continuously mapped Tertiary sedimentary units shown on plate 2. The geological and geophysical evidence are in agreement; the Coipasa strip does not exist as a strike-slip fault system, because it offsets neither geology nor gravity or magnetic anomalies.

Mineral Deposit Models

By Steve Ludington, G.J. Orris, Dennis P. Cox, Keith R. Long, *and* Sigrid Asher-Bolinder

Introduction **64**
Metallic mineral deposits unrelated to igneous activity **64**
- Sediment-hosted copper deposits **64**
- Basaltic copper deposits **66**
- Sandstone uranium deposits **66**
- Sediment-hosted gold deposits **66**
- Syntectonic antimony and related deposits **67**
- Gold placer deposits **67**

Metallic mineral deposits related to igneous activity **69**
- Bolivian polymetallic veins **69**
- Polymetallic replacement deposits **75**
- Distal disseminated silver deposits **75**
- Porphyry and epithermal deposits **75**
  - Porphyry copper deposits **75**
  - Porphyry gold deposits **75**
  - Quartz-alunite veins **79**
  - Quartz-adularia veins **79**
  - Hot-spring gold and hot-spring mercury deposits **80**
  - Epithermal manganese deposits **80**
  - Interrelationships **80**
- Volcanogenic uranium and rhyolite-hosted tin deposits **80**

Nonmetallic and industrial mineral deposits **80**
- Deposits associated with saline and alkaline lakes and salars **81**
  - Brines **81**
  - Salts **86**
  - Borates **86**
  - Hectorite **87**
  - Sedimentary zeolites **87**
  - Lacustrine diatomite **87**
- Barite veins **88**
- Dimension stone **88**
- Fumarolic sulfur **88**

FIGURES

36. Map showing the extent of Tertiary and Cretaceous sedimentary rocks that host sediment-hosted copper deposits **65**
37. Map showing distribution of some syntectonic antimony deposits **68**
38. Histogram showing phosphorus content of volcanic and intrusive rocks **71**
39. Map showing distribution of Tertiary Bolivian polymetallic vein deposits **74**
40. Metallogeny of Bolivian polymetallic vein deposits **76**
41. Map showing absolute ages of Bolivian polymetallic vein deposits **78**
42. Map showing location of salars and alkaline or saline lakes **85**
43. Photograph showing solfataric alteration at Mina Juanita **89**

TABLES

8. Location, metallogeny, and age of Tertiary polymetallic vein deposits **70**
9. Maximum fluid inclusion homogenization temperatures and salinities of selected Bolivian polymetallic vein deposits **73**
10. List of selected named Bolivian salars and lakes **82**

INTRODUCTION

Descriptive mineral deposit models are tools that are used in both mineral exploration and mineral-resource assessment. They consist essentially of lists of characteristics that can be used both to classify the mineral deposits and occurrences they represent, and to predict geologic environments where undiscovered deposits may exist.

In this section, we present models that represent the spectrum of mineral deposits that we either have identified in the study area, or have reason to believe may be present there. Some of the models are identical to previously documented deposit types, for example, quartz-alunite gold deposits (Berger, 1986b). Others, such as Bolivian polymetallic vein deposits and syntectonic antimony deposits, have been defined as a result of this study. Each discussion includes a description of the geologic environment that is permissive for the occurrence of these mineral deposits. In the last sections of this bulletin, we define the areas, or permissive domains, in which deposits of the various types may be present on the Altiplano and in the Cordillera Occidental, and make subjective estimates of the undiscovered resources contained in the domains.

METALLIC MINERAL DEPOSITS UNRELATED TO IGNEOUS ACTIVITY

In this discussion, metallic mineral deposits are defined as those for which the metal resource is extracted from the constituent minerals of the deposit by smelting or another extractive process. This contrasts with nonmetallic mineral deposits, in which the constituent minerals of the deposits are the valuable resource, and can be concentrated by physical separation, or other similar procedures.

We begin by describing a group of deposit types whose genesis bears no apparent or direct relation to igneous activity. The geologic environments for these types of deposits can often be specified with a great degree of precision, because, although not necessarily strictly syngenetic, they formed as the result of geologic processes occurring throughout broad regions of the Earth's crust, processes that often leave many other clues in the rocks. Thus, on a regional basis, it is relatively easy to define permissive environments for this class of deposits.

SEDIMENT–HOSTED COPPER DEPOSITS

Sediment-hosted copper deposits are statabound concentrations of copper sulfide minerals or native copper in sedimentary rocks (Cox, 1986e). Typical ore minerals are chalcocite, bornite, and other sulfur- and iron-poor copper sulfides. These deposits are commonly associated with continental redbeds but the deposits themselves are localized in reduced (green, gray, or white colored) parts of the redbed sequence or in laminated carbon-rich shales or algal carbonate rocks that overlie the redbeds. Sedimentary rocks hosting these deposits commonly form in association with evaporites in epicontinental rift basins within 30° of the paleoequator (Kirkham, 1989).

The formation of a sediment-hosted copper deposit requires six factors: 1, a source of copper (detrital rock grains in the redbeds); 2, a brine to dissolve copper and form a stable copper chloride complex (may be derived from evaporites); 3, an oxidizing environment (ferric iron in the redbeds or subaerial basalt) to maintain stability of the copper chloride complex; 4, permeable rocks through which the copper-rich brine can move to a site of deposition; 5, a source of energy to cause fluids to flow (basin compaction or diapir intrusion); and 6, a reductant to cause deposition of native copper and, where the ore mineral is chalcocite, a source of sulfur. The reductant can be in the form of fossil plant or algal remains, liquid petroleum, or natural gas.

The major sediment-hosted copper districts of the world, including Zaire and Zambia, Germany and Poland, and Michigan exhibit similar characteristics. Fine-grained, laminated, carbonaceous sedimentary strata formed by shallow-marine transgression and tidal-facies deposition overlie the redbeds. The laminated rocks act as an efficient trap for copper sulfides and their great lateral extent permits the formation of very large stratabound deposits. The black Nonesuch Shale overlying the red Calumet Conglomerate in the White Pine deposit, Mich., is an example of this scenario.

Redbed environments are widely distributed in Tertiary sedimentary rocks of the Altiplano and Cordillera Occidental (fig. 36), but the absence of a marine transgressive sequence effectively rules out the possibility of world-class deposits. Deposit tonnages on the Altiplano are, in most cases, limited by the small size of the reductant traps available. Traps that control mineralization on the Altiplano are accumulations of leaf-trash in fluvial channels, or possibly, pockets of oil or gas in the pore space of sandstone hosts. The largest deposits that occur on the

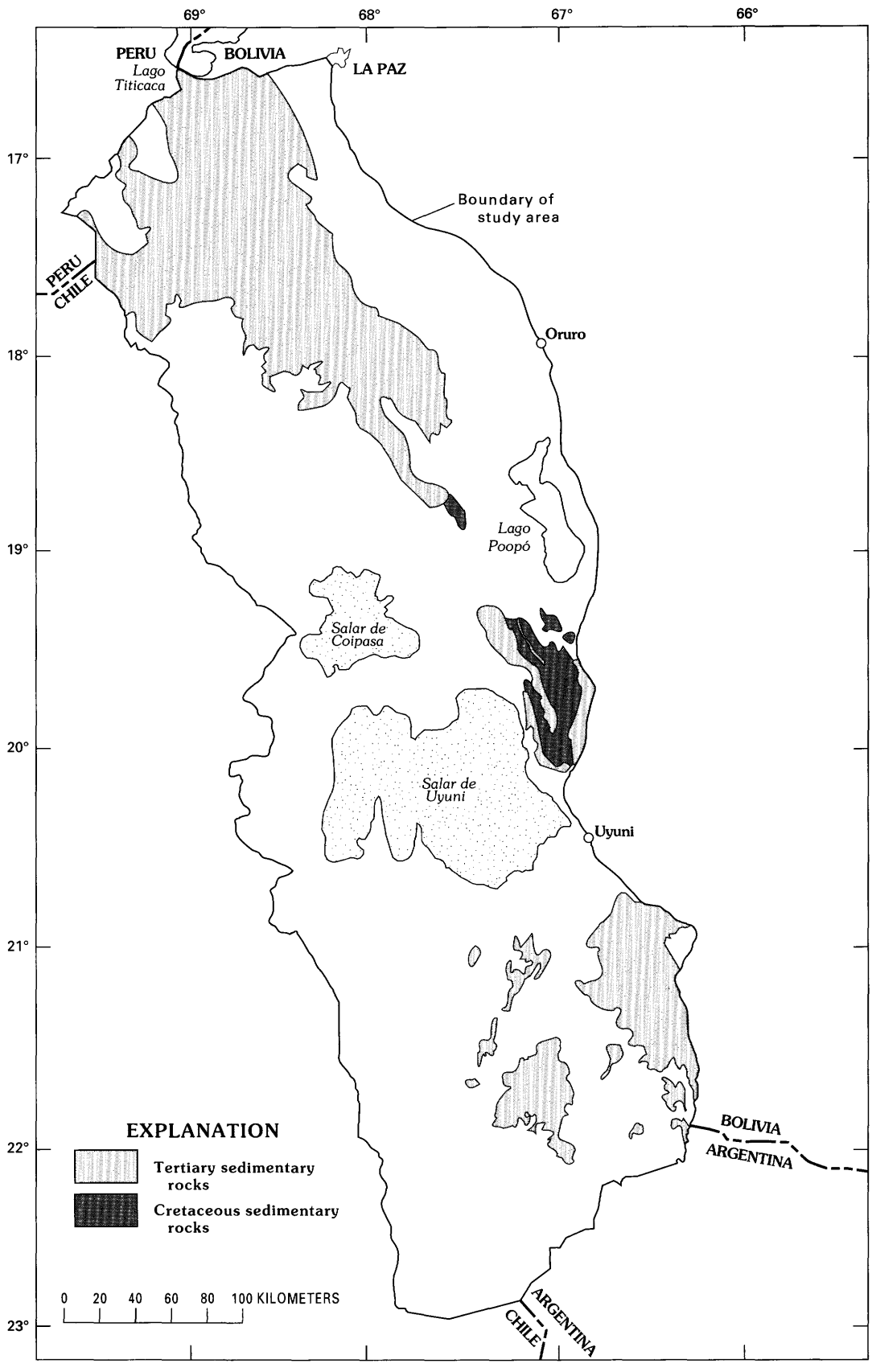


Figure 36. Map showing the extent of Tertiary and Cretaceous sedimentary rocks that contain sediment-hosted copper deposits, Altiplano and Cordillera Occidental, Bolivia.

Altiplano result from special geologic conditions, mainly related to factor 5, that cause large volumes of brine and reductant to be focused into a depositional site; such conditions include elevated temperature and fluid flow related to gypsum diapirs (Corocoro, Chacarilla). Basalt interbedded with the redbeds (Azurita) may be related to factor 1, providing an especially rich source of copper for the circulating brine. A contact between redbeds and overlying tuff appears to have controlled deposition of sulfides at Avaroa and other deposits in Sud Lípez.

BASALTIC COPPER DEPOSITS

Basaltic copper deposits (Cox, 1986d) are genetically related to sediment-hosted copper and can be expected in the same geologic environment. The deposits consist of native copper and copper sulfides contained in veins, amygdales, and in the matrix of breccias in basaltic volcanic rocks. Subaerial basalt, because it degasses upon extrusion, is commonly devoid of reduced sulfur. Copper-rich brine can therefore migrate through fractures and interflow breccias in basalt flows in the same manner as through redbeds. The basalt also is a source of copper because of its intrinsic high copper content. Basaltic copper deposits form where brines are diluted or where they encounter reducing fluids in cavities in basalt or in pore spaces in overlying sedimentary rocks. The Azurita deposit in the Turco area is the most important example in the study area. Additional examples, such as the Tambillo deposit, are known to exist in the Sevaruyo area, and areas of subaerial basalt interlayered with Tertiary sedimentary rocks occur northwest and south of Lake Poopó (fig. 36).

SANDSTONE URANIUM DEPOSITS

Sandstone uranium deposits (Turner-Peterson and Hodges, 1986) form in oxidized sedimentary rocks where fluids derived from humic acids transport uranium in solution. The uranium source is thought to be granitic rocks in the basement or detrital grains of rhyolitic ash in the sediments. Chemical analysis of samples collected during this study of the sediment-hosted copper deposits showed uranium contents of 1–15 ppm (app. B). Lack of a source of uranium in the sedimentary or basement rocks probably accounts for the paucity of deposits. Although one uranium prospect is reported (Murillo and others, 1969) in the Pululos area in Sud Lípez, we were unable to confirm this.

SEDIMENT–HOSTED GOLD DEPOSITS

The geologic characteristics of sediment-hosted gold deposits have been described by many authors (Radtke, 1985; Bonham, 1989; Berger and Bagby, 1991). Although deposits of this type, also known as Carlin-type deposits, have been mined for nearly 50 years, most of the known deposits were discovered within the last 25 years. Worldwide, the total endowment of gold is very high in these deposits; for example, in Nevada, this endowment almost certainly exceeds 2,500 tonnes of gold (Ludington and others, 1991).

These deposits are typically formed in carbonaceous, silty, carbonate rocks, and associated jasperoids. The ore minerals are disseminations of very fine grained pyrite and carbonaceous material, that may be accompanied by marcasite, arsenopyrite, realgar, orpiment, and stibnite. Gold is present as micron-sized particles. Sedimentary host rocks may include silty dolomite, limestone, siltstone, sandstone, conglomerate, and argillite. Base metals usually are found in very low concentrations. Although the shapes of orebodies are often highly irregular, faults are an important factor in channelizing fluids and localizing ore. Hydrothermal alteration consists of decalcification, silicification, and argillization, along with development of a stockwork of thin quartz veinlets, particularly in strongly silicified rocks and jasperoids.

Explanations about the genesis of Carlin-type deposits are sharply divergent. The relatively low temperatures (<250 °C) and the low intensity of hydrothermal alteration in these deposits makes traditional interpretation of field relations very difficult, and much remains to be learned about them. In detail, the distribution of mineralization is very distinctive; discrete, high-grade veins are virtually unknown in these deposits, and throughgoing, open vertical fracture systems that may reached the surface may not have been present during their formation. The hydrothermal fluids responsible for gold deposition are high in dissolved carbon dioxide and low in chloride, and are believed to have a deep-seated, connate, or highly exchanged meteoric source. In North America, most of the deposits are found in regions where Paleozoic or Mesozoic overthrusting caused rapid burial of sedimentary rocks, perhaps providing for the preservation and transport of associated formational and ground waters to depth (Berger and Henley, 1989). The relationship of these deposits to granitoid plutons is also a matter of debate. One group (Sillitoe and Bonham, 1990; Berger and Bagby, 1991) feels that they are vitally important, and that sediment-hosted gold deposits are genetically related to skarn deposits. Others (Hofstra and others, 1991) see sediment-hosted gold deposits forming in response to thermal gradients unrelated to plutonism.

On the Altiplano, the Paleozoic sedimentary rocks that form the basement to the Tertiary basins and volcanic fields could contain sediment-hosted gold deposits. There are no confirmed examples of this deposit type in all of South America, although some deposits bear strong resemblance, such as Silica del Hueso, Chile (Camus, 1990), and Purísima Concepción, Peru, which is probably a

distal disseminated silver deposit (see description that follows) (Alvarez and Noble, 1988). Nevertheless, the overthrusting and thickening that occurred, both during the Miocene development of the main Andean Orogen, and during pre-Mesozoic deformation of the Paleozoic sedimentary rocks, provides a likely environment for these deposits in parts of the Altiplano. Any deposits formed in the Miocene or later are probably still deeply buried, but they could be exposed in uplifted Paleozoic outcrops.

SYNTECTONIC ANTIMONY AND RELATED DEPOSITS

A group of more than 500 antimony and antimony-gold deposits are found along the entire length of the Cordillera Oriental in Bolivia. In this study, we refer to these deposits, described by Lehrberger (1988), as syntectonic antimony deposits. Figure 37 shows the approximate location of the more important of these deposits. Bolivia produces about 10,000 tonnes per year of antimony, primarily from these deposits, and has been the world's leading antimony producer since 1976.

These deposits consist of quartz-carbonate (often dolomite) veins that fill pressure shadows at the crests of folds in Ordovician and Silurian sedimentary rocks. The gangue minerals are accompanied by stibnite, pyrite, arsenopyrite, and minor jamesonite, sphalerite, chalcopyrite, galena, berthierite ($FeSb_2S_4$) and locally, native gold. Vein quartz is characterized by fluid inclusions that contain both water and carbon dioxide. Thus, the deposits appear to be similar to those in the Murchison Range in northeastern South Africa described by Pearton and Viljoen (1986), and to deposits in the Canadian cordillera described by Madu and others (1990). Lehrberger (1988) classed at least 14 of the deposits he studied as gold-antimony deposits, including several in the southern Cordillera Oriental, immediately adjacent to the Altiplano. We have no information whether the antimony deposits in Bolivia that do not produce gold have been tested for the presence of gold.

Low-sulfide gold-quartz vein deposits (Berger, 1986c) are found in a similar environment in other parts of the world. These deposits consist of quartz veins with gold, minor amounts of sulfide and telluride minerals, and, rarely, scheelite. Quartz-carbonate alteration around the veins is a distinctive feature of these deposits, as well as ore-forming fluids rich in carbon dioxide and low in chloride, as shown by studies of fluid inclusions. Most examples of this deposit type have formed in higher grade metamorphic terranes than the Paleozoic sedimentary rocks of the Altiplano, however, some of the gold-bearing quartz veins described by Ahlfeld and Schneider-Scherbina (1964) are pre-Mesozoic, and may be low-sulfide gold-quartz veins. Riera (1989) describes veins in the Cordillera Oriental that probably correspond to this deposit type. One deposit on the Altiplano, Iroco (app. A), may be a low-sulfide gold-quartz vein. Two pre-Tertiary gold deposits (San Jorge and San Bernardino) are being developed in the Cordillera Oriental (Matthews, 1991). In addition, Tistl and Schneider (1986) describe some apparently stratiform gold-tungsten deposits from the northern Cordillera Oriental, just northeast of the Altiplano, that they postulate are related to metamorphic processes.

Deposits of these types are not known to exist in the Paleozoic rock outcrops on the Altiplano, but the abundance of the syntectonic antimony deposits immediately to the east, and the wide geographic distribution of both antimony and gold-quartz veins suggests that they could have formed in Paleozoic rocks that underlie the Altiplano.

GOLD PLACER DEPOSITS

Gold placer deposits consist of grains or nuggets of native gold in alluvial, eolian, eluvial, and (or) glacial sediments and their consolidated equivalents. A concise description of the deposit type is given by Yeend (1986). The material composing the placers may have its sources locally, or as distant as tens of kilometers. The concentration of heavy minerals that forms the deposit is the result of mechanical and chemical processes over time (Boyle, 1979). The deposits are commonly Cenozoic in age, and are often derived from erosion of gold-bearing deposits, such as epithermal, sediment-hosted, or low-sulfide gold-quartz deposits, porphyry copper deposits, copper skarns, polymetallic vein and replacement deposits, and older placer deposits. In some areas where no sources are known, the gold has been theorized to have been eroded and concentrated from black shales or tuffaceous rocks with very low disseminated gold contents.

Most placer gold is actually electrum, and contains some silver, as well as base metals. The content of these impurities commonly decreases with increasing distance from the source. Placer deposits may also contain varying amounts of platinum-group metals, and other heavy minerals, such as pyrite, garnet, or rutile.

Few placer deposits are known in the study area. Whether this is due to the fact that they have not been extensively searched for, or because of the low precipitation and erosion rates is not known, but coarse, conglomeratic Quaternary deposits are also uncommon. Placer deposits in Sud Lípez were observed to be composed of silt, sand, and gravel that contains as much as 5 percent by volume of angular, white to translucent quartz. Some of this quartz contains iron oxide pseudomorphs of pyrite, but no visible gold was seen.

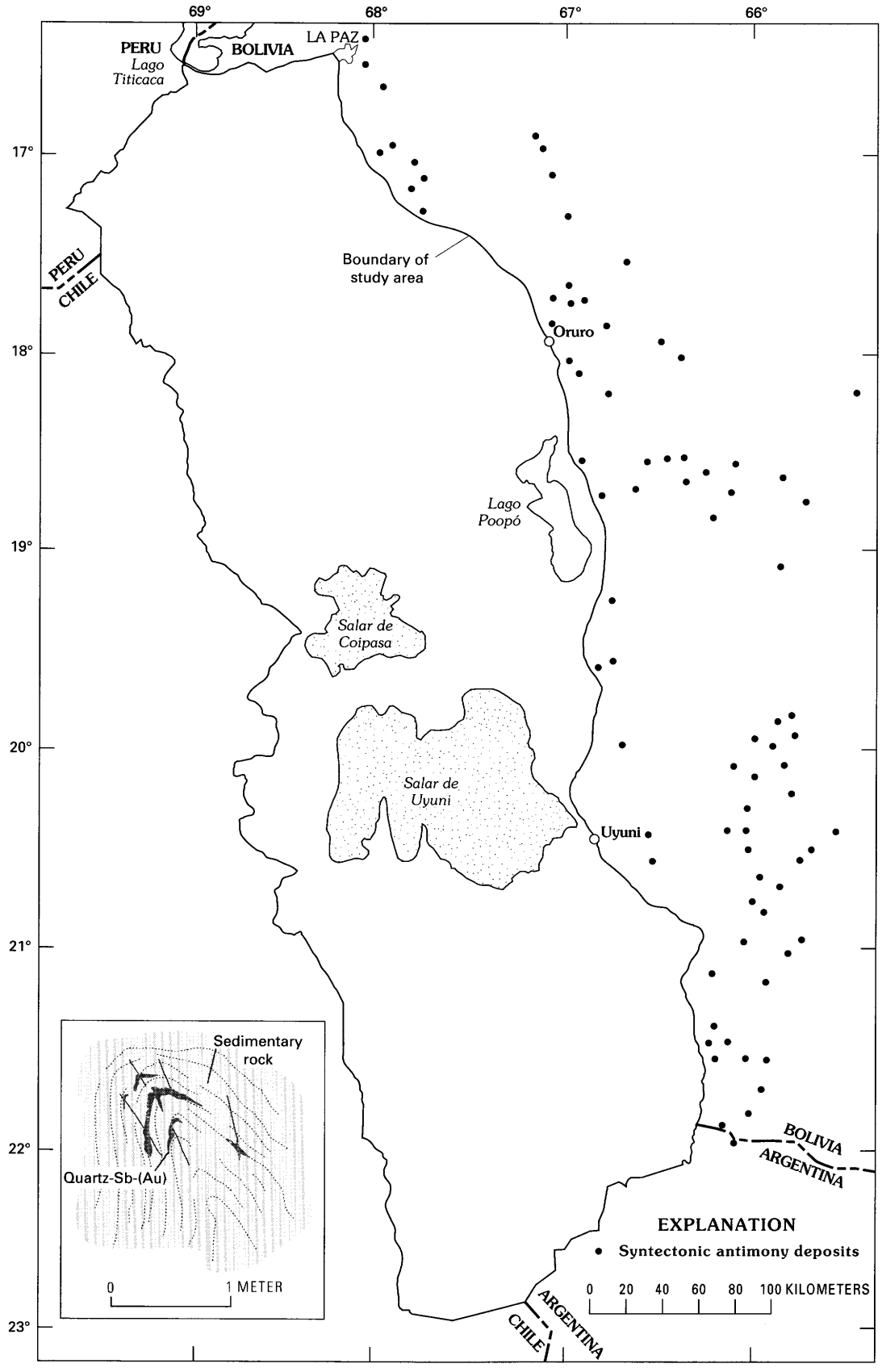


Figure 37. Map showing distribution of some syntectonic antimony deposits near the Altiplano, Bolivia. Modified from Lehrberger (1988). Inset is sketch showing form of mineralization in syntectonic antimony deposits (dark) in sedimentary rocks (light).

METALLIC MINERAL DEPOSITS RELATED TO IGNEOUS ACTIVITY

Mineral deposits that are directly related to igneous activity owe their ultimate origin to processes that began deep in the Earth's crust, or even below it, in the mantle. As such, the geologic terranes in which they may occur are sometimes difficult to define with precision. On the other hand, because they are related to localized thermal anomalies, they may be easier to recognize where they do occur.

We discuss here one very important deposit type for Bolivia, that we term Bolivian polymetallic veins. Following this, we show how hydrothermally altered young volcanic rocks may be indicative of several types of precious-metal-bearing deposits. Finally, we discuss two deposit types, volcanogenic uranium and rhyolite-hosted tin, that are relatively less important.

BOLIVIAN POLYMETALLIC VEINS

The extraction of mineral wealth has dominated Bolivia's economy for more than 400 years. Throughout that long history, most of Bolivia's mineral production has come from a particular group of ore deposits. For three hundred years, huge amounts of silver were produced from dozens of vein deposits, primarily in the Cordillera Oriental. This production, along with that from Mexico and Peru, was of such a magnitude that, for more than a century, it altered the course of European history and politics. During the 19th century, as many of these mines were exhausted of ore that was easy to find and mine, tin became an important metal in the world's economy, and there followed a century (1870–1970) during which Bolivia was often the world's most important producer of tin. Both the silver and tin were produced from the same group of mineral deposits; we call this deposit type Bolivian polymetallic veins.

Polymetallic veins, in the sense of vein deposits that contain a wide variety of metals, are found throughout the world in many types of geologic environments. In this report, we use the term, Bolivian polymetallic vein deposits, to refer to a specific group of vein and veinlet deposits related to mesozonal and epizonal intrusions.

General models for polymetallic veins have been presented in Cox (1986c) and Sangster (1984). However, the examples used to illustrate this deposit type are very small; do not contain metals such as tin, tungsten, and bismuth; and probably formed at depths of several kilometers. They bear little similarity to the large Bolivian deposits we describe here. Summary models and discussions of polymetallic vein deposits that correspond to the Bolivian type, in part based on deposits in Japan, can be found in Nakamura and Hunahashi (1970), Grant and others (1977, 1980), Imai and others (1978), and Togashi (1986).

Bolivian polymetallic vein deposits consist of veins, usually in groups, and often with swarms of smaller veins and veinlets, that contain an assemblage that includes some or all of the following minerals: sphalerite, galena, cassiterite, pyrrhotite, pyrite, arsenopyrite, chalcopyrite, stibnite, stannite, tetrahedrite, wolframite, arsenopyrite, native bismuth, bismuthinite, argentite, native gold and complex sulfosalt minerals (for example, teallite, frankeite, and cylindrite). Some deposits have been principally exploited for tin, some for silver, and a few have been considered important for their tungsten, bismuth, and (or) antimony. One deposit, the Kori Kollo mine of Inti Raymi, is presently being mined primarily for gold. Cadmium and indium are being produced as byproducts at the Carguaicollu deposit (Matthews, 1991). Table 8, while not exhaustive, lists 54 of these deposits, their principal metals, and what is known about their absolute ages.

Host rocks do not appear to be an important control on the occurrence of these deposits, which are found in sedimentary, metasedimentary, volcanic, and intrusive rocks. In Bolivia, the distribution of the polymetallic vein deposits spans two distinct host rock terranes, the Paleozoic sedimentary and metasedimentary terrane of the Cordillera Oriental, and the series of Tertiary basins filled with primarily continental sedimentary and volcanic rocks, which constitutes the Altiplano.

Most of the Bolivian polymetallic vein deposits are intimately related to andesitic to dacitic intrusions, and rarely, to volcanic rocks, including dome-flow complexes. Most of the intrusions are stocks; a few deposits are related to dike swarms. A partial compilation of data about these igneous bodies is presented in Saavedra and Shimada (1986).

The composition of the intrusive rocks associated with the deposits appears to be restricted to intermediate compositions between 60 percent and 70 percent SiO_2. Only a few unaltered rocks associated with mineralization were found to exceed 70 percent SiO_2; they are from the Todos Santos and Escala districts. Aside from these extreme compositions, the rest of the samples from polymetallic mineralized areas appear to belong to the same population as all the rest of the Cenozoic igneous rocks in the study area, regardless of location or age. There are at least three possible explanations for these observations: 1, sampling was inadequate to discern important chemical differences between the rocks; 2, no significant differences exist; or 3, important differences may be found only in the trace constituents of the rocks. The third explanation remains unexplored.

One subtle difference exists that may or may not be significant. Figure 38 is a histogram showing P_2O_5 contents for the same suite of rocks portrayed in figures 7 and 8. This histogram suggests that the older Miocene lavas, that are

Table 8. *Location, metallogeny, and age of Tertiary polymetallic vein deposits in the Altiplano and Cordillera Oriental, Bolivia*

[Deposits are listed from north to south in 1:250,000 quadrangles. Deposits preceded by • are in the study area. Principal commodities, subjectively judged, shown in **bold**. Ages in Ma, rounded to whole numbers. Leaders (--) indicate no data]

Deposit or district	Quadrangle name	Principal metals	Intrusion age	Mineral age
• Tiwanaku	La Paz	**Pb**-Zn-**Ag**-Cu	13	13
Viloco	SE 19-04	**Sn**-Cu-**W**-Mo	24	--
Caracoles	SE 19-04	**Sn**-**Bi**-W	24	23
• Berenguela	Charaña	**Pb**-**Zn**-Ag-**Cu**-**Cd**	--	<26
• La Joya	Corocoro	Pb-Zn-Ag-**Cu**-**Au**-Bi	14	
Chicote	Cochabamba	Zn-**Sn**-Cu-**W**	--	--
Kami	Cochabamba	Pb-Zn-Ag-**Sn**-**W**	--	--
Colquiri	Cochabamba	Pb-**Zn**-Ag-**Sn**-Cu	23	--
• Kori Kollo	Cochabamba	Pb-Zn-**Ag**-Sn-**Au**	15	15
Colcha	Cochabamba	Pb-Zn-Ag-**Sn**-Sb	--	--
• San José	Cochabamba	**Pb**-Zn-**Ag**-**Sn**-Sb	16	15
• Negrillos	Corque	Pb-Zn-**Ag**-Cu	--	<21
• Carangas	Corque	Pb-Zn-**Ag**	--	<15
Japo	Uncia	Zn-**Sn**-Cu	--	--
Morocacala	Uncia	Pb-**Zn**-Ag-**Sn**-Bi	24	20
Cuyuma	Uncia	Pb-Zn-**Ag**	--	--
Huanuni	Uncia	Zn-**Sn**	--	--
Poopó	Uncia	**Zn**-**Ag**-**Sn**-W	--	--
Monserrat	Uncia	Pb-**Zn**-**Ag**-**Sn**	--	--
Llallagua	Uncia	Pb-Zn-Ag-**Sn**-Bi-W	21	20
Avicaya-Bolívar	Uncia	Pb-**Zn**-Ag-**Sn**-Cu-Bi-Sb	--	--
María Teresa	Uncia	Pb-Zn-Ag-**Sn**-Cu-W	--	--
Maragua	Aiquile	Pb-Zn-**Ag**-**Sn**	--	--
Colquechaca	Aiquile	**Pb**-Zn-**Ag**-**Sn**-Bi	22	21
• Todos Santos	Salinas de Garci Mendoza	Pb-Zn-**Ag**	--	<6
• María Luisa	Salinas de Garci Mendoza	Pb-Zn-**Ag**-Au	--	--
Carguaicollo	Río Mulato	**Zn**-**Ag**-**Sn**-**Sb**	--	--
Porco	Río Mulato	**Pb**-**Zn**-**Ag**-**Sn**	--	--
Malmisa	Sucre	**Sn**-Mo	--	--
Colavi	Sucre	Zn-Ag-**Sn**-Cu-Bi-W	--	--
Huari Huari	Sucre	**Zn**-Ag-**Sn**-Sb	--	20
Cerro Rico	Sucre	Pb-**Zn**-**Ag**-**Sn**-Cu-**W**-Sb	--	13
Illimani	Sucre	**Pb**-Zn-**Ag**-Cu	--	--
Sta. Rosa de Kasiri	Sucre	**Pb**-Zn-**Ag**-Cu	--	--
El Asiento	Uyuni	Pb-Zn-**Ag**-**Sn**	--	--
Pulacayo	Uyuni	**Pb**-**Zn**-**Ag**-**Cu**-**Bi**	--	--
Ubina	Uyuni	Zn-**Ag**-**Sn**-Cu-**W**-Sb-Au	--	--
Tasna	Uyuni	Zn-Ag-**Sn**-Cu-**Bi**-**W**-Au	--	16
Chorolque	Uyuni	Zn-Ag-**Sn**-Cu-**Bi**-**W**	--	16
• Chocaya	Uyuni	**Pb**-**Zn**-**Ag**-**Sn**	14	13
• San Cristobal	San Pablo de Lípez	Pb-Zn-**Ag**	--	9
• Tatasi	San Pablo de Lípez	**Pb**-**Zn**-**Ag**-Sn-Bi-Sb	16	--
• San Vicente	San Pablo de Lípez	Pb-**Zn**-**Ag**-Sn-Cu-Au-Sb	18	--
• Escala	San Pablo de Lípez	Pb-Zn-**Ag**	--	<15
• Santa Isabel	San Pablo de Lípez	Pb-Zn-**Ag**-**Sn**-Bi-Sb	--	<15

Table 8. *Location, metallogeny, and age of Tertiary polymetallic vein deposits in the Altiplano and Cordillera Oriental, Bolivia*--Continued

Deposit or district	Quadrangle name	Principal metals	Intrusion age	Mineral age
• Todos Santos	San Pablo de Lípez	Pb-Zn-**Ag**-Sb	--	<15
• Buena Vista	San Pablo de Lípez	Pb-Zn-**Ag**-Au-**Sb**	--	11
• Bonete	San Pablo de Lípez	Pb-Zn-**Ag**-**Bi**	--	<15
• Esmoraca	San Pablo de Lípez	Pb-Zn-Ag- Sn-**Bi**-**W**-**Au**	--	<15
• Morokho	San Pablo de Lípez	Pb-Zn-**Ag**	--	<15
• San Antonio	San Pablo de Lípez	Pb-Zn-**Ag**-Au	--	<15
• Jaquega	San Pablo de Lípez	Pb-Zn-**Ag**	--	<15
Isca Isca	Tarija	**Pb**-Zn-Ag-**Sn**-Cu-**W**	--	--
Choroma	Tarija	**Pb**-Zn-**Ag**-Au	--	--

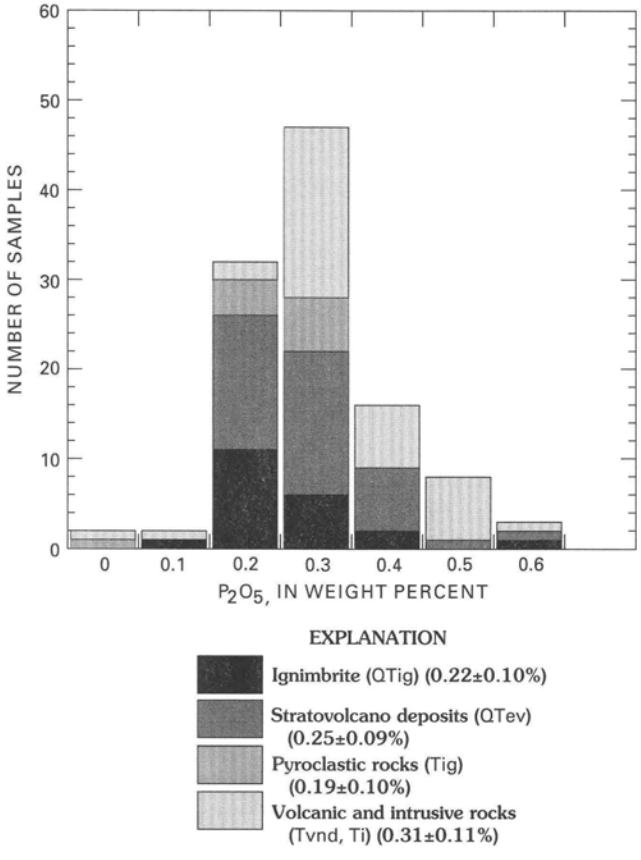


Figure 38. Histogram showing phosphorus content of volcanic and intrusive rocks from the Altiplano and Cordillera Occidental, Bolivia. Numbers in parentheses are mean and standard deviation of P_2O_5 contents.

associated everywhere with the polymetallic vein deposits, are noticeably enriched in phosphorus. More extensive and systematic sampling is needed to confirm this possibility.

Worldwide, there seem to be few restrictions on the age of polymetallic vein deposits, although significant deposits are rare in Precambrian rocks. In Bolivia, deposits of three age groups are present. Triassic deposits are found associated with Triassic peraluminous plutons in the Cordillera Real, which is the northernmost portion of the Cordillera Occidental in Bolivia, east and north of our study area. A group of deposits with Oligocene ages is associated with the Quimsa Cruz batholith, southeast of La Paz. Most of the deposits appear to be Miocene in age. San Cristobal, dated at 8.5 Ma, is the youngest known to date, but Todos Santos may be younger yet. Because we have no evidence of Triassic igneous activity on the Altiplano, we believe that deposits of this age are unlikely to be found outside their known area of occurrence in the Cordillera Oriental.

The veins and veinlets that constitute Bolivian polymetallic vein deposits appear to fill primarily tension fractures related to the emplacement of an associated intrusion; there are few examples of mineralization emplaced in major faults that are related to regional tectonism. In the Cordillera Oriental, there is a tendency for veins to be normal to anticlinal axes. In Sud Lípez, the majority of the veins trend approximately east-west. Replacement of wallrocks along narrow fissures was the mode of deposition of early stages of mineralization, followed by open-space filling in the later stages in many deposits (Turneaure, 1960a, 1971). The vertical and horizontal extent of many of these deposits is impressive; at Cerro Rico de Potosí, the mineralized interval is nearly 2 km long and the lowest workings are more than 900 m below the uppermost; the lower extent of mineralized rock has not been determined (Bernstein, 1989). On the basis of fluid inclusion filling temperatures and salinities (Grant and others, 1980; Sugaki and others, 1985, Kelly and Turneaure, 1970), and on stratigraphic reconstructions, it is likely that most of the Bolivian polymetallic vein deposits formed at depths of 0.5–2 km beneath the surface.

The relationship of Bolivian polymetallic vein deposits to other deposit types is not totally clear. Reed (1986a) includes Caracoles as an example of the Sn vein deposit type; Caracoles is one of a group of northern deposits that is apparently lacking in base metals, however other geologic characteristics fail to distinguish this group from the others. Reed (1986b), Grant and others (1977, 1980), and Sillitoe and others (1975) include deposits at Chorolque, Llallagua, and elsewhere as examples of the porphyry Sn deposit type. We regard these "porphyry"

deposits, like other deposits where the distribution of veins and veinlets has made bulk mining feasible, (for example, Toldos, Kori Kollo, and Tasna), as large-tonnage, bulk-mineable examples of polymetallic veins. The spacing of fractures seems to be the most important difference. Although this difference can be very important to the mining economics of a deposit, it has little to do with predicting permissive or favorable environments, or with exploration criteria.

The mineralogy of these deposits is extremely complex. The deposits have been lucrative areas for mineral collectors for hundreds of years. Those interested in the complex mineralogy of these deposits should examine the exhaustive mineralogical tables and detailed mine descriptions in Ahlfeld and Schneider-Scherbina (1964), Turneaure (1960a), and Sugaki and others (1981, 1986), as well as the listing by Alarcón and Kitakase (1987). Many of the metals found in these deposits (Sn, W, Bi) are commonly associated with high-temperature deposits that derive a major portion of their metals directly from associated magmas during their formation.

Perhaps the most significant aspect of the vein mineralogy is the relative paucity of nonsulfide gangue minerals. Veins generally consist of 90 volume percent or more sulfide minerals; pyrite, marcasite and pyrrhotite are the major sulfides. A few deposits have abundant quartz, barite, or manganese carbonate in the vein assemblage. Notable is the vein deposit at Mesa de Plata, in the San Antonio de Lípez area, where, at the present level of erosion, the veins contain abundant barite and quartz (more than 70 volume percent), some of it amethystine. However, at a depth of a few hundred meters, the same veins consist primarily of pyrite, with only minor quartz or barite. Sillitoe (1988) suggests that this upward change in vein mineralogy from massive sulfides to barite-quartz or barite-chalcedony is a general feature of this deposit type, and that it represents the transition from the porphyry to the epithermal environment.

Ore minerals are generally present in discrete veins, that range from 10 cm to more than 2 m in width (most deposits), as well as in groups, splays, or swarms of small veinlets (for example, at Llallagua, Chorolque, and Toldos). Veinlet swarms are not generally intersecting stockworks, but tend to be parallel sets of veinlets, or sheeted veins, that do not intersect significantly. The veins and veinlets are closely associated in space with small dacitic stocks or dike swarms, and, in many deposits, for example, Toldos and Mesa de Plata, mineralized veins are confined to the intrusion.

Quartz-sericite-pyrite is the most characteristic hydrothermal alteration assemblage. Many of the Bolivian polymetallic vein deposits display alteration envelopes with dimensions of tens to hundreds of meters, where the wallrock is bleached white because of replacement of the groundmass by quartz and sericite, and stained red and brown, because of the oxidation of disseminated pyrite and other sulfide minerals. The apparent strength of alteration is, in part, a function of the original nature of the host rock. In the dacites, biotite phenocrysts are almost always pseudomorphically replaced by sericite. In Upper Quehua ash-flow tuffs, the original rocks are soft and white, and the effects of hydrothermal alteration may be hard to discern megascopically. At a few deposits, notably Toldos, biotite phenocrysts appear to be stable in this assemblage, although secondary hydrothermal biotite has not been recognized. Additional minerals that may occur in this assemblage include tourmaline, fluorite, calcite, and siderite. At most deposits, argillic and (or) advanced argillic assemblages (which may contain alunite) are found in the upper and outer portions of the deposit. This alteration may be extremely difficult to distinguish from supergene argillic alteration, formed by acid leaching from dissolution of disseminated pyrite that originally formed in a quartz-sericite-pyrite assemblage.

The total volume of rock affected by veining and alteration in some of these systems can be very large, on the order of several cubic kilometers. The altered area in the Chocaya district, on the eastern border of the Altiplano, is several kilometers in diameter, as can be seen on plate 3, image E.

Extensive studies of fluid inclusions associated with Bolivian polymetallic vein deposits have been made by Kelly and Turneaure (1970), Grant and others (1980), and Sugaki and others (1985). These fluid-inclusion studies show an evolution from early, very hot (>400 °C) brines (halite-saturated), to later, cooler, less saline fluids. Table 9 summarizes some of the observations of these and other authors.

Figure 39 shows the geographic distribution of polymetallic vein deposits in southwestern Bolivia. Figure 40 shows what is known about the metallogenic variability among these deposits. The patterned areas that include deposits with similar metallogenic character should not be interpreted as "mineral belts;" they are meant only to highlight the information. Previously, many workers have focused on tin and have not considered the polymetallic deposits on the Altiplano. Although there is a relative scarcity of tin and tungsten in the western group of deposits on the Altiplano, a detailed analysis of figure 40 reveals complex patterns that make it difficult to relate variations in mineralogy and elemental abundance within the polymetallic deposits to any known or suspected chemical differences in the underlying crust. There is significant cassiterite in the Santa Isabel district, which is clearly on the Altiplano, however Pulacayo and Choroma are prominent examples of Cordilleran deposits that lack tin. In addition, Lehmann and others (1988, 1990) have shown that Bolivian Paleozoic clastic metasedimentary rocks do not exhibit anomalously high tin or boron concentrations; they suggest that the tin enrichment in Bolivian dacite-hosted systems is

Table 9. *Maximum fluid inclusion homogenization temperatures and salinities of selected Bolivian polymetallic vein deposits*

[Temperatures in °C and salinites in weight percent NaCl equivalent. Leaders (--) indicate no data.]

Deposit	Maximum temperature	Maximum salinity	Reference
Matilde	283	--	Sugaki and others (1985)
Trinidad	427	47.1	Sugaki and others (1985)
Milluni	321	--	Sugaki and others (1985)
Milluni	407	--	Kelly and Turneaure (1970)
Kellhuani	363	26.0	Sugaki and others (1985)
Kellhuani	307	--	Kelly and Turneaure (1970)
Chojlla	311	--	Sugaki and others (1985)
Chicote	385	--	Kelly and Turneaure (1970)
Llallagua	481	--	Kelly and Turneaure (1970)
Llallagua	>400	>26	Grant and others (1980)
Viloco	494	55.4	Sugaki and others (1985)
Caracores	455	50.6	Sugaki and others (1985)
Colquiri	383	6.4	Sugaki and others (1985)
Colquiri	405	--	Kelly and Turneaure (1970)
La Joya	550	50	Zamora (1989)
Kori Kollo	>320	>26	Zamora (1989)
San José	353	10.1	Sugaki and others (1985)
San José	526	--	Kelly and Turneaure (1970)
San José	398	<26	Argandoña (1989)
Trinacria	422	26.0	Sugaki and others (1985)
Morococala	408	31.4	Sugaki and others (1985)
Huanuni	405	26.0	Sugaki and others (1985)
Avicaya	413	36.6	Sugaki and others (1985)
Bolivar	327	--	Sugaki and others (1985)
Catavi	399	8.6	Sugaki and others (1985)
Colquechaca	407	37.1	Sugaki and others (1985)
Potosí	371	19.7	Sugaki and others (1985)
Illimani	311	9.5	Sugaki and others (1985)
Kumurana	413	20.4	Sugaki and others (1985)
Caracota	342	--	Sugaki and others (1985)
Pulacayo	248	--	Kelly and Turneaure (1970)
Tasna	499	50.4	Sugaki and others (1985)
Tasna	446	--	Kelly and Turneaure (1970)
Chorolque	509	53.2	Sugaki and others (1985)
Chorolque	>500	>40	Grant and others (1980)
Chocaya	379	11.9	Sugaki and others (1985)
Tatasi	345	10.6	Sugaki and others (1985)
San Vicente	385	8.9	Sugaki and others (1985)
Buena Vista	305	5.8	Sugaki and others (1985)
Mesa de Plata	317	16.1	Sugaki and others (1985)

made possible by low-oxygen fugacities during magmatic differentiation. Thus, to relate the distribution of metals among the polymetallic vein deposits to chemical differences in the underlying crust seems speculative, at best. We believe that all the deposits shown on figures 39 and 40 conform to a single type.

Of greater significance in delineating permissive areas for the occurrence of undiscovered deposits is the distribution of ages of the deposits, shown on figure 41. The Tertiary deposit ages appear to become younger from north to south in Bolivia, but this pattern may be illusory because the majority of the deposits are undated. Because pre-Tertiary polymetallic vein deposits are present in the northern part of the Cordillera Oriental, and because Paleozoic and Mesozoic magmatism is known in Chile, to the west, there is some reason to expect the possible existence of pre-Tertiary polymetallic deposits on the Altiplano. However, no older magmatic rocks are exposed in any of the pre-Tertiary outcrops on the Altiplano, and the probability that some are concealed and yet to be discovered seems extremely low. Most of the Bolivian polymetallic vein deposits shown on figure 41 are of Miocene age, and

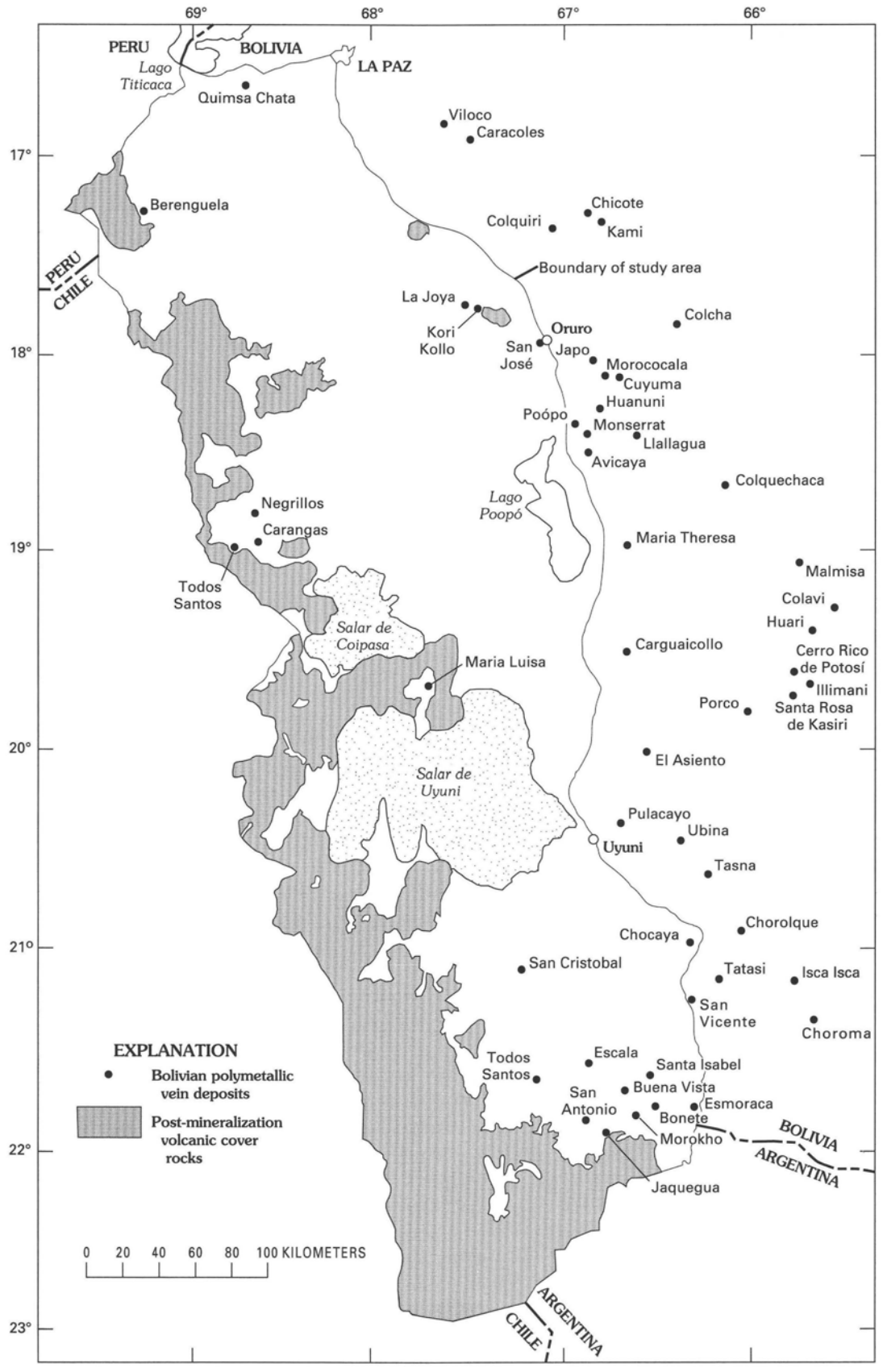


Figure 39. Map showing distribution of Tertiary Bolivian polymetallic vein deposits on the Altiplano and in the Cordilleras Oriental and Occidental, Bolivia.

this appears to be true for all the deposits on the Altiplano. Thus, undiscovered Miocene or Oligocene polymetallic systems might occur where rocks of Miocene or older age crop out.

POLYMETALLIC REPLACEMENT DEPOSITS

Elsewhere in the world, polymetallic replacement deposits (Morris, 1986) are commonly associated with, and sometimes appear to be fed by, polymetallic veins. It is interesting to speculate that some rich polymetallic replacement deposits might have resulted, had some of the Bolivian polymetallic mineralized systems encountered large amounts of carbonate rock during their development. Sillitoe (1988) suggests that replacement deposits are possible near at least two of the known deposits, Tatasi and Tasna (fig. 39). If carbonate rocks were common as host rocks for polymetallic systems like those described here, we would expect to find polymetallic replacement deposits. The paucity of carbonate host rock argues against the occurrence of any replacement deposits.

DISTAL DISSEMINATED SILVER DEPOSITS

Vein and replacement deposits that form around igneous intrusions are sometimes associated with disseminated silver and gold mineralization localized on the extreme periphery of the ore-forming system, typically in fine-grained clastic rocks and carbonates. These deposits, termed distal disseminated silver deposits (Cox and Singer, 1990) are commonly mined by open-pit and heap-leaching methods and resemble the previously mentioned, bulk-mineable sediment-hosted gold deposits, from which they differ in that silver is commonly more abundant than gold, and manganese and base metals are prominent in their geochemical signature.

There are numerous examples of this deposit type in the western United States, such as at Cove and Taylor, Nev. In South America, an example can be found at the Purísima Concepción deposit in the Yauricocha mining district, Peru (Alvarez and Noble, 1988), where 200,000 tonnes of ore containing about 3 ppm gold is disseminated in tightly folded Cretaceous fine-clastic sedimentary rocks 0.5 km from the granodiorite stock associated with the Yauricocha base-metal replacement ore bodies. Silver (about 30 ppm) is positively correlated with abundant manganese which occurs as rhodochrosite.

These ores, typically fine grained and darkened by carbonaceous material are difficult to recognize except by chemical analysis, and we believe there is a small chance that undiscovered deposits may be present on the peripheries of polymetallic vein districts in Bolivia.

PORPHYRY AND EPITHERMAL DEPOSITS

Porphyry Copper Deposits

Porphyry copper deposits (Cox, 1986a) consist of stockworks of quartz veins that contain chalcopyrite with or without bornite as the primary ore minerals, and are found in hydrothermally altered porphyries and their adjacent wallrocks. They are found worldwide at convergent plate boundaries, and many of the world's best-known examples occur in the Andes (Titley and Beane, 1981). Large numbers of important porphyry copper deposits are found in nearby Chile, Argentina, and Peru, in some cases only a few kilometers from the Bolivian border.

Redwood (1987a) predicted that porphyry copper deposits may underlie polymetallic vein deposits on the Altiplano, as well as the many altered areas in the Cordillera Occidental. This supposition assumes that most of the polymetallic vein deposits are epithermal, and formed near the paleosurface, above an underlying porphyry deposit. However our field observations and other more recent studies (Sillitoe, 1991) suggest to us that the polymetallic veins systems are, in general, not epithermal. On the contrary, they represent, and are generally emplaced in, the porphyry environment. The prevalence of sericitic alteration, the intrusive nature of most of the associated igneous rocks, and the prevalence of high-temperature (>350 °C), halite-saturated fluid inclusions at studied localities all indicate that these deposits should not be classified as epithermal. Perhaps the extremely thick crust under the Altiplano and Cordillera Oriental is, in some way, responsible for a different metallogeny in petrochemically similar rocks.

Although there is a chance that porphyry copper deposits might underlie some of the altered areas in very young volcanic rocks in the Cordillera Occidental, they would be relatively deeply buried, probably more than 1 km. We believe the probability of encountering porphyry copper deposits on the Altiplano or in the Cordillera Occidental is very small.

Porphyry Gold Deposits

Recent exploration discoveries in the southern Andes of Chile have led to the recognition of a new deposit type, porphyry gold, that contains very large tonnages of low-grade gold ore (Rytuba and Cox, 1991). These deposits consist of a stockwork of quartz veinlets in and beneath dacitic and andesitic stratovolcanoes in continental and oceanic island arcs. Most ore formed within 1 km of the paleosurface. The deeper parts of these deposits are characterized by potassic (biotite stable) and phyllic alteration. The upper parts may include precious- or base-

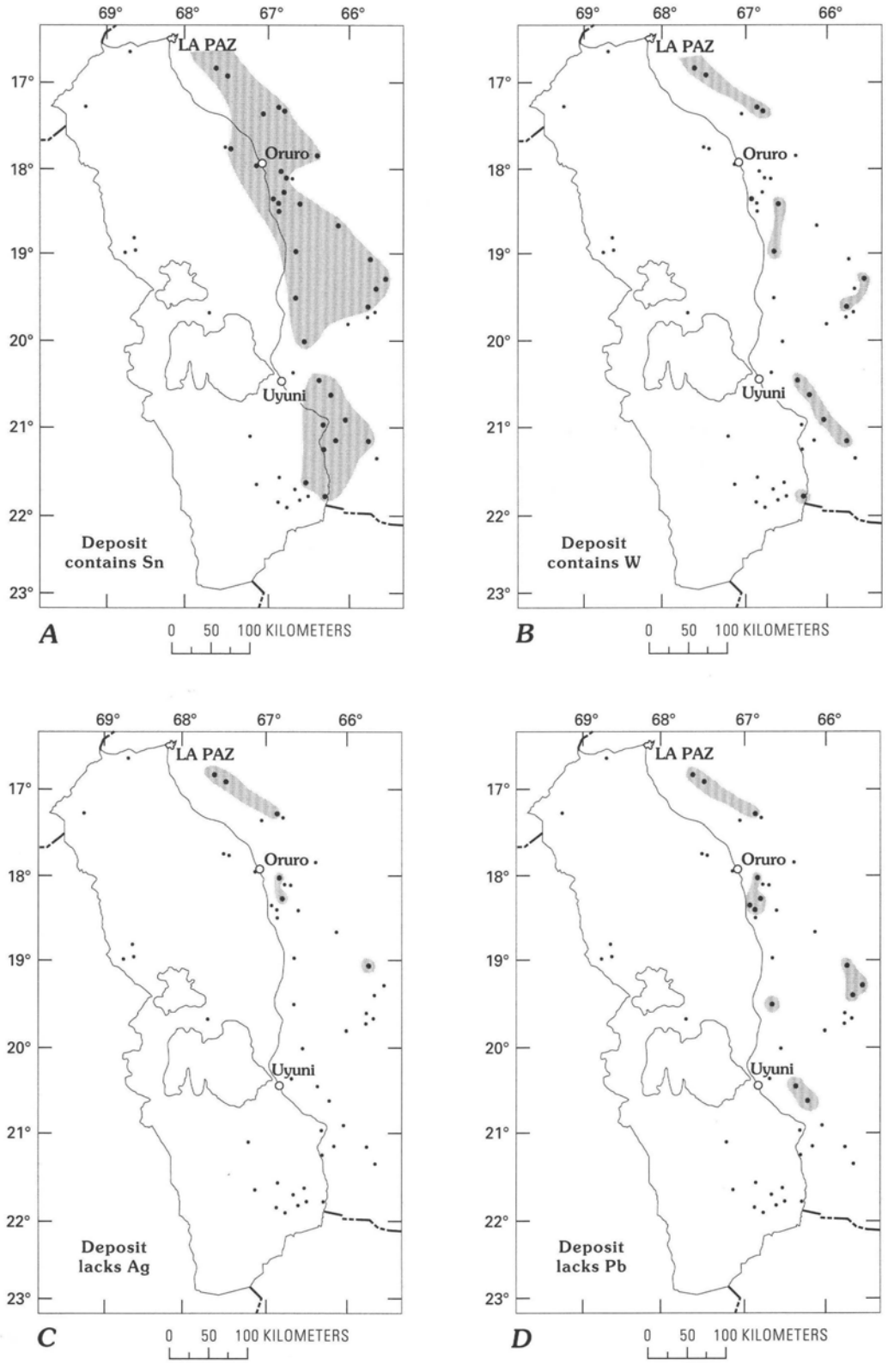
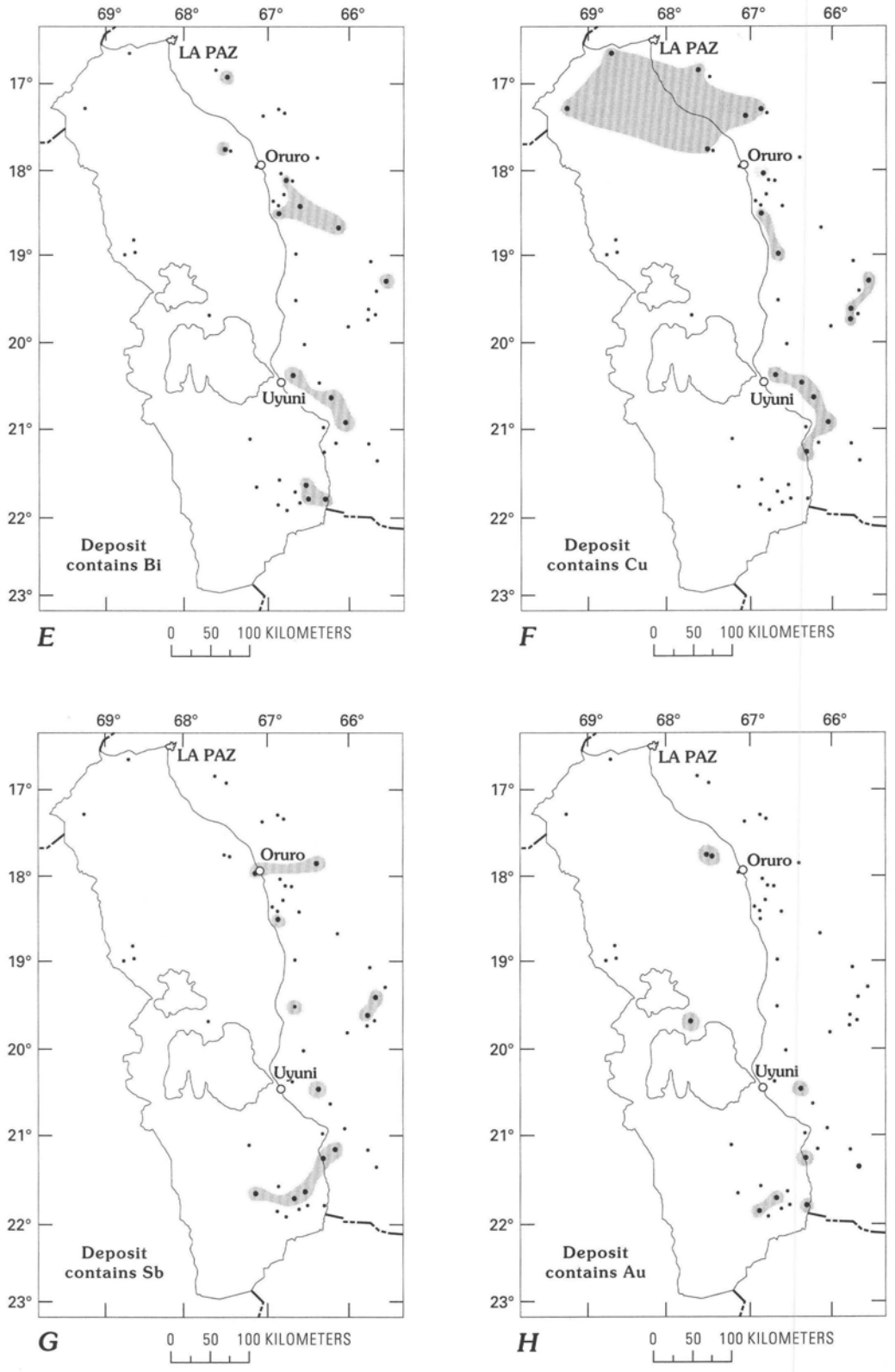


Figure 40 (above and facing page). Metallogeny of Bolivian polymetallic vein deposits on the Altiplano and in the Cordilleras Oriental and Occidental, Bolivia. Shaded areas and larger dots indicate deposits that *A*, contain Sn; *B*, contain W; *C*, lack significant Ag; *D*, lack significant Pb; *E*, contain Bi; *F*, contain Cu; *G*, contain Sb; and *H*, contain Au. Shaded areas around deposits with similar metallogenic character should not be interpreted as "mineral belts"; they are meant only to highlight the information. Commodity information is subjective in some cases, and is gleaned from many literature sources, as well as this investigation.



metal-rich veins, as well as hot-spring deposits of mercury or sulfur. Pervasive alteration near the paleosurface is primarily argillic and advanced argillic, with alunite as a common alteration mineral. The lower parts may be related to or grade into porphyry copper deposits. It is important to note that the uppermost parts of porphyry gold, quartz-adularia vein, quartz-alunite vein, and polymetallic vein systems are difficult to distinguish from each other.

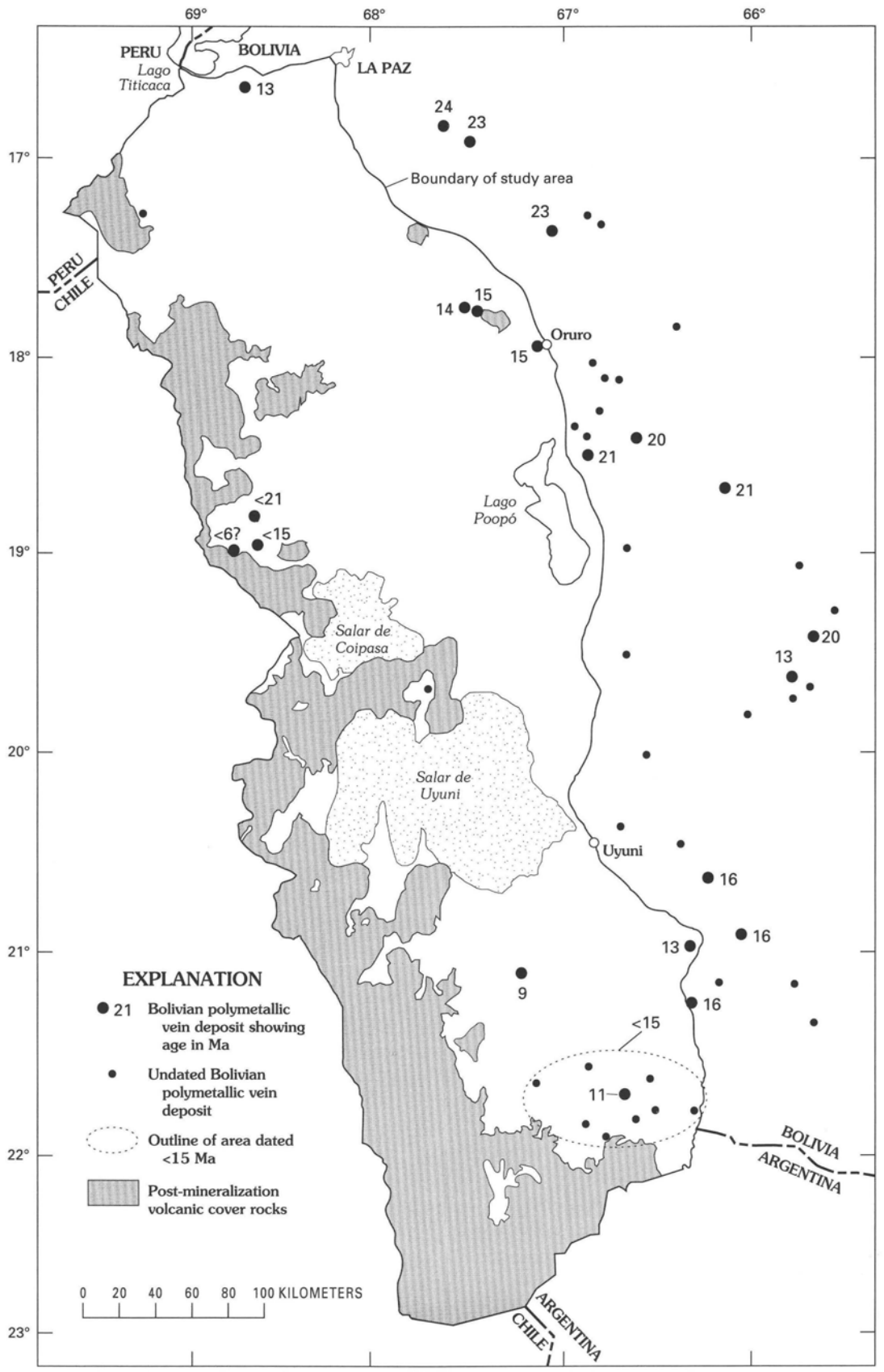


Figure 41. Map showing absolute ages of Bolivian polymetallic vein deposits on the Altiplano and in the Cordilleras Oriental and Occidental, Bolivia. All ages in Ma. Shaded area as on figure 39.

Although no porphyry gold deposits are known in Bolivia, they might occur in any of the volcanic rocks of the central Andes. Because they have not been found in the older volcanic terrane (pl. 1, Tvnd), that has been relatively well explored for Bolivian polymetallic vein systems, we believe they are very likely to be found only in the younger volcanic terrane (pl. 1, QTv, QTig).

Quartz-Alunite Veins

Epithermal quartz-alunite gold deposits have been described in summary fashion by Berger (1986b), and, under the name acid-sulfate-type deposits, in longer form by Heald and others (1987).

These deposits consist of epithermal veins or groups of veins that typically contain enargite and pyrite, with or without covellite. Gold is present as electrum, and various silver-bearing sulfosalts and, commonly, bismuthinite are also present. Hydrothermal alteration associated with these deposits is characterized by advanced argillic alteration assemblages, often featuring alunite, kaolinite, and (or) pyrophyllite. Gold-to-silver ratios and base-metal abundances are quite variable, although copper is typically the most abundant base metal. The mineralized area is usually roughly equidimensional and centered on a volcanic or hypabyssal intrusive center. Often, the age of mineralization is similar to, and within the cooling history of, the age of the associated intrusive rocks. Most deposits have had structural controls for intrusion and mineralization; caldera ring fractures are a common site for emplacement. Most formed at paleodepths of less than 1 km. Limited isotopic data suggests a local magmatic source for most of the sulfur and lead in these deposits, as well as an important component of magmatic water.

In many parts of the world, quartz-alunite gold deposits appear to be related to porphyry intrusions, some of which may be porphyry copper systems. Summitville, Colo. and the gold-poor alteration cap at Red Mountain, Ariz. are apparently the upper parts of porphyry copper systems. At El Indio, Chile, a gold-rich quartz-alunite vein system appears to grade downward into a deposit not unlike the Bolivian polymetallic veins described previously (Walthier and others, 1985). In addition, gold-poor volcanic-hosted enargite replacement deposits (Sillitoe, 1983; Cox, 1986b) are found in similar environments.

One deposit on the Altiplano, Laurani, fits the quartz-alunite vein model extremely well (Garzón, in press; this volume). Enargite is the major ore mineral at Laurani, and alunite is an important constituent of intensely developed argillic alteration. The deposit is hosted in an intermediate-composition dome or stock that was emplaced at 8.4 Ma (Redwood and Macintyre, 1989). The Coniri fault, that separates Cretaceous and Paleozoic sediments, served as a structural control for the deposit.

Other epithermal prospects and altered areas on the Altiplano, which are described later in this volume, are better assigned to other models. For example, the gold-rich polymetallic deposit at Kori Kollo has alunite veins that may contain some precious metals, but they occur very late in the paragenesis and are not an essential part of the development of the system. Alunite is also found in the upper parts of alteration zones in many of the younger stratovolcanoes of the Altiplano, for example at the María Elena and Milenka prospects. Some of these occurrences are related to volcanogenic sulfur deposits, while others, which are poorly explored, may eventually be shown to be porphyry gold deposits.

Thus, it is difficult to speculate if and where more deposits like Laurani might be found. The Coniri fault in the Laurani area may have helped to localize the deposit, but the absence of exposed faults cannot be used to eliminate other areas, because faults in basement rocks, such as the Coniri fault, are seldom exposed on the Altiplano. Indeed, the probability that there are undiscovered, well-exposed quartz-alunite deposits is low. However, vast portions of the Altiplano consist of thick volcanic rocks that could easily conceal slightly older mineral deposits. Any of the volcanic terranes of the Altiplano might host quartz-alunite vein deposits.

Quartz-Adularia Veins

Epithermal quartz-adularia gold deposits have been described in summary fashion in Cox and Singer (1986), where they are divided into three subtypes, Creede, Comstock, and Sado. The geologic and grade and tonnage data that supports this subdivision are presented in Mosier and others (1986). Under the name adularia-sericite-type deposits, they are described in detail by Heald and others (1987).

These deposits consist of epithermal veins or groups of veins that typically have a sulfide assemblage that includes argentite, tetrahedrite, tennantite, and variable amounts of galena and sphalerite. Gold, as electrum, is usually present. Hydrothermal alteration associated with these deposits is characterized by sericitic and argillic alteration assemblages, along with adularia and carbonate; primary alunite associated with the main stage of mineralization is absent. Gold-to-silver ratios and base-metal abundances are quite variable. The mineralized area is often elongate, and some of the systems are very large, with vein systems many kilometers long. The age of mineralization can be the same as, or may be distinct from the emplacement of any associated igneous centers, which are commonly andesitic to dacitic stratovolcanoes. Structural controls for intrusion and mineralization are complex; caldera ring and radial fracture settings are not uncommon, yet some deposits occur remote from any caldera. Most deposits formed at paleodepths of less than 1 km, with many

forming within a few hundred meters of the paleosurface. Isotopic data suggests nonmagmatic sources for most of the water, sulfur, and lead in these deposits.

Sillitoe (1991) suggests that some quartz-adularia deposits are related to porphyry gold, copper, or copper-molybdenum deposits, but many of them in the western United States, although commonly associated with centers of Tertiary volcanism, appear unrelated to any known porphyry systems, or associated skarn and replacement deposits.

No deposits in Bolivia have been identified that fit the characteristics of quartz-adularia deposits very well. However, vast parts of the Altiplano consist of thick sequences of volcanic rocks that could easily conceal slightly older mineral deposits, and as in the case of quartz-alunite vein deposits, the young volcanic rocks might contain quartz-adularia vein deposits.

Hot-Spring Gold and Hot-Spring Mercury Deposits

Hot-spring gold deposits are defined by Berger (1986a), and hot-spring mercury deposits by Rytuba (1986). These deposits represent the uppermost portions of epithermal systems, and formed within a few tens to hundreds of meters of the surface. They can form above either quartz-alunite, or quartz-adularia deposits, and thus, they will be found in the same regions as those two deposit types. No deposits that fit either of these descriptive models are known in Bolivia, even though the younger volcanic terrane (pl. 1, QTev, QTig) seems permissive. Indeed, the lack of available mercury for amalgamation was a serious problem for 16th and 17th century Bolivian miners, and they transported mercury great distances by mule from the large deposits at Huancavelica, Peru.

Epithermal Manganese Deposits

Epithermal manganese deposits (Mosier, 1986) consist of veins, or groups of veins, that are emplaced in continental subaerial volcanic sequences. The veins consist of rhodochrosite or manganocalcite, along with quartz, barite, and sometimes, zeolite minerals. Most of these deposits are closely associated with epithermal precious-metal deposits, and they form in the same environment. In the study area, two examples are known, the Negra mine (app. A) and Mina Granada at Cerro Puquisa, which is described in the section on Geology of known mineral deposits.

Interrelationships

All the deposit types discussed in this subsection, porphyry gold, quartz-alunite vein, quartz-adularia vein, hot-spring, and epithermal manganese, are interrelated. That is, they tend to form as parts of large, complex, hydrothermal systems. In some districts, one type will be more important, but the presence of one of these types implies the possibility for the occurrence of many or all of the others. In addition, the upper parts of all these systems can appear very similar. Large areas of pervasive alteration in the upper levels of volcanic rock provide few clues as to the exact nature of the deposits that may lie below. Thus, it seems inappropriate to attempt to subdivide the areas where these deposit types are likely to occur. On the Altiplano of Bolivia, altered rocks that suggest the presence of one or more of these deposit types are common; good examples of the actual deposits are rare, probably in large part because erosion has not yet exposed any young deposits that may exist.

VOLCANOGENIC URANIUM AND RHYOLITE–HOSTED TIN DEPOSITS

Uranium is found in a variety of volcanic environments, but is almost universally associated only with highly evolved, silicic volcanic rocks (Goodell, 1985; Locardi, 1985; Wenrich, 1985). Several deposits are known on, and immediately adjacent to the Altiplano, in the highly evolved Los Frailes volcanic field (Leroy and others, 1985; Pardo-Leyton, 1985).

Rhyolite-hosted tin deposits, which are formed by condensation of vapors evolved from cooling lavas, also occur exclusively in highly evolved rhyolites (Reed and others, 1986). Examples of this type of mineralization are described in Ahlfeld and Schneider-Scherbina (1964) from the Los Frailes volcanic field, just east of the Altiplano.

Both of these deposit types are likely to be found in Bolivia only in the highly evolved Los Frailes and Morococala volcanic fields.

NONMETALLIC AND INDUSTRIAL MINERAL DEPOSITS

Models and methods for modeling industrial mineral deposits are in the process of being developed. Existing deposit models are described in a manner similar to metals, but in the long run a different format may have to be developed. One of the major problems in developing deposit models for industrial minerals is our lack of geologic understanding of the processes and conditions under which many of these deposits form. Industrial minerals do not have the glamour appeal of most metals and there has been relatively little research on these deposits compared with metals. Industrial minerals are typically regarded as low-value common minerals, but many of the materials are in fact not low in value or common; the total value of industrial minerals greatly exceeds that of metals.

Some characteristics are relatively unique to modeling industrial mineral deposits, for example, many surficial industrial mineral deposits, including some that are being exploited, are in the process of forming and we are attempting to define and describe deposits that are not yet fully developed. Other industrial mineral deposits are products of alteration and erosion processes working on rocks that meet a certain set of chemical or physical preconditions which are not fully understood. A large number of industrial "minerals" are actually industrial materials and (or) chemical compounds that may be present in trace amounts in a host rock or that may constitute such a large part, as much as 90 percent of the rock, that the ore may be a distinctive rock type of its own. Despite these drawbacks, most models for industrial minerals can be developed in a manner similar to metals; descriptive and grade-tonnage relationships can be described and generalized.

DEPOSITS ASSOCIATED WITH SALINE AND ALKALINE LAKES AND SALARS

Most of the industrial mineral deposit types that are permissive given the geology of the Bolivian Altiplano and Cordillera Occidental are associated with the formation and evolution of the more than 200 alkaline and saline lakes in closed basins (table 10). There are deposit types associated with the presence of lakes such as sedimentary clays or sand and gravel deposits and deposits such as lacustrine diatomite, carbonates, and some borate deposits that are associated with particular lake chemistries. Some deposit types are formed through evaporative processes including lacustrine brines enriched in lithium, boron, potassium, or magnesium and a variety of soluble minerals including halite, gypsum, sylvite, ulexite and other borate minerals, and sodium carbonates and sulfates. Still other deposit types are products of the interaction of saline-alkaline lake water with felsic to intermediate volcanic rocks; these deposit types would include sedimentary zeolites or hectorite. Figure 42 shows the location of many of the saline and alkaline lakes and playas discussed in this section, and in the section on Geology of known mineral deposits.

When considering deposits directly related to the environment of saline and alkaline lakes and playas, the form and grade of mineralization can change within a short time, a problem not commonly encountered with metals. The proportion of brine to soluble salt is a fragile equilibrium that can be rapidly altered by relatively minor changes in pH, density, temperature, and (or) pressure. The saturation level of the brine may change as a result of the same forces and lead to seasonal or localized precipitation of salts that may be resorbed by the brine in weeks or months.

The presence of multiple commodities in the same environment occurs with both metallic and nonmetallic mineral deposits. For example, with the nonmetallic deposits, there may be a problem determining if the lithium-enriched zone of a playa is a different deposit type than the boron-enriched zone of the same playa; or it may be unclear if the boron in a brine enriched in boron, lithium, magnesium, sodium, carbonate, and potassium is different in form or origin from the boron in a brine enriched in boron and carbonate only. The lakes and salars of Bolivia represent a wide variety of combinations of elements commonly concentrated in these types of systems. Small differences in the lithology of a catchment basin, the presence or absence of a thermal spring, and the amount of runoff in the basin can affect the presence or absence of a specific element in lake or playa waters. To simplify the following discussion, the various salts and brines are discussed as if they occur independently, but we acknowledge that in reality each of these deposit types interacts within a complex system.

Brines

Evaporation of closed basin lake waters can lead to concentration of some elements in the remnant brine as well as to deposition of relatively soluble salts. Compounds that have been produced from marine and continental lacustrine brines include potassium, magnesium, boron, lithium, bromine, iodine, sodium sulfate, sodium nitrate, sodium carbonate, and sodium chloride. With the exception of bromine, iodine, and nitrate, these commodities are present in elevated concentrations in one or more of Bolivia's lakes and salars. Most of the potential for brines is in Tertiary to Quaternary basins with surface playas and (or), in the case of sodium carbonate and boron, alkaline lakes.

Lithium is most commonly enriched in chloride brines of basins draining felsic- to intermediate-composition volcanic rocks or continental saline sedimentary rocks (Asher-Bolinder, 1991a). Brines have become an increasingly important source of lithium, and it is currently being extracted from brines at Silver Peak playa, Nev., and at Searles Lake, Calif. An average brine content of greater than 0.03 percent lithium in a large, porous aquifer is considered to be potentially economic. Known deposits cover several tens of square kilometers in aquifers that extend to 200 m below ground surface. Springs contributing lithium to these systems commonly have lithium-to-sodium ratios exceeding 1:100 (Asher-Bolinder, 1991a). Salar de Uyuni, Bolivia, is the largest lithium brine resource in the world and has been actively prospected in the recent past. Many other lakes and salars on the Altiplano and in the Cordillera Occidental have elevated lithium contents including Salar de Coipasa and its inflow from Río Sabaya, Laguna Loromayu, Laguna Cachi, Lagunas Pastos Grandes, and Laguna Busch o Kalina. Areas permissive for the

Table 10. *List of selected named salars and lakes on the Altiplano and in the Cordillera Occidental, Bolivia*

[Only those lakes shown on the Cerro Zapaleri, Cochabamba, Corque, La Paz, Nevados Payachata, Río Mulato, Salinas de Garci Mendoza, Uyuni, Villa Martin, Volcán Juriques, Volcán Ollague 1:250,000 quadrangles are listed. Salars or lakes with mapped areas less than 1 km^2 are indicated with an *. References: 1, Ballivian and Risacher, 1981; 2, Risacher, 1976; 3, Echenique and others, 1978; 4, Risacher and Miranda, 1976; 5, Ericksen and Salas O., 1989; 6, Risacher and others, 1984; 7, Servant-Vildary, 1978a, 1978b; 8, Rettig and others, 1980; 9, Risacher and Fritz, 1991; 10, Risacher, 1978; 11, Ericksen and others, 1978]

Name	Reference(s)
La Paz quadrangle	
Lago Titicaca	
Laguna Aripuno	
Laguna Cabrahuani	
Laguna Jayu Kkota*	
Laguna Khara Kkota	
Laguna Kkota*	
Laguna Kollpa Kkota*	
Laguna Laramkkota*	
Laguna Mat Kkota*	
Laguna Milluni	
Laguna Parina Kkota*	
Laguna Sora Kkota	
Laguna Taypi Chaka	
Charaña quadrangle	
Laguna Chungara	
Corocoro quadrangle	
Laguna Achiri	
Laguna Blanca*	
Laguna Chijmo Kkota*	
Laguna Chulluncani*	
Laguna Churuputo	
Laguna Kkota Pata	
Laguna Kkotana	
Laguna Lima Kkota	
Laguna Parco Kkota	
Laguna Phuchu Phuchu	
Laguna Tanapaca	
Laguna Zapamaya*	
Cochabamba quadrangle	
Laguna Chiri Huarina*	
Laguna Jancho Kkota*	
Laguna Khara Kkotana*	
Laguna Khoa Churo*	
Laguna Khollpa Kkota	
Laguna Kkota Pata*	
Laguna Kollpa Kkota	
Laguna Sorka Kkota*	
Nevados Payachata quadrangle	
Laguna Chiar Kkota*	
Laguna Inca Ingenio*	
Corque quadrangle	
Laguna Andapata	
Laguna Anocara	
Laguna Anto Kkota	
Laguna Canasa	
Laguna Chica Micaya	
Laguna Copachamaya*	
Laguna Jachcha Huaña*	
Laguna Jankho Kkota	
Laguna Jaya Kkoya	
Laguna Jayu Kkota	2; 4; 10
Laguna Khara Kkota*	
Laguna Khara Kkotalla*	
Laguna Khellu Kkota*	
Laguna Kirquiza*	
Laguna Kkota Cancha	
Laguna Kkota Sayaña	
Laguna Kollpa Khara	
Laguna Mallcu Kkota	
Laguna Melchor Kkota	
Laguna Pakkollu	
Laguna Parina Kkota*	
Laguna Sacabaya	
Laguna Seca	
Laguna Sicoko Kkota	
Laguna Tujsa Kkota	
Laguna Uma Sayaña*	
Laguna Wila Khara	
Lagunas Jayu Kkota	
Uncia quadrangle	
Lago Poopó	1; 7
Lago Uru Uru	
Laguna Jankho Kkota	
Laguna Kkotaña*	
Laguna Salade*	
Salinas de Garci Mendoza quadrangle	
Laguna Berta Khara	
Laguna Calcha*	
Laguna Challuma*	
Laguna Huaña Toro*	
Laguna Huara Huar Kkota*	
Laguna Huaramuar Kkota*	
Laguna Irupata Kkotaña*	
Laguna Jamachuma*	
Laguna Jankho Taque*	
Laguna Jaruma Khara	
Laguna Jayu Kkota	
Laguna Khasoj Saya	
Laguna Lamaniquima	
Laguna Malloc Challa	
Laguna Quichar Kkotaña	
Laguna Tropen Kkota	
Salar de Coipasa	1; 5; 11

Table 10. *List of selected named salars and lakes*—Continued

Name	Reference(s)
Río Mulato quadrangle	
Lago Poopó	1; 7
Laguna Anti Kkota*	
Laguna Charajayu Kkota*	
Laguna Chihua Kkota*	
Laguna Chihuana Kkota*	
Laguna Chira Kkota	
Laguna Corpo Kkota	
Laguna Hiare	
Laguna Huacuyo*	
Laguna Huancarani Kkota	
Laguna Itoro	
Laguna Jamach Kkota*	
Laguna Jankho Kkota	
Laguna Jarruma	
Laguna Jayo Kkota	
Laguna Jayu Kkota *	
Laguna Jayuma	
Laguna Jiskha Huanapa*	
Laguna Khara Kkota	
Laguna Khasilla	
Laguna Kkotathek	
Laguna Kocha Pampa*	
Laguna Lagunillas	
Laguna Orkho Khasilla*	
Laguna Parco Kkota	
Laguna Pequereque	
Laguna Prestia	
Laguna Quisa Vinto	
Laguna Sevaruyo	
Laguna Taypi Kkota*	
Laguna Vengalla*	
Laguna Wara Wara	
Laguna Wila Kkota*	
Villa Martin quadrangle	
Laguna Rosada*	
Salar de Empexa	1; 2; 4; 5; 11
Salar de la Laguna	1; 10
Salar Laguani	1; 5; 10
Salar de Uyuni	1; 5; 8; 11
Uyuni quadrangle	
Laguna Allita	
Laguna Anayuri*	
Laguna Butajani*	
Laguna Chacavi	
Laguna Chilchasi*	
Laguna Colorada*	
Laguna Huayllapata*	
Laguna Jatun Khocha*	
Laguna Khara Kkota*	
Laguna Kocha Grande	
Laguna Khocha Phi Ro*	
Laguna Kollpa Kkota	
Laguna Kusmani	
Laguna Vela Kkota*	
Laguna Vila Kkota	
Laguna Wila Kkota	
Salar de Uyuni	1; 5; 8; 11
Volcán Ollague quadrangle	
Laguna Balivian*	9
Laguna Blanca (Oeste)*	
Laguna Cachallcha*	
Laguna Cachi	1; 4; 6; 9; 10
Laguna Cañapa	1; 2; 5; 9; 10
Laguna Capina	1; 4; 9; 10
Laguna Chiar Kkota	1; 2; 4; 9; 10
Laguna Chulluncani	1; 9
Laguna Hedionda (Norte)	1; 2; 4; 9; 10
Laguna Honda (Norte)*	1; 9
Laguna Khara	1; 3; 9; 10
Laguna Ramaditas	1; 2; 4; 9; 10
Laguna Pujio*	9
Laguna Tarha*	
Laguna Turquiri*	9
Laguna Turuncha	
Laguna Yapi	
Lagunas Pastos Grandes	1; 2; 5; 9; 10
Salar de Chiguana	1; 10
Salar de Ollague	
San Pablo de Lípez quadrangle	
Laguna Achata	
Laguna Chijlla Khasa*	
Laguna Chuan	
Laguna Cuevas*	
Laguna Huaylla Khara	
Laguna Khocha	
Laguna Khosko	
Laguna Murusa	
Laguna Novillo	
Laguna Potrero	
Laguna Puca	
Laguna Puca Khocha	
Laguna Salitre	
Laguna Vena*	
Laguna Yapi	
Volcán Juriques quadrangle	
Laguna Colorada	1; 9
Laguna Guayaques	
Laguna Jachi*	
Laguna Lagunillas	9

Table 10. *List of selected named salars and lakes*—Continued

Name	Reference(s)
Laguna Puripica Grande	9
Laguna Verde	1; 9
Salar de Challviri	1; 9; 10
Cerro Zapaleri quadrangle	
Laguna Alto Tuilis*	
Laguna Arenal	
Laguna Bateitas*	
Laguna Blanca*	
Laguna Busch o Kalina	9
Laguna Callejon	
Laguna Campo Grande	
Laguna Carancho*	
Laguna Catalcito	9
Laguna Celeste	
Laguna Champa*	
Laguna Chipapa*	
Laguna Chojllas	9
Laguna Colorada*	
Laguna Corante	
Laguna Coruto	9
Laguna Fraile*	
Laguna Galera*	
Laguna Guacha*	
Laguna Hedionda (Sur)	1; 3; 9
Laguna Honda (Sur)*	1; 9
Laguna Huira Sokha*	
Laguna Khastor	
Laguna Khonchu	
Laguna Kollpa	1; 3; 9; 10
Laguna Larga*	
Laguna Loromayu	9
Laguna Luriques	9
Laguna Mama Khumu	9
Laguna Morejon	
Laguna Pelada	9
Laguna Peñitas Blancas*	
Laguna Seca*	
Laguna Sombrerito*	
Laguna Sombrerituyoj*	
Laguna Thiuyoj*	
Laguna Totoral	9
Laguna Tucunqui	
Laguna Tullu Jara	
Lagunas Hoyito*	

occurrence of lithium-enriched brines would consist of sequences of Tertiary to Quaternary continental sediments with a surface playa and contemporaneous volcanic rocks to supply a source of lithium.

The boron in saline-alkaline lakes and salars in closed or semi-closed basins is thought to originate from thermal springs associated with felsic- to intermediate-composition volcanic rocks. Alternatively, the boron may be leached from volcanic rocks. The boron content of the lake or salar is elevated through the process of evaporation. No published information was found on the level of boron concentration needed for a brine to be potentially economic. Brines are not a major source of boron production, but boron is a coproduct of brine operations at Searles Lake, Calif. and Lake Inder, U.S.S.R. and is planned as a byproduct of Salar de Atacama, Chile, brine operations. Many of Bolivia's lakes and salars have elevated boron contents including, among others, scattered localities in the Salar de Uyuni, Laguna Chojllas, Laguna Busch o Kalina, Laguna Loromayu, the vicinity of Río Sabaya in the northern Salar de Coipasa, Laguna Chiar Kkota, and Laguna Cachi. Other boron-enriched brines might form in Tertiary to Quaternary basins containing alkaline lakes, saline lakes, or playas with associated contemporaneous volcanic rocks to supply a source of boron.

Natural sodium carbonate or soda ash is subordinate to synthetic soda ash in terms of world supply. Most natural soda ash is produced in North America and production is dominated by trona production from the Green River, Wyo. lacustrine deposits. The content of natural sodium carbonate in lake waters is attributed to a variety of sources including thermal-spring activity. Ground water draining igneous and metamorphic terrains yields alkaline solutions that are relatively chlorine and sulfate poor; sodium may be derived from leaching of feldspars or sodium-rich rocks and carbon dioxide from organic matter and the atmosphere (Mannion, 1975). Sodium carbonate is produced from concentrations in brine as low as 0.8 percent sodium carbonate, but most production is from brines containing 4–11 percent sodium carbonate. Sodium carbonate is produced from brine at Searles Lake, Calif., and Lago Texcoco, Mexico, and is planned at Sua Pan, Botswana. In Bolivia, past production from brine at Laguna Cachi was not economically sustainable (Ahlfeld and Schneider-Scherbina, 1964; Mannion, 1975). Other lakes and salars in Bolivia containing elevated sodium carbonate contents in brine include Laguna Kollpa, Laguna Hedionda Sur, and Laguna Khara.

Like sodium carbonate, most sodium sulfate is produced by synthetic methods, although production from natural sources is important in North America, the U.S.S.R., Turkey, Argentina, and Spain (Harben and Bates, 1990). Like waters enriched in sodium carbonate, sodium sulfate waters are believed to drain areas of igneous and metamorphic rocks. Seasonal drops in temperature may lead to crystallization of mirabilite on the surface of sodium sulfate brines; warming leads to resolution of the mirabilite into the brine. Several lakes in Saskatchewan, Canada produce sodium sulfate from lake brines; sodium sulfate is also produced from brines of Great Salt Lake, Utah, Searles Lake, Calif., Laguna del Rey, Mexico, and Tersakan Lake, Turkey. Brines containing elevated sodium sulfate contents in Bolivia include those at Laguna Cañapa, Laguna Chulluncani, and Laguna Hedionda Norte.

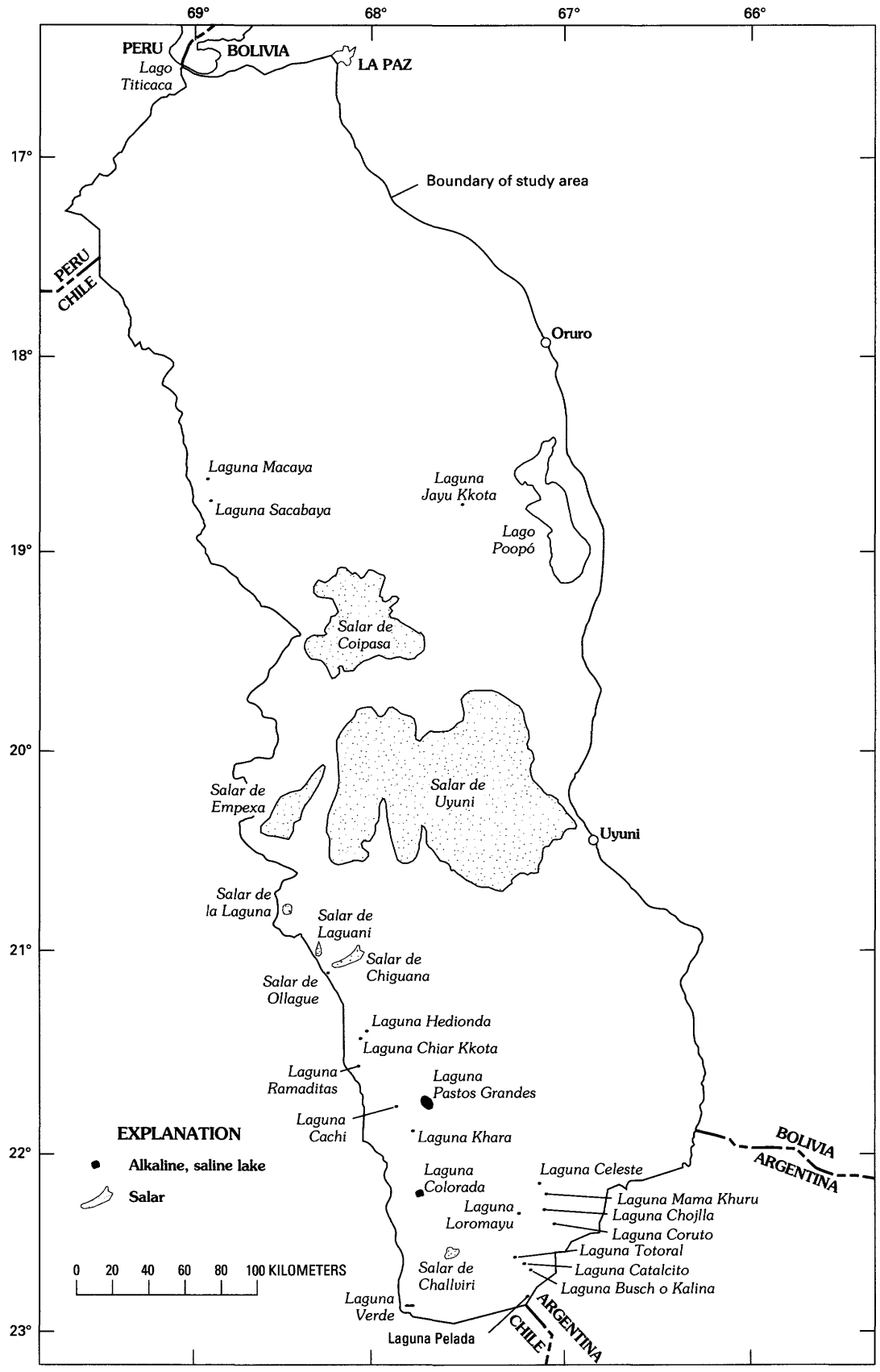


Figure 42. Map showing location of salars and alkaline or saline lakes on the Altiplano and in the Cordillera Occidental, Bolivia, visited during this study and (or) discussed in the text.

Potash production from brines is of minor importance on a world scale, but important locally. Potash is produced from brines of Great Salt Lake, Utah, Searles Lake, Calif., Bonneville Salt Flats, Utah, and Lake Mcleod, Australia. The Bolivian lakes and salars containing elevated potassium contents include, among others, Laguna Hedionda Norte, Laguna Capina, Laguna Chulluncani, and Salar de Uyuni.

Salts

In addition to brines, most saline and alkaline lakes are edged or partially encrusted by precipitates related to their brine composition. Salars, or playas, often have no brines at the surface and are easily identified by expanses of surficial white salts and clays. The most common precipitate is halite or rock salt. Playa halite deposits are commonly bedded and deposits are known in the western United States that are over 30 m thick (Papke, 1976). When buried relatively deeply, these continental salt deposits will be deformed into dome structures, much like marine bedded salt. Worldwide, continental halite deposits are of little importance compared with salt mined from marine deposits or extracted from sea water. Locally, continental evaporite deposits of salt may be a major source of production. In Bolivia, halite occurs in the Late Tertiary-Quaternary salar and saline-lake deposits and in sequences of older Tertiary lacustrine sediments. There are no marine evaporites known. Salar de Uyuni is estimated to contain more than 64 billion metric tons of halite in its crust. Other recent salars contain smaller resources. Mina de Jayuma de Llallagua, on the northern Altiplano, exploits a relatively thick sequence of gypsum and halite from the Tertiary Chacarilla Formation to produce halite.

Like halite, deposits of gypsum are common on the Altiplano and in the Cordillera Occidental. These lacustrine deposits occur in the same geologic contexts as the halite deposits. Gypsum has been identified in the salt crusts of Laguna Cañapa, Salar de Empexa, Laguna Honda Norte, Laguna Jayu Kkota, Lagunas Pastos Grandes and other saline lakes and salars. Gypsum occurs in the Tertiary Chacarilla Formation at Jayuma de Llallagua and is mined at the Crucero mine from the Oligocene-Miocene Totora Formation.

Lithium is most likely to be valuable when it is a brine constituent. Lithium ore minerals are unlikely to be found in an evaporitic sedimentary environment; instead, lithium will be incorporated into the crystal structures of clays and others minerals. Lithium does impart some unique characteristics to clays (see hectorite discussion), but these forms are not of interest for their lithium contents.

The main potassium minerals are sylvite, carnallite, kainite, and langbeinite; commonly combinations of these or other potassium chlorides and sulfates will occur. Because potassium is highly soluble, potassium salts only form under conditions of extreme evaporation. Because of extensive reserves of marine potash, continental lacustrine deposits are rarely exploited, and, when they are mined, they are mined for potash-bearing brines. In Bolivia, sylvite has been identified at Laguna Kollpa and Salar de Uyuni, but the deposits are not large. Sylvite has also been identified in minor amounts in older Tertiary halite deposits. Continental lacustrine sediments with abundant halite are permissive for potassium salts.

Sodium carbonate most commonly precipitates as the minerals trona, natron, or thermonatrite in the Bolivian salars and alkaline lakes. In young playa and alkaline-lake deposits, natron tends to form crystals in cool, wet environments. Thermonatrite will form powdery efflorescences at the surface. Relatively massive and hard deposits of trona will be deposited around the shores or at the bottom of shallow alkaline lakes (Mannion, 1975). Sodium carbonate minerals are commonly mixed with other salts, especially sulfates and chlorides. The occurrence of extensive deposits of trona, nahcolite, or other sodium-carbonate-bearing minerals in Bolivia similar to the Green River, Wyo. deposits is not considered to be likely from the available data, although it is possible. Small- to moderate-sized deposits may be associated with the development and desiccation of recent alkaline lakes.

Sodium sulfate mineralization is widespread on the Altiplano and in the Cordillera Occidental. The most common identified mineral form is mirabilite. Mirabilite contains approximately 56 percent water and is known for its spontaneous loss of water (Weisman and Tandy, 1975). At temperatures below 29.8 °F, mirabilite will precipitate from sodium sulfate brines. Preservation of sodium sulfate deposits over time requires interstratified layers of less soluble salts and clays. In Bolivia, mirabilite and tenardite have been identified at Laguna Cañapa. Mirabilite has been noted at Laguna Colorada, Laguna Hedionda Norte, and Laguna Honda Norte. At Salar de la Laguna, small amounts of sodium sulfate have been produced intermittently. Sodium sulfate is widely distributed throughout the Altiplano and Cordillera Occidental, but known surficial resources are relatively small in terms of total tonnage. Any additional resource would need to be at depth.

Borates

Borate mineralization is one of the most promising of the deposit types associated with saline-alkaline lakes and salars. Ulexite is the most widespread of the borate minerals in Bolivia where it forms efflorescences at or near the surface of playas and at the edges of saline and alkaline lakes; this is the most common occurrence mode for ulexite. On a worldwide basis, ulexite is commonly found mixed with colemanite (at depth, colemanite is more abundant than ulexite), less commonly with borax and proberite, and at times with a wide variety of other borate minerals some of which may be considered to be contaminants for purposes

of mining. A variety of processes have been proposed for world occurrences of borate minerals including deposition as spring aprons, precipitation from stratified alkaline lakes, and precipitation as an evaporite. In Bolivia, these environments often overlap and in the past may have succeeded one another.

While we have little information about the shape or depth of the basins on the Altiplano and in the Cordillera Occidental, we do know that geologic conditions have been permissive for the development of borate deposits for moderate periods of time on several occasions during the Tertiary and Quaternary. Using a model based on worldwide occurrences of borate deposits with surficial deposits of ulexite (Orris, 1991), the following generalizations can be made. If borate deposits occur below or peripheral to the surface playas and lakes, the mineralization is most likely to be a mixture of colemanite and ulexite; borax and proberite may occur in varying amounts. The mineralization in a basin is most likely to consist of several small- to moderately sized bodies that are spatially associated and at varying depths. Colemanite and borax have been recognized in Bolivia, although no references to proberite have been found. Small bodies of borax, colemanite, and ulexite have been mined from Salar de Challviri and borax and colemanite have been reported in small amounts at the surface of several sites. This information supports the hypothesis of mineralization at depth.

Hectorite

Hectorite is a lithium-rich smectite that differs from standard montmorillonite in that aluminum is virtually absent in the crystal structure, lithium substitutes for magnesium, and fluorine substitutes for hydroxyl groups. This leads to a smectite with excellent gelling properties. Hectorite is postulated to form in one of three ways: alteration of vitric volcanic rock to lithium-rich smectite; precipitation from lithium-enriched lake waters; or incorporation of lithium into existing smectites (Asher-Bolinder, 1991b). Each of these genetic models is characterized by the presence of silicic volcanic rocks, lacustrine sedimentation, abundant magnesium, lithium-enriched fluids (saline, alkaline lake), a closed basin, and an arid environment. Known hectorite deposits are spatially associated with evaporite deposits of borates and gypsum, sedimentary zeolite deposits, calcium carbonates, and other bentonite deposits. Hectorite, although rarely mined, can be a high unit-value mineral with, among others, uses in the cosmetic industry, and for drilling muds.

Sedimentary Zeolites

Sedimentary zeolites have not been identified in the study area; however, little work has been done on the Quaternary and Late Tertiary lacustrine sedimentary units and associated tuffs. Zeolites have been identified in amygdales of a Quaternary basaltic unit in the Charaña basin by Eduardo Soria-Escalante (oral commun., 1990). Zeolites may form during early diagenesis of rhyolitic to dacitic vitric tuffs in closed basins (Sheppard, 1991; Sheppard and others, 1987). As summarized from Sheppard (1991), over periods of thousands to hundreds of thousands of years, zeolites crystallize from the reaction of the vitric tuff with saline, alkaline pore water trapped during lacustrine sedimentation. The saline lake water in these systems is of the sodium carbonate-bicarbonate type with a pH of 9 or greater. The deposits may be concentrically zoned from unaltered volcanic glass to alkali-rich, silicic zeolites to analcime and then to potassium feldspar in the central part of the basin.

Sedimentary zeolite deposits in closed basins may be composed of a wide variety of zeolite species, but are especially notable as a source of chabazite, erionite, and phillipsite. The age range of known deposits of this type throughout the world is late Paleozoic to Holocene; most of these deposits are Cenozoic. Other deposit types spatially associated with this deposit type include bedded lacustrine evaporites (halite, trona, borates), diatomite, and lacustrine carbonates and clays.

The closed basins of the Bolivian Altiplano and Cordillera Occidental have been commonly occupied by alkaline lakes and salars during the Holocene to recent times. Indications are that extensive sequences of lacustrine evaporites have been deposited periodically in the same basins or earlier basins since the early Tertiary. These lacustrine deposits have formed in the presence of continuing volcanic activity. It is therefore logical to presume that conditions have been locally favorable for formation of sedimentary zeolite deposits at various times. It is likely that several deposits of this type will be identified as larger scale mapping of the lacustrine volcaniclastic deposits is completed.

Lacustrine Diatomite

Diatomite is a light-colored sedimentary rock composed of the siliceous skeletal remains of microscopic aquatic plants called diatoms. Lacustrine diatomite deposits form in fresh to brackish water in basins near active volcanism (Shenk, 1991). It is widely held that the large quantity of silica necessary for large accumulations of diatomite is silica released by the weathering and decomposition of silica-rich volcanic rocks. The silica is transported as runoff, ground water, and through systems of springs. Basinal characteristics necessary for thick accumulations of diatomite include "(1) extensive, shallow basins for photosynthesis; (2) an abundant supply of soluble silica and nutrients; (3) an absence of toxic or growth-inhibiting constituents; (4) sustained high rates of diatom

reproduction; (5) minimal clastic, chemical, and organic contamination; and (6) a low-energy environment for preservation of the delicate diatom structure" (Shenk, 1991). Lacustrine diatomite deposits are commonly associated with lacustrine evaporite deposits, especially gypsum and trona.

Occurrences of diatomite are common on the Altiplano and in basins of the Cordillera Occidental. Diatoms have been reported in superficial sediments of Lago Poopó (Servant-Vildary, 1978a). Diatoms have also been found in Quaternary Tauca Formation rocks east and north of Uyuni, near Culluri west of Lago Poopó and at Escara north of Salar de Coipasa. Diatoms are also reported in the following formations of Quaternary age: in the Charaña Formation at Charaña; in the Lauca Formation at Lauca and Tres Cruces; in the Ulloma Formation at Calacoto and Nazacara; in the Minchin Formation northwest of Salar de Uyuni at Chuca Khaua; in the Quaternary Vito Formation at Vito south of Salar de Uyuni; and in Holocene surficial sediments at Ayo Ayo and Toponoco (Servant-Vildary, 1978b). In Sud Lípez, diatomite has been reported to occur at Laguna Honda Norte and Laguna Colorada (Ballivian and Risacher, 1981).

BARITE VEINS

Barite is known to occur in veins in the study area. Throughout the world, epigenetic barite commonly occurs along faults, fractures, and shear zones in a wide variety of host rocks (Clark and Orris, 1991). Barite deposits are commonly spatially and (or) genetically associated with major base- and precious-metal deposits including sediment-hosted Au-Ag, sedimentary exhalative Zn-Pb, polymetallic veins, epithermal Au-Ag, and Kuroko massive sulfide deposits, as well as a wide variety of industrial mineral deposit types including evaporites. Barite mineralization commonly forms zones peripheral to these other deposit types. Barite veins commonly have widths ranging from a few centimeters to tens of meters and lengths ranging from tens of meters to more than 1 km.

Most of the known occurrences of barite in veins on the Altiplano and in the Cordillera Occidental are spatially and genetically associated with polymetallic vein mineralization; examples include barite mineralization in the San Cristobal and Jaquegua areas. Several occurrences of barite are known just outside of the study area including a small barite mine in Devonian rocks near the La Paz-Palca road which is mined for the paint industry in La Paz, barite and barite-mercury veins in Devonian sandstone near Huarina that are mined for use in drilling mud, and barite veins in Ordovician rocks south of Anzaldo (Ahlfeld and Schneider-Scherbina, 1964).

DIMENSION STONE

Dimension stone is rock, commonly attractive to the eye, that is quarried for use in specialized dimensional applications, such as building stone, monumental stone, flagging, roofing and mill-stock slate, curbing and paving stone, and a variety of other uses. Desirable dimension stone characteristics include chemical and physical invulnerability, as well as an attractive appearance. Appearance is commonly judged using homogeneity of mineralization, grain size, and color; eye appeal being the dominant consideration. About three-fourths of the dimension stone market is met by rocks of igneous origin and indiscriminately termed "granites;" marble, limestone, slate, and sandstone compose most of the rest of the dimension stone market. Attractive, good quality dimension stone can command a world market. For example, black granite from Uruguay is sold in Asia and travertine and marble from the Carrara district of Italy is renowned and used throughout the world.

Two major rock types, andesite and travertine are quarried for use as dimension stone in Bolivia; other rock types are mined for strictly local use as building stone. The use of stone as a building material on the Altiplano has its roots in pre-Incan civilization. The major granite production is from the Comanche quarry, operated by Compañía Minera del Sur, where a fine-grained, equigranular, medium-gray andesite is quarried for use as paving stone in La Paz. Additional production of 7 cm by 7 cm paving stones for shipment to Belgium is planned. The intrusive body is small with nonperpendicular curvilinear jointing and limited reserves.

At least three quarries in the study area have produced travertine for use as building stone, the Mirzapani Quarry near Berenguela de Pacajes, the Lomitas Quarry near Sicasica, and a quarry near Soniquera for which no name is known. The travertine is a carbonate sinter deposited by springs and typically has a banded translucent appearance. Some of the material from the Mirzapani Quarry is sold as onyx marble. These travertines take a good polish and commonly resemble true onyx.

It is difficult to consider all of the possible sources for dimension stone; in a general sense any rock has some potential for use as a building or paving material. Local use of building stone is dictated by the availability of materials that are relatively easy to shape for a specific use, as well as the level of need for durability. In contrast, material suitable for shipping any distance must exhibit a natural beauty, as well as more measurable characteristics, such as resistance to chemical and physical erosion.

FUMAROLIC SULFUR

Fumarolic sulfur deposits are the best inventoried of the industrial mineral deposit types in Bolivia, probably

because they are easy to identify and relatively simple to mine. The following discussion of fumarolic sulfur deposits is taken largely from Long (1991). Fumarolic sulfur deposits are commonly composed of surficial sublimates, open-space fillings and replacements of native sulfur in the vent areas of volcanoes. The sulfur mineralization is hosted by porous volcaniclastic rocks and lava flows, and less commonly by underlying or adjacent sedimentary rocks. In the solfataric alteration zones where deposits are found, the host rock is replaced by quartz, sulfur, and minor calcite; in the areas of most intense alteration, the host rock is reduced to alunite and clay. Other minerals found in fumarolic sulfur deposits include orpiment, realgar, manganese-bearing minerals, pyrite (wet climate), and gypsum (dry climate). Fumarolic sulfur deposits are not likely to survive weathering and are commonly Late Miocene to Recent in age.

In Bolivia, the largest known fumarolic sulfur deposit is Mina Susana, which has been reported by mine personnel to contain 40 million tonnes of 48–54 percent sulfur ore, as well as 280 million tonnes of 18–35 percent sulfur ore. Fumarolic sulfur deposits are found at or near the summits of active volcanoes and large zones of solfataric alteration have commonly been exposed by glaciation which removed relatively unaltered outer lavas (fig. 43). The ore typically consists of disseminated fine-grained sulfur in a matrix of white clay (kaolinite? and (or) bentonite?) and alunite; many of the deposits have active fumaroles where sulfur is being precipitated. Some deposits, such as Mina Susana have zones of large clear crystals of remobilized sulfur. Other minerals deposited by these systems include arsenic minerals, commonly orpiment and realgar, and hydrothermal manganese minerals. Gypsum has been reported as a gangue mineral at several sulfur mines, but was not observed during this study.

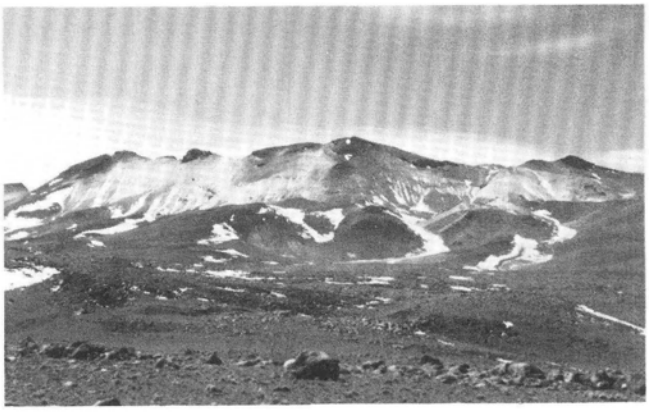


Figure 43. Solfataric alteration at Mina Juanita forms the irregular light-colored area at the summit of Cerro Amarillo, Sud Lípez, Potosí, Bolivia.

Geology of Known Mineral Deposits

Introduction **95**
Copper deposits in sedimentary rocks *by* Dennis P. Cox, Raul Carrasco, Orlando André-Ramos, Alberto Hinojosa-Velasco, *and* Keith R. Long **95**
- Introduction **95**
- San Silvestre area **95**
  - Ana María mine **97**
  - Vatutin mine **97**
  - La Incognita mine **97**
  - María Elena mine **97**
  - Palmira mine **97**
  - La Casualidad-San Fransisco mine **97**
  - San Silvestre mine **97**
  - Tres Amigos mine **97**
  - Virgen de Fatima mine **97**
- Chacoma area **97**
  - Chacoma mine **98**
  - Las Mercedes mine **98**
- Corocoro area **98**
  - Porvenir mine **98**
  - Llallagua mine **98**
  - María Elena-Victoria mine **98**
  - Pisaqueri (Anaconda) mine **98**
  - Americas Unidas mine **99**
  - Transvaal mine **99**
  - Pontezuelo mine **99**
  - Corocoro district **99**
  - Veta Verde mine **101**
- Callapa area **101**
  - El Hogar mine **101**
  - Noe group **101**
  - San Agustín mine **102**
  - San Francisco prospect **102**
  - San Miguel mine **102**
- Chacarilla area **102**
  - Chacarilla district **102**
  - Esperanza mine **103**
  - La Encontrada mine **103**
- Chuquichambi area **103**
  - Llanquera-San Miguel prospects **103**
  - Santa María prospect **103**
- Turco area **103**
  - Santa Clara mine **103**
  - Azurita mine **103**
  - Corona de España mine **104**
  - Cuprita mine **104**
  - Chihuirari mine **104**
- Sevaruyo area **104**
  - Amistad mine **105**

Concepción prospect **105**
Tambillo mine **105**
Uyuni area **105**
Koholpani mine **105**
Puntillas mine **105**
Iñes mine **105**
Esmeralda area **105**
Esmeralda and San Pedro mines **105**
San Pablito occurrence **105**
Mesa Verde occurrence **105**
Ucrania prospect **106**
Huancané mine **106**
Rosario prospect **106**
Ladislao Cabrera mine **106**
Serranía de las Minas area **106**
Farellón mine **106**
Cerro Colorado (Negra) mine **106**
25 de Julio (Peña Blanca) mine **106**
Copacabana mine **106**
Bartolo mine **106**
Avaroa area **106**
Avaroa mine **107**
Bolívar mine **107**
Mantos Blancos mine **107**
El Morro mine **107**
Linares mine **107**
Cerro Negro mine **107**
Aguilar mine **107**
Alianza mine **107**
Sucre mine **108**
Argentine border area **108**
Aviadora mine **108**
Campanario occurrence **108**
Deposits related to stratovolcanoes **108**
Introduction **108**
Altered areas **108**
Wara Wara prospect (Cerro Phasa Willkhi) *by* James C. Ratté, B.M. Gamble, *and* Alberto Hinojosa-Velasco **108**
María Elena prospect (Cerro Culebra) *by* James C. Ratté, B.M. Gamble, Edwin H. McKee, Eduardo Soria-Escalante, *and* Raul Carrasco **110**
Milenka prospect (Cerro Curumaya) *by* James C. Ratté, B.M. Gamble, Eduardo Soria-Escalante, *and* Raul Carrasco **112**
Cerro Puquisa *by* Eduardo Soria-Escalante *and* René Enriquez-Romero **112**
Iñexa prospect (Intersalar Range) *by* Eduardo Soria-Escalante *and* René Enriquez-Romero **114**
Cerro Eskapa *by* Donald H. Richter, W. Earl Brooks, Nora Shew, Alberto Hinojosa-Velasco, *and* Angel Escobar-Diaz **116**
Cerro Cachi Laguna *by* W. Earl Brooks, Donald H. Richter, Alberto Hinojosa-Velasco, *and* Angel Escobar-Diaz **118**
Cerro Poderosa-Cerro Amarillo *by* Donald H. Richter, W. Earl Brooks, Angel Escobar-Diaz, *and* Alberto Hinojosa-Velasco **119**
Fumarolic native sulfur deposits **122**
Cerro Saca Sacani *by* B.M. Gamble, James C. Ratté, Raul Carrasco, *and* Eduardo Soria-Escalante **123**
El Desierto area *by* G.J. Orris, Sigrid Asher-Bolinder, Eduardo Soria-Escalante , *and* René Enriquez-Romero **123**
Mina Olca *by* G.J. Orris, Sigrid Asher-Bolinder, Eduardo Soria-Escalante, *and* René Enriquez-Romero **123**

Mina Susana *by* G.J. Orris, Sigrid Asher-Bolinder, Eduardo Soria-Escalante, *and* René Enriquez-Romero **124**
Bolivian polymetallic vein deposits **125**
Introduction **125**
Quimsa Chata (Tiahuanacu) district *by* Orlando André-Ramos *and* Keith R. Long **125**
Berenguela district *by* Alan R. Wallace **129**
La Joya district *by* Keith R. Long, Steve Ludington, Edward A. du Bray, Orlando André-Ramos, *and* Edwin H. McKee **131**
Todos Santos district *by* B.M. Gamble, James C. Ratté, Raul Carrasco, Eduardo Soria-Escalante, *and* Edwin H. McKee **136**
Salinas de Garci Mendoza district *by* James C. Ratté, B.M. Gamble, Raul Carrasco, *and* Eduardo Soria-Escalante **143**
Sonia-Susana area *by* B.M. Gamble, James C. Ratté, Eduardo Soria-Escalante, *and* Raul Carrasco **151**
San Cristobal district *by* Donald H. Richter, W. Earl Brooks, Steve Ludington, Alberto Hinojosa-Velasco, Angel Escobar-Diaz, Edwin H. McKee, *and* Nora Shew **153**
Comunidad Todos Santos area *by* Steve Ludington *and* Edward A. du Bray **157**
Escala district *by* Donald H. Richter, W. Earl Brooks, Dennis P. Cox, Nora Shew, Elizabeth A. Bailey, Alberto Hinojosa-Velasco, *and* Angel Escobar-Diaz **159**
Santa Isabel district *by* Donald H. Richter, W. Earl Brooks, Angel Escobar-Diaz, *and* Alberto Hinojosa-Velasco **161**
Buena Vista area *by* Steve Ludington, Gerald K. Czamanske, Raul Carrasco, Alberto Hinojosa-Velasco, *and* Edwin H. McKee **164**
Cerro Bonete area *by* Donald H. Richter, Steve Ludington, W. Earl Brooks, Edward A. du Bray, René Enriquez-Romero, Elizabeth A. Bailey, Alberto Hinojosa-Velasco, Gregory E. McKelvey, Eduardo Soria-Escalante, *and* Angel Escobar-Diaz **166**
Morokho area *by* Steve Ludington, Edward A. du Bray, Gregory E. McKelvey, *and* Eduardo Soria-Escalante **174**
San Antonio de Lípez area *by* Steve Ludington, Edward A. du Bray, Donald H. Richter, *and* Gerald K. Czamanske **176**
Esmoraca area *by* Steve Ludington, Edward A. du Bray, Gregory E. McKelvey, Eduardo Soria-Escalante, *and* Gerald K. Czamanske **179**
Jaquegua area *by* Steve Ludington, Edward A. du Bray, *and* Eduardo Soria-Escalante **182**
Other metallic deposits **184**
Introduction **184**
La Española prospect *by* Eduardo Soria-Escalante *and* Rubén Terrazas **184**
Pachekala prospect *by* Steve Ludington, Edward A. du Bray, *and* Eduardo Soria-Escalante **187**
Laurani area *by* Steve Ludington *and* Edward A. du Bray **189**
Kiska prospect *by* Steve Ludington, Edward A. du Bray, *and* Edwin H. McKee **191**
Chinchilhuma volcano area *by* Eduardo Soria-Escalante *and* René Enriquez-Romero **192**
San Francisco mine *by* Donald H. Richter, W. Earl Brooks, Angel Escobar-Diaz, *and* Alberto Hinojosa-Velasco **194**
Mineral deposits associated with lakes and salars **195**
Introduction **195**
Laguna Sacabaya *by* Sigrid Asher-Bolinder, Eduardo Soria-Escalante, Eduardo Camacho, *and* William Blacutt **196**
Salar de Coipasa *by* G.J. Orris, Sigrid Asher-Bolinder, Eduardo Soria-Escalante, *and* René Enriquez-Romero **196**
Salar de Empexa *by* G.J. Orris, Sigrid Asher-Bolinder, Eduardo Soria-Escalante, *and* René Enriquez-Romero **197**
Salar de la Laguna *by* G.J. Orris, Sigrid Asher-Bolinder, Eduardo Soria-Escalante, *and* René Enriquez-Romero **197**
Laguna Hedionda Norte *by* G.J. Orris, Sigrid Asher-Bolinder, Eduardo Soria-Escalante, *and* René Enriquez-Romero **198**
Laguna Chiar Kkota *by* G.J. Orris, Sigrid Asher-Bolinder, Eduardo Soria-Escalante, *and* René Enriquez-Romero **199**
Lagunas Pastos Grandes *by* G.J. Orris, Sigrid Asher-Bolinder, Eduardo Soria-Escalante, *and* René Enriquez-Romero **199**

Laguna Cachi *by* G.J. Orris, Sigrid Asher-Bolinder, Eduardo Soria-Escalante, René Enriquez-Romero, *and* E.A. Bailey **199**
Laguna Capina *by* G.J. Orris, Eduardo Soria-Escalante, Sigrid Asher-Bolinder, *and* René Enriquez-Romero **200**
Laguna Celeste *by* G.J. Orris, René Enriquez-Romero, *and* Eduardo Soria-Escalante **201**
Laguna Colorada *by* G.J. Orris, Sigrid Asher-Bolinder, Eduardo Soria-Escalante, René Enriquez-Romero, *and* E.A. Bailey **201**
Laguna Mama Khumu *by* G.J. Orris, René Enriquez-Romero, *and* E.A. Bailey **202**
Laguna Chojllas *by* G.J. Orris, Eduardo Soria-Escalante, *and* René Enriquez-Romero **202**
Laguna Loromayu *by* Sigrid Asher-Bolinder, Eduardo Soria-Escalante, *and* G.J. Orris **203**
Laguna Coruto *by* G.J. Orris, René Enriquez-Romero, *and* Eduardo Soria-Escalante **203**
Salar de Challviri *by* G.J. Orris, Sigrid Asher-Bolinder, Eduardo Soria-Escalante, *and* René Enriquez-Romero **204**
Laguna Catalcito *by* Sigrid Asher-Bolinder *and* Eduardo Soria-Escalante **204**
Laguna Busch o Kalina *by* Sigrid Asher-Bolinder *and* Eduardo Soria-Escalante **205**
Laguna Verde *by* G.J. Orris, Sigrid Asher-Bolinder, Eduardo Soria-Escalante, René Enriquez-Romero, *and* E.A. Bailey **205**
Other industrial mineral deposits **206**
CORDEOR clay pit *by* Sigrid Asher-Bolinder, Eduardo Soria-Escalante, *and* G.J. Orris **206**
Mina Comanche *by* G.J. Orris, Sigrid Asher-Bolinder, Raul Carrasco, *and* Marcelo Claure Zapata **207**
Mina Santa Rosa *by* G.J. Orris, Sigrid Asher-Bolinder, *and* Orlando André-Ramos **207**
Volcán Quemado *by* Sigrid Asher-Bolinder *and* Eduardo Soria-Escalante **208**
Barrero sodium carbonate plant *by* Sigrid Asher-Bolinder, G.J. Orris, Eduardo Soria-Escalante, *and* René Enriquez-Romero **208**
El Desierto sulfur plant *by* G.J. Orris, Sigrid Asher-Bolinder, Eduardo Soria-Escalante, *and* René Enriquez-Romero **208**
Mina Susana sulfur plant *by* G.J. Orris, Sigrid Asher-Bolinder, Eduardo Soria-Escalante, *and* René Enriquez-Romero **209**
Laguna Kollpa sodium carbonate plant *by* Sigrid Asher-Bolinder *and* Eduardo Soria-Escalante **209**

FIGURES

44. Map showing areas of known sediment-hosted copper deposits **96**
45. Geologic sketch map and cross section of the Corocoro area **100**
46. Geologic sketch map and cross section of the Veta Verde area **101**
47. Geologic sketch map and cross section of the Chacarilla area **102**
48. Geologic sketch map and cross section of the Azurita deposit **104**
49. Sketch map and cross section of Cerro Phasa Willkhi composite stratovolcano **109**
50. Sketch map and cross section of the María Elena altered area **111**
51. Sketch map and lateral view of Cerro Curumaya area **113**
52. Geologic sketch map and cross section of the Paco Kkollu area **114**
53. Sketch map and diagrammatic cross section of a manganese vein, Granada mine area **115**
54. Geologic sketch map and cross section of the Iñexa area **115**
55. Sketch map of the Cerro Eskapa area **117**
56. Sketch map of the Eskapa copper mine area **118**
57. Sketch map of the Cerro Poderosa-Cerro Amarillo area **120**
58. Map showing location of known fumarolic native sulfur deposits **121**
59. Sketch map of the Saca Sacani area **124**
60. Photograph showing unaltered dacitic lavas above solfatarically altered area **125**
61. Map showing geology, mines, and sample localities in the Quimsa Chata district **127**
62. Map showing geology and location of mines in the Berenguela district **130**
63. Geologic map and cross section of the La Joya district **133**
64. Generalized geologic map of the Todos Santos district **137**
65. Sketch map and cross section of the Todos Santos area **139**
66. Sketch map of underground workings at the Todos Santos mine **140**
67. Sketch map showing geology and sample localities in the Carangas and Negrillos areas **141**
68. Geologic map of Cerro Espíritu Santo, Carangas **142**

69. Sketch map of the Negrillos area **142**
70. Sketch map of Salinas de Garci Mendoza district **144**
71. Photograph showing view south from Cerro Husachata **146**
72. Photograph showing view of Cerro Kancha from north **147**
73. Cross section of the Guadalupe mine **147**
74. Photograph showing dumps of the La Deseada mine on the north slopes of Cerro Husachata **149**
75. Sketch map of the Sonia-Susana area **152**
76. Sketch of pyritic shear zone, Sonia-Susana area **153**
77. Generalized geologic map of the San Cristobal district **154**
78. Diagrammatic cross section through the Toldos mine **156**
79. Map showing geology in the Comunidad Todos Santos area **158**
80. Sketch map of the Escala district **159**
81. Sketch map of the principal workings at the Escala mine **160**
82. Sketch map of the Santa Isabel district **162**
83. Diagrammatic cross section through the Candelaria mine area **163**
84. Geologic map of the Mercedes mine area **165**
85. Map showing geology in the Buena Vista area **165**
86. Map showing geology and location of mineral deposits in the Cerro Bonete area **168**
87. Diagrammatic sketch of geologic relationships at Bolívar mine **171**
88. Map showing mine workings and sample localities, Colorados de Bolivia mine **172**
89. Map showing geology in the Morokho area **174**
90. Plot showing silver and lead values for mineralized samples at Mina Himalaya **175**
91. Geologic map of the San Antonio de Lípez area **177**
92. Plot showing gold and silver values for channel samples from the El Mestizo prospect **178**
93. Map showing geology in the Esmoraca area **180**
94. Map and cross section showing geology, alteration, and sample localities in the Jaquegua area **183**
95. Plot showing relationship of silver and lead values in samples from the Jaquegua area **183**
96. Map and cross section of the La Española area **186**
97. Map showing geology of the Pachekala prospect **188**
98. Map showing geology of the Laurani area **190**
99. Map showing geology of the Kiska prospect **192**
100. Map and cross section of the San Salvador and Aguilani mines at Chinchilhuma volcano **193**
101. Schematic cross section showing geologic relationships in the San Francisco mine area **194**
102. Photograph showing wind erosion at Salar de la Laguna **198**
103. Photograph showing Laguna Cachi **200**
104. Photograph shwoing Laguna Celeste **201**
105. Photograph showing sulfur concentrate at the El Desierto sulfur plant **209**

TABLES

11. Chemical analyses of mineralized and altered rocks, Cerro Eskapa area **118**
12. Chemical analyses of altered rocks, Cerro Cachi Laguna area **119**
13. Chemical analyses of altered rocks, Cerro Poderosa-Cerro Amarillo area **120**
14. Native sulfur deposits and occurrences **122**
15. Major polymetallic districts that have been studied extensively **126**
16. Chemical analyses of altered and mineralized rocks, Quimsa Chata area **128**
17. Chemical analyses of mineralized rocks, La Joya district **135**
18. Status of mines and prospects, Todos Santos district **137**
19. Chemical analyses of mineralized and altered rocks, Todos Santos district **141**
20. Status of mines and prospects, Salinas de Garci Mendoza district **143**
21. Chemical analyses of mineralized and altered rocks, Salinas de Garci Mendoza district **148**
22. Chemical analyses of mineralized rocks and altered rocks, Sonia-Susana area **153**
23. Principal mines and prospects, San Cristobal district **155**
24. Chemical analyses of altered and mineralized rocks, San Cristobal district **156**
25. Chemical analyses of mineralized rocks, Comunidad Todos Santos area **158**
26. Chemical analyses of altered and mineralized rocks, Escala area **161**
27. Chemical analyses of altered and mineralized rocks, Candeleria mine area **164**

28. Summary description of mines and prospects, Cerro Bonete area 167
29. Chemical analyses of altered and mineralized rocks, Cerro Bonete area 170
30. Selected chemical analyses of mineralized rocks, Morokho area 175
31. Chemical analyses of mineralized rocks, Esmoraca area 181
32. Chemical analyses of mineralized rocks, Jaquegua district 184
33. Chemical analyses of mineralized rocks, La Española area 185
34. Chemical analyses of mineralized rocks, Laurani area 191
35. Chemical analyses of mineralized rocks, Chinchilhuma area 194
36. Chemical analyses of vein and slag, San Francisco mine area 195

INTRODUCTION

The first step in a mineral resource assessment is the documentation and classification of known mineral deposits and occurrences. All available data on mines, prospects, and mineral occurrences on the Altiplano and in the Cordillera Occidental, Bolivia was compiled. Data on selected deposits have been verified and complemented by field observations. These data are summarized in appendix A which is keyed to localities plotted on plate 6. Unlike traditional compilations which group mineral occurrences by commodity, the data in appendix A and on plate 6 is organized according to deposit type, using the classification of Cox and Singer (1986). Where sufficient data were available, known deposits were assigned to specific metallic and nonmetallic mineral deposit types; otherwise, they were categorized as unassigned. Recognition of the deposit types found in the study area led to the development of the geological criteria by which areas permissive for their occurrence were delineated (pls. 7, 8).

The mineral deposit data listed in appendix A contains selected information and principal sources from the Mineral Resource Data System (MRDS) computer file of the U.S. Geological Survey. Drawn from hundreds of published and unpublished sources, the data in MRDS were supplemented with field observations made during visits to many of the sites in 1990–91. During the course of the study, members of the team made numerous visits to specific mineral deposits, prospects, and occurrences. This section includes descriptions of those sites visited, as well as information gleaned from the published and unpublished literature. In addition, some sites are described because of their importance, even though they were not visited, or the visit was only superficial, resulting in no new data.

Complete MRDS data records are available to the public either as hard copy or as computer files. For further information, contact:

Mineral Resources Data System
U.S. Geological Survey, Mail Stop 920
12201 Sunrise Valley Road
Reston, VA 22092, USA

COPPER DEPOSITS IN SEDIMENTARY ROCKS

By Dennis P. Cox, Raul Carrasco, Orlando André-Ramos, Alberto Hinojosa-Velasco, *and* Keith R. Long

INTRODUCTION

More than 80 sediment-hosted copper and basaltic copper deposits and districts are known in the Tertiary sedimentary rocks of the Altiplano. They are described in the following section in order of their location from north to south and grouped in informally named areas for easy reference. These areas are shown on figure 44. Individual deposits are located in relation to small villages and other features not shown on the 1:500,000-scale map. These features can be found on 1:250,000-scale topographic maps of Bolivia.

SAN SILVESTRE AREA

The San Silvestre area is the northernmost cluster of sediment-hosted copper deposits on the Altiplano. Lying south and southwest of Guaqui, the San Silvestre area is an alignment of small stratabound deposits that coincides with the southwest flank of an westnorthwest-striking anticlinorium composed of lower Tertiary sandstone and conglomerate of the Tiahuanacu or Huayllamarca Formation. Rocks along the southwest side of this structure are not exposed, but a concealed thrust fault is inferred to underlie the alluvium. An exposure of Paleozoic and Cretaceous sedimentary rock is located north of Jesus de Machaca in the central part of the area, and small exposures of Cretaceous rocks are found on strike to the west of Guaqui. The older rocks, whether exposed in the cores of anticlines or in uplifted fault blocks, do not seem to control the distribution or size of copper deposits in Tertiary sedimentary strata. Typically chalcocite replaces woody material in stream channels in these deposits. The best documented deposits in this area include the Ana María, Vatutin, La Incognita, María Elena, Palmira, La Casualidad-San Francisco, San Silvestre, Tres Amigos, and Virgen de Fatima mines.

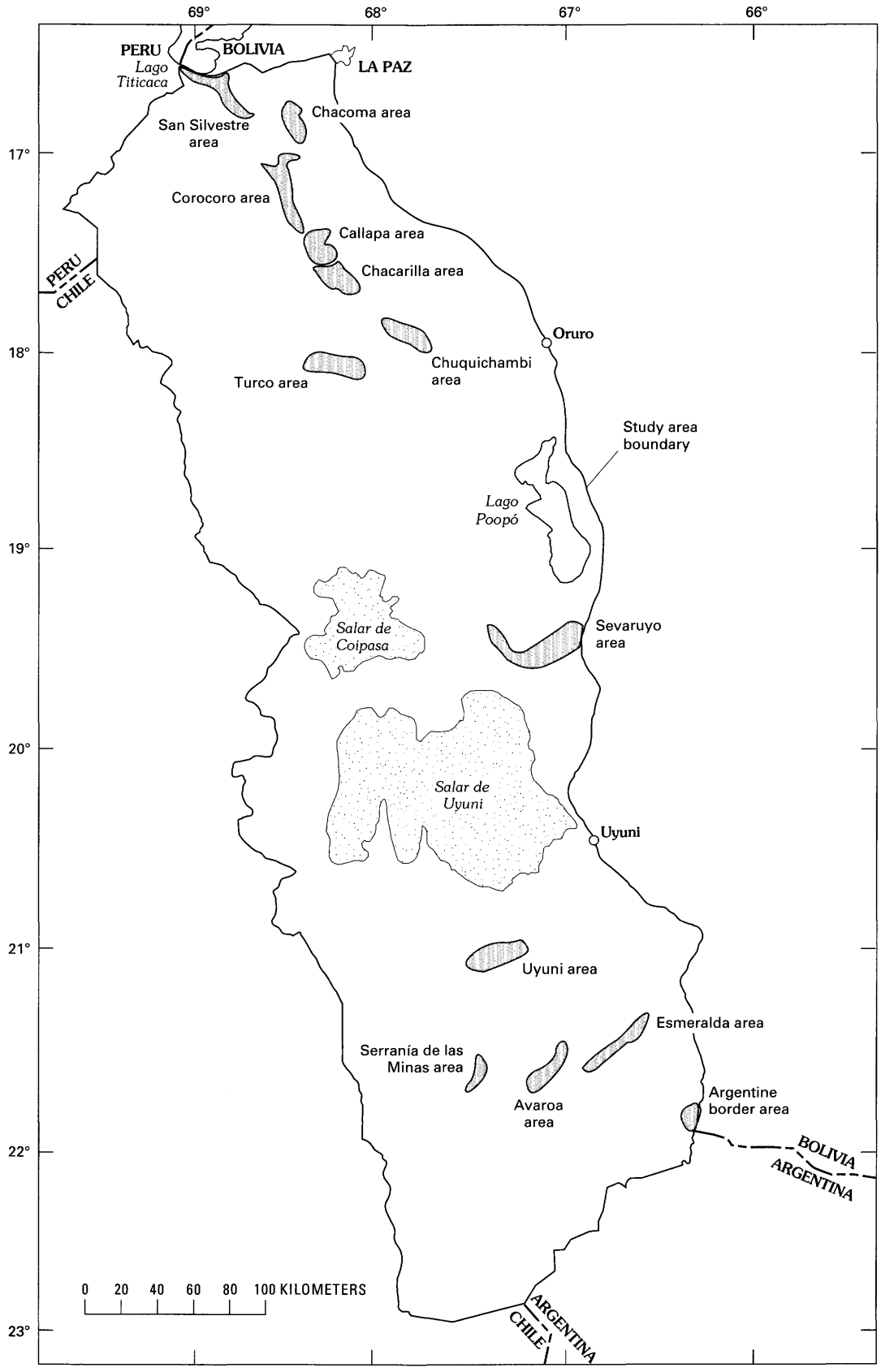


Figure 44. Map showing areas of known sediment-hosted copper deposits described in the text, Altiplano and Cordillera Occidental, Bolivia.

Ana María Mine

The Ana María mine is located near Jankomarca. Lenses, as thick as 80 cm strike N. 60°–86° W. and dip 20°–45° northeast; they contain chalcocite, malachite, and azurite as replacements of fossil plants in sandstone. The host rock is sandstone with thin interbeds of siltstone belonging to Huayllamarca Formation. The strata are folded in a northwest-trending anticline. The mine has an adit 150 m long and a shaft. It produced 485 tonnes of ore and concentrate containing 3–17 percent copper between 1959 and 1967 (Vargas, 1967; Guerra and Ascarrunz, 1964b).

Vatutin Mine

The Vatutin mine is located near Jankomarca and the Ana María mine. Malachite and azurite occur in lenses 50 cm thick, containing plant fossils. The host rock is Huayllamarca Formation exposed on the flank of a northwest-trending anticline. Samples contain 3.6–12.3 percent copper (Vargas, 1967).

La Incognita Mine

The La Incognita mine is located 6 km S. 69° E. of Guaqui. Copper minerals replace organic matter in the Tiahuanacu Formation sandstone. Beds strike N. 73° W., and dip 55°–78° north. Samples contained 1.4–16.1 percent copper (Vedia and Llanos, 1965).

María Elena Mine

The María Elena mine, located in the community of Laguacollo near the San Silvestre mine, has a small mill and concentrator. Seven mantos, as much as 180 m in length and 0.6–1.4 m thick, strike N. 60° W. and dip 16°–65° south. Chalcocite, azurite, and malachite replace organic matter in the Huayllamarca Formation sandstone. Samples collected over a 0.3–1.4 m width contained 0.3–11.94 percent copper, averaging 8.13 percent. The mine produced 6–8 tonnes of concentrate per month in 1967 (Zapata and Delgadillo, 1968; Zapata, 1987; Vargas, 1967).

Palmira Mine

The Palmira mine is located near Chapicollo. Mantos strike N. 62°–72° W. and dip 62°–68° northeast. Chalcocite, malachite, azurite, and cuprite replace organic matter in the Tiahuanacu Formation sandstone. One of the adits is 48 m long. Samples contained 0.25–9.25 percent copper (Caro and Vargas, 1963).

La Casualidad-San Fransisco Mine

The La Casualidad-San Francisco mine is near the Siempre Adelante mine. Lenses, 0.9–1.9 m thick, strike about N. 80° E. and dip 30°–65° southwest, and contain chalcocite, covellite, malachite, and azurite replacing organic matter in sandstone. The host strata are medium- to coarse-grained sandstone of the Huayllamarca Formation on the west flank of an anticline near a northwest-trending reverse fault of regional extent. In 1967, the mine produced 2 tonnes of concentrate per month (Vargas, 1967).

San Silvestre Mine

The San Silvestre mine is located near Kanku Likiliki, 2 km southeast of the María Elena mine. Ten mantos, 120–150 m long, 0.3–1.0 m thick, strike N. 60° W. and dip 27° southwest. Chalcocite replaces organic matter in the Huayllamarca Formation sandstone on the east flank of an anticline. Samples contain 7.11–11.4 percent copper (average grade 2.15 percent copper with 60 g/t silver). Between 1964 and 1967, the mine produced 171 tonnes of concentrates with copper grades of 10–30 percent. Reserves in 1967 were 28,000 t, grade unknown (Guerra and Ascarrunz, 1964d, Zapata and Delgadillo, 1968).

Tres Amigos Mine

The Tres Amigos mine is located near the Virgen de Fatima mine. Small mantos 10–40 cm thick strike N. 40°–80° E. and dip 30°–35° southeast. Chalcocite, azurite, and malachite replace fossil plants in sandstone. Samples contain 4.9–10.4 percent copper (Vargas, 1967).

Virgen de Fatima Mine

The Virgen de Fatima mine is located 5 km west of the road between Laja and Tiahuanacu near the Tres Amigos mine. Mantos 300 m long and 0.05–2.0 m thick strike N. 40°–80° E. and dip 30°–35° southeast. Chalcocite, azurite, and malachite replace organic matter in sandstone and conglomerate of Huayllamarca Formation. Mineralization is more intense in the direction of the Loria Kollu intrusion. Samples contain 0.65–11.1 percent copper. In 1974, this mine produced 17 tonnes of concentrates containing 22 percent copper. Ore reserves in 1968 were about 40,000 tonnes, grade not reported (Zapata and Delgadillo, 1968).

CHACOMA AREA

The Chacoma area is situated 15 km west of Viacha and extends along the northeast flank of the regional anticlinorium. Most of the deposits are found in sandstone and conglomerate of the Tiahuanacu Formation near its contact with the younger Coniri Formation. As in the San Silvestre area, chalcocite typically replaces plant materials

in conglomerate. There are many small deposits in this area; the best documented include the Chacoma and Las Mercedes mines.

Chacoma Mine

The Chacoma mine is located 1 km north of Estancia Chacoma Grande, 100 m east of the highway from Viacha to Corocoro. It is developed on four mantos, 60 cm thick and 60–450 m long. The mineralization follows lenses of gray sandstone and shale with fossil wood that are enclosed in red sandstone of the Tiahuanacu Formation on the overturned flank of a fold. Mine workings consist of a small inclined shaft and prospect pits. A sample collected from the dump contained 5.98 percent copper (Zapata, 1987).

Las Mercedes Mine

The Las Mercedes mine is located 4.5 km S. 10° W. of Estación Chacoma Grande. Stratabound copper mineralization occurs in the Tiahuanacu Formation. No description of the deposit is available.

COROCORO AREA

The Corocoro area includes the Corocoro district, containing the most productive of all of the sediment-hosted copper deposits on the Altiplano. It also includes all of the deposits situated on or near the contact between lower Tertiary red lutite, sandstone, gypsum, and minor conglomerate (Ballivian and Huayllamarca Formations and equivalents, locally referred to as Ramos Formation; pl. 1, Ts1) and the middle Tertiary tan to reddish sandstone and conglomerate of the Caqiaviri and Totora Formations (locally referred to as Vetas Formation; pl. 1, Ts2). This contact extends 40 km from a point near the Pisaqueri deposit southsoutheastward through Corocoro to the Veta Verde mine (figs. 45–46). Except where disturbed by faulting, the contact is an angular unconformity (Entwistle and Gouin, 1955; Rutland, 1966) with a 50°–55° difference in dip. Both the lower and middle Tertiary strata are folded and, locally, the lower Tertiary beds are overturned. Diapirs originating from lower Tertiary, or possibly upper Cretaceous evaporites pierce these fold structures (pl.1, Tdp). They appear in outcrop as friable masses of gypsum and gypsiferous shale totally lacking in bedding or other sedimentary structure and are assigned to the Jalluma or Chuquichambi Formation. This material may represent a cap rock over deeper salt diapirs. A salt intrusion was encountered by drilling in the Corocoro district in 1976 at a depth of 386 m (Hernan Uribe, oral commun., 1990). The largest copper deposits are located a few kilometers from these diapirs and may owe their formation to increased flow of warm, copper-bearing brine along the diapir flanks. Brine springs are active near the south flank of the Jalluma diapir 15 km south of Corocoro. From north to south, the most important sediment-hosted copper deposits include the Porvenir, Llallagua, María Elena-Victoria, Pisaqueri (Anaconda), Americas Unidas, Transvaal, Pontezuelo, and Veta Verde mines and the Corocoro district.

Porvenir Mine

The Porvenir mine is located northwest of the Pisaqueri mine. Chalcocite, covellite, and malachite replace organic matter in sandstone (probably belonging to the Vetas Formation) that strikes N. 15° E. and dips 15° northwest. Some hand-picked ore contained 18 percent copper and 122 g/t silver (López and Murillo, 1963a).

Llallagua Mine

The Llallagua mine is located 4 km south of Estación Comanche. Stratabound copper mineralization occurs in the Huayllamarca Formation. Samples contain as much as 10 percent copper (Carrasco, 1962).

María Elena–Victoria Mine

The María Elena-Vicotria mine, located 1.5 km west of Antaquira, lies 25 km west of the main trend of deposits and is developed on an irregular lense of ore 500 m long and 1.3 m thick in rocks probably belonging to the Totora Formation. The lens strikes N. 25°–35° W. and dips 15°–80°southwest. Cuprite mineralization is more apt to occur in coarse-grained rather than fine-grained sandstone. The deposit was drilled in 1975; 300,000 tonnes of ore with unspecified grade was outlined (Terrazas, 1975).

Pisaqueri (Anaconda) Mine

The Pisaqueri (Anaconda) mine is located 5 km northwest of Estación General Ballivian and is near the trace of the same unconformity that controls mineralization in the Corocoro district. East-dipping red lutites of the Ballivian Formation (Ramos) crop out in a gully east of the mine, and west-dipping sandstone and conglomerate of the Caquiaviri Formation (Vetas) are found in a trench 30 m west. Southeast of the mine is small diapir of gypsum. Native copper and cuprite replace clay minerals in the matrix of Ramos-type sandstone, locally occurring as nodules, 5–20 mm in diameter. Chalcocite occurs southwest of the unconformity, presumably in Vetas-type rocks. The average grade of the ore is 3–4 percent copper. Samples collected during a visit in 1990 contained >2 percent

copper, 50 ppm silver, 30 ppm lead, 0.012 ppm gold, and 4 ppm uranium (app. B, sample 90BCX014). Small cement-copper production ceased in 1975 (Carrasco, 1962; Ljundgren and Meyer, 1964; Bernal, 1979). This area appears to be favorable for undiscovered deposits because all of the elements of a Corocoro district are present. The thin alluvial cover in this broad valley could conceal a major new district. No record of any subsurface exploration is known.

Americas Unidas Mine

The Americas Unidas mine is located 5 km north-northwest of Corocoro near the Río Pontezuelo. In a zone 2,500 m long, there are 19 lenses as thick as 4 m separated by more than 10 m of barren rock. Bedding strikes N. 30°–40° W. and dips 40°–60° southwest. Chalcocite, covellite, cuprite, malachite, and azurite are associated with organic material in sandstone and conglomerate of the Caquiaviri or Vetas Formation (Bernal, 1979, however, states that the deposit is in the Ballivian Formation). An ore sample collected during our visit in 1990 contained 6 percent copper, 10 ppm silver, 100 ppm lead, and 7 ppm each of uranium and thorium (app. B, sample 90BCX004). The large mill foundation present on the property appears out of proportion to the small number and size of mine workings (Bernal, 1979).

Transvaal Mine

The Transvaal mine is located 5 km N. 5° W. of Corocoro on the flank of a large gypsum diapir. Mantos as thick as 45 cm occur in Ramos-type sandstone. Bedding strikes N. 10° W. and dips 45° northeast (Guerra and Ascarrunz, 1964e).

Pontezuelo Mine

The Pontezuelo mine is located 6 km north of Corocoro. Mantos, 0.6–1.5 m thick, strike N. 20°–30° W., and dip 50°–65° southwest. They contain chalcocite, azurite, and malachite as replacement of organic matter in sandstone of the Totora Formation (Vargas, 1967).

Corocoro District

The Corocoro district is located on the Ferrocarriles del Estado, 130 km southwest of La Paz, and 340 km from the port of Arica, Chile. Individual mines are the Toledo, operated since 1940; Tancani-Libertad, 3 km north of Corocoro, abandoned for many years; Challcoma, 4 km south of Corocoro; Buen Pastor, mined for silver between 1840 and 1860; and the Capilla, Copacabana, Estrella, Guallatiri, Malcocoya, Remedios, San Angel, San Agustín, San Geronimo, Santa Rita, Santa Rosa, Viscachani, and Yanabarra mines.

Stratabound copper ores are localized along a N. 20° W. striking, steeply dipping to vertical, unconformable contact between west-dipping tan to reddish sandstone and conglomerate of the Caquiaviri Formation (Vetas Formation) on the west and east-dipping red lutite and shale of the older Ballivian Formation (Ramos Formation) on the east (fig. 45). Three km north of Corocoro, the vertically dipping unconformity is marked by abundant limonite in beds of the Ramos Formation. Vetas-type strata west of the contact contain many small angular clasts of banded opal and chalcedony presumably derived from the underlying Ramos Formation. One sample of basal coarse sandstone in the Vetas Formation near the contact collected during our visit in 1990 contained anomalous amounts of silver and base metals (app. B, sample 90BCX003).

The two formations have been sharply upwarped along the flanks of a large diapir composed of Jalluma Formation gypsum and shale. Bedding in the Ramos Formation, because of its 55° angular discordance to the unconformity, is overturned. A fault follows the unconformity throughout much of the district. One rich ore shoot, the Dorado, is this fault zone.

Vetas Formation ore material is mainly chalcocite impregnations of the sandstone-conglomerate matrix; Ramos Formation ores contain mainly native copper and cuprite in disseminations and sheets. Chalcocite and native copper replace the clay and carbonate matrix of the clastic rocks, and native copper pseudomorphically relaces aragonite. Entwistle and Gouin (1955) proposed on sedimentological evidence that copper deposits in the Ramos Formation were formed early, and were reworked by erosion and sedimentation to form the sulfide ore in the Vetas Formation. We suggest that both were formed in a single period probably coincident with diapir intrusion. The presence of native copper in the Ramos is consistent with its history of erosion and oxidation of contained sulfide minerals prior to the deposition of the Vetas Formation. Deposition of chalcocite in the Vetas Formation was presumably favored by the presence of sulfide as pyrite or H_2S in the lower parts of that formation.

Rich silver ores are locally present. The Buen Pastor ore body contained copper sulfides, native copper, domeykite, and native silver and produced over 500 tonnes of silver between 1840 and 1860; also found in the district are minor bornite, covellite, chalcopyrite, galena, sphalerite, stromeyerite, and tennantite. Gangue minerals are gypsum, anhydrite, barite, aragonite, celestite, and minor chalcedony, alunite and clay minerals. The ore is said to contain about 15 g/t of silver per one percent of copper. One

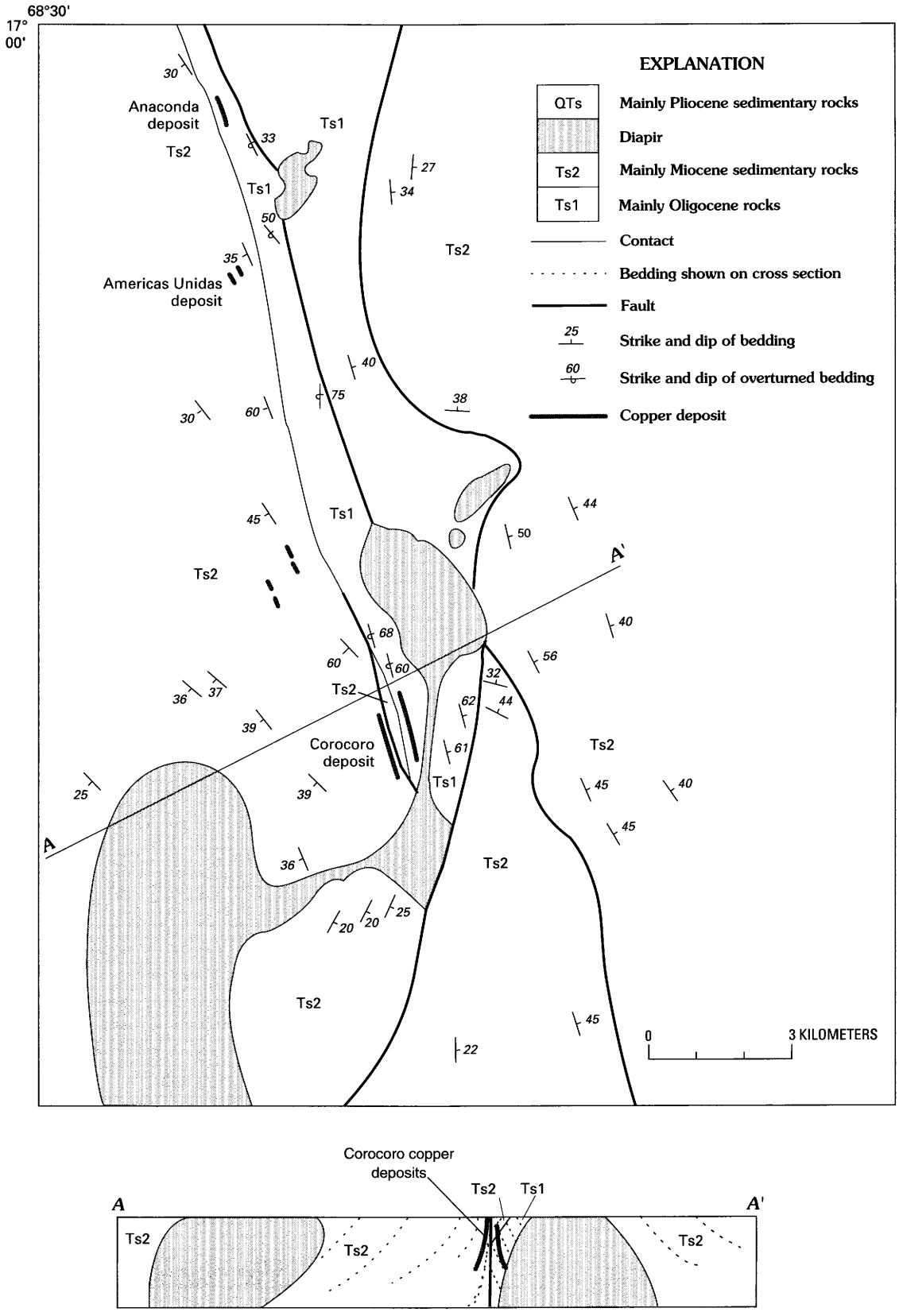


Figure 45. Geologic sketch map and cross section of the Corocoro area, Bolivia. Ts1, Ballivian Formation; Ts2, Totora and Kollu Kollu Formations. Geology modified from unpublished maps of Servicio Geológico de Bolivia and Yacimientos Petrolíferos Fiscales de Bolivia.

sample collected during our visit in 1990 contained >2 percent copper, 150 ppm lead, 7 ppm silver, and 1.4 ppm uranium (app. B, sample 90BCX007).

The last production from the district was in 1987. The Corocoro deposits produced over 7,000,000 tonnes of copper ore (Entwistle and Gouin, 1955). Reserves as of 1952 in deep undeveloped parts of the district totalled 468,000 t (L.P. Entwhistle, written commun. 1990). A note in Engineering and Mining Journal Metals Week (Jan. 14, 1974) described a shaft-sinking project aimed at development of 840,000 tonnes containing 3.75 percent copper. This was suspended when the shaft encountered massive halite at 368 m (Hernan Uribe, oral commun., 1990).

Other references to the Corocoro district are Sundt (1915), Steinmann (1916), Singewald and Berry (1922), Berton (1937); Ahlfeld and Schneider-Scherbina (1964), Ljundgren and Meyer (1964); Flint (1986); Pélissonier (1964); and Kohanowski (1944).

Veta Verde Mine

The Veta Verde mine is located 25 km southwest of Corocoro, 4 km west of Comunidad Choque Puju. Deposits consists of four mantos that crop out over a distance of 2.5 km on the southwest flank of a large diapir of gypsum and shale. The mantos follow a structure that closely resembles the unconformity that controls mineralization at Corocoro (fig. 46). The west-dipping Totora Formation hosts chalcocite, native copper, silver, and arsenic minerals and lenses rich in galena locally as thick as 50 cm. East-dipping Ballivian Formation hosts cuprite and domeykite mineralization and is lower grade. Chalcocite and bornite replace anhydrite cement in sandstone. Secondary copper minerals are found in vertical fractures around orebodies. Samples contain as much as 36 percent copper, 15 percent lead, 16–65 g/t silver, and 26 percent iron. Between 1921 and 1962, the mine produced 769 tonnes of hand-picked ore containing 15.2 percent copper. Reserves, estimated in 1963, were 50,000 tonnes with copper grade of 0.5–6.0 percent (Schneider-Scherbina, 1963; López and Murillo, 1963c; Meyer and Murillo, 1961).

CALLAPA AREA

The Callapa area includes numerous small deposits on the south flank of a complex uplift of lower Tertiary rocks referred to as the Huayllamarca Formation, middle Tertiary rocks of the Totora Formation, and small diapirs of gypsum and shale of the Jalluma Formation. This structure is a continuation of the uplifts in the Corocoro area but is sharply deflected to a nearly easterly strike. The principal mines in the area include the El Hogar, San Agustín, and San Miguel mines, Noe group, and San Francisco prospect.

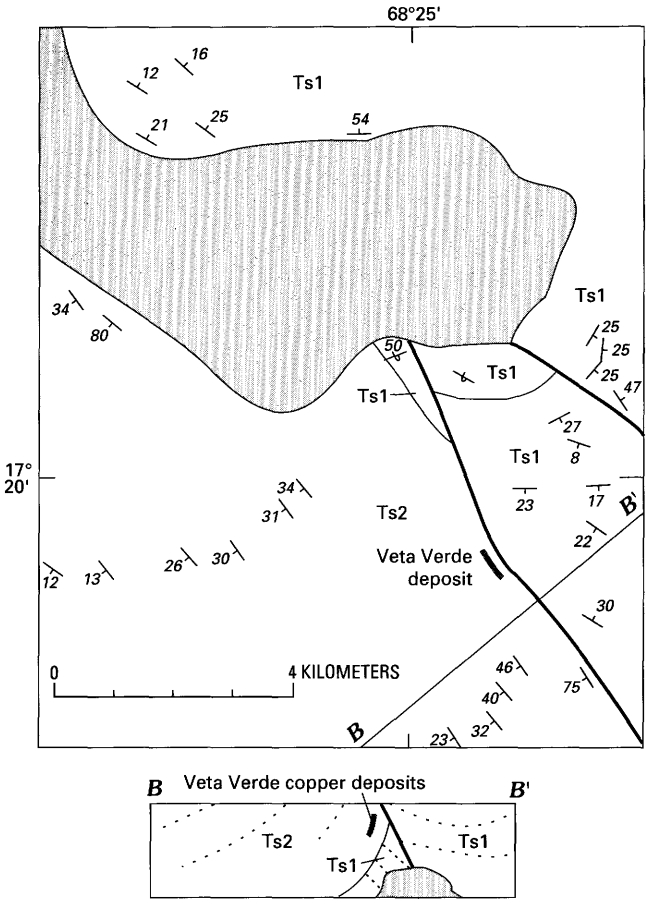


Figure 46. Geologic sketch map and cross section of the Veta Verde area, Bolivia. For explanation see figure 45. Ts1, Ballivian Formation; Ts2, Totora and Kollu Kollu Formations. Geology modified from unpublished maps of Servicio Geológico de Bolivia and Yacimientos Petrolíferos Fiscales de Bolivia.

El Hogar Mine

The El Hogar mine is located 8 km north of Callapa, near the Copacabana, Carmen, Dinamita, Pucara, and Gran Poder mines. At El Hogar, the Gloria, San José, and Santiago mantos, as long as 2,000 m, strike N. 70° W. and dip 60° north. Their average grades are 3.63, 1.99, and 5.28 percent copper, respectively. Deposits are localized near a N. 70° W. striking thrust fault. The El Hogar, Copacabana, and Carmen deposits are in the Huayllamarca Formation in the upper plate of the thrust; the Dinamita, Pucara, and Gran Poder are in the Totora Formation of the lower plate. El Hogar produced 17.6 tonnes of hand-picked ore containing 19.2 percent copper in 1958–59 (Meyer and Murillo, 1961).

Noe Group

The mines of the Noe group, located 5 km northwest of Callapa, are the Pinquillani, La Exploradora, El Carmen, 16 de Julio mines, and, south of Río Desaguadero, the

Chiguana mine. Also included are the Cachu, Clara Rosa, Concesiones, and Portachuro mines. Five mantos strike N. 45° W. and dip 30°–50° southwest. Native copper occurs in rocks of the Totora Formation, which are uplifted along the south flank of a diapir containing gypsum and shale of the Jalluma Formation. Samples contained 8.7 percent copper, 0.45 percent lead, 1.85 percent sulfur, and 30 g/t silver (Meyer and Murillo, 1961).

San Agustín Mine

The San Agustín mine is located 8 km N. 5° E. of Ulloma at Willa Khañuta. Mantos, 5 cm to 1.1 m thick, strike N. 10° W. and dip 30° northeast. Copper minerals replace cement in fluvial channels in the Totora Formation sandstone. The mine produced 3 tonnes of ore containing 6.8 percent copper in 1969 (Meyer and Murillo, 1961).

San Francisco Prospect

The San Francisco prospect is located 10 km southeast of Callapa. Chalcocite, cuprite, and malachite replace organic matter in sandstone of the Totora Formation (Meyer and Murillo, 1961).

San Miguel Mine

The San Miguel mine is located 4 km N. 10° E. of Callapa. Copper minerals occur in sandstone of the Totora Formation. Bedding strikes N. 40° W. and dips 45° southwest. Samples contained as much as 4.07 percent copper, 97 g/t silver, and 0.02 g/t gold. The mine produced 30 tonnes of ore containing 6.5 percent copper in 1971 (Vedia and others, 1971).

CHACARILLA AREA

The Chacarilla area contains the Chacarilla district, the second most productive copper district on the Altiplano, as well as a few small deposits to the west. Deposits occur in sandstone and conglomerate of the Huayllamarca and Totora Formations that is upwarped by a northnorthwest-trending diapir of gypsum and shale (Chuquichambi Formation) as shown on figure 47. The Chacarilla deposits are situated around the north end of the diapir. No deposits are recorded around the southeast part of this structure, which would otherwise be considered as favorable for undiscovered deposits. Mine workings in the area include the Chacarilla district and Esperanza and La Encontrada mines.

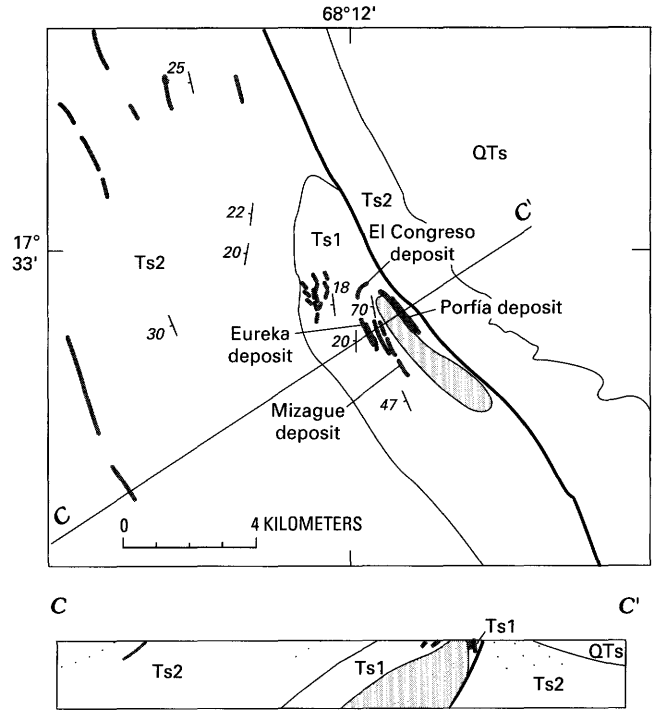


Figure 47. Geologic sketch map and cross section of the Chacarilla area, Bolivia. For explanation see figure 45. Ts1, Huayllamarca Formation; Ts2, Totora Formation; QTs, Umala Formation. Geology modified from Meyer and Murillo (1961).

Chacarilla District

The Chacarilla district is located 19 km southeast of Callapa. The principal mines are the Porfía on the overturned northeast flank developed on three mantos that dip 80° southwest; the Congreso, near the axis of the diapir on the northwest, the Amigo, Borda, and Esperanza on the west side with four mantos dipping 20° west; the Eureka, San Fermin, and Tiviña on the southwest flank with four mantos dipping 17°–22° southwest; and, to the southeast on the same trend, the Mizague mine with eight mantos dipping 30°–45° southwest. Chalcocite is the most important ore mineral at the Porfía and El Congreso mines, and locally forms pseudomorphous replacements of gypsum(?). Native copper, cuprite, bornite, and chalcopyrite are also known in the district. Gangue minerals are gypsum and minor celestite and pyrite. Uranium mineralization is associated with yellowish altered shale and gypsum of the Chuquichambi Formation. One sample collected during our visit in 1990 from a uranium prospect in the Chuquichambi Formation contained 11 ppm thorium and 15 ppm uranium (app. B, sample 90BCX020). Production by Dowa Mining Company between 1963 and 1976 was 1,457,000 tonnes of ore containing 2.55 percent copper. Reserves in the district total 1,187,000 tonnes of ore containing 2.78 percent copper. This estimate includes 813,000 tonnes of possible ore in the El Congreso area containing 3 percent copper. Analytical data from ore samples collected during our visit in 1990

(samples 90BCX017, 18, 19a) are shown in appendix B. Important references to the Chacarilla district are Ahlfeld and Schneider-Scherbina (1964); Ljundgren and Meyer (1964); and Meyer and Murillo (1961).

Esperanza Mine

The Esperanza mine is located 4 km south of Callapa. Mineralization is semicontinuous and stratabound and extends for 30 km to the southeast. At Esperanza, five mantos, averaging 2 m thick, strike N. 40° W. and dip 40° southwest. Chalcocite, malachite, and azurite replace organic matter in Totora Formation sandstone. The mine produced 5.3 tonnes of hand-picked ore averaging nearly 30 percent copper in 1959 (Meyer and Murillo, 1961).

La Encontrada Mine

The La Encontrada mine is located west of the Chacarilla district. Mantos with copper mineralization strike N. 15°–38° W. and dip 25°–32° southwest on the west flank of a northwest-striking anticline. The mine produced 630 tonnes of hand-picked ore containing 25 percent copper between 1956 and 1964 (Guerra and Ascarrunz, 1964c).

CHUQUICHAMBI AREA

The Chuquichambi area contains a few small copper deposits in the Huayllamarca Formation. Outcrops of Chuquichambi Formation occupy the core of an anticline surrounded by beds of the Huayllamarca Formation. These outcrops differ from previously noted exposures of the Chuquichambi Formation in that they show well developed, strongly folded, stratification. Mine workings in the area include the Llanquera-San Miguel and Santa María prospects.

Llanquera-San Miguel Prospects

The Llanquera-San Miguel prospects are located in the Serranía de Huayllamarca near Llanquera. Chalcocite, malachite, and azurite are observed in a manto extending discontinuously for more than 10 km in the Huayllamarca Formation. The manto strikes N. 50° E. and dips 40° south. Gypsum beds of the Chuquichambi Formation occur to the east. Ore reserves in 1958 were 325,000 tonnes containing 5 percent copper (López, 1958).

Santa María Prospect

The Santa María prospect is located on the east flank of the Serranía de Huayllamarca southwest of Huaylla Marca. Mantos in the Huayllamarca Formation strike N. 55°–58° W., dip 40°–50° southwest, and contain azurite and malachite. Copper mineralization also occurs in a vein striking N. 12° E. and dipping 49° northwest. Gypsum beds of the Chuquichambi Formation occur to the east (Vedia and Gonzales, 1970).

TURCO AREA

The Turco area is a cluster of sediment-hosted copper and basaltic copper deposits offset to the west from the more or less continuous belt of deposits extending from Corocoro to Chuquichambi. The area contains a variety of deposits in host rocks of different ages and types including the most important example of a basaltic copper deposit, Azurita. Basalt flows are present in the Azurita Formation and light-colored tuff beds are abundant in the Turco Formation. Copper deposits are known in the Huayllamarca, Azurita, and Turco Formations. Mines in the area include the Santa Clara, Azurita, Corona de España, Cuprita, and Chihuirari mines.

Santa Clara Mine

The Santa Clara mine is located 22 km N. 35° W. of Turco. One manto, 30 m long and 30–40 cm thick, occurs in red-brown arkosic and tuffaceous sandstone and white dacitic tuff of the Turco Formation. The manto strikes N. 40° W., dips 30°–40° northeast, and exhibits chalcocite in layers 5–10 cm thick that contain as much as 20 percent copper. Reserves in 1971 were 1,330 tonnes containing 4.9 percent copper (Kuronuma, 1971).

Azurita Mine

The Azurita mine is located 17 km northeast of Turco. The ore deposit is in two red-brown conglomerate beds, 0.8–1.5 m thick, in a red lutite sequence in the lowermost part of the Azurita Formation. The mineralized beds lie between two flows or sills of basalt and the mineralization is coextensive with the basalt over a distance of 2 km (fig. 48). Five mantos are known; the largest is 140 by 150 m, 1.6 m thick, and mined to a depth of 120 m and another is 75 m long and worked to a depth of 60 m. Cuprite and native copper are the main ore minerals in these mantos and late vertical veinlets of cuprite-tennantite-celestite cross the bedding. Locally the basalt is altered to chlorite and calcite and mineralized with cuprite. In May, 1990, production was from a pit 10 m by 4 m by 2 m deep exposing an irregular vein of well-crystallized cuprite and native copper roughly concordant with bedding; this vein locally cuts sharply across strata in 0.5 m steps. The vein, 2–5 cm thick, is marked by a 20–50 cm halo of bleached conglomerate. Production from 1948 to 1962 was 70,000 tonnes

containing 3.5–4.0 percent copper (Schneider-Scherbina, 1963). Proven plus probable reserves in 1963 were 750,000 tonnes containing 4.0 percent copper (C.M. Tschanz, written commun., 1963). In 1971, an estimate of 660,000 tonnes at 2.2 percent copper was given by Kuronuma (1971). One sample collected during our visit in 1990 contained more than 2 percent copper, 150 ppm silver, 200 ppm vanadium, and 7 ppm uranium (app. B, sample 90BCX023).

Corona de España Mine

The Corona de España mine is located 5 km northeast of Turco and contains native copper and cuprite in five or six mantos 10–38 m long and 0.2–1.0 m thick in sandstone and tuff of the Turco Formation. The mantos strike N. 47° W. and dip 15°–73° northeast. In 1969, the mine produced 3 tonnes per month of hand-picked ore containing 17–30 percent copper. Ore in sight at that time totaled 4,200 tonnes containing 3.25 percent copper (Barrios and Prevost, 1970; Kuronuma, 1971).

Cuprita Mine

The Cuprita mine is located 20 km southeast of Turco. The deposits are in lenses 5–50 m in diameter, spaced 50–300 m apart, along a strike length of more than 5 km. The host rocks are red-brown conglomerates in the Azurita and Huayllamarca Formations. The strata dip 40°–80° on the flanks of a north-trending anticline and syncline. The folds have been disrupted by northeast- and northwest-trending reverse faults. The ore minerals consist mainly of cuprite and native copper disseminated in the sandstone matrix. Chalcedony, tinted blue by copper minerals, occurs with the ore. Chalcocite ore is known in a small manto in the uppermost part of the Turco Formation 2 km northeast of Cuprita (Schneider-Scherbina, 1963). Estimates of reserves for four separate lenses total 138,000 tonnes at 2.0 percent copper (Kuronuma, 1971; Georgi, 1958). One sample collected during our visit in 1990 contained more than 2 percent copper, 20 ppm silver, and 1.5 ppm uranium (app. B, sample 90BCX026).

Chihuirari Mine

The Chihuirari mine is located 25 km northnortheast of Totora. It is developed on a small manto that is 8 m long, 5–8 cm thick, strikes N. 36° W., and dips 52° northeast in Huayllamarca Formation sandstone.

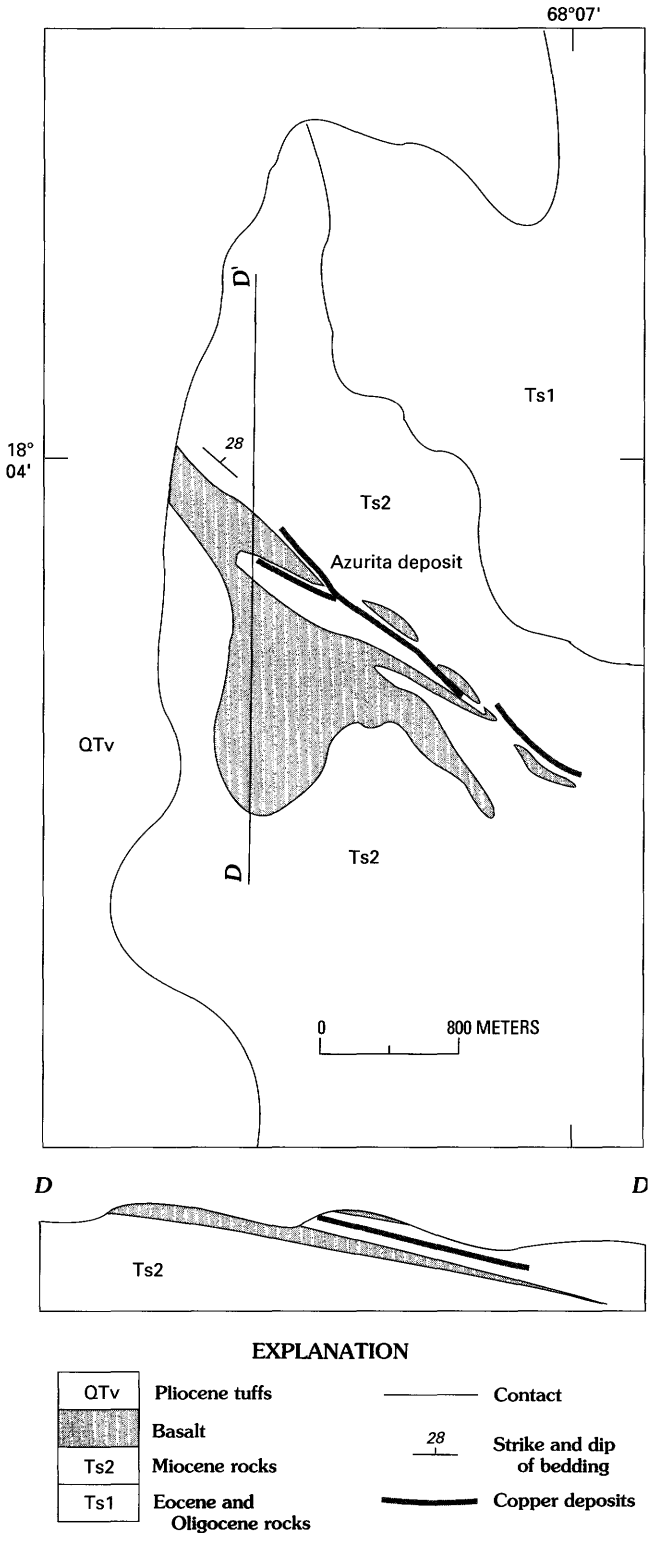


Figure 48. Geologic sketch map and cross section of the Azurita deposit, Bolivia. Ts1, Huayllamarca Formation; Ts2, Turco and Azurita Formations; QTv, Mauri Formation. Geology modified from Schneider-Scherbina (1963).

SEVARUYO AREA

The Sevaruyo area lies between Lago Poopó and Salar de Uyuni. It contains a few sediment-hosted copper and basaltic copper deposits localized in middle Tertiary sandstone of the Chamarra and Totora Formations and

basalt in the Totora and Tambillo Formations. These rocks are exposed in a series of northwest-trending folds involving underlying redbeds of Cretaceous age. No deposits are known in the Cretaceous redbeds. Mines in the area include the Amistad and Tambillo mines and the Concepción prospect.

Amistad Mine

The Amistad mine, located 8 km southwest of Sevaruyo, is developed on copper-bearing mantos that are 250–450 m long and 0.7–2.0 m thick. Copper minerals are found in bleached zones of the Chamarra Formation sandstones. Ore reserves estimated in 1969 were 3,541 tonnes of ore containing 4.66 percent copper (Murillo and others, 1969).

Concepción Prospect

The Concepción prospect is located 2 km southeast of Cajuata. Native copper, cuprite, and malachite occur in an irregular stockwork 40 m long and 1.5 m thick in basalt of the Tambillo Formation. A sample from a 30-cm zone contained 10.9 percent copper (Murillo and others, 1969).

Tambillo Mine

The Tambillo mine is located 3.5 km N. 40° W. of Tambo Tambillo. Copper minerals are disseminated in basalt of the Totora Formation (Schneider-Scherbina, 1963).

UYUNI AREA

The Uyuni area contains widely scattered deposits in restricted outcrop areas of the Lower Quehua, San Vicente, and Potoco Formations on the south side of Salar de Uyuni. Mines in the area include the Koholpani, Puntillas, and Iñes mines.

Koholpani Mine

The Koholpani mine is located 35 km northeast of Culpina. Chalcocite, malachite, and azurite occur in a manto 20–90 cm thick in calcareous conglomerate of the lower Quehua Formation. Beds strike N. 30° E. and dip 8°–10° west. Samples contain as much as 4.3 percent copper (Servicio Geológico de Bolivia, 1971y).

Puntillas Mine

The Puntillas mine is located 20 km west of San Cristobal. Malachite, tenorite, and chrysocolla occur in 2 mantos and one vein in the upper part of the San Vicente Formation. One manto is 50 m long and 10 cm thick; the second is 20 m long and 3 cm thick. They both strike N. 15° E. to north-south and dip 40° west. The vein strikes N. 60° W., dips 11° southeast, and is 3–28 cm wide. Chalcedony is also reported in the deposit. Reserves estimated in 1971 total 1,756 tonnes at 7.72 percent copper (Servicio Geológico de Bolivia, 1971ll).

Iñes Mine

The Iñes mine, located 5 km south of Puntillas mine, and 20 km west of San Cristobal, is developed in small lenses of chalcocite, tenorite, malachite, azurite, and chrysocolla. The lenses occur in gypsum-bearing Potoco Formation sandstone exposed on the west flank of a northwest-trending anticline. Reserves in 1970 totaled 15,137 tonnes at 3.75 percent copper (Servicio Geológico de Bolivia, 1971w).

ESMERALDA AREA

The Esmeralda area contains several small deposits hosted by sandstone and conglomerate of the Potoco and Lower Quehua Formations. These units are folded in a north-trending anticline and syncline. The principal mines and prospects include the Esmeralda and San Pedro mines, San Pablito and Mesa Verde occurrences, Ucrania prospect, Huancan´a mine, Rosario prospect, and Ladislao Cabrera mine.

Esmeralda and San Pedro Mines

The Esmeralda and San Pedro mines are located 7 km N. 72° W. of Cerrillos. Chalcocite, cuprite, and tenorite occur in mantos 0.3–1.8 m thick that strike N. 70°–80° E. and dip 22°–40° north. The host rock is sandstone of the Potoco Formation on the northwest flank of the Kellu Kellu anticline. The mantos are disrupted by faulting (Bassi, 1980).

San Pablito Occurrence

The San Pablito occurrence is located northeast of the Mesa Verde mine and consists of native copper, chalcocite, and malachite in conglomerate of the Lower Quehua Formation exposed on the east flank of the Kellu Kellu anticline (Servicio Geológico de Bolivia, 1971gg).

Mesa Verde Occurrence

The Mesa Verde occurrence is located 6.5 km N. 40° W. of Cerrillos. Chalcocite and copper carbonates are disseminated in conglomerate of the Lower Quehua

Formation on the east flank of the Kellu Kellu anticline. Nearby basalt is altered and contains secondary pyrite and chlorite (Servicio Geológico de Bolivia, 1971gg).

Ucrania Prospect

The Ucrania prospect is located 5.5 km west of Cerrillos. Malachite, azurite, and chrysocolla occur in sandstone of the Potoco Formation (Servicio Geológico de Bolivia, 1971tt).

Huancané Mine

The Huancané mine is located 6 km S. 70° W. of Cerrillos. Chalcocite and native copper are disseminated in mantos 30 m long that strike N. 12° W. and dip 20° east. The mine produced 5 tonnes of hand-picked ore containing 15–18 percent copper in 1969 (Servicio Geológico de Bolivia, 1969).

Rosario Prospect

Workings at the Rosario prospect, located 6.5 km S. 55° W. of Pululus, follow a mineralized zone 10 by 25 by 2 m that contains hematite concretions with cores of malachite. A chalcocite vein 13 cm wide occurs nearby (Servicio Geológico de Bolivia, 1971mm).

Ladislao Cabrera Mine

The Ladislao Cabrera mine is located about 3 km south of the Escala mine. Chrysocolla and malachite occur in a manto as thick as 96 cm in sandstone of the Potoco Formation. Altered tuff is reported at the locality.

SERRANIA DE LAS MINAS AREA

The Serranía de las Minas area contains a group of small copper deposits localized in sandstone of the Potoco and San Vicente Formations on the west flank of a large thrusted block of Ordovician siltstone and phyllite. Mines in Tertiary rocks in the area include the Farellón, Cerro Colorado (Negro), 25 de Julio (Peña Blanca), Copacabana, and Bartolo.

Farellón Mine

The Farellón mine is located in the north part of the Serranía de las Minas. Mantos of sandstone cemented by calcite, malachite, and azurite are cut by fractures that contain chalcocite, azurite, malachite, tenorite, cuprite, hematite, and manganese oxides. The host rock is reported to be the Cretaceous Cayara Formation, however unpublished mapping by GEOBOL does not show any rocks of that age in the area. In 1969, the mine produced 5 tonnes per month of hand-picked ore containing 35 percent copper (Servicio Geológico de Bolivia, 1971t).

Cerro Colorado (Negra) Mine

The Cerro Colorado (Negra) mine, located 10 km east of Lago Yapi, is developed in mantos in the San Vicente Formation as thick as 36 cm that strike N. 25°–30° E. and dip 60°–65° southeast. They contain chalcocite, malachite, and chrycocolla and a sericitic, ferruginous cement. Colluvium near the mine contains clasts of copper ore (Servicio Geológico de Bolivia, 1971n).

25 de Julio (Peña Blanca) Mine

The 25 de Julio mine is located 5 km northnortheast of Comunidad Mallcu. It exposes steeply dipping veins as thick as 25 cm that cut conglomerate of the San Vicente Formation. The veins contain native copper, cuprite, malachite, azurite, chrysocolla, hematite, and limonite (Servicio Geológico de Bolivia, 1971a).

Copacabana Mine

The Copacabana mine is located 12 km north of Mallcu Cueva. Malachite and chrysocolla form mantos 0.1–1.0 m thick in sandy conglomerate of the San Vicente Formation. The mantos strike N. 30° E. Chalcocite, bornite, malachite, and chrysocolla also occur in east-west vertical veins 5–15 cm wide (Servicio Geológico de Bolivia, 1971q).

Bartolo Mine

The Bartolo mine is located 9 km north of Mallcu Cueva. The ore bodies include several mantos that contain chalcocite, malachite, chrysocolla, azurite, and covellite. They strike N. 30° E., dip 35°–54° southeast, and occur in the San Vicente Formation on the west flank of a syncline. Reserves in 1971 totaled 2,400 tonnes at 3.55 percent copper (Servicio Geológico de Bolivia, 1971h).

AVAROA AREA

The Avaroa area contains the largest sediment-hosted copper deposit in Sud Lípez, the Avaroa mine, as well as several smaller deposits that are situated a few meters to 100

m below an unconformable contact between sandstone of the Lower Quehua Formation and younger tuff. The sandstones are deformed by a series of northeast-trending anticlines and synclines. The deposits contain chalcocite and are characterized by high levels of arsenic. To the south near the Cerro Todos Santos volcanic center, the deposits become richer in arsenic, antimony, lead, and zinc. The principal mines in the Avaroa area include the Avaroa, Bolívar, Mantos Blancos, El Morro, Linares, Cerro Negro, Aguilar, Alianza, and Sucre mines.

Avaroa Mine

The Avaroa mine, the largest in the area, is located 44 km west of San Pablo de Lípez. The copper deposits occur in redbeds immediately below a flat-lying sequence of tuffs. The redbeds are light-reddish-brown sandstone and minor red lutite of the Lower Quehua Formation. There is a 5°–10° angular discordance between the tuff and the sedimentary strata. All of the mine workings are located within a few meters of the tuff-sandstone contact. Chalcocite has partly replaced the sandstone matrix in mantos 0.5–3.0 m long and 10–20 cm thick. The mantos are cut by steeply dipping fractures that strike N. 30°–50° E. and contain chalcocite and bornite. Native copper, cuprite, azurite, malachite, tenorite, and chrysocolla are also present. Calcite and celestite form veins and concretions following the copper zone. Black chalcedony is present in surficial rubble. Reserves in 1972, based on limited sampling, totaled 450,000 tonnes of ore containing 5.0 percent copper (Bassi, 1980; Vedia and Cortez, 1966a). One sample collected during our visit in 1990 contained more than 2 percent copper, 15–20 ppm silver, 200 ppm arsenic, 50–100 ppm lead, 200–700 ppm zinc, and 7 ppm uranium (app. B, sample 90BCX030).

Bolívar Mine

The Bolívar mine, located 8 km west of the Avaroa mine, is on three mantos in sandstone of the Lower Quehua Formation that strike N. 54° E. and dip 5°–7° southeast. These mantos contain chalcocite, chalcopyrite, and malachite partly replacing fossil plants. Reserves in 1971 totaled 9,500 tonnes of ore at 2.7 percent copper (Servicio Geológico de Bolivia, 1971i).

Mantos Blancos Mine

The Mantos Blancos mine is located 2 km from the Avaroa mine. Chalcocite is disseminated in mantos with an average thickness of 50 cm that strike N. 20° E. and dip 5°–8° southeast. Veins of quartz, chalcocite, bornite, and chalcopyrite also occupy normal faults that strike N. 30° E., dip 70°–75° east. The faults have a 1.8 m throw and extend for 700 m. Host rock for the mantos and veins is the Lower Quehua Formation. Reserves in 1971 totaled 27,000 tonnes at 4.1 percent copper (Servicio Geológico de Bolivia, 1971dd).

El Morro Mine

The El Morro mine is located southwest of the Mantos Blanco mine. Chalcocite, malachite, and azurite occur in several mantos 10–45 cm thick that strike N. 15°–22° E. and dip 7°–8° northwest and in veins 6–60 cm wide that strike N. 70° W. and dip 65°–81° northeast. The host rock is sandstone of the Quehua Formation exposed on the flank of a broad syncline. Reserves in 1971 were 3,034 tonnes at 3.09 percent copper (Servicio Geológico de Bolivia, 1971r).

Linares Mine

The Linares mine is located near the 25 de Julio mine near Cerro Negra. Chalcocite, bornite, and malachite are disseminated in a zone 15 cm thick and 300 m long in sandstone of the Lower Quehua Formation. The host rocks strike N. 5°–15° E. and dip 15°–42° southeast on the flank of an anticline. Reserves in 1971 were 169 tonnes of ore at 9.5 percent copper (Servicio Geológico de Bolivia, 1971aa).

Cerro Negro Mine

The Cerro Negro mine is located near the Linares mine. Bornite, malachite, and azurite occur in sandstone of the Lower Quehua Formation near the Linares anticline. Ore reserves are 92 tonnes containing 9.4 percent copper (Servicio Geológico de Bolivia, 1971aa).

Aguilar Mine

The Aguilar mine is located 56 km west of San Pablo de Lípez. The ores consist of chalcocite, bornite, malachite, and chrysocolla disseminated in a sandstone bed overlain by an impermeable shale in the Lower Quehua Formation. The strata strike N. 30°–54° W. and dip 4°–6° northeast on the flank of a broad anticline. In 1969, the mine produced 5 tonnes per month of hand-picked ore containing about 15 percent copper (Servicio Geológico de Bolivia, 1971c). One sample collected during our visit in 1990 contained 5.3 percent copper, 5 ppm silver, and 8.5 ppm uranium (app. B, sample 90BCX032).

Alianza Mine

The Alianza mine is located 16 km southwest of the Avaroa mine. Mantos in sandstone of the Lower Quehua

Formation have a calcite, chlorite, and limonite cement, and are cut by small fractures containing chalcocite, bornite, and chalcopyrite. A larger fault contains galena, chalcopyrite, and tetrahedrite that are probably related to hydrothermal fluids from the late Tertiary or Quaternary volcanic center 5 km south. Ore reserves are 2,000 tonnes of ore containing 4.36 percent copper (Servicio Geológico de Bolivia, 1971d). One sample collected during our visit in 1990 contained 4.8 percent copper, 30 ppm silver, 700 ppm arsenic, 50 ppm germanium, and 9.6 ppm uranium (app. B, sample 90BCX031).

Sucre Mine

The Sucre mine is located southeast of the Alianza mine. Mantos in sandstone as thick as 15 cm and in conglomerate as thick as 50 cm contain malachite and chrysocolla. Host rock is the San Vicente Formation on the flank of a N. 13° E. trending anticline. Reserves in 1970 were only 4 tonnes of ore with 10 percent copper (Servicio Geológico de Bolivia, 1971ss).

ARGENTINE BORDER AREA

The Argentine border area contains deposits localized in Tertiary sandstone and conglomerate of the San Vicente Formation and basalt of the Rondal Formation on the west flank of an uplift of Ordovician rocks. Occurrences in the area include the Aviadora mine and Campanario occurrence.

Aviadora Mine

The Aviadora mine is located 1.5 km N. 60° E. of Pueblo Viejo. Chalcocite, native copper, and copper carbonates occur with calcite and quartz in fissures in basalt of the Rondal Formation (Servicio Geológico de Bolivia, 1971f).

Campanario Occurrence

At the Campanario occurrence, located 6.5 km S. 12° E. of Pueblo Viejo, bornite, covellite, malachite, and azurite with quartz and calcite impregnate fissures in conglomerate and basalt of the San Vicente Formation (Servicio Geológico de Bolivia, 1971l).

DEPOSITS RELATED TO STRATOVOLCANOES

INTRODUCTION

Quaternary to late Miocene (about 7 Ma) stratovolcanoes and their distal deposits (pl. 1, QTev) cover more than 24,000 km^2 in the study area. Many of the eruptive centers that have been identified in the area exhibit pronounced bleached and altered areas, some of which contain deposits of native sulfur (figs. 4, 58); one, Cerro Eskapa, contains an unusual copper deposit. All are potential sites of hydrothermal systems that may have deposited base- and (or) precious-metals.

ALTERED AREAS

More than 130 conspicuous, light-colored altered areas were identified, either by ground observation or on satellite images, in the summit areas of many of the volcanic centers (see section on Remote sensing). Most of these altered areas are less than 2 km in diameter and restricted to the immediate volcanic vent area. Others, such as at Cerro Amarillo in the Volcán Juriques 1:250,000-scale quadrangle and Cerro Phasa Willkhi in the Corque 1:250,000-scale quadrangle, may cover more than 20 km^2 and occur as a chain or group of volcanic vents. The alteration may have involved no more than the leaching of certain elements from the rocks, but in areas of stronger alteration the rocks may be silicified, argillized, and pyritized. Limonite staining is locally common and alunite is present in some of the altered areas.

Eight of these young, high-level altered areas were briefly examined and sampled during the course of this study. With the exception of minor barite mineralization in the Cerro Eskapa altered area, no veins or mineralized structures were observed in any of the areas. Geochemical analyses, on the other hand, do show that trace amounts of precious metals occur locally, suggesting that an epithermal gold and (or) silver resource may be present.

WARA WARA PROSPECT (CERRO PHASA WILLKHI)

By James C. Ratté, B.M. Gamble, *and* Alberto Hinojosa-Velasco

Summary

The Wara Wara prospect (app. A, no. 103) is a large, complex area of hydrothermal alteration in an eroded composite stratovolcano. In the southern part of the altered area, the character of the alteration indicates a fumarolic or hot-spring environment represented by widespread and intense silicification (opalization) and alunitization. No ore minerals or vein structures were observed, but the extent and intensity of the altered rocks warrants systematic geochemical sampling and detailed geologic mapping.

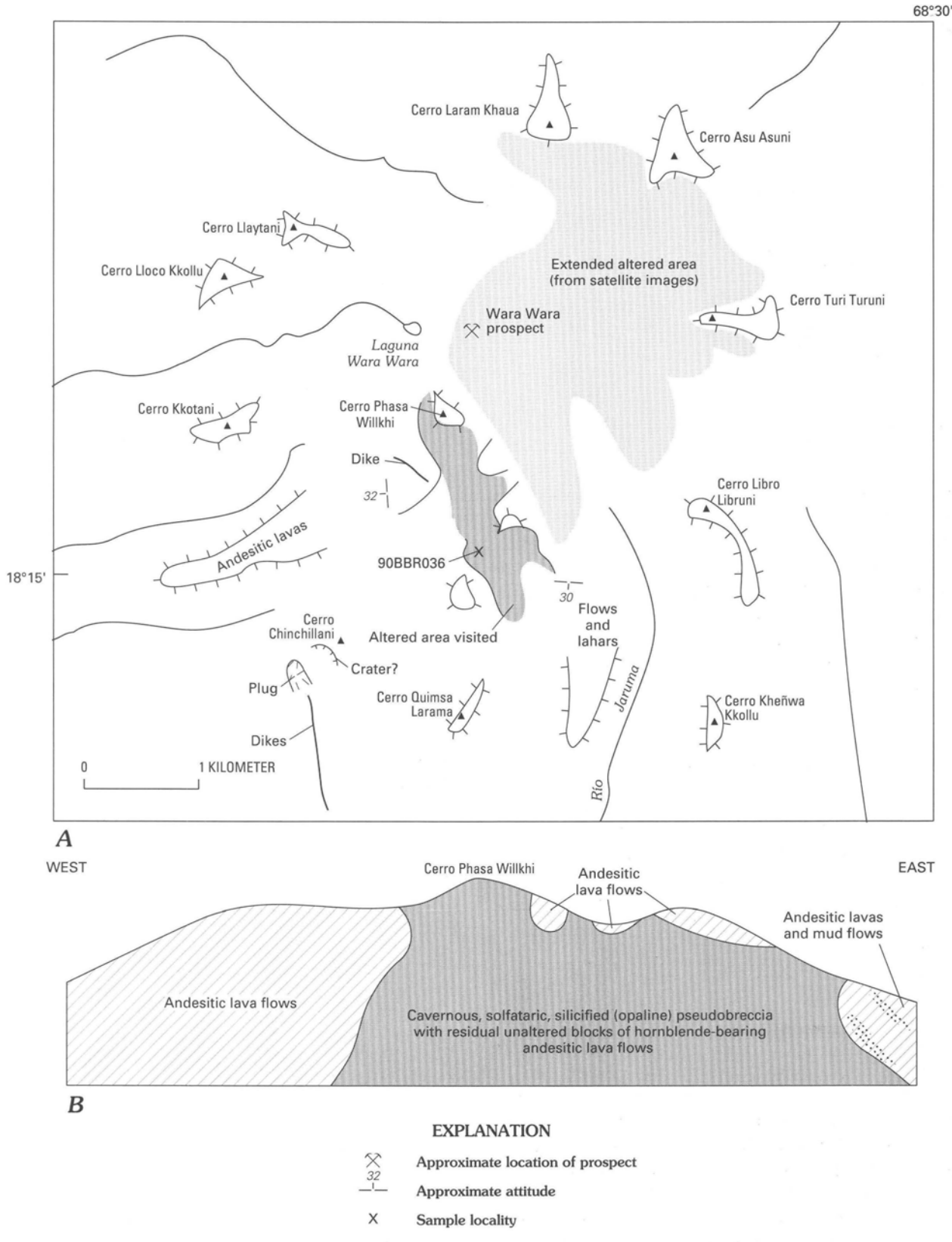


Figure 49. Cerro Phasa Willkhi composite stratovolcano, Bolivia. *A*, Sketch map showing approximate extent of altered volcanic rocks as interpreted from satellite photos. Drainage from Estancia Rica 1:50,000-scale quadrangle. Hachured lines outline upper contours of major peaks. *B*, Diagrammatic cross section of Cerro Phasa Willkhi.

Introduction

A precious-metal prospect known as Wara Wara is located in the summit area of the stratovolcano Cerro Phasa Willkhi about 35 km west of the village of Turco in the Corque 1:250,000-scale quadrangle (fig. 49). The prospect, at an elevation of about 4,870 m, consists of workings of unknown extent in an extensive altered area. Assays of as much as 0.04 g/t gold, 1 g/t silver, 30 ppm arsenic, and 18 ppm antimony are reported from the prospect. The geologic map of the Sajama 1:100,000-scale quadrangle (Ponce and Avila, 1965b) includes all of the altered area and most of the Cerro Phasa Willkhi stratovolcano. A part of the altered area was examined in September 1990; the remote prospect, however, was not visited.

Geologic Setting

Phasa Willkhi is a composite stratovolcano chiefly of dacite or andesite composition that probably overlies a foundation of early Miocene to late Oligocene Mauri Formation ignimbrites. The altered rocks, which underlie as much as 10–20 km^2 in the eroded summit area of the volcano, consist of hornblende-bearing andesitic to dacitic lava flows, mudflows, and volcaniclastic breccias. A plug and related dike, representing a small subsidiary intrusion, cut volcanic rocks on the south flank of the volcano near Cerro Chinchillani.

Geology and Mineral Deposits

Altered rock is first exposed on the volcano at about 4,700 m in the valley southeast of the saddle at 4,910 m (fig. 49), where ledges on the west side of the valley have the appearance of a highly silicified (opalized) cap. Higher, in the saddle, the silicified rock is a cavernous breccia, derived from alteration of the hornblende-bearing andesite, which is preserved as pseudoclasts of centimeter-size to large outcrop masses. Samples collected at this locality (app. B., samples 90BBR036a, c, d, e, h) are slightly anomalous in lead (30–50 ppm); all contain less than 0.05 ppm silver. The altered rock is dominantly yellow to white opal, with areas of massive clay(?), and quartz and alunite. No pyrite or other sulfides were observed, but abundant fine-grained, yellow, crystalline jarosite(?), and iron oxide stains are present. Where the silicified rock is intensely fractured, the fractures parallel joints and layering in unaltered outcrops. The siliceous, cavernous, and brecciated character of the altered rocks suggest a high-level solfataric or hot-spring environment above a cooling intrusion. A composite grab sample of argillized and iron-stained float (app. B, sample 90BBG040) collected near the head of Quebrada Khuymiri on the south flank of the stratovolcano contained 0.16 ppm silver but no other anomalous metal concentrations.

MARIA ELENA PROSPECT (CERRO CULEBRA)

By James C. Ratté, B.M. Gamble, Edwin H. McKee, Eduardo Soria-Escalante, *and* Raul Carrasco

Summary

The María Elena prospect (app. A, no. 177) consists of an extensive area of silicification in an apparent subvolcanic intrusion exposed at the top and along the western and southern flanks of Cerro Culebra. No veins were observed, and the gold and silver values reported from the area may represent disseminated mineralization in a shallow stock or in highly altered silicic dikes and sills. More sampling and detailed geologic mapping are recommended for a better evaluation of the area.

Introduction

Cerro Culebra is a composite stratovolcano, probably of late Miocene age, that is located about 6.5 km south and slightly east of the village of Todos Santos in the Cordillera Occidental. The María Elena prospect consists of an extensive altered zone extending south from the summit area. No workings were seen or are reported to occur in the area, and no mineralized structures were observed. Minería Técnica Consultores Asociados (MINTEC) explored the area in 1987 and found trace amounts of precious metals but apparently nothing has been done in the area since then. The only published information on the area is the Todos Santos 1:100,000-scale geologic map (Ponce, Avila, Delgadillo and others, 1967). The area was visited in September 1990 to examine and sample the altered area.

Geology and Mineral Deposits

Examination of the altered area was confined to the south side of Cerro Culebra where a glacial valley trends southeast from the central part of the volcano. On the northeast side of the cirque valley, the mountain consists largely of a yellowish-white, altered subvolcanic intrusion in the core of the volcano (fig. 50). A distinct but irregular contact between the altered intrusion and a roof of dark-gray andesitic-dacitic lavas is present near the east end of the ridge, and remnants of the lava flows are also preserved along the mountain crest. The plagioclase-phyric lava flows in the roof of the intrusion have been invaded by numerous narrow sills and dikes of fine-grained, silicified rhyolite containing oxidized pyrite and perhaps jarosite. The main

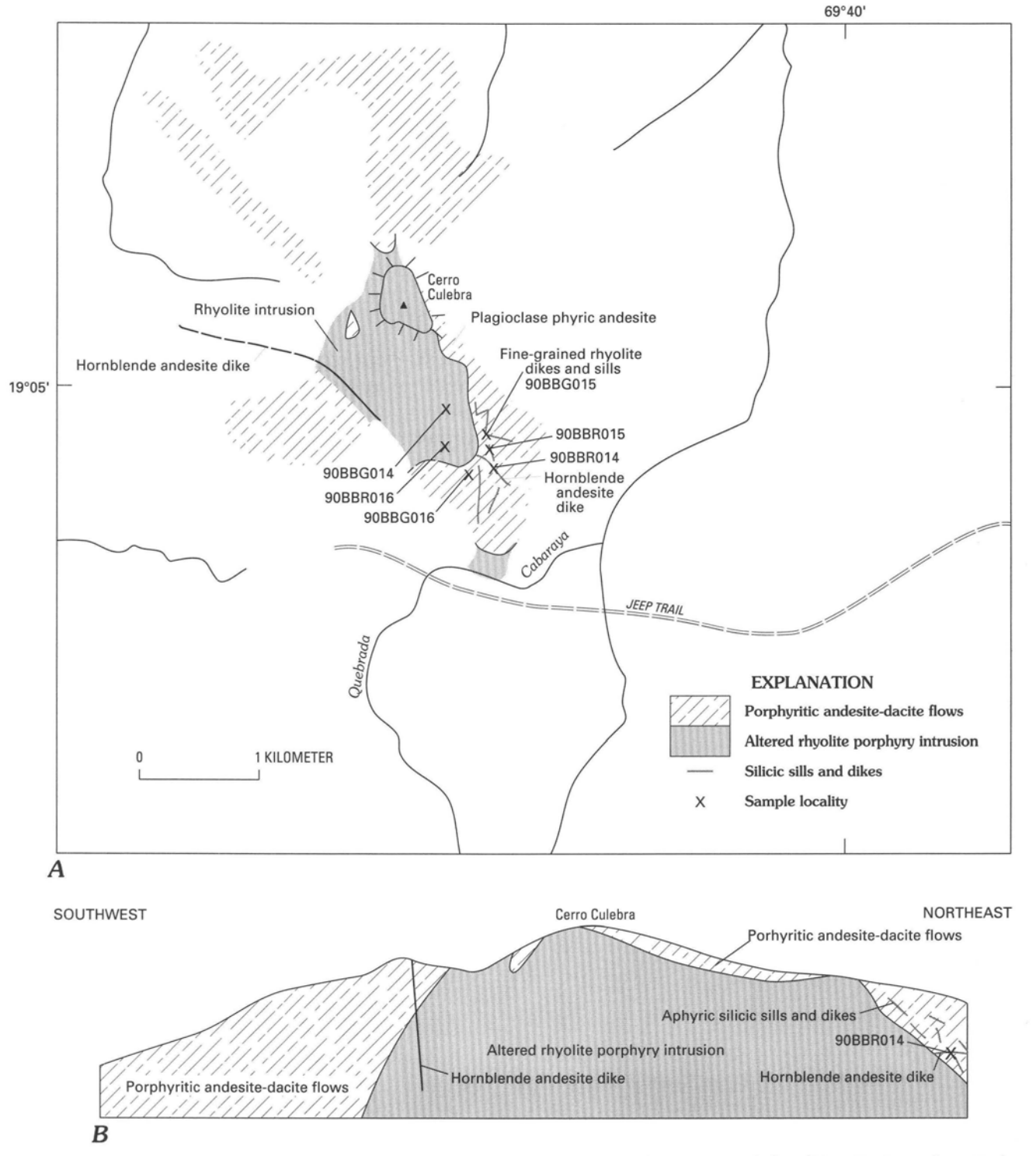


Figure 50. María Elena altered area on Cerro Culebra, Bolivia. *A*, Sketch map showing sample localities. Drainage from Todos Santos (5836 I) 1:50,000-scale quadrangle. *B*, Diagrammatic southwest-northeast cross section through Cerro Culebra.

intrusive mass has a relict texture that indicates it was a spherulitic, porphyritic rhyolite(?) containing feldspar phenocrysts, 2–4 mm long, that are now altered to a white mineral. The rock is now strongly silicified to yellow and gray opal, and locally contains small pockets of white clay(?) and finely crystalline coatings of yellowish-pink jarosite(?). The porphyritic intrusion, the rhyolite dikes and sills, and the volcanic roof rocks are all cut by a 5–10 m thick, dark-gray, fine-grained, hornblende-bearing andesite dike, that can be traced for several kilometers across the

southern and western slopes of Cerro Culebra (fig. 50). Hornblende from this dike has yielded a K–Ar age of 6.3±0.2 Ma (app. C), thus limiting the age of the silicic intrusion and related alteration.

During exploration in the area, MINTEC geologists obtained a number of samples that contained 0.1–0.5 g/t gold; silver values were generally less than 1 ppm. Samples collected during this study (app. B, samples 90BBG014, 15a, b, c, 16a, b; 90BBR015, 16) from the main intrusive body and the satellitic dikes and sills all contain less than 0.002 ppm gold and a maximum of 0.7 ppm silver.

MILENKA PROSPECT (CERRO CURUMAYA)

By James C. Ratté, B.M. Gamble, Eduardo Soria-Escalante, *and* Raul Carrasco

Summary

Milenka (app. A, no. 173) is a prospect on Cerro Curumaya consisting chiefly of argillically altered rock in the core of an eroded stratovolcano. No ore minerals were observed. Systematic sampling of the altered rocks and a more thorough study of the geologic setting are needed to evaluate the area.

Introduction

The Milenka prospect is an altered area south of the summit of the volcano Cerro Curumaya (fig. 51). The volcano is located about 12 km due west of the village of Todos Santos in the central Cordillera Occidental. Previous exploration by MINTEC revealed gold values as high as 0.2 g/t, but very low silver values, less than 1 g/t. The altered area was examined in September 1990.

Geology

Cerro Curumaya is an eroded stratovolcano, probably of late Miocene age, flanked by extensive glacial moraines. Lava flows of hornblende-plagioclase-pyroxene andesite vitrophyre crop out along the ridge between the two main cirques on the south side of the volcano above the moraines. Above these lavas, at about 4,840 m, a frothy lava flow or intrusive dacite vitrophyre containing fresh biotite and 65.9 percent SiO_2 (app. B, sample 90BBR020) is exposed. Altered rocks from the base of the cliffs on the east side of the cirque and in iron oxide-stained rock knobs and ribs cropping out of talus beneath the cliffs appear to be the same biotite-bearing vitrophyre suggesting that the upper flows of the volcano and its core, or plug, may be more siliceous than the flows lower on the flanks. These altered rocks (app. B, samples 90BBR021a, b, c, d) contain a maximum of 0.7 ppm silver and 50 ppm lead. Float samples of variably silicified, argillized, and iron oxide-stained rock were also collected (app. B, samples 90BBG018a, b, c, d; fig. 51). These samples were collected from an extensive altered area that underlies the cliffs at the head of the cirque. The samples contain as much as 10 ppm silver and 50 ppm lead; gold was not detected at the limit of determination (0.002 ppm).

CERRO PUQUISA

By Eduardo Soria-Escalante *and* René Enriquez-Romero

Summary

Puquisa volcano contains a hydrothermally altered area (app. A, no. 205) that could be associated with an epithermal precious-metal deposit. However, geochemical studies and geologic mapping are needed to better evaluate the mineral-resource potential. The nearby Granada manganese deposit may have some potential as a source of high-grade manganese ore from veins buried under a cover of Quaternary lacustrine deposits.

Introduction

Cerro Puquisa is apparently a small cone on the northwest flank of Cerro Caltama (4,936 m), a larger stratovolcano in the Cordillera Occidental between Salar de Uyuni and the Chilean border, in the Villa Martin 1:250,000-scale quadrangle. An altered area was observed on Cerro Puquisa by Ludington and Soria-Escalante during a flight over the area in October 1990 and it was examined in December 1990, as was the Granada manganese mine, south of the village of Canquella.

Geologic Setting

Cerro Puquisa appears typical of many of the smaller composite cones in the Cordillera Occidental. A late Miocene age is assigned to the volcano mostly on the basis of the well-developed glacial deposits on its flanks. The lavas of the Puquisa and Caltama cones overlie a thick sequence of older volcanic rocks consisting chiefly of dacitic pyroclastic flows, tuffs, and volcaniclastic rocks that were probably deposited in a subaqueous environment.

Altered Area

An area of argillic and silicic alteration, that may be associated with the emplacement of a subvolcanic intrusion, occurs under and around Paco Kkollu (fig. 52), a hill on the western slope of Cerro Puquisa. Although no outcrops of

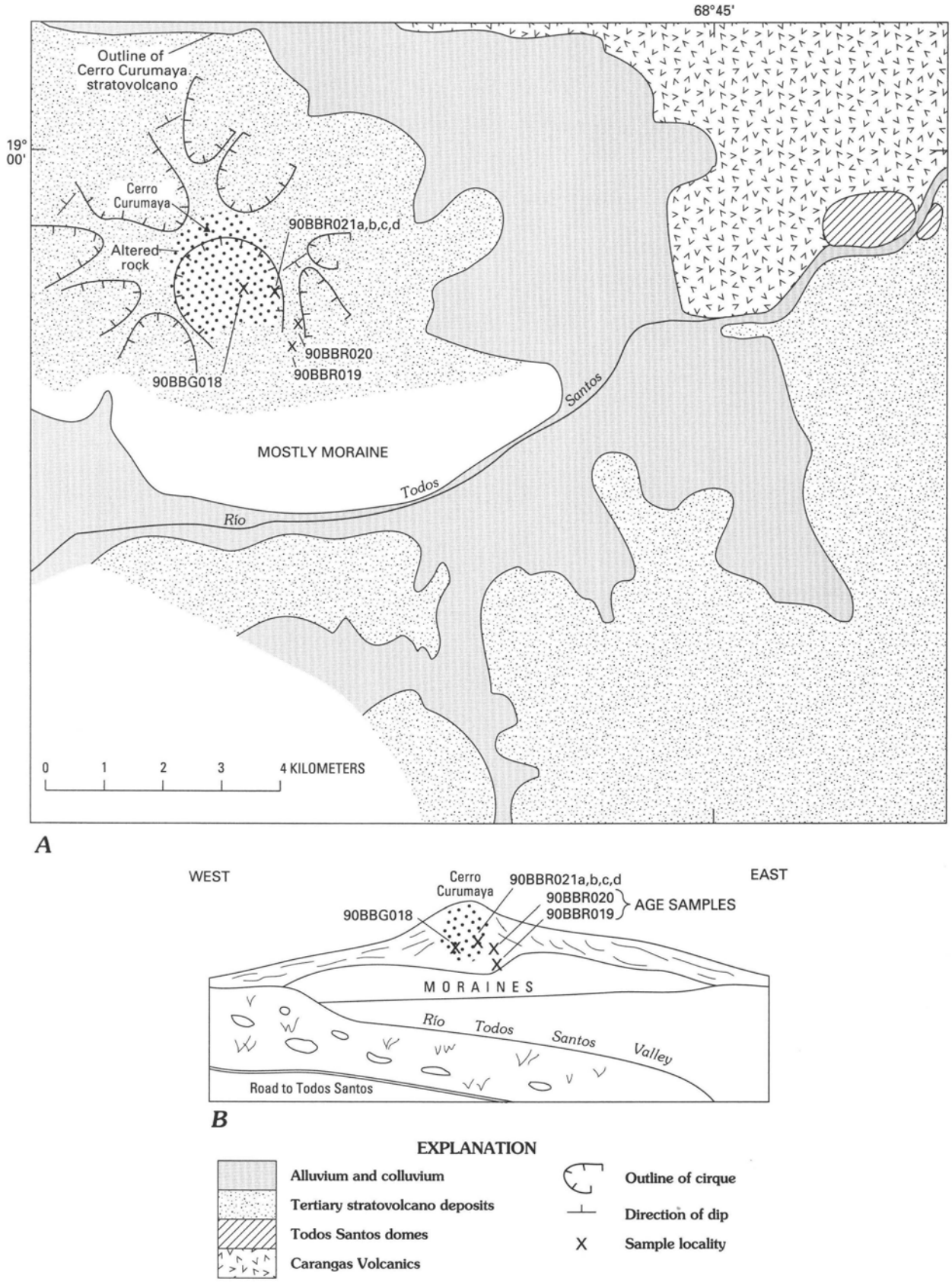


Figure 51. Cerro Curumaya area, Bolivia. *A*, Sketch map showing sample localities. Drainage from Todos Santos (5836) 1:100,000-scale quadrangle. *B*, Sketch of Cerro Curumaya from the south, showing altered area.

unequivocal subvolcanic rock have been found, there is an aureole of very intense silicic alteration in the pyroclastic rocks peripheral to the hill. Primary textures in the rock of Paco Kkollu and surrounding area have been completely modified or obliterated. Limonite-rich veinlets occur locally; however, no sulfides or other ore minerals were observed. A northeast-trending shear zone, which occurs in the outer fringe of the alteration aureole, may have played a role in the localization of the alteration. Seven samples (90BES037, 39–44) were taken from the altered area. Neither gold nor silver was detected at the limits of determination (gold, 0.002 ppm; silver, 0.045 ppm), and no other anomalous elements were noted.

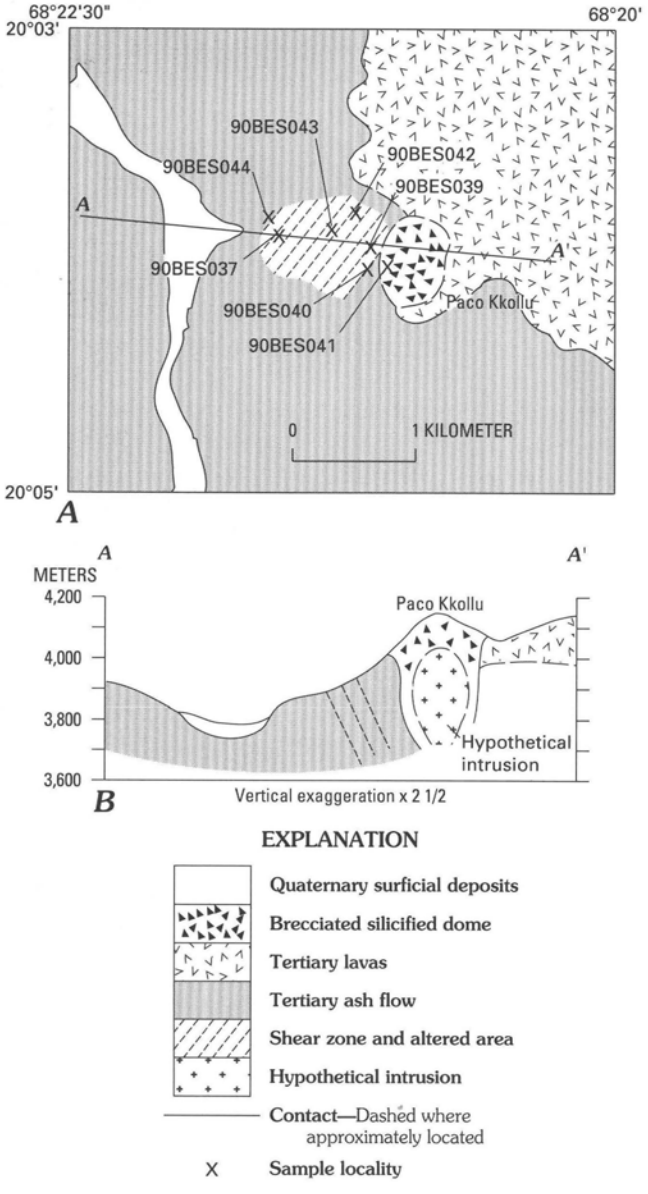


Figure 52. Paco Kkollu area on Cerro Puquisa, Bolivia. *A*, Sketch map showing geology and sample localities. *B*, Cross section through Paco Kkollu.

Granada Mine

A series of veins of high-grade manganese ore (app. A, no. 209) occur 5 km south of the village of Canquella and about 13 km southeast of the altered area on Cerro Puquisa. The veins have been mined on a limited scale in the past, but are currently inactive; the last reported owner was A. Quezada (Donoso, 1959).

Host rock for the veins is a sequence of volcaniclastic and pumice-rich pyroclastic deposits interbedded with various amounts of sedimentary rocks. The sedimentary rocks are fine grained and finely laminated, and contain abundant worm tubes, suggesting that the entire sequence was deposited in a lacustrine environment.

The veins occupy a series of north-trending fractures and faults that exhibit dextral strike-slip displacement. Locally, thicker pods of manganese minerals occur at flexures in the fracture-fault system (fig. 53*A*). Manganese minerals also extend out from the veins along bedding planes in the host volcaniclastic and pyroclastic rocks (fig. 53*B*). Ore minerals consist of reniform pyrolusite, psilomelane, and minor limonite-hematite; chalcedony is a common gangue mineral. The veins contain as much as 50 percent impurities, consisting chiefly of rock and pumice fragments. A sample analyzed by Donoso (1959) contained 41.60 percent MnO_2, 45.76 percent SiO_2, 2.34 percent Fe_2O_3, and 0.16 percent phosphorus.

The mineralization at the Granada mine is apparently of hot-spring origin. Manganese-rich cement in the overlying Quaternary stromatolitic limestones (fig. 53*B*) suggest that the hot-spring activity persisted until recently.

IÑEXA PROSPECT (INTERSALAR RANGE)

By Eduardo Soria-Escalante *and* René Enriquez-Romero

Summary

The Iñexa prospect (app. A, no. 195) is a hydrothermally altered area in the eroded vent area of a Late Tertiary stratovolcano. It has interest as a possible precious-metal deposit, but there is no evidence of ore mineralization and the results of geochemical sampling were not encouraging.

Introduction

The Iñexa prospect is in the Intersalar Range about 30 km west of the village of Salinas de Garci Mendoza between Salar de Coipasa and Salar de Uyuni in the Salinas

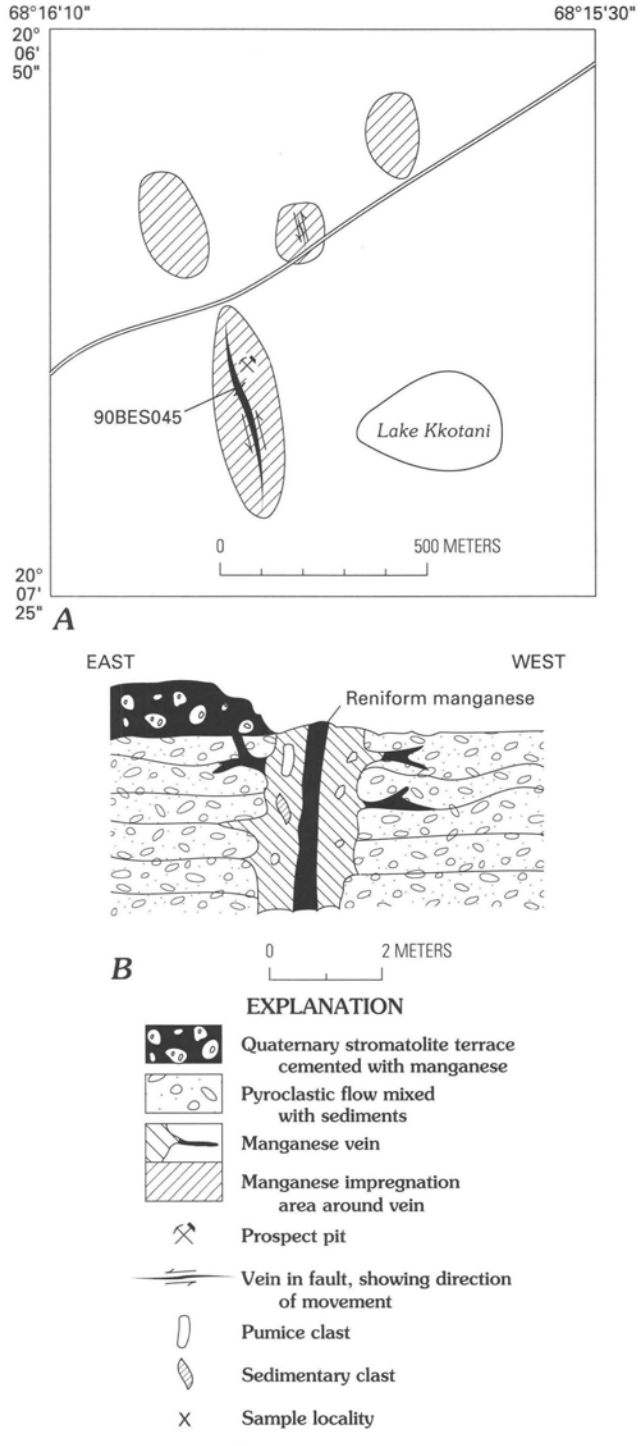


Figure 53. Mineralized areas of manganese, Granada mine area, Bolivia. *A*, Sketch map showing sample locality. *B*, Diagrammatic section through a manganese vein.

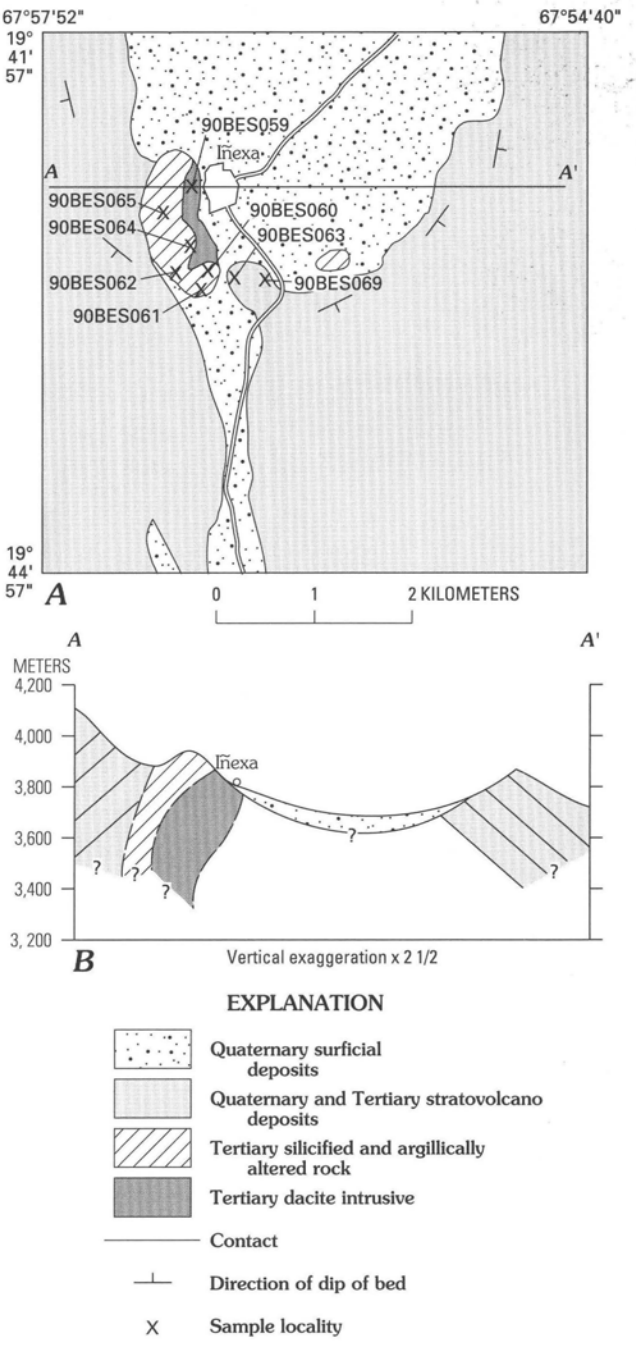


Figure 54. Iñexa area, Bolivia. *A*, Sketch map showing geology and sample localities. *B*, Cross section through the Iñexa area.

de Garci Mendoza 1:250,000-scale quadrangle. The prospect has been explored and sampled by MINTEC, but there is no known published information on the area. The area was examined in December 1990.

Geologic Setting

The Intersalar Range is composed of a number of late Miocene and younger stratovolcanoes aligned in an east-west trend, normal to the general trend of the Cordillera Occidental. In the range, stratovolcano lavas (pl. 1, QTev) overlie a sequence of ash flows and volcaniclastic rocks of the Tagua Formation (pl 1., Tvnd) of middle Tertiary(?) age. Near the village of Iñexa the stratovolcano lavas are chiefly hornblende-biotite dacite flows and fragmental rocks.

Geology and Mineral Deposits

At the Iñexa prospect, intense silicic and argillic alteration occurs in a brecciated dome-like area (fig. 54). The hornblende-biotite dacite lavas appear to have been intensely sheared and silicified by the emplacement of a shallow hornblende dacite intrusion. No ore minerals were observed in the area but boxwork textures and abundant limonite indicate that sulfides had been present. Unconfirmed reports of high silver values at the prospect were not confirmed by analyses of our geochemical samples (app. B, samples 90BES059–65, 69) showed only very low precious-metal values. Sample 90BES063 contained 0.07 ppm silver, and sample 90BES059 contained barely detectable gold (0.002 ppm). Base metal values were low.

CERRO ESKAPA

By Donald H. Richter, W. Earl Brooks, Nora Shew, Alberto Hinojosa-Velasco, *and* Angel Escobar-Diaz

Summary

The Eskapa mine (app. A, no. 260) is a small, near-surface, volcanic-hosted low-temperature copper deposit. A very limited mining operation producing high-grade material may be economically feasible, especially during times of high copper prices, however, there does not appear to be a significant copper resource and the potential for finding additional deposits is probably low.

The altered area in the vent complex of Cerro Eskapa (app. A, no. 259) is a possible example of a high-level epithermal quartz-adularia deposit. Although gold and silver values from surface samples are low, the extent and intensity of alteration should encourage an investigation of the mineral resource in the subsurface.

Introduction

Cerro Eskapa (5,145 m) is a late Tertiary strato-volcano approximately 125 km southwest of the city of Uyuni and 18 km northwest of the village of Alota in Sud Lípez province in the Volcán Ollague 1:250,000-scale quadrangle. The areas of interest are an inactive copper mine low on the flank of the volcano and a very conspicuous hydrothermally altered area in the eroded central vent complex (fig. 55). The copper mine and altered area on the volcano were examined in October 1990.

Geology and Mineral Deposits

Volcano Cerro Eskapa and its twin Cerro Khala Katin, to the northeast, occur in a large field of Quaternary and late Tertiary stratovolcanoes north of Pastos Grande caldera. The volcanoes were built on ash flows of the Miocene to Pleistocene Ignimbrite Formation (pl. 1, QTig) and volcaniclastic rocks of the Upper Quehua Formation (pl. 1, Tig).

Eskapa Mine

The Eskapa mine (app. A, no. 260) is a small, possibly unique, copper vein deposit on the north flank of Cerro Eskapa at an elevation between 4,200 and 4,250 m (fig. 55). The deposit was probably discovered and mined in Spanish colonial times and, according to local sources, was mined in 1968 and 1971 by a small, local cooperative; present ownership is unknown.

Development consists of 2 small glory holes, which open downward into a series of underground workings of unknown dimension, and a short adit that terminates at a 15-m-deep shaft (fig. 56). The workings occur in a broad and somewhat irregular broken and brecciated zone, trending about N. 10° W., in a massive dacite or rhyolite porphyry lava flow or dome.

The ore minerals are chiefly tenorite (black amorphous oxide of copper), chrysocolla, and minor malachite. The tenorite and chrysocolla occur as colorful botryoidal layers, as thick as 1 cm, and in small irregular veins coating fragments and filling space between fragments in the broken brecciated zone. Malachite occurs locally as thin layers of bright-green crystals lining small open spaces. White to pale-green, chalky calcite is a local gangue mineral, generally filling some of the larger interstitial space between fragments and blocks. Size of the blocks and fragments in the broken brecciated zone ranges from about 1 cm to more than 2–3 m. Other metals in the copper-rich veins (table 11, sample 90BDR035a) include some silver (30 ppm) and modest amounts of lead (3,000 ppm).

The host dacite porphyry contains phenocrysts of sanidine, plagioclase, biotite, and minor quartz in a light-gray cryptocrystalline groundmass that locally has undergone vapor phase crystallization. The SiO_2 content of a sample of typical dacite porphyry is 63.8 percent (app. B, sample 90BDR035). Biotite from the same sample yielded a K–Ar age of 6.3±0.1 Ma (app. C).

Altered Area

A large area of white to tan, chiefly argillic alteration (app. A, no. 259) covers more than 12 km^2, high in the eroded center of the volcano. The original composition of

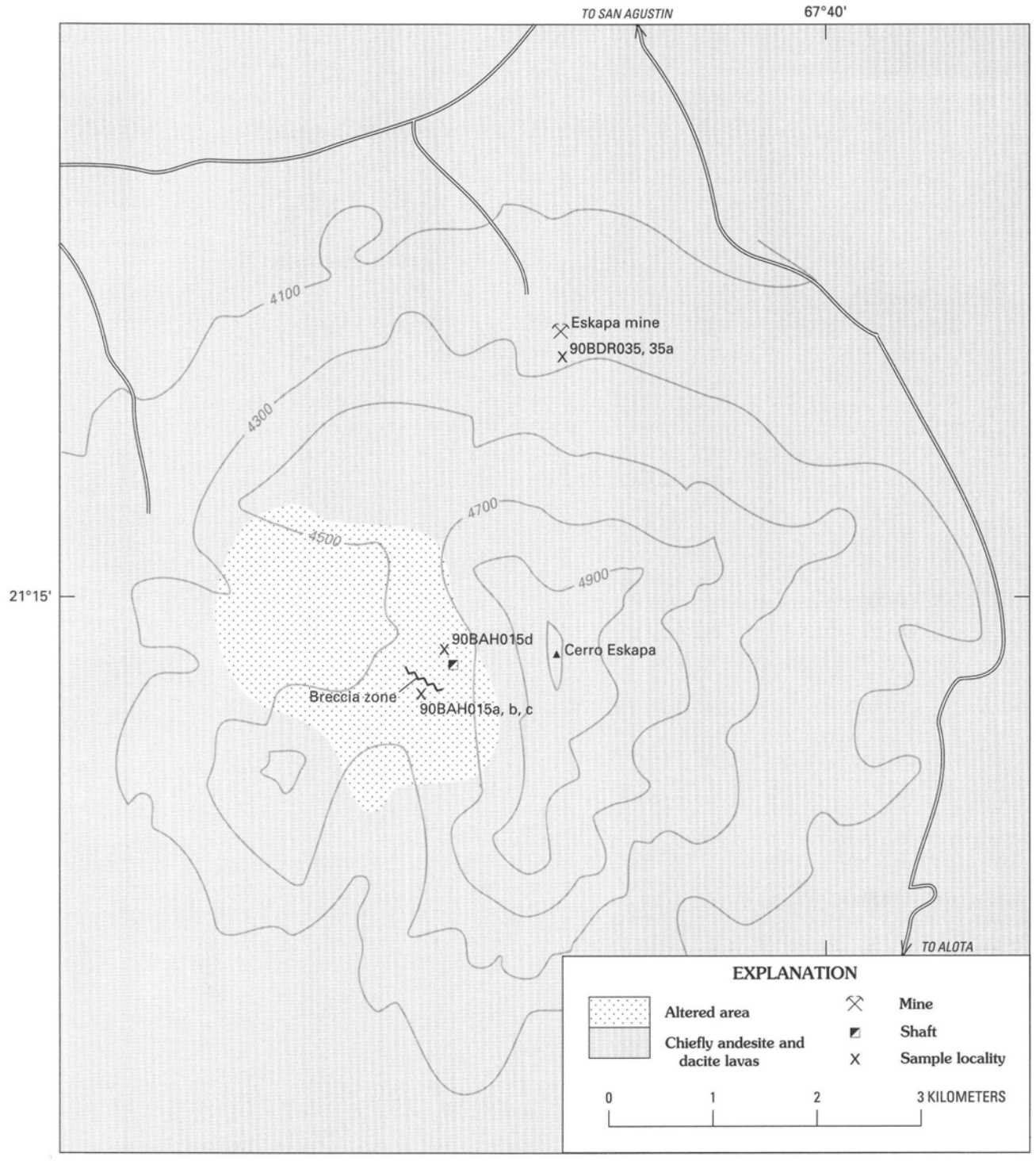


Figure 55. Sketch map of Cerro Eskapa area, Bolivia, showing location of Eskapa mine, altered area, and sample localities. Topography from Estancia Sora (6030 II) 1:50,000-scale quadrangle.

the altered rock is believed to have been predominantly dacite. Quartz is the only remaining primary mineral; feldspar sites are filled with clay and sericite(?) or alunite(?), and mafic minerals are either absent or replaced by clay minerals.

Prospecting activity in the altered area appears to have been largely restricted to a northwest-trending zone of brecciation (fig. 55) marked by strong iron staining and the local occurrence of bladed crystals of barite in a breccia cement. A 10-m-deep shaft, at an elevation of about 4,600

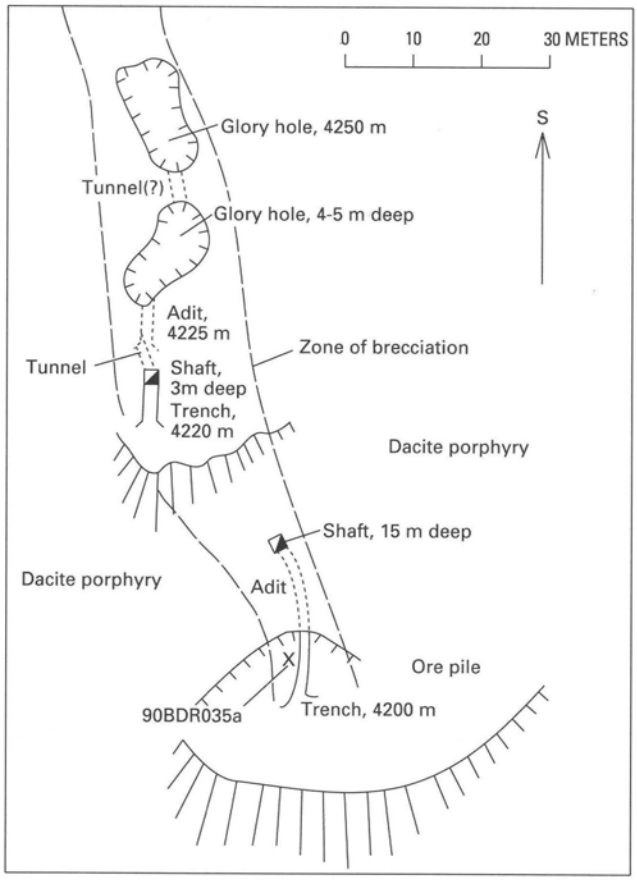


Figure 56. Sketch map of the Eskapa copper mine area, Bolivia.

m, and a number of shallow pits explore about 30 m of the breccia zone. Three samples collected from the breccia zone (90BAH015a, b, c) contain as much as 0.20 ppm gold, 400 ppm silver, 790 ppm arsenic, 7,700 ppm antimony, and 44 ppm tellurium (table 11; app. B). About 80 m northeast of the breccia zone, a 20 m-deep shaft has been sunk in an area of pronounced chalcedony deposition. Sample 90BAH015d, collected from the tailings at this shaft, contains 33 ppm silver, 3,400 ppm lead, 210 ppm arsenic, 3,800 ppm antimony, and 4.6 ppm mercury (table 11; app. B).

In 1917, H.G. Officer visited the altered area on Cerro Eskapa and referred to it as the Cuidado silver mine. He prepared a sketch map of the area and collected 15 samples for analysis (Officer, 1917a). Little has changed in the more than 70 years since his visit. Officer noted the presence of a house and spring, which we did not see, and estimated the depth of the lone shaft at 50 m, more than twice the depth of our estimate. Of significance perhaps, is one of Officer's samples which contained 5.54 oz/short ton gold and 30.5 oz/short ton silver. Unfortunately, the location of this sample is only given by the cryptic statement that it was collected "lying near an open pit". The 14 other samples collected by Officer, which are all specifically located, contained a maximum of a trace of gold and 4.4 oz/short ton silver.

CERRO CACHI LAGUNA

By W. Earl Brooks, Donald H. Richter, Alberto Hinojosa-Velasco, *and* Angel Escobar-Diaz

Summary

The summit of Cerro Cachi Laguna contains a large area of solfataric alteration (app. A, no. 282). Minor native sulfur is present locally, but no other ore minerals or vein structures were observed or have been reported. In addition, geochemical sampling did not indicate any significant metal anomalies. On the basis of these surface criteria, the area is considered to have little potential for precious-metal deposits.

Table 11. *Chemical analyses of mineralized and altered rocks, Cerro Eskapa area, Bolivia*

[All results in parts per million (ppm). Complete analyses in appendix B. Sample 90BDR035a, chrysocolla vein; sample 90BAH015a, barite-rich altered breccia; sample 90BAH015b, barite-rich altered breccia; sample 90BAH015c, barite-rich altered breccia; sample 90BAH015d, silicified volcanic rock]

Sample no.	Au	Ag	Pb	Zn	Cu	As	Sb	Te
90BDR035a	<0.002	30	1,200	140	150,000	<30	190	<0.05
90BAH015a	.20	400	180	40	49	790	7,700	44.0
90BAH015b	.002	51	45	25	<0.3	85	310	10.2
90BAH015c	<.004	<0.45	<5.0	29	<.3	33	20	.4
90BAH015d	<.002	33	3,400	36	4.1	210	3,800	17.0

Table 12. *Chemical analyses of altered rocks, Cerro Cachi Laguna area, Bolivia*

[All results in parts per million (ppm). Sample descriptions, methods, and complete analyses in appendix B. Gold in all samples was <0.002 ppm. Sample 90BEB003a, altered dacite; sample 90BEB003B, altered dacite; sample 90BEB003D, composite sample of altered volcanic rock]

Sample no.	Ag	Pb	As	Tl
90BEB003a	1.4	790	390	3.50
90BEB003b	0.64	120	72	2.15
90BEB003d	<0.45	340	900	4.25

Introduction

Cerro Cachi Laguna is a partly dissected stratovolcano in the Volcán Ollague 1:250,000-scale quadrangle approximately 42 km southwest of the village of Alota in Sud Lípez province. The bowl-shaped summit area of the volcano encloses a brightly colored altered zone that was examined in October 1990.

Geology and Mineral Deposits

Cerro Cachi Laguna is a moderate-sized (about 40 km^3) volcanic cone built in the interior of the large Pastos Grande caldera which formed about 5–7 m.y. ago (Baker and Francis, 1978). The cone is composed chiefly of lava flows, flow breccias, and mudflows of andesitic and dacitic composition. A large, unaltered dacite porphyry dome occurs on the west side of the summit depression. The dacite contains 64.3 percent SiO_2 (app. B, sample 90BDR038) and contains phenocrysts of plagioclase and minor hornblende, biotite and pyroxene in a trachytic groundmass of biotite and feldspar. Unaltered lavas exposed in the cliffs peripheral to the summit altered area are also chiefly dacite porphyries containing phenocrysts of plagioclase, hornblende, and biotite. In the altered area, which covers about 6 km^2, the rocks are bleached, argillized, and locally stained by iron oxide. Our traverse through the altered zone ended at a small, 2–3 m^2 sulfur prospect pit at an elevation of 5,000 m, where sparse, small (<2 cm) masses of native sulfur and clay(?) minerals are scattered throughout the bleached rocks. No evidence of any recent exploration activity was observed. Three samples (90BEB003a, b, d) of altered rock collected along the traverse for geochemical analysis contained only a trace of silver (as much as 1.4 ppm) but as much as 900 ppm arsenic and 790 ppm lead (table 12).

CERRO PODEROSA–CERRO AMARILLO

By Donald H. Richter, W. Earl Brooks, Angel Escobar-Diaz, *and* Alberto Hinojosa-Velasco

Summary

The large solfataric and hydrothermally altered area on Cerro Poderosa-Cerro Amarillo (app. A, no. 317) is poorly exposed. Although no ore minerals were observed and geochemical sampling did not show any significant metal anomalies, the area warrants more sampling and detailed geologic mapping to better evaluate the metallic mineral resource. Three sulfur deposits occur in the apparent western extension of the altered area suggesting that similar deposits may be present elsewhere.

Introduction

A large (>20 km^2) altered area extends between Cerro Poderosa and Cerro Amarillo, two remnant stratovolcanoes, about 45 km south of Laguna Colorada in the Volcán Juriques 1:250,000-scale quadrangle (fig. 57). The altered zone may extend to the west across the Amarillo-Poderosa ridge where three native sulfur deposits are known to occur. The altered area was examined and sampled in October 1990.

Geology and Mineral Deposits

The Cerro Poderosa-Cerro Amarillo altered area is rather poorly exposed, especially at elevations below about 5,500 m. Our investigation was restricted to the northeast part of the altered area where three broad arroyos that join to form an extensive alluvial fan drain the altered zone (fig. 57). The terrain above the drainages is relatively gentle and mostly covered by colluvial rubble. Examination of rock fragments in two of the arroyos, suggests that the dominant rock type in the altered area was originally a dacite porphyry, possibly from a large dome-flow complex. The rock is now very light gray to pinkish gray in color and consists of clay minerals replacing feldspar phenocrysts, jarosite(?) crystals lining small cavities, and rare fresh smoky quartz crystals in a dense silicified (opaline) matrix. Limonite-staining is conspicuous in the area indicating spotty concentrations of oxidized pyrite. The geochemical results of a 100-m-long and a 50-m-long sample traverse (samples 90BDR040a, c, respectively) across two of the

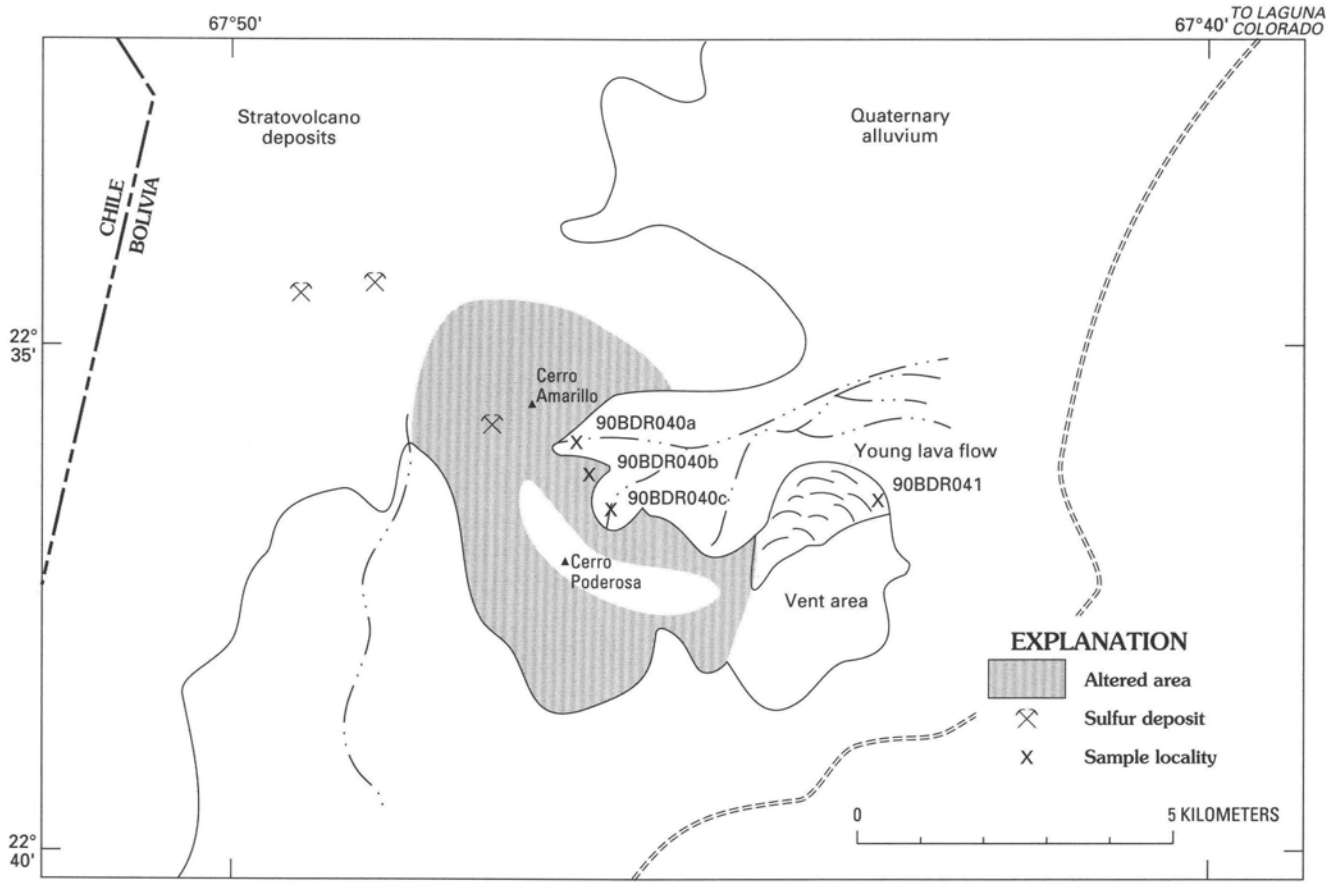


Figure 57. Sketch map of the Cerro Poderosa-Cerro Amarillo area, Bolivia, showing altered rocks, sample localities, and sulfur prospects. Drainage from Volcán Juriques 1:250,000-scale quadrangle.

Table 13. *Chemical analyses of altered rocks, Cerro Poderosa-Cerro Amarillo area, Bolivia*

[All results in parts per million (ppm). Sample descriptions, methods, and complete analyses in appendix B. Gold is <0.002 ppm in all samples. Sample 90BDR040a, 100-m-long composite sample of altered volcanic rock; sample 90BDR040b, silicified breccia; sample 90BDR040c, 50-m-long composite sample of altered volcanic rock]

Sample no.	Ag	Pb	Zn	Cu	As	Sb	Sn
90BDR040a	1.7	270	54	2,000	75	11	<10
90BDR040b	<.45	130	25	61	15	<6.0	<10
90BDR040c	<.45	56	25	<0.30	15	<6.0	15

arroyos are shown in table 13. Neither composite sample contains more than a trace of silver (2 ppm), but sample 90BDR040a contains 2,000 ppm copper, and sample 90BDR040c, surprisingly contains 15 ppm tin. A highly altered bedrock knob exposed between the two sampled arroyos appears to be a different type of volcanic rock. It is only slightly porphyritic with small, sparse feldspar phenocrysts completely altered to sericite or clay minerals in a dense alunite(?)-silica matrix. No mafic minerals or quartz were observed. A sample from a brecciated, limonite-stained part of the outcrop contained <0.45 ppm silver and moderate amounts of lead (table 13, sample 90BDR040b).

The altered area is capped by post-alteration lava flows that may have been erupted from a vent 4 km east of Cerro Poderosa. This vent was also the source of a small and very young, lobate-shaped dacite flow (fig. 57). The dacite flow (65.1 percent SiO_2) is porphyritic containing abundant, fresh phenocrysts of plagioclase and very sparse altered biotite and hornblende phenocrysts (app. B, sample 90BDR041).

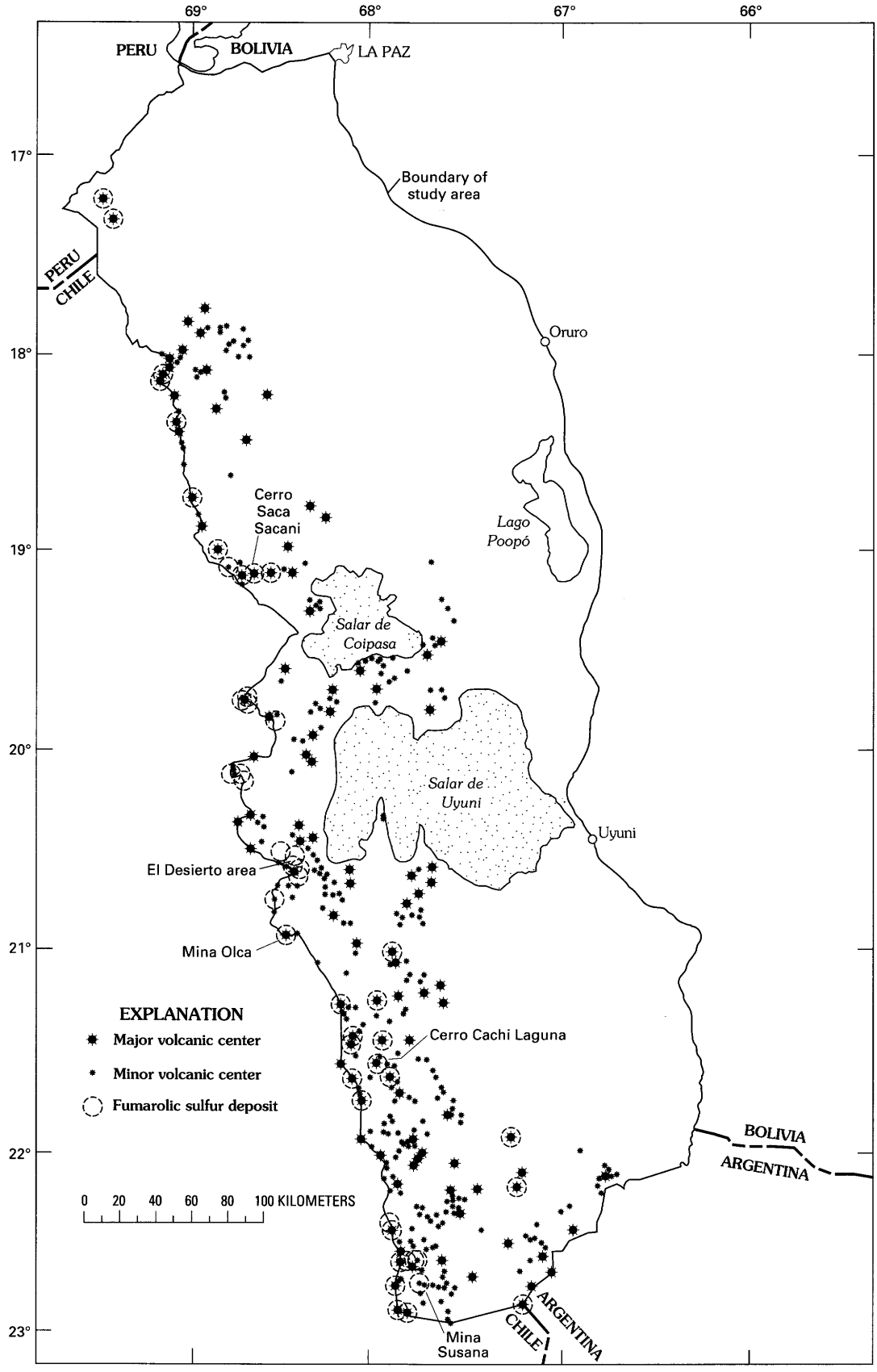


Figure 58. Map showing location of known fumarolic native sulfur deposits, Altiplano and Cordillera Occidental, Bolivia.

Table 14. *Native sulfur deposits and occurrences in the Cordillera Occidental and southern Altiplano, Bolivia*

[Underlined mine name denotes known production. Leaders (--) indicate no specific mine name]

Map no.	Mine or prospect name	Stratovolcano
	Charaña quadrangle	
1	—	Cerro Serkhe
2	—	Cerro Huaricuna
3	El Desierto	Cerro Sinejani
	Corocoro quadrangle	
4	—	Cerro Suni Khava
	Nevados Payachata quadrangle	
5	—	Cerro Parinacota
6	—	Nevado Quimsa Chata
7	—	Nevados Payachata
	Corque quadrangle	
8	—	Cerro Paquentica
9	—	Nevado Sajama
	Salinas de Garci Mendoza quadrangle	
10	—	Cerro Cumi
11	—	Cerro Saca Sacani
12	—	Cerro Tunupa
13	—	Nevado Candelaria
14	—	Cordillera Sillajquay
15	—	Volcán Sillillica
16	10 de Noviembre	Cerro Cabarayo
17	Anita	Cerro Cabarayo
	Villa Martin quadrangle	
18	Golden Hill	Cerro Catalma
19	—	Cerro Tankhani
20	Concepción	Cerro Cayte
21	María Eugenia	Cerro Cayte
22	Milluri	Volcán Ocaña
23	San Pablo de Napa	Cerro Roko Kkollu
24	Victoria	Cerro Cayte
25	—	Volcán Iruputuncu
26	Tres Rayas, Carlota	Volcán Olca
	Volcán Ollague quadrangle	
27	—	Cerro Ascotan
Ramaditas		
28	—	Cerro Cachi Laguna
29	—	Cerro Caquella
30	Corina	Cerro Tapaquilcha
31	El Triunfo	Cerro Cañapa
32	—	Cerro Chiquana
33	Luz Marina	Cerro Cañapa
34	Victoria	Cerro Cañapa
35	Santa Rosa	Volcán Ollague
	Volcán Juriques quadrangle	
36	—	Cerro Pabellon
37	—	Cerro Sairecabur
38	—	Cerro Tocor Puri
39	Juanita	Cerro Amarillo
40	Rosario del Rey	Cerro Rosario del Rey
41	Rosita	Cerro Amarillo
42	SanVicente	Cerro Amarillo
43	Susana	Cerro Rio Amargo
44	—	Volcán Juriques
45	—	Volcán Llicancahur
46	Nelly	Cerro Aguas Calientes
47	Bienvenida	Cerro Bienvenida
48	Cahuana	Cerro Cahuana
49	Carmen	Cerro Amarillo
	Cerro Zapaleri quadrangle	
50	—	Cerro Piedras Grande
51	—	Cerro Soniquera
52	Cristóbal Colón	Cerro Zapaleri
53	—	Cerro Dulce Nombre
54	Uturuncu	Cerro Uturuncu

FUMAROLIC NATIVE SULFUR DEPOSITS

At least 54 native sulfur occurrences were recognized in high-level altered zones in stratovolcanoes in the study area (fig. 58, table 14). These deposits are mostly small, fumarolic open-space fillings and replacements, that were deposited from sulfur-charged volcanic gases in the immediate area of a volcanic vent. The native sulfur occurs both as relatively pure masses and as disseminations, generally in a highly altered volcanic rock. Trace amounts of arsenic, antimony, and selenium are generally present in the sulfur and in a few deposits the minerals orpiment (As_2S_3) and realgar (AsS) have been reported. Gypsum, clay minerals, opaline silica, and alunite(?) are common associated gangue minerals.

During the past twenty years, at least 16 of the deposits were mined (table 14), generally by small, labor-intensive mining cooperatives. Currently only a few are sporadically active. Production from individual deposits has probably been less than a few thousand tonnes and reserves for individual deposits are generally on the order of 5,000–100,000 tonnes of ore grading as high as 50–60 percent sulfur. A notable exception is the Susana mine, the largest known sulfur deposit in Bolivia, which is currently producing about 12,000 tonnes a month and has a reported reserve of 40 million tonnes of ore with grades of 48–54 percent sulfur. Four sulfur deposits were visited during this investigation.

CERRO SACA SACANI

By B.M. Gamble, James C. Ratté, Raul Carrasco, *and* Eduardo Soria-Escalante

Summary and Conclusions

Cerro Saca Sacani consists of several, small, native sulfur prospects (app. A, no. 179) near the Chilean border. Fine- to coarse-grained sulfur occurs as disseminations and clots in argillized and alunitized andesite. The small size of the deposit and its remote location suggests that it is unlikely to be exploited other than for small-scale local use.

Introduction

A previously unreported native sulfur prospect occurs on the west flank Cerro Saca Sacani, an eroded stratovolcano near the Chilean border, about 16 km southeast of the village of Todos Santos in the Salinas de Garci Mendoza 1:250,000-scale quadrangle. The prospect was examined in September 1990.

Geology and Mineral Deposits

Cerro Saca Sacani is part of an east-west belt of stratovolcanoes that extends from Cerro Pariani in the east, through Cerro Cabarayo, and west into Chile. Examination of float and rare outcrop in the area of the prospect and in the upper part of the volcano indicates that the volcanic host rock is largely a sequence of high-silica andesite lava flows and subordinate volcanic breccias. In the vicinity of the prospect, the rocks are strongly argillized and weakly to moderately iron stained. Locally, the alteration is a mixture of fine-grained alunite, gypsum, and clay minerals.

Native sulfur is exposed in two areas, at an elevation between 5,200 and 5,300 m, on a very steep, largely talus covered hillside (fig. 59). Each mineralized area is about 5 m by 10 m in size, however, sulfur-bearing rock may continue under the extensive talus cover. The uppermost and richest mineralized area has been explored by a prospect pit 3 m wide by 3 m deep. Sulfur mineralization occurs as coarse, irregular clots, as much as 10 cm across, and as fine-grained disseminations in strongly argillized andesite(?). The sulfur does not occur in veins or veinlets nor does its deposition appear to be localized by fractures or any other structures. Rather it appears that the sulfur is the result of vapor-phase crystallization or possibly some type of replacement process.

The second, and smaller, prospect lies about 40–50 m below the first. The native sulfur is entirely fine grained and disseminated in argillized and alunitized rock.

The grade of the deposits ranges from 10 to 40 percent native sulfur, although laborious hand-sorting, common at other deposits in the area, could recover higher-grade material.

EL DESIERTO AREA

By G.J. Orris, Sigrid Asher-Bolinder, Eduardo Soria-Escalante, *and* René Enriquez-Romero

Summary and Conclusions

The El Desierto area (app. A, no. 218) contains producing fumarolic sulfur mines with extensive low-grade resources.

Introduction

The El Desierto area is in the Departament of Potosí, Provincia Daniel Campos in the Villa Martin 1:250,000-scale quadrangle, and consists of the El Desierto and Concepción mines, a mill facility, and a company village. The operation is run by Empresa Minera Clavijo Ltda. (EMICLA). The operation supplies 2,000 tonnes of sulfur per year to the sugar industry. The mine only produces to order. This site was visited in August 1990.

Geology and mineralization

The El Desierto fumarolic sulfur deposits are at the southern end of Salar de Empexa; this was once one of the highest grade deposits in Bolivia with ore from the Old mine, which is uphill from the current workings, running as high as 80 percent sulfur. Much of the mine area is part of a debris avalanche, and occurs in hummocky terrain at relatively low elevations. Other ore has been found in areas of fumarolic activity and is at least partly in place. The ore supplied to the processing plant has a grade of 40 percent sulfur and contains minor clay and manganese. The many pits and other workings seem to suggest hand sorting of the ore. Apparent reserves are 3,000,000 tonnes of 33–50 percent sulfur.

MINA OLCA

By G.J. Orris, Sigrid Asher-Bolinder, Eduardo Soria-Escalante, *and* René Enriquez-Romero

Summary and Conclusions

Mina Olca is a small, low-grade fumarolic sulfur deposit (app. A, no. 248) a few meters from the Chilean border that was mined in the past. The deposit is too small for large-scale development and the ore is of such low grade that small-scale mining is unlikely to be profitable.

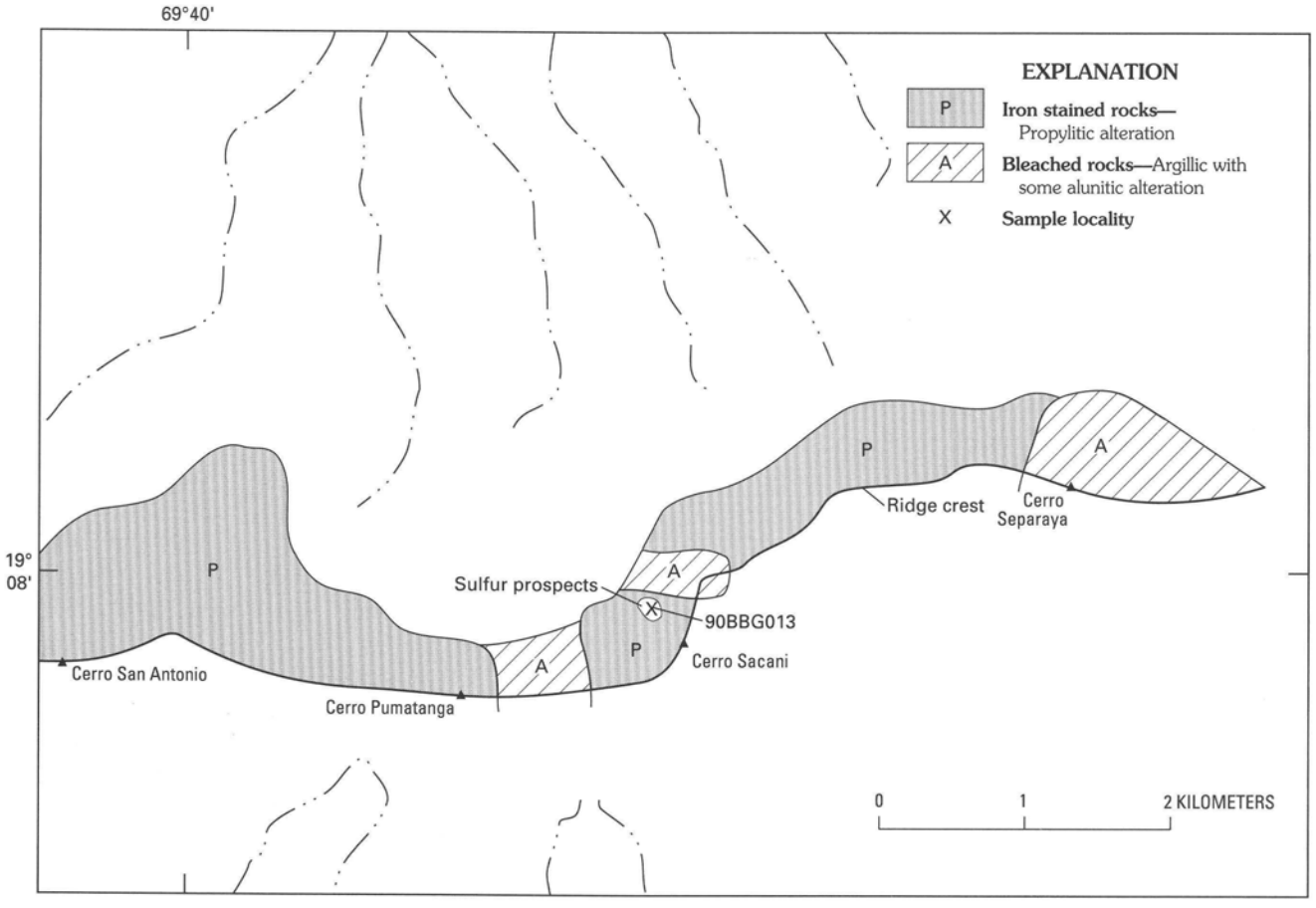


Figure 59. Sketch map of the Saca Sacani native sulfur deposit area, Bolivia. Drainage from Todos Santos (5836 I) 1:50,000-scale quadrangle.

Introduction

Mina Olca is near the summit of Volcán Olca in the Departament of Potosí, Provincia Nor Lípez in the Villa Martin 1:250,000-scale quadrangle. The inactive mine, tens of meters from the Chilean border, is accessible by steep roads that may be blocked by snow in the winter. It was examined in August 1990.

Geology and Mineral Deposits

Two principal zones of solfataric alteration are exposed on Volcán Olca. The western zone contains an active fumarole and was not visited. In the eastern zone, solfataric alteration is exposed over an area 30 m by 100 m, and at least two small patches (<10 m in diameter) of altered rocks occur along the access road at lower elevations. The fumarolic ore mineralization occurs as disseminations of native sulfur in a matrix of highly argillized basaltic andesite(?). The basaltic andesite is underlain by dacitic to rhyolitic volcanic flows, and is overlain by agglomerate exhibiting extensive iron oxide- and manganese oxide-staining. The manganese oxide-staining extends into the top of the sulfur-bearing zone. Ahlfeld and Schneider-Scherbina (1964) estimated that Mina Olca contained 200,000 tonnes of sulfur ore with grades of 55 percent sulfur. The mine was active from 1962 to 1981. Current reserves are limited, and the ore grade in the eastern zone probably averages less than 35 percent sulfur.

MINA SUSANA

By G.J. Orris, Sigrid Asher-Bolinder, Eduardo Soria-Escalante, *and* René Enriquez-Romero

Summary and Conclusions

Mina Susana (app. A, no. 323), the largest known fumarolic sulfur deposit in Bolivia, currently produces about 12,000 tonnes of sulfur per month; there are plans to expand production in the near future. The total sulfur

resource at Mina Susana is very large, and may exceed 250 million tonnes of ore with grades as high as 35 percent sulfur.

Introduction

Mina Susana is located in the Department of Potosí, Provincia Sud Lípez. The main workings of the mine are at an elevation of about 5,400 m on the southwest flank of Cerro Río Amargo in the Volcán Juriques 1:250,000-scale quadrangle. The concession containing Mina Susana, which is controlled by HORSU S.A., covers a total of 32 km^2 and includes an area of low-grade mineralization at the so-called Nelson site on the southeast flank of the volcano. The mine was examined in August 1990.

Geology and Mineral Deposits

Mina Susana is mined by open-pit methods and the ore is trucked to Campamento Mina Horsu where it is processed to 99+ percent sulfur. Most of the product is shipped west to Chile and from there to markets primarily in Argentina and Brazil. G. Garron, Director of HORSU S.A., reported (oral commun., 1990) that Mina Susana has been in intermittent production for about 40 years and currently produces about 12,000 tonnes of sulfur concentrate per month; he also reported reserves to be 40 million tonnes of ore with grades of 48–54 percent sulfur, as well as possible reserves of 280 million tonnes with grades of 18–35 percent sulfur. Estimates of total past production were unavailable. Earlier estimates of reserves and resources may be found in Ballivian and Barrios (1969).

Pyroclastic rocks in the volcanic vent area at the top of Cerro Río Amargo are the host rocks for the sulfur deposit. A large area, greater than 1,000 m in one direction, of solfataric alteration is capped by a relatively unaltered dacitic lava (fig. 60). The alteration is composed of disseminations and pockets of native sulfur, white to pale-pink clay believed to be largely kaolinite and alunite, and scattered patches of limonite and hematite. Most of the ore consists of disseminated sulfur in a highly argillized host; the grades range from less than 10 percent to more than 50 percent sulfur and are extremely variable over short distances. In places, especially along fractures, remobilized sulfur forms patches of clear, crystalline sulfur. Ballivian and Barrios (1969) report the presence of orpiment and realgar, but none was seen during the visit. However, scattered loose pieces of clear, orange crystalline material on the floor of the pit and along the haulage road suggest an elevated arsenic content in some of the remobilized sulfur zones.

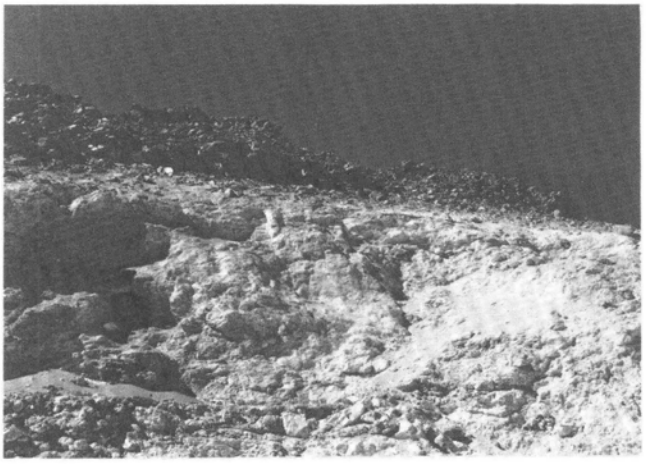


Figure 60. Unaltered dacitic lavas above solfatarically altered area near summit of Cerro Río Amargo, Mina Susana area, Bolivia.

BOLIVIAN POLYMETALLIC VEIN DEPOSITS

INTRODUCTION

We include in this section descriptions of field visits to the deposits that we believe fit the description of Bolivian polymetallic vein deposits presented in the section on Mineral deposit models. These deposits are of Middle and Late Miocene age, and are related to intrusions and, in some cases, volcanic rocks of dacitic composition. In some cases, the reports that follow refer to individual deposits (such as, Jaquegua), and in other cases, entire districts are described together (such as, San Antonio de Lípez).

San José de Oruro, Chocaya (Animas, Siete Suyos), Tatasi-Portulagete, and San Vicente-Monserrat are important polymetallic districts that occur in or very near the study area, however they were not included as part of this study because they are either presently or were recently operating properties of the Corporación Minera de Bolivia (COMIBOL). Each of these districts is relatively well described in the existing literature (table 15) and is the subject of large numbers of detailed, unpublished COMIBOL reports.

QUIMSA CHATA (TIAHUANACU) DISTRICT

By Orlando André-Ramos *and* Keith R. Long

Summary

The Quimsa Chata district (app. A, no. 14) consists of veins of lead, zinc, and silver in an altered Miocene dacite

Table 15. *Major polymetallic districts in and near the Altiplano and Cordillera Occidental, Bolivia, that have been studied extensively and are therefore not described in this report*

Deposit	Reference
San José de Oruro	Ahlfeld and Schneider-Scherbina (1964) Campbell (1942) Chace (1948) Flores-Balcazar (1979) Lindgren and Abbott (1931) Pinto (1989e) Saavedra and Shimada (1986) Thormann (1960) Turneaure (1960a, b)
Chocaya (Animas, Siete Suyos)	Ahlfeld and Schneider-Scherbina (1964) Borja and others (1989) Buerger and Maury (1927) Grant and others (1979) Koeberlin (1926) Pinto (1988a) Pinto (1988c) Saavedra and Shimada (1986)
Tatasi-Portulagete	Ahlfeld and Schneider-Scherbina (1964) Grant and others (1979) Meave (1966) Pinto (1988d) Rivas (1975) Roberts (1899) Saavedra and Shimada (1986)
San Vicente-Monserrat	Ahlfeld and Schneider-Scherbina (1964) Pinto (1988c) Pinto (1989c) Saavedra and Shimada (1986) United Nations Development Program (1989a)

sill that intrudes early Tertiary sandstone and conglomerates. Individual vein systems are long but narrow, and are unevenly mineralized.

Introduction

The Quimsa Chata (Tiahuanacu) district lies on the north flank of Cerro Quimsa Chata, in the Serranía de Tiwanaku, 10 km S. 15° E. of the town of Tiwanaku and 55 km S. 20° W. of La Paz. Polymetallic precious- and base-metal veins occur in an altered Miocene dacite sill that intrudes early Tertiary Tiahuanacu Formation sandstone. Mineralization is confined to northeast-trending vein systems exploited in Spanish colonial times and during the 1930's.

Previous geologic studies include a brief description by Ahlfeld (1954), a two day visit by the German Geological Mission to Bolivia (Schneider-Scherbina, 1961b), reconnaissance geologic mapping at 1:100,000 scale by the Servicio Geológico de Bolivia (GEOBOL) (Requena and others, 1963), recent prospecting by Minería Técnica Consultores Asociados (MINTEC), radiometric-age dating (Redwood and Macintyre, 1989), and two undergraduate theses (Acland, 1989; Paton, 1989). The area was visited as part of this study in July 1990.

Geologic Setting

The Quimsa Chata district is in the central, and topographically highest, part of the Serranía de Tiwanaku, a northwest-trending mountain range south of Lake Titicaca (fig. 61). Most of the mines in the district are hosted by an altered biotite dacite porphyry multiple sill that was intruded along the northwest flank of a northeast-trending anticline which folds sandstones, conglomerates, and shales of the Paleocene to Eocene Tiahuanacu Formation. The contact between dacite and sediments is generally brecciated and irregular and dacites near the contact contain many inclusions of sedimentary rock fragments. Blocks and slivers of sediments are found in the intrusive body and are often fault bounded. In places, gypsum has been intruded along faults at the contact between sediments and dacite. The sill is elongate in the direction of N. 70° W. and covers an area of about 15 km^2. The sediments strike N. 50°–70° E. and dip 35°–50° northwest.

The dacite is pervasively sericitized and locally argillized. Veins have selvages of intense sericitization, pyritization, and kaolinization. Silicified and pyritized dacite is found on the dumps. The dacite is cut by 5–50 m wide dikes of altered dacite to andesite, oriented N. 70° W. and N. 40° E. Some of these dikes were intruded along faults that bound blocks of sediments in the dacite.

Mineral Deposits

At least four vein systems occur, all striking N. 45°–60° E., dipping steeply to the northwest, 500–900 m apart, in the central part of the district, between Cerro Nasa Poke and Cerro Potosí. An outlying vein system, oriented east-west, occurs on the northwest flank of Cerro Aramani, at the extreme northwest end of the dacite sill. Placer deposits, apparently of fluvioglacial origin are found in the vicinity of Cerro Chuñu Rahui. Gypsum has been mined at a location northwest of the Potosicollo mine.

Veins are 0.1–1 m wide, average about 0.4 m wide, and occur along narrow zones of alteration that are as long as 2.5 km. Veins consist of quartz, pyrite, barite, tourmaline, and sulfides; galena, sphalerite, chalcopyrite, and tetrahedrite are the principal ore minerals. Schneider-Scherbina (1961b) suggested a paragenesis of pyrite-silica alteration of dacite, followed by veins of chalcopyrite and sphalerite, and then by veins of barite-galena-tetrahedrite associated with the younger altered dikes. An alternative explanation would be that the district is zoned from a silica-pyrite core with copper-zinc rich veins passing outwards into barite-lead-silver veins.

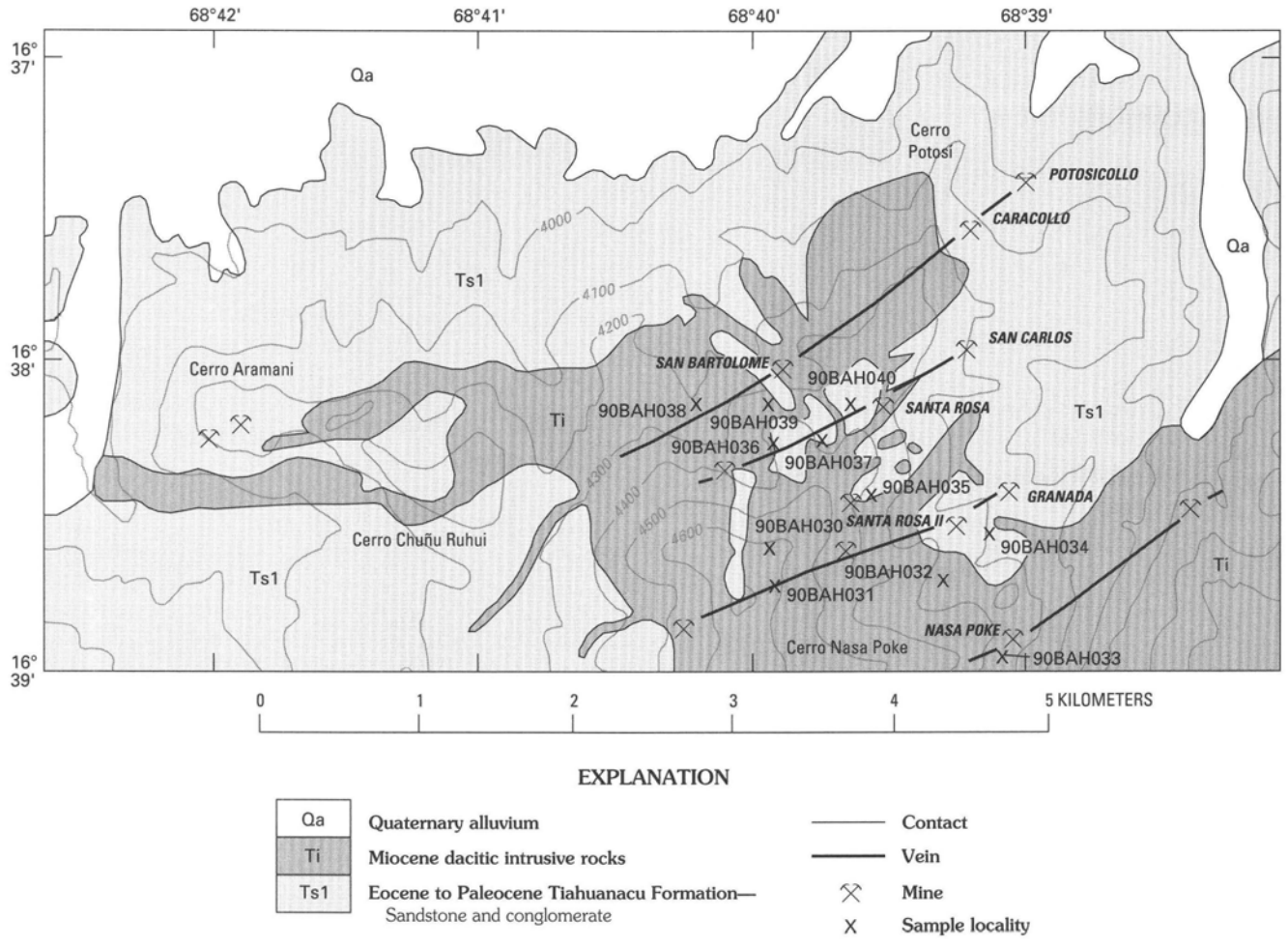


Figure 61. Map showing geology, mines, and sample localities in the Quimsa Chata (Tiahuanacu) district, Bolivia. Geology modified from Acland (1989) and Requena and others (1963). Contour interval, 100 m; base modified from the Tiwanaku (5844-III) 1:50,000-scale quadrangle.

The northernmost vein system runs through the San Bartolomé, Caracollo, and Potosicollo mines, for a total length of about 1,900 m. Nothing is known about the San Bartolomé mine which appears to be hosted by dacite. The Caracollo mine occurs in bleached sandstone near the dacite-sediment contact. Exposed in a 3,000 m^3 open pit are malachite, azurite, and cuprite in pockets and as stockwork veinlets in sandstone. The Potosí mine is an open pit, 70 m long, 50 m wide, and 12 m deep, that exposes a breccia pipe in bleached and sericitized sandstone. Pockets and stockwork veinlets of galena, chalcopyrite, barite, and sparse pyrite, sphalerite and silver minerals occur in the breccia.

Five hundred meters to the southeast another vein system runs through the Santa Rosa mine, San Carlos mine, and an unnamed mine to the southwest, for a length of 1,700 m. Veins occur in a zone of intense kaolinization 0.45 m wide. The Santa Rosa mine is a 70-m long open pit, 30 m deep, in a 25-m wide block of bleached sandstone surrounded by dacite. Veinlets of galena and sphalerite, 1–10 cm wide, occur along with disseminated pyrite in the sandstone. The San Carlos mine is located just outside the dacite intrusion in sandstone and conglomerate. Veinlets, 2–10 cm wide, of galena, sphalerite, pyrite, chalcopyrite, malachite, azurite, siderite, limonite, and barite cut sediments.

About 800 m to the southeast is another vein system that runs between the Granada and Carmen adits over a length of 2.2 km. Ahlfeld (1954) described the veins as consisting mostly of drusy pyrite with associated native gold. The veins also contain galena, sphalerite, chalcopyrite, arsenopyrite, and barite and cut kaolinized and pyritized dacite. Schneider-Scherbina (1961b) estimated that 20,000 t of dump material occurred around the Granada and Carmen adits. Some of the dumps contain fragments of silicified dacite.

At the Nasa Poke mine, 900 m southeast of the Granada-Carmen vein system, a vein of sphalerite of unknown length cuts sericitized sandstone and dacite. Various prospects expose small galena and sphalerite veins, for example at Santa Rosa II. The east-west veins at Cerro

Aramani in the extreme northwest part of the district are 0.2 m wide and contain sphalerite, galena, and chalcocite. The placers at Cerro Chuñu Rahui yielded one sample with 66.4 mg/m^3 of gold.

Geochemical Analyses

Schneider-Scherbina (1961b) obtained four assays of dump material from the Granada-Carmen vein system. Three samples of pyritic copper-silver ore yielded 2.90, 3.20, and 3.55 percent lead; 1.05, 21.20, and 13.55 percent zinc; 1.00, 1.85, and 1.85 percent copper; and 460, 100, and 630 g/t silver, respectively. A sample of barite-lead-zinc ore yielded 4.45 percent lead, 5.30 percent zinc, 6.7 percent copper, and 2,160 g/t silver. These data contradict Schneider-Scherbina's (1961b) distinction between an early generation of pyrite-copper-silver ore on the Granada-Carmen vein system and a younger generation of barite-lead-zinc ore along the other vein systems to the northwest. The samples of pyrite-copper-silver ore clearly carry significant values in lead and zinc, and have less copper than the so-called barite-lead-zinc ore. In fact, these assay data, and data on vein mineralogy, are consistent with a vertical zonation from pyrite-massive sulfide veins upwards into barite-sulfide veins, a characteristic pattern of Bolivian polymetallic vein deposits.

Assays by MINTEC yielded generally less than 2 g/t silver and less than 0.01 g/t gold, with a few samples as high as 430 g/t silver and 0.54 g/t gold. Our analyses (table 16) show values of as much as 15 percent zinc, 3 percent lead, and 2,100 ppm silver, with trace amounts of copper, arsenic, antimony, and bismuth. Gold values are very low, generally less than 0.15 g/t, but sample 90BAH037 with 15 percent zinc has 0.7 ppm gold. Tin contents are no greater than 10 ppm.

Age of Deposits

According to Redwood and Macintyre (1989), clasts of dacite porphyry are found in the upper Pliocene Tamuco Formation conglomerates, making the dacite sill Miocene in age. Sericite from a vein selvage yielded a K–Ar date of 13.4±0.5 Ma. Sanidine from an altered dacite dike that cuts the dacite sill yielded a K–Ar date of 11.0±0.5 Ma. Evernden and others (1977) dated unaltered biotite from the dacite sill as 12.6 Ma, but Redwood and MacIntyre (1987) were unable to locate dacite at the reported sample site and no unaltered biotite could be found in the intensely altered dacite sill. Redwood and Macintyre (1989) suggest that the age of intrusion, alteration, and mineralization of the sill occured at about 13 Ma, followed by a second event of intrusion and alteration at about 11 Ma.

Conclusion and Recommendations

The Quimsa Chata district is typical of the Bolivian polymetallic vein deposit type, with lead, zinc, and silver as the principal metals of economic interest. Mineralization is largely confined to four northeast-trending vein zones in an altered Miocene dacite sill and Tiahuanacu Formation sandstones. Veins are narrow and lack continuity. Acland (1989) reports that disseminated silver mineralization occurs in altered zones between veins, however, sampling by MINTEC found this mineralization to be of low grade. The predominance of quartz- and barite-bearing veins suggests that only the upper levels of a Bolivian polymetallic vein system are exposed. Potential exists for the discovery of massive sulfide veins at depth.

Table 16. *Chemical analyses of altered and mineralized samples from the Quimsa Chata (Tiahuanacu) district, Bolivia*

[All results in parts per million (ppm). Sn is ≤10 ppm in all samples. Sample descriptions, methods, and complete results in appendix B]

Sample no.	Au	As	Bi	Sb	Zn	Cu	Pb	Ag
				Nasa Poke				
90BAN033	0.10	450	4.6	100	450	1,200	3,800	35
				Granada				
90BAN032	0.02	35	7.7	9.3	11	13	430	4.2
90BAN034	.10	65	66	18	790	220	720	26
				Santa Rosa				
90BAN037	0.70	96	53	7,000	3,600	48	68,000	400
90BAN039	.004	57	2.5	49	70	140	460	6.8
90BAN040	.004	14	<.6	48	15	7.1	2,800	3.7
				Santa Rosa II				
90BAN030	0.15	150	29	82	30	21	1,500	2,100
90BAN031	.008	49	110	160	160	15	370	9.7
90BAN035	.026	100	4	3	46	42	770	7

BERENGUELA DISTRICT

By Alan R. Wallace

Introduction

The Berenguela district (app. A, nos. 126, 127, 131–137) is located approximately 35 km northeast of where the borders of Chile, Peru, and Bolivia intersect, at the headwaters of Río Berenguela. The district includes numerous sediment- and volcanic-hosted veins that were worked during Spanish colonial times, as well as several undeveloped occurrences that were encountered during the present study. No mining activity has taken place since World War II. The locations of the major mines are shown on figure 62.

The district was first studied in detail by Schneider-Scherbina (1962b) and the geology of the district and surrounding region was mapped by Sirvas (1964). Informal subdivisions of the Mauri Formation are those used on the published geologic maps of Kriz (1963a, b). During the present investigation, the geology was again mapped in order to place the mineral deposits in a geologic context, and the veins and dumps were examined. The discussion that follows includes proposed stratigraphic revisions based on that mapping, however the revisions are not reflected on figure 62.

Geologic Setting

The rocks of the Berenguela district are broadly divisible into Eocene to Oligocene continental sedimentary rocks and Miocene volcanic, volcaniclastic, and intrusive rocks. The older sedimentary rocks include the red quartz arenites and mudstones of the Berenguela Formation (pl. 1, Ts1) and black to red arkoses of what previously was described as part 1 and part of part 3 of the Mauri Formation (pl. 1, Tvnd). The Mauri-Berenguela contact is disconformable to unconformable. The Mauri (Mauri 2) contains sills or flows of two-pyroxene and plagioclase porphyritic andesites which have been dated at about 26 Ma (Lavenu, 1986). Subrounded cobbles of Cretaceous granites and Proterozoic metamorphic rocks are common in conglomerate layers in both formations.

The younger volcanic-rich units, previously included in Mauri 3, 5 and 6 on the east side of the district and the Cerke Formation (pl. 1, QTev) on the west, represent dynamic and rapid basin filling immediately east of an active explosive volcanic source. The units on the east side of the district include interbedded sandstones, conglomerates, reworked tuffaceous sediments and pyroclastic airfall deposits. A pyroxene andesite flow (Mauri 4) has been dated at about 26 Ma, whereas a tuff higher in the section (Mauri 6) has an age of 10 Ma (Lavenu, 1986); we consider the andesite age to be incorrect, based on geologic and stratigraphic relationships in the region. Westward, the stratigraphic section contains considerably more pyroclastic deposits and dacite mudflow deposits, which were derived from a chain of volcanoes that includes Cerros Cerke and Hauricunca. Eastward, the younger rocks disconformably overlie the lower part of Mauri 3, and to the west, they unconformably overlie Mauri 1 and the Berenguela Formation. In the central part of the district, isolated remnants of a locally derived, trough-filling sedimentary breccia overlie the Berenguela and Mauri 1.

Rhyolite, rhyodacite, and dacite plugs, domes, and dikes were emplaced into all of the sedimentary and volcaniclastic units in the western part of the area, and ages probably range from about 15 to 5 Ma, on the basis of existing ages and new ideas about stratigraphic relationships. These rocks, as well as the surrounding volcaniclastic units, were included in the Cerke Formation shown on the geologic map of the Santiago de Machaca quadrangle (Kriz, 1963b). The youngest unit in the area is the Perez Ignimbrite (pl. 1, QTig), which has been dated at 2 Ma (Evernden and others, 1977). It was erupted somewhere to the southwest, and has an estimated total volume of more than 150 km^3.

The Berenguela district is in a westnorthwest-trending right-lateral fault system which produced broad flexures and normal fault systems from probably pre-Mauri through middle Miocene time. The tectonic activity was responsible for the observed unconformities and vein systems in the district, as well as the prominent broad structural dome in the area.

Mineral Deposits

The mineral deposits of the Berenguela district include cadmium-rich veins in the Berenguela and lower Mauri Formations and cadmium-poor veins in the younger volcaniclastic and intrusive rocks.

Deposits in Sedimentary Rocks

The sediment-hosted veins in and near the town of Berenguela occur in steep normal faults and fractures that are products of the regional right-lateral fault system; intersections of two of the principal fracture sets created the best ground preparation for mineralization. These faults occur principally in the upper part of the Berenguela Formation, but they also extend into the lower Mauri Formation. The wallrocks are bleached and somewhat porous adjacent to the veins.

Workings originally developed during the Spanish colonial period principally exploited silver in the oxide zone which is less than 30 m thick throughout most of the district (Sirvas, 1964). Malachite and azurite are common

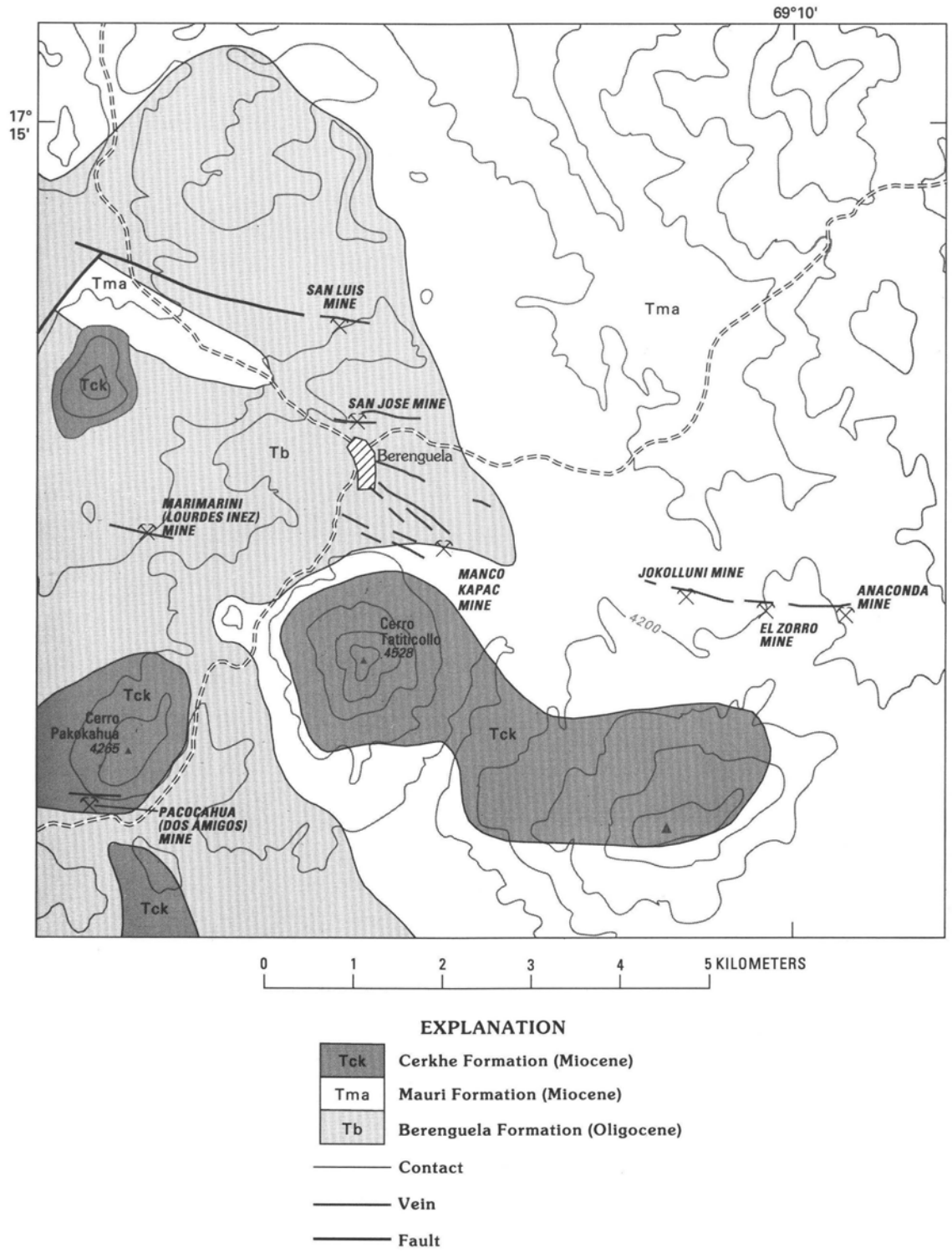


Figure 62. Map showing geology and location of mines in the Berenguela district, Bolivia. Geology modified from Kriz (1963b). Contour interval, 100 m; base modified from Berenguela (5742 II) 1:50,000-scale quadrangle.

secondary minerals in many of the dumps and some samples contain minor amounts of chalcedony and barite. Mining at the San Luis, Manco Kapac, and Marimarini (Lourdes Inez) mines during the twentieth century, exploited the deeper sulfide zones; minerals found on dumps include finely banded sphalerite, greenockite, barite, and galena, with local tennantite, chalcocite, chalcopyrite, and marcasite. No district-wide mineral zonation was noted. Marcasite was

found only at the San José mine, where it is abundant; the absence of jarosite in virtually all dumps suggests that iron sulfides in the primary ores are rare. Most ore occurs in fractures, but disseminated secondary copper carbonates indicate some intergranular dissemination into the altered wallrocks. Movement along the fractures both before and after mineralization suggests that the ore was deposited during the formation of the fracture systems, possibly during the Oligocene.

The Jokolluni, El Zorro, and Anaconda mines are located along an east-trending fault, 4 km eastsoutheast of Berenguela. The Jokolluni mine is in the lower part of Mauri 3 and is identical to deposits near the village of Berenguela. Twentieth century mining exploited the sulfide zone, and the mineralogy and textures appear to be identical to those near Berenguela. The El Zorro and Anaconda mines are two of many prospects along the fault to the east. The El Zorro mine is in andesites of Mauri 4, and the Anaconda mine is in sandstones and conglomerates of Mauri 5. On the geologic map of the Charaña quadrangle (Kriz, 1963a), both are mislocated and all deposits, including the El Zorro and the Anaconda, are within 1 km of the Jokolluni mine (fig. 62). No deposits are present along the fault to the west of the Jokolluni mine in the upper part of Mauri 5, or in Mauri 6.

Deposits in Volcanic Rocks

Mineral deposits are present in the younger volcaniclastic and volcanic rocks at the Pacocahua (Dos Amigos) mine and on Cerro Tatitocollo. The Pacocahua (Dos Amigos) is in a vein 2 km southwest of Berenguela along the road to Charaña. The vein follows a N. 70° W. fault which dips steeply to the southwest. A rhyolite dike was emplaced along the fault prior to mineralization and slickensides indicate continued fault movement. The rhyolite forms the footwall; sedimentary rocks of the Berenguela Formation form the hanging wall. All rocks are altered to a quartz-sericite assemblage and quartz is the dominant gangue mineral. Tennantite, galena, pyrite, and sphalerite were observed on the dumps; Sirvas (1964) reported pearcite. Both fault and silica-cemented hydrothermal breccias are common along the vein. Recent carbonate-bearing low-temperature waters have formed a line of travertine aprons along the fault zone.

Cerro Tatitocollo is 1 km south of the village of Berenguela and displays several small prospect pits of probable Spanish colonial age. The lower half of the conical hill is composed of sedimentary rocks and andesites of Mauri 1 and 2, which are overlain unconformably by volcaniclastic and tuffaceous rocks probably equivalent in age to Mauri 5 or 6. The dominant sedimentary rock is an epiclastic breccia- to pebble-conglomerate composed primarily of subangular rhyolite fragments in a coarse sand matrix. All rocks were intruded by flow-banded rhyolite plugs. Mineralization was concentrated along north-trending fractures in the breccia. Hydrothermal fumarolic breccias were localized along the fractures, and silicification increases towards these zones. Anomalous values of silver, copper, arsenic, zinc, lead, and antimony have been reported from this zone, which is no more than a few hundred meters wide in maximum dimension; gold occurs in a small area southwest of the silver-base metal zone. None of this mineralization can be genetically tied to any specific intrusive rocks.

Additional mineralized zones were encountered in rhyolite domes several kilometers west of Berenguela and near Cerro Vilacollo, 8 km west of the town. The rhyolite domes are sericitically altered and contain abundant fractures filled with pyrite; no prospect pits or workings were encountered along these fractures. An altered area near Cerro Vilacollo was noted on satellite images, and, when examined, found to contain sericitically altered dacites, with visible pyrite. A mineralized zone was reported to occur on the east side of Cerro Cerke, but poor weather conditions prevented us from visiting it; from a distance, it does appear to have strong hematitic alteration.

Conclusions

The majority of known deposits in the Berenguela district are in the Tertiary continental sedimentary rocks of the Berenguela Formation. The veins are localized at fracture intersections; mining exploited only the upper parts of the veins, which may continue to depth. Unlike the Corocoro district to the east, there is no field evidence for a pre-vein stratiform copper-silver deposit in the district. The volcanic-hosted deposits are relatively small; the one on Cerro Tatitocollo may be amenable to bulk mining methods if sufficient reserves can be identified. The deposits on Cerro Tatitocollo are silver rich, and gold is apparently very scarce.

LA JOYA DISTRICT

By Keith R. Long, Steve Ludington, Edward A. du Bray, Orlando André-Ramos, *and* Edwin H. McKee

Summary

The La Joya district (app. A, nos. 51–54) consists of several polymetallic vein deposits that formed in Miocene dacite stocks and the Silurian sedimentary rocks that they intrude. These deposits include one, at Cerro Kori Kollo, that has been developed into a mine estimated to contain almost 150 tonnes of gold and 1,000 tonnes of silver. The potential for discovery of more ore in the district is excellent.

Introduction

The La Joya district consists of a number of polymetallic vein deposits emplaced in Miocene dacite stocks and their Paleozoic sedimentary wallrocks. The district is located about 40 km northwest of Oruro, at the eastern edge of the Altiplano, along the southwest shore of ephemeral Lago Soledad. The mineral deposits are exposed on several small hills and one large hill (Cerro La Joya) that rise above a flat plain that consists of Quaternary lacustrine and alluvial sediments. The district is about 30 km west of the paved highway from La Paz to Oruro, and is reached by excellent all-weather roads. Previous geologic studies include brief descriptions by Ahlfeld and Schneider-Scherbina (1964), Redwood (1987b), Jimenez and others (1988), and Zamora (1989). A recent abstract describing new developments in the district was published by Anzoleaga and others (1990).

History

The oldest workings in the district are believed to date from the 19th century. A small copper mine operated on Cerro La Joya from 1952 until 1980, recovering copper by leaching oxide ore. In the mid-1970's, a Canadian firm, exploring for gold in the Altiplano, cut a tunnel into Cerro Kori Kollo that intersected sulfide mineralization. Reserves of this ore were estimated in 1976, but because the ore was thought to be refractory, the enterprise was abandoned. A geologist from that company remained in Bolivia, and, in the late 1970's, interested Empresa Minera Unificada in the property. Rotary drilling in 1980–82 on 40 m centers established that the deposit contained about 10,000,000 t of oxide ore at a grade of about 1.65 g/t of gold and 20 g/t of silver. Inti Raymi S.A. was established as a joint venture with WestWorld of Texas, and a small mine and pilot plant were built that produced about 7 kg of gold per month. Metallurgical tests indicated amenability of the ore to cyanide heap-leaching and by 1985, a new leach facility was built at San Andres. Subsequently, another leach facility was added at Chuquiña. The new facilities have increased production capacity to 4,000 t per day. Battle Mountain Gold has entered the joint venture and now holds an 85 percent interest in Inti Raymi S.A. Recent development has focused on exploration of reserves of sulfide ore at Kori Kollo, and as of summer 1991, a feasibility study has been completed, and plans for development of the sulfide orebody are underway.

Geologic Setting

Mineralized rock is found on four hills, Cerro Kori Kollo, Cerro Llallagua, Cerro Quiviri (La Barca), and Cerro La Joya, which rise up out of Quaternary cover southwest of Lago Soledad (fig. 63). These hills are cupolas on a large intrusive body of dacitic composition (pl. 1, Ti) that invades quartzites, siltstones, and shales of the Silurian Catavi Formation (pl. 1, Pzs). Drilling has revealed outward-flaring contacts on the cupolas, and many of the outcrops of Silurian sediments are best considered as roof pendants.

Three of the hills, Cerros Kori Kollo, Llallagua, and Quiviri, are aligned along a northnorthwest trend, but each has been interpreted to be displaced to the west along northwest-trending normal faults, although no direct evidence has been demonstrated for these faults. Cerro La Joya, 5 km to the west, and much larger than the other three, has no obvious structural controls. Between these two igneous centers (La Joya and Kori Kollo-Llallagua-Quiviri) is a range of low hills composed of Catavi Formation that exhibits little indication of mineralization. The district lies along the Viacha lineament (Servicio Geológico de Bolivia, 1979), which appears to control other middle to late Miocene dacitic stocks, volcanic centers, and mineralized centers.

Five samples, three from Cerro La Joya (samples 90BSL004, 47, 48) and two from Cerros Llallagua (sample 90BSL040), and Quiviri (sample 90BSL046), were collected that demonstrate the original character of the dacite intrusions in the district. Complete chemical data for these rocks is in appendix B. The 5 samples range in silica content from about 63 to about 67 weight percent, on an anhydrous basis. All 5 samples are porphyritic, with phenocrysts of quartz, feldspar, biotite, and hornblende; each has a very fine grained groundmass, as befits their subvolcanic nature. Most of them exhibit conspicuous vitric melt inclusions in the quartz phenocrysts. None of the samples are truly fresh; all exhibit varying degrees of propylitic alteration, oxidation, and sulfidization.

Mineral Deposits

Polymetallic vein deposits are found on all four hills. The mineralized rock on Cerros Kori Kollo, Llallagua, and Quiviri can be interpreted as being the result of the activity of a single hydrothermal system. La Joya deposits are somewhat different, and probably represent a separate, though related, event.

Cerro Kori Kollo

Cerro Kori Kollo consists entirely of highly sericitized dacite which hosts the oxide and sulfide orebodies that currently are being mined by open-pit methods or are under development. The ore consists of an oxidized cap of extremely variable thickness (as thick as 70 m), that is separated from sulfide ore by a weak chalcocite enrichment blanket. The host rock consists of two textural facies, a coarse- and a fine-grained dacite porphyry. The coarse-grained facies contains phenocrysts of quartz (as much as 15

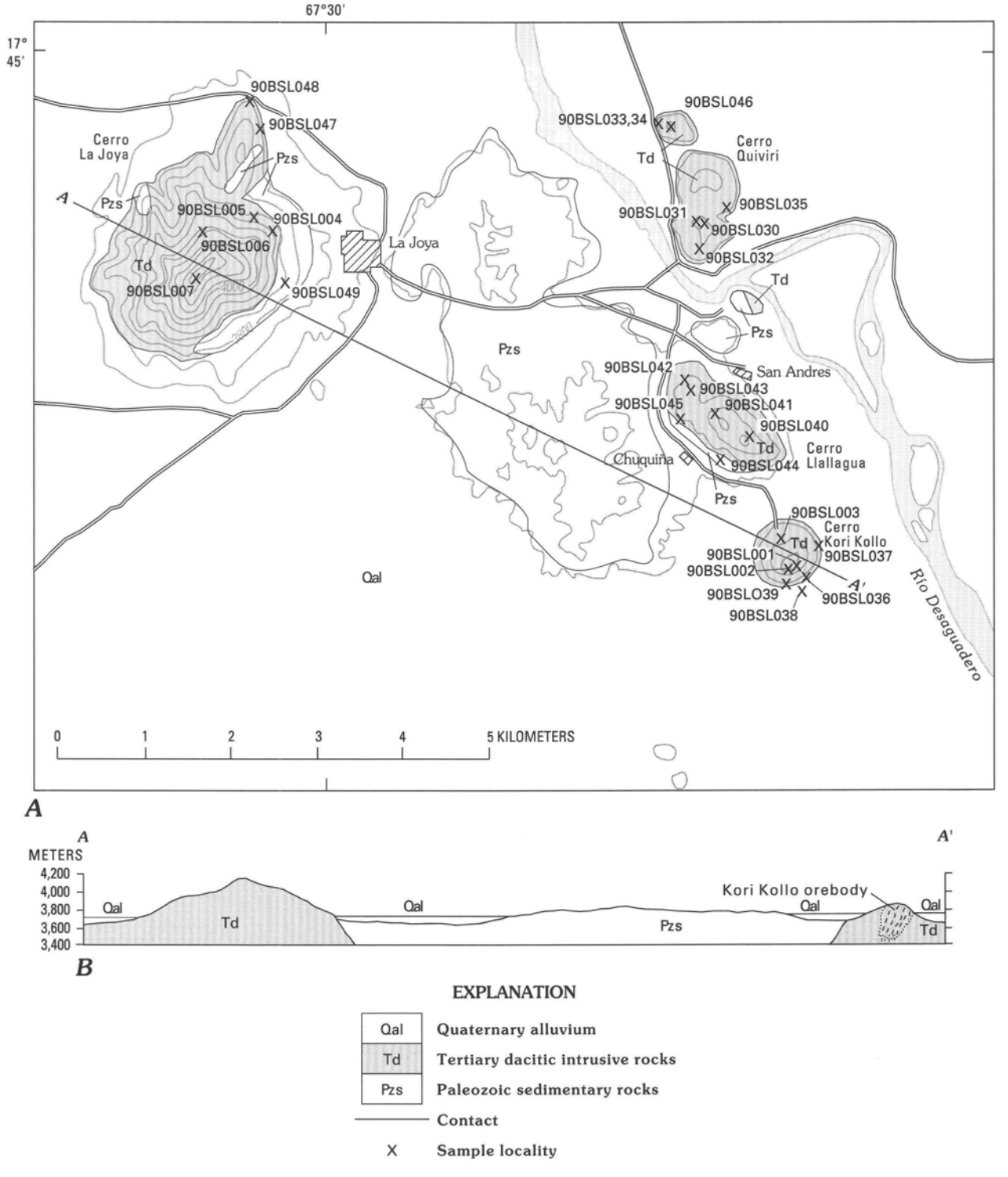


Figure 63. La Joya district, Bolivia. *A*, Map showing geology and sample localities. Geology is modified from unpublished mapping by Inti Raymi. Contour interval, 40 m; base modified from the Soledad (6140 IV) and Cerro La Joya (6040 I) 1:50,000-scale quadrangles. *B*, Cross section through the La Joya district.

percent), relict feldspar (as much as 25 percent) and a trace of biotite, in a very fine grained groundmass that has been altered to a mass of quartz, sericite, and pyrite. The total percentage of phenocrysts ranges from about 20 percent to about 50 percent, and their size, although variable, may be as large as about 1 cm. The fine-grained facies contains the same phenocryst population, in about the same proportions, but the maximum size is only about 3–4 mm. Contact

relationships between the two facies are ambiguous and there may have been two nearly contemporaneous intrusions from the same magma chamber. Highly altered, but recognizable, cognate inclusion swarms are present in both facies.

The main control of mineralization is a set of fractures that trend N. 10° E. to N. 20° E., dip 75°–85° northwest, and are found throughout the hill. The veins and veinlets that fill these fractures are parallel and do not form a stockwork; they range in thickness from a hairline to almost 1 m, but most range from 20 mm to 2 cm. In the central part of Cerro Kori Kollo, a 200 m-wide zone of increased fracture density has localized the higher grade portion of the orebody. Several zones of tectonic or hydrothermal breccia are found in this fracture zone and these host higher-grade material in the oxidized zone only.

The fractures on Cerro Kori Kollo are filled with an assemblage of sulfides that includes major pyrite and lesser amounts of arsenopyrite, chalcopyrite, galena, sphalerite, tetrahedrite, stibnite, and electrum. Realgar has been noted in these veins and stannite has been detected at deeper levels (Hugo Alarcón, written commun., 1990). Microscopic evidence suggests that these sulfides both filled the open fractures and replaced the walls of the veins. There is virtually no quartz in this set of veins. The veins constitute 1–2 percent of the rock volume in ore zones.

Approximately two-thirds of the gold in the ore resides in these veins, whereas one-third is associated with disseminated pyrite. The silver-to-gold ratio for the entire deposit is about 6:1, based on a 1.15 g/t cutoff grade. The eastern and western boundaries of the ore zone result from a lower density of mineralized fractures away from the axis of mineralization. To the north and south of the ore zone, the degree of fracturing decreases in the coarser grained facies of the dacite.

A set of low-angle fractures crosscuts the older mineralized fractures; the low-angle fractures contain primarily an assemblage of quartz and alunite, with very low, if any, precious-metal values.

In the lower, and possibly, outer parts of the deposit, marcasite appears to replace pyrite in the groundmass of the rock and also appears in the vein paragenesis. The appearance of marcasite in the rock generally corresponds to a rapid decrease in grade of the ore, to below economic values.

Hydrothermal alteration, which may be contemporaneous or slightly earlier than vein formation, is entirely phyllic, with virtually complete replacement of the rock by quartz, sericite, and pyrite, except for quartz phenocrysts. The disseminated pyrite forms 5–20 percent of the rock. Some of the rock can be considered silicified (samples 90BSL003, 90BDR001a), containing as much as 85 percent silica. However, this is not the result of fine quartz veins, but simply to large amounts of fine-grained quartz in the altered groundmass.

Cerro Llallagua

Cerro Llallagua, just northwest of Cerro Kori Kollo, is the site of the old San Andres mine (fig. 63). The dacite facies on Cerro Llallagua is similar to rocks at Cerro Kori Kollo and diamond drilling has shown that the bodies are continuous at depth. Mineralization consists of high-grade sulfide veins (Central, Aviadora, and Maruja) that fill northeast-trending fractures. These veins are 1–2 m wide and extend to depths of at least 200 m. Gold values apparently decrease with depth. There are closely spaced, mineralized fractures, similar to those on Cerro Kori Kollo, throughout much of the dacite outcrop on the hill. About 80 exploration holes have been drilled, and, although they show that gold grades are significantly lower on Cerro Llallagua, the overall style and intensity of mineralization is very similar to that at Kori Kollo. The silver-to-gold ratio at Cerro Llallagua is similar to that at Cerro Kori Kollo, ranging from about 6:1 to about 10:1. Higher grade, oxidized ore on Cerro Llallagua may be mined in the future.

Cerro Quiviri (La Barca)

Cerro Quiviri, like Cerro Llallagua, contains northeast-trending mineralized fractures in altered dacite. A roof pendant of altered and mineralized Catavi Formation makes up the southern flank of the hill. The overall style of mineralization is similar to the two southern hills, although the distribution of mineralized rock is quite erratic; there is much almost fresh rock on Cerro Quiviri. The grade of the mineralized rock is distinctly lower, and the silver-to-gold ratio is similar to or lower than that found on the other two hills.

Cerro La Joya

Cerro La Joya stands alone 6 km to the northwest of Cerro Kori Kollo and is the site of the old Carmen and San Pablo mines (fig. 63). The hill is composed primarily of dacite that has intruded Catavi Formation sediments. The sediments, as well as the dacite, are altered and cut by sulfide veins. Most of the dacite is propylitically altered, but there are some sericitized parts. It is cut by a few aplite dikes (sample 90BSL005).

The upper part of the hill is composed of a breccia that consists of subrounded to subangular clasts of dacite in a dark-gray, fine-grained matrix that contains tourmaline; the breccia is cut by sulfide veins. Another cryptic breccia body is found on the southern flank of the hill; it is composed of rounded clasts of Catavi Formation.

The upper, mineralized part of the hill has not yet been extensively explored, but the mineralization is similar to other areas in the district; the silver-to-gold ratio is apparently about 3:1 in the oxidized zone, and much higher in the sulfide veins.

Geochemical Analyses

At least 16 mineralized samples from both the oxide and sulfide zones were collected in the La Joya district and some of the more important results of analyses of those samples are presented in table 17. Complete analyses and sample descriptions can be found in appendix B.

The data in the table clearly demonstrate the polymetallic nature of the deposits in the La Joya district. The high tin and bismuth contents show similarities between the deposits at La Joya and other Bolivian polymetallic deposits. In addition, sample 90BSL002 contains 30 ppm tungsten; sample 90BSL049a contains 150 ppm tungsten; and samples 90BSL030, 6, and 7 contain 2,000 or more ppm boron; tourmaline was identified in sample 90BSL030 in the field.

Arsenic and antimony values are quite variable. Nevertheless, both elements appear to be anomalous, even at long distances from economic precious-metal mineralization.

Copper values are remarkably low; an exception is sample 90BSL049a, which was collected from the San Pablo mine dump, historically known as a copper mine, at Cerro La Joya.

Although our sample density is too low to make definitive statements, there are interesting hints of district-wide, south-to-north zoning shown by lead, zinc, and, possibly arsenic and antimony. Lead is high in the Kori Kollo deposit, much lower on Cerro Llallagua, and high again on Cerro Quiviri. Arsenic and antimony values show a similar pattern, although it is much less clear. Zinc behaves antithetically to this pattern and is highest in the samples from Cerro Llallagua.

Fluid Inclusions

Observations on fluid inclusions in quartz phenocrysts from rocks in the La Joya district have been made by Zamora (1989), Hugo Alarcón, written commun. (1990), and Alarcón and Villalpando (1991). Virtually all of the samples contain secondary inclusions characterized by liquid, vapor, and a daughter crystal of halite. Only in the upper parts of the Kori Kollo deposit, in the oxidized zone where the average salinity is 18 percent, are lower salinity inclusions found. Average homogenization temperatures for the various deposits are Kori Kollo (sulfide zone), 320 °C; Kori Kollo (oxide zone), 317 °C; Llallagua, 267 °C; Quiviri, 255 °C; and La Joya, 348 °C. The upper part of Cerro La Joya has the hottest, most saline inclusions; they range from 30 to 50 percent NaCl equivalent and have a range of homogenization temperatures from 300 °C to 550 °C, with an average of about 400 °C.

Many of the quartz phenocrysts also display distinctive melt inclusions that are psuedo-cubic in shape; some are as large as 50 μ. Some of these inclusions appear to be totally vitric, displaying only isotropic glass and a vapor bubble.

Age of Deposits

Redwood (1987b) has shown that the age of intrusion of the La Joya pluton and mineralization of the stock at Kori

Table 17. *Chemical analyses of mineralized rocks from the La Joya district, Bolivia*

[All results in parts per million (ppm). Sample descriptions, methods, and complete results in appendix B]

Sample no.	Au	Ag	Pb	Zn	Cu	As	Sb	Sn	Bi
				Cerro Kori Kollo					
90BSL001	2.8	11	780	2.8	8.8	940	100	20	27
90BSL002	1.8	12	50	13	10	17	11	50	3.0
90BSL003	.1	6.7	9.9	1.4	1.8	11	12	70	.76
90BSL036	4.70	46	5,200	26	11	710	57	70	19
90BSL037	0.012	0.5	33	16	7.8	34	7.4	70	1.5
				Cerro Llallagua					
90BSL042	0.10	2.7	200	1200	20	660	29	<10	3.1
90BSL043	.002	1.3	730	790	9.6	35	3.9	15	<.6
90BSL044	<.002	1.3	29	430	42	14	47	<10	2
90BSL045	.004	.48	80	1300	4.2	54	12	<10	<.6
				Cerro Quiviri					
90BSL030	0.012	2.8	400	16	5.6	80	4.5	<10	7.4
90BSL031	.034	8.8	1,700	26	19	320	21	50	1.8
90BSL032	2.8	35	37,000	1.3	15	490	4,300	30	<.6
90BSL035	1.55	12	1,100	1.1	42	800	190	150	3.1
				Cerro La Joya					
90BSL006	0.022	0.15	14	<0.03	8	46	2.2	<10	5.2
90BSL007	.020	.54	14	1.5	14	200	6.2	30	15
90BSL049a	3.10	2,100	1,900	75	3,300	1,500	8,900	100	6,400

Kollo are indistinguishable. A K–Ar date for biotite from fresh dacite on the northern side of Cerro La Joya yielded an age of 14.3±0.4 Ma, whereas an age determined on sericite from the orebody at Kori Kollo was 15.7±0.5 Ma. We dated a sample (90BSL110) of the flat, crosscutting quartz-alunite veins that was provided by Kirk Schmidt, of Battle Mountain Gold; the age obtained, 4.7±0.2 Ma, puts a minimum constraint on the mineralization age. If all of these dates are correct, they indicate an extremely long-lived hydrothermal system.

Grade and Tonnage

Development drilling done by Inti Raymi S.A. during 1989 and 1990 has demonstrated the existence of a large precious-metal resource at Cerro Kori Kollo. The recently announced geologic resource for the sulfide zone is 58.7 million tonnes, with a grade of 2.32 g/t gold and 13.8 g/t silver. The oxide zone contains an additional 6 million tonnes at 1.86 g/t gold and 24.7 g/t silver. Mineable reserves are approximately 10–20 percent less, at similar grades. Data for lead, zinc, and other metals are not available. Drilling on Cerros Llallagua, Quiviri, and La Joya does not permit actual tonnage estimates, but, at least at Cerro Llallagua, it indicates that substantial mineable reserves exist.

Conclusions and Recommendations

The La Joya district contains substantial gold and silver resources. These occur in polymetallic vein deposits that, except for the high gold grade, are similar to other polymetallic deposits in the Cordillera Oriental and on the Altiplano. Geologic features such as outward-flaring contacts, the presence of tin and tourmaline, and the high homogenization temperatures and salinity of the fluid inclusions demonstrates that these deposits did not form near the surface in a volcanic environment, but at considerable pressure and depth, in an environment more akin to that of porphyry copper deposits than to that of epithermal precious-metal deposits.

TODOS SANTOS DISTRICT

By B.M. Gamble, James C. Ratté, Raul Carrasco, Eduardo Soria-Escalante, *and* Edwin H. McKee

Summary and Conclusions

Mineral deposits in the Todos Santos district (app. A, nos. 168, 169, 171, 175) occur in the Carangas Formation, a sequence of interlayered andesitic lava flows and silicic pyroclastic rocks, and related domes and shallow intrusions. Three mineralized areas were examined, the Todos Santos mine, Cerro Espíritu Santo at Carangas, and Negrillos.

The deposit at the Todos Santos mine is related to a rhyolite dome and associated tuffs and breccias. The source of the mineralization appears to be a northnortheast-trending fault that cuts the narrow belt of mineralization in argillized tuffs and breccias along the east side of the dome. The mineralization is predominantly disseminated and low grade, not exceeding 5 percent total metallic minerals. Our analyses show as much as 200 ppm silver, 1.5 percent lead, and 1 percent zinc. Gold was not detected in any samples, at the lower limit of determination (0.002 ppm). Compañía Minera del Sur (COMSUR) has estimated ore reserves at 1 million tonnes at 0.7 g/t gold and 70 g/t silver by drilling. Because of the structural localization of mineralization, there appears to be little potential for additional reserves.

The deposit at Carangas consists of dikes and small intrusive bodies of rhyolite and breccia bodies with clasts of the same rhyolite that cut lithic tuffs of the Carangas Formation. Our brief examination of the upper parts of Cerro Espíritu Santo failed to detect visible mineralization. However, analyses of the breccia, altered lithic tuffs, and quartz veins and veinlets show silver values between 1 and 700 ppm, as well as 150–7,000 ppm lead, and 200–700 ppm zinc. Gold was not detected at the lower limit of determination (0.002 ppm). The extent of this mineralization is not known. Detailed sampling and drilling are necessary to fully evaluate this deposit.

Mineralization was not observed in the workings near the village of Negrillos. Dump material, however, contained quartz-galena-sphalerite-pyrite-pyrolusite veins as thick as 5 cm. Analyses of this material show as much as 0.10 ppm gold, 1,000 ppm silver, greater than 2 percent lead, greater than 1 percent zinc, and 7,000 ppm copper. The veins are unlikely to be economic unless their size or density is considerably greater than suggested by material on the dumps. Disseminated mineralization was not observed. Detailed sampling of underground exposures should give some idea of the quality of disseminated mineralization and will indicate if further work is needed.

Although the known deposits in the Todos Santos district appear to be too small and (or) too low grade for profitable production, potential for additional deposits exists in the area. Numerous Spanish colonial era prospects, including the Paco Kkollu prospect, occur on the north flank of Cerro Jankho Willkhi, and the top of the hill was being drilled as a disseminated silver target. A small rhyolite intrusion was found about 6 km north of Negrillos, and although not altered or mineralized, its presence indicates that other unmapped intrusions may be present. Geologic mapping, and geochemical sampling of all rock types, particularly domes, intrusions, and altered volcanic rocks, is recommended. It should be kept in mind that disseminated mineralization may not be readily visible.

Introduction

The Todos Santos district is about 20 km east of the Bolivia-Chile border and about 240 km west of Oruro. The district includes three inactive mining areas, Todos Santos, Carangas, and Negrillos, and several known prospects (fig. 64; table 18), all chiefly volcanic hosted, silver-rich polymetallic veins and disseminations.

As part of the present investigation the three mineralized areas were examined briefly. Additional information on these areas is available from Ahlfeld and Schneider-Scherbina (1964) (Todos Santos and Carangas), Guerra and others (1965b) (Negrillos), Ahlfeld (1967) (Carangas), and McNamee (1988) (Todos Santos and Carangas). Although there is no current production from these three mineralized area, the Todos Santos deposit is being explored by COMSUR, and the Paco Kkollu prospect near Negrillos is being drilled by Pan Andean S.A.

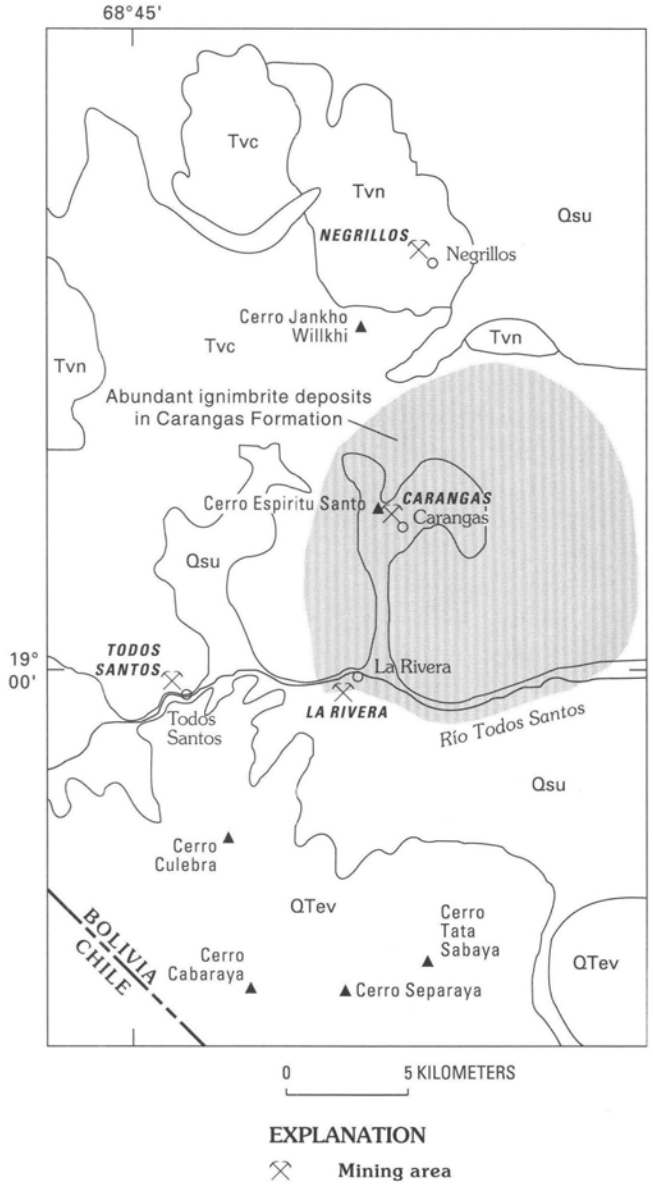


Figure 64. Generalized geologic map of Todos Santos district, Bolivia. Tvn, Negrillos Formation; Tvc, Carangas Formation; QTev, stratovolcano deposits; Qsu, surficial deposits.

Table 18. *Status of mines and prospects in the Todos Santos district, Bolivia*

Mineralized area	Status
Todos Santos	Inactive mine with Spanish colonial era workings and 2,350 m of modern workings; reserves reported to be 10^6 t with 0.07 g/t Au and 70 g/t Ag.
Carangas	Several inactive mines with adits and prospect pits; reserves unknown
Negrillos	Several inactive mine with one adit 50-100 m long and Spanish colonial era prospects; reserves unknown
Paco Kkollu	Active prospect, currently under exploration by Pan Andean S.A.

Geologic Setting

Host rocks for the mineral deposits of the Todos Santos district are a sequence of interlayered andesitic lava flows and breccias, silicic pyroclastic rocks, lava domes, and related(?) shallow intrusions referred to as the Carangas Formation (Ponce and Avila, 1965b; Ponce, Avila, and Delgadillo, 1967) or the Carangas volcanic field (McNamee, 1988). The Carangas Formation, probably of Miocene to Oligocene age (pl. 1, Tvnd), is exposed over an area of several hundred square kilometers mainly east and north of the village of Todos Santos. Biotite from a phenocryst-rich plagioclase-biotite ash-flow tuff (sample 90BBR010) in the upper(?) part of the Carangas Formation has a K–Ar age of 21.7±0.7 Ma (app. C). The Carangas Formation is overlain on the west and south by andesitic and dacitic lavas apparently erupted from a number of younger (Quaternary and late Tertiary) stratovolcanoes that are mostly aligned with the north-south chain of volcanoes paralleling the Bolivia-Chile border. South of the Todos Santos district, however, the younger stratovolcanoes occur in an east-west belt that separates the district from the extensive lowlands of Salar de Coipasa.

Several anticlines and synclines are shown in the Carangas Formation on the 1:100,000-scale geologic maps of the Carangas and Todos Santos quadrangles (Ponce and Avila, 1965b; Ponce, Avila, and Delgadillo, 1967), but at least one of these folds is apparently the result of drag along a major fault. This fault is one of several parallel faults that cut the Carangas Formation, and it is possible that many of the fold axes shown are fault related and not necessarily indicative of compressional tectonics.

The Carangas Formation is thickest in the circular area outlined on figure 64; the eruptive centers for the ignimbrites found in the formation are probably located within that area. The ignimbrites have an extensive regional distribution, are several hundred meters thick locally, and are probably caldera related. No attempt was made to distinguish between outflow and intracaldera facies during this brief reconnaissance and any speculation on the location of a caldera related to this sequence of ash-flow tuffs would be premature.

Mineral Deposits

Todos Santos

The Todos Santos deposit consists mainly of small veins and disseminations localized in or near a N. 10° E. trending fault or fault zone that cuts across tuffs and breccias near the eastern margin of a dome-shaped body of rhyolite (fig. 65). The rhyolite was interpreted as a rhyolite stock (Ahlfeld and Schneider-Scherbina, 1964) and more recently as a rhyolite dome (McNamee, 1988). Our examination substantiated the intrusive-extrusive origin of the rhyolite, but more importantly focused on the fault zone as the main structural control of mineralization. In addition, a fairly extensive block-and-ash deposit, intruded by a smaller rhyolite dome east of Río Todos Santos, was identified.

The main Todos Santos dome consists of a central intrusive-extrusive body of flow-banded, marginally brecciated, almost aphyric rhyolite, about 1 km in diameter. The dome intrudes through the vent of earlier tuffs and breccias, which probably formed a related cone or tuff ring (fig. 65). Thin-bedded tuffs exposed locally on the east flank of the dome appear to be waterlain deposits, perhaps deposited in a central or satellitic crater of the pyroclastic cone or tuff ring. A vitrophyre zone several meters wide borders the dome; on the east side the vitrophyre is devitrified and hydrated, but it is much less altered on the west side. The marginal vitrophyre appears to dip more steeply on the east side than on the west. Samples of the crystalline dome and glassy margin show SiO_2 contents of 76.9 and 75.8 percent respectively, on a normalized anhydrous basis (app. B, samples 90BBG004 and 3, respectively).

A smaller, bulbous, rhyolite dome, about 200–300 m in diameter, is exposed on the east side of Río Todos Santos, where it apperars to intrude a coarse block-and-ash flow of pumiceous, biotite-rich rhyodacite. Biotite from this block-and-ash flow has given a new K–Ar age of 6.1±0.2 Ma (app. C, sample 90BBR004a), essentially the same as the age of a hornblende andesite dike that is part of the Cerro Culebra stratovocano that encroaches on the Todos Santos area from the south. Lava flows from Cerro Culebra overlap the Carangas Volcanics along Río Todos Santos southwest of the main Todos Santos rhyolite dome (fig. 65). The extent of the 6.1 Ma-old block-and-ash flow along Río Todos Santos south and west of the main Todos Santos rhyolite dome, as well as the relationships between the block-and-ash flow, the Carangas Volcanics, and the rocks from Cerro Culebra need to be mapped in further detail. However, the apparent intrusive contact between the smaller rhyolite dome and the block-and-ash flow east of Río Todos Santos indicates that the smaller dome, and thus, also the main Todos Santos rhyolite dome, are younger than 6.1 Ma.

The Todos Santos deposit, currently being explored by COMSUR, consists of a main mineralized zone about 350 m long as defined by the old workings. The mineralized zone is localized along a N. 10° E. fault or fault zone that cuts across the eastern flank of the Todos Santos dome and dips about 75° west into the dome (figs. 65, 66). The footwall of the fault is best exposed along the northern extension of the fault zone, where it consists of andesite flows overlain successively by a heterogeneous explosion breccia and a homogeneous rhyolite breccia. The breccia is like that of the main dome, but is probably a separate intrusion. The hanging wall of the fault consists largely of pyroclastic breccia layers of a tuff ring or cone that preceded dome emplacement. The bedded pyroclastic breccias dip as much as 60° where they have been dragged adjacent to the fault zone and are apparently the host rocks for most of the ore.

The host rocks for the mineralization are strongly argillized tuffs and breccias. Because of the intensity of alteration, the nature of the host rock at some underground localities was unclear. The ore minerals consist of disseminated pyrite, yellow sphalerite, and a dark-gray metallic mineral, probably tetrahedrite. Mineralization is uneven; some areas lack visible metals and others contain as much as 1 percent. The richest mineralization is in an area of strongly argillized and faulted explosion breccia. The argillized rock here is very plastic and gougy, and is cut by 3 or 4 faults, trending chiefly N. 10°–20° E., and dipping 20°–35° northwest, along a 15 m section of one of the crosscuts. Mineralization in this zone consists of about 2–3 percent very fine to fine-grained, disseminated pyrite, an unidentified dark metallic mineral, and minor sphalerite. The lithic clasts in the breccia appear to be more silicic (silicified?) and more mineralized than the matrix.

Only one veinlet was found underground. The veinlet is discontinuous, as thick as 2 cm, trends N. 80° W., dips 70° north, and consists entirely of fine-grained specular hematite. Extensive Spanish colonial era workings extend along the trend of this veinlet, suggesting that the veinlet thickened in places, or possibly anastamozed. Other Spanish colonial workings in the mine area suggest the presence of other veins or veinlets.

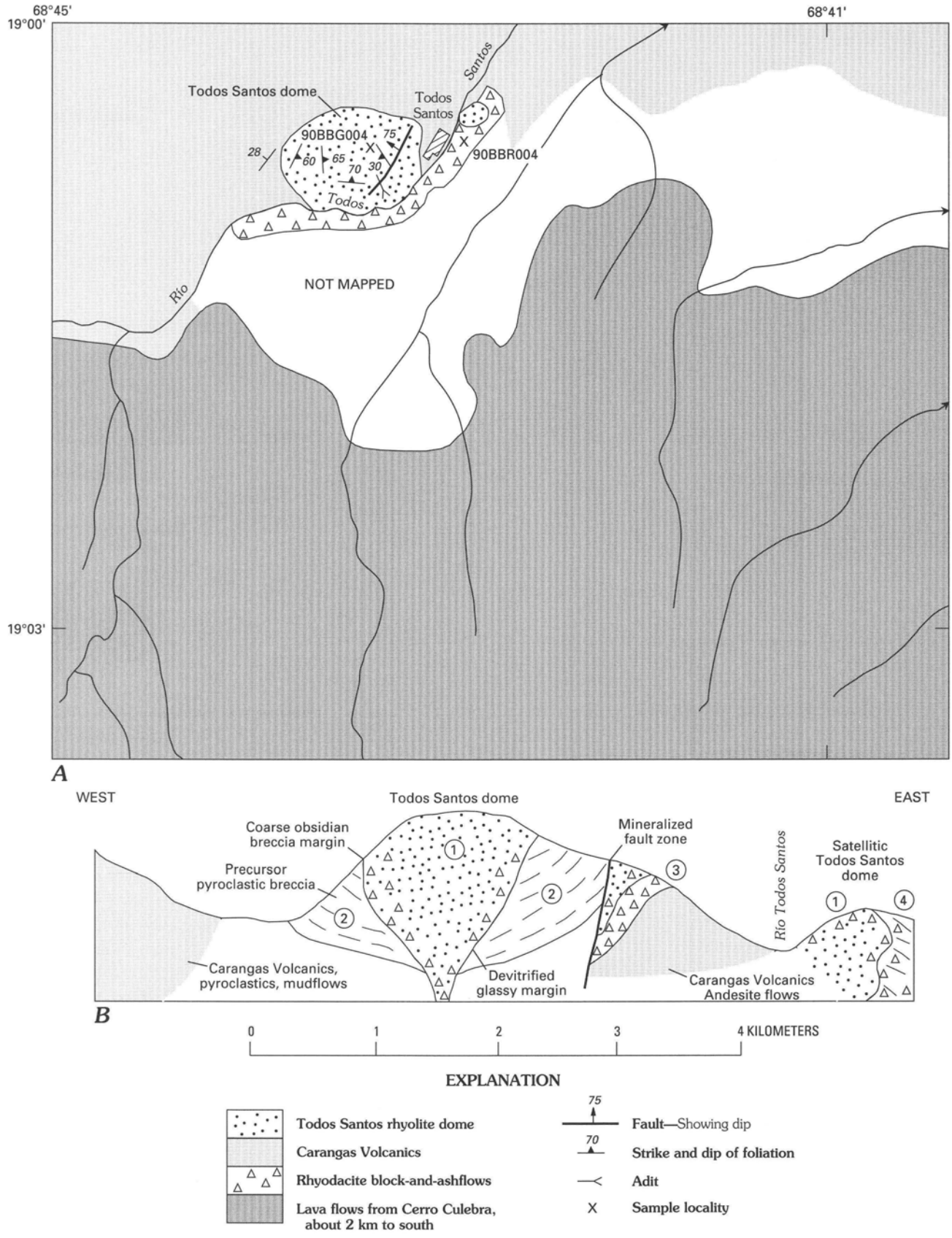


Figure 65. Todos Santos area, Bolivia. *A*, Sketch map showing generalized geology, mineralized fault zone, and sample localities. Area is in Todos Santos (5837 III) 1:50,000-scale quadrangle. *B*, Diagrammatic east-west cross section through the Todos Santos rhyolite dome. 1, largely aphyric, flow-banded and flow folded, locally brecciated rhyolite; 2, volcaniclastic breccia and tuffs; 3, heterogeneous explosive breccia; and 4, coarse ash and block flow.

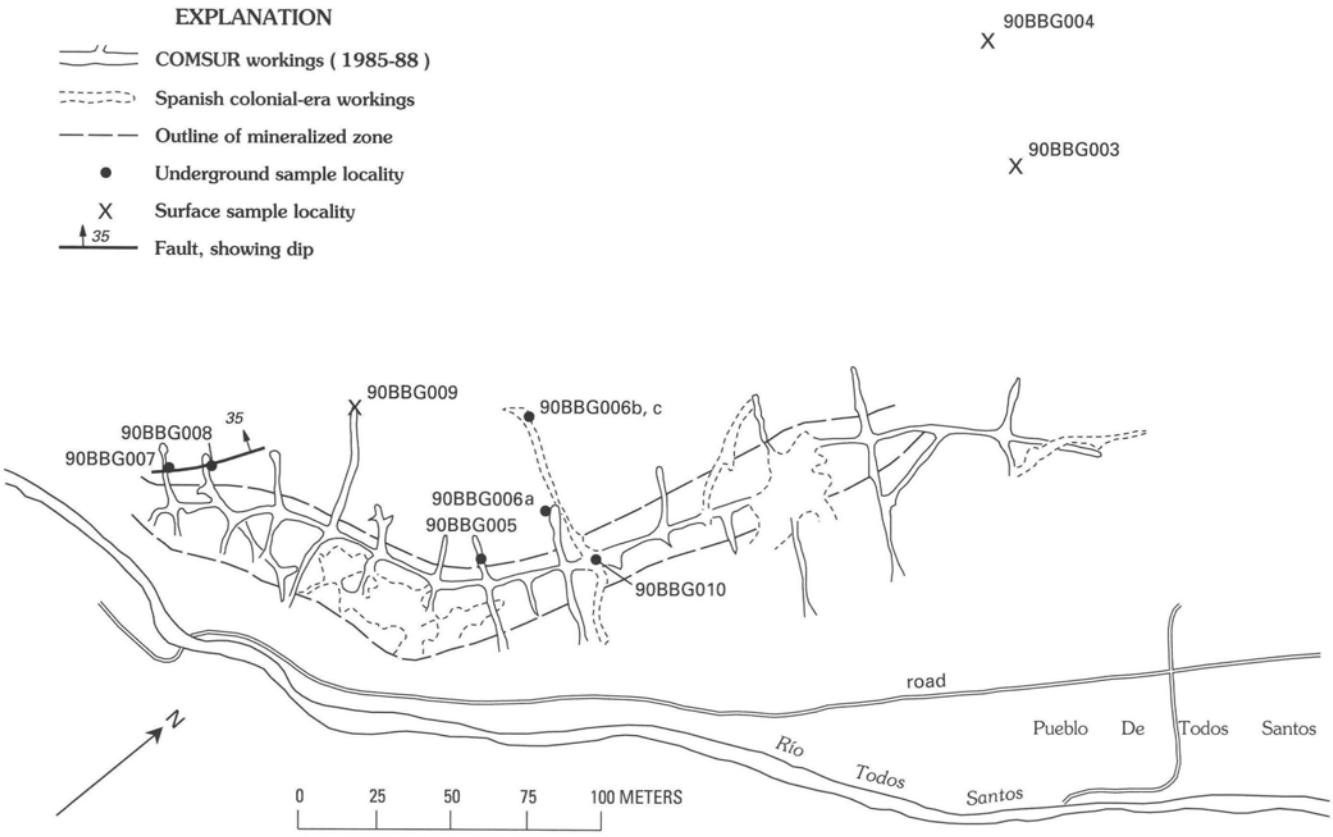


Figure 66. Sketch map of underground workings at the Todos Santos mine, Bolivia, showing outline of mineralized zone and sample localities. Map modified from McNamee (1988).

Disseminated ore (samples 90BBG005a, 5b, 6b, 6C, 7, 8, 9a, 9b, 10b) contains 2–200 ppm silver, 50–15,000 ppm lead, and 700–10,000 ppm zinc (table 19). A sample of the hematite veinlet (90BBG010a) contains 200 ppm silver, 1,000 ppm lead, and 2,000 ppm zinc. None of these samples contain gold above the lower limit of determination (0.002 ppm). A N. 45° E. mineralized fracture in the footwall of the main fault zone contains 69 ppm silver (table 19, sample 90BBR003).

A mining engineer informed us that between 1985 and 1988, COMSUR excavated 2,347 m of drifts and crosscuts and drilled 48 holes totalling 2,773 m. Recoverable ore reserves are estimated to be 1 million tonnes of 70 g/t silver and 0.07 g/t gold.

Carangas

Deposits near the village of Carangas are exposed on two low hills and consist of small silver-rich polymetallic veins as thick as 12 cm and disseminations in pyroclastic rocks of the Carangas Formation proximal to small rhyolitic intrusions and breccias (fig. 67). The deposit was apparently mined in Spanish colonial times and is currently being explored by COMSUR. As evident from the number and size of the dumps, the westernmost hill, Cerro Espíritu Santo, probably has the most significant deposits. The hill was mapped by McNamee (1988) and was the only area visited during this investigation.

Cerro Espíritu Santo (fig. 68) consists chiefly of an argillized dacitic lithic tuff containing as much as 5–10 percent propylitically altered andesite clasts as much as 5 cm across and about 10–15 percent quartz, feldspar, and biotite phenocrysts. Two zones of intense alteration, trending about N. 70° W., occur in the tuff. The lower altered zone is strongly fractured, locally silicified, and conspicuously stained by iron and manganese oxides. The upper altered zone is similar but no silicification was observed. The dominant fracture attitude is about N. 70° W. and vertical. Samples of the altered tuff (90BBG020, 21) contain as much as 50 ppm silver, 5,000 ppm lead, and 500 ppm zinc (table 19).

Near the top of Cerro Espíritu Santo the lithic tuff is intruded by a rhyolite dike, small bodies of rhyolite, and numerous dense masses of rhyolite breccia. The rhyolite dike (sample 90BBG024) contains about 5 percent feldspar, 3 percent quartz, and 1 percent biotite phenocrysts in an aphanitic groundmass; the dike has been silicified, as shown by its normalized SiO_2 content of more than 80 percent (app. B). Biotite from this sample was dated by the K–Ar method and gave an age of 15.4±0.5 Ma (app. C). Flow

Table 19. *Chemical analyses of mineralized and altered rocks from Todos Santos district, Bolivia*

[All results in parts per million (ppm). Sample 90BBG011a contains 0.008 ppm Au; sample 90BBG011b contains 0.10 ppm Au; all other samples contain <0.001 ppm Au and <10 ppm Sn. Sample descriptions, methods, and complete results in appendix B]

Sample no.	Ag	Pb	Zn	Cu
90BBG003	<0.05	50	<200	5
90BBG004	.5	50	<200	5
90BBG005a	50	7,000	10,000	20
90BBG005b	7	3,000	2,000	30
90BBG006b	30	10,000	3,000	150
90BBG006c	50	3,000	3,000	50
90BBG007	5	1,000	200	50
90BBG008	200	15,000	10,000	50
90BBG009a	5	100	700	70
90BBG009b	2	50	700	15
90BBG010a	200	1,000	2,000	100
90BG010b	20	5,000	5,000	70
90BBG011a	300	20,000	5,000	3,000
90BBG011b	1,000	>20,000	>10,000	7,000
90BBG012	700	>20,000	>10,000	1,500
90BBG020	1	150	200	10
90BBG021	50	5,000	500	15
90BBG022a	300	7,000	700	100
90BBG023	50	3,000	<200	30
90BBG025a	200	5,000	500	50
90BBG025b	10	1,000	700	20
90BBG025c	700	7,000	500	100
90BBR003	69	4,110	460	460

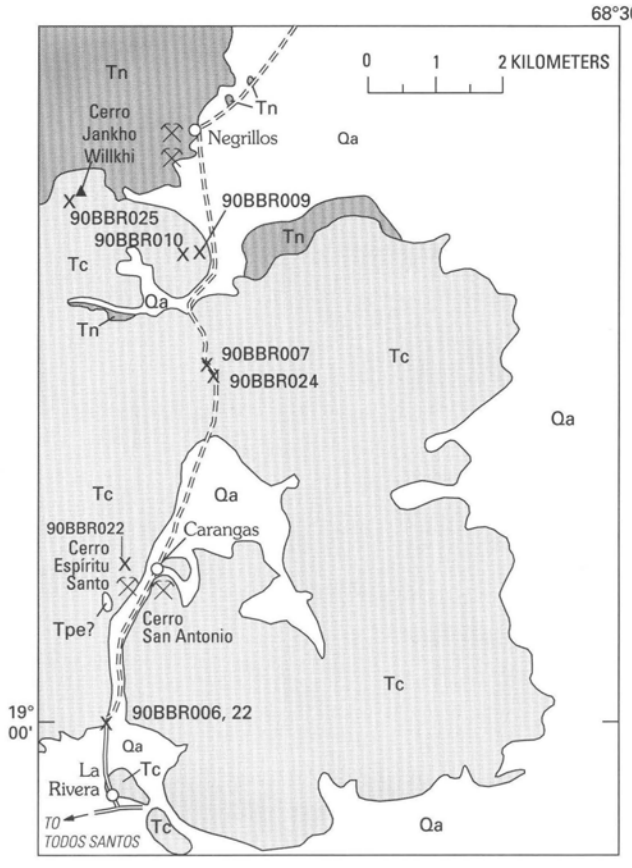


Figure 67. Sketch map showing geology and sample localities in the Carangas and Negrillos area, Bolivia. Geology simplified from Ponce and Avila (1965b) and Ponce, Avila, and Delgadillo (1967). Qa, Quaternary alluvium; Tc, Carangas Formation; Tn, Negrillos Formation; Tpe, Perez Formation (ignimbrite, younger than Carangas Formation).

banding is ubiquitous and parallels the orientation of the dike. The rhyolite breccias (pipes?) range in size from 5 m by 6 m to as much as 15 m by 30 m in plan view. Clasts range in size from a few millimeters to as much as 1.5 m in diameter and are subrounded rhyolite porphyry, similar in composition to the dike and small intrusive bodies. The clasts constitute 30–60 percent of the breccia and are generally argillized and locally silicified. A few small, altered clasts may have been derived from the lithic tuff host rock sequence. The breccia matrix is iron oxide stained quartz and (or) silicified rock flour, which makes the breccia exceedingly dense and resistant to erosion. The breccia (samples 90BBG022a, 23) contains as much as 300 ppm silver, 7,000 ppm lead, and 700 ppm zinc (table 19).

Numerous steep, narrow pits and trenches, many dating from Spanish colonial times, are present on Cerro Espíritu Santo. They all appear to be in lithic tuff and are 5–20 m deep. The largest working is a glory hole that is apparently connected to a series of underground workings. Only one quartz veinlet thicker than 1 cm and one quartz vein, 3–5 cm thick, were observed in the workings; both were stained with manganese oxide, but neither contained visible metallic minerals. The quartz is clear, has an open-space texture, and appears to be epithermal in origin. Samples of the veinlet and vein (90BBG025a, b, c) contain as much as 700 ppm silver, 5,000 ppm lead, and 700 ppm zinc (table 19). Gold does not exceed 0.002 ppm in any of the samples from Cerro Espíritu Santo.

Negrillos

Mineral occurrences near the town of Negrillos consist of silver-bearing veins, veinlets, and breccia fillings in andesitic lava flows and volcanic breccia. These volcanic rocks may be part of the Carangas Formation, or they might be related to younger stratovolcanoes. The mineralized area has been explored by two adits and numerous small prospects, many of which apparently date from Spanish colonial times (fig. 69). The area is presently inactive; Empresa Minera La Plata is the current owner.

Only the largest adit, southwest of Negrillos, and several small prospects were examined in detail during this investigation. The adit trends N. 20° W. and is about 135 m

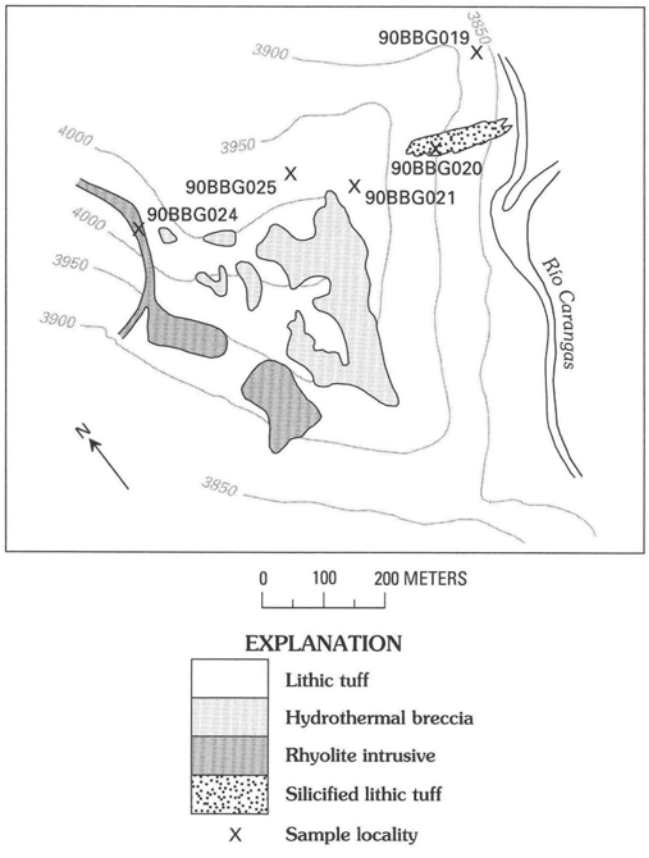


Figure 68. Geologic map of Cerro Espíritu Santo, Carangas, Bolivia, showing sample localities. Modified from McNamee (1988).

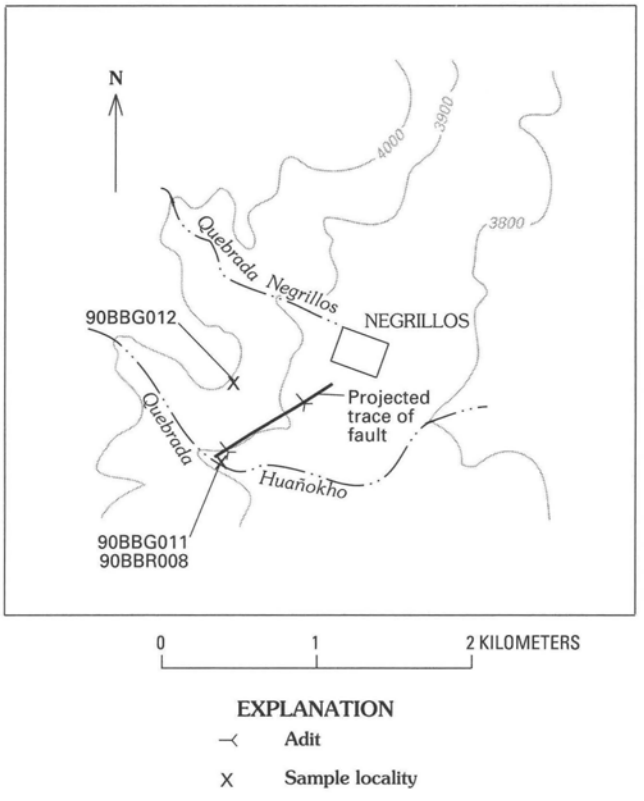


Figure 69. Sketch map of the Negrillos area, Bolivia, showing sample localities. Base from Negrillos (5837 I) 1:50,000-scale quadrangle.

long. At its end is a shaft at least 20 m deep, and at 125 m is an inclined winze heading N. 55° W. and at least 10–15 m deep. At about 130 m, a small overhead stope about 15–20 m high follows a fault trending N. 80° E., dipping 65° north. Along the fault is a 20–30 cm thick zone of plastic, gougy, altered volcanic rock that is strongly stained with manganese oxide and cut by thin (<2 mm) quartz veinlets. The volcanic rock in the immediate hanging wall is intensely argillized and contains about 1 percent disseminated pyrite. No other mineralization was seen in these workings.

Abundant mineralized rock on the dump at the portal of the adit presumably came from the shaft at the end of the adit. Judging from the dump material, there are two main types of mineralization, which appear to grade into each other. One is pyrolusite-quartz-pyrite veinlets and breccia fillings and the other is quartz-galena-sphalerite-pyrite-pyrolusite-cerrusite veinlets and veins as thick as 5 cm. Both types commonly exhibit open-space growth, and euhedral crystals of quartz, sphalerite, and cerrusite are common. Host rock for the mineralized dump material is a pale-green to light-gray, bleached and argillized lithic volcanic rock of uncertain type. Some pyrolusite veinlets are also present in sparse basaltic material on the dump. Host rock at the portal of the adit is an andesite breccia with a normalized SiO_2 content of 59.2 percent (app. B, sample 90BBR008). Samples of mineralized material on the dump (sample 90BBG011a, 11b) contain 0.008–0.10 ppm gold; 300–1,000 ppm silver; >20,000 ppm lead; 5,000 to >10,000 ppm zinc; and 3,000–7,000 ppm copper (table 19).

Several nearby prospects are aligned along a N. 60°–80° E. trend over a distance of about 1 km. This trend is approximately parallel to the strike of the fault encountered underground, suggesting that the fault is probably a major control of mineralization.

Several prospects, evidently dating from the Spanish colonial era, are located on the ridge between Quebradas Negrillos and Huañokho. These apparently exploited vertical fractures that trend N. 70°–80° W., but no mineralization was seen along any of the fractures. One of the dumps contained some quartz-galena-sphalerite-pyrolusite vein material. A composite grab sample of mineralized material from this dump contains 700 ppm silver, >20,000 ppm lead, >10,000 ppm zinc, and 1,500 ppm copper (table 19, sample 90BBG012).

Country rock in this area is a coarse volcanic breccia (debris flow?) containing andesitic blocks as much as 2.5 m across. In several localities, the breccia is overlain by an andesitic(?) lava flow. Both rock types are propylitically

altered throughout the immediate area and argillized as much as 15 cm from fractures.

Paco Kkollu Prospect

The Paco Kkollu silver prospect (fig. 67, locality 90BBR025) is located about 4 km westsouthwest of Negrillos on the south side of Cerro Jankho Willkhi. A number of old Spanish diggings are present on the north flank of Cerro Jankho Willkhi. The prospect is currently being drilled by Pan Andean S.A. and is a possible large volume, disseminated silver prospect (Peter Matthews, Pan Andean S.A., oral commun., 1990). Rocks on the old dumps are reported to contain as much as 400 g/t silver, and altered rock near the drill site as much as 100–150 g/t silver.

At the drill site, near the top of Cerro Jankho Willkhi, the rock is a light-tan, vuggy or vesicular-textured rhyolite(?) containing sparse, unaltered, sanidine crystals 1–2 mm long, and numerous small voids of rectangular shape, many of which are filled with a soft brown clayey material. The vesicular appearance is derived from the leaching of some pre-existing mineral, most likely feldspar. The highly silicified rock also contains sparse white mica, probably replacing original biotite.

SALINAS DE GARCI MENDOZA DISTRICT

By James C. Ratté, B.M. Gamble, Raul Carrasco, *and* Eduardo Soria-Escalante

Summary and Conclusions

Polymetallic base and precious metal veins in the Salinas de Garci Mendoza district (app. A, nos. 188, 189, 191–194) are localized along approximately east-west and northwest-trending fracture zones and dikes. There is no active mining in the district today and past production, as indicated by the size of dumps and extent of workings, probably was small. A recent evaluation of reserves at the Guadalupe mine by a private mining company estimated 2,500,000 tonnes of ore averaging 0.4 g/t gold, and 280 g/t silver; similar reserves were estimated for the La Deseada mine.

Better knowledge of the mineral potential of the Salinas de Garci Mendoza district will come from further exploration of known veins that have been exploited in the past, mainly in the southern part of the district, and exploration of similar, but largely untested, silicified fracture zones on and around the highly silicified Cerro Kancha porphyritic dacite intrusion in the northern part of the district. Although several geochemical samples of vuggy silica rock collected at Cerro Kancha during this study failed to show significant precious or base metals, the many similarities between this altered intrusion and epithermal, quartz-alunite gold mineralization at Summitville, Colo. probably warrants a detailed geochemical survey of Cerro Kancha and the surrounding area.

Table 20. *Status of mines and prospects in the Salinas de Garci Mendoza district, Bolivia*

Mine or prospect	Status
Cangura (Cerro Kancha)	MINTEC prospect; area of vuggy silica rock (Stewart Redwood, oral commun., 1990).
La Deseada	Inactive mine; in situ reserves of 2.5 million tonnes, 0.4 g/t Au; 280 g/t Ag; dump reserves of 30,000 t, 0.4 g/t Au, 400 g/t Ag; underground workings about 30 m (Uribe, 1989).
Guadalupe	Inactive mine; in situ reserves, 2.5 million tonnes, 0.4 g/t Au, 280 g/t Ag; dump reserves of 20,00 t, 0.4 g/t Au, 400 g/t Ag; underground workings include 20 m shaft and an adit (Uribe, 1989).
Maria Luisa	Inactive mine; COMIBOL property; drilling reported but reserves not available; extensive underground workings (500-1,000 m?).
San Miguel	Inactive mine; drilling reported, but reserves not available; underground workings about 300 m.
Margarita	Inactive mine; drilling reported, but reserves not available; underground workings about 700-800 m.

Introduction

The Salinas de Garci Mendoza district is in the Intersalar Range, between Salar de Uyuni and Salar de Coipasa, about 260 km southsouthwest of Oruro. Polymetallic silver and base-metal veins occur in a highly eroded, complex volcanic terrain that underlies the late Miocene to Quaternary stratovolcanoes that dominate this mountainous region. The principal mines in the district (table 20; fig. 70) are the María Luisa, San Miguel, Margarita, Guadalupe, and La Deseada. All mines in the district are currently inactive.

Previous geologic studies include reconnaissance geologic mapping at the scale of 1:100,000 (Alarcón and Cadima, 1967; Alarcón and others, 1967), a report on the

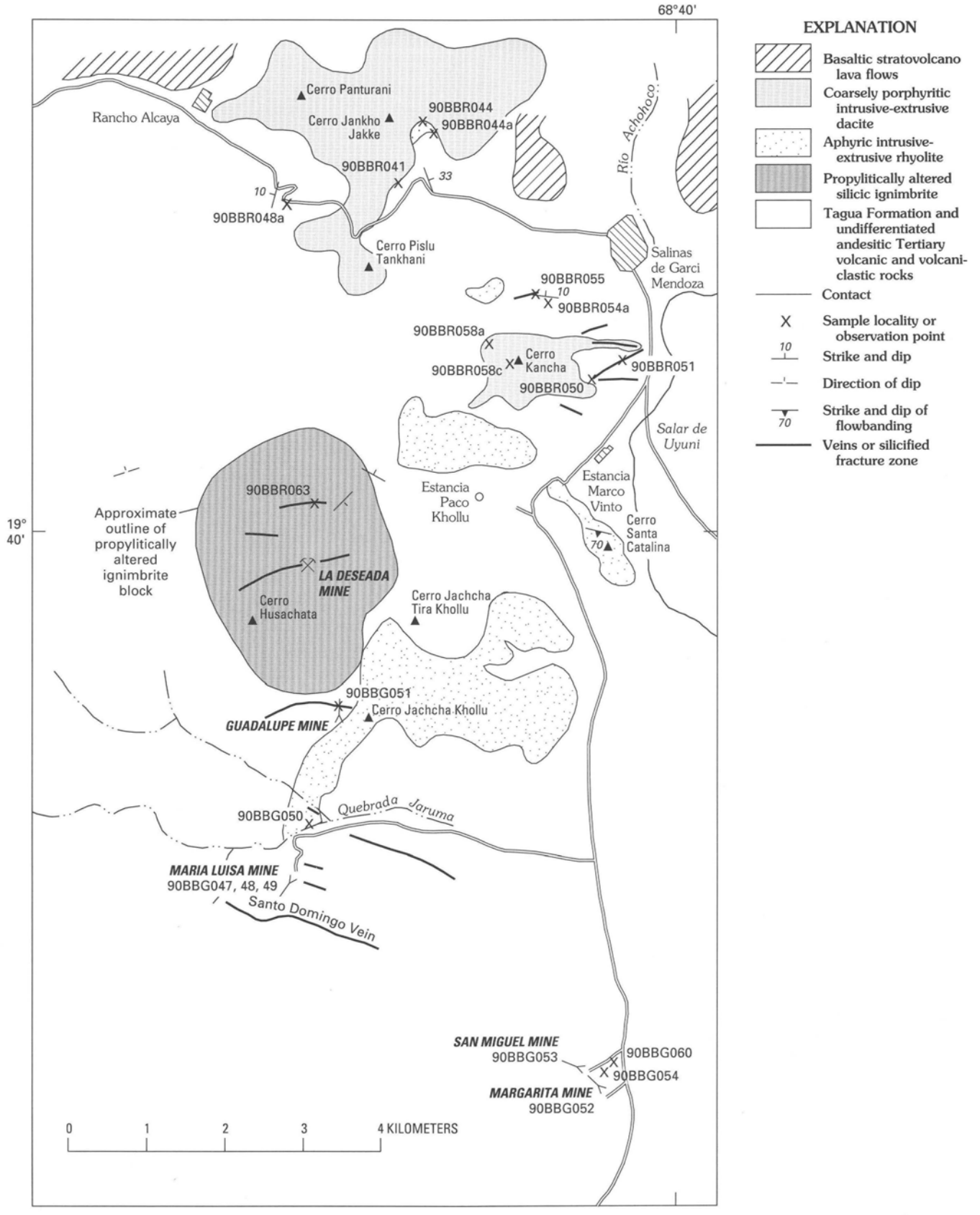


Figure 70. Sketch map of Salinas de Garci Mendoza district, Bolivia, showing outline of some major intrusive-extruisive bodies, the Cerro Husachata ignimbrite block, vein structures, and principal inactive mines. Outline of rhyolite at Cerro Jachcha Khollu, north and east of the María Luisa mine, modified from Sillitoe (1988, fig.7).

geology, mineral deposits, and hydrothermal alteration in the district (Medina and others, 1988), and an evaluation of the María Luisa veins by Sillitoe (1988); the latter two studies were conducted by the United Nations Development Program (UNDP). In general, the brief field examination conducted during the present study largely confirmed the earlier studies. However, new observations from a visit in September 1990 are presented here relative to the geologic setting of the Salinas de Garci Mendoza district, particularly in the northern part. We did not visit the area around Cerro Jachcha Tira Khollu, east of the Guadalupe mine, and have relied on the descriptions of Medina and others (1988) and Sillitoe (1988) for these and other areas not visited.

Geologic Setting

The Salinas de Garci Mendoza district is in the central part of the easternmost of two northeast-trending volcanic ranges in the Intersalar Mountains (Medina and others, 1988). Both ranges consist mainly of volcanic rocks ranging in age from Miocene to Quaternary (Baker and Francis, 1978). In the district, an older sequence of andesitic lava flows and breccias, tuffs, and volcaniclastic sedimentary rocks (pl. 1, Tvnd) are intruded and overlain by several small to moderately large bodies of intrusive-extrusive rhyolite and coarsely porphyritic dacite (fig. 70). The aggregate exposed thickness of the older volcanic sequence is about 700 m. It is overlain by roughly an equal thickness of andesitic and basaltic lava flows from younger stratovolcanoes of late Miocene to Quaternary age (pl. 1, QTev), whose imposing cones dominate the surrounding landscape, as at Cerro Tunupa, south of the district (fig. 71). Flows from the stratovolcanoes give radiometric ages ranging from 1.8±0.2 Ma (biotite) on the north flank of Cerro Tunupa to 4.5±0.3 Ma (biotite) for flows from Cerro Coracora, north of Salinas de Garci Mendoza (Baker and Francis, 1978; Medina and others, 1988). In the southern part of the district, south of Quebrada Jaruma, the older volcanic rocks have been tentatively divided into the Tagua Formation, consisting of lava flows, tuffs, and volcaniclastic sedimentary rocks, about 200 m thick, and an overlying sequence of undifferentiated lava flows and tuffs (Medina and others, 1988, fig. 2, unit Tnd-1). The polymetallic vein deposits at the María Luisa, San Miguel, and Margarita mines are hosted in both of these older volcanic rock sequences.

North of Quebrada Jaruma, the Tagua Formation and undifferentiated volcanic rocks (Medina and others, 1988, fig. 2, unit Tnd-1) are overlain and intruded by discrete domal bodies of largely aphyric rhyolite and coarsely porphyritic dacite. The rhyolite occurs in a large body around Cerro Jachcha Khollu and in several other mappable bodies at Cerro Santa Catalina, and north and south of Cerro Kancha (figs. 70, 72; Sillitoe, 1988). A rhyolite dike along the road between Salinas de Garci Mendoza and Rancho Alcaya is probably only one of numerous such dikes in the area.

Intrusive and (or) domal accumulations of coarsely porphyritic dacite occur mainly at Cerro Kancha and in the Cerro Jankho Jakke-Cerro Pislu Tankhani-Cerro Panturani intrusive-extrusive body, southwest and northwest of the village of Salinas de Garci Mendoza, respectively. The Cerro Jankho Jakke massif is largely unaltered except for a conspicuous area of white, chalky, montmorillonitic alteration at the margin of the body southeast of Cerro Jankho Jakke (fig. 70, locality 90BBR044). Unaltered dacite is found at locality 90BBR041 (fig. 70). Large phenocrysts of orthoclase, quartz and albite-oligoclase, with dimensions of 0.5–3 cm, constitute about 30 percent of the rock; euhedral mafic phenocrysts of hornblende, biotite, sphene, and apatite are generally less than 0.5 mm in size, and commonly occur as microphenocrysts in a very fine grained, gray, granular groundmass. Accessory zircon also is present. The dacite contains about 64 percent SiO_2, on an anhydrous basis (app. B), and is chemically similar to other Miocene dacites collected from the study area.

In contrast with the unaltered dacite at Cerro Jankho Jakke, the dacite intrusion of Cerro Kancha (fig. 72), is extremely altered and leached; most of the upper 100–200 m of the mountain is reduced to a vuggy silica rock from which almost all original constituents except silica have been removed. However, its similarity to the unaltered coarsely porphyritic dacite is shown by the relict porphyritic texture, which is particularly evident in places where remnants of advanced argillic alteration are preserved and the original feldspar phenocrysts are replaced by alunite and (or) kaolinite. Alunite was also identified in a thin section of sample 90BBR058a, collected from the northwest margin of the intrusion (fig. 70). Native sulfur is present in the leached casts of feldspar phenocrysts in the vuggy silica rock over much of the mountain.

Several silicified fracture zones (veins?, dikes?) form conspicuous ribs that are more or less radial to the eastern end of the mountain; other fractures are parallel to the northern edge of the intrusion on the lower north slopes of Cerro Kancha. The fracture zones commonly have argillically altered borders around vuggy silica cores.

During this study of the Salinas de Garci Mendoza district, a large ignimbrite block, generalized on figure 70 as a subcircular body about 3 km in diameter that includes Cerro Husachata, was recognized. Beneath Cerro Husachata, the tuff is about 600 m thick, contains about 10–20 percent small (<1–2 mm) plagioclase phenocrysts, and was probably moderately to densely welded prior to alteration. The ignimbrite and much of the surrounding andesite is highly propylitized and eutaxitic pumice in the tuff is conspicuous as green chloritic streaks. The ignimbrite also is a lithic-rich tuff and contains abundant andesitic and dacitic to rhyolitic inclusions ranging from lapilli size to

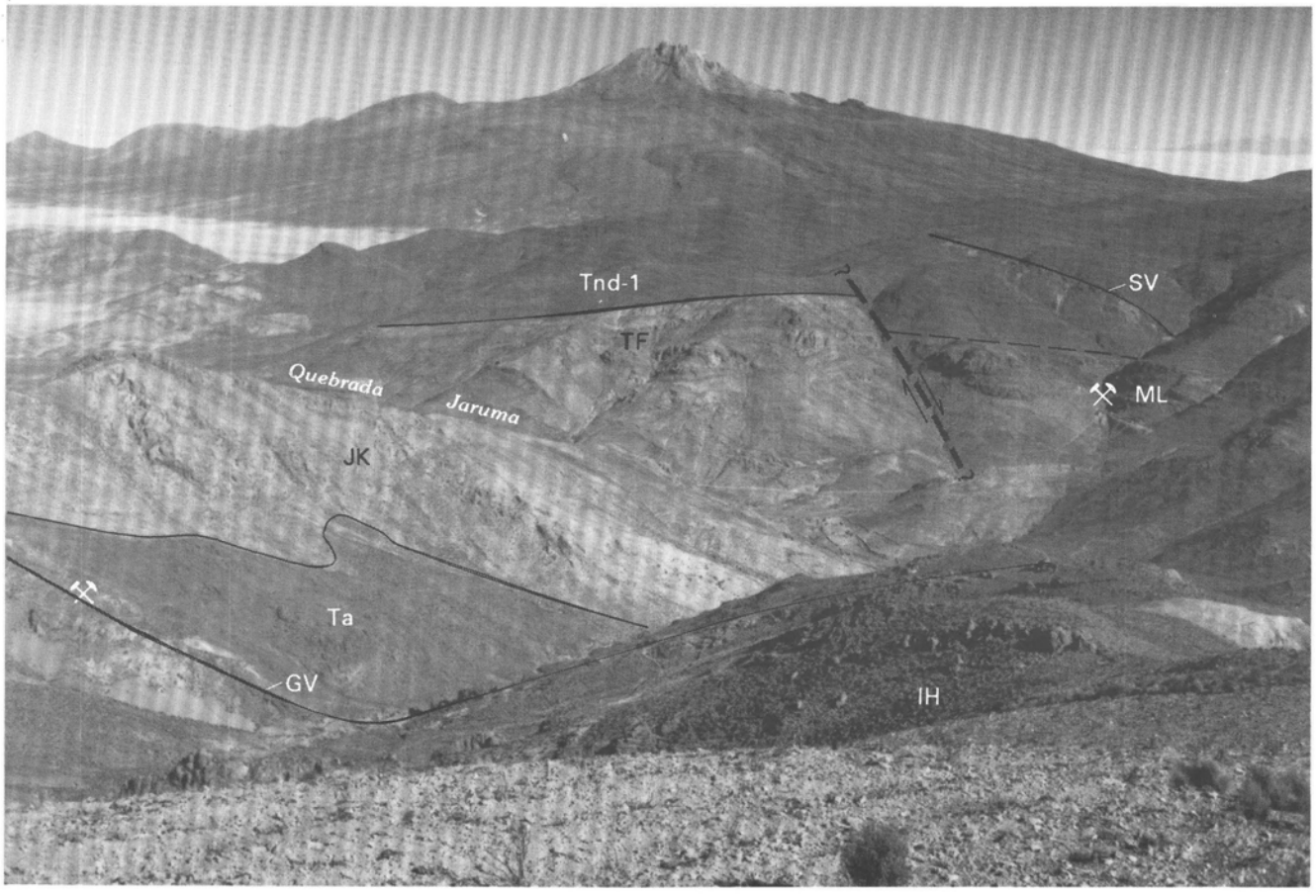


Figure 71. View south from Cerro Husachata, Salinas de Garci Mendoza district, Bolivia. In foreground, north of Quebrada Jaruma: JK, intrusive-extrusive rhyolite of Jachcha Khollu; Ta, andesitic lava flows and breccias; IH, ignimbrite of Cerro Husachata; and GV, Guadalupe vein. South of Quebrada Jaruma: ML, María Luisa mining camp; SV, Santo Domingo vein; TF, Tagua Formation; and Tnd-1, undivided Tertiary volcanic rocks of Medina and others (1988). In background, the stratovolcano Cerro Tunupa, which is dated at 1.8–2.5 Ma. Arrows indicate direction of movement along fault.

megabreccia blocks many meters long. The abundance and size of lithic inclusions appears to increase toward the contact with surrounding andesitic flows and breccias in the northeastern sector of the ignimbrite block.

Understanding the stratigraphic and structural relationships of the geologic units described here relative to major volcanic structures, such as a stratovolcano complex, with or without an associated ash-flow tuff caldera, will require additional detailed geologic mapping.

Mineral Deposits

Guadalupe Mine

The ore minerals at the Guadalupe mine occur in three dacite dikes (Uribe, 1989) that intrude andesitic rocks along the southeast margin of the large ash-flow block at Cerro Husachata. The principal dike is 1,000 m long, 8–10 m wide, trends N. 85° E., and dips 80° north. The other dikes are shorter (100 m, 150–200 m) but about the same width. There is a shaft about 20 m deep on the principal dike (fig. 73). Near the shaft, the dike is strongly silicified to a light-gray, sugary textured rock; argillized feldspar phenocrysts can be recognized locally. At least one discrete, 3–4 cm wide, quartz vein containing 1–3 percent pyrite was observed in the dike. Otherwise, the dike contains less than 1 percent pyrite and rare grains of a dark-gray, metallic mineral tentatively identified as enargite. According to Uribe (1988), the dikes contain, or are accompanied by, "tectonic breccias cemented by ferrous material." We did not see this breccia. The location of the Guadalupe mine is incorrectly shown near the southern edge of the Salinas de Garci Mendoza 1:100,000-scale geologic map (Alarcón and Cadima, 1967), but is correctly shown on the Alianza 1:50,000-scale topographic map.

Sulfide minerals are exposed in an inclined adit slightly downhill from the shaft. The adit trends almost due north and apparently intersects the downdip projection of the dike. Intensely silicified rock with a variable sulfide content also occurs in a zone at least 5 m wide in a northerly direction and at least 7 m wide in an easterly direction. The

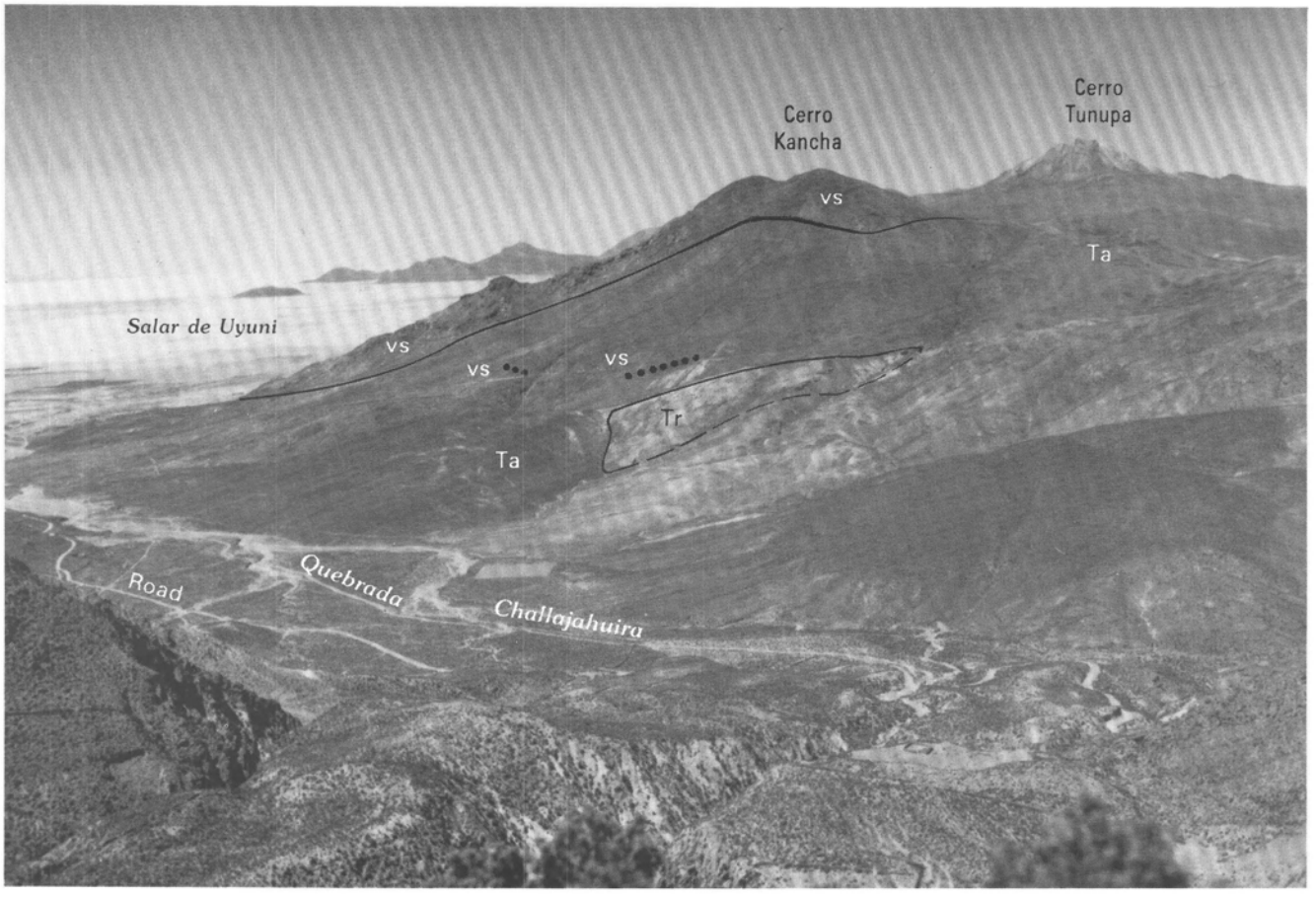


Figure 72. View of Cerro Kancha, Salinas de Garci Mendoza district, Bolivia, from north, showing distribution of vuggy silica rock (vs) altered from coarsely porphyritic dacite intrusion of Cerro Kancha, and smaller vuggy silica fracture zones on lower, colluvium-mantled slopes. Tr, aphyric, flow-banded rhyolite dome; Ta, andesitic lava flows and breccias.

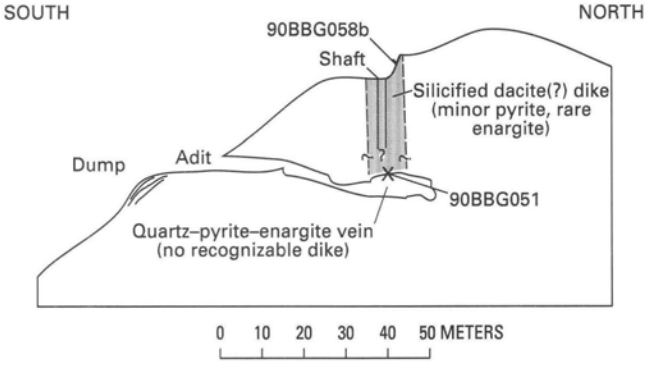


Figure 73. Cross section of the Guadalupe mine, Bolivia.

protolith of the silicified rock could not be determined; the altered rock is virtually 100 percent quartz, sulfides, and locally, patches of white clay minerals. The patches of clay minerals are a few millimeters across to about 3–5 cm across, that appear to be argillized breccia fragments of unknown origin. The sulfide content is as high as 20–25 percent pyrite and 5 percent enargite and averages about 5 percent pyrite and 2–3 percent enargite. Higher-grade material on the dump contained as much as 30 percent pyrite and 20 percent enargite. Samples from the dike (90BBG058b), underground mineralization (90BBG051a), and mineralized material collected from the dump (90BBG051b) contain 86–450 ppm silver, 0.1–0.9 ppm gold, 350–30,000 ppm copper, and anomalous amounts of lead, zinc, and tin (table 21).

Altered rocks at the Guadalupe mine include the argillized and silicified dike, and propylitized and locally argillized country rocks. In the dike, argillization is recognizable only where silicification is not strong. Argillized country rocks are confined to sheared areas near the portal of the adit.

The country rocks are andesite lava flows and flow breccias (Medina and others, 1988, fig. 2, unit Tnd-1). Near the shaft, the andesite is a purple lava flow containing 10–15 percent plagioclase and hornblende phenocrysts; near the portal of the adit, it is a green to purple flow breccia with rounded, andesitic clasts as much as 15 cm across.

Uribe (1989) reports grades as high as 16.6 g/t gold and 660 g/t silver with an average of 0.4 g/t gold and 325 g/t silver for the brecciated dikes and 0.4 g/t gold and 452 g/t

Table 21. *Chemical analyses of mineralized and altered rocks from the Salinas de Garci Mendoza district, Bolivia*

[All results in parts per million (ppm). Sample descriptions, methods, and complete results in appendix B]

Sample no.	Au	Ag	Pb	Zn	Cu	Sn
90BBG047	0.55	1,000	6,500	10,000	360	<10
90BBG048a	.10	82	1,100	10,000	530	<10
90BBG49a	.85	1,400	59,000	5,800	1,400	<10
90BBG050b	.004	11	440	390	14	<10
90BBG051a	.65	86	320	110	4,500	15
90BBG051b	.90	450	550	47	30,000	700
90BBG052a	2.1	20	58,000	3,300	130	<10
90BBG052b	.006	1.4	310	1,100	18	<10
90BBG052d	1.05	1,200	110,000	500	2,000	<10
90BBG053a	.05	14	85,000	5,000	6.3	<10
90BBG053b	.002	.87	250	550	8	<10
90BBG054	.01	.045	1,900	1,700	8.8	<10
90BBG058b	.1	150	420	40	350	15
90BBG058c	.002	.29	8.5	1,700	100	<10
90BBR048a	<.002	.55	5.4	15	25	<10
90BBR050	<.002	.34	15	9.3	3.8	<10
90BBR051	<.002	<.045	4.9	8.5	3	<10
90BBR054a	<.002	<.045	12	5.8	1.5	<10
90BBR055	<.002	.7	14	8	6.8	<10
90BBR058c	<.002	<.045	4.4	2.5	2.7	<10
90BBR063	.074	65	6,100	190	120	<10

silver for the dumps. Grade and tonnage calculations (Uribe, 1989), assuming a 1,000 m length, 10 m width, and 100 m depth, provide an estimate of 2,500,000 tonnes of 0.4 g/t gold and 280 g/t silver for the dike, with an additional 20,000 tonnes of 0.4 g/t gold and 400 g/t silver in the dumps.

La Deseada Mine

The western part of the silicified fracture zone that the La Deseada mine exploits was examined during this study. The La Deseada mine, which was not visited during this study, is developed in a mineralized dacite dike containing sphalerite and galena in a quartz-barite-pyrite gangue (Uribe, 1989; fig. 74). The dike strikes about due east, dips 80° north, is about 10 m wide, and is more than 1 km long. As much as 30 m of workings are present along the structure. About 80 m south of the principal dike, two smaller dikes about 600 m long and 2–2.5 m wide, contain azurite and malachite in a quartz-pyrite gangue. Uribe (1989) reports 5–15 m chip samples across the principal dike yielded grades ranging from 0.07 to 3.52 g/t gold and 51 to 436 g/t silver; with an average for 9 samples (without the 3.52 g/t gold assay) of 0.23 g/t gold and 218 g/t silver. Interestingly, Uribe (1989) obtained identical reserves for the La Deseada mine as he did for the Guadalupe mine: 2,500,000 tonnes of 0.4 g/t gold and 280 g/t silver. Dump reserves were calculated at 30,000 tonnes at 0.4 g/t gold and 400 g/t silver.

Where examined on the north side of Cerro Husachata, the La Deseada "vein" consists of vuggy silica rock that is about 15–30 m wide. Downslope to the north, on Wila Sirca Loma, a similar, but weaker, silicified fracture zone cuts the ash-flow tuff and has been prospected at several places. The quartz-rich core of this N. 70° W. trending structure is about 0.5 m wide, and a sample from the core (90BBR063) contained 0.074 ppm gold, 65 ppm silver, 120 ppm copper, 130 ppm molybdenum, 6,100 ppm lead, and 190 ppm zinc (table 21).

María Luisa Mine

The María Luisa mine is on the Santo Domingo vein, a fault-localized zone of silica flooding and discrete quartz veins that is at least 2 km long. The vein-structure ranges from less than 1 m to almost 6 m wide, and averages about 2 m wide. Where examined underground, it strikes east-west and dips steeply north to vertical. At the surface however, the vein has a strike of about N. 75° W. (Medina and others, 1988). Gougy clay seams 3–15 cm wide are locally present along the vein walls and in the vein proper.

Overall the vein averages about 2–3 percent pyrite and 1 percent other metallic minerals including sphalerite,



Figure 74. Dumps of La Deseada mine on the north slopes of Cerro Husachata, Bolivia. IH, ignimbrite of Cerro Husachata; LDV, outcrop of La Deseada vein.

minor chalcopyrite, and black to silvery black minerals (galena, freibergite, stephanite, and covellite were identified by Ahlfeld and Schneider-Scherbina, 1964). Locally, small areas of the vein contain as much as 20 percent pyrite and an equal amount of the other metallic minerals. The metallic minerals are fine grained, rarely more than 2 mm across, and occur as disseminations and as clots 1–5 cm across. Quartz is by far the dominant gangue mineral; it is white to dark gray, has a massive to sugary texture, and contains as much as 10 volume percent open-space cavities. These cavities are lined with small clear, quartz crystals as long as 5 mm, and locally contain colorless to white, bladed barite(?) crystals that are as long as 5 mm. Some cavities are filled with unknown clay minerals. A smaller subsidiary vein at the María Luisa mine is 20–60 cm wide, trends N. 40° W., dips 60° northeast, and contains 10–40 percent metallic minerals.

Country rocks exposed at the portal of the mine, and in underground exposures near the portal, are propylitically altered andesitic lava flows. Further underground, the host rocks of the vein are fine-grained volcaniclastic rocks of the Tagua Formation. The country rocks are variably silicified for as much as 1 m from the veins and locally contain an estimated 1 percent disseminated pyrite and lesser amounts of dark minerals. Geochemical samples collected from the underground exposures of the veins (table 21, 90BBG047, 48a, 49) contain 82–1,400 ppm silver, 0.1–0.85 ppm gold, 1,100–59,000 ppm lead, 5,800–10,000 ppm zinc, and 360–1,400 ppm copper. A large rhyolitic body, possibly a dome or shallow intrusion, is exposed on the north side of Quebrada Jaruma (fig. 70), approximately 750 m north of the portal to the María Luisa mine. This rock is white, flow banded, and contains a few percent quartz and feldspar phenocrysts in a very siliceous, aphanitic groundmass. The attitude of the flow banding is somewhat variable, but mostly very steep. The rhyolite body is about 0.5 km wide in an east-west direction, and extends 2–3 km to the north beneath Cerro Jachcha Kkollu, which is immediately east of the Guadalupe mine. Sillitoe (1988, fig. 7) suggests it broadens to the east and north. A small adit and dump are present at creek level near the center of the rhyolite body. Some of the fragments on the dump consist of sparse quartz veinlets cutting the rhyolite; no metallic minerals were observed. A sample of the rhyolite with quartz veinlets (90BBG050b) contains 11 ppm silver, 0.004 ppm gold, 440 ppm lead, and 390 ppm zinc (table 21).

Margarita and San Miguel Mines

The Margarita and San Miguel mines, approximately 5 km southeast of the María Luisa mine, are on the same mineralized structure and their underground workings are connected by raises. The San Miguel workings are parallel to, and about 50 m higher than, the Margarita workings. There are approximately 700 to 800 m of workings at the Margarita mine and approximately 275 to 300 m of workings at the San Miguel mine.

The deposit consists of discontinuously silicified and mineralized vertical shear zones trending chiefly N. 45° W. to N. 75° W. One shear zone has an attitude of N. 80° E. and dips 80° north to vertical. The width of the shear zones range from 50 cm to 6 m; they consist of thin (1–3 cm) gougy slip planes in highly argillized and variably silicified country rock. The host rocks are intercalated tuffs and volcaniclastic rocks of the Tagua Formation that strike northeast and dip moderately (10°–45° northwest).

Mineralization is discontinuous across the width and along the strike of the shear zones. The longest continuously mineralized section was heavily timbered and about 50–70 m long. The mineralized part of the shears contain from 3 percent to about 90 percent metallic minerals, but averages about 20–30 percent. Galena and sphalerite are the dominant sulfides and a few percent pyrite is invariably present. The sphalerite is yellow to brown in color, and commonly, a rim of brown sphalerite can be seen as an overgrowth on earlier yellow sphalerite. The sulfides are fine to coarse grained and occur as disseminated grains, massive intergrowths, and in discrete quartz veins as wide as 10 cm. Quartz is the dominant gangue mineral. Clots and masses of white clays (argillized wallrock?) are locally abundant and ankerite (dolomite?) is locally present in small amounts. Several varieties of quartz are present. Most common is massive to banded, colorless, white, or red (hematitic) with small open-space cavities containing small (<3 mm long) euhedral quartz crystals and locally, ankerite crystals. One vein observed in a mineralized section consisted of an outer band of terminated amethyst crystals (5–8 mm long) with an inner, open-space-filling band, as wide as 2 cm, of massive, white quartz. Small grains and clots of galena and pyrite were present along the outer margin of the amethyst band.

Rocks of the host Tagua Formation at the San Miguel and Margarita mines are mostly propylitically altered, both underground and at the surface. Strong argillic alteration is locally present adjacent to the veins and extending outward for 1–2 m. In the shear zones, intensely argillized host rock can be recognized locally, with or without a silicification overprint. Silicified rocks appear to be confined to the shear zones and to parallel, fracture-controlled, quartz veins. In one crosscut, several silicified shear zones, 50 cm to 2 m wide, were present over a distance of about 12 m. One of these contained about 3 percent galena and 1 percent sphalerite.

Samples of the veins (90BBG052a, 53a) contain 14–20 ppm silver, 0.05–2.1 ppm gold, 5–9 percent lead, and 3,300–5,000 ppm zinc. A selected high-grade sample from the dump of the Margarita mine (90BBG052d) contains 1,200 ppm silver, 1.05 ppm gold, 11 percent lead, 500 ppm zinc, and 2,000 ppm copper. Samples of the country rock (90BBG052b, 53b) collected within 1 m of the vein contain low level anomalies of silver, gold, lead, and zinc (table 21).

Two other silicified fracture zones were observed on the surface within 150 m of the portal of the San Miguel mine; they are 8 and 12 m wide and consist of individual quartz veins as wide as 25 cm separated by variably propylitic, argillic, silicic, and sericitically altered volcaniclastic rocks. The silicified zones trend N. 50° to 60° W. and dip vertically. Iron- and manganese-oxide stain is common, but no metallic minerals were observed. A sample of one of these silicified zones has low level anomalies of silver, gold, lead, and zinc (table 21, sample 90BBG054).

Cerro Kancha Area

The highly altered intrusive rocks on Cerro Kancha have a number of features in common with worldwide epithermal gold deposits, for example, those at Summitville, Colo. (Steven and Ratté, 1960; Stoffregen, 1987). These features include the coarsely porphyritic dacitic intrusion; extreme silicification and leaching of the porphyritic rock to produce a vuggy silica rock; and associated alunitic-advanced argillic and pervasive propylitic alteration zones. As at Summitville, some of the feldspar casts and other voids in the vuggy silica rock are filled with native sulfur. The silica contains tiny gray blotches, which were too small for identification in a polished section by ore microscopy, but examination by the scanning electron microscope identified them as leucoxene, after sphene. Very fine grained pyrite is present in some specimens containing dense vein-type silica, but pyrite is absent or oxidized in most of the vuggy silica rock. Five geochemical samples collected from the vuggy silica rock on Cerro Kancha and from satellitic silicified fracture zones showed no detectable gold at the limit of determination (0.002 ppm), and only minimal silver contents of as much as 0.7 ppm (table 21, samples 90BBR048a, 50, 51, 54a, and 55). Thus, significant mineralization does not appear to be associated with the silicified dacite intrusion at Cerro Kancha, but a more systematic geochemical sampling survey for low-grade gold is recommended.

Other Deposits

Three abandoned mines are shown on the Salinas de Garci Mendoza geologic map, the Candelaria copper mine, northwest of Cerro Kancha, and two lead mines on the northeast and southeast flanks of Cerro Kancha (Alarcón

and Cadima, 1967). These mines were not found during this investigation of the area and they are not mentioned by Medina and others (1988).

SONIA–SUSANA AREA

By B.M. Gamble, James C. Ratté, Eduardo Soria-Escalante, *and* Raul Carrasco

Summary and Conclusions

Several large altered areas, known collectively as the Sonia-Susana area (app. A, nos. 164, 166, 167), occur chiefly in andesitic or dacitic lava flows and flow breccias of the Negrillos Formation. Propylitic alteration is widespread, and argillization and silicification may be locally present. Unmineralized quartz-pyrite veins are locally present. Reconnaissance geochemical sampling of altered rocks reveals the presence of low level gold, silver, lead, and zinc anomalies, and suggests that the area has potential for epithermal precious-metal deposits and possibly for polymetallic vein deposits.

Introduction

The Sonia-Susana area lies near the Bolivia-Chile border, about 20 km west of Negrillos. The area is in the Julo (5837 IV) and Cerro Capitán (5837 III) 1:50,000-scale quadrangles, which are in the southwest corner of the Corque 1:250,000-scale quadrangle. The area covers most of an eroded stratovolcano complex mapped as Negrillos Formation on the 1:100,000-scale geologic map of the Carangas quadrangle (Ponce and Avila, 1965a). These volcanics (pl. 1, Tvnd) are presumed to be late Oligocene or early Miocene and are part of the Western Volcanic Zone of the Andes. Numerous occurrences of extensive hydrothermal alteration, reported to contain silver, lead, copper, gold, arsenic, and antimony, occur in the area. A traverse into the area along Río Pacokhaua was made in September 1990. This examination served to confirm the presence and extent of highly altered rocks.

Geology and Mineral Deposits

The northeastern mountain slopes between Negrillos and Estancia Juramani appear to consist of interlayered tuffs and lava flows (pl. 1, Tvnd) that may be an extension of the Carangas Formation.

Northeast of Estancia Viluyo (fig. 75), a thick sequence of interlayered tuffs and volcaniclastic rocks of the Carangas Formation strikes northwest and dips 40°–45° northeast. Hot springs at Estancia Viluyo are probably related to a fault of uncertain trend that separates these rocks from the eroded stratovolcano complex of the Negrillos Formation to the southwest.

Composite float samples of argillized and silicified tuff(?) were collected at locality 90BBG033 (fig. 75) that were apparently derived from the large altered area to the south and east. However, the samples (90BBG033a, b) do not have anomalous metal contents (table 22). The rocks southwest of the fault are mainly andesitic to dacitic lava flows, locally interlayered with volcaniclastic rocks and tuffs. What appears to be a massive, plagioclase-phyric, andesitic intrusion occurs at locality 90BBR030 (fig. 75).

Upstream (southwest) of this andesitic intrusion, the rocks along both sides of the valley are generally propylitized and locally argillized and silicified. In some places, quartz phenocrysts as much as 0.5 cm across were observed in the altered rocks and a variety of igneous rock types are undoubtedly present in this altered area.

On the west flank of Loma Santa Catalina (fig. 75), the andesite flows and flow breccia are locally argillized, silicified, fractured, and (or) brecciated. The argillization is clearly an overprint on regional propylitic alteration. In the few good outcrops present, the fracturing appears to be truly random; there are numerous orientations with no single attitude predominating. Where the rocks are brecciated, the matrix is locally silicified and consists of rock flour mixed with fine-grained iron oxides. A few quartz-pyrite veinlets were observed in one outcrop. A few pieces of float with quartz veinlets were also observed, and one piece of float contained a 4-cm thick, vuggy, brecciated quartz vein. All of the quartz appears to be epithermal vein quartz, however no samples contained any visible sulfide minerals other than pyrite. Samples of these altered rocks contain as much as 0.038 ppm gold, 10 ppm silver, and 1,500 ppm lead (fig. 75; table 22, samples 90BBG030, 31, 32a, b, c).

At localities 90BBG029 and 90BBR028, a shear zone in propylitically altered andesite was sampled (fig. 76). The central part of the shear is a vein 50–80 cm thick that strikes N. 80° E. and dips 85° south. The vein is an intensely oxidized, vuggy to boxwork-textured mass of iron oxides; no other metallic minerals remain in the vein. The andesite is brecciated and strongly argillized for as much as 2 m on both sides of the vein. Pyrite is common in the brecciated zone, occurring as thin (<1 mm wide) veinlets and fracture coatings. Beyond this breccia zone, the andesite is strongly fractured and contains sparse fine-grained pyrite. One sample of the vein and breccia contains 0.024 ppm gold, 3 ppm silver, and 2,000 ppm zinc (table 22, sample 90BBG029).

Further south, towards Cerro Wila Willkhi, is an extensive area of yellowish-white to red altered rocks that was not visited. A sample of altered andesite(?) float collected north of this altered area contains disseminated pyrite and specular hematite. This sample contains 0.004

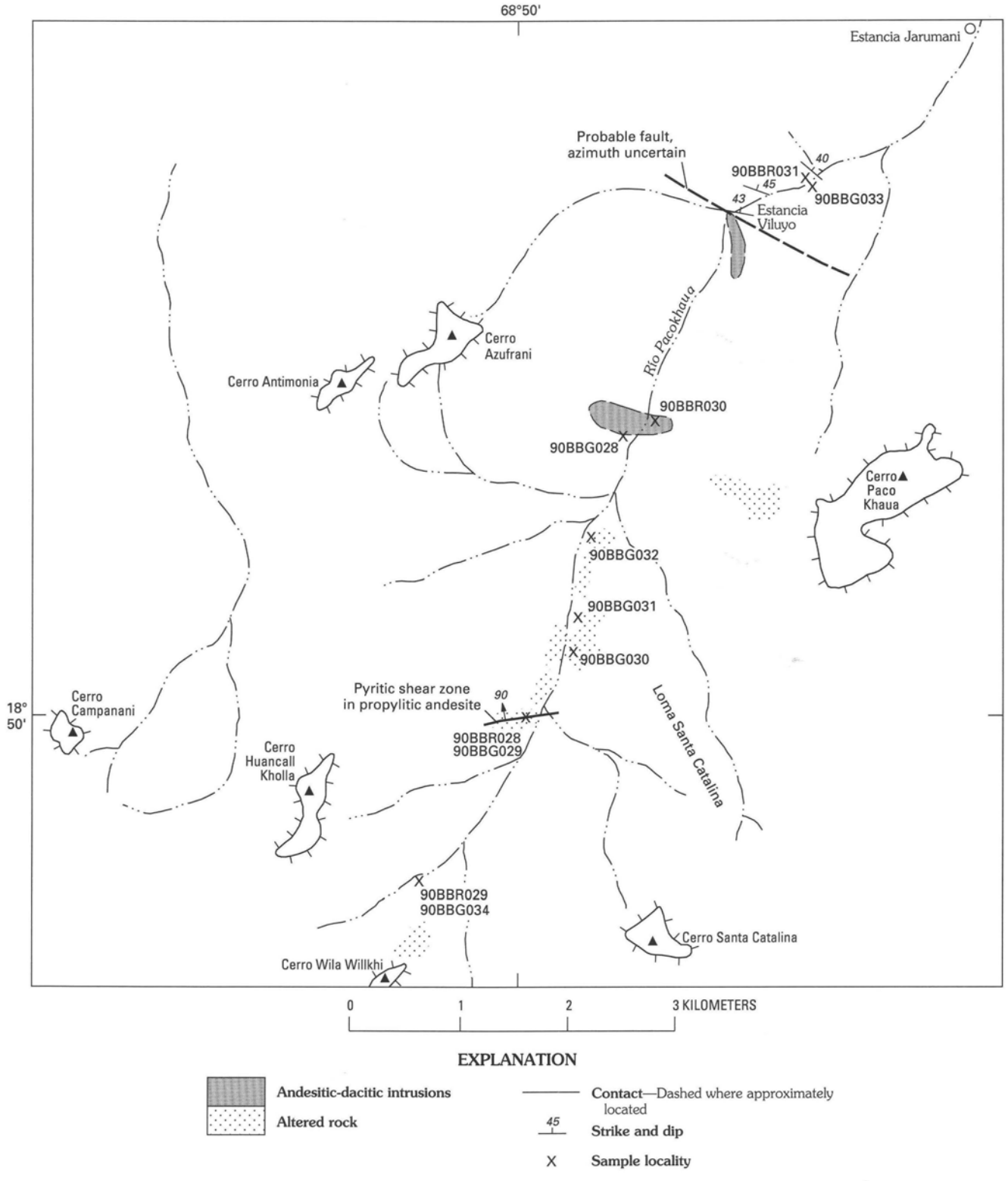


Figure 75. Sketch map of the Sonia-Susana area, Bolivia, showing selected geographic features, sample localities, and areas of altered rocks and intrusions. Outline of major peaks shown by hachured lines. Area is in the Julo (5837 IV) and Cerro Capitán (5837 III) 1:50,000-scale quadrangles.

Table 22. *Chemical analyses of mineralized and altered rocks, Sonia-Susana area, Bolivia*

[All results in parts per million (ppm). Sample descriptions, methods, and complete results in appendix B]

Sample no.	Au	Ag	Pb	Zn	Cu	Sn
90BBG029	0.024	3	50	2,000	200	15
90BBG030	.004	2	100	300	50	<10
90BBG031	.006	10	1,500	200	100	10
90BBG032a	.004	5	1,500	200	100	<10
90BBG032b	.038	5	50	<200	150	20
90BBG032c	.018	1	100	<200	150	<10
90BBG033a	<.002	<.045	5.1	5.6	.68	<10
90BBG033b	<.002	<.045	.6	.96	.82	<10
90BBG034	.004	.32	27	180	310	<10
90BBR029	<.002	<.05	10	<200	10	<10

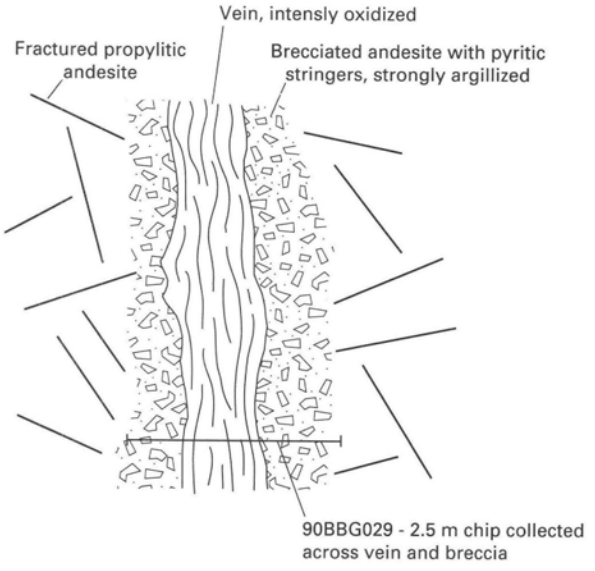


Figure 76. Sketch of pyritic shear zone at sample locality 90BBG029, Sonia-Susana area, Bolivia.

ppm gold and 310 ppm copper (table 22, sample 90BBG034). A large mine dump could be seen from this locality, and may correspond to one of the mine symbols shown on Ponce and Avila (1965a).

SAN CRISTOBAL DISTRICT

By Donald H. Richter, W. Earl Brooks, Steve Ludington, Alberto Hinojosa-Velasco, Angel Escobar-Diaz, Edwin H. McKee, *and* Nora Shew

Summary

The San Cristobal district (app. A, nos. 236–239) appears to be typical of polymetallic districts in the western and southern part of the study area; tin is largely absent and the gold content appears to be negligible. All known mineral deposits in the district occur in subvolcanic rocks whose textures and geologic relationships suggest intrusion at shallow depths.

Several exposed, but unexplored, areas of intrusive rocks occur in the district, and it is probable that others may be present beneath the extensive colluvial cover. The ore reserves at the Toldos mine, the only currently producing property in the district, are estimated to be 3 million tonnes containing about 120 g/t silver. Although it is unlikely that undiscovered vein deposits in this district are distinctly larger or richer than those known, there may be considerable potential for additional moderate-sized stockwork deposits similar to the Toldos deposit.

Introduction

The San Cristobal district is approximately 80 km southwest of Uyuni at the western edge of the great plain drained by Río Grande de Lípez in the San Pablo de Lípez 1:250,000-scale quadrangle. It includes 8 known polymetallic vein deposits that have been worked intermittently since the discovery of silver in the area early in the 17th century (table 23; fig. 77). At the present time only the Toldos deposit is being mined. The Toldos deposit was visited briefly in May and again in September 1990.

The district was studied in some detail by Jacobson and others (1969) in 1966. The present investigation is concerned chiefly with the Toldos deposit, where low-grade ore is being mined by Empresa Minera Yana Mallcu S.A. with a combination of open-pit and underground block-caving techniques; the silver is recovered by cyanide heap leaching. Brief descriptions of the other deposits are presented; more detailed descriptions are available in Jacobson and others (1969).

Geologic Setting

The deposits in the San Cristobal district are clustered near the center of a deeply eroded Tertiary eruptive-

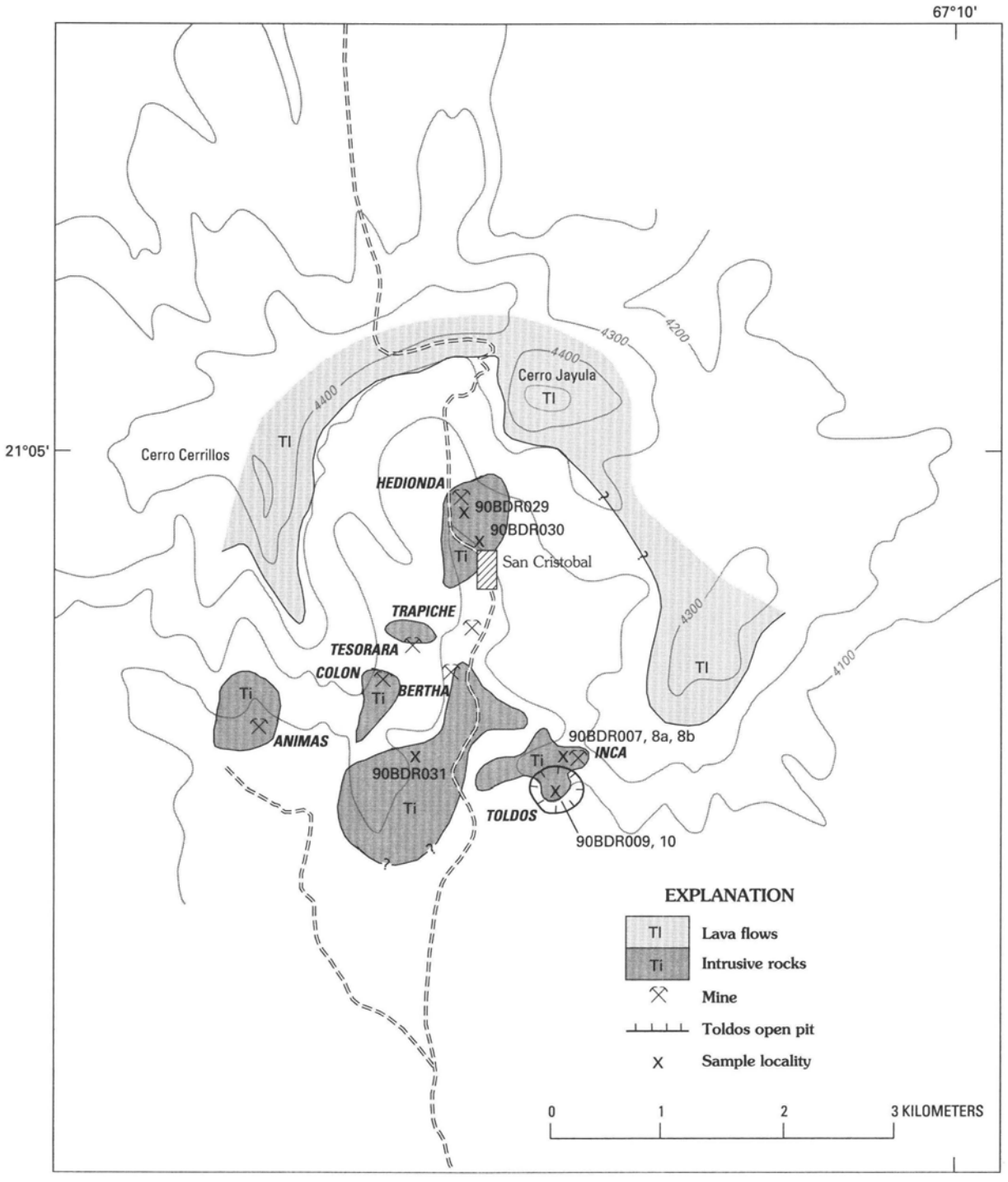


Figure 77. Generalized geologic map of the San Cristobal district, Bolivia, showing principal mines and sample localities. Contour interval, 100 m; base modified from the San Cristobal (6130 I) 1:50,000-scale quadrangle. Geology modified from Jacobsen and others (1969).

intrusive complex, approximately 20 km in diameter. Its high point is an arcuate ridge, 4,400 m above sea level, that is drained to the south by Quebrada Toldos.

The complex consists chiefly of a number of subvolcanic stocks (pl. 1, Ti) that intrude red sandstone, shale, and conglomerate of the lower Tertiary Potoco Formation (pl. 1, Ts1) and volcaniclastic rocks of the unconformably overlying Miocene Upper Quehua Formation (pl. 1, Tig). Post- and probably syn-intrusive dacitic tuffs and flows (pl. 1, Tvnd) overlie, or interlayer with, Upper Quehua rocks on the north flank of the complex. Sedimentary rocks of the Miocene to Oligocene Lower Quehua Formation do not

Table 23. *Principal mines and prospects in the San Cristobal district, Bolivia*

Mine or prospect	Status
Animas	Inactive; previously productive. Main tunnel about 80 m long.
Bertha	Inactive. Tunnel 195 m long.
Colon	Inactive. Small, accessible workings 25 m in length.
Hedionda	Inactive. Oldest mine in district. Three adits, extensive old underground workings.
Inca	Inactive. Contiguous to the Toldos mine.
Tesorera	Inactive.
Toldos	Active. Open-pit and block-caving mining operation. Extensive old underground workings.
Trapiche	Inactive. No veins exposed in 305 m of underground workings.

appear to be present in the area. There may be, however, some problems with this stratigraphic interpretation. For example, some unpublished mapping by GEOBOL does not show any Potoco Formation in the area, and all redbeds are considered to be part of the Lower Quehua Formation. It is evident that additional studies are needed to understand the stratigraphic relationships.

Two types of subvolcanic intrusive rocks are recognized in the district, andesite porphyry and dacite porphyry. The andesite porphyry, which contains about 62 percent SiO_2 (app. B, sample 90BDR031), forms the largest known intrusion in the area and consists of plagioclase and altered hornblende phenocrysts in a greenish-gray, generally propylitized, microcrystalline groundmass. The dacite porphyry contains 64–68 percent SiO_2 (app. B, samples 90BDR008a, 8b, 10, 30) and consists of plagioclase, hornblende, biotite, and occasional quartz phenocrysts in a micro- to cryptocrystalline groundmass. Both porphyries, even those that in the field appear unaltered, contain 8–10 percent K_2O and only 1–3 percent Na_2O, indicating strong potassic alteration of the groundmass. At the Toldos deposit, the dacite porphyry appears to intrude and form the core of a larger mass of andesite porphyry, but elsewhere the age relationships of the two intrusive units are not known. Additional analyses of intrusive rocks from the San Cristobal district are given by Arellano (1991). K–Ar dates on biotite from altered dacite porphyry (sample 90BDR010) in the Toldos open pit and from fresh dacite porphyry (sample 90BDR030) collected north of the village of San Cristobal yielded ages of 8.5±0.3 Ma and 8.0±0.1 Ma, respectively (app. C).

Ore minerals occur in veins, stockworks, and disseminations in hydrothermally altered intrusive rocks, associated intrusive breccias, and locally, their host sedimentary and volcaniclastic rocks. Intrusive dacite porphyry, however, is the principal host rock for the ore deposits. Hydrothermally altered rocks in the area are widespread and are prominent on satellite imagery (pl. 3, image F).

Description of Deposits

Toldos Deposit

The Toldos deposit was described by Jacobson and others (1969) as a series of northeast-trending near vertical veins that were being mined over lengths as much as 300 m on several levels. These veins, now largely mined out on accessible levels, were as thick as 1 m, but probably averaged less than 30 cm thick. They contained chiefly hematite, barite, siderite, and locally minor quartz and magnetite. The chief ore minerals were native silver and stromeyerite (Ahlfeld and Schneider-Scherbina, 1964) and, locally, small amounts of chalcopyrite, pyrite, arsenopyrite, pyrargyrite, and polybasite. This low-sulfide assemblage is similar to that observed in the contiguous Inca deposit, where Jacobson and others (1969) reported that the veins contained chiefly barite and hematite.

The deposit currently being mined consists of a stockwork of silver-bearing pyrite veins and veinlets that cut the argillized dacite porphyry between the mined out major veins (fig. 78). A mineralized pipe-like intrusive(?) breccia is also present near the center of the dacite porphyry. In addition to pyrite, the present operator has noted the presence of galena, sphalerite, and tetrahedrite in the stockwork veins, suggesting that sulfide minerals are more common than reported by Jacobsen and others (1969). Mine personnel indicated that grades range from about 50 g/t silver near the top of the orebody (now mined out) to more typical grades of 150 g/t silver at the levels being mined in April-October 1990. The results of an analysis of a 2 kg sample of crushed, run-of-mine ore collected in May 1990 are shown in table 24 (sample 90BDR009). The orebody is approximately 100 m wide by 200 m long by 50 m deep and contains about 3 million tonnes of ore reserves with an estimated average grade of about 120 g/t silver. An additional 4 million tonnes of probable ore (down to level 0) is indicated, according to mine staff personnel.

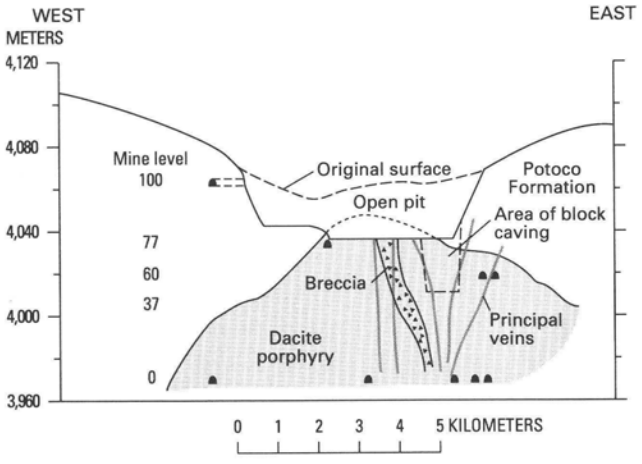


Figure 78. Diagrammatic cross section through the Toldos mine, Bolivia, showing some geologic relationships and old and new workings. Black symbols indicate tunnel entrances. Modified from cross section provided by Yana Mallcu S.A. (written commun., 1990).

Other Deposits

The Animas mine exploited a body of hydrothermally brecciated dacite about 300 m long, in which the matrix is sporadically replaced by argentiferous galena and sphalerite.

The Bertha mine is on a vein, 1–80 cm thick, consisting of pyrite, sphalerite, and galena. It strikes about N. 70° W. and dips 34°–64° north in volcaniclastic rocks of the Upper Quehua Formation.

The Colon mine exposes two irregular veins, consisting of massive barite and traces of galena, in altered Upper Quehua Formation. In 1966, about 25 m of mine working were accessible (Jacobsen and others, 1969).

The Hedionda mine exploited a number of small veins, 1–3 cm wide, and a body of disseminated pyrite, galena, sphalerite, and native silver of unknown dimensions that is localized along the contact of an altered intrusive dacite porphyry. A sample of sulfide-rich ore from the Hedionda (Dewitt adit) mine dump contained 2,600 ppm silver and more than 6 percent lead (table 24, sample 90BDR029).

The Inca mine, as known in 1966, exposed a series of barite-hematite veins striking northwesterly (Jacobsen and others, 1969). It was recognized as being near, and related to, the Toldos deposit and in 1990, parts of the Inca mine were exposed in the open pit of the Toldos mine. The metal contents of a 5-cm-wide vein sample (90BDR007) and two grab samples (90BDR008a, b) from the old Inca mine workings, collected during our visit in May 1990, are shown in table 24.

The Tesorera mine explored a mineralized fault zone as wide as 0.5 m that strikes N. 55° E. The fault zone contains pyrite and galena, and separates altered Upper Quehua agglomerate and intrusive dacite porphyry. The dacite porphyry contains disseminated pyrite.

The Trapiche mine explored an area beneath some earlier unnamed workings. No veins are cut by the 305 m of workings, although several unmineralized faults are exposed that may represent roots of veins above.

Table 24. *Chemical analyses of altered and mineralized rocks from the San Cristobal district, Bolivia*

[All results in parts per million (ppm). All samples contain <0.002 ppm Au, except 90BDR029, which contained 0.014 ppm. All samples contain <10 ppm Sn. Sample descriptions, methods, and complete results in appendix B]

Sample no.	Ag	Pb	Zn	Cu	Sb	As	Bi
			Inca mine				
90BDR007	24	14,000	550	57	47	260	16
90BDR008a	.25	87	340	.82	1	4.1	<6
90BDR008b	.68	310	500	1.8	2.4	6.7	<6
			Toldos mine				
90BDR009	48	4,900	770	85	49	130	0.81
90BDR010	14	790	1,300	21	13	6.5	<6
			Hedionda mine				
90BDR029	2,600	64,000	>17,000	410	1,100	1,100	<6
90BDR029a	30	3,100	7,400	26	6.1	480	9.3

COMUNIDAD TODOS SANTOS AREA

By Steve Ludington *and* Edward A. du Bray

Summary

The Comunidad Todos Santos area (app. A, nos. 367, 368) contains widespread silver-lead-zinc and antimony mineralization in veins and closely spaced veinlets, associated with a group of dacite intrusions into sedimentary rocks of the Potoco and Lower Quehua Formations. Geochemical results show that there is some gold associated with these deposits; because the area is poorly known, there is potential for the discovery of gold, silver, lead, and zinc resources.

Introduction

The Comunidad Todos Santos area contains two groups of mineral deposits, one group of veins that are apparently valuable only for antimony and possibly gold and one group that consists of silver-lead-zinc veins. The deposits are located to the south of Comunidad Todos Santos in the Sud Lípez region of the southern Altiplano. Comunidad Todos Santos is about 140 km from Uyuni and is reached by relatively good roads. Both groups of veins are presently being worked on a very small scale by local cooperatives. Neither large-scale mining nor regional exploration are active in the district, and we have been unable to find any information about the past mining history of the area. Likewise, we have found no references to previous studies in the area, other than a brief mention in Ahlfeld and Schneider-Scherbina (1964). The area was visited in October 1990. While in the area, we investigated the igneous rocks associated with the deposits and sampled easily accessible vein systems.

Geologic Setting

Comunidad Todos Santos is the most westerly of the mining camps in the Sud Lípez region. The deposits are related to a group of dacitic stocks (pl. 1, Ti) that intrude continental clastic rocks of the Lower Tertiary Potoco Formation (pl. 1, Ts1) and volcaniclastic sandstones of the Miocene Lower Quehua Formation (pl. 1, Ts2). The Potoco beds are strongly deformed in the vicinity of the stocks, apparently as a result of their forceful intrusion. The Potoco Formation is exposed in the area only where it has been folded upward on the margins of the intrusions (fig. 79).

The dacite that crops out on the west side of the area contains phenocrysts of plagioclase, biotite, and quartz in a microcrystalline groundmass (app. B, sample 90BSL067). It is one of the most silica-rich dacites in Sud Lípez, containing about 69 weight percent, on an anhydrous basis. A sample of fresh dacite on the east side of the area contains phenocrysts of hornblende, plagioclase, and quartz in a microcrystalline groundmass and is very low in silica, about 58 percent (app. B, sample 90BSL073). The mass of dacite directly south of Comunidad Todos Santos was not visited, but, as viewed from a distance, subhorizontal banding suggests that it may be made up of volcanic rocks (fig. 79).

Mineral Deposits

Two mineralized areas were studied during our visit. Southwest of Comunidad Todos Santos, along an unnamed quebrada, there is an east-west trending zone of stibnite veins almost 2 km long. Known as the Antonio sector, this zone of veins has been exploited sporadically along its length by shallow workings. These narrow, weakly developed siliceous veins contain minute amounts of stibnite and pyrite. Alteration related to this set of veins is minimal, and nowhere do the veins appear to be thicker than a few centimeters; however, the zone is easily recognized because the dark-red Potoco beds have been bleached white adjacent to the structure. Two samples were taken from these veins. They contain substantial amounts of silver, lead, and antimony and gold as high as 3.3 ppm (table 25, samples 90BSL066, 68). The presence of 660 ppm of molybdenum in sample 90BSL066 is notable, as molybdenum is not commonly enriched in Bolivian polymetallic vein deposits.

Southeast of Comunidad Todos Santos, a different mineralized system is exposed. The historic mine at Almacén was not visited, but alteration in that area appears to be well developed, and veins crop out over several square kilometers. Sample 90BSL070 (fig. 79) was collected from a mine dump near a small community. The mineralized rock appears to have been transported there for processing, so the source of the dump material is not known. The sample consists primarily of pyrite, galena, and sphalerite, and contains anomalous silver, lead, zinc, copper, and antimony (table 25).

In the vicinity of sample localities 90BSL071 and 90BSL072, there is a poorly exposed area of altered dacite that seems to be characterized by small sulfide veins and veinlets that form a stockwork in places. Iron-oxide stain is prevalent in this area, but we were unable to map the extent of alteration. Sample 90BSL071 is primarily composed of pyrite, with colloform bands of sphalerite and galena, as well as a sparse calcite gangue. The samples collected in this area yielded silver values as high as 390 ppm and substantial amounts of lead and zinc (table 25). The area just north of sample locality 90BSL073 is also altered and stained by iron oxides.

Table 25. *Chemical analyses of mineralized rocks from the Comunidad Todos Santos area, Bolivia*

[All results in parts per million (ppm). Sn is <10 ppm, and Bi is <0.6 ppm in all samples. Sample 90BSL066 contains 660 ppm Mo. Sample descriptions, methods, and complete results are in appendix B]

Sample no.	Au	Ag	Pb	Zn	Cu	As	Sb
90BSL066	0.05	13	1,100	850	48	2,500	840
90BSL068	3.3	32	1,100	<30	180	<6	86,000
90BSL070	.01	39	49,000	8,800	440	14	380
90BSL071	<.002	390	100,000	300	250	<6	110
90BSL072	.004	59	920	>1,600	82	130	43

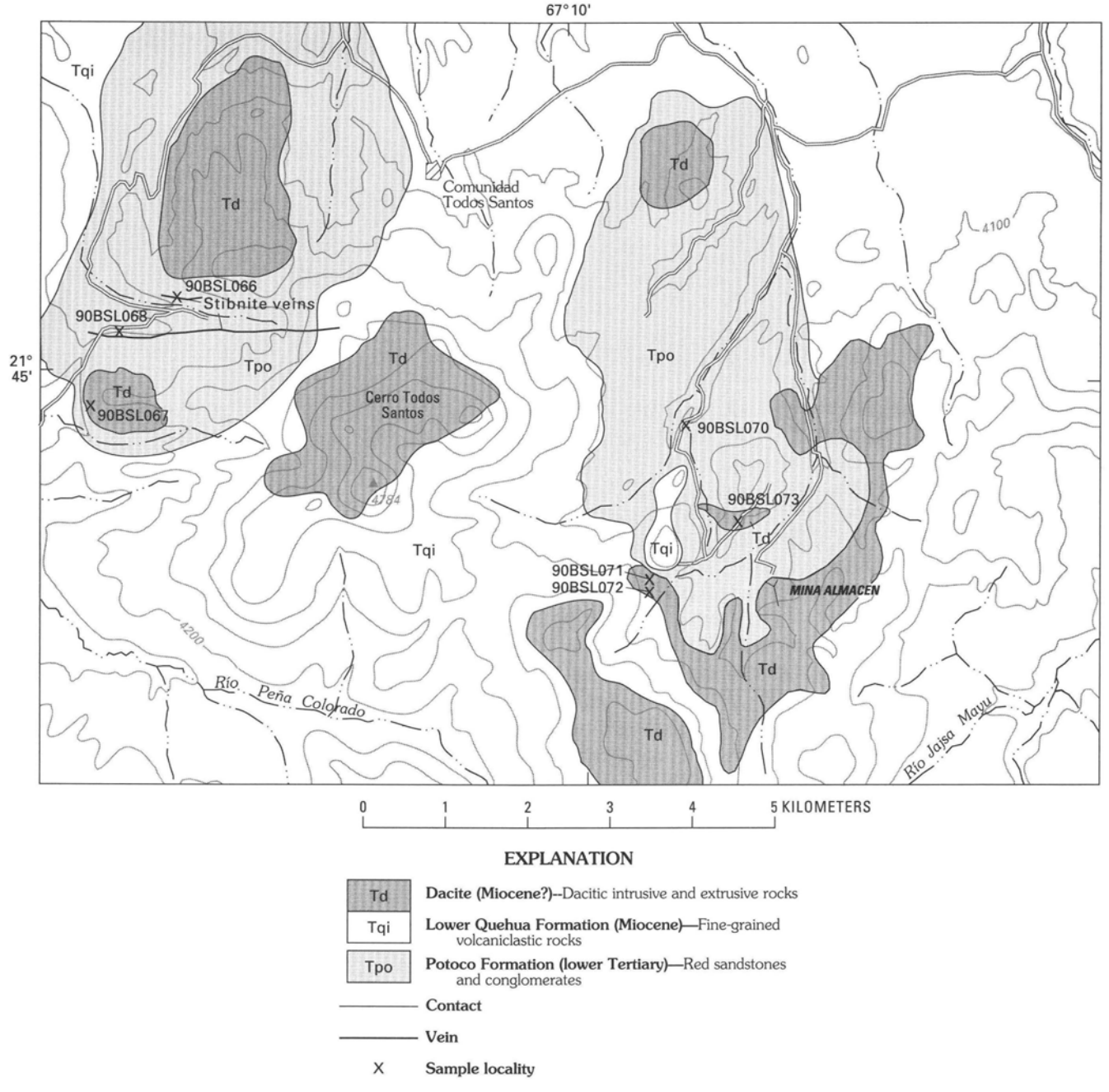


Figure 79. Map showing geology and sample localities in the Comunidad Todos Santos area, Bolivia. Geology modified from unpublished mapping by the Servicio Geológico de Bolivia. Contour interval, 100 m; base modified from the Comunidad Todos Santos (6128-I) 1:50,000-scale quadrangle.

Conclusions and Recommendations

The Comunidad Todos Santos area exhibits widespread mineralization and alteration, especially in the eastern part of the area, west and southwest of Mina Almacén. Although gold values are low in samples from the area, the widespread anomalous silver values (as much as 390 ppm) suggest that systematic sampling of the area might lead to the discovery of bulk-mineable silver-lead-zinc ore. The relatively high gold content (3.3 ppm) of one of the samples from stibnite veins suggests that further sampling of that area is also warranted.

ESCALA DISTRICT

By Donald H. Richter, W. Earl Brooks, Dennis P. Cox, Nora Shew, Elizabeth A. Bailey, Alberto Hinojosa-Velasco, *and* Angel Escobar-Diaz

Summary

The Escala deposit (app. A, no. 384) is a polymetallic vein deposit in a subvolcanic rhyolite porphyry of Miocene age. It contains only small amounts of tin and gold, similar to many other polymetallic deposits in the southern Altiplano. The rhyolite porphyry host rock is of limited extent and is generally well exposed; altered fracture-shear zones containing ore-bearing veins are apparently limited to the area of known mineralization. Ore reserves at the Escala mine are small and the district as a whole does not appear to be favorable for the discovery of additional near-surface deposits. However, there may be some potential for new discoveries at depth on structures that do not reach the surface.

The deposit at the Rosario mine is a volcanic-hosted copper deposit of very small size and potential. Although additional copper deposits associated with the basaltic andesite of Cerro Achacana may be present, they probably would be similar in size and grade to the Rosario deposit.

Introduction

The Escala district is approximately 125 km south of Uyuni in the San Pablo de Lípez 1:250,000-scale quadrangle between Río San Pablo and Río Escala (fig. 80).

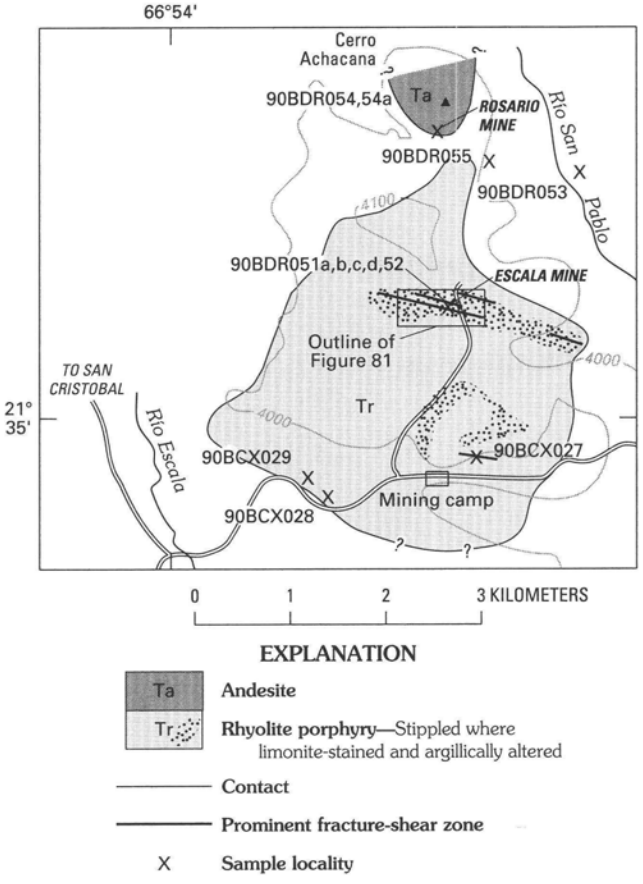


Figure 80. Sketch map of the Escala district, Bolivia, showing some geologic features and sample localities. Geology modified from unpublished mapping by the Servicio Geológico de Bolivia. Contour interval, 100 m; base modified from Mina Escala (6229 III) 1:50,000-scale quadrangle.

The area contains two very different deposits, the Escala mine, a polymetallic vein deposit that is currently in production, and the Rosario mine, a small, inactive, volcanic-hosted copper deposit. The district was examined in October 1990.

Geologic Setting

The region is underlain by poorly consolidated sedimentary and volcaniclastic rocks of the Oligocene and Miocene Lower and Upper Quehua Formations (pl. 1, Ts2, Tig, respectively). Biotite from a monolithologic, dacitic, volcanic debris flow in the upper part of the Upper Quehua Formation yielded a K–Ar age of 18.2±0.3 Ma (app. C, sample 90BDR053). The sedimentary and volcaniclastic rocks are intruded by a subvolcanic rhyolite porphyry and either intruded by, or interlayered with, a basaltic andesite intrusion or massive lava flow.

Fresh rhyolite porphyry, sampled about 2 km north of the Escala mine, contains abundant phenocrysts of rounded quartz, plagioclase, sanidine, and fresh biotite in a dense pinkish-gray microcrystalline feldspathic groundmass; SiO_2 content is about 76 percent, on an anhydrous basis (app. B, sample 90BDR055). Biotite from this sample yielded a K–Ar age of 18.0±0.2 Ma (app. C). Most of the rhyolite porphyry in the area, however, is pervasively propylitized and locally argillized, sericitized, and iron oxide stained. The conspicuous, bleached, white, altered areas, locally associated with silicification, are generally confined to zones of pronounced fracturing, shearing, and local brecciation. These zones occur where there are many small, limonite-filled veins and fractures.

The basaltic andesite at the Rosario deposit is a dark-gray, dense rock containing abundant, small phenocrysts of plagioclase and large, fresh clinopyroxene phenocrysts in a dark intergranular groundmass, consisting largely of plagioclase and opaque minerals; it contains about 52.2 percent SiO_2 (app. B, sample 90BDR054). Veinlets and microfractures in the rock are filled with limonite and other opaque minerals. Neither the age nor the contact relationship with the rhyolite porphyry intrusive is known. The basaltic andesite appears to have either intruded or flowed upon Lower Quehua strata inasmuch as a basaltic andesite debris apron occurs in the Upper Quehua section proximal to the basaltic andesite outcrop. The basaltic andesite is locally brecciated but otherwise shows no evidence of the intense alteration exhibited by the rhyolite porphyry.

Mineral Deposits

Escala Mine

The Escala mine, called the Crosca mine by Alfaro (1989), was first mined in Spanish colonial times. It is now controlled by COMIBOL and is currently being operated by a small mining cooperative. The area was studied in 1970 by the Servicio Geológico de Bolivia (1971s) and more recently by Sugaki and others (1986).

The mine consists of a number of pits, trenches, and underground workings scattered over more than 2 km^2 of altered rhyolite porphyry. The principal mineralization and present mining activity is restricted to 2 major fracture and (or) shear zones that are accessible by a single extensive series of underground workings, referred to locally as Socavón C (fig. 81). Some of the mine tailings from Spanish colonial times are being reprocessed.

Ore minerals occur in veins in the argillized, sericitized, and silicified fracture and shear zones in the rhyolite porphyry. The two major zones, which trend N. 50°–55° W. and dip 75°–85° northeast, range from less than 1 m to more than 4 m thick and are as long as 500 m. The mineralized

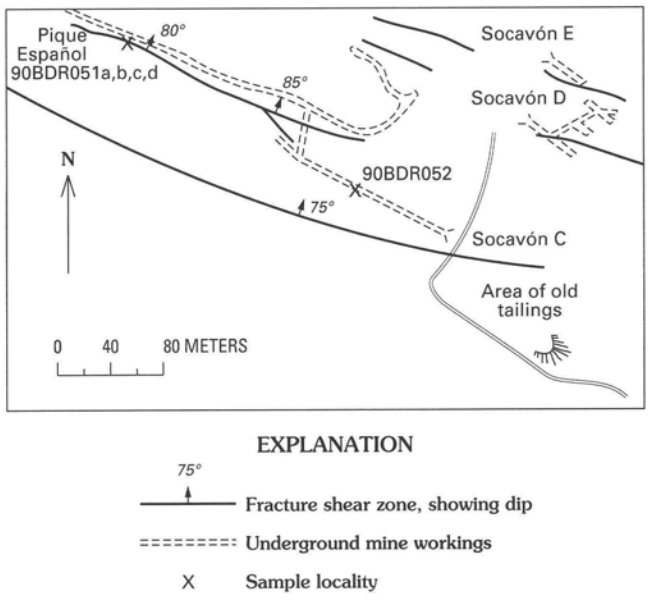


Figure 81. Sketch map of the principal workings at the Escala mine, Bolivia, showing sample localities. Modified from Servicio Geológico de Bolivia (1971s).

veins are discontinuous and generally are subparallel to the trend of the fracture and shear zones. Veins may be as thick as 30 cm and tend to occur in argillized and (or) seriticized rhyolite porphyry rather than in areas of strong silicification. The ore minerals are galena, sphalerite, pyrite, marcasite, arsenopyrite, and minor chalcopyrite, pyrrhotite, tetrahedrite, jamesonite, and semseyite (Sugaki and others, 1986); gangue is sparse and generally consists of limonite, quartz, and siderite. Alfaro (1989) mentions that in the oxidized zone, goethite and jarosite occur in multidirectional veins in association with galena boxworks. Disseminated pyrite also occurs locally throughout the zones of argillic alteration. A sample of sulfide-rich ore collected underground from an 8 cm thick vein in the southernmost fracture-shear zone (fig. 81), contained 950 ppm silver and 36 percent lead (table 26, sample 90BDR052), and a high-grade sample of ore from Pique Español in the northern fracture-shear zone contained 410 ppm silver and 14 percent lead (table 26, sample 90BDR051c). Argillized porphyry (sample 90BDR051a) and silicified vein material (sample 90BDR051b), also collected from near Pique Español in the northern fracture-shear zone, contained 8.7 and 1.4 ppm silver, respectively (table 26). According to the present manager of the cooperative, the hand-sorted ore has an average grade of approximately 15 percent lead, 30 percent zinc, and 200 g/t silver. Ore reserves are probably a few thousand tonnes.

A smaller vein set occurs 0.5 km east of the mining camp in an irregularly shaped area of limonite staining and argillization (fig. 80). The veins, which trend approximately westnorthwest, are 5–20 cm thick. A sample of sulfide-rich

Table 26. *Chemical analyses of altered and mineralized rocks from the Escala area, Bolivia*

[All results in parts per million (ppm). Sample 90BDR054a contains 87 ppm Bi. Sample 90BCX029 contains 150 ppm B. Sample descriptions, methods, and complete results are in appendix B. Sample 90BDR051a, argillized fracture shear zone; sample 90BDR051b, silicified fracture-shear zone; sample 90BDR051c, sulfide-rich vein; sample 90BDR052, sulfide-rich vein; sample 90BDR054a, chrysocolla vein; sample 90BCX027, 5 cm-thick, sulfide-bearing vein; sample 90BCX028, sericite alteration; sample 90BCX029, copper-stained sericite alteration]

Sample no.	Au	Ag	Pb	Zn	Cu	As	Sb	Sn
				Escala mine				
90BDR051a	0.014	8.7	400	64	<0.3	20	<6	15
90BDR051b	.002	1.4	140	39	<.3	66	6.7	<10
90BDR051c	.016	410	140,000	>17,000	1,900	60	370	30
90BDR052	.046	950	360,000	35,000	2,500	500	2,800	50
90BCX027	.04	1,200	70,000	110	1,100	<38	1,800	100
90BCX028	<.002	.14	120	51	7.5	21	1.4	<10
90BCX029	<.002	38	370	18	97,000	<110	<100	<10
				Rosario mine				
90BDR054a	<0.002	92	2,600	940	78,000	<10	120	<10

material from one of the smaller veins contained 1,200 ppm silver and 100 ppm tin, in addition to high grades of lead and zinc (table 26, sample 90BCX027). Also of interest is a band of intense sericitic alteration at least 200 m wide that trends east-west across the southwest side of the rhyolite porphyry. This alteration was sampled in a roadcut and found to contain as much as 38 ppm silver and 370 ppm lead (table 26, sample 90BCX028). Parts of this band of alteration also show prominent copper-oxide staining and a sample of this material contained more than 9 percent copper (table 26, sample 90BCX029).

Rosario Mine

The Rosario mine, located approximately 2 km north of the Escala mine, is a small copper deposit in a basaltic andesite dome, intrusive, or flow of Cerro Achacana (fig. 80). The deposit is controlled by COMIBOL, but is inactive and from all appearances probably has not been worked for many years. The workings consist of a single, wide shaft or large pit, about 8 m deep; its floor is inclined 40° north.

Ore minerals, consisting chiefly of layered and massive chrysocolla and locally crystalline malachite, occur as very irregular fillings between blocks and smaller fragments of broken and locally brecciated basaltic andesite. The copper minerals are generally associated with masses of colorful red to gray jasper and agate. A random sample of copper minerals from the tailings pile near the shaft contained almost 8 percent copper, 92 ppm silver, and small amounts of lead, zinc, and bismuth (table 26, sample 90BDR054a). The deposit at the Rosario mine may have more potential value as a source of ornamental stone than as a copper resource. The type and form of the mineralization at the Rosario mine appears similar to that observed at the Eskapa mine.

Other Deposits

During our visit to the district, a local miner was observed panning gravel in Río San Pablo near the Rosario mine (fig. 80). He showed us a cup of black sand containing more than 20 flakes of gold, including a small nugget about 2 mm in diameter. The source of the gold-bearing gravel is not known.

SANTA ISABEL DISTRICT

By Donald H. Richter, W. Earl Brooks, Angel Escobar-Diaz, *and* Alberto Hinojosa-Velasco

Summary

Three highly altered dacitic subvolcanic intrusions in the Santa Isabel district (app. A, nos. 398, 400) host a number of polymetallic vein deposits that have been developed by two mines. The largest mine, the Candelaria, has been worked intermittently since Spanish colonial times and is currently under development to mine sulfide ore.

The apparent presence of substantial amounts of tin and gold in the same mineralized system is somewhat remarkable and noteworthy. Moreover, the presence of gold in conjunction with large volumes of untested, pervasively altered rock make the Santa Isabel district an attractive exploration target.

Introduction

The Santa Isabel district, located approximately 135 km southsoutheast of Uyuni in the San Pablo de Lípez

1:250,000-scale quadrangle, includes a number of polymetallic vein deposits that have been developed by two mines, the Candelaria and Mercedes mines (fig. 82). The Candelaria mine and a small gold and tin placer deposit are currently active. The mine area was examined in October 1990.

Geologic Setting

The oldest rocks in the Santa Isabel district are a series of red pebble conglomerates, sandstones, and shales that resemble strata of the early Tertiary Potoco Formation, but which Medina and Ibáñez (1988b) placed in the lower Miocene to Oligocene San Vicente Formation (pl. 1, Ts2). These beds exhibit a regional dip of 15° to the southwest and are overlain unconformably by volcaniclastic rocks of the Miocene Upper Quehua Formation (pl. 1, Tig). Along the southern border of the district a sequence of dark basaltic or basaltic andesite lavas, called Rondal Lavas (pl. 1, Tvnd) by Medina and Ibáñez (1988b), unconformably overlie the redbeds. Rondal Lava elsewhere on the Altiplano has been dated at 23.5 Ma (Kussmaul and others, 1975). The entire layered sequence is intruded by at least 3 shallow dacitic stocks (pl. 1, Ti) that, together with much of the surrounding host rock, are pervasively altered. Although supergene processes have converted disseminated sulfides to secondary limonite and have obscured the nature of much of the primary alteration, argillic, propylitic, and sericitic assemblages have been recognized (Medina and Ibáñez, 1988b).

The least altered dacite porphyry observed during our visit was at the south end of the Cerro Santa Isabel intrusion (fig. 82). It contains phenocrysts of rounded and embayed, locally inclusion rich, quartz, saussuritized feldspar, and abundant fresh to highly altered biotite in a cryptocrystalline groundmass that locally is flooded by fine-grained quartz; SiO_2 content is 67.6 percent (app. B, sample 90BDR061c). The K_2O content of the dacite is 10.8 percent suggesting that, as in the case of the dacite porphyry in the San Cristobal district, this probably represents intense potash replacement of the groundmass rather than high primary K_2O concentrations.

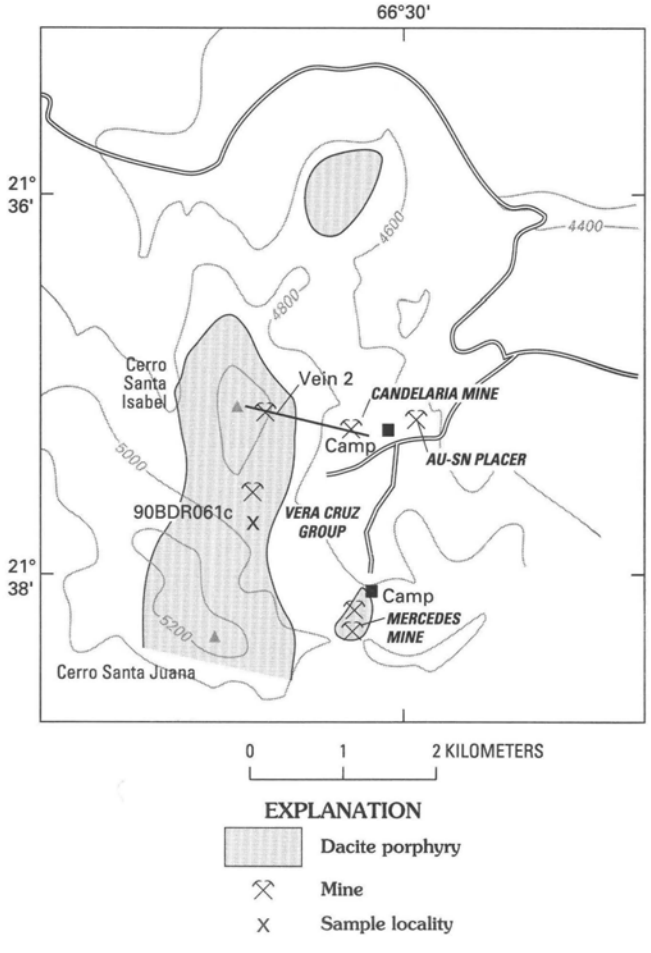


Figure 82. Sketch map of the Santa Isabel district, Bolivia, showing known intrusive rocks and localities of mines and placer deposits. Geology modified from unpublished mapping by the Servicio Geológico de Bolivia. Contour interval, 200 m; base modified from Cerro Santa Isabel (6229 II) and Cerro Yana Orkho (6329 III) 1:50,000-scale quadrangles.

Mineral Deposits

Candelaria Mine

The Candelaria mine, sometimes referred to as the Santa Isabel mine, includes most of the east flank of Cerro Santa Isabel (fig. 82). The deposit was discovered and mined in Spanish colonial times; much of the extensive underground development is the result of mining done during the late 1800's and until 1908 by the Nueva Compañía de Lípez. The present owner, W. Huarachi, acquired the property in 1961 and is preparing the mine for the production of silver, gold, tin, and base metals.

The mine includes extensive underground workings that follow individual vein-filled fracture zones in the highly altered and locally brecciated dacite porphyry of Cerro Santa Isabel (fig. 83). The major veins or vein groups from north to south, are the Silver Mine vein, Vein 2, Escalera vein, the Consuelito vein group, and the Vera Cruz vein group. Vein 2, largest and most productive of the veins to date, has been developed on at least 5 levels, or more than 300 m vertically, and it probably extends to the surface for an additional 200 or more meters. Vein 2 has been explored horizontally for 465 m and is inferred to be at least 800 m long (Segurola and others, 1987). Vein 2 and the Consuelito vein group strike between east-west and N. 65° W. and dip 70°–85° southwest. The Escalera vein strikes N. 50°–70° W. and dips 80°–85° southwest, whereas the Vera Cruz veins strike N. 80° E. and dip 80° southeast. The veins range

in thickness from 15 to 180 cm; Vein 2 is the thickest and most consistent. In addition to the principal veins, there are many smaller veins present and, locally, some mineralized structures may be concentrated enough to be exploited by bulk-mining techniques.

The primary ore minerals include sphalerite, galena, arsenopyrite, chalcopyrite, cassiterite, stannite, tetrahedrite-tennantite, pyrargyrite, fizelyite (a lead-silver-antimony sulfide), native gold, and petzite (Sugaki and others, 1986). In the oxidized zone (above about 4,700 m), anglesite, cerussite, oxides of zinc, cassiterite, silver minerals, and native gold are present. Pyrite, quartz, and calcite are the principal gangue minerals in the sulfide zone and limonite, jarosite, hematite, alunite, opal, quartz, and kaolinite in the oxide zone. The highest apparent concentration of tin minerals is on the Candelaria level of Vein 2. High gold values of 18 g/t across 1.5 m, as well as silver values as high as 1,800 g/t have recently been found in the Consuelito vein group (W. Huarachi, oral commun., 1990). During our visit we sampled a 6-cm-thick, sulfide-rich part of the Escalera vein (sample 90BDR061), a 10-cm-thick part of the Consuelito 1 vein (sample 90BDR061a), and the 1.5-m-thick, gold-rich Consuela vein (sample 90BDR061b). Partial results of analyses of these samples are shown in table 27; complete analyses are available in appendix B. Silver values as high as 1,200 ppm and tin as high as 300 ppm were found, but the high gold values reported for the Consuela vein could not be confirmed by our sampling. The maximum we obtained was 0.55 ppm (sample 90BDR061).

Studies by the Fondo Nacional de Exploración Minera (Segurola and others, 1987) report a measured ore reserve of 141,000 tonnes and an inferred reserve of more than 550,000 tonnes for Vein 2, the Escalera vein, and the Consuelito vein group. Grades in Vein 2 range from 400 g/t silver, 2.1 percent lead, 1.0 percent tin, and 3.5 g/t gold in the oxidized zone (121,000 known and inferred tonnes) to 155 g/t silver, 4.4 percent zinc, 1.8 percent lead, 0.655 percent tin, and 0.13 g/t gold in the sulfide zone (67,000 measured and inferred tonnes). In the Consuelito vein group, the grade of 105,000 tonnes of known and inferred ore is 494 g/t silver, 4.6 percent zinc, 6.7 percent lead, and 0.3 percent tin. Additional data on production during the early 1960's and some grade figures and ore reserves as of 1964 are available from Caro (1964a).

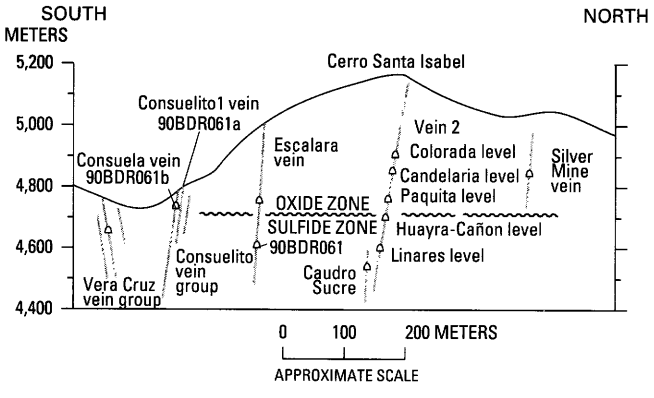


Figure 83. Diagrammatic cross section through the Candelaria mine area, Bolivia, showing principal veins, mine levels, and sample localities. Open triangles indicate tunnel entrances.

In addition to the vein deposits, Sugaki and others (1986) mention an area of fracture filling and veins in a brecciated zone of intense argillic alteration just south of Cerro Santa Isabel. The location may correspond to the area around the Vera Cruz vein group, south of Cerro Santa Isabel (fig. 82). Pyrite, chalcopyrite, and chalcocite are described as occuring in veins and fractures and as disseminations in the host rock. We were unable to confirm the presence of these stockworks during our investigation.

Mercedes Mine

The Mercedes mine is 2 km south of the Candelaria mine on the eastern slopes of Cerro Santa Juana and, like the Candelaria mine, was first worked in Spanish colonial times. Later it was reactivated and worked until 1908 by the Nueva Compañía de Lípez; in 1961, W. Huarachi acquired the property. The mine was not visited during this investigation; information presented here is from Medina and Ibáñez (1988b) and the Servicio Geológico de Bolivia (1971ff).

The workings at the Mercedes mine explore a limited exposure (about 2 km^2) of altered dacite porphyry and its contact zone with mafic flows of Rondal Lava. The workings consist principally of 3 crosscuts (recortes) and 2 inclined shafts (piques) in the southern part of the dacite intrusive and numerous pits and trenches in the northern (Goya) part (fig. 84).

The dacite porphyry host rock is pervasively altered. Bands of argillic alteration are intercalated with propylitized rock, and the degree of argillization appears to be a function of fracture density. Also, the biotite and feldspar phenocrysts in the dacite tend to be sericitized where fracture density is high. Principal fracture orientation is N. 40°–80° E.; a secondary set trends N. 20°–60° W. Most of the veins tend to occupy fractures of the principal set, however, near the contact between dacite and Rondal Lavas, the veins trend N. 60°–80° W.

At Pique Español I (fig. 84), an inclined shaft follows a 30-cm-thick vein that trends N. 40° E. and dips southwest. It chiefly contains quartz, pyrite, and galena. Twenty meters from the collar of the shaft, the vein is cut by a subparallel, northwest-trending system of veinlets with an aggregate thickness of about 60 cm. These veins contain sphalerite in addition to quartz, pyrite, and galena. On the surface they crop out as limonite and (or) jarosite stringers in the mafic Rondal Lavas. Silver values range from 150 to 348 g/t in the veins. In both the Recorte I and Pique Español II workings, the veins are oxidized and consist largely of limonite; they

Table 27. *Chemical analyses of altered and mineralized rocks from the Candelaria mine area, Santa Isabel district, Bolivia*

[All results in parts per million (ppm). Sample descriptions, methods, and complete results in appendix B. Sample 90BDR061, sulfide-bearing Escalera vein; sample 90BDR061a, sulfide-rich Consuelito vein; sample 90BDR061b, 1.5-m-long sample across Consuela vein]

Sample no.	Au	Ag	Pb	Zn	Cu	As	Sb	Sn	Bi
90BDR061	0.55	30	950	>17,000	550	5,200	46	300	110
90BDR061a	.028	1,200	150,000	>17,000	390	8,400	1,500	300	<6
90BDR061b	.038	29	4700	>17,000	120	1,500	60	100	58

range from 2 to 15 cm in thickness and trend generally N. 60°–80° W. Silver values as high as 520 g/t have been reported. Numerous limonite-quartz veins (stockwork?) occur in the northern (Goya) exposed part of the dacite porphyry, but values reported from this area are less than 80 g/t silver and 2.0 percent lead. No gold analyses are available.

Gold-Tin Placer Deposit

A small placer deposit is currently being mined in the principal drainage through the Candelaria mine area (fig. 82). Both tin and gold are reportedly being recovered from the operation, but no details are available.

BUENA VISTA AREA

By Steve Ludington, Gerald K. Czamanske, Raul Carrasco, Alberto Hinojosa-Velasco, *and* Edwin H. McKee

Summary

The Buena Vista area (app. A, nos. 392–394) contains several polymetallic lead-zinc-silver-antimony veins that occur in pyroclastic rocks of the Miocene Upper Quehua Formation. Unlike most Bolivian polymetallic deposits, these veins are not locally associated with dacitic intrusions. The veins contain significant amounts of gold; their subsurface limits are unknown.

Introduction

The Buena Vista area consists of one major and several minor lead-zinc-silver veins that apparently were discovered and first worked in Spanish colonial times. The veins are hosted in dacitic ash-flow tuffs, agglomerates, and lava flows of the Miocene Upper Quehua Formation. The principal mine, the Buena Vista, is located about 5 km south of the village of San Pablo de Lípez, capital of the province of Sud Lípez, and about 210 km from Uyuni (fig. 85). The area is located in the San Pablo de Lípez (6228 I) 1:50,000-scale quadrangle, at altitudes ranging from about 4,400 m to 4,800 m. The access road from San Pablo de Lípez is in excellent condition as far as the Buena Vista mine; we did not visit the two upper mines, Leoplán and Pulacayito. In 1990, the Buena Vista mine was being operated on a small scale by a local mining cooperative. Buena Vista and Pulacayito are COMIBOL properties. Leoplán is owned by San José de Berque, and was producing silver and antimony concentrates on a small scale in 1970, but the present state of activity is unknown. Previous studies of the area include those of Jiménez (1971), Sugaki and others (1986), and Ibáñez and Medina (1988). The area was visited in May 1990.

Geologic Setting

The deposits in the Buena Vista area are hosted entirely in the Miocene Upper Quehua Formation (pl. 1, Tig). At the Buena Vista mine, the rocks consist almost entirely of several layered outflow sheets of ash-flow tuff on the northern flank of the Morokho volcanic center, from which they were probably derived. Jiménez (1971) reports that, higher in the stratigraphic section, breccias, agglomerates, and lava flows of the same dacitic composition occur. No intrusive rocks are in evidence in the immediate vicinity.

Mineral Deposits

Ore deposits in the area occur as parallel polymetallic veins that are sulfide-rich and lack significant quartz or other nonsulfide gangue. Jiménez (1971) states that the principal ore minerals are stibnite, galena, and sphalerite, with lesser amounts of chalcopyrite, argentite, and pyrargarite. In some areas of the vein, stibnite reportedly forms almost 100 percent of the vein filling. Siderite, quartz, realgar, and orpiment were noted as gangue minerals. Sugaki and others (1986) report chalcopyrite, arsenopyrite, electrum, argentite, jalpaite (Ag_3CuS_2), famatinite

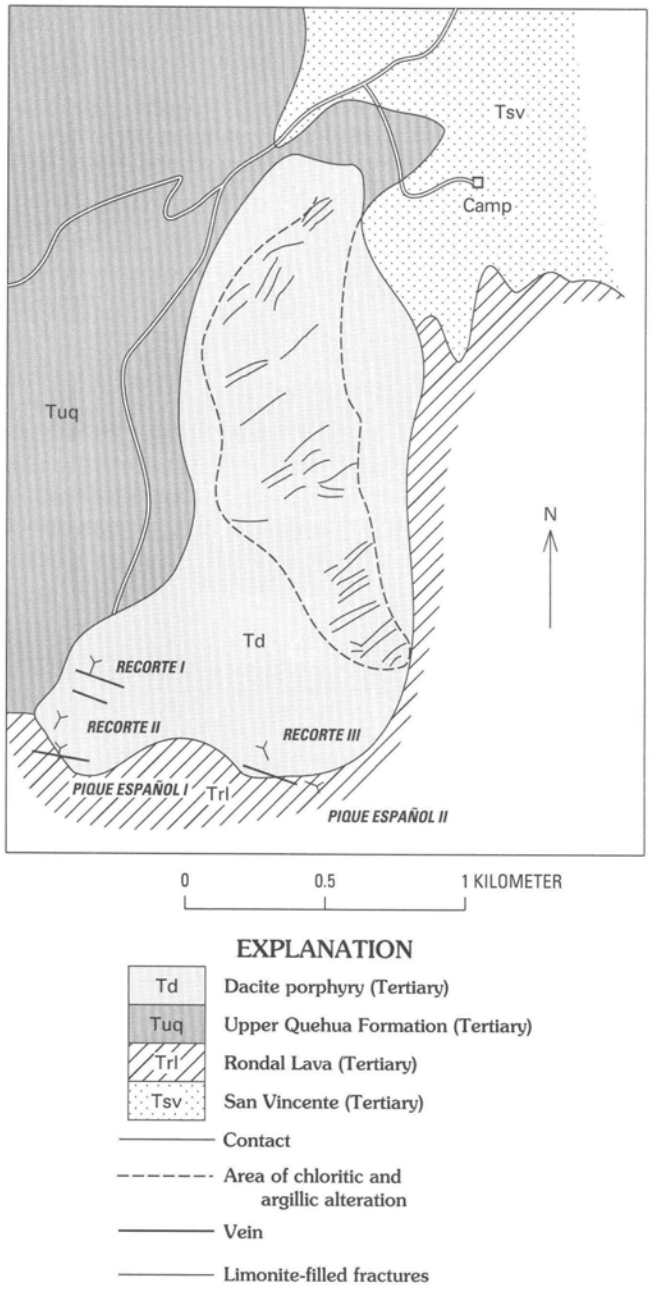


Figure 84. Geologic map of the Mercedes mine area, Bolivia. Modified from Medina and Ibáñez (1988b). Area is in the Cerro Santa Isabel (6229 II) and Cerro Yana Orkho (6329 III) 1:50,000-scale quadrangles.

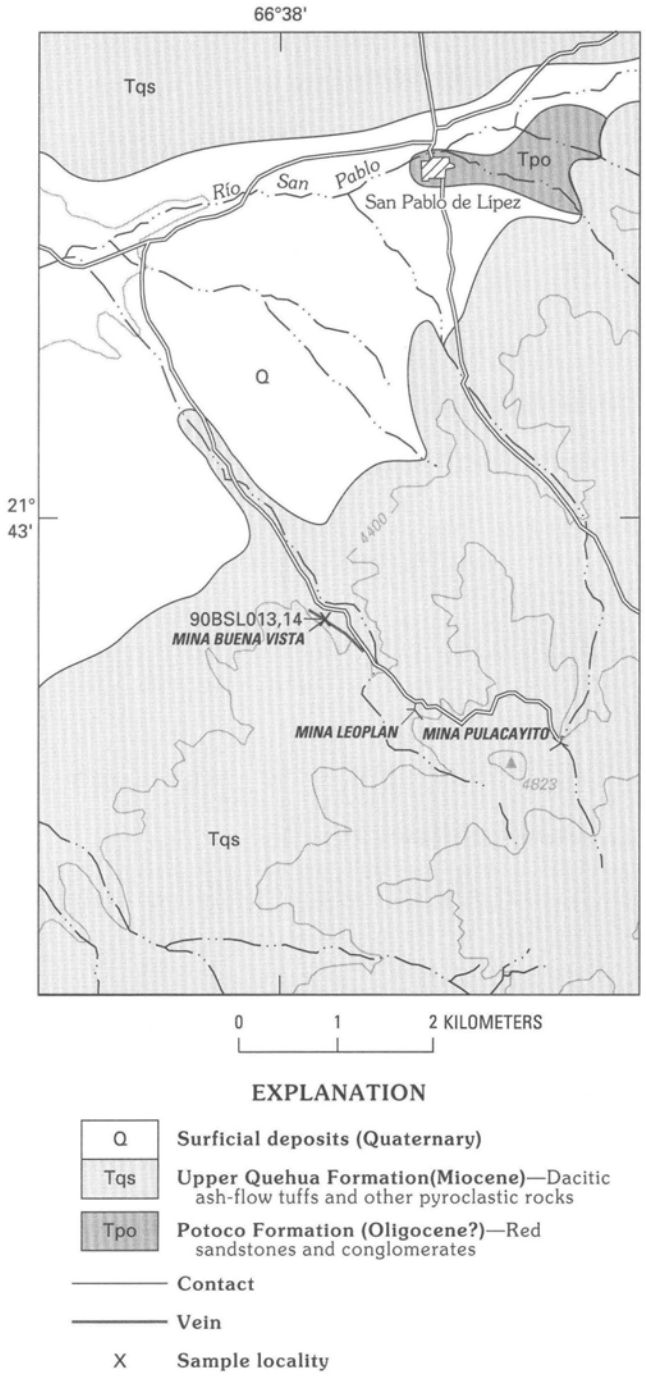


Figure 85. Map showing geology and sample localities in the Buena Vista area, Bolivia. Geology modified from Ibañez and Medina (1988b). Contour interval, 200 m; base modified from the San Pablo de Lípez (6228-I) 1:50,000-scale quadrangle.

(Cu_3SbS_4), tennantite, tetrahedrite, bournonite ($PbCuSbS_3$), boulangerite ($Pb_5Sb_4S_{11}$), fizelyite ($Pb_5Ag_2Sb_8S_{18}$), and semseyite ($Pb_9Sb_8S_{21}$) in addition to galena, sphalerite, and pyrite.

Sulfide minerals identified in a sample (90BSL013) of material taken from Buena Vista mine dumps include pyrite, sphalerite, galena, a Pb-Sb sulfide (boulangerite?), and tetrahedrite-freibergite. Textures of the tetrahedrite suggest that it formed late, and, in part, by reaction among the original minerals in the vein. The galena contains no discernible exsolution phases; the sphalerite contains less than 1 percent iron.

The veins at Buena Vista, of which Jiménez (1971) recognized at least ten, all trend approximately N. 75° W.

and dip steeply to the north; they range in thickness from 1 cm to about 1 m. The lateral extent of the larger veins is at least 500 m.

Various workings exploited these veins and details can be found in Jiménez (1971). Ahlfeld and Schneider-Scherbina (1964) report that the workings were known to extend to depths of 300 m.

The one high-grade sample (90BSL013) of vein material collected contains 9 ppm gold, 700 ppm silver, 3,000 ppm copper, 500 ppm cadmium, and several percent lead and zinc, as well as 1,000 ppm arsenic and approximately 1 percent antimony. Tin, bismuth, and tungsten were not detected. Complete analytical results are in appendix B. A sample of the altered ash-flow tuff that forms the walls of the vein (90BSL014) contained 700 ppm zinc, 150 ppm lead, 100 ppm antimony, and 15 ppm silver, indicating that there is some disseminated mineralization. Interestingly, the wallrock sample also contained 150 ppm boron, suggesting that tourmaline may be part of the alteration assemblage, at least locally.

Jiménez (1971) reports the results of extensive sampling of the veins. Recalculated to a mining width of 80 cm, some typical grades are gold, 0–5 g/t; silver, 10–50 g/t; lead, 1–10 percent; zinc, 2–15 percent; and antimony, 0.5–2 percent. Ibáñez and Medina (1988) describe one of five holes drilled by COMIBOL in 1980. The hole was drilled normal to the mineralized structures at a declination of -35°, and reached depths of 190 m below the surface. Although no major vein was intersected, altered and mineralized Upper Quehua tuffs were encountered, and individual samples contained as much as 5 g/t gold, 123 g/t silver, and several percent lead and zinc. We have no information on the other drill holes.

The veins at Buena Vista are enveloped in two long (as much as 4 km), narrow (5–120 m) zones, in which the host tuffs are extensively altered to aggregates of quartz, sericite, and pyrite (Jiménez, 1971). There is surprisingly little oxidation of the pyrite and the altered rocks are not prominent, either on the ground or on satellite images.

An age of 11.3±0.6 Ma was reported (Instituto de Geología Economica, 1985) for alteration sericite associated with one of the veins at the Buena Vista mine. During our site visit, we collected apparently similar material (tuff altered to an aggregate of quartz, sericite, and pyrite) about 50 cm from the margin of the vein (90BSL014). The age determined for our sample, 11.1±0.3 Ma (app. C), is concordant with the earlier date, and would seem to confirm the age of mineralization at Buena Vista. This is at least 3 Ma younger than the emplacement of the youngest of the tuffs in the Upper Quehua Formation dated by Kussmaul and others (1975).

Conclusions and Recommendations

Polymetallic vein deposits in the Buena Vista area are extensive, and of potentially mineable grades. The presence of significant amounts of gold in the ore is notable. Exploration underground or by diamond drilling is necessary to determine if substantial amounts of bulk-mineable material are present.

CERRO BONETE AREA

By Donald H. Richter, Steve Ludington, W. Earl Brooks, Edward A. du Bray, René Enriquez-Romero, Elizabeth A. Bailey, Alberto Hinojosa-Velasco, Gregory E. McKelvey, Eduardo Soria-Escalante, *and* Angel Escobar-Diaz

Summary

The Cerro Bonete area (app. A, nos. 401–414) contains two distinct groups of mineral deposits that occur in a large volcanic center of Miocene age. The first contains only silver, lead, and zinc, while the second consists of veins with important contents of copper and bismuth. In addition, several large altered areas contain sulfide veins with untested precious-metal contents.

Introduction

The Cerro Bonete area, approximately 140 km south of Uyuni, in the San Pablo de Lípez 1:250,000-scale quadrangle, includes part of a large volcanic complex of Miocene age. It covers about 60 km^2 and includes at least 14 mines and prospects, all chiefly silver- or bismuth-rich polymetallic vein deposits. Currently there is no mining activity in the area.

The area was visited in September and November 1990. Four specific deposits were examined, Bolívar, La Salvadora, Colorados de Bolivia (Rosario I), and Santa Rosa, all in the southern part of the area. In addition, several samples of float were collected from the large, pervasively altered area centered on Cerro Colorado (also known as Cerro Pucasalle) in the south-central part of the area. Information presented here on other workings is from GEOBOL and the United Nations Development Project (UNDP), as well as a thesis by Valencia (1973), and unpublished mapping by German Núñez.

Geologic Setting

The Cerro Bonete area was last mapped by Valencia (1973), and in reconnaissance fashion by GEOBOL geologists almost 30 years ago. Many new concepts in volcanology have been introduced since the area was last studied. Most of the rocks in the higher parts of the area are

Table 28. *Summary description of mines and prospects in the Cerro Bonete area, Bolivia*

Mine	Description	Mineralogy
	Cerro Colorado (western) area	
Pampa Guadalupe	No known production, 3 adits	Chrysocolla, siderite
Pucasalle	7,000 tonnes ore mined from 350 m adit	Galena, sphalerite, pyrite, quartz
Rosario II	No known production, 2 adits	Galena, quartz
Santa Rosa	3 main adits, one 250 m long	Galena, sphalerite, tetrahedrite, pyrite, quartz, barite, hematite
Herreria	No data	No data
Bonete	No known production, only small workings.	Galena
Barrahuayco	Dumps indicate production; 2 adits, larger is 200 m long.	Galena, pyrite, limonite, quartz
	Bismuth-bearing (eastern) area	
Bolívar	Major producer, extensive workings	Bismuthinite, pavonite, chalcopyrite, aikinite, pyrite, quartz, ankerite, siderite
Colorados de Bolivia	No known production, workings to 70 m, flooded.	Chalcopyrite, pyrite, bismuthinite
San Julián	No known production, 2 adits	Bismuthinite, galena, quartz
La Salvadora	Major producer, 2 adits	Bismuthinite, pavonite, pyrite, quartz
Dos Martillos	No known production, 1 adit	Bi and Ag minerals
San José	No known production, 1 adit	Bi and Ag minerals
La Moza	No known production, 1 adit	Bi and Ag minerals, quartz, pyrite, barite, limonite
Lipeña	No known production; 7 adits, largest 40 m.	Bismuthinite, chalcopyrite, quartz, pyrite, barite, hematite

dacitic intrusions and lava flows (pl. 1, Tvnd) that cut and overlie almost horizontal pyroclastic beds of the Upper Quehua Formation (pl. 1, Tig). The dacite at the Bolívar mine is apparently part of a dome-flow that was extruded onto the surface. Similarly, the summit of Cerro Bonete is probably composed of surficial lava flows. The altered rock that forms much of the southern part of the area (Cerro Colorado) is probably intrusive and may, in fact, be the source of some of the extrusive volcanic rocks in the area. Jiménez and Núñez (1988) describe Cerro Puca Orkho, between Cerros Colorado and Bonete, as a vent breccia. It is quite possible that these dacitic lava flows and intrusions largely hide one or more calderas that could have been the sources for the voluminous Upper Quehua ash-flow tuffs that underlie the area. Kussmaul and others (1975) includes dates that appear to place the age of these ash-flow tuffs of the Upper Quehua Formation between 24.0±0.9 Ma and 14.6±0.6 Ma.

Mineral Deposits

The deposits in the area can be divided into two groups: (1) The deposits in the western part of the area (Pampa Guadalupe, Pucasalle, Rosario II, Santa Rosa, Herrería, Bonete, Barrahuayco) have relatively simple mineralogies and apparently contain primarily lead, zinc, and silver. Many of these deposits are proximal to the large altered area centered on Cerro Colorado. (2) Eight deposits (San Julián, Colorados de Bolivia, Bolívar, La Salvadora, Dos Martillos, San José, Lipeña, La Moza) feature bismuth as an important metal in the assemblage. All of these deposits are east and north of, and probably not related to, the Cerro Colorado center. Some characteristics of these deposits are summarized in table 28, and their locations are shown on figure 86.

Pampa Guadalupe Mine

The Pampa Guadalupe mine is located immediately southeast of the summit of Cerro Colorado, above 5,000 m. The workings, consisting of adits on three levels, are relatively small and show no evidence of recent exploration. The chief characteristics of interest are the presence of copper, in the form of chrysocolla, along with colloidal silica (chalcedony?) and siderite, as reported by Jiménez and Núñez (1988).

Pucasalle Mine

Mina Pucasalle is located a little more than 1 km southeast of Cerro Colorado. The mine area contains several workings and a main adit reported to be 350 m long. The size of the workings indicate considerable activity in the area, however, little is known of the early history of the mine. Information on Mina Pucasalle is from Servicio Geológica de Bolivia (1971kk), Jiménez and Núñez (1988), and German Núñez (written commun., 1990).

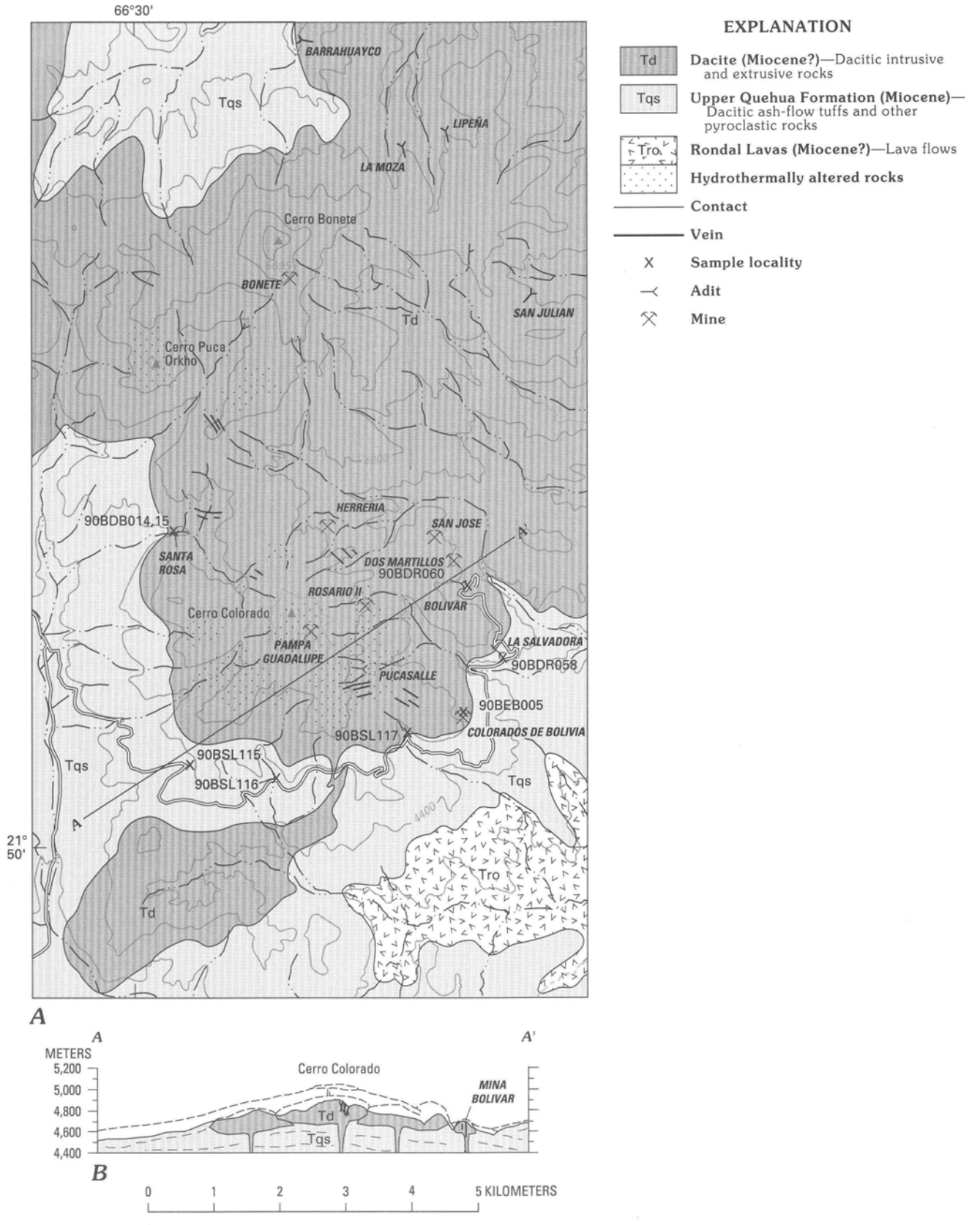


Figure 86. Geology and location of mineral deposits in the Cerro Bonete area, Bolivia. *A*, Geology modified from unpublished mapping by the Servicio Geológico de Bolivia. Contour interval, 200 m; base modified from La Ciénega (6328 IV) 1:50,000-scale quadrangle. *B*, Cross section through Cerro Colorado area. Dashed lines represent pre-erosion configuration.

The host rocks for the ores are primarily dacite intrusions containing phenocrysts of biotite, quartz, and plagioclase. Some pyroclastic rocks are also reported. Silicic, sericitic, and propylitic alteration have affected the surrounding area. Samples of the altered rocks generally contain chlorite, sericite, and iron oxides. Veins in the area are described as "rosario" or brecciated, perhaps the result of continued hydrofracturing in a longlived hydrothermal system, or to local post-mineralization tectonism. The main working is along a vein system that strikes N. 78° E., dips 58°–85° north, and is as thick as 35 cm. Galena and sparse sphalerite occur in the vein along with limonite, pyrite, and quartz. Numerous small fractures cut the rocks in the main adit peripheral to the principal vein. Only one fault, with minimal offset, cuts the principal vein. In the southwestern part of the area, there are several northwest-trending, 15–40 cm-thick veins with steep dips to the east. Limonite is present in most of these veins but no sulfides have been found.

More than 60 samples from the main adit yielded the following results: silver, 20–960 ppm with a mean of 165 ppm; lead, 0.4–33.2 percent with a mean of 5.5 percent; zinc, 0.6–15.6 percent with a mean of 4.6 percent; and traces of copper (Servicio Geológico de Bolivia ,1971kk).

The results of chemical analyses from the mine area, combined with the large volumes of dump material, suggest that this mine was an important silver producer in Spanish colonial times. The Pucasalle and Pampa Guadalupe mines are located centrally in the large alteration zone surrounding Cerro Colorado.

Rosario II Mine

The Rosario II mine is located just east of the summit of Cerro Colorado, in the center of the altered area. The workings are small and largely caved, but they apparently followed some north-trending veins. Galena and quartz occur on the dumps (Jiménez and Núñez, 1988).

Santa Rosa Mine

Mina Santa Rosa is located about 2 km northwest of Cerro Colorado. The deposit is a polymetallic vein system with silver, lead, zinc, and minor copper, that cuts Tertiary dacite and dacite breccia. Workings date from Spanish colonial times. Prior to 1970, geochemical and geophysical surveys were carried out in the area by the Servicio Geológico de Bolivia (1971qq).

The host dacites contain phenocrysts of biotite, plagioclase, and quartz which when altered are green to gray and may contain sericite and hematite. The mine area includes 4 adits and smaller prospect pits. There are two structural systems; the most important consists of veins that strike N. 50°–60° W. and dip southwest. The second is a fracture system with sparse mineralization that strikes N. 76° E. and dips northwest. Results of analyses of over 150 samples of mineralized material from the area yielded silver values of 20–1,720 ppm, with a mean of 211 ppm; and lead values of 0.12–15.2 percent, with a mean of 1.7 percent (Servicio Geológico de Bolivia, 1971qq). It is estimated that dumps in the area have a total volume of 13,000–14,000 m^3, and may contain as much as 250 ppm silver and 0.82–7.24 percent lead. The ore minerals include argentiferous galena, tetrahedrite, and sphalerite in a gangue of quartz, barite, pyrite, and hematite (Sugaki and others, 1986). Malachite and azurite were reported from one of the smaller workings.

Minas Esperanza and Segunda Esperanza are small workings that may be considered to be part of the Santa Rosa area. During July and August 1967, 2 tonnes of ore were mined from these now abandoned deposits (Cortez and Kuronuma, 1969).

Mina Esperanza is a 35 m-long adit that follows a gouge zone in dacite that trends N. 50° W. and dips 80° southwest. The zone is from 5–50 cm thick and the only macroscopic evidence of mineralization in the clay and limonite gouge zone was a 7 cm by 4 cm galena sample. Segunda Esperanza is smaller, perhaps 1 m in length, and is flooded. It also follows a northwest striking, 80 cm-thick gouge zone that dips northeast. Pyrite, iron oxides, and clay are present. Analyses for 6 samples from both workings are lead, 0.002–0.02 percent and silver, 40–200 g/t. Two samples (90BDB014, 15) were collected in November 1990 and the results are shown in table 29.

Geochemical and geophysical exploration by GEOBOL indicate a possible mineralized northwest-trending structure at shallow depths. The size and mineral content of the dumps justify further examination of the Mina Santa Rosa area.

Herrería Prospect

Herrería is a small prospect on the northern fringe of the Cerro Colorado alteration zone. Almost nothing is known of the area or the extent of the workings.

Bonete Mine

Mina Bonete is a small prospect southeast of Cerro Bonete, that consists of small workings, trenches, and prospect pits; little is known of its history (Servicio Geológico de Bolivia, 1971j).

The host rocks for the veins are lithic tuffs, dacite, and dacite breccia which are exposed in sparse outcrops. Fractures in the area strike N. 70° W., N. 80° E., and N. 25° W. and are commonly filled with iron oxides and some disseminated galena. In areas where hydrothermal alteration is strongest, the veins are 0.2–2 m thick, however, where alteration is weaker they are only 1–10 cm thick. Analyses of 12 samples from the veins produced results in the range from 20 to 280 g/t silver and 0.20 to 6.65 percent lead. Bismuth was searched for, but not detected.

Table 29. *Chemical analyses of altered and mineralized rocks from the Cerro Bonete area, Bolivia*

[All results in parts per million (ppm). Sample descriptions, methods, and complete results in appendix B]

Sample no.	Lithology	Au	Ag	Pb	Zn	Cu	As	Sb	Sn	Bi
				La Salvadora						
90BDR058	Vein	<1.5	15,000	58,000	4,200	5,000	140	190	<10	120,000
90BDR058b	Dacite breccia	<1.5	70	510	380	370	380	650	<10	190
				Mina Bolívar						
90BDR060	Vein	<1.5	90	5,200	1,000	24,000	970	160	<10	26,000
90BDR060b	Dacite	<10	<.5	200	500	<5	<200	<100	<10	<10
				Colorados de Bolivia						
90BEB005a	Dacite breccia	<1.5	330	9,100	3,400	100	720	770	<10	130
90BEB005b	Dacite breccia	<1.5	62	600	200	140	580	120	<10	61
90BEB005c	FeO vein	<1.5	41	1,000	250	190	570	89	<10	180
90BEB005d	Dacite breccia	<1.5	46	4,900	640	100	210	64	<10	68
				Cerro Colorado altered zone						
90BSL115	Dacite	<0.002	0.56	53	55	6.3	85	68	10	<0.6
90BSL116	Dacite	<.002	.74	330	44	4.9	29	35	<10	<.6
90BSL117	Dacite	<.002	6.6	26	22	4.0	58	19	<10	5.4
				Mina Santa Rosa						
90BDB014	Sulfide vein	<0.002	38	12,000	480	130	330	92	<10	14
90BDB015	Sulfide vein	<.002	11	3,300	310	28	320	57	<10	38

Barrahuayco Mine

Mina Barrahuayco is the northernmost of the polymetallic stockwork vein systems in the Cerro Bonete area. Originally developed by Spanish explorers, this mine has been a COMIBOL property since 1952 and was most recently worked during 1967 and 1971 by the Lípez Mining Company (Servicio Geológica de Bolivia, 1971g; Medina and Ibáñez, 1988a).

The deposits occur in altered dacite that is somewhat bleached or propylitically altered to shades of pale green or yellowish brown. The area of alteration at Barrahuayco is small, less than 1 km^2, and the workings consist of a principal adit (flooded) and a smaller adit. Both adits follow a northwest-trending, steeply dipping (75°–90°) vein system. A zone of silicic to argillic alteration as wide as 100 m parallels the veins in the main adit. The stockwork nature of this deposit is a result of the dense fractures, as many as 15 per meter, that strike northwest, northeast, and east-west. Propylitic alteration is apparent west of the main workings where fractures are 10 per meter; alteration generally decreases to the north. The veins contain galena, barite, pyrite, limonite, blue-green copper oxides, and quartz.

The highest silver analysis, 5,840 g/t, came from a sample from P-17, the smaller of the workings. The range of results from the two workings are silver, 60–5,840 g/t; lead, 3.2–17 percent; and zinc, 1–33.4 percent. An estimate of 10–16 million tonnes was made for the stockwork in the Barrahuayco area, on the basis of the distribution of alteration.

Cerro Colorado Alteration Zone

A large altered area is centered on Cerro Colorado (fig. 86; pl. 3, image G). It is very conspicuous from a distance and appears to be an intrusive-extrusive complex, primarily of dacitic composition, that has undergone strong hydrothermal alteration.

Three samples of float from this complex were collected (90BSL115, 116, 117). Megascopically, they all appear to be igneous rocks of uncertain origin that have undergone strong phyllic alteration. Under the microscope, samples 90BSL115 and 90BSL117 appear to be fine-grained quartz porphyries with few textural features to distinguish between intrusive and extrusive origin. Both samples are strongly altered and no original minerals other than quartz remain. Both sericite and jarosite, presumably an oxidation product of pyrite, are widely disseminated in the groundmass. Former mafic minerals cannot be recognized. Sample 90BSL116 shows laminae that may indicate it was a lava flow. The groundmass is extremely fine grained and appears to have formed by devitrification of an original glassy matrix. Sericite is not abundant, except as a pseudomorphic replacement of biotite, and jarosite is much less abundant than in the other two samples. Geochemical analysis of these three samples showed extremely low levels of mineralization; gold was not detected, and silver values are no more than a few parts per million (table 29).

German Núñez of the UNDP is conducting a geochemical study of the samples collected by Jiménez and Núñez (1988) from the Cerro Colorado altered zone and preliminary results were provided to us (Enrique Arteaga

and German Núñez, written commun., 1990). Similar to our geochemical results, the values are low, and not as favorable as might be expected, given the appearance of the area. Most silver values are 1–10 ppm and gold values are all less than 0.01 ppm. Nevertheless the large volume of pervasively altered rock suggests that a large and vigorous hydrothermal system was active here.

Cerro Puca Orkho Alteration Zone

South of Cerro Bonete and north of Cerro Colorado are two alteration zones on Cerros Puca Orkho and Khellu Orkho about which little is known (fig. 86). Alteration on Cerro Puca Orkho is silicic to propylitic, covers an area of approximately 1 km^2, and, on the basis of the orange-red colors, seems to be the more intensely altered of the two (Jiménez and Núñez, 1988; G. Núñez, written commun., 1990). The two zones are prominent on satellite images (pl. 3, image G), although not as large as the one centered on Cerro Colorado to the south. We did not see or visit either of these areas.

Small outcrops of hydrothermal breccia are reported to occur in the altered zones, and it is likely that the brecciation was caused by the same processes that caused the alteration. The flanks of Cerros Puca Orkho and Khellu Orkho are covered with breccia boulders as much as 1 m in diameter. Veins of milky quartz and opal form a stockwork. Silicification has affected the rocks and generally only the quartz remains unaltered. However, in some samples biotite appears either fresh or secondary; oxidation has eliminated pyrite leaving many boxwork structures and the iron oxides that cause the distinct red-orange color of the area (Jiménez and Núñez, 1988).

Bolívar Mine

Historically, the Bolívar mine has been the largest and most productive mine in the area. It was worked in Spanish colonial times and was last operated in 1979, by Empresa Minera Unificada, S.A. (EMUSA). It is now the property of COMIBOL.

The deposit consists principally of a single, near vertical vein, trending N. 86° W. and ranging in thickness from 10 to 25 cm; it was mined on 3 levels, between about 4,400 and 4,500 m in elevation (Jiménez and Núñez, 1988). One extremely rich ore shoot, 45 m long and 70 m in vertical extent, was evidently the main source of ore prior to 1964. The ore minerals include pavonite $(Ag,Cu)(Bi,Pb)_3S_5$ (Harris and Chen, 1975), bismuthinite, chalcopyrite, pyrite, and aikinite ($PbCuBiS_3$); gangue minerals are quartz, ankerite, and siderite. The deposit is considered to be unique because pavonite, here a major ore mineral, is not found in exploitable quantities elsewhere in the world (Ahlfeld and Schneider-Scherbina, 1964).

Although Ahlfeld and Schneider-Scherbina (1964) reported that the deposit was worked out in 1964, the mine continued to operate until 1979. During its last years, the average grade of ore was about 0.3 percent bismuth, 0.2 percent lead, and 300 g/t silver; the concentrate that was produced contained 12 percent bismuth, 6 percent lead, 9,000 g/t silver, and 4 g/t gold (Hernán Uribe, oral commun., 1990). Ore grades prior to this time are not available, but undoubtedly were much higher. For example, in 1965 an informal GEOBOL memorandum mentions a 10,000 tonne block of ore below the 4,400 m level that had an average grade of 2.7 percent bismuth, 4.5 percent copper, and 1,165 g/t silver. A bismuthinite-rich sample collected from a Spanish colonial era dump contained 480 ppm silver and almost 3 percent bismuth (table 29, sample 90BDR060).

The Bolívar deposit is one of few in the study area that appears to be emplaced in an extrusive volcanic dome rather than in a subvolcanic stock (fig. 87). The dome was emplaced in a vent over a series of inwardly dipping layered vent breccias. The veins occur in the throat of the dome, at least 300 m below the original surface. The dome is a dacite porphyry that contains phenocrysts of embayed quartz, plagioclase, and fresh to totally altered biotite in a cryptocrystalline groundmass; SiO_2 content is about 65 percent (app. B, sample 90BDR060b). Much of the dacite is propylitized, especially near the Bolívar and La Salvadora mines.

Colorados de Bolivia Mine

Mina Colorados de Bolivia (or Rosario I) is located in the southern part of the Cerro Bonete area, a few kilometers southeast of the Pucasalle mine. The area is small, less than 1 km^2, and consists of three main workings. The descriptions of this mine are from Servicio Geológico de Bolivia (1971p) and a brief visit in October 1990.

The deposits exploited by these workings are breccias with a copper- and bismuth-bearing matrix. The host rock for the breccia zones is a biotite dacite that contains

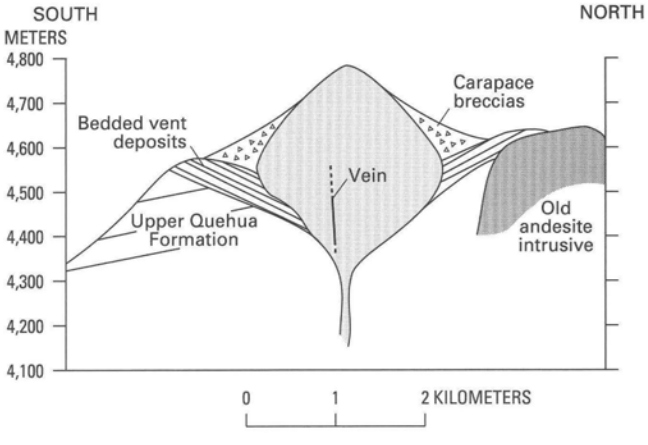


Figure 87. Diagrammatic sketch of geologic relationships at the Bolívar mine, Cerro Bonete area, Bolivia.

phenocrysts of quartz, plagioclase, and biotite. Accessory minerals include apatite and zircon. Propylitic, sericitic, and argillic alteration has affected the area near the mine.

There are three main workings in the area (fig. 88). The first, referred to as X–24, is a 70 m-long, east-west trending, flooded adit that follows a 1 m-thick limonitic breccia zone that dips 70° north. Pyrite, chalcopyrite, and sparse bismuthinite are present on the dumps. The second, known as V, is an adit that was 36 m long and followed a limonite stained, 2 m-thick breccia zone. The adit is now caved and only about 3 m are accessible. Pyrite was the only sulfide mineral found on the dump. The third working is an unnamed trench that follows a N. 80° W., steeply north dipping breccia zone that is approximately 2 m thick. Samples from the tailings and along the walls of the unnamed trench contain pyrite, chalcopyrite, and bismuthinite that occur in the matrix of the breccia.

Analyses reported by the Servicio Geológico de Bolivia (1971kk) for samples collected from the three workings are silver, 20–450 ppm, with a mean of 150 ppm; lead, 0.6–4.4 percent, with a mean of 1.8 percent; and zinc, 0.7- 2.1 percent, with a mean of 1.2 percent. Analyses on grab samples from the dumps and from along the wall of the trench yielded silver values that range from 41 to 330 ppm and lead values that range from 600 to 9,100 ppm (samples 90BEB005a, b, c, d; table 29).

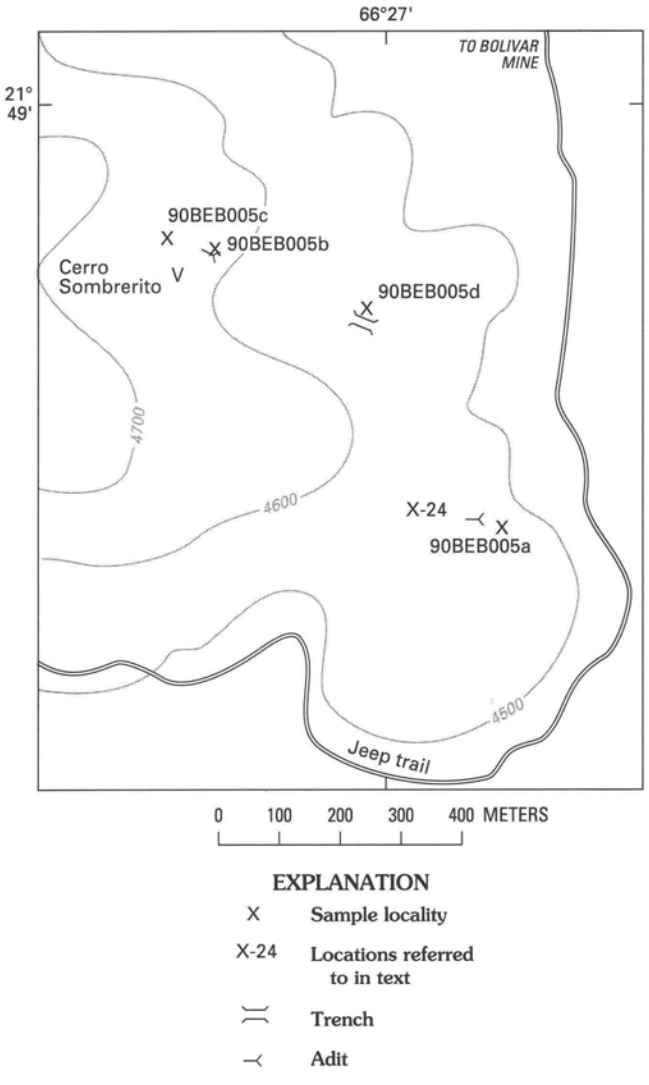


Figure 88. Map showing mine workings and sample localities at the Colorados de Bolivia mine, Bolivia. Contour interval, 100 m; base modified from La Ciénega (6328 IV) 1:50,000-scale quadrangle.

San Julián Mine

Mina San Julián is approximately 4 km east of Cerro Bonete and is a silver-rich polymetallic vein system. Stone archways suggest that the workings date back to Spanish colonial time, however, work since that time has been sporadic. The only source of information for Mina San Julián is Servicio Geológico de Bolivia (1971pp).

The San Julián workings consist of two accessible adits and several other now caved workings. The adits follow the east-west trend of veins, which consist of quartz and iron oxides, are 20 cm to 1.2 m thick, and occur in biotite dacite. Selvages as thick as 2 m contain galena, quartz, and iron oxides. The dacite is typically pale green and contains calcite and sericite as products of hydrothermal alteration.

Analyses of samples from the veins and selvages in the accessible adits are silver, 20–2460 g/t; lead, 0.2–22.2 percent; bismuth, 0.01–0.2 percent. There are no reserve estimates for Mina San Julián.

La Salvadora

The La Salvadora mine exploited a vein that is in the same dacite dome that hosts the Bolívar deposit. Like the Bolívar deposit, the La Salvadora consists of a single vertical vein trending east-west and ranging in thickness from 10 to 20 cm (Jiménez and Núñez, 1988). It was mined from two adits (elevation 4,350–4,400 m), one of which had been backfilled from within; the other was flooded at the time of our visit. Fifty meters northeast of the main workings, an altered breccia zone in dacite porphyry, trending N. 80° W. and dipping 80° S, has been explored by a 10 m-long adit.

No data are available on the mineralogy or the grade of the ore in the vein. A sample of quartz-, pavonite- and bismuthinite-bearing vein material collected from the dump of the lower adit contained 15,000 ppm silver and 12 percent bismuth (table 29, sample 90BDR058), and a 1 m-wide chip sample across the breccia zone exposed in the short adit contained 70 ppm silver, 510 ppm lead, and 190 ppm bismuth, although no sulfide minerals are evident (table 29, sample 90BDR058b).

Dos Martillos, San José Prospects

The Dos Martillos and San José workings are small, consisting of little more than shallow prospect pits and trenches with small dumps. Both deposits reportedly contain bismuth and silver minerals; at San José, the vein strikes N. 70° W., and at Dos Martillos, the vein strikes N. 40° W. The host rock in the area of these prospects is probably altered dacite and the structural setting of the mineralization is similar to that at other mines in the vicinity.

La Moza Mine

Mina La Moza is one of three mines in the northern part of the Cerro Bonete area. Nearby mines with similar settings include Mina Barrahuayco and Mina Lipeña. The deposit was discovered by Spanish explorers; the mine has been a COMIBOL property since 1952 and was worked by the Lípez Mining Company in 1967 and 1971. Information on this mine is from Servicio Geológico de Bolivia (1971z) and Medina and Ibáñez (1988a).

The country rock is quartz-plagioclase-biotite dacite. There is argillic to silicic alteration that grades into propylitic alteration in the mine area.

The La Moza mine area contains 11 prospect pits and one adit. Veins in the P–41 adit are 1–5 cm thick and contain limonite and sparse pyrite. The major vein system strikes northeast (N. 11°–58° E.) and dips 32°–48° west; a subordinate vein system strikes northwest (N. 36°–49° W.) and dips 10°–48° north. This variety of fracture orientations results in a crude stockwork. The fractures are most dense in the silicic-argillic zone (10 per meter) and decrease toward the propylitic zone. The fractures are as wide as 10 cm and contain limonite, quartz, barite, and sparse pyrite in addition to unknown silver and bismuth minerals.

Analyses from the P–41 adit are silver, 60–1,240 g/t; lead, 0.8–1.2 percent; and bismuth, trace to 0.2 percent. However, analyses from unknown localities in the vicinity yielded values as high as 3,360 g/t silver, 1.1 percent lead, and 4.6 percent bismuth. The estimated reserves of stockwork ore at the La Moza deposit are 19 to 44 million tonnes.

Lipeña Mine

Mina Lipeña exploits a polymetallic stockwork vein system that contains bismuth, copper, and silver. Work in the area dates back to the Spanish explorers; the mine has been a COMIBOL property since 1952. In 1967, the Lípez Mining Company carried out exploration in the area and later formed a cooperative venture named Santa Ana, but work in the area was sporadic and appears to have stopped by 1970. Information about this mine is from Servicio Geológico de Bolivia (1971bb) and Medina and Ibáñez (1988a).

The ores occur in subvolcanic intrusive rocks that have been variously described as dacite, quartz andesite, biotite dacite, and biotite rhyolite. Primary minerals in these rocks include quartz, sanidine, plagioclase, and biotite. Sericite, calcite, and chlorite are present as alteration products.

The Lipeña deposit appears to be larger than either the La Moza or Barrahuayco deposits. The same style of alteration—silicic, silicic to argillic, grading into propylitic— is present at all three. Fractures in altered areas are as dense as 12 per meter. Veins contain bismuthinite, chalcopyrite, and limonite. The strike of the fractures and veins is variable but is commonly N. 60°–80° W. with near vertical dips. The largest vein reported in the area is about 5 m thick, strikes N. 80° W., and has a gangue of quartz, barite, and pyrite. Specularite veins, 1–10 cm thick, occur in the south-central part of the area.

Analyses of samples from the seven adits in the area yielded the following ranges: bismuth, 0.02–0.58 percent; copper, 0.15–4.8 percent; and silver, 40–250 g/t. Of the workings in the area, only the vein exposed at the P-9 working has significant copper. This vein strikes N. 80° E., dips 63° south, and contains chalcopyrite, malachite, and azurite along with pyrite, limonite and quartz. An estimate of 35–106 million tonnes of stockwork material of unknown grade was made for the area (Servicio Geológico de Bolivia, 1971bb).

Alluvial Gold

Alluvial gold has been reported in various drainages south of the Cerro Bonete area and in drainages south of San Pablo de Lípez. Mining activity usually peaks during the rainy season when the runoff is high. The gold particles are typically less than 0.5 mm in size, but some larger flakes have been found; their morphology indicates little transport. Gold and mercury-gold amalgam have also been found in drainages in the area, especially north of Guadalupe. It is possible that the mercury-gold amalgam and mercury date from Spanish colonial times. Information on gold in the Cerro Bonete area is described in Jiménez and Núñez (1988).

The source of the gold is believed to be from altered areas in the Cerro Bonete area or from Cerro Aguilar, 10 km southwest of Cerro Bonete and outside of the area studied (German Núñez, oral commun. 1990). Gold also has been reported in concentrate taken from Mina Bolívar (Hernán Uribe, oral commun., 1990).

Conclusions and Recommendations

The bismuth reserves in the Cerro Bonete area may well be largely exhausted; nevertheless, material with significant silver and bismuth values remains on the dumps. The precious-metal potential of the two large altered zones,

Cerro Colorado and Puka Orkho, has not yet been adequately evaluated. The large size of these hydrothermally altered areas remains intriguing. The assays reported for the Barrahuayco and La Moza deposits deserve verification, as do the large size estimates for Barrahuayco, La Moza, and Lipeña.

MOROKHO AREA

By Steve Ludington, Edward A. du Bray, Gregory E. McKelvey *and* Eduardo Soria-Escalante

Summary

Mineral deposits in the Morokho area (app. A, nos. 395, 396) consist of silver-, lead-, zinc-, and tin-bearing veins and veinlets, that are emplaced in Miocene dacite intrusions and lava flows. The deposits occur in a large hydrothermally altered area. The extent of exploration in the area is very limited and there is significant potential for the existance of polymetallic resources.

Introduction

The Morokho area contains one major (Mina Himalaya) and several minor lead-zinc-silver veins that were discovered sometime prior to 1865, when the mine was first worked (Servicio Geológico de Bolivia, 1971u). The Himalaya mine is located near the headwaters of Río Morokho, about 7 km west of the village of Guadalupe, at an altitude of about 4,700 m. The area is in the San Antonio de Esmoruco (6228 II) 1:50,000-scale quadrangle, about 230 km southwest of Uyuni and about 25 km south of San Pablo de Lípez. The last 2 km of the access road from Guadalupe are impassable to vehicles. Previous studies on the area include those of Zubrzycki and Murillo (1958a), and of Servicio Geológico de Bolivia (1971u). The area was visited in November 1990.

Geologic Setting

The deposits at the Himalaya mine are hosted in Miocene dacitic rocks (pl. 1, Tvnd and (or) Ti), which are massive and lack internal characteristics or other features that might indicate they originated as lava flows (fig. 89). We believe that most of these rocks actually are hypabyssal stocks or sills. Near the upper parts of the Morokho massif (above 5,000 m), the rocks appear to have more clearly defined, subhorizontal fabrics and partings, suggesting that the upper dacites are lava flows. The dacites appear to both intrude and flow out over ash-flow tuffs of the Miocene Upper Quehua Formation (pl. 1, Tig).

Only one sample of fresh dacite was collected in the area. Petrographic examination of the dacite shows it to be porphyritic, with a total phenocryst content of 30–40 percent. The phenocrysts consist of feldspar, biotite, and,

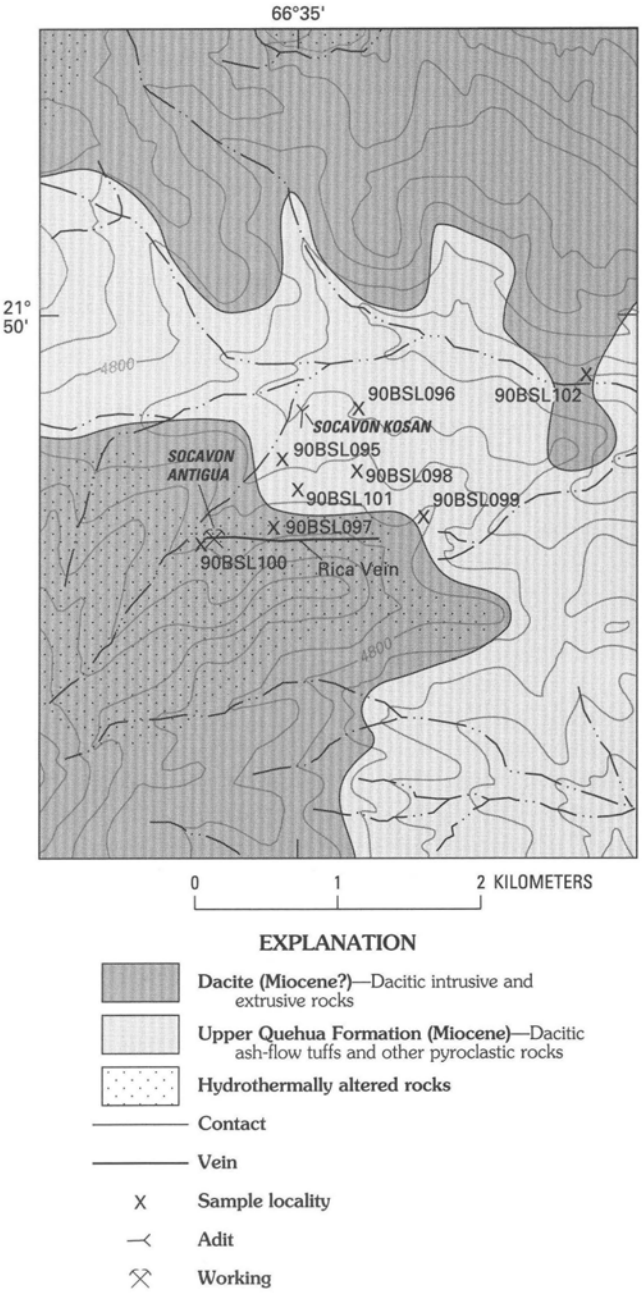


Figure 89. Map showing geology and sample localities in the Morokho area, Bolivia. Geology is modified from unpublished mapping by the Servicio Geológico de Bolivia. Contour interval, 100 m; base modified from San Antonio de Esmoruco (6228 II) and San Pablo de Lípez (6228 I) 1:50,000-scale quadrangles.

Table 30. *Selected chemical analyses of mineralized rocks from the Morokho area, Bolivia*

[Values reported in ppm. All samples contain <2 ppm Bi. Sample descriptions, methods, and complete results in appendix B]

Sample no.	Au	Ag	Pb	Zn	Cu	As	Sb	Sn
90BSL095	0.028	320	21,000	>16,000	88	1,300	9,100	>1,000
90BSL097	.004	2.4	26	37	5.6	769	180	50
90BSL098	.002	.58	52	57	9.5	920	110	20
90BSL099	<.002	<.045	23	26	10	18	49	<10
90BSL100a	<.002	.1	25	9.2	2.1	18	30	150
90BSL101	<.002	.054	17	64	10	17	19	<10

less commonly quartz in a medium-gray aphanitic to microcrystalline groundmass. The silica content is, on an anhydrous basis, about 66 weight percent (app. B, sample 90BSL102).

Mineral Deposits

Veins

The known ore deposits in the area occur as continuous, polymetallic veins that are sulfide-rich, but contain quartz and abundant manganese carbonate gangue. Principal sulfide minerals present are pyrite, marcasite, chalcopyrite, and galena, as well as an unknown silver-bearing species (pyrargyrite?) (Servicio Geológico de Bolivia, 1971u). The veins all trend about east-west and dip steeply to the south. The entire lateral extent of the veined area may be as much as 3 km. Three principal veins, all less than 1 m thick, are identified in the Morokho area, the principal one being the Rica vein.

Two principal mine workings exploited these veins (fig. 89). The principal working is called Socavón Kosan, and was driven almost 1,000 m southward from its mouth, at an elevation of about 4,650 m. Socavón Kosan intercepts what is believed to be the Rica vein at its southern end, almost 500 m below the surface. The tunnel is now inaccessible. The other working, Socavón Antiguo, follows the Rica vein for about 25 m at an altitude of almost 5,000 m. Details of the mine workings are presented in Servicio Geológico de Bolivia (1971u).

Results of chemical analyses of 85 samples of veins and altered rock are available in Servicio Geológico de Bolivia (1971u). The samples were collected both underground and at the surface. Lead, zinc, and silver all appear to exhibit lognormal distributions. The median concentrations are silver, 12 ppm; lead, 0.92 percent; and zinc, 1.8 percent. The maximum values are silver, 584 ppm; lead, 9.0 percent; and zinc, 31.2 percent. In these 85 samples, silver and lead are not well correlated (fig. 90), suggesting that a substantial part of the silver present occurs in minerals other than galena. Sample 90BSL095, collected from the dump at the mouth of Socavón Kosan, contains large amounts of silver, lead, zinc, arsenic, antimony, and tin (table 30); gold is present in very small quantities (0.028 ppm).

Hydrothermal alteration

A large area of about 4 km^2 of hydrothermally altered rock (fig. 89) can be seen in the field and on satellite images (pl. 3, image G). The altered rock, primarily intrusive dacite, is distinctly red and orange, presumably the result of oxidation of pyrite disseminations and fracture fillings in the rock. Judging from the size of the fragments of altered rock in the talus, the fracture spacing ranges from about 5 to 50 per meter.

Samples 90BSL097, 98, 99, and 100a are samples of sericitized dacite cut by goethite-jarosite veins; they contain anomalous abundances of as much as 2.4 ppm silver, 920 ppm arsenic, 180 ppm antimony, and 50 ppm tin (table 30). Sample 90BSL100a shows almost complete replacement of

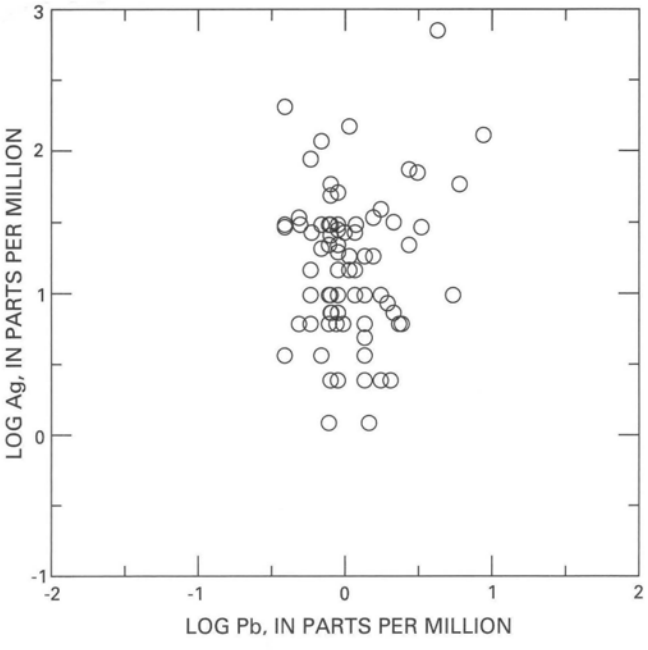


Figure 90. Plot showing silver and lead values for mineralized samples collected by Servicio Geológico de Bolivia (1971u) at Mina Himalaya, Bolivia.

all phenocrysts (except quartz) and the groundmass by sericite; there are no fluid inclusions in the quartz phenocrysts. Sample 90BSL101 is a brecciated dacite with iron oxides and barite and does not appear to be mineralized, although it is strongly affected by sericitic alteration.

Another large altered area, about 5–8 km to the north, that includes the Mulato deposit (Servicio Geológico de Bolivia, 1971ii) can be seen on plate 3 (image G). It is at least as large as the one near Mina Himalaya, but it was not visited as part of this study.

Conclusions and Recommendations

The volumes of altered rock in the Morokho area, as well as in the Mulato area to the north, are very large; each area crops out over several square kilometers. Our limited geochemical sampling was not encouraging, and precious-metal contents of the altered and oxidized rock appear to be quite low. Nevertheless, the altered areas are very large, and will remain attractive exploration targets until further sampling is done.

SAN ANTONIO DE LIPEZ AREA

By Steve Ludington, Edward A. du Bray, Donald H. Richter, *and* Gerald K. Czamanske

Summary

The San Antonio de Lípez area (app. A, nos. 378–381) contains at least 4 potentially important mineral deposits. One of them, Mesa de Plata, is a typical Bolivian polymetallic vein deposit that may contain substantial silver, lead, and zinc resources. Two others, El Mestizo and Machu Socavón, have considerable potential as large, low-grade precious-metal deposits. All of the deposits appear to be related to a large, Miocene, dacitic volcanic center.

Introduction

The San Antonio de Lípez area contains at least 4 separate mineralized systems in the northern part of Cerro Lípez, a Miocene dacitic volcanic center that intrudes and overlies pyroclastic rocks of the Upper Quehua Formation. The area is located in the San Antonio de Lípez (6228 III) 1:50,000-scale quadrangle, at altitudes of about 4,500 m and higher. It is about 200 km from Uyuni, on all-weather roads. The area includes the Mesa de Plata polymetallic vein deposit, which was apparently one of the first silver discoveries by the Spaniards in Alto Perú (modern Bolivia), in the middle part of the 16th century, when it became the site of major mining endeavors. At that time, as many as 15,000 people lived in San Antonio de Lípez and worked in the mines of Mesa de Plata, which were abruptly abandoned a few years later when rich silver ore was discovered at Cerro Rico de Potosí. Mesa de Plata has not been worked since, with the exception of a brief rejuvenation in 1866–74 (Ahlfeld and Schneider-Scherbina, 1964). The area was visited in May and November 1990.

Geologic Setting

Cerro Lípez is a very large volume dacitic volcanic center. Dacites of the center (pl. 1, Tvnd) appear to cut and overlie the voluminous ash-flow tuffs of the Miocene Upper Quehua Formation (pl. 1, Tig). However, the rubbly nature of outcrops in the area render relative age determinations somewhat ambiguous, and it is possible that Upper Quehua deposits are younger than some of the dacites of Cerro Lípez. In the western part of the area, dacites are emplaced directly on the sedimentary rocks of the Lower Quehua Formation (pl. 1, Ts2), and the tuffs of the Upper Quehua are missing.

The nature of the Cerro Lípez volcanic center is also somewhat ambiguous. Our brief investigations in the area were not sufficient to determine if the Cerro Lípez center is the remains of a cluster of stratovolcanoes composed of coalesced lava flows and related shallow intrusive masses or the deeply eroded roots of a caldera system. The great volume of numerous, monotonous, seemingly older dacitic ash-flow tuffs of the Upper Quehua Formation, and the inability to identify sources for these rocks, suggests that the tuffs may have been erupted in caldera-forming eruptions from the dacite centers. Volcanic centers such as Cerro Lípez may have been the source of these tuffs; the volcanic rocks currently exposed at Cerro Lípez may represent caldera-filling lava flows, their associated shallow intrusions, and the subvolcanic roots characteristic of this type of volcanic system. As seen on satellite images (pl. 3, image G), the Cerro Lípez volcanic center has a distinctive ovoid shape and a general morphology not unlike the younger Panizos caldera to the southeast on the Bolivia-Argentina border. Only careful field mapping can clarify these relationships.

Mineral Deposits

Mesa de Plata

Mesa de Plata, located immediately adjacent to the ruins of the ancient city and the modern village of San Antonio de Lípez (fig. 91), was actively mined very early during the Spanish tenure in the area. The deposit is

described in some detail by Sugaki and others (1986), and, at present, is under active exploration by COMIBOL.

Mesa de Plata consists of a series of veins that trend almost east-west, dip steeply to the south, and cut pervasively altered intrusive(?) dacite. The veins are as thick as 3 m and consist of pyrite, quartz, marcasite, sphalerite, galena, hematite, and barite, as well as lesser amounts of chalcopyrite, arsenopyrite, tetrahedrite, magnetite, greenockite (CdS), aikinite ($PbCuBiS_3$), native silver, argentite, polybasite ($(Ag,Cu)_{16}Sb_2S_{11}$), pyrargarite, and stephanite (Ag_5SbS_4). Sphalerite in the veins contains from 0.2 to 1.3 weight percent iron and from 0.6 to 1.2 weight percent cadmium (Sugaki and others, 1986). A dump sample of a quartz-rich vein collected from the surface showed both chalcedonic and crystalline quartz, with scattered grains of galena, pyrite, and very fine grained sphalerite and covellite (sample 90BSL022a).

Two-phase, liquid-vapor fluid inclusions in quartz from the veins have homogenization temperatures (uncorrected for pressure) of from 149 °C to 317 °C and salinities

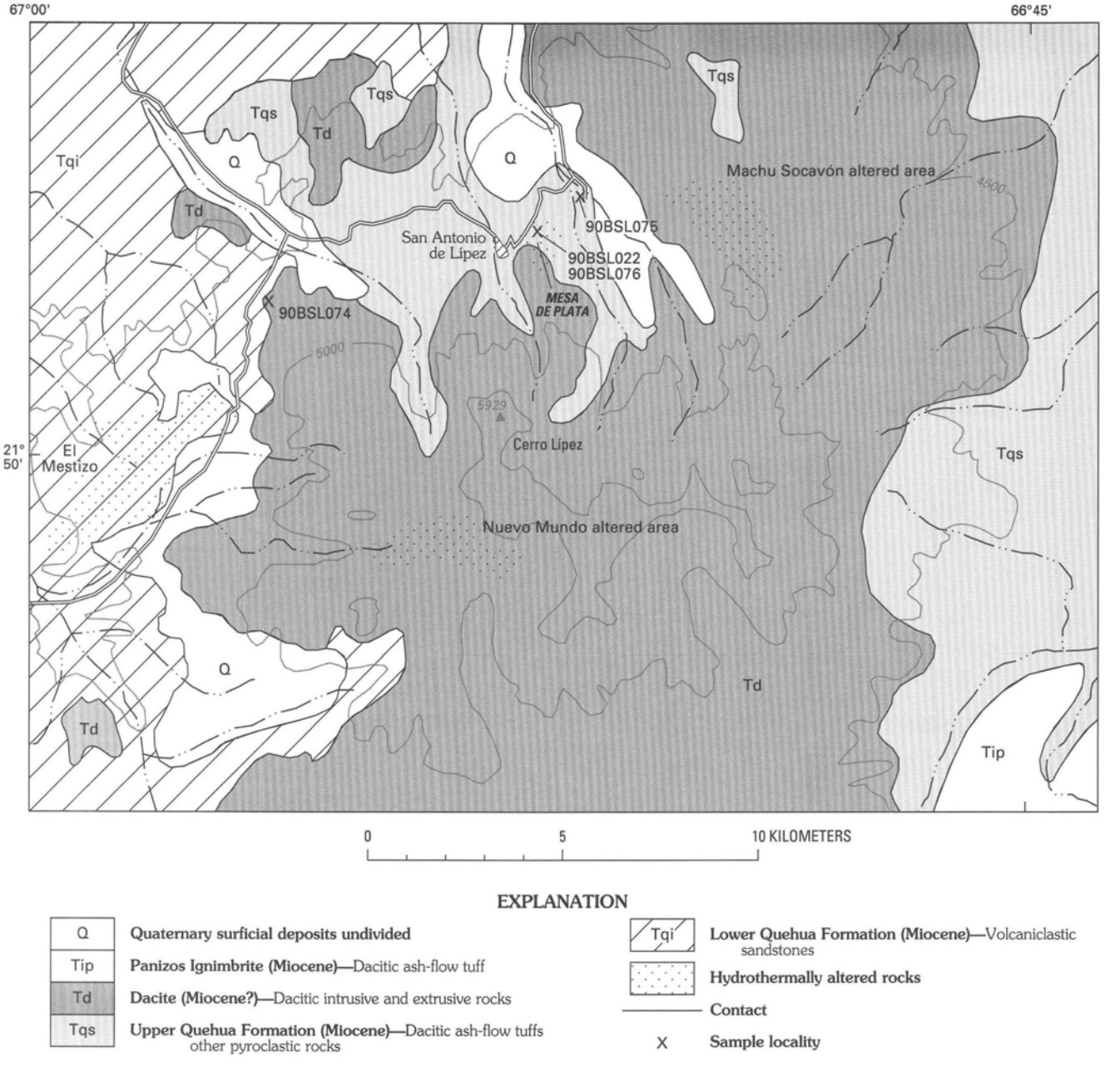


Figure 91. Map showing geology, mineral deposits, and altered areas in the San Antonio de Lípez area, Bolivia. Contour interval, 500 m. Geology generalized from unpublished mapping by the Servicio Geológico de Bolivia.

of from 1.2 to 18.9 weight percent NaCl equivalent (Sugaki and others, 1986). We observed no fluid inclusions in the vein-filling quartz in sample 90BSL022a.

The grade of ore from the mine is reported to be 200 to 240 g/t silver, 1.2 to 2.6 percent lead, and 0.5 to 3.4 percent zinc (Sugaki and others, 1986).

A sample of pervasively altered dacite from the mine dump contains mostly very fine grained clays, probably a result of supergene alteration (sample 90BSL076). Iron oxide pseudomorphs suggest that the dacite porphyry originally contained phenocrysts of both biotite and hornblende. Quartz and feldspar phenocrysts are also present. Altered dacite from the surface above the deposit is similar, although the quartz phenocrysts display a small number of liquid and vapor fluid inclusions and pseudo-cubic melt inclusions (sample 90BDR022). Sample 90BSL076 contains anomalous amounts of silver (0.9 ppm), lead (1,400 ppm), zinc (160 ppm), arsenic (240 ppm), and antimony (170 ppm); sample 90BDR022 contains anomalous silver (8.5 ppm) and lead (3,400 ppm). Complete analyses for both samples can be found in appendix B.

At the surface, the veins are primarily quartz, barite, and hematite. At depth, the amount of pyrite and other sulfides increases substantially. Thus, Mesa de Plata, especially when it is better known at depth, may clearly demonstrate the transition from mesothermal to epithermal environments.

El Mestizo Prospect

El Mestizo is a large area (several square kilometers) of stockwork veins and veinlets entirely in Lower Quehua Formation sediments that dip homoclinally to the north. The prospect is located on the western edge of the Cerro Lípez volcanic center (fig. 91). The large alteration zone is prominent on satellite images (pl. 3, image G). The description of this prospect is based entirely on the reports of Pinto (1988b, 1989a); we examined a few outcrops in May 1990, but collected no samples.

The area is intensely fractured, with two sets of near-vertical fracture directions predominating: N. 30°–40° E. and N. 60°–80° E. The fractures are filled with quartz, barite, and pyrite; stibnite occurs locally. Covellite, bornite, and marcasite have been identified microscopically. Fracture density is from 5–10 to 20–30 per meter. The rock is silicified and in much of the area contains disseminated pyrite and sphalerite. At the surface, all of the pyrite has been weathered to hematite; this supergene alteration has also affected the silicate minerals in the rock, which is bleached white and stained brown and yellow. Most of the groundmass is now composed of kaolinite and illite. The stockwork area is traversed by a 900 m-long shear zone (Socavón Alcida) that trends N. 75° E. This zone contains numerous veins and veinlets as wide as 1 m and was the site of sporadic mining by cooperatives in the 1980s.

Samples from the stockwork zone reported in Servicio Geológico de Bolivia (1971hh) contained values of 3–7 g/t gold and 30–180 g/t silver, whereas samples from the Socavón Alcida shear zone contained values of as much as 5 g/t gold and 34 percent antimony. Samples reported in Pinto (1989a) yielded results that are more than an order of magnitude lower (fig. 92).

Nevertheless, the UNDP has conducted further exploration and sampling continues to be done in the area. El Mestizo remains an important exploration target because of the large area of altered rock and the consistent, if low, precious-metal values. Ultimately, the prospect must be tested at depth to determine if surficial weathering processes have significantly leached or enhanced the metal contents.

Machu Socavón

Machu Socavón is a very large altered area that is located about 6 km east of San Antonio de Lípez (fig. 91). On the satellite images (pl. 3, image G), it is one of the most prominent altered areas in Sud Lípez. Available information comes from Alfaro (1989) and López and Pinto (1990).

The area consists of dacite dome-flows, intrusions, and pyroclastic rocks that cut and overlie pyroclastic rocks of the Upper Quehua Formation. A distinctive "sanidine porphyry" was also noted. Alfaro (1989) describes "phreatic breccias" that are cut by veinlets of cryptocrystalline dark silica, as well as siliceous sinter composed of chalcedony and opal. Mineralization is reportedly localized by north-south structures. A single chemical analysis of a vein 0.15 m wide, reported by Alfaro (1989), gave the following results:

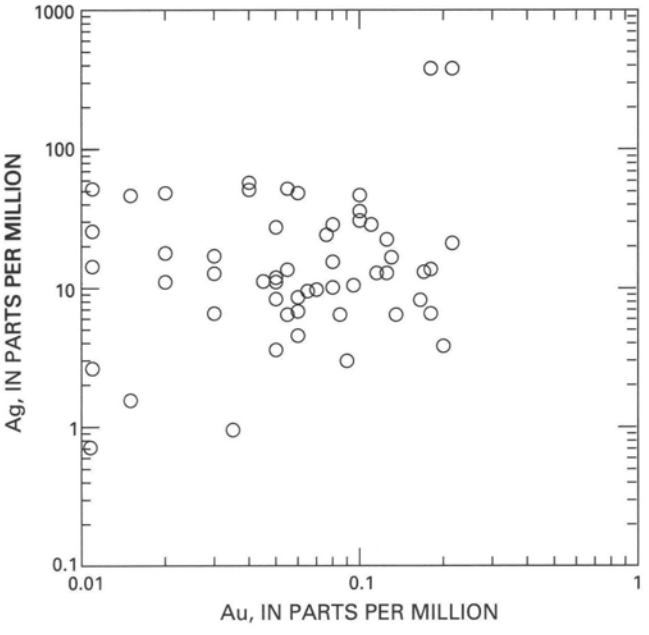


Figure 92. Plot showing gold and silver values for thirty-nine 10–15 kg channel samples reported in Pinto (1989a) for the El Mestizo prospect, San Antonio de Lípez area, Bolivia.

gold, 104 g/t; silver, 800 g/t; and lead, 6.2 percent. However, analyses of samples collected by Flores (1988) reported by López and Pinto (1990) were not as high. Sixteen samples yielded silver contents less than 1.2 ppm and gold contents less than 0.005 ppm, and 4 samples yielded silver values between 9 and 100 ppm and gold values between 0.01 and 0.03 ppm.

Alfaro (1989) described widespread hydrothermal alteration throughout the area, however López and Pinto (1990) were unable to confirm this description; they describe only localized phyllic alteration, and imply that the widespread highly visible alteration is largely supergene.

On the basis of conflicting and sketchy information, it seems clear that Machu Socavón should be explored further to determine the nature of this large altered area.

Nuevo Mundo

Our knowledge of the Nuevo Mundo deposit comes from Servicio Geológico de Bolivia (1971jj) and from López and Pinto (1990). Near the heart of the Cerro Lípez volcanic center, Nuevo Mundo is a vein that contains chalcopyrite, tennantite, and chalcocite in a gangue of quartz, pyrite, calcite, barite, and hematite. The vein occurs on the western end of a prominent altered area, as seen on satellite images, and is emplaced in what López and Pinto (1990) recognized as a composite volcanic cone that is extensively pyritized.

A summary of previous sampling shows important amounts of precious metals, as much as 4.73 g/t gold and 2,620 g/t silver (López and Pinto, 1990) . The Nuevo Mundo area is extremely difficult of access, lying at altitudes in excess of 5,200 m and 10 km or more from vehicular access. Nevertheless, the high precious-metal values yielded by the geochemical sampling indicate that the area should be explored further.

Conclusions and Recommendations

The known mineral deposits in the San Antonio de Lípez area are extremely varied, and the large size of several of the hydrothermal systems is notable. All of them, except for Mesa de Plata, which is relatively well known, require further exploration, both at the surface and at depth.

ESMORACA AREA

By Steve Ludington, Edward A. du Bray, Gregory E. McKelvey, Eduardo Soria-Escalante, *and* Gerald K. Czamanske

Summary

The Esmoraca area (app. A, nos. 420–425) contains several gold-, bismuth-, and tungsten-bearing polymetallic vein deposits emplaced in Miocene dacite intrusive and volcanic rocks and the underlying Tertiary sedimentary rocks. The size of the known veins is limited, and the area is poorly explored. However, large areas have been affected by hydrothermal alteration, and the area is favorable for the discovery of additional mineral resources.

Introduction

The Esmoraca area contains a number of generally east-west trending, tungsten-bearing polymetallic veins that have been worked intermittently since at least the nineteenth century. The area is in the southernmost part of the study area, about 10 km from the Bolivia-Argentina border. The village of Esmoraca, located on Río Esmoraca about 8 km above its confluence with Río San Juan de Oro, is about 75 km from Tupiza, the nearest town. The road is in good condition for most of the way from Tupiza; the last 15 km are traversed by driving up the dry riverbeds of Ríos San Juan de Oro and Esmoraca. The area is located in the Esmoraca (6328 I), La Cienega (6328 IV), Khuchu (6329 II), and Cerro Yano Orkho (6329 III) 1:50,000-scale quadrangles, at altitudes between 3,900 and 5,000 m. In the past, this area has been a source of, successively, gold and silver, bismuth, and, most recently, tungsten. Bismuth was discovered in the area in 1880, and mining began in 1900. One of the deposits, the Pueblo Viejo mine, is owned and is currently being operated by San José de Berque Ltda. as a tungsten mine, producing 30–40 tonnes of concentrates per month. Previous studies include work by Ahlfeld and Schneider-Scherbina (1964) and Pinto (1989d). The area was visited in November 1990.

Geologic Setting

The veins in the Esmoraca area occur in the easternmost of the large dacitic volcanic centers (pl. 1, Tvnd) in the Sud Lípez area; the highest peak in the area is Cerro Galán, at 5,347 m (fig. 93). This massif is the least known of all the dacitic centers in Sud Lípez. At Esmoraca, the dacites appear to be intrusive; sills of dacite can be seen intruding the underlying sedimentary rocks. From a distance, subhorizontal banding, high on the mountain, suggests that volcanic rocks are present at higher altitudes. Ahlfeld and Schneider-Scherbina (1964) also noted the presence of tuffs. Several dacitic dikes were noted during our visit. The underlying sedimentary rocks are red shales, sandstones, and conglomerates of either the middle Tertiary San Vicente Formation or the lower Tertiary Potoco Formation (pl. 1, Ts1). The area lies a few kilometers west of the structural margin of the Altiplano, a large, north-

south trending fault that exposes Paleozoic sedimentary rocks (pl. 1, Pzs) on the east side. This fault is apparently a west-verging reverse fault related to thrusting of the main Andean orogen.

Mineral Deposits

There are numerous veins in the Esmoraca area. Most veins trend about east-west, are relatively thin (less than 1 m) and have a mineral assemblage that consists of various combinations of bismuthinite, matildaite, hematite, pyrite, chalcopyrite, wolframite, sphalerite, and gold, in a predominantly quartz gangue. Ahlfeld and Schneider-Scherbina (1964) reported emplectite ($CuBiO_2$) in veins at an unknown locality, high in the central part of the Galán massif, as well as a quartz-tourmaline-pyrite-wolframite vein at an unknown locality.

Pueblo Viejo Mine

Mina Pueblo Viejo is on the central vein in the area, is owned by San José de Berque Ltda., and is the only mine in the area currently operating. The vein at Pueblo Viejo trends slightly north of west and has been exploited on at least 3 levels over a vertical range of more than 100 m; the workings are almost 1.5 km long. Exploratory workings below the lowermost (Santa Elisa) level of the mine have encountered the veins emplaced in redbeds beneath the floor of the igneous complex.

Samples from dumps at two levels of the mine show substantial amounts of gold (as much as 15 ppm), copper (as much as 1.2 percent), and bismuth (as much as 0.9 percent), as well as interesting values for tin and tungsten (table 31).

Petrographic examination of sample 90BSL092a, collected from dumps at the lowest working level of the mine, showed a vein filled with radiating quartz crystals,

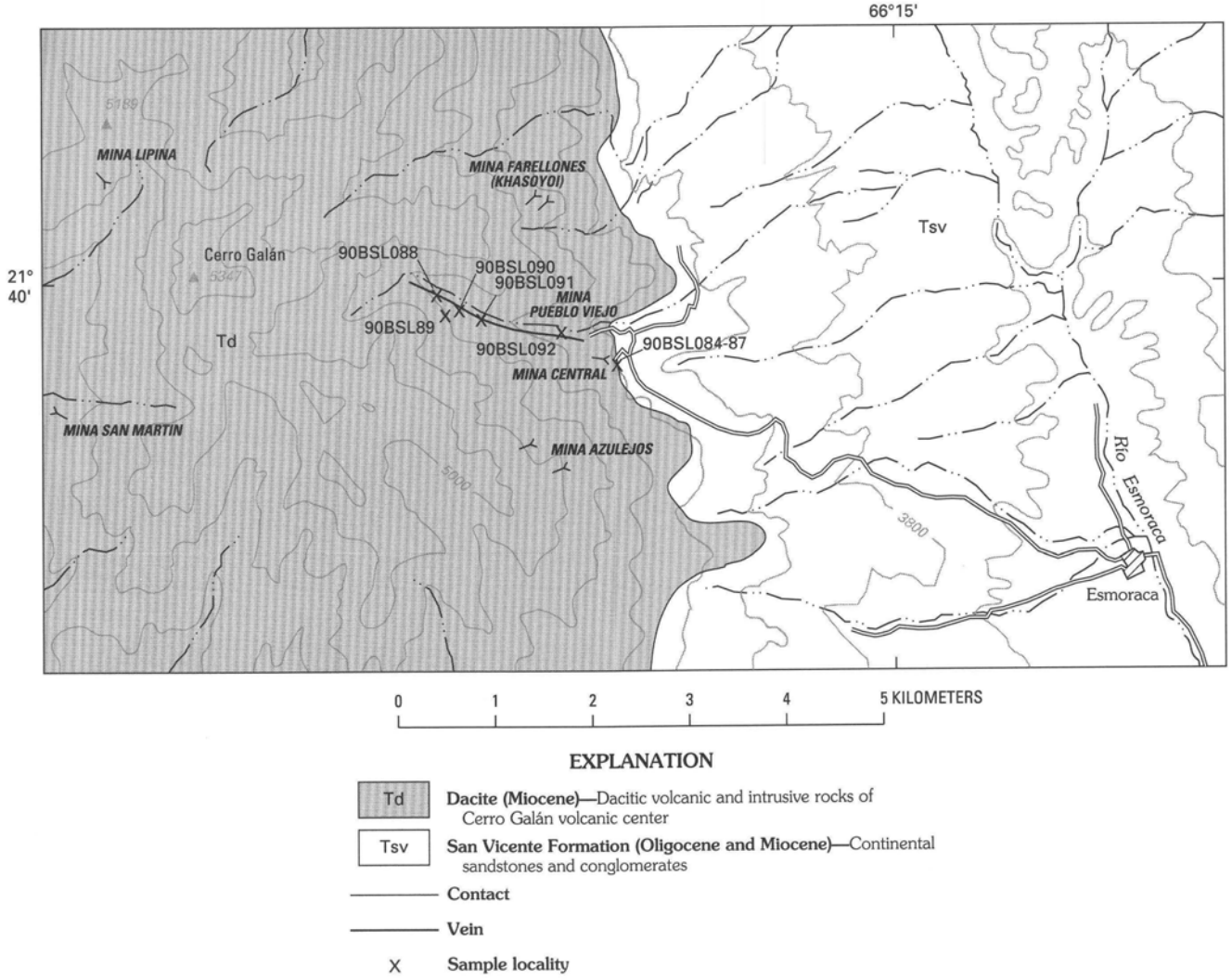


Figure 93. Map showing geology and sample localities in the Esmoraca area, Bolivia. Geology modified from unpublished mapping by the Servicio Geológico de Bolivia. Contour interval, 100 m; base modified from Esmoraca (6328 I), La Cienega (6328 IV), Khuchu (6329 II), and Cerro Yano Orkho (6329 III) 1:50,000-scale quadrangles.

Table 31. *Chemical analyses of mineralized rocks from the Esmoraca area, Bolivia*

[All values in parts per million (ppm). Sample 90BSL084c contains 25 ppm Mo and sample 90BSL092a contains 50 ppm Mo. Sample descriptions, methods, and complete results in appendix B]

Sample no.	Au	Ag	Pb	Zn	Cu	As	Sb	Sn	Bi	W
Dump, Mina Central										
90BSL084a	1.2	5.9	2,500	320	8,400	160	120	700	24,000	700
90BSL084b	1.5	4.6	2,800	140	5,200	540	290	700	61,000	700
90BSL084c	.1	4.7	70	130	6,300	74	44	700	530	500
Dump, Mina Pueblo Viejo										
90BSL088a	0.004	2.3	20	2.7	3.3	15	3.8	30	22	100
90BSL088b	.004	.63	85	6.1	12	43	8.2	100	6.3	70
90BSL088c	2.10	22	100	23	12,000	120	30	30	9,000	150
90BSL092a	15.0	14	69	75	6,400	60	37	1000	88	3,000
Altered dacites										
90BSL085	<0.002	0.27	50	130	44	20	7.5	70	20	50
90BSL086	.15	18	770	183	350	140	32	30	1,000	100
90BSL087	<.02	.1	49	96	41	35	14	<10	12	<20
90BSL089	.002	.08	2.8	3.6	3.9	<.6	<.6	15	<.6	<50
90BSL090	<.15	.09	2.8	250	34	1.5	.75	<10	<.6	<20
90BSL091	<.002	.43	17	11	29	63	19	15	35	<20

pyrite, tourmaline, and hematite. Wolframite occurs as sparse, subhedral crystals and irregular grains about 100 to 200 μ across. Average cation proportions of manganese-to-iron-to-tungsten, based on a limited number of semiquantitative scanning electron microscopic determinations, were 5:21:74. In some areas, concentrations of small cassiterite grains were noted, as well as rare chalcopyrite. Sample 90BSL088a, from the uppermost level of the mine, contained only quartz, pyrite, and tourmaline. Quartz in both samples contains small fluid inclusions consisting of liquid and vapor.

Central Mine

Located a few hundred meters south of Mina Pueblo Viejo, Mina Central exploited a 4 m-wide zone containing 4 narrow veins; this zone was worked in the past for a few tens of meters. Development of mineralized rock was reportedly sporadic along these structures, consisting primarily of pyrite, with traces of chalcopyrite and bismuthinite. Analyses of some samples collected previously by COMIBOL yielded gold values between 4 and 68 g/t (Pinto, 1989d). Another nearby structure that contains specular hematite, pyrite, chalcopyrite, chalcocite, bornite, and enargite yielded gold values of 3–20 g/t. Samples that we collected from the dump of this mine (table 31) showed important amounts of gold, copper, bismuth, and tin.

Petrographic examination of sample 90BSL084a, also collected from the dump at Mina Central, showed it to consist primarily of quartz, pyrite, and iron oxides, with substantial amounts of bismuthinite and chalcopyrite. Sphalerite and wolframite were noted in trace amounts.

Azulejos Mine

Mina Azulejos is situated at about 4,800 m, 1 km south of Mina Pueblo Viejo (fig. 31). It apparently consisted of two narrow (15–30 cm), east-west trending veins that were worked for several hundred meters. The veins contained pyrite, chalcopyrite, bismuthinite, and a little gold and were explored on only one level (Pinto, 1989d).

Farellones (Khasoyoj) Mine

Located a few hundred meters north of Mina Pueblo Viejo, little is known of the veins at this mine, except that they carry hematite and pyrite, and yielded values in bismuth, tin, and tungsten (Pinto, 1989d).

Other Mines

Two other mines, San Martin and Lipina, are shown on the topographic maps, both about 4 km west of the Pueblo Viejo area, on the west side of the volcanic complex. They are inaccessible by vehicle, and nothing was found about them in the literature.

Alteration

Hydrothermal alteration is widespread throughout the entire volcanic massif; the alteration exhibits a wide range of colors when seen from a distance and on satellite images. In the vicinity of the mines visited, the alteration is pervasive, and varies from propylitic to phyllic. Petrographic examination of samples 90BSL085, 86, 89, 90, and 91 showed biotite invariably altered to mixtures of

chlorite and sericite; feldspar was replaced by sericite in varying degrees. All of these samples contain saline, halite-bearing fluid inclusions in the quartz phenocrysts. Many of the samples contain anomalous amounts of various metals, including gold values as high as 0.15 ppm (table 31).

Conclusions and Recommendations

The Esmoraca area is one of the least known of the polymetallic districts in the study area. Gold-bearing bismuth-tungsten veins are found over a wide area and large amounts of rock have been subjected to pervasive hydrothermal alteration. Although detectable amounts of gold are common in this area, the known veins are unlikely to yield large, new resources. Nevertheless, the area must be mapped geologically and altered rocks sampled in order to determine the potential for bulk-mineable deposits.

JAQUEGUA AREA

By Steve Ludington, Edward A. du Bray, *and* Eduardo Soria-Escalante

Summary

The Jaquegua area (app. A, no. 382) consists of a number of silver-bearing barite-manganese-quartz veins that intrude tuffs and clastic rocks of the Miocene Upper Quehua Formation. Widespread silver-bearing veins and large amounts of sericitic alteration suggest that the Jaquegua area may be the site of a major hydrothermal system, most of which is still unexposed.

Introduction

The Jaquegua area consists of a number of vertical, east-west trending barite-manganese-sulfide veins that have produced ore since Spanish colonial times. The area was worked extensively in the 16th century, and may have been the second place in the Lípez area, after San Antonio, populated by the Spaniards. The veins are hosted in ash-flow tuffs and debris flows of the Upper Quehua Formation. The area is located on the north bank of Río San Antonio, in the San Antonio de Lípez (6228 III) and San Antonio de Esmoruco (6228 II) 1:50,000-scale quadrangles. It is located about 250 km southwest of Uyuni and about 45 km south of San Pablo de Lípez. The road that descends from the Altiplano to the bottom of the canyon of Río San Antonio is impassable to vehicles the last 3 km, although it could be repaired relatively easily. The area apparently includes concessions belonging to both COMIBOL and private parties. Previous studies include those by Servicio Geológico de Bolivia (1971x) and Zubrzycki and Murillo (1958b), although the area has received relatively little study, apparently because of its remoteness. The area was visited in November 1990.

Geologic Setting

Almost flat-lying ash-flow tuffs, their reworked equivalents, and debris flows of the Upper Quehua Formation (pl. 1, Tig) host the deposits in the Jaquega area (fig. 94). The Upper Quehua Formation in this area is principally composed of numerous ash flows, some of which may have cooled together as compound cooling units. The tuffs, which are weakly welded and poorly indurated biotite dacites, contain abundant relatively unflattened pumice blocks and in many places contain abundant lithic fragments of older dacite porphyries. The tuffs are relatively crystal poor, and contain phenocrysts of biotite, feldspar, and rare quartz, many of them broken (sample 90BSL079).

The Upper Quehua Formation is at least 300 m thick in the area. Tuffs of the Upper Quehua Formation are overlain to the northwest of the area by dacitic lava flows from the Cerro Lípez volcanic center. To the south, across Río San Antonio, the tuffs appear to be covered by outflow tuff from the Panizos caldera to the southeast.

In the northern part of the area, the tuffs are overlain and intruded by plagioclase-biotite-quartz dacite lavas and stocks (pl. 1, Tvnd). These dacite lava flows and stocks are petrographically similar to those exposed elsewhere in Sud Lípez. The phenocryst assemblage in dacite sample 90BSL083 is virtually identical to that in the tuffs.

The tuffs have locally been reworked; the resulting deposits are well-sorted, fine-grained tuffaceous sedimentary rocks. Rare debris flows also crop out at several places, principally low in the stratigraphic section. These rocks are poorly sorted conglomerates that principally contain clasts (3–15 cm) of older dacite porphyries. Contact relationships suggest that underlying ash-flow deposits were scoured during debris flow deposition.

Mineral Deposits

The Jaquegua area is characterized by a large number of silver-bearing veins, many of which have been mined at some unknown time in the past (fig. 94). Servicio Geológico de Bolivia (1971x) reported on twelve separate veins, in a study that covered only part of the district. Most veins strike almost east-west, although a few in the northern part of the area trend northwesterly; most dip almost vertically. Many of the veins have widths in excess of 1 m. They are remarkable for their persistence and many can be traced for

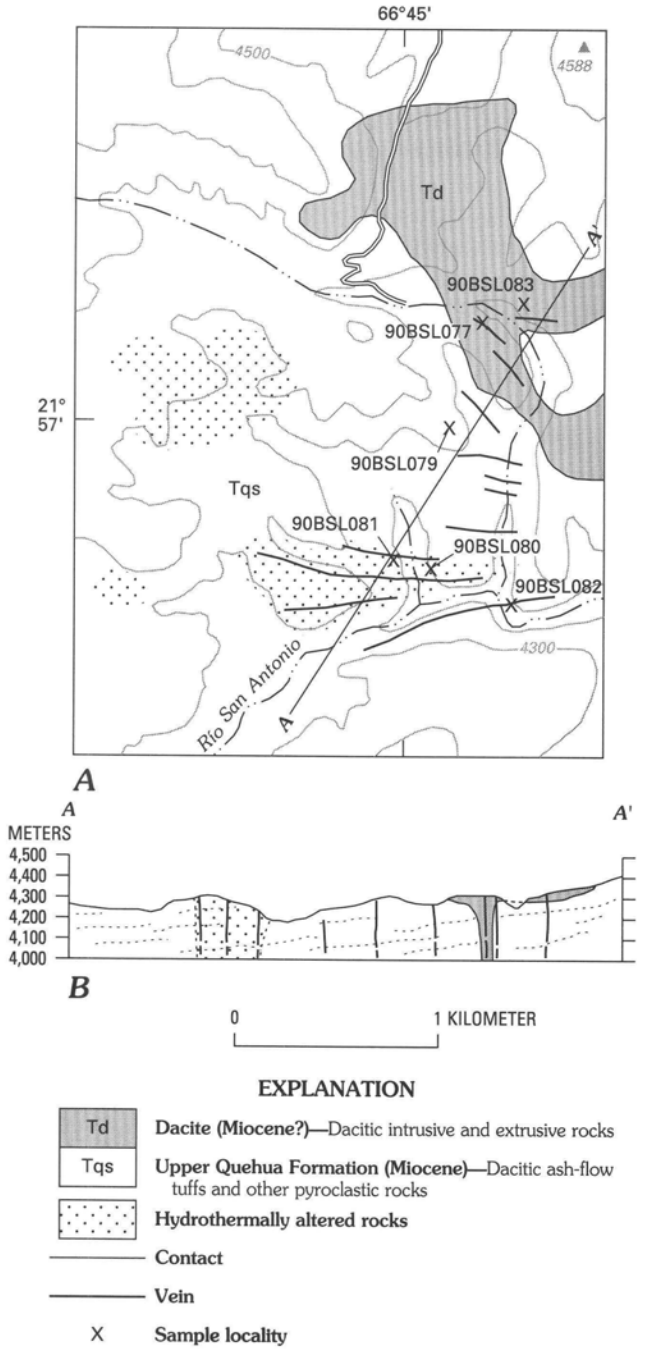


Figure 94. Geology, alteration, and sample localities in the Jaquegua area, Bolivia. *A*, Map showing geology mapped by Ludington and du Bray. Contour interval, 100 m; base modified from the San Antonio de Lípez (6228 III) and San Antonio de Esmoruco (6228 II) 1:50,000-scale quadrangles. *B*, Cross section through area.

several kilometers. Barite, manganese oxides, and galena are the most common vein minerals. The prominent barite and manganese minerals are reminiscent of the deposits at San Cristobal and Mesa de Plata. Sphalerite, argentite, and quartz are less common (Zubrzycki and Murillo, 1958b).

GEOBOL collected 200 samples in the area and analyzed them for silver, lead, and zinc (Servicio Geológico de Bolivia, 1971x). These samples were collected primarily from veins in underground workings and surface outcrops, although some samples of altered rock were also collected. Lead and zinc concentrations in the samples approximate log normal distributions, however too many silver values were below the lower limit of determination to evaluate. The median concentrations are silver, 3 ppm; lead, 0.5 percent; and zinc, 0.8 percent. The maximum values are silver, 79 ppm; lead, 27.3 percent; and zinc 5.24 percent. Lead and zinc are not correlated at all, whereas lead and silver show a strong positive correlation, except for a few anomalous samples that appear to be enriched in silver (fig. 95). These anomalous samples are probably the result of supergene silver enrichment; the correlation of lead and silver in the majority of the samples suggests that silver occurs primarily in galena. Zubrzycki and Murillo (1958b) obtained similar results on a smaller number of samples. However, they analyzed one composite dump sample for which they obtained a gold concentration of 0.8 ppm. We collected three samples of barite-manganese veins (fig. 94). The geochemical results in table 32 are generally in agreement with the earlier studies, although very little gold was detected.

Hydrothermal alteration associated with the vein system is widespread. Previous workers have all mentioned that the altered rocks can be clearly seen from a great distance. We concur that the volume of altered rock in the

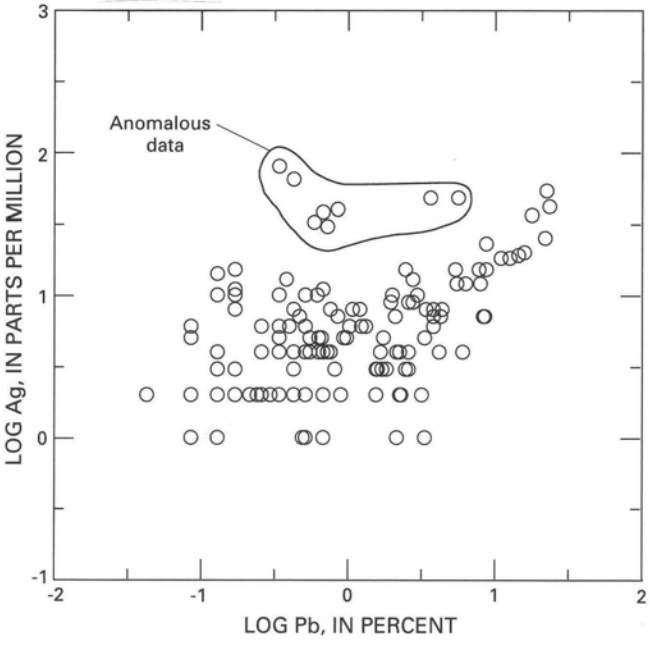


Figure 95. Plot showing relationship of silver and lead values in samples reported in Servicio Geológico de Bolivia (1971x) for the Jaquegua area, Bolivia. Samples enriched in silver are outlined as anomalous data; there is good correlation between lead and silver in the remainder of the samples.

Table 32. *Chemical analyses of mineralized rocks from the Jaquegua district, Bolivia*

[All values in parts per million (ppm). Sample 90BSL082 contained 0.014 ppm Au. All samples contain <100 ppm Cu, <10 ppm Sn, and <6 ppm Bi. Sample descriptions, methods, and complete results in appendix B]

Sample no.	Ag	Pb	Zn	Cu	As	Sb	Mn
			Ash-flow tuff				
90BSL079	0.051	27	58	10	23	0.98	500
90BSL080	11	11,000	>1,600	38	280	96	700
			Dacite				
90BSL083	0.29	55	13	8.9	6.3	50	700
			Barite veins				
90BSL077	150	3,400	430	9	30	26	>5,000
90BSL081	340	37,000	2,300	65	300	230	>5,000
90BSL082	390	130,000	<0.3	<0.3	<6	800	>5,000

district is impressive. Servicio Geológico de Bolivia (1971x) reported that sericite was the most abundant alteration mineral, followed by clay minerals.

Conclusions and Recommendations

Silver-bearing veins and hydrothermal alteration are scattered over more than 10 km^2 in the Jaquegua area. The persistence and extent of the mineralization and alteration indicate the presence of a possible major hydrothermal system, which is probably largely buried at depths of a few tens to hundreds of meters. The district is largely unexplored and systematic sampling of the veins and wallrocks, including analysis for gold, is necessary to determine if mineable material is present.

OTHER METALLIC DEPOSITS

INTRODUCTION

Metallic deposits whose affinity with specific mineral deposit types is either not clear, or that belong to deposit types not discussed in the first three parts of this section are included in this section. It is our belief that most of the deposits classed as uncertain will be shown ultimately to be either polymetallic vein deposits or epithermal precious-metal deposits.

LA ESPAÑOLA PROSPECT

By Eduardo Soria-Escalante *and* Rubén Terrazas

Summary

The La Española prospect is emplaced in a shallow subvolcanic or volcanic environment. It is composed of two intensively argillized bodies with propylitic envelopes. Highly silicified shear zones in the argillic alteration contain disseminated gold and silver mineralization as well as disseminated sulfides (pyrite, galena, sphalerite). It is likely that this deposit will be developed.

Introduction

La Española is the northern and westernmost deposit in the Bolivian Cordillera Occidental (app. A, no. 122). The area was first discovered and mined for silver in Spanish colonial times at the old Santa Rosa mine, now abandoned. Located in the Thola Kkollu (5642-II) 1:50,000-scale quadrangle, the area is 187 km west of La Paz and 5–6 km east of the Bolivia-Peru border. It can be reached by a well maintained dirt road that runs between La Paz and southern Peru.

The deposits of the area are poorly known and there is no published information available. The La Española prospect presently is under evaluation by EXPROMIN. Two short visits were made to the area, one with EXPROMIN personnel.

Geologic Setting

The La Española deposit is emplaced in a northwest-southeast trending strip of volcanic and volcaniclastic rocks; the Abaroa Formation (pl. 1, Tvnd), is surrounded by younger volcanic rocks of Upper Miocene Cerke and Sinejavi volcanics (pl. 1, QTev). The Abaroa Formation is a sequence of alluvial facies, mudflows, and fragmental volcaniclastics of reworked volcanic material and pyroxene-bearing andesite lava flows. The rocks of the Abaroa Formation are the oldest in the area (22–14 Ma, Evernden and others, 1977; 18–13 Ma, Lavenu and others, 1989); they represent the back-arc, proximal facies of the Western Andean continental arc in Neogene times. Further east, towards the center of the Altiplano, the Mauri Formation is the contemporaneous, distal equivalent of the Abaroa Formation.

Table 33. *Selected chemical analyses of mineralized rocks from the La Española area, Bolivia*

[All values reported in parts per million (ppm). Sample descriptions, methods, and complete results in appendix B. All samples contain <25 ppm As, <1 ppm Sb, <3 ppm Bi. Sample 90BES029 contains 500 ppm B; sample 90BES032 contains 30 ppm Sn]

Sample no.	Au	Ag	Pb	Zn	Cu
90BES006	<0.002	3.1	220	12	25
90BES007	<.002	2.8	<20	18	40
90BES008	.066	13	55	44	3.9
90BES009	.25	390	54	14	37
90BES010	<.002	2.1	55	230	20
90BES011	<.15	<.045	7.6	32	25
90BES012	<.15	<.045	6.9	22	31
90BES013	<.15	<.045	4.6	24	24
90BES029	<.002	.42	<3.8	2.0	18
90BES030	<.002	.24	32	3.3	5.2
90BES031	<.002	.059	2.9	35	17
90BES032	.008	.28	26	7.1	31

Several dacitic intrusions and volcanic domes and flows, like those at Mariajichu, Milluni, and Ayruchu (fig. 96), are emplaced in the La Española area. These dacites have a phenocryst assemblage of plagioclase, hornblende, and biotite, with almost no quartz. A last extrusive episode emplaced the dacitic volcanic dome at Thola Kkollu, which probably represents the youngest magmatic event in the area (fig. 96).

Two previously unpublished K–Ar dates were taken by M. Macintyre (Scottish Universities Research Reactor Centre) at the Milluni dome and at a small biotite dacite dome that is emplaced on the northern side of the Mariajichu dome. Hornblende from the first sample, a volcanic andesite, provided an age of 11.2±0.7 Ma. Biotite from the latter sample, an intrusive dacite, provided an age of 11.8±0.8 Ma.

Field relationships suggest that an important episode of dacitic magmatism occurred about 11 Ma (Milluni, Ayruchu domes). The propylitic alteration affecting the Mariajichu dome suggest that alteration occurred after 11 Ma, before the young, fresh, dacitic cupola (Late Miocene?) that intrudes the top of San Gerónimo (fig. 96).

Description of Deposits

Mineralization at La Española is hosted in two bodies of highly argillized and locally silicified rock (fig. 96). The Abaroa Formation is disturbed and propylitized around the altered bodies suggesting an intrusive contact. An upper level, domelike, shallow felsic intrusion is inferred, but the exact nature and composition of the host rock is obscured by intense alteration. The Mariajichu dome (fig. 96), of propylitized, dacitic composition was emplaced south of the mineralized bodies.

There are two areas of interest, Santa Rosa and San Gerónimo, located in each of the domelike bodies that are being investigated for development (fig. 96). At Santa Rosa, a highly argillized core is surrounded by a propylitic zone. Sericitic alteration has been identified in several areas around the southern part of the altered body; sericite may have been more widespread before weathering. In the argillic area, a predominant shear zone that trends between N. 75° E. and east-west, is locally intensively silicified and mineralized with disseminated pyrite, sphalerite, and galena. These silicified areas are intensively sheared and generally have low concentrations of microcrystalline disseminated gold. Another set of shear planes, trending about N. 45° E., is also locally silicified. Dikes and a set of narrow silica veins (10 cm) with massive sulfides and high silver values also occur in the area. The silicification appears to be younger than the argillic alteration. No visible gold has been found in drainage sediments or in the host rock.

Mineralization in the San Gerónimo area consists of a similarly argillized body with a propylitic envelope. The argillic core is intruded by a fresh dacitic stock (fig. 96). A N. 60° E. trending shear zone appears to be developed in a silicified stockwork that is mineralized with pyrite and barite; anomalous gold and silver are present. The stockwork was mined by the Spanish at the base of the hill. Jarosite and well crystallized alunite are present in surface outcrops. San Gerónimo probably represents a higher level hydrothermal system than Santa Rosa. Silicification again appears to be younger than argillic alteration. Flakes of gold have been found in the drainage downstream from San Gerónimo. A set of veins that trends N. 80° W., bearing

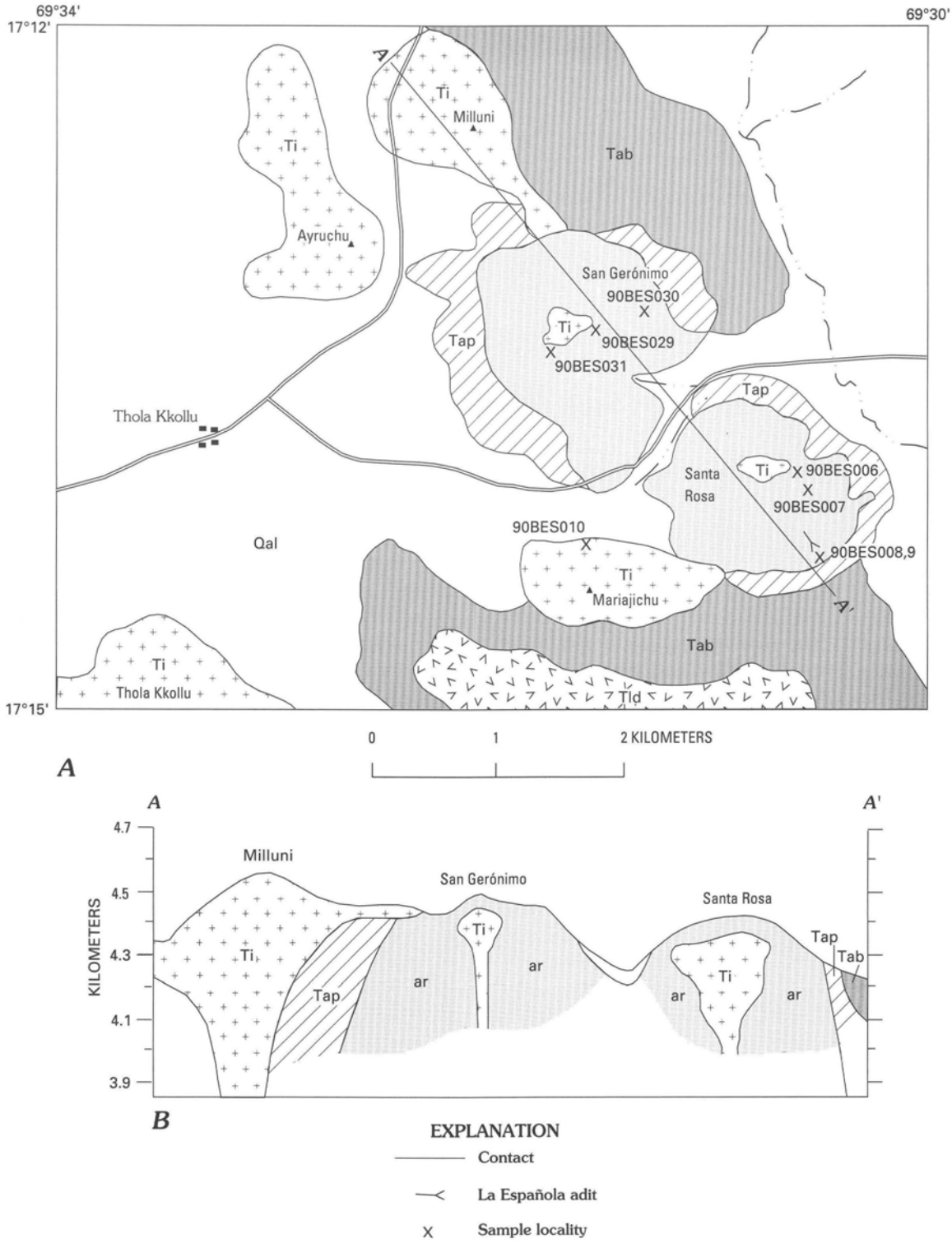


Figure 96. The La Española area, Bolivia. *A*, Map showing geology and sample localities. Geology mapped by Eduardo Soria-Escalante. Qal, Quaternary alluvium; Tld, Tertiary dacitic lavas; Ti , Tertiary intrusives of dacitic composition; Tap, propylitized Abaroa Formation; Tab, Abaroa Formation. *B*, Cross section through Santa Rosa and San Gerónimo; ar, argillic alteration with silicified shear zones.

pyrite, galena, sphalerite, and barite, with anomalous concentrations of gold and silver, is emplaced in the foothills west of San Gerónimo.

Geochemical results for selected samples are shown in table 33. Twelve samples were analyzed, seven from the altered areas at Santa Rosa (samples 90BES006–9) and San

Gerónimo (samples 90BES029–31), and five from less altered domes and flows in the vicinity. Sample localities are shown on figure 96, except for samples 90BES011, 12, 13 and 32, which were collected north and south of the area shown on the figure. Complete results and sample descriptions are found in appendix B.

The samples from Santa Rosa are of argillized and silicified rock that is oxidized and shows boxwork textures after sulfide minerals. The two samples of altered rock (samples 90BES006, 7; fig. 96; table 33) showed only minor enrichment in lead and silver, whereas samples 90BES008 and 90BES009, from a high-sulfide vein at the La Español an adit showed precious-metal contents as high as 0.25 ppm gold and 390 ppm silver.

Three samples from San Gerónimo (samples 90BES029–31, fig. 96) are of slightly silicified, argillized rock, with fresh sulfides. These samples had only slight enrichment in silver, and gold values as high as 0.008 ppm (table 33).

The generally low base metal and tin contents of these samples (table 33; app. B) suggests that the La Española system is more closely related to epithermal precious-metal deposits than to Bolivian polymetallic vein deposits, and it may represent the outer fringes of a porphyry gold system.

The remaining samples do not clearly show enrichment in any ore elements, except for sample 90BES010, a sample from the Mariajichu dome that contains 2.1 ppm silver. This sample is weakly affected by propylitic alteration, but most of the remaining samples appear to be fresh.

Conclusions

La Española prospect seems to be an example of a deposit in a volcanic or shallow subvolcanic environment that contains disseminated sulfides, gold, and silver associated with silicic alteration. Detailed study of the deposit may provide a useful model for similar felsic altered bodies intruding the Abaroa Formation, observed in areas further south (for example, Cerro Chillahua at Estación Abaroa). Other prospects in the vicinity are typical examples of epithermal mineralization in volcanic settings (for example, Antacahua, Sinejavi, Cerke).

PACHEKALA PROSPECT

By Steve Ludington, Edward A. du Bray, *and* Eduardo Soria-Escalante

Summary

The Pachekala prospect consists of a group of gold-bearing breccias with an unusual matrix of magnetite and (or) hematite with or without apatite formed in a large pluton of intermediate composition that intrudes Tertiary sedimentary rocks. The presence of this deposit suggests the possibility for a previously unsuspected deposit type on the Altiplano, similar to gold deposits in New Mexico and Chile.

Introduction

The Pachekala prospect (app. A, no. 36) is about 60 km southwest of La Paz and is located in the Collana (5943 III) and Estación General Ballivián (5942 IV) 1:50,000-scale quadrangles. The area can be reached by the road that connects Viacha and Corocoro. The prospect is reached by relatively new exploration roads from a point just west of Comanche (fig. 97). The prospect was discovered and explored during the 1980's. We visited the area in November 1990, guided by Craig McEwan of Minería Técnica Consultores Asociados (MINTEC).

Geologic Setting

Cerro Miriquiri (4,842 m) is a composite intrusion of about 8 km^2 that consists primarily of andesite porphyry that is intruded by a dacite porphyry (pl. 1, Ti). The Comanche intrusion (fig. 97), which has been quarried extensively for paving blocks and building stone, is a sill of andesite that crops out to the northeast of the main intrusion (Redwood and Macintyre, 1989). Three K–Ar ages on hornblende have been determined by Evernden and others (1977) and McBride (1977); their average age is 16.7 Ma, consistent with the stratigraphic evidence.

Redwood and Macintyre (1989) report extensive propylitically altered rock at Miriquiri, as well as local zones of phyllic and silicic alteration. One sample collected from the southern part of Cerro Miriquiri (app. B, sample 90BDB010) contains about 64 percent SiO_2 on an anhydrous basis and is weakly propylitically altered; in contrast the sill on Cerro Comanche (app. B, sample 90BDB011) is quite fresh and slightly more mafic (about 61 percent SiO_2 on an anhydrous basis). Near the top of Cerro Miriquiri, some rocks are preserved that are probably volcanic in origin; their distribution has not been mapped.

Mineral Deposits

At the northwestern base of Cerro Miriquiri, an unusual brecciated zone is exposed; clasts of dacite are set in a matrix of intergrown magnetite and apatite. One sample of breccia with a magnetite-apatite matrix from this area contains no anomalous metals (app. B, sample 90BSL119). Rocks surrounding the breccia do not appear to be mineralized or altered.

Near the top of the Cerro Miriquiri, fractured and brecciated volcanic and intrusive rocks are cut by veins of

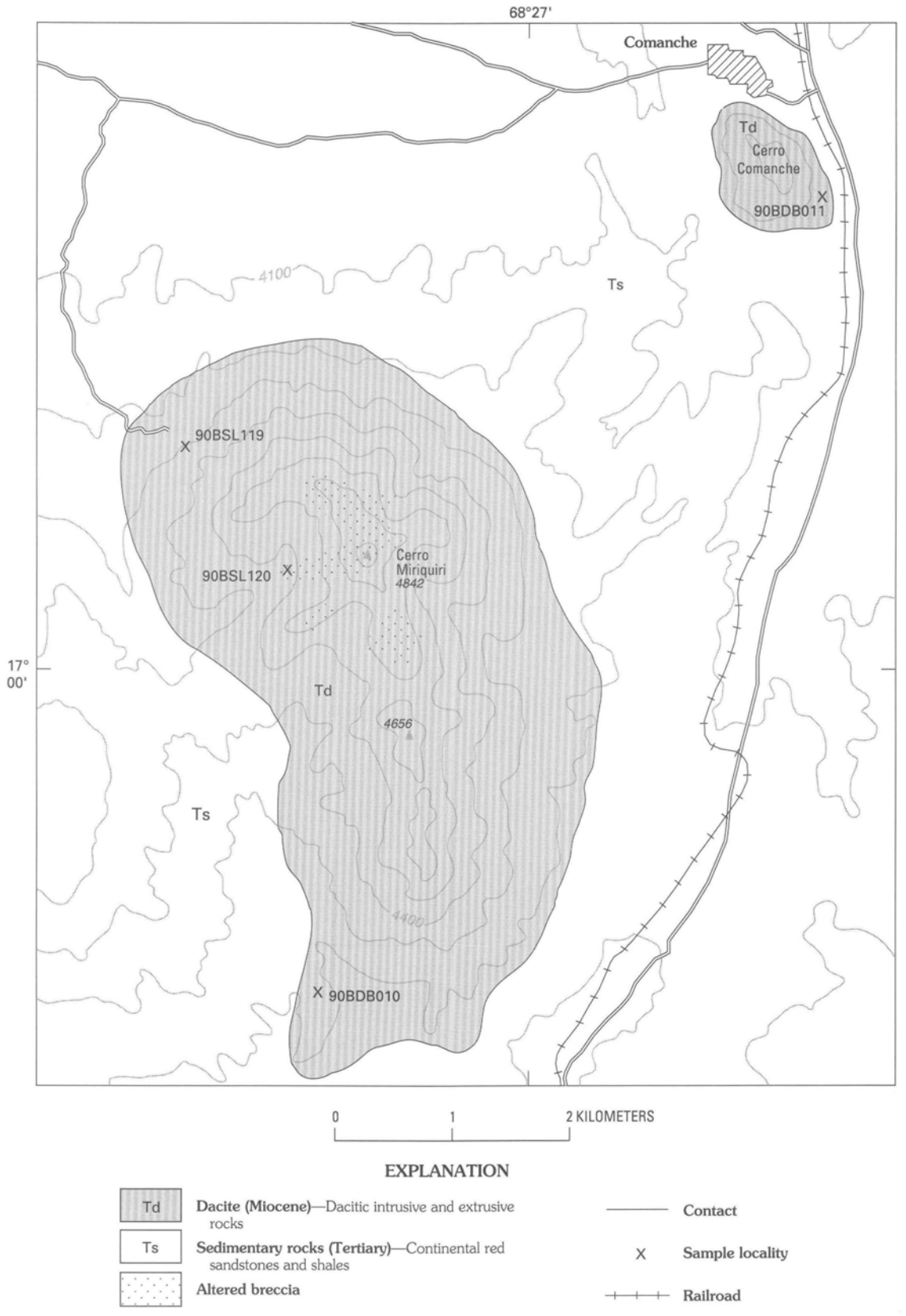


Figure 97. Map showing geology and sample localities in the area of the Pachekala prospect, Bolivia. Contour interval, 100 m. Geology modified from unpublished mapping by Servicio Geológico de Bolivia. Topographic base from the Collana (5943 III) and Estación General Balliván (5942 IV) 1:50,000-scale quadrangles.

specular hematite, with minor magnetite, barite, and apatite. This mineral assemblage also makes up the groundmass of the breccia, that in places is strongly developed and matrix supported. Surface samples contain as much as 5 g/t gold (Craig McEwan, oral commun., 1990). Gold contents in the area are highly erratic, and the geometry of the brecciated bodies is very irregular. Four relatively shallow (<100 m) diamond drill holes near the top of Cerro Miriquiri encountered gold mineralization at depth, but the assay results did not warrant further development. One sample of specular hematite breccia from this area contains 0.66 ppm gold and 1,500 ppm barium, but little else of interest (app. B, sample 90BSL120).

Conclusions and Recommendations

The presence of gold mineralization in hematitic breccias is reminiscent of the deposit at Cerrillos, New Mex. (Wright, 1983), where breccias related to a Mesozoic monzonite have been successfully mined for gold. Magnetite- and hematite-rich rocks are also found at the Marte porphyry gold deposit, in the Maricunga district, Chile (Sillitoe, 1991). Although the major part of the Cerro Miriquiri deposit may have been lost to erosion, its existence raises the possibility for other such deposits on the Altiplano.

LAURANI AREA

By Steve Ludington *and* Edward A. du Bray

Summary and Conclusions

The Laurani area is a typical quartz-alunite vein deposit, hosted in a Late Miocene volcanic center, emplaced along the Coniri fault, which separates Cretaceous redbeds from Paleozoic sedimentary rocks. In addition to the high-grade copper-gold veins, there is potential for bulk-mineable ore in the deposit; it is actively under development.

Introduction

The Laurani area (app. A, no. 48) consists of several quartz-alunite veins that cut Late Miocene volcanic rocks. The volcanic complex is located about 100 km south of La Paz, at the eastern edge of the Altiplano, near Sica Sica, and is reached by a gravel road from the Interamerican Highway. The district is located on the Chijmuni (6041 IV) 1:50,000-scale quadrangle, and the deposits are situated at an elevation of about 4,000 m on the slopes of Cerro Capaja (4,362 m). The deposits in the Laurani area have been mined for silver and copper since the 17th century. The area is currently under development as a joint venture that includes United Mining Corporation, Reno, Nev. Previous studies include those of Schneider-Scherbina (1961a), Ahlfeld and Schneider-Scherbina (1964), and a recent report by Garzón (in press). We visited the property in November 1990.

Geologic Setting

The Laurani area deposits are located in an isolated Late Miocene volcanic complex (8.4 Ma; Redwood and Macintyre, 1989), on the eastern edge of the Altiplano. The volcanic complex (pl. 1, QTev) overlies and intrudes Paleozoic sedimentary rocks on the east (pl. 1, Pzs) and Cretaceous redbeds on the west (pl. 1, Ks). The Paleozoic and Cretaceous rocks were juxtaposed by movement on the Coniri fault, which may have localized emplacement of the Laurani volcanic center (fig. 98). Redwood and Macintyre (1989) suggest that the dacitic to andesitic volcanic rocks exposed in the Laurani massif represent the base of a deeply eroded stratovolcano. Studies by Garzón (in press) suggest that this center is composed of a number of dacitic domes, plutons, lava flows, and a pyroclastic complex of enigmatic character.

The volcanic rocks include dacites, andesites, and hydrothermally altered breccias. The dacites include phenocrysts of plagioclase, biotite, and large, strongly resorbed quartz, in a medium-gray aphanitic to microcrystalline groundmass. Sample 90BSL054 (app. B) displays fresh biotite, but the plagioclase phenocrysts are moderately altered to sericite, and the rare hornblende phenocrysts are altered almost beyond recognition. The dacite porphyry also includes distinctive disc-shaped mafic enclaves and rare potassium feldspar megacrysts as long as 10 cm.

Shallowly dipping contacts between the dacite and underlying Paleozoic and Cretaceous sedimentary rocks suggest that at least part of the dacite is a series of lava flows. However, the massive nature and apparent thickness of the dacite, the relative abundance and coarse grain size of crystals, the lack of internal flow fabric, and the absence of basal breccia suggest that some of the dacite forms sills that may coalesce in three dimensions to form a dacite stock at the core of the Laurani massif.

The andesites, which also may be intrusive, occur only in the most intensively altered, central part of the complex. Quartz phenocrysts are much less abundant in the andesite, but details of the petrography are obscured by strong hydrothermal alteration.

Various types of breccia and pyroclastic rocks that crop out in the upper parts of the Laurani center are intensely altered. Some of the breccias are clearly reworked pyroclastic deposits that include clasts of Paleozoic and Tertiary sedimentary rocks. Other, interlayered breccias

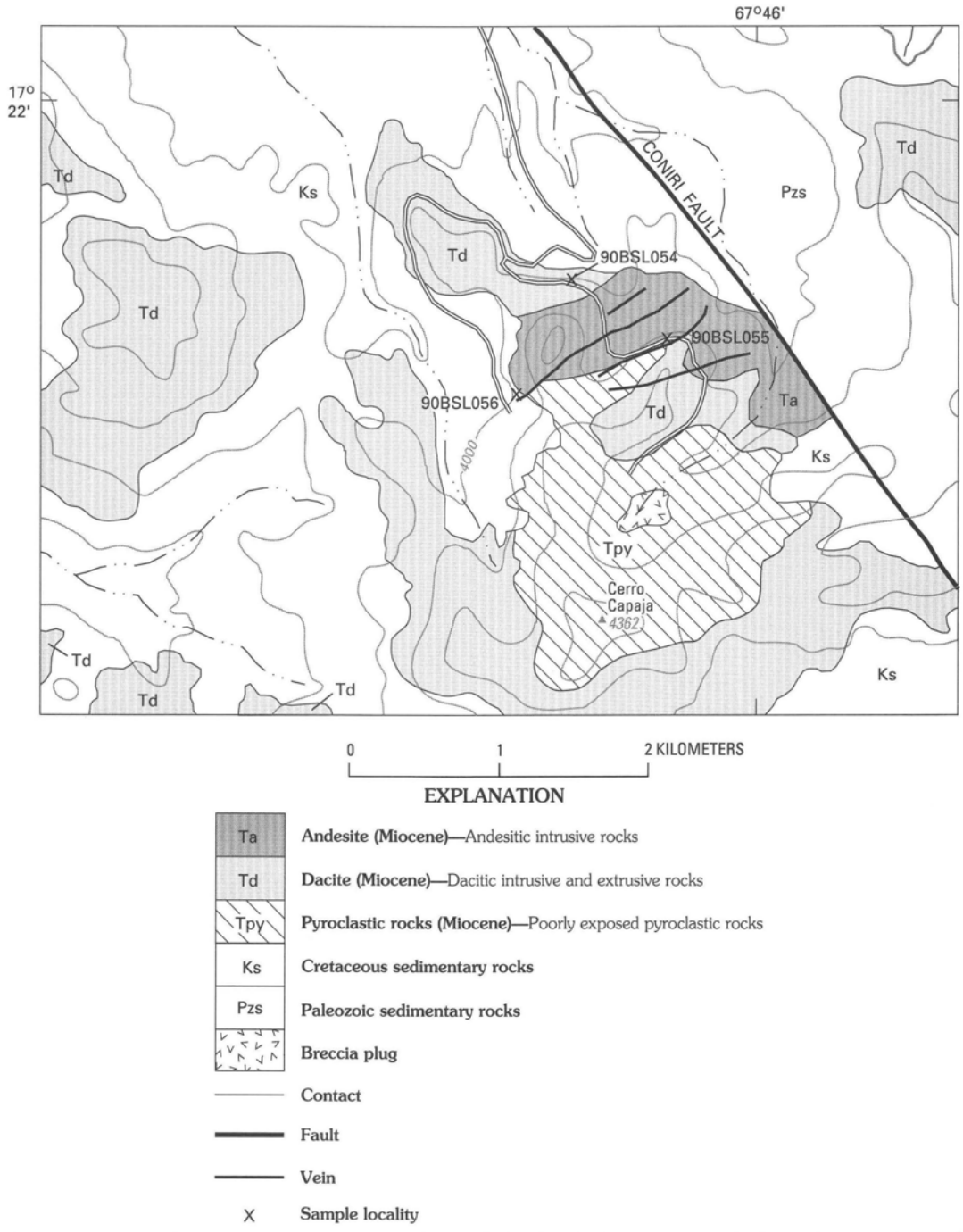


Figure 98. Map showing geology and sample localities for the Laurani area, Bolivia. Contour interval, 100 m. Geology modified from Garzón (in press). Topographic base from Chijmuni (6041 IV) 1:50,000-scale quadrangle.

appear to be severely altered, primary pyroclastic flow breccias that display some of the textural characteristics of caldera-related megabreccias.

Mineral Deposits

The ore deposits in the Laurani area consist of a series of subparallel veins that trend eastnortheast to northeast across the center of the district (fig. 98). They are zoned around a center of intense quartz-alunite alteration (Schneider-Scherbina, 1961a). Closest to the alteration center is a zone characterized by abundant auriferous pyrite and traces of cassiterite. Further out, the primary minerals are enargite, tennantite, and pyrite. Finally, at the extreme northeast end of the mineralized zone, galena, sphalerite, and silver sulfosalts are the primary minerals. Gangue

Table 34. *Chemical analyses of mineralized rocks from the Laurani area, Bolivia*

[All results in parts per million (ppm). Sample descriptions, methods, and complete results in appendix B]

Sample no.	Au	Ag	Pb	Zn	Cu	As	Sb	Sn
90BSL055	1.20	38	520	130	22,000	890	1,100	100
90BSL056	.004	.37	16	7.1	98	91	8.8	<10

minerals include barite, quartz, pyrite, marcasite, alunite, and siderite; barite and alunite are most common in the inner zone, while marcasite and siderite are characteristic of the peripheral zone.

In addition, Schneider-Scherbina (1961a) delineated four temporal phases of mineralization: (1) pyrite-gold-cassiterite (oldest), (2) lead and zinc sulfides and copper sulfosalts, (3) copper-antimony sulfosalts, and (4) copper-precious metal seleno-tellurides (youngest).

Two mineralized samples were collected at Laurani (fig. 98), and the results of analysis are shown in table 34. Sample 90BSL055 is a high-grade vein sample from a dump; sample 90BSL056 is altered and mineralized wall-rock collected a few meters from the edge of a vein. The very high copper and antimony contents of the vein sample are characteristic of quartz-alunite deposits.

The veins near the center of the Laurani area have continuity for at least 2 km and locally, are several meters thick. Garzón (in press) reports that there is disseminated and stockwork mineralization present in the wallrock adjacent to the veins.

Hydrothermal alteration is zoned; there is no published map that shows the distribution of the various facies. A central zone of intense quartz-alunite alteration is reflected in narrow bodies of quartz-alunite rock that immediately border the important veins. Outward from this, an advanced argillic assemblage flanks most of the major veins. Large portions of the Laurani area are altered to quartz and sericite, and, especially at the northeastern periphery, an outermost zone of propylitic alteration is developed.

Historically, the mine was worked primarily for silver and gold, until the twentieth century, when hand-sorted copper ore with a substantial gold content was recovered. Recently, development consisting of drilling and tunneling by United Mining Corporation has been directed toward outlining an ore body that can be mined by bulk methods. Although this exploration has, as yet (December 1990), not been directed toward depths greater than 100 m, the company had developed a geologic projection of approximately 2 million tonnes of ore, with an average grade of 2.5 g/t gold, 220 g/t silver, and 1 percent copper.

Conclusions and Recommendations

The Laurani area is a typical quartz-alunite vein deposit that apparently contains substantial amounts of gold, silver, and copper. The future of the area will be dependent on development work on mineralized areas related to the known deposit. Little indication exists for additional separate deposits in the area.

KISKA PROSPECT

By Steve Ludington, Edward A. du Bray, *and* Edwin H. McKee

Summary and Conclusions

The Kiska prospect is a 13.6 Ma-old mineralized system of indeterminate type that crops out on an isolated hill southwest of the La Joya district. The host rocks are very strongly altered, and contain an abundance of fluid inclusions. Although the samples we collected showed only traces of precious metals, the prospect is being actively explored.

Introduction

The Kiska prospect (app. A, no. 50) consists of a hill of strongly silicified Paleozoic sedimentary rock. Numerous quartz-jarosite veins cut the silicified sedimentary rocks, as well as some small porphyry intrusions. The hill rises about 50 m above a flat plain, about 9 km southwest of Cerro La Joya, on the Llanquera (6040 II) 1:50,000-scale quadrangle. The area is being actively explored by EXPROMIN. Previous exploration appears to have been minimal, and no mention of the area has been found in the literature. The area was visited in October 1990.

Geologic Setting

The Kiska prospect appears to be underlain by Paleozoic rocks (pl. 1, Pzs) that consist of sandstones and siltstones with a few calcareous layers, similar to the sedimentary rocks exposed a few kilometers to the northeast, in the La Joya district (fig. 99). No faults were noted. The sediments are intruded by at least two, possibly more, small bodies of dacite porphyry. Although the porphyry mineralogy has been affected by hydrothermal alteration, it appears similar to other Miocene dacites on the

Altiplano. The dacite consists of quartz and feldspar phenocrysts in a very fine grained groundmass.

Mineral Deposits

Mineralized rock at Kiska consists of a true stockwork of fine-grained veinlets of silica, with or without jarosite, hematite, and alunite ranging in thickness from hairline cracks to about 2 cm. The entire hill has been affected by hydrothermal alteration, which is strongest at the north end and appears to weaken to the south. The alteration minerals are all very fine grained, and consist primarily of quartz, jarosite, which we interpret to represent the oxidation of original pyrite, and lesser amounts of very fine grained clay minerals, alunite, and sericite. The dacite porphyry is also altered and veined, and contain much the same alteration suite as the sedimentary rock. Quartz grains in both the groundmass and in veins in both rock types contain extremely abundant and diverse types of fluid inclusions. The most abundant are large vapor inclusions (as large as 100 μ) which make up a significant portion of the volume of the quartz. Also abundant are inclusions that consist of liquid, a vapor bubble, and a halite crystal. We interpret the fluid inclusion evidence to suggest that the rocks encountered a large volume of boiling brine, that was depositing quartz, sericite, and pyrite.

Two samples were analyzed; sample 90BSL052 is a composite sample of the altered and veined sedimentary rock and sample 90BSL053 is of the mineralized dacite porphyry intrusion (app. B). Both samples contained only traces of precious metals; gold as high as 0.44 ppm and silver as high as 1.1 ppm.

In a few places, the mineralized veins are cut by younger veins consisting primarily of alunite. One sample of this material (app. B, sample 90BSL109) was kindly provided by Douglas Smith of ASARCO. The sample showed an alteration suite adjacent to the vein that is similar to the other rocks on the hill. The vein consists of intergrown coarse, bladed alunite and jarosite. Alunite from this sample was dated at 13.6±0.5 Ma by the K–Ar method (app. C), thus providing a minimum age for the deposit.

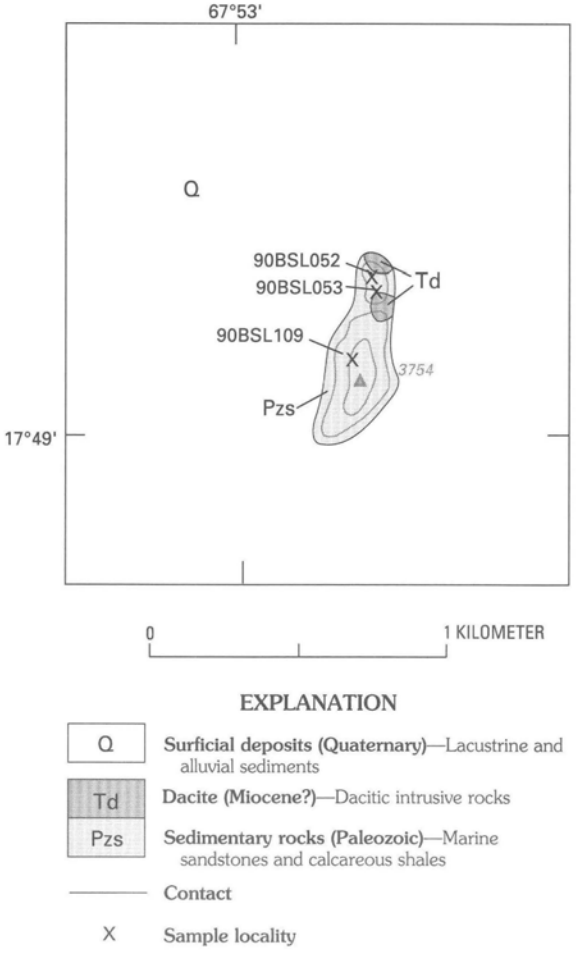


Figure 99. Map showing geology and sample localities at the Kiska prospect, Bolivia. Contour interval, 20 m. Topographic base from the Llanquera (6040 II) 1:50,000-scale quadrangle.

Conclusions and Recommendations

The strong pervasive alteration and remarkable density of fluid inclusions marks the Kiska prospect as the site of a robust hydrothermal system. Although two samples yielded only trace amounts of precious metals, geologists with EXPROMIN have found more encouraging results, and, as of this writing (March 1991), the prospect is being drilled. The age of mineralization is nearly identical to those in the nearby La Joya district.

CHINCHILHUMA VOLCANO AREA

By Eduardo Soria-Escalante *and* René Enriquez-Romero

Introduction

Chinchilhuma is a volcano located in the Cordillera Occidental (app. A, no. 204). Several small deposits on its flanks have been mined since Spanish colonial times; San Salvador and Aguilani are the best known of the deposits. A visit was made to the area in December 1990. There was no activity in the area and mining facilities are very rudimentary and old.

Geologic Setting

The Chinchilhuma district is located on the flanks of an eroded volcano. Although there is no radiometric age

determination on the lava flows, an Upper Miocene age is tentatively assigned based on its very eroded morphology. Well developed glacial deposits are located on the east and southeast flanks of the edifice. Recent hot-spring deposits, chiefly calcareous sinter, cover the floor of the glacial valley.

The country rock consists of hornblende-bearing dacite lava and fragmental flows. These rocks are cut by a shallow intrusion of probable rhyolitic composition, which is locally bordered by zones of intense brecciation and hydrothermal alteration.

Mineral Deposits

Mineralization in the district is located in two main areas, the San Salvador and Aguilani mines (fig. 100). Several minor occurrences are located on the eastern flanks of the volcano.

The San Salvador mine consists of a set of sulfide veins with northwest-southeast strike and almost vertical dip. Two workings are located in the same structure, a vein of massive pyrite, galena, and sphalerite. Some malachite was found on the dumps. Intense silicic and argillic alteration and brecciation is associated with the mineralization.

Samples for geochemical analysis were taken from dumps (table 35, samples 90BES049–50, 53–55), and the results show gold values as high as 1.2 ppm and silver as high as 67 ppm, as well as variable and substantial amounts of copper, lead, and zinc. Two samples of mineralized, altered wallrock (samples 90BES051, 52) yielded gold values as high as 0.3 ppm and silver as high as 150 ppm. Although tin has been reported from this mine (Sanjinés, 1968b), we found no cassiterite on the dumps; the geochemical samples showed some tin in 3 samples (app. B, sample 90BES053, 30 ppm; sample 90BES054, 70 ppm; sample 90BES055, 50 ppm).

Three samples (app. B, samples 90BES046–48) of igneous rocks from the Chinchilhuma area were not visibly mineralized, but contained detectable gold and silver (table 35) suggesting that disseminated mineralization may be present in the area.

At the Aguilani mine, a porphyry stock, probably an apophysis of the one exposed in San Salvador, is intensively brecciated and silicified. At the base of the outcrop, there is a northwest-southeast trending manganese vein. The dumps of the Aguilani mine are very old and consist mainly of alteration products; no solid pieces of ore were found. Judging from the size of the dumps, the Aguilani mine had only very minor production.

Three samples (app. B, samples 90BES056–58) showed gold values as high as 0.16 ppm, silver values as high as 4.3 ppm, and moderate amounts of lead and zinc (table 35).

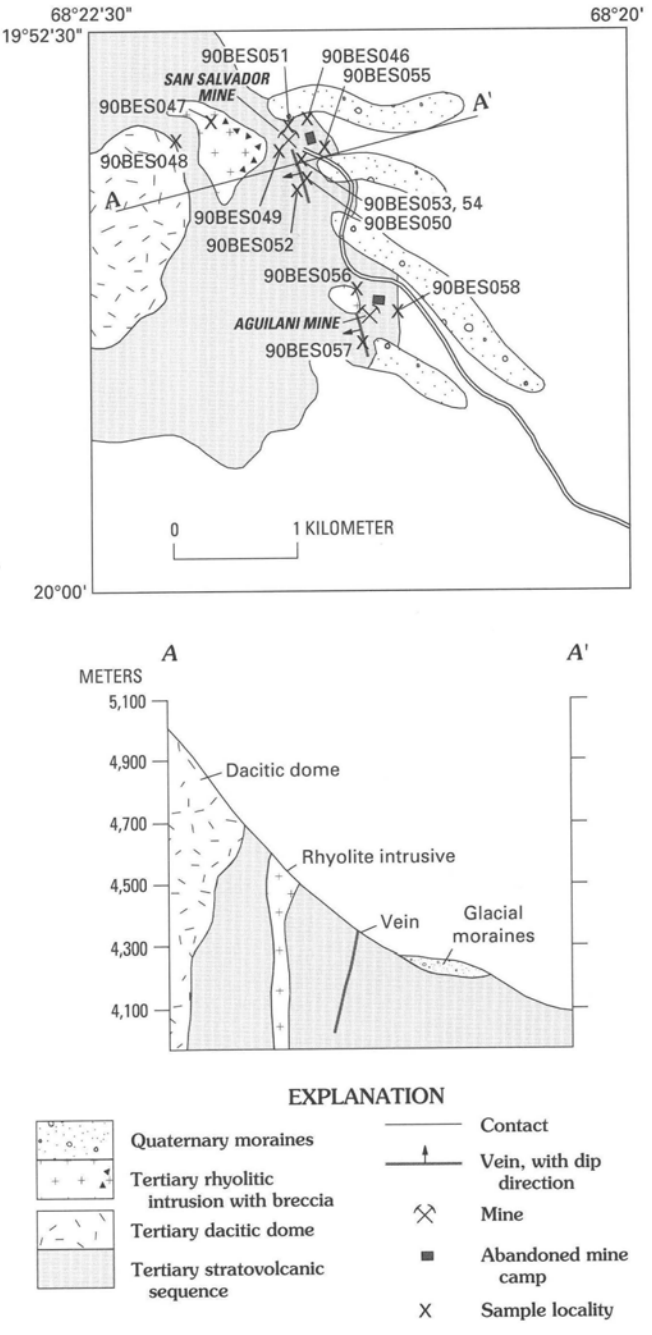


Figure 100. San Salvador and Aguilani mines at Chinchilhuma volcano, Bolivia. *A*, Map showing geology and sample localities. *B*, Cross section of the San Salvador area at Chinchilhuma volcano.

Conclusions

The Chinchilhuma district contains polymetallic veins that crop out on the eastern flanks of the Chinchilhuma volcano. A set of northwest-southeast veins were mined in a limited way at the Aguilani mine and at the San Salvador mine. The deposits in the Chinchilhuma area appear similar to those in the Salinas de Garci Mendoza

Table 35. *Chemical analyses of mineralized rocks from the Chinchilhuma area, Bolivia*

[All values reported in parts per million (ppm). Sample descriptions, methods, and complete results in appendix B]

Sample no.	Au	Ag	As	Sb	Pb	Zn	Cu
90BES046	0.006	2.9	<0.6	<0.6	20	0.79	0.19
90BES047	<.002	1.2	2.5	0.94	110	18	2.1
90BES048	<.002	<.45	.79	<.6	2.2	85	11
90BES049	<.004	<.045	4.6	1.6	7.6	160	.89
90BES050	.20	25	53	13	7,100	>1,300	260
90BES051	.028	150	28	62	280	28	18
90BES052	.30	14	130	18	3,300	36	190
90BES053	1.20	22	17	12	7,200	9,300	990
90BES054	.40	67	35	12	980	4,900	6,900
90BES055	.008	7.5	8.1	180	51,000	170	25
90BES056	.006	4.3	27	4.5	2200	330	140
90BES057	<.002	.66	17	.98	550	300	2.7
90BES058	.016	.14	7.3	<.6	260	>1,300	22

district, and are related to a similar porphyritic intrusion. Mineralized rock may be concealed beneath glacial deposits in the southern and northern flanks of the Chinchilhuma volcano, and the significant precious-metal contents of veins and altered rock in this area suggest that further exploration is warranted.

SAN FRANCISCO MINE

By Donald H. Richter, W. Earl Brooks, Angel Escobar-Diaz, *and* Alberto Hinojosa-Velasco

Summary and Conclusions

The San Francisco mine was probably exploited for silver; however, the absence of known intrusive rocks, coupled with a lack of any hydrothermal alteration and encouraging metal values, suggests that the mineral resources of the area are negligible.

Introduction

An ancient mine, referred to locally as the San Francisco mine (app. A, no. 356), occurs 15 km southeast of the village of Alota, in the San Pablo de Lípez 1:250,000-scale quadrangle. It was apparently discovered, and probably last worked, in Spanish colonial times; present ownership is not known. The mine area was examined in September 1990.

Geologic Setting

The mine occurs on top of a 4,050 m-high ridge which is underlain by volcaniclastic rocks of the Miocene Upper Quehua Formation (pl. 1, Tig) that unconformably overlie red mudstones of the early Tertiary Potoco Formation (pl. 1, Ts1). Both units are unconformably overlain by younger ash-flow tuffs, probably of the Pliocene Ignimbrite Formation (pl. 1, QTig; fig. 101).

Mineral Deposits

The host dacite ash-flow tuff is moderately welded and crystal rich; it contains phenocrysts of plagioclase, biotite, quartz, and hornblende and minor lithic fragments in a shard-rich eutaxitic matrix. It contains about 66 percent SiO_2, on an anhydrous basis (app. B, sample 90BDR034). A

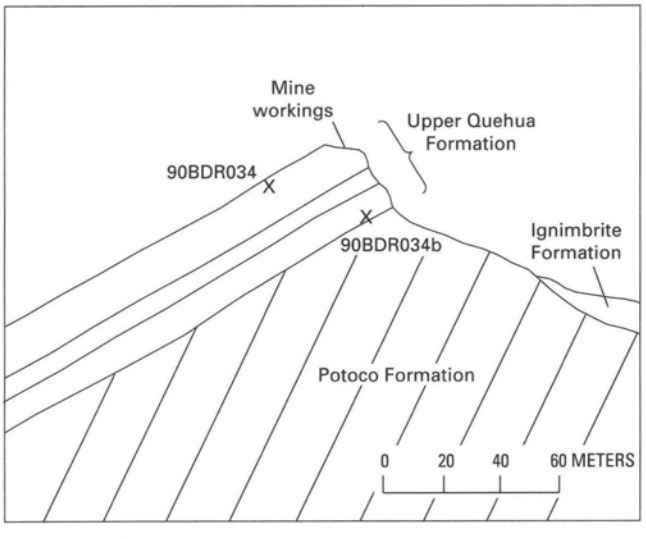


Figure 101. Schematic cross section showing geologic relationships in the San Francisco mine area, Bolivia.

Table 36. *Chemical analyses of vein and slag, San Francisco mine area, Bolivia*

[All results in parts per million (ppm). Sample descriptions, methods, and complete analyses in appendix B. Sample 90BDR034a, 3 cm-thick vein; sample 90BDR034c, chips of vein material; sample 90BDR034d, old smelter slag]

Sample no.	Au	Ag	Pb	Zn	Cu	As	Sb	Sn
90BDR034a	<0.002	580	1,500	8,000	120	150	34	<10
90BDR034c	.022	83	360,000	340	71	5,200	2,100	<10
90BDR034d	<.002	24	410	920	8,800	300	150	50

second ash-flow tuff, which is exposed below the mine workings is, crystal- and pumice-rich and contains phenocrysts of plagioclase, altered biotite, and minor quartz in an ash and shard-rich matrix. Pumice clasts in the tuff typically exhibit dark margins.

Mine workings consist chiefly of a number of pits, trenches, and short adits, and are scattered over an area about 125 m long by 25 m wide. The workings are all in a coarsely brecciated ash-flow tuff in the Upper Quehua Formation and appear to follow very irregular, dark-colored veins and veinlets that are interstitial to the fragments. At the north end of the disturbed area, a shaft, inclined 40° and trending N. 60° W., follows the basal contact of the ash flow to a depth of at least 20 m. No veins or ore minerals were observed in the shaft. The veins exposed in the surface workings are narrow, and none thicker than 5 cm were observed. They appear to consist chiefly of very fine grained dark-brown to black manganiferous limonite or goethite. A 3 cm-thick vein sample (90BDR034a) contained 580 ppm silver and 1,500 ppm lead, whereas sample 90BDR034c, also of vein material from the dump, is extremely lead and arsenic rich, and contains 0.022 ppm gold (table 36). Pieces of glassy slag (sample 90BDR034d), which are scattered through the area and apparently come from an old nearby smelter (not located), were found to contain about 9 percent copper and 50 ppm tin.

Although the physical appearance of the mine area is not encouraging, and alteration is not widespread, the geochemical results from sampling indicate this area merits further investigation.

MINERAL DEPOSITS ASSOCIATED WITH LAKES AND SALARS

INTRODUCTION

The Altiplano and Cordillera Occidental have many saline and alkaline lakes, as well as the world's largest salar. Many industrial minerals are associated with these environments. The brines are commonly enriched in lithium, boron, potassium, or other components. The mineable salts of the salars may include many minerals, some of which are halite, gypsum, trona, natron, mirabilite, ulexite, colemanite, and borax. There are more than 200 alkaline and saline lakes and salars (table 10) on the Bolivian Altiplano ranging in size from less than 1 km^2 to more than 9,000 km^2 and they represent one of Bolivia's greatest resources. Much work has been done to evaluate lithium and other nonmetallic resources in some of these lakes and salars by personnel of Servicio Geológio de Bolivia (GEOBOL), George Ericksen of the U.S. Geological Survey (USGS), and François Risacher of France's L'Office de la Recherche Scientifique et Technique de Outre-Mer (ORSTOM), as well as others. This investigation focused special attention on lakes and salars that have not been well studied but might have some economic potential, even on a small scale. In addition, lakes and salars that we felt could contribute to the understanding of the deposit type and were of geologic interest were studied. Most of the lakes and salars visited were in the southern part of the study area. At most sites, a brine sample from the lake or salar and a water sample from one or more inflow sources such as springs or rivers were collected. An attempt was made to characterize the composition and extent of any associated evaporite deposits and samples were collected for analysis. Spatially associated springs were sampled where possible to investigate the relationship between spring geochemistry and salar brine compositions. Geologic and topographic evidence indicating higher lake stands was noted. Because it is the most thoroughly studied salar in Bolivia (Ballivian and Risacher, 1981; Ericksen and others, 1978; Risacher, 1989), no work was done at Salar de Uyuni during this study. The sites visited are discussed from north to south.

The winter following our field work, a paper on the geochemistry of Bolivian lakes and salars was published (Risacher and Fritz, 1991). It was not possible to incorporate all of their detailed information; additional information is available from this source.

LAGUNA SACABAYA

By Sigrid Asher-Bolinder, Eduardo Soria-Escalante, Eduardo Camacho, *and* William Blacutt

Summary

Laguna Sacabaya is a saline lake with elevated boron levels in its brine and occurrences of cottonball ulexite in its near-surface sediments. Borates were produced in the past from the southern playa. The economic potential in the immediate vicinity of Laguna Sacabaya is considered to be limited to small-scale mining of ulexite. The waters are of geologic interest because of the high cadmium, iron, titanium, and zinc levels.

Introduction

Laguna Sacabaya is located near the base of Cerros Poquentica and Tunapa, Departament of Oruro, Provincia Atahuallpa, and is in the Corque 1:250,000-scale quadrangle (app. A, nos. 161, 162). A small amount of borate has been produced from the southern playa. This site was visited in August 1990. Cottonball ulexite, lacustrine mud, water from two springs that feed the lake, and lake water from the south end of the lake were sampled.

Geology and Mineral Deposits

Laguna Sacabaya occurs near the base of Cerro Tarina in the Cordillera Occidental, possibly occupying a local structural sag. The lake is fed by at least two springs and by runoff from Cerro Poquentica and Cerro Tarina, and is drained by Río Kajachi Jahuira when it is at relatively high levels. One spring on the west end of the lake was sampled, as was warm water emerging from a basalt flow at the south end of the lake (35 °C). Results of analyses of the western spring waters (pH, 7.7) were 23.200 ppm B; 0.040 ppm Ba; 172 ppm Ca; 87 ppm K; 5.590 ppm Li; 116 ppm Mg; 0.020 ppm Mn; 1,010 ppm Na; 0.060 ppm Ni; 48.8 ppm Si; and 3.390 ppm Sr. Results of analyses of filtered water from the warm spring were 39.600 ppm B; 258 ppm Ca; 1 ppm Fe; 164 ppm K; 11.100 ppm Li; 191 ppm Mg; 1,750 ppm Na; 52.7 ppm Si; 4.210 ppm Sr; and 0.070 ppm Zn.

The lake surface is typical of a playa with wet mud rimming shallow water. When visited, the lacustrine sediments were water saturated to a depth of 85 cm. An analysis of filtered lake brine (pH, 7.6) was 41.200 ppm B; 268 ppm Ca; 0.010 ppm Cd; 2 ppm Fe; 171 ppm K; 11.500 ppm Li; 198 ppm Mg; 1,820 ppm Na; 0.030 ppm Ni; 54.7 ppm Si; 4.380 ppm Sr; 0.040 ppm Ti; and 0.070 ppm Zn. The color of the muds is commonly light gray with traces of darker organic-rich material. Analysis of one mud sample showed 15 percent Ca; 2.8 percent Al; 1.2 percent K; 18 percent Si; 1 percent Mg; 2 percent Na; 150 ppm Li; 1,500 ppm Sr; and 600 ppm B. In places, the muds have a strong odor of hydrogen sulfide. Evaporite mineralization was largely limited to halite and ulexite efflorescence in the surrounding deposits and dunes of fine volcanic ash and pumice. One sample collected from a stockpile of ulexite ore had 7.4 percent Ca; 1.4 percent Mg; 1.2 percent Si; 14 percent Na; 300 ppm Li; 2,200 ppm Sr; and 78,000 ppm B.

SALAR DE COIPASA

By G.J. Orris, Sigrid Asher-Bolinder, Eduardo Soria-Escalante, *and* René Enriquez-Romero

Summary

Salar de Coipasa has produced minor amounts of salt and borates; in the northwest part of the salar, halite is currently being produced from the surface and minor borate production has probably occurred at the southern end. The brines of Salar de Coipasa are relatively enriched in aluminum, boron, barium, calcium, cobalt, potassium, lithium, magnesium, manganese, and strontium. The Río Sabaya drainage is promising for borate, lithium, and other evaporite-brine exploration. Basic mapping and exploration work are needed to evaluate its potential for more significant production.

Introduction

Salar de Coipasa is in the Departament of Oruro, Provincia Atahuallpa, and is in the Garci de Mendoza 1:250,000-scale quadrangle (app. A, nos. 183, 184, 186, 187). Compared with the neighboring salars of Empexa and Uyuni, Salar de Coipasa is relatively unstudied, especially the northern part. The northern part of the playa system was visited in August 1990 and identification and characterization of inflow sources was conducted. In August 1990 it was possible to drive across the western portion of the salar.

Geology and Mineral Deposits

Previous work at Salar de Coipasa is described in Ballivian and Risacher (1981) and Risacher (1984). The salt crust mineralization at Salar de Coipasa includes halite,

gypsum, and ulexite. Brines are also present. The margin of the salar crust is composed of a mixture of clay, gypsum, and ulexite, whereas the central crust consists of halite at the surface. There was no surface runoff entering the Coipasa basin from the Chilean Andes during our visit, although remote sensing images from 1986 indicate major water and sediment inflow from this direction.

Samples collected include one brine and one spring sample. The brine sample from the surface at Jachapsu contained 0.009 ppm Al; 88.200 ppm B; 0.290 ppm Ba; 1,610 ppm Ca; 0.030 ppm Co; 3,500 ppm K; 105 ppm Li; 1,730 ppm Mg; 0.670 ppm Mn; 861 ppm Na; 23.4 ppm Si; and 21.500 ppm Sr. The sample collected from a warm spring on the playa near the island of Cerro Villa Pucarani contained 30.700 ppm B; 0.040 ppm Ba; 818 ppm Ca; 478 ppm K; 9.420 ppm Li; 470 ppm Mg; 5.050 ppm Mn; 2,500 ppm Na; 16.1 ppm Si; and 3.690 ppm Sr. A second warm spring, collected less than 1 m from the first, was rimmed by a black substance that may be manganese. Both springs released an odorless gas, possibly carbon dioxide which is common in this environment.

A major part of our work was the collection of samples characterizing the chemical composition of the inflows to Salar de Coipasa. One well at Pisiga Sucre was slightly anomalous in manganese (0.030 ppm). One sample from Río Laca Jahuira had a pH of 7.8 and contained 6,700 ppm total dissolved salts, as well as, 0.020 ppm Ti; 0.050 ppm Ni; and 0.110 ppm Ba. Water from Río Sabaya, collected a few kilometers north of where it enters Salar de Coipasa contained 0.007 ppm Al; 244 ppm B; 0.190 ppm Ba; 685 ppm Ca; 2,560 ppm K; 105 ppm Li; 1,360 ppm Mg; 1,990 ppm Na; 0.043 ppm Si; 24.300 ppm Sr; and a pH of 7.5, all of which are highly anomalous values. Water from Río Largo contained 0.030 ppm Ti; a tributary to Río Khoto, also sampled, had unremarkable water chemistry.

SALAR DE EMPEXA

By G.J. Orris, Sigrid Asher-Bolinder, Eduardo Soria-Escalante, *and* René Enriquez-Romero

Summary

Salar de Empexa has been fairly well studied in the past. We sampled one of the hot springs that feeds the salar because it may be a source for the boron in the salar; the sample was enriched in boron, lithium, sodium, manganese, molybdenum, silicon, and vanadium. Salar de Empexa was reportedly mined for borates (1900–41), but production levels and totals are not known. Exploration by GEOBOL in the 1960's indicated no remaining potential; Ballivian and Risacher (1981) comment on the absence of borates.

Introduction

Salar de Empexa is in the Departament of Potosí, Provincia Daniel Campos, and is in the Villa Martin 1:250,000-scale quadrangle (app. A, no. 214). GEOBOL explored for borates in the 1960's with negative results. Most of a visit in August 1990, was spent sampling one hot spring that feeds Salar de Empexa.

Geology and Mineral Deposits

Earlier studies of Salar de Empexa are described in Ballivian and Risacher (1981) and Risacher and Miranda (1976). Salar de Empexa is described as having a crust composed primarily of gypsum with halite, clay, calcite, and minor sodium sulfate. In the areas of Boratera Laqueca and Boratera Isma, ulexite was reportedly mined from ore beds that were 30–40 cm thick. Along the road to Abra de Napa, prominent stromatolitic terraces occur about 5 m above the road. During our visit, we sampled a hot spring at the southern end of the salar where the road to El Desierto crosses the Quebrada Malpaso. The hot spring was boiling at a temperature of 78 °C because of elevation. The hot-spring water contained 32.200 ppm B; 0.060 ppm Ba; 6.6 ppm Ca; 0.125 ppm K; 11.400 ppm Li; 6.2 ppm Mg; 0.120 ppm Mn; 0.020 ppm Mo; 1,580 ppm Na; 0.030 ppm Ni; 142 ppm Si; 2,600 ppm Sr; and 0.100 ppm V. The pH of the spring water was 8.3.

SALAR DE LA LAGUNA

By G.J. Orris, Sigrid Asher-Bolinder, Eduardo Soria-Escalante, *and* René Enriquez-Romero

Summary

Salar de la Laguna is a dry lake with sodium sulfate and sodium carbonate mineralization. No brine chemistry is known from this salar, but the water could be expected to have elevated boron, lithium, and strontium contents based on a sample of inflow waters. The large amount of wind erosion that occurs at this salar decreases any potential for economic mineralization. Any significant potential for economic mineralization would exist at depth, provided the basin morphology is favorable.

Introduction

Salar de la Laguna, also known as Boratera la Laguna, is in the Departament of Potosí, Provincia Nor

Lípez, and is in the Villa Martin 1:250,000-scale quadrangle (app. A., nos. 244, 245). The salar lies at the foot of Volcán Olca. Small amounts of sodium sulfate have been produced intermittently from this salar by residents of San Pedro Quemez. A visit was made in August 1990.

Geology and Mineral Deposits

Salar de la Laguna is a dry lake where sodium sulfate, natron, gypsum, and halite are the dominant evaporite minerals. Much of the surface material is very fine grained. One sample of the gypsum-halite-thenardite crust collected in 1990 had 6.7 percent Ca; 4.5 percent K; 4.6 percent Mg; 10 percent Na; 140 ppm Li; 460 ppm Sr; and 1,300 ppm B. During our visit, a large cloud of white dust was raised by high winds from the surface of the salar (fig. 102). The potential loss of material by wind erosion is quite large, because the windy season lasts from approximately April through November. We were unable to collect a brine sample.

One sample collected from a hot spring that feeds Salar de la Laguna indicated that the hot spring had a pH of 7.9 and a temperature of 40 °C. This sample contained 3.200 ppm B, 117 ppm Ca, 73 ppm K, 0.190 ppm Li, 68.7 ppm Mg, 236 ppm Na, 85.6 ppm Si, 0.550 ppm Sr, and 0.070 ppm V.

The basin in which Salar de la Laguna is located has a basement of late Miocene(?) pyroclastic rocks from an unknown source. Younger dacitic to andesitic volcanics cover the area surrounding the basin. The area has experienced recent volcanism; there are active fumaroles at Volcán Olca and Volcán Iruputuncu and hot springs at the contacts between lava and pyroclastic rocks.



Figure 102. Wind erosion of sodium salts at Salar de la Laguna in Provincia Nor Lípez, Departament of Potosí.

LAGUNA HEDIONDA NORTE

By G.J. Orris, Sigrid Asher-Bolinder, Eduardo Soria-Escalante, *and* René Enriquez-Romero

Summary

Laguna Hedionda Norte is a small saline lake with thenardite- and ulexite-bearing evaporite crusts, and brine containing slightly anomalous amounts of lithium, boron, and potassium. There is no known production from this lake and its potential is believed to be low.

Introduction

Laguna Hedionda Norte, also known as Laguna Hedionda, is in the Departament of Potosí, Provincia Sud Lípez, and in the Volcán Ollague 1:250,000-scale quadrangle (app. A, nos. 265, 266, 270, 275). A small lake in the Volcán Juriques 1:250,000-scale quadrangle is also named Laguna Hedionda, but is referred to as Laguna Hedionda Sur. Laguna Hedionda Norte occurs at the base of Cerro Papellón in the valley between the volcanoes Cerro Tapaquillcha and Cerro Cañapa and is less than 1 km from Laguna Chiar Kkota. The lake has a surface area of approximately 0.5 km^2. A major source of surface water to the lakes and salars of the valley is Río Tapaquillcha near the northeast border of the valley. A visit was made in August 1990 and brine and mineral samples were collected.

Geology and Mineral Deposits

Laguna Hedionda Norte lies above Pastos Grandes pyroclastic flows in a sag created by intersecting lava flows and domes in the valley between Cerro Tapaquillcha and Cerro Cañapa. Surface water inflow to the basin drains areas of young lavas and sulfur deposits associated with the volcanoes. Laguna Hedionda Norte is probably a remnant of a larger older lake that extended from Laguna Hedionda Norte southsouthwest to Laguna Ramaditas (Ballivian and Risacher, 1981). The lake is small and saline; brines contain 20.4 ppm B; 2,090 ppm Na; 14.9 ppm Li; 298 ppm Ca; 122 ppm silica; and 113 ppm Mg (Ballivian and Risacher, 1981).

The evaporite minerals at Laguna Hedionda Norte include thenardite and mirabilite, halite, gypsum, diatomite, clay, and minor ulexite. Native sulfur occurs in mud about 10 cm below the surface evaporites. It is not clear if the sulfur is of biogenic origin, associated with fumarolic activity, or a reduction product of gypsum. Analysis of a sample of the thenardite-bearing surface crust showed 25 percent Na; 1.1 percent Ca; 880 ppm As; 410 ppm Li; and

680 ppm B. The gypsum-halite-sulfur mud had 11 percent Ca; 7.3 percent Na; 6,400 ppm As; 840 ppm Li; 1,300 ppm Sr; and 13,000 ppm B.

LAGUNA CHIAR KKOTA

By G.J. Orris, Sigrid Asher-Bolinder, Eduardo Soria-Escalante, *and* René Enriquez-Romero

Summary

Laguna Chiar Kkota is a small saline lake and salar with no known production. The lake brine is relatively enriched in sodium, boron, lithium, and potassium. Surface mineralization includes gypsum, halite, calcite, and ulexite. This occurrence has little economic significance at this time.

Introduction

Laguna Chiar Kkota is in the Departament of Potosí, Provincia Sud Lípez, and is located in the Volcán Ollague 1:250,000-scale quadrangle (app. A, nos. 267, 268, 269). The lake occupies a valley formed by lava flows and domes from the neighboring volcanoes Cerro Tapaquillcha and Cerro Cañapa and is less than 1 km from Laguna Hedionda Norte. The site was visited in August 1990, but no samples were collected.

Geology and Mineral Deposits

Laguna Chiar Kkota overlies pyroclastics of the Pastos Grandes caldera. It is probable that the lake is a remnant of an older larger lake that extended from Laguna Hedionda Norte southsouthwest to Laguna Ramaditas (Ballivian and Risacher, 1981). Laguna Chiar Kkota is a saline lake (pH, 8.3) with a small salar area. Inflow waters drain pyroclastics, young lava flows, and sulfur deposits associated with the volcanoes. The brine contains 238 ppm B; 23,800 ppm Na; 2,380 ppm K; 168 ppm Li; 1,240 ppm Ca; and 1,085 ppm Mg (Ballivian and Risacher, 1981). The evaporite crust contains gypsum, halite, calcite (limestone), clays, ulexite, and sodium sulfate, as well as native sulfur produced from reduction of gypsiferous sediments by bacteria (Ballivian and Risacher, 1981). Risacher (1976) also reports the presence of minor sylvite. Risacher and Miranda (1976) classify the lake as a sodium chloride type, but give no other geologic or geochemical information.

LAGUNAS PASTOS GRANDES

By G.J. Orris, Sigrid Asher-Bolinder, Eduardo Soria-Escalante, *and* René Enriquez-Romero

Summary

Lagunas Pastos Grandes is a large saline lake and salar complex in a caldera. The brines have no economic potential at this time.

Introduction

Lagunas Pastos Grandes is in the Departament of Potosí, Provincia Sud Lípez and in the Volcán Ollague 1:250,000-scale quadrangle (app. A, nos. 280, 281). The area encompassed by Lagunas Pastos Grandes includes saline lakes, marshes, and areas of evaporitic salt deposition. A visit to the area was made in August 1990.

Geology and Mineral Deposits

Lagunas Pastos Grandes are a series of lakes, salt crusts, and pampas in a caldera. Surface water inflow to the basin drains areas of rhyolitic rocks to the west and ignimbrites to the east. In addition, at least 12 thermal springs feed the west side of the basin (Ballivian and Risacher, 1981). Minerals in the crust include halite, gypsum, clay, ulexite, and calcite. A sample of this crust collected in 1990 had 3.7 percent Al; 3.5 percent Ca; 1.8 percent K; 1.4 percent Mg; 15 percent Na; 750 ppm Li; 1,200 ppm B; and 17 percent Si. Ballivian and Risacher (1981) reported a brine analysis that contained 1.64 g/L Li; 101 g/L Na; 945 mg/L B; 14.2 g/L K; 3.1 g/L Ca; and 3.48 g/L Mg. Two inflow sources, a spring and a small stream, were sampled as part of this study. The spring on the north side of the basin had a pH of 7.1 and contained 1.100 ppm B; 9.5 ppm Ca; 7 ppm K; 0.780 ppm Li; 4.4 ppm Mg; 69 ppm Na; 27.1 ppm Si; and 0.150 ppm Sr. The stream contained 0.600 ppm B; 41 ppm Ca; 6 ppm K; 0.080 ppm Li; 14.5 ppm Mg; 18 ppm Na; 0.130 ppm Ni; 42.8 ppm Si; and 0.190 ppm Sr; as well as a pH of 7.7. The stream drains an area largely underlain by the Ignimbrite Formation. Additional discussion of Lagunas Pastos Grandes may be found in Risacher and Miranda (1976) and Risacher (1984).

LAGUNA CACHI

By G.J. Orris, Sigrid Asher-Bolinder, Eduardo Soria-Escalante, René Enriquez-Romero, *and* E.A. Bailey

Summary

Laguna Cachi is an alkaline lake and salar currently being mined for sodium carbonate (trona). Brines at this site

are enriched in sodium carbonate, boron, lithium, potassium, molybdenum, fluorine, and tungsten. The main ore mineral is trona. Ulexite and halite are also present. Ballivian and Risacher (1981) estimate a total trona resource of 18 million tonnes of sodium carbonate on the basis of chemical analyses of the brine.

Introduction

Laguna Cachi, also referred to as Cachi Laguna, is in the Departament of Potosí, Provincia Sud Lípez, and is located in the Volcán Ollague 1:250,000-scale quadrangle (app. A, nos. 283, 284). It is an alkaline lake at the western base of Cerro Pabellón-Cachi Laguna, but it also receives runoff from the western sides of Cerro Pastos Grandes and Cerro Cachi Laguna, as well as from a large area to the south and southeast of Cachi Laguna Loma. Trona, thermonatrite, and (or) natron was mined and processed at this site in 1958–60. The lake is currently being mined by Empresa Minera Clavijo Limitada (EMICLA), although processing is not being done at the old plant site at Laguna Cachi but at Barrero's Mina Corina site, 25 mi north. The site was visited during August 1990 and brine and salt samples were collected.

Geology and Mineral Deposits

Laguna Cachi, located on the west flank of the Pastos Grandes caldera, overlies late Miocene pyroclastic flows from the caldera. The surface water inflow originates in ignimbrites to the west and volcanic domes to the east. The waters also drain fumarolic sulfur deposits such as the one at Cerro Cachi Laguna. Laguna Cachi is a shallow alkaline lake (pH, 10.5) possessing a patchy surface crust (fig. 103). In places, the crust has relatively high relief compared with the smooth surfaces of many of the Bolivian salars. These roughly surfaced winter crusts have been reported to be composed of natron, thermonatrite, and halite. Most of the sodium carbonate material observed during a visit to the site was probably natron; the samples collected proved to be very unstable and converted to a watery mush over a period of days. The evaporite deposits along the western and northern shoreline contained trona, clay, diatomite, halite, and ulexite. One sample of trona collected in 1990 from a stockpile adjacent to the lake had 0.06 percent Ca; 2.9 percent Na; 2,500 ppm As; 720 ppm Li; 2,500 ppm B; and 0.42 percent Si. One sample of the evaporite crust contained 6.4 percent Al; 3.6 percent Ca; 2.6 percent K; 1.7 percent Mg; 5.8 percent Na; 830 ppm As; 330 ppm Li; 1,000 ppm B; and 26 percent Si.

The brine of Laguna Cachi has been analyzed by Ballivian and Risacher (1981) and by Risacher and others (1984). Additional information on Laguna Cachi may be found in Risacher (1984), Risacher and Miranda (1976), and Ahlfeld and Schneider-Scherbina (1964). Ranges of values for select elements include 216–2,500 ppm B; 177–848 ppm Li; 20,900–92,000 ppm Na; 7,290–35,600 ppm K; 4.9–10 ppm Ca; 25–50 ppm Mo; 40–70 ppm F; 11–20 ppm W; and 438–2300 ppm As. The wide range of values may be the result of seasonal changes, brine stratification, sampling areas nearer and farther from inflow sources, or a combination of all of these factors. The molybdenum, tungsten, and arsenic values are high for natural waters and may indicate the presence of mineralization enriched in these elements in the drainage basin of Laguna Cachi (Risacher and others, 1984). A brine sample collected as part of this study had values intermediate to the ranges of concentrations found by previous analyses. Ahlfeld and Schneider-Scherbina (1964) report that the salt crust was 47.3 percent sodium carbonate; 11 percent sodium bicarbonate; 11 percent sodium sulfate; and 7 percent sodium chloride.

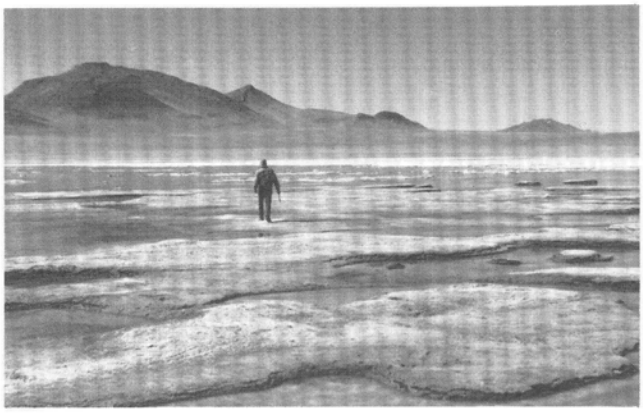


Figure 103. Laguna Cachi is an alkaline lake in Provincia Sud Lípez. The salt crust is composed of natron, thermonatrite, and halite.

LAGUNA CAPINA

By G.J. Orris, Eduardo Soria-Escalante, Sigrid Asher-Bolinder, *and* René Enriquez-Romero

Summary

Laguna Capina is a saline lake and salar with ulexite and halite mineralization and brines enriched in boron, lithium, sodium, and potassium. Minor and intermittent ulexite and probertite production has taken place.

Introduction

Laguna Capina is in the Departament of Potosí, Provincia Sud Lípez, and is in the Volcán Ollague

1:250,000-scale quadrangle (app. A, nos. 287, 288). Laguna Capina is also known as Capina and Boratera de Capina in the literature. A minimum of 1 km^2 of the 40 km^2 surface area of the salar has been disturbed by surface mining. Terra Ltda. has a 1.448 hectare concession at Laguna Capina and is presently mining ulexite and probertite. Total production of ulexite from May 1989, through 1990 was 18 tonnes containing 30 percent B_2O_3. Probertite production since November 1989, has grades of 42 percent B_2O_3. The average production grade on a dry basis is 32 percent B_2O_3. The refining process consists of leaching the ore with sulfuric acid to produce boric acid (H_3BO_3) that is 99.8 percent pure. Reserves are estimated at 8 million tonnes B_2O_3; this estimate is significantly larger than that of Ballivian and Risacher (1981). During a visit in August 1990, no work was in progress.

Geology and Mineral Deposits

Laguna Capina is a saline lake and salar with a fine-grained halite-gypsum crust that overlies late Cenozoic pyroclastic flows from the Pastos Grandes caldera; brines contain boron, lithium, and potassium. Most of the surface water flowing into the basin originates in pyroclastic flows and younger volcanics to the southwest near Laguna Colorada. Ulexite occurs near the periphery of the salar and extends towards the center of the basin. The ulexite ore forms a layer as thick as 60 cm and locally contains as much as 50 percent mudstone. The brines of Laguna Capina are reported by Ballivian and Risacher (1981) to have a pH of 8.6 and to contain 280 ppm B; 8,500 ppm Na; 1,460 ppm K; 193 ppm Li; 800 ppm Ca; and 260 ppm Mg. Risacher and Miranda (1976) found that the lithium content of clays and borates exceeded that of the brine; that the boron content of the evaporite minerals and lacustrine sediments exceeded that of the brine by at least an order of magnitude; and that lacustrine sediments and precipitates had high (2,700–7,500 ppm) potassium values.

LAGUNA CELESTE

By G.J. Orris, René Enriquez-Romero, *and* Eduardo Soria-Escalante

Summary

Laguna Celeste is a saline lake that contains 24 ppm B and 7.7 ppm Li in the water.

Introduction

Laguna Celeste is in the Departament of Potosí, Provincia Sud Lípez, and is in the Cerro Zapaleri 1:250,000-scale quadrangle (app. A, no. 346). The lake lies in the foothills of Cerro Uturuncu. During a visit in August 1990, the lake had clear water and the shoreline was rimmed by ice as thick as 1 m.

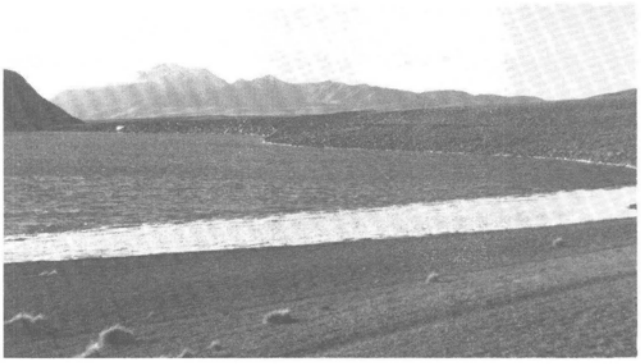


Figure 104. Laguna Celeste is an alkaline lake in Provincia Sud Lípez with no evaporitic precipitates. The white material at the shoreline is composed of blocks of ice, some of the blocks are as thick as 1 m.

Geology and Mineral Deposits

Laguna Celeste occurs in a small basin overlying pyroclastic flows of the Ignimbrite Formation. Laguna Celeste is one of the few lakes in the Sud Lípez that had no surficial salt precipitates around its periphery during site visits in 1990 (fig. 104); in addition none are indicated on the topographic maps of the area. The present lake does not occupy all of its basin, but surficial deposits left by higher lake stands consist of light-brown argillaceous sediments with no noticeable salt content. The surface water inflow to Laguna Celeste originates from snow and (or) springs on the northeast side of Cerro Uturuncu, a volcano with an active fumarole and a sulfur mine; the surface water also drains areas of other pyroclastic rocks. A water sample collected from the southern part of the lake had a pH of 9.0 at 0 °C. On site the total dissolved solids were measured using a meter at 1,600 ppm and later analysis indicated a content of 24.400 ppm B; 7.700 ppm Li; 8.2 ppm Ca; 200 ppm K; 85.3 ppm Mg; 985 ppm Na; 12.6 ppm Si; and 40 ppm Sr.

LAGUNA COLORADA

By G.J. Orris, Sigrid Asher-Bolinder, Eduardo Soria-Escalante, René Enriquez-Romero, *and* E.A. Bailey

Summary

Laguna Colorada is a saline lake which has limited surface potential for small-scale production of sodium sulfate. There is some potential for diatomite deposits in the basin, as well as for borate and sodium sulfate deposits at depth.

Introduction

Laguna Colorada is in the Departament of Potosí, Provincia Sud Lípez and in the Volcán Juriques 1:250,000-scale quadrangle (app. A, nos. 290, 291, 292, 293, 295). It is one of the largest lakes in Sud Lípez and has a large contiguous playa, Playa Huayllajara. There is no known production from this site.

Geology and Mineral Deposits

Laguna Colorada occupies a basin overlying pyroclastic flows of the Ignimbrite Formation. The lake is bordered to the north by young andesitic volcanoes, Cerro Chijlla and Volcán Chico, and to the west by a Miocene volcanic complex. Laguna Colorada is a saline lake with evaporite crusts around the edges that are composed of trona, thenardite and mirabilite, halite, and ulexite. Rimming the western edge of the lake are small islands of white minerals, primarily thenardite with ulexite and halite, that rise as much as 3 m above the water level. Other lacustrine sediments and evaporites in the basin include trona, clay, sodium sulfate, and diatomite. The current lake occupies a small portion of its closed basin and the water is distinctly reddish purple when seen from a distance. A sample of thenardite-bearing material collected from the white islands in 1990 had 25 percent Na; 21 ppm Li; and 700 ppm B. A sample of the ulexite-halite mineralization had 7.7 percent Ca; 15 percent Na; 1.1 percent Si; 10,000 ppm As; 2,200 ppm Li; 410 ppm Sr; and 83,000 ppm B.

A sample of the brine at Laguna Colorada taken 25 m offshore in 1990 contained 9.600 ppm B; 2.560 ppm Li; 569 ppm Na; 55.8 ppm Si; and 0.070 ppm V. The pH registered 7.7 and the total dissolved solids content was 1,120 ppm. This sample was collected in an area with no ice or salt cover and the open water may not have had an ice or salt crust because of inflow from a nearby spring. Ballivian and Risacher (1981) collected a sample which had total dissolved solids of 100 g/L and a pH of 8.5.

One warm spring feeding Laguna Colorada at its northwestern end had a temperature of 21 °C, a pH of 7.5, and 300 mg/L total dissolved solids. The warm spring contained 0.460 ppm Li; 42.2 ppm Si; and 1.900 ppm B.

LAGUNA MAMA KHUMU

By G.J. Orris, René Enriquez-Romero, *and* E.A. Bailey

Summary

Laguna Mama Khumu is a saline lake that has been mined for borates, specifically ulexite. Potential for additional borates at depth or in other parts of the basin is possible, but dependent on the unknown parameters of basin depth and morphology.

Introduction

Laguna Mama Khumu is in the Departament of Potosí, Provincia Sud Lípez, and in the Cerro Zapaleri 1:250,000-scale quadrangle (app. A, nos. 247, 248). Most of the water inflow to Laguna Mama Khumu is from Cerro Uturuncu to the west and from Cerro Khastor to the southeast. Rectangular pits from which ulexite was mined occur in the east-central part of the salar. During a visit in August 1990, some ore was piled next to the pits.

Geology and Mineral Deposits

Laguna Mama Khumu is a saline lake with a total dissolved solids content of 280 ppm. Ulexite occurs in layers 30–80 cm thick below a 2 cm thick halite-gypsum-kainite ($4KCl \cdot 4MgSO_4 \cdot 11H_2O$) crust. The very fine grained kainite was identified by E.A. Bailey of the USGS using X-ray diffraction. The ulexite is underlain by clays. Some of the ulexite that has been mined from the rectangular pits has small, bright-yellow and orange patches of native sulfur. An analysis of brine from a location more than 200 m from the ulexite mineralization contained 4.900 ppm B; 26.8 ppm Ca; 15 ppm K; 1.290 ppm Li; 8.5 ppm Mg; 248 ppm Na; 39.8 ppm Si; and 0.410 ppm Sr; and had a pH of 7.3. One sample of the evaporite crust contained 17 percent Ca; 7.1 percent Na; 170 ppm As; 440 ppm Li; 580 ppm Sr; and 29,000 ppm B. A grab sample of ore material from one of the pits had 18 percent Ca; 7 percent Na; 1,500 ppm As; 430 ppm Li; 720 ppm Sr; 27 ppm V; 13,000 ppm B; and 2.9 percent Si.

LAGUNA CHOJLLAS

By G.J. Orris, Eduardo Soria-Escalante, *and* René Enriquez-Romero

Summary

Laguna Chojllas is a saline lake that has anomalous concentrations of boron, lithium, barium, and strontium.

Laguna Chojllas and its basin should be considered for further study.

Introduction

Laguna Chojllas is in the Departament of Potosí, Provincia Sud Lípez, in the Cerro Zapaleri 1:250,000-scale quadrangle (app. A, no. 349). Overflow from Laguna Coruto enters Laguna Chojllas by way of Río Puntas Negras. Additional water may enter the basin from Río Khenwal. A short visit was made in August 1990.

Geology and Mineral Deposits

Laguna Chojllas, a saline lake-salar complex, occupies a structural sag overlying pyroclastic and volcaniclastic sequences of the Ignimbrite Formation. The basin is bordered by the Cerro Khastor dome and lava flows, the dome of Cerro Puntas Negras, and the Loromayu massif. Much of the surface water entering the basin drains sequences of volcaniclastic rocks. Springs also supply water to the basin. A brine sample contained 141 ppm B; 65.800 ppm Li; 0.210 ppm Ba; 20.500 ppm Sr; 714 ppm Ca; 3,260 ppm Na; 355 ppm K; 30.4 ppm Si; and 179 ppm Mg; and had a pH of 8.1. One of the springs feeding Laguna Chojllas had a pH of 7.0.

LAGUNA LOROMAYU

By Sigrid Asher-Bolinder, Eduardo Soria-Escalante, *and* G.J. Orris

Summary

Laguna Loromayu is a saline lake with unusual morphology and uncertain evolution that has very high concentrations of boron, lithium, magnesium, sodium, potassium, strontium, and barium relative to other brine and water samples collected as part of this study. Additional study is required to understand the nature and potential of this lake.

Introduction

Laguna Loromayu is in a remote part of the Departament of Potosí, Provincia Sud Lípez, and in the Cerro Zapaleri 1:250,000-scale quadrangle (app. A, nos. 337, 338). During a visit in August 1990, there was little ice on the lake and the lake appeared to have a depth greater than 5 m.

Geology and Mineral Deposits

Laguna Loromayu is a saline lake (pH, 8.5) emplaced in a depression with near vertical walls and overlying late Cenozoic pyroclastic flows. Its morphology suggests a maar-like structure, possibly related to a resurgent collapse. The south end of the lake is fed by at least two springs emanating from Cerro Bravo; additional inflow may occur near the north end. The lake has only sparse salts around its edge, but a single sample of the lake water showed very high concentrations of a large suite of elements. The water sample collected in 1990 contained more than 500 ppm B; 0.220 ppm Ba; 12,300 ppm K; 608 ppm Li; 1,040 ppm Mg; 2,550 ppm Na; 29.500 ppm Sr; and 422 ppm Ca. The boron and lithium contents reported by Risacher (1984) were substantially larger than the values shown by our analysis.

LAGUNA CORUTO

By G.J. Orris, René Enriquez-Romero, *and* Eduardo Soria-Escalante

Summary

Laguna Coruto is a saline lake and salar complex that is anomalous in boron and lithium. The occurrence of lake terraces, gravels, and salts at elevations well above the current lake level indicate Laguna Coruto is a remnant of a much larger lake. Some spring waters feeding the basin are highly anomalous with respect to boron, lithium, and other components found in the lacustrine brine. The brines are not sufficiently enriched in any element to indicate economic potential, but Laguna Coruto occupies a relatively large basin that could contain more enriched brines or potentially economic evaporite deposits. More study is needed.

Introduction

Laguna Coruto is in the Departament of Potosí, Provincia Sud Lípez, and in the Cerro Zapaleri 1:250,000-scale quadrangle (app. A, no. 352). The salar is remote and difficult to reach, although there is an old encampment with a very small population still present. The lake waters occupy the southeastern part of the basin, while the northnorthwestern part is covered by salt deposits.

Geology and Mineral Deposits

Laguna Coruto is located in a structurally controlled basin along the Bolivia-Argentina border and overlies pyroclastics rocks of the Ignimbrite Formation. Younger

dacitic-andesitic volcanic rocks overlie the pyroclastics and border the lake to the south and east. Laguna Coruto is a saline lake which has extensive salt flats developed in the northwestern part of the basin. Most of the surface water inflow to the basin drains pyroclastic sequences north and east of the lake, is from springs at the contacts of lavas and pyroclastics, and (or) drains areas of intense solfataric alteration. In Bolivia, a minimum of 13 springs comprise source waters for the basin. Overflow from the Laguna Coruto basin enters Laguna Chojllas by way of Río Puntas Negras.

A brine sample from the lake with a pH of 8.5 and a total dissolved solids content of 1,270 ppm, contained 3.400 ppm B; 1.160 ppm Li; 58.1 ppm Si; 95 ppm Na; 0.040 ppm Ni; 13 ppm K; 11.7 ppm Ca; and 0.170 ppm Sr. A water sample from one of the springs on the west side of the basin had a pH of 7.7; 8.900 ppm B; 5.040 ppm Li; 2.100 ppm Sr; 29 ppm K; 458 ppm Na; 107 ppm Ca; 18.6 ppm Mg; 0.030 ppm Ni; 35.1 ppm Si; and 0.050 ppm Ba. The spring sample had higher contents of most elements than the brine sample. It is possible that the brine sample was taken near a freshwater source that was not visible or that the lake was stratified and an upper and less saline layer was sampled.

Much of the salt crust at Laguna Coruto appears to be composed of halite, clay, and fine-grained, powdery gypsum. A sample of this crust collected in 1990 contained 3.5 percent Al; 8.1 percent Ca; 1.4 percent K; 1.1 percent Mg; 3.1 percent Na; 300 ppm Li; 2100 ppm B; and 25 percent Si.

SALAR DE CHALLVIRI

By G.J. Orris, Sigrid Asher-Bolinder, Eduardo Soria-Escalante, *and* René Enriquez-Romero

Summary

Salar de Challviri has had minor production of borate minerals. Borax and colemanite have been identified, as well as ulexite efflorescence typical of many of the salars in the Andes. Potential for additional borate mineralization below the identified surface mineralization is dependent on the parameters of basin depth and subsurface basin morphology, which are not known at present.

Introduction

Salar de Challviri is in the Departament of Potosí, Provincia Sud Lípez, and is located near the east-central edge of the Volcán Juriques 1:250,000-scale quadrangle (app. A, nos. 305, 307, 309, 310, 311). The salar is extensive and has several areas of relatively fresh water which probably originate from springs. Borates have been produced at some time in the past from this salar. GEOBOL conducted an exploration program at this salar in the 1960's, but no details are known about the program or its results. Ballivian and Risacher (1981) estimated reserves at a minimum of 2.4 million tonnes of ulexite. A short visit was made in August 1990.

Geology and Mineral Deposits

Salar de Challviri is located in a basin that overlies pyroclastic flows of the Ignimbrite Formation. In other directions, the salar is bordered by the andesitic to dacitic volcanics of Cerro Boratera de Challviri and the Putana-Polques volcanic complex. Salar de Challviri is largely composed of evaporite crusts with little water at the surface. Surface water inflow to the basin drains ignimbrites to the south and the andesitic to dacitic volcanics to the north and west. In addition to halite, borate minerals, commonly ulexite and borax, are relatively abundant in lenses of variable thickness and have been the targets of past production. Colemanite is also present. In the southeastern part of the salar, prospect pits and mounds of discarded salts are present in an area where the surficial crust is very rough, with relief ranging from 10 to 18 cm. The mineralization in the pits in this area occurs approximately 10 cm below the surface and extends to a depth of approximately 27 cm. Three mineral forms occur: a smooth shiny white ulexite; a delicate finely crystalline material that may be borax; and ulexite cottonballs. Much of the ulexite is mixed with silty sediment and detritus. A sample of ulexite-bearing material collected in 1990 had 8.1 percent Ca; 9.8 percent Na; 3.9 percent Si; 620 ppm Li; 4,300 ppm Sr; and 100,000 ppm B. The surface crust had 4.2 percent Ca; 22 percent Na; 0.26 percent Si; 2,300 ppm Li; 460 ppm Sr; and 49,000 ppm B. Salar de Challviri is discussed in Ballivian and Risacher (1981) and Cadima and Lafuente (1969).

LAGUNA CATALCITO

By Sigrid Asher-Bolinder *and* Eduardo Soria-Escalante

Summary

Laguna Catalcito is a remote, very small, slightly saline lake containing boron, lithium, and nickel. The lake is too small to have brines with economic potential; the lack of precipitates precludes small-scale mining.

Introduction

Laguna Catalcito is in the Departament of Potosí, Provincia Sud Lípez, and is in the Cerro Zapaleri 1:250,000-scale quadrangle (app. A, no. 335). The lake is a small body of water at the base of Cerro Totoral that is fed by Río Novillito, which in turn is fed by a chain of very small lakes that descend from a spring issuing from lava on the side of Cerro Totoral. No published information was found for this site that was visited in August 1990.

Geology and Mineral Deposits

Laguna Catalcito occupies a structural basin overlying late Cenozoic pyroclastic flows. Younger volcanics of the Cerro Totoral dome border the lake to the north and west. Laguna Catalcito is a slightly saline lake with a pH of 7.6. A single analysis of the water contained 0.070 ppm Ni; 3.170 ppm Li; and 6.600 ppm B. The lake has a gravelly margin without evaporite minerals. However, the current lake level (4,555 m by altimeter) is approximately 5 m below the highest associated terrace (4,560 m) and 1 m below an intermediate terrace, suggesting that the boron, lithium, and nickel contents of the water have probably been enhanced by evaporative processes.

LAGUNA BUSCH O KALINA

By Sigrid Asher-Bolinder *and* Eduardo Soria-Escalante

Summary

Laguna Busch o Kalina has anomalous values for boron, calcium, potassium, lithium, molybdenum, sodium, strontium, and titanium. The current lake is a remnant of a much larger and deeper lake.

Introduction

Laguna Busch o Kalina is on the southernmost part of the Altiplano in the Departament of Potosí, Provincia Sud Lípez, and is in the Cerro Zapaleri 1:250,000-scale quadrangle (app. A, no. 336). No production is known from this salar. The salar is remote and access is difficult along a poorly defined dirt track. The northeastern edge of the lake was visited in August 1990.

Geology and Mineral Deposits

Laguna Busch o Kalina occupies a structural basin in pyroclastic flows. Volcanic domes rim the northern and southern boundaries of the basin. Laguna Busch o Kalina is a saline lake with no evaporite precipitate around or on its eastern edge, but extensive salar and (or) sand areas are shown to the west and southwest on unpublished GEOBOL maps of the Cerro Zapaleri 1:250,000-scale quadrangle. Surface water inflow to the basin is largely from the dacitic lavas of the domes and from an ignimbrite plateau to the west. One brine sample was collected from the lake, but there were high winds and the turbid, yellow, and opaque water was contaminated by some of the bottom sediment. The chemistry of this sample is nevertheless anomalous in several elements; it contained 500 ppm B; 200 ppm Li; 20 ppm Sr; 1,110 ppm K; 2,780 ppm Na; 526 ppm Ca; 0.13 ppm Ti; and 0.13 ppm Mo; and the pH was 7.9. A sample of inflow water from Cerro Colino at the east end of the lake had a pH of 7.5 and a very low content of dissolved solids.

Laguna Busch o Kalina is a remnant of a more extensive lake as indicated by lacustrine sediments to the southwest and west of the present lake. Several older lake terraces can be identified above the present water level. In August 1990, the lake level registered an elevation of 4,445 m on an altimeter. A first terrace of sand was measured at 4,446 m, a second terrace of sand and ignimbrite registered at 4,450 m, a third terrace of carbonate-cemented gravel was at 4,482 m, and a probable fourth terrace registered at 4,485 m. Calcium carbonate coats the surface of the gravel between the second and third terraces; no carbonate cement was present above the fourth terrace.

LAGUNA VERDE

By G.J. Orris, Sigrid Asher-Bolinder, Eduardo Soria-Escalante, René Enriquez-Romero, *and* E.A. Bailey

Summary

Laguna Verde is a saline lake in the extreme southwestern part of Bolivia. There has been no known production from this lake and the brines are not currently economic.

Introduction

Laguna Verde is in the Departament of Potosí, Provincia Sud Lípez, and in the Volcán Juriques 1:250,000-scale quadrangle less than 5 km from the Bolivia-Chile border (app. A, nos. 320, 321). Laguna Verde occupies part of a closed basin that receives most of its water inflow from Ríos Blanco and Amargo. A relatively major east-west road runs along the northern shore of Laguna Verde and serves as the most important export route to Chile where goods can be

transported to the port of Antofagasta by a major road and railroad. A sulfur plant that processes ore from the Mina Juanita (Río Blanco) mine is located above the southern shore. The plant and mine are the property of EMICLA. A few shallow pits have been dug in the sediments 2–4 m above the current lake level, but no production is known.

Geology and Mineral Deposits

Laguna Verde is located in a basin defined by the flanks of the volcanoes Juriques, Llicancahur, and Sairecabur on the border with Chile. Laguna Verde is a saline lake that occupies less than 50 percent of its basin. A sample of the lake brine (pH, 7.8) contained 20.800 ppm B; 94 ppm Ca; 37 ppm K; 6.350 ppm Li; 44.9 ppm Mg; 0.651 ppm Na; 50.4 ppm Si; 1.840 ppm Sr; and 0.070 ppm V. The boron and lithium values are very similar to those reported by Ballivian and Risacher (1981) and Risacher (1984). The surrounding lacustrine sediments have minor halite at the surface which overlies clay, ash, and limestone. The limestone is exposed about 3 m above the current lake level. It is a fine-grained, thinly bedded material, containing interbedded organic matter. A sample of the limestone collected in 1990 had 35 percent Ca; 3,700 ppm Mn; 350 ppm As; 76 ppm Li; and 2,700 ppm Sr. The limestone is immediately overlain by a layer of friable white ash with minor fine-grained carbonate. The shaly limestone may be suitable for use as flagstone, although the nearest possible markets would be in Chile.

OTHER INDUSTRIAL MINERAL DEPOSITS

A variety of other types of nonmetallic mineral deposits were visited during August 1990, however, it was not possible to visit all of the known mines and occurrences. The following sites, including one lake deposit classified as a freshwater lake by Risacher (1991), one peat occurrence, and two travertine deposits, were visited and sampled, but are only briefly described.

Laguna Totoral is in the Departament of Potosí, Provincia Sud Lípez, and is in the Cerro Zapaleri 1:250,000-scale quadrangle. The site was visited in August 1990. The lake sits at the base of Cerro Totoral and has a gravel covered rim at a barometric altitude of 4,465 m. An older shoreline composed of carbonate-coated gravel is cut into the ignimbrite at 4,470 m. Laguna Totoral appears to be deep and has many water plants, but no ice or chemical precipitates. A water sample contained 1.900 ppm B; 20.3 ppm Ca; 0.330 ppm Li; 1.4 ppm Mg; 114 ppm Na; 49.9 ppm Si; and 0.130 ppm Sr; and the lake has a pH of 8.1. The lake was free of ice in August, which indicated that the lake must have at least one warm spring in its inflow area, although the topographic map shows no springs or streams providing inflow or outflow.

One peat deposit near Sepultures was sampled in August 1990. The peat deposit is located in Departamento La Paz, Provincia Pacajes, and is in the Charaña 1:250,000-scale quadrangle. It occurs in a bofedal (a high, open meadow) characterized by clumps and pillars of moss and peat, small shrubs, and water-dependent vegetation. Peat deposits have some potential for the occurrence of uranium; they also may be a source of fuel, or used as a soil amendment in a terrane with poorly developed soils. The sample of peat from Sepultures contained 5.4 ppm Th, 3.9 ppm U, and 250 ppm V. Bofedals occur in many areas of the Cordillera Occidental and there may be other peat deposits in the study area.

Two travertine quarries were sampled, one a few kilometers south of Soniquera and the other at Mirzapani. Travertine from both localities is translucent and hard, has been used as building stone, and is suitable for ornamental uses. The travertine from Soniquera is banded and could be classified as onyx marble.

CORDEOR CLAY PIT

By Sigrid Asher-Bolinder, Eduardo Soria-Escalante, *and* G.J. Orris

Summary

The CORDEOR clay pit is in an extensive Quaternary lacustrine deposit of illitic clay 1.3 m thick and suitable for manufacture of bricks and tiles. Reserves of clay in the lacustrine rocks in 1984 were approximately 2,000,000 tonnes.

Introduction

The clay pit of the Corporación de Desarrollo de Oruro (CORDEOR) is located approximately 3 km south-southeast of Caracollo in the Departament of Oruro, Provincia Cercado (app. A, no. 56). This mine is situated in a clay deposit that extends from Caracollo to Oruro, a distance of approximately 30 km. The clay is largely composed of illite and is used locally in the manufacture of bricks and tiles. The quarry is approximately 500 m by 200 m in area. In August 1990, a stockpile of clay was piled on three sides of the quarry and estimated to contain 5,500 m^3 of clay.

Geology and Mineral Deposits

A deposit of Quaternary lacustrine nonswelling clay occurs along the western front of the Cordillera Oriental for

30 km between Caracollo and Oruro. At the CORDEOR workings, the lacustrine deposits consist of detritus derived from the Paleozoic rocks to the east. The mined clays are pale reddish brown to light brown and are nonswelling. The mined clay-bearing horizon has a basal layer of fine sand that grades upward into a 1.3 m interval of silt and clay that contains less than 2 percent volcanic ash. The clay-bearing horizon is underlain by a 30-cm-thick bed of sandstone of which approximately 5 percent is conglomeratic. The sandstone unit is underlain by 1 m of fluvial conglomerate with well-rounded clasts composed mainly of sedimentary rock and vein quartz in a sandy matrix. A sample of clay collected in 1990 had 11 percent Al, 5.1 percent Fe, 3.4 percent K, 1.1 percent Mg, 120 ppm Li, and 130 ppm V. Montes de Oca (1982) estimated that there were approximately 2,000,000 tonnes of illitic clay reserves in lacustrine sediments between Caracollo and Oruro.

MINA COMANCHE

By G.J. Orris, Sigrid Asher-Bolinder, Raul Carrasco, *and* Marcelo Claure Zapata

Summary

Light- to medium-gray paving stone is produced by COMSUR at Mina Comanche from a small body of Miocene andesite.

Introduction

Mina Comanche is in the Departament of La Paz, Provincia Pacajes and is in the La Paz 1:250,000-scale quadrangle (app. A, no. 35). The Mina Comanche quarry is located adjacent to the railroad and a major road from Viacha to Corocoro. Current mining operations produce paving stone. Rectangular blocks with a textured surface are produced for the La Paz market. The mine maintains an inventory of 20,000 m^3 of standard paving stone. COMSUR also markets paving blocks in Belgium. Most of the stone is rough finished by hand texturizing, but some stone is sent to La Paz for polishing.

Geology and Mineral Deposits

Mina Comanche is located in a Miocene andesite 40 km southsouthwest of Viacha (see description of Pachekala prospect). The andesite is fine grained, equigranular, commonly homogeneous, and contains about 20 percent quartz. The stone ranges from light to medium gray in color. The jointing and fracturing in this rock is curvilinear; nonperpendicular jointing is usually not desirable for dimension stone operations. Perpendicular jointing simplifies the process of producing square and rectangular blocks for construction and monument uses. There is some clay, sericite, and limonite developed along some fracture surfaces, commonly 0.1–3 cm thick. In addition, the weathered andesite has a limonitic rind less than 10 mm to 1 cm deep.

MINA SANTA ROSA

By G.J. Orris, Sigrid Asher-Bolinder, *and* Orlando André-Ramos

Summary

The Mina Santa Rosa has an occurrence of kaolin, a product of the argillization process that accompanied the formation of hydrothermal polymetallic veins near the contact of Miocene sediments and dacite. It is unlikely that the kaolin mineralization at this site is economic, but it is possible that similar hydrothermal kaolin might be of economic interest elsewhere.

Introduction

Mina Santa Rosa is located in the Departament of La Paz, Provincia Ingavi, about 13 km southsoutheast of Tiahuanacu (app. A, no. 13). Hydrothermal kaolin occurs associated with polymetallic veins where sandstone and other sediments are intruded by dacite. Access to the mine is provided by a dirt road. Mina Santa Rosa was visited in July 1990. MINTEC appears to have done some work in the area, but no information was available. Workings at the mine are surficial. No published geologic studies on the argillic alteration were located.

Geology and Mineral Deposits

In the mine area, Miocene dacite intrusions emplaced in the Miocene Tiahuanacu Formation sediments have led to formation of polymetallic vein systems and accompanying argillic alteration (see description of Quimsa Chata district). Inclusions of sandstone and mudstone in the dacite are present in the vicinity and in the mine area there is a strong hydrothermal overprint.

Hydrothermal kaolin occurs in the area of the mine in moderate quantities. The kaolin contains approximately 20–25 percent silica and the iron oxide content ranges from about 0 to approximately 5 percent. Limonitic staining, goethite, and pyrolusite are concentrated chiefly in the

immediate vicinity of the dacite contact and along shear and fracture surfaces. Vugs at the dacite-clay interface contain copper minerals, limonite, pyrolusite, and jarosite(?). The alteration is roughly zoned from the contact out as follows: relatively unaltered dacite; clay-goethite-limonite alteration; clay-quartz-pyrite-limonite; clay-quartz-limonite; and kaolin-quartz.

VOLCAN QUEMADO

By Sigrid Asher-Bolinder *and* Eduardo Soria-Escalante

Summary

Volcán Quemado is of interest because of workings near its base where welded tuff has been quarried for local use as building stone. At the summit of the volcano is an occurrence of well sorted glassy volcanic sand in dunes that may have some potential for use as an abrasive, an additive in concrete, and as aggregate. There is little economic potential for use of the tuff as a construction material except in limited local use for building construction.

Introduction

Volcán Quemado occurs in the Departament of Oruro, Provincia Atahuallpa, and is in the Corque 1:250,000-scale quadrangle (app. A, nos. 158, 159). The volcanic pumice-ash occurrence and the welded tuff workings were visited in August 1990.

Geology and Mineral Deposits

Volcán Quemado is a Quaternary volcano with a dome in its crater and upper slopes that are covered with loose whitish-gray pumice and ash. The west lip of the crater is overlain by light-gray to white dunes composed of volcanic sand. The dunes are 300 m long and 100 m wide. The depth of the dunes is unknown, but may be 5–10 m.

Near the western base of Volcán Quemado is an outcrop of light-pinkish gray welded tuff that has been quarried for local use as building stone. The outcrop is approximately 50 m by 30 m. The tuff has curvilinear joints and appears in places to have been noticeably weathered despite its presumably young age.

BARRERO SODIUM CARBONATE PLANT

By Sigrid Asher-Bolinder, G.J. Orris, Eduardo Soria-Escalante, *and* René Enriquez-Romero

Summary

The plant, operated by Barrero, is a trial plant for processing sodium carbonate from Laguna Cachi. A possible market for the sodium carbonate is the lithium carbonate precipitation plant at Salar de Atacama, Chile.

Description

A visit was made to the plant in August 1990. It is located about 7 km east of Laguna Hedionda Norte in the Volcán Ollague 1:250,000-scale quadrangle. Sodium carbonate from Laguna Cachi is brought to this site for processing. Two tonnes of raw sodium carbonate ore is dissolved in water from a nearby stream. The brine is then brought to a boil in a large shallow tank while being stirred regularly. The boiling produces a precipitate enriched in sodium carbonate that is put into a settling tank. The precipitate is washed and placed in a lower tank for further precipitation. The top of the resulting sodium carbonate precipitate is removed and placed in the lowest tank to heat and dry. Finally, the sodium carbonate is crushed, screened, and bagged for transport. On average, the original 2 tonnes of raw sodium carbonate ore yields 150 kg of finished product. The fuel used in this plant is yareta, a dense woody, low-growing plant native to the Altiplano.

EL DESIERTO SULFUR PLANT

By G.J. Orris, Sigrid Asher-Bolinder, Eduardo Soria-Escalante, *and* René Enriquez-Romero

Summary

The El Desierto sulfur plant is operated by Empresa Minera Clavijo Ltda. (EMICLA). The plant produces sulfur only to order at the current time; current production amounts to approximately 60 tonnes of sulfur per month, although capacity is 800 tonnes per month. The plant was visited in August 1990.

Description

The El Desierto sulfur plant, located at the southeastern end of Salar de Empexa, has a capacity of 800

tonnes of sulfur concentrate per month, but currently produces approximately 60 tonnes per month and only in response to orders. The plant is the major supplier of sulfur to the Bolivian sugar industry which requires about 2,000 tonnes of sulfur per season of sugar production. Raw sulfur ore is fed to one of two autoclaves; the typical ore feed is presently 40 percent sulfur from old spoil piles near the plant. The material discarded on dumps after processing contains 20 percent sulfur. Oil is added to the sulfur slurry in the autoclaves and, after about 45 minutes, the slurried sulfur concentrate is then drained into cooling ponds. The sulfur concentrate is then broken into blocks and stacked to await shipment (fig. 105). The plant is fueled by yareta brought from the northwest side of Salar de Empexa, a distance of 15–20 km.

MINA SUSANA SULFUR PLANT

By G.J. Orris, Sigrid Asher-Bolinder, Eduardo Soria-Escalante, *and* René Enriquez-Romero

Summary

The Mina Susana sulfur plant is an active processing plant operated by HORSU S.A. Currently the Mina Susana plant produces 600–700 tonnes per month of more than 99.5 percent sulfur concentrate; there are plans to increase production.

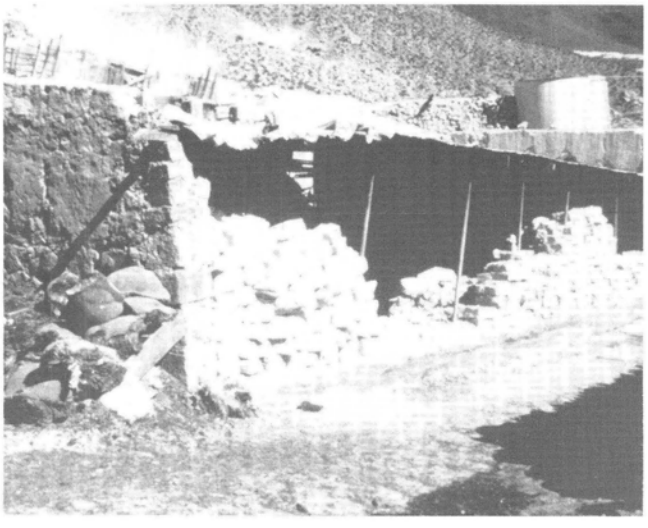


Figure 105. Blocks of sulfur concentrate awaiting shipment at EMICLA's plant at El Desierto, at the southeastern end of Salar de Empexa.

Description

The Mina Susana sulfur plant processes sulfur ore from Mina Susana in the Volcán Juriques quadrangle, Departamento Potosí, Provincia Sud Lípez. The extraction is an autoclave process; each autoclave has a capacity of 1,600 kg and 1.5 tonnes of sulfur ore can be processed by each autoclave in 40 minutes. The plant produces on average 600–700 tonnes per month of sulfur concentrate at more than 99.5 percent sulfur. During a visit in August 1990, the plant had four autoclaves and HORSU was building a flotation step to allow processing of lower grade ore. The plant has run as many as 2 shifts daily when ore and fuel are both in good supply. Current feed to the plant contains 35–38 percent sulfur; 1.5 tonnes of this ore produces 100–200 kg of sulfur concentrate, which is shipped directly west to Chile.

LAGUNA KOLLPA SODIUM CARBONATE PLANT

By Sigrid Asher-Bolinder *and* Eduardo Soria-Escalante

Summary

The Laguna Kollpa sodium carbonate plant is a small cooperative that produces about 20 tonnes of sodium carbonate per month.

Description

The Laguna Kollpa sodium carbonate plant is run by a cooperative that produces sodium carbonate for the La Paz Fiambi Plant. The plant is located on the shore of Laguna Kollpa in Departamento Potosí, Provincia Sud Lípez. After the wind blows away the shallow cover of water on the lake, 10–15 cm of sodium carbonate is removed from the surface. No beneficiation is done at the site and trucks transport approximately 10 tonnes per load. The plant produces as much as 20 tonnes of sodium carbonate per month.

Application of Economic Evaluations to Deposit Models

By Donald I. Bleiwas *and* Robert G. Christiansen, U.S. Bureau of Mines

Introduction **211**
Evaluation method **211**
Epithermal quartz-adularia deposits **212**
Bolivian polymetallic vein deposits **213**
Lacustrine borate deposits **216**
Conclusions **217**

FIGURES

106. Flowsheet of U.S. Bureau of Mines Minerals Availability Program evaluation procedure **211**
107. Gold grade and gold price relationship to attain a 0 and 15 percent discounted cash flow rate-of-return for a hypothetical heap-leach operation **212**
108. Gold grade and gold price relationship to attain a 0 and 15 percent discounted cash flow rate-of-return for a conventional flotation agitation tank leaching operation and Merrill-Crowe plant **213**
109. Impact of specified gold grades and gold market price on discounted cash flow rate-of-return for a hypothetical heap-leach operation **214**
110. Impact of specified gold grades and gold market price on discounted cash flow rate-of-return for a hypothetical agitation tank leaching operation **214**
111. Impact of silver price on discounted cash flow rate-of-return for a Bolivian polymetallic vein deposit **215**
112. Comparison of discounted cash flow rate-of-return with variations of metal prices for a Bolivian polymetallic vein deposit **215**
113. Comparison of discounted cash flow rate-of-return analyses at full equity, one-third equity and, used and reconditioned equipment for a Bolivian polymetallic vein deposit **215**
114. Sensitivity of colemanite grade and market price to attain specified discounted cash flow rate-of-return for a hypothetical lacustrine borate deposit **216**
115. Impact of colemanite concentrate value on discounted cash flow rate-of-return for a hypothetical lacustrine borate deposit **216**
116. Sensitivity of royalties on discounted cash flow rate-of-return for a hypothetical lacustrine borate deposit **217**

TABLES

37. Evaluation parameters for open-pit operation using heap leaching to recover gold from epithermal quartz-adularia vein deposits **212**
38. Evaluation parameters for conventional flotation agitation tank leaching operation and Merrill-Crowe plant to recover gold from epithermal quartz-adularia vein deposits **213**
39. Evaluation parameters for underground cut-and-fill operation to recover metals from a Bolivian polymetallic vein deposit **214**
40. Evaluation parameters for hypothetical open-pit operation to recover colemanite from a lacustrine borate deposit **216**

INTRODUCTION

Personnel of the U.S. Bureau of Mines (BOM), Minerals Availability Field Office (MAFO) performed an economic analysis for selected mineral deposit types found on the Altiplano and in the Cordillera Occidental, Bolivia. This section briefly summarizes the results of engineering, economic evaluations, and sensitivity analyses, performed at the prefeasibility level, based on hypothetical grades and resource estimates provided by the U.S. Geological Survey (USGS). Evaluations and analyses were performed for three tonnage and grade models. One is a combination of the data for the Comstock and Sado epithermal quartz-adularia deposits (Cox and Singer, 1986); these deposits are valuable primarily for gold. The second is the subjective tonnage and grade model developed during this study for Bolivian polymetallic vein deposits; these are valuable primarily for silver and tin. The third tonnage and grade model uses data from lacustrine borate deposits presented in the section on Undiscovered nonmetallic deposits. The development of the economic evaluations and associated sensitivity analyses are intended to illustrate the importance of identifying significant factors and their effects on the economics of potential mining projects or exploration targets in Bolivia. Economic analyses were performed to determine the long-run price at which the primary commodity must be sold in order to recover all costs of production, including a pre-specified discounted cash flow rate-of-return (DCFROR), less any byproduct revenues. Economic analyses were also performed to approximate the expected DCFROR and resulting net present value of the property, given specified commodity prices. The results of sensitivity analyses can be of importance as a tool for developing exploration strategies, for investors, and for government policy makers attempting to attract foreign and domestic investment.

EVALUATION METHOD

A flowsheet of the BOM Minerals Availability Program (MAP) evaluation procedure illustrates the initial identification of deposit models through the execution and interpretation of sensitivity analyses (fig. 106). Hypothetical grades and resources for the development of base models in this study were developed on the basis of field work, analytical methods, geologic analogs, and literature searches by members of the USGS and the Servicio Geológico de Bolivia (GEOBOL). Engineering and economic analyses, performed by the BOM, were developed for three mine-to-marketable-product models: (1) epithermal quartz-adularia, (2) Bolivian polymetallic vein, and (3) lacustrine borate deposits. In order to perform DCFROR and sensitivity analyses, it was necessary to estimate the capital and operating costs of recovering the primary commodity and any associated byproducts. Actual ore characteristics could have significant effects on selection of technology and equipment, reagent consumption, and metallurgical recoveries, all of which impact costs.

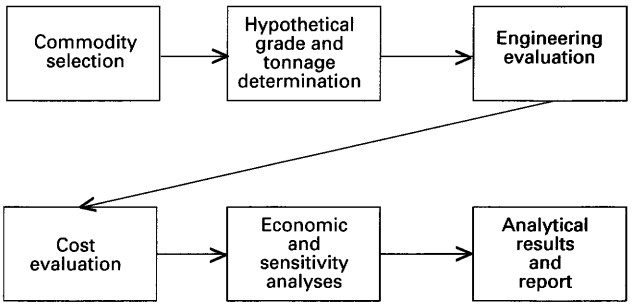


Figure 106. Flowsheet of U.S. Bureau of Mines Minerals Availability Program evaluation procedure.

Engineering parameters, such as mine design and mining method, mine recovery and dilution, waste-to-ore ratios, equipment selection, processing methods, and metallurgical recoveries, were selected on the basis of grade and resource data provided by the USGS and analogous operations in Bolivia, except in the case of colemanite, for which the base model was developed using data from operations in the United States and Turkey.

The evaluations, performed in U.S. dollars, utilize 1990 Bolivian cost estimates for labor, materials, equipment, transportation, and other important components. Most of the costs were collected in Bolivian currency (Boliviano) and converted to U.S. dollars at a 3:1 ratio.

Capital cost estimates used for the calculations include exploration, mine development, mine and mill plant and equipment, and infrastructure (for example, access roads, powerlines, waterwells). They do not include costs for purchasing land, reclamation and environmental requirements, townsites, or any permitting associated with mining activities. Costs were derived from analogous operations in Bolivia, for which actual costs and engineering data were available; from BOM and GEOBOL data and utilization of the BOM's Cost Estimating System (CES), which was adjusted to reflect Bolivian costs for labor, fuel, supplies, and equipment; and other U.S. and Bolivian sources of information.

Operating costs include infrastructure, mining, beneficiation, transportation, and post-mill treatment (toll smelting and refining charges). The estimates were developed using costs for labor, materials, and supplies in Bolivia and information sources listed previously. Costs and terms for treatment of concentrates at smelters and refineries were based on actual contracts in force during the study (1990–91). The CES program was also used to develop mining and beneficiation operating costs.

It was assumed that the investments required for production of the modeled mines were developed at full equity, therefore there were no interest charges included in

Table 37. *Evaluation parameters for open-pit operation using heap leaching to recover gold from epithermal quartz-adularia vein deposits*

[Metal prices used in analyses: gold, $350/oz; silver, $4.00/oz]

ECONOMIC PARAMETERS (1990 US$)

Capital Investments	million $
Infrastructure	$3.1
Mine	3.2
Beneficiation	2.7
TOTAL	$9.0

Production costs	$/t ore	$/oz Au
Infrastructure	$0.25	$2.20
Mine	4.65	41.20
Beneficiation	11.30	100.20
Post mill processing[1]	0.40	3.35
Transportation	0.10	0.85
TOTAL	$16.70	$147.80

[1]Includes cost of silver recovery ($0.30/oz) and a 98 percent pay for.

ENGINEERING AND TECHNICAL PARAMETERS

Mine Type: Open pit
Ore processing method: Cyanide heap leach with Merrill-Crowe plant
Annual ore production: 195,000 t
Waste-to-ore ratio: 2:1
Gold feed grade: 5.4 g/t
Silver feed grade: 59.4 g/t
Overall gold recovery: 65 percent
Overall silver recovery: 45 percent
Average annual gold production: 22,000 oz
Average annual silver production: 168,000 oz

the base models. A sensitivity analysis illustrating the impact of interest charges on the economics of the Bolivian polymetallic vein model is presented later.

Applicable depreciation periods, taxes, and royalties, in accordance with current Bolivian laws, were estimated for all of the evaluations. Sensitivity of the economics of each operation to taxes and royalties are discussed in greater detail later.

The data were entered into the BOM computerized, economic mine simulator program (MINSIM). This program is used to either approximate an expected DCFROR, or determine the long-run price at which the primary commodity must be sold to recover all costs of production, including a prespecified DCFROR on investment, less any byproduct revenues. Utilizing the program, the economic sensitivity of the evaluations to selected variables can be determined and illustrated graphically. The results of these analyses can assist in the development of exploration and (or) investment programs and can provide information for government policy makers in the development of an investment environment that may attract foreign and (or) domestic investors. Favorable economic policies could result in the generation of tax revenues, increased employment, and foreign exchange earnings.

EPITHERMAL QUARTZ–ADULARIA DEPOSITS

Several economic sensitivity analyses, including comparison of technologies, sensitivity to grades, and varying the market price for gold, were performed on the epithermal quartz-adularia deposit type. Technical data for the tonnage and grade model are listed in table 37. Economic evaluations were performed varying the feed grade of gold for a Bolivian open-pit operation using heap leaching and a Merrill-Crowe facility to recover gold and silver. The silver grade was not changed because it represented only a minor portion of total revenues.

The relationship between gold grade and market prices required to attain specified rates-of-return from the hypothetical heap-leach operation is shown in figure 107. In

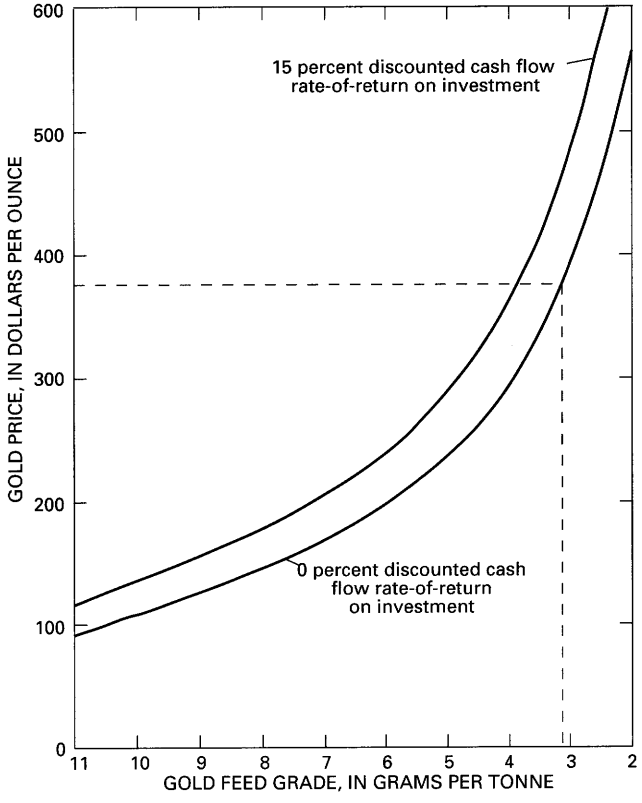


Figure 107. Gold grade and gold price relationship to attain a 0 and 15 percent discounted cash flow rate-of-return (DCFROR) for a hypothetical heap-leach operation. Dashed line shows that using the gold market price at the time of the study in 1990 ($374/oz), the property could operate above 0 percent DCFROR at average gold grades slightly above 3 g/t.

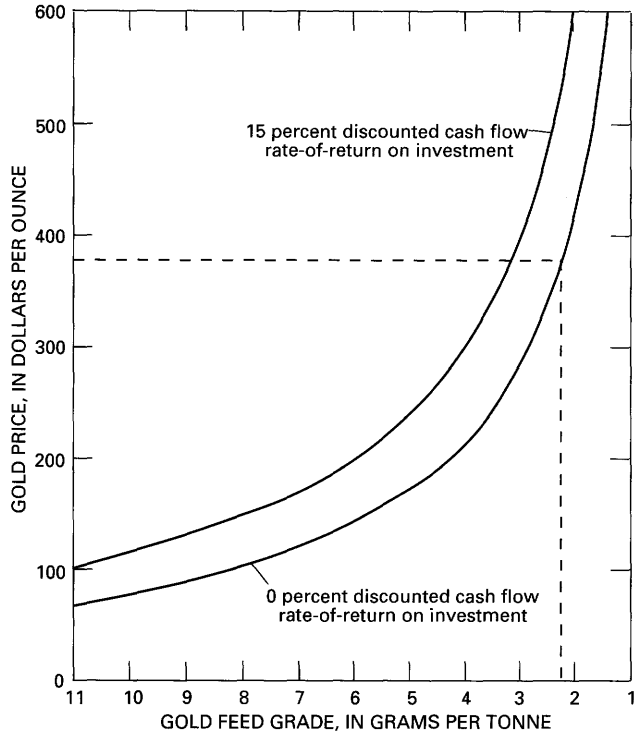


Figure 108. Gold grade and gold price relationship to attain a 0 and 15 percent discounted cash flow rate-of-return (DCFROR) for a conventional flotation agitation tank leaching operation and Merrill-Crowe plant. Dashed line shows that using the gold market price at the time of the study in 1990 ($374/oz), the property could operate above 0 percent DCFROR at average gold grades above 2.3 g/t.

Table 38. *Evaluation parameters for conventional flotation agitation tank leaching operation and Merrill-Crowe plant to recover gold from epithermal quartz-adularia vein deposits*

[Metal prices used in analyses: gold, $350/oz; silver, $4.00/oz]

ECONOMIC PARAMETERS (1990 US$)

Capital Investments	million $
Infrastructure	$3.1
Mine	3.2
Beneficiation	11.9
TOTAL	$18.2

Production costs	$/t ore	$/oz Au
Infrastructure	$0.25	$2.15
Mine	4.65	36.70
Beneficiation	7.45	58.80
Post mill processing[1]	0.80	3.35
Transportation	0.10	0.85
TOTAL	$13.25	$101.85

[1]Includes cost of silver recovery ($0.30/oz) and a 98 percent pay for.

ENGINEERING AND TECHNICAL PARAMETERS

Mine Type: Open pit
Ore processing method: Conventional flotation, agitation leach, Merrill-Crowe plant
Annual ore production: 195,000 t
Waste-to-ore ratio: 2:1
Gold feed grade: 5.4 g/t
Silver feed grade: 59.4 g/t
Overall gold recovery: 73 percent
Overall silver recovery: 65 percent
Average annual gold production: 24,700 oz
Average annual silver production: 242,000 oz

order for the open-pit operation outlined in table 37, which had a gold feed grade of 5.4 g/t, to produce at a 0 percent DCFROR, a gold price of approximately $220/oz is required; in order to receive a 15 percent DCFROR, a gold price of approximately $268/oz over the 5 year mine life is necessary. At the gold market price at the time of the study ($374/oz), the property could operate above a 0 percent DCFROR at average gold grades slightly above 3 g/t (fig. 107).

A similar sensitivity analysis, analyzing conventional flotation, agitation tank leaching and a Merrill-Crowe plant is shown on figure 108. Technical data for the tonnage and grade model is provided in table 38.

At the modeled feed grade of 5.4 g/t, a price of approximately $165/oz of gold is required to achieve a 0 percent DCFROR and a price of $225/oz to achieve a 15 percent DCFROR. Based on a market price of $375/oz, the property could earn a positive rate-of-return at all gold grades above 2.3 g/t (fig. 108). With an ore feed grade of 3.25 g/t , a 15 percent DCFROR could be earned.

The results of analyses performed to determine the sensitivity of rates-of-return to selected gold feed grades (2.5, 3.5 and 5.4 g/t) and gold market price for the hypothetical heap-leach operation are shown on figure 109. A DCFROR of slightly more than 40 percent would be received using a gold feed grade of 5.4 g/t and slightly less than 15 percent using a gold feed grade of 3.5 g/t and a price of $375/oz for gold.

The results of analyses performed to determine the sensitivity of the conventional gold model with agitation tank leaching to a similar analyses are shown on figure 110. The hypothetical operation would also receive a 40 percent DCFROR over the 5 year mine life. The tank-leach operation could potentially be profitable at lower grades than the heap-leach operation.

BOLIVIAN POLYMETALLIC VEIN DEPOSITS

The Bolivian polymetallic vein deposit type, described in the section on Mineral deposit models, was modeled using an underground cut-and-fill operation accessed by a 350-m vertical shaft and 1,000 m of horizontal drifts and crosscuts with 7 stopes developed prior to production. The engineering and economic analyses are

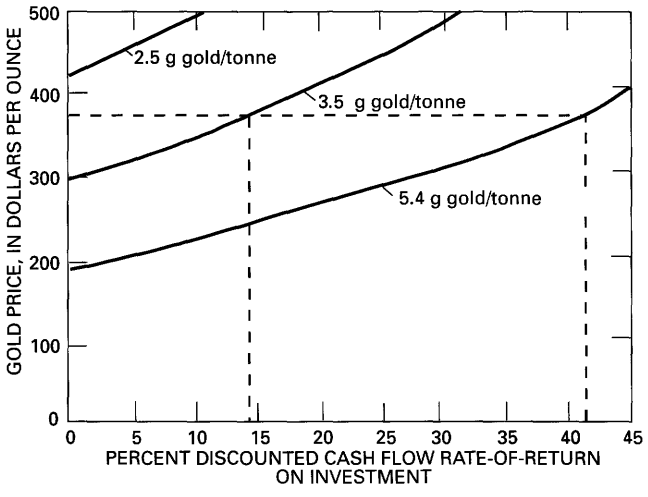


Figure 109. Impact of specified gold grades and gold market price on discounted cash flow rate-of-return (DCFROR) for a hypothetical heap-leach operation. Dashed line shows the percent DCFROR on investment at 2.5, 3.5, and 5.4 g/t using the gold market price at the time of the study in 1990 ($374/oz).

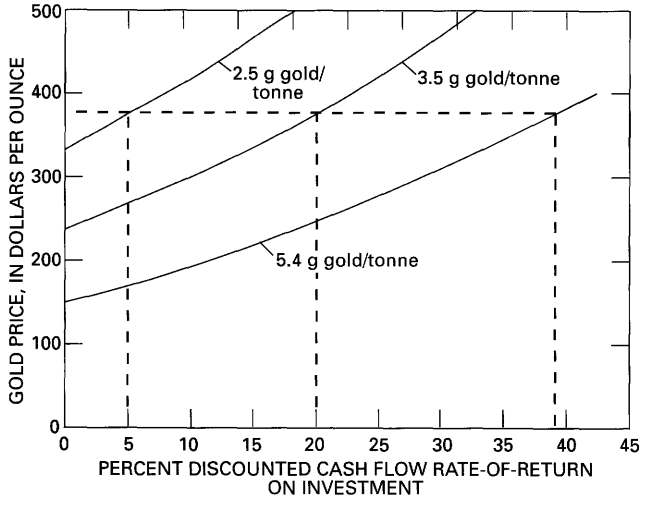


Figure 110. Impact of specified gold grades and gold market price on discounted cash flow rate-of-return (DCFROR) for a hypothetical agitation tank leaching operation. Dashed lines show the percent DCFROR on investment at 2.5, 3.5, and 5.4 g/t using the gold market price at the time of the study in 1990 ($374/oz).

based on current mining practices and associated costs in Bolivia; they assumed that a 2-year preproduction period would be necessary and the operation would continue in production for 20 years. Table 39 provides engineering and economic parameters utilized in the evaluation of Bolivian polymetallic veins.

Three sensitivity analyses were performed: (1) sensitivity to metal prices; (2) sensitivity to new versus used and reconditioned equipment; and (3) investment at one-third equity.

Table 39. *Evaluation parameters for underground cut-and-fill operation to recover metals from a Bolivian polymetallic vein deposit*

[Metal prices used in analyses: zinc, $0.80/lb; silver, $4.00/oz; lead, $0.40/lb]

ECONOMIC PARAMETERS (1990 US$)

Capital Investments	million $
Infrastructure	$ 3.1
Mine	6.9
Beneficiation	3.0
TOTAL	$13.0

Production costs	$/t ore	$/lb Zn
Infrastructure	$ 0.35	$.01
Mine	21.25	.23
Beneficiation	7.00	.08
Post-mill processing	18.00	.19
Transportation costs	8.50	.09
TOTAL	$55.10	[1]$.60

[1]Cost would be $0.70/lb when adjusted for 85 percent zinc pay for.

ENGINEERING AND TECHNICAL PARAMETERS

Mine Type: Underground cut-and-fill
Ore processing method: Flotation
Annual ore production: 130,000 t
Zinc feed grade: 4.8 percent
Silver feed grade: 135 g/t
Lead feed grade: 0.95 percent
Overall zinc recovery: 90 percent
Overall lead recovery: 70 percent
Overall silver recovery: 80 percent
Average annual zinc production: 5,600 t
Average annual silver production: 450,000 oz
Average annual lead production: 865 t

The price of zinc required to achieve a specified DCFROR as the market price of silver is adjusted is illustrated on figure 111. The price of lead was constant because lead contributes less than 5 percent to the total revenue of the operation. The price of silver does not appear to have a significant impact on the price of zinc required to meet a specific rate-of-return.

Another way to demonstrate the comparative impact of revenues from silver and zinc is the construction of histograms (fig. 112). The prices of zinc and silver were adjusted and the profitability (DCFROR) of the operation is shown to be more dependent on the price of zinc than on the price of silver.

Economic analyses were also performed comparing the economic sensitivity of the mining operation developed at full equity; at one-third equity with the balance borrowed at 15 percent interest, paid back over 10 years; and on the basis of reconditioned and used equipment (purchased at 100 percent equity). It was assumed that used and (or) reconditioned mining and beneficiation equipment could be purchased at approximately 60 percent of the cost of new equipment. Estimated operating costs for mining and ben-

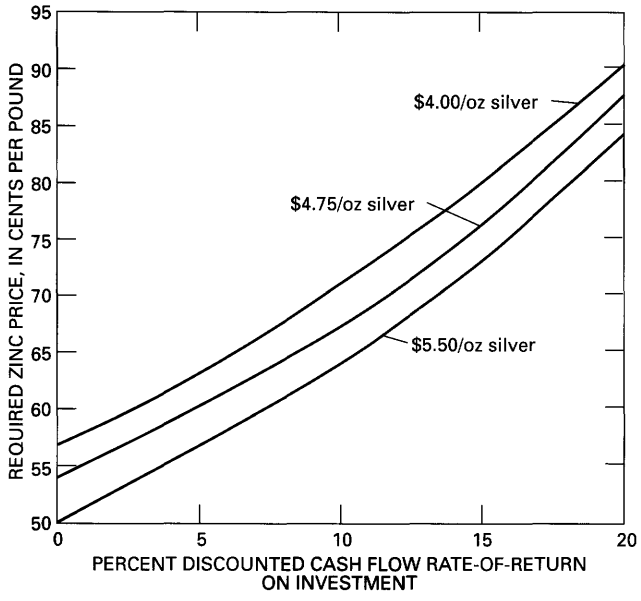


Figure 111. Impact of silver price on discounted cash flow rate-of-return for a Bolivian polymetallic vein deposit.

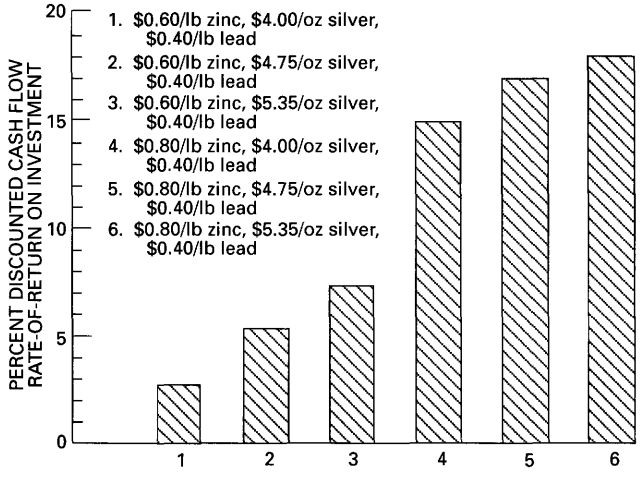


Figure 112. Comparison of discounted cash flow rate-of-return with variations of metal prices for a Bolivian polymetallic vein deposit.

eficiation were increased by 30 percent over the tonnage and grade model, in order to reflect the expense and loss of efficiency resulting from increased repair and maintenance presumed necessary on the equipment.

At full equity, development of the deposit requires lower zinc prices to meet pre-specified DCFRORs than at one-third equity, until a 9 percent DCFROR is exceeded (fig. 113). This relationship indicates that leveraging the cost of the operation at interest rates (in this case 15 percent) below the hurdle rate specified by the investor is generally advantageous. The analysis based on used and reconditioned equipment are similar; development of the theoretical operation at full equity, is economically advantageous until the DCFROR exceeds about 16 percent, after which the required price for zinc is higher.

Economic evaluations were performed comparing the currently emplaced royalty, or "regalia" tax, with a proposed optional tax system. This analysis was completed before the recent (spring 1991) changes in the mining and tax laws were enacted. The "regalia" tax is payable on notional (presumptive) profit, after deductions for notional production costs and notional realization expenses. Notional, or presumptive, production and realization costs are determined by the Bolivian government and imputed for determination of royalty payments. The costs are specific to certain metals. The "regalia" tax system is punitive to high-cost operations, especially during periods of low market prices. The current Bolivian tax laws do not permit deductions for exploration, development, and mine safety costs. As a result, mining interests have not expended large sums in these categories. The intent of the proposed optional tax system is to encourage investment in Bolivia's mineral sector, and especially to attract larger operations, which have more attendant capital risk. The proposed optional tax system would be comparable to that in effect in a number of other countries, such as the United States, Australia, and Canada, and would be based on a 2.5 percent basic tax on net sales, plus 20 percent tax on net profits (after deductions). This proposed tax system would also allow deductions previously not permitted, including investments for development of offsite locations. The intent of the proposed tax system is to encourage new investments and reinvestments resulting in expansion of Bolivia's mining sector. Small mining companies and cooperatives may elect to use the "regalia" tax format because of its simplicity and because they would be unable to take advantage of allowable deductions with only small reinvestments.

The results of the DCFROR analysis indicate that the optional tax system would benefit mining operations, especially those with higher operating costs. Tax savings for

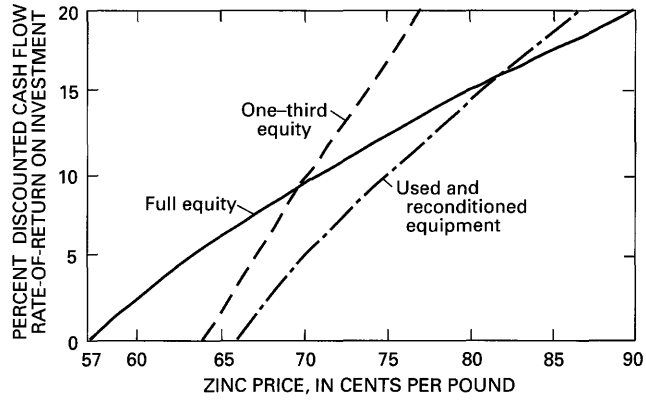


Figure 113. Comparison of discounted cash flow rate-of-return analyses at full equity, one-third equity, and used and reconditioned equipment for a Bolivian polymetallic vein deposit.

Table 40. *Evaluation parameters for hypothetical open-pit operation to recover colemanite from a lacustrine borate deposit*

[Concentrate market price: colemanite, $350/t of 42% B_2O_3]

ECONOMIC PARAMETERS (1990 US$)

Capital investments	million $
Infrastructure	$0.5
Mine	12.0
Beneficiation	4.0
TOTAL	$16.5

Production costs	$/t ore	$/t concentrate
Infrastructure	$0.24	$0.64
Mine	9.30	24.80
Beneficiation	15.50	41.34
Transportation	50.20	133.87
TOTAL	$75.24	$200.65

ENGINEERING AND TECHNICAL PARAMETERS

Mine type: Open pit
Ore processing method: Conventional flotation, drying, and bagging
Annual ore production: 200,000 t
Waste-to-ore ratio: 5:1
Colemanite ore grade: 22.5 percent B_2O_3
Overall colemanite recovery: 70 percent
Average annual colemanite concentrate production: 75,000 t
Colemanite concentrate grade: 42 percent B_2O_3

the evaluated polymetallic vein deposits with the optional tax system, was approximately 30 percent over the current "regalia" tax system.

LACUSTRINE BORATE DEPOSITS

The results of the DCFROR analyses and related sensitivity studies for lacustrine borate deposits are based on the economic and engineering parameters that are presented in table 40. Results of analyses were compared to the January 1990 market price of $350/t for 42 percent B_2O_3 Turkish colemanite concentrate. Sensitivity analyses included determination of DCFROR by varying the market value of the colemanite concentrate, impact of grades, and effects of royalties on DCFROR.

The tonnage and grade model was evaluated using a grade comparable to those of colemanite ores exploited in the U.S. and Turkey (23 percent B_2O_3). However, additional analyses were performed in order to determine the sensitivity of a potential operation to average feed grades and the market price required to attain a 0 and 15 percent DCFROR. Results of the analyses indicate that ore grades would need to exceed approximately 15 percent B_2O_3 in order to achieve a 0 percent DCFROR and 19 percent B_2O_3 in order to achieve a 15 percent DCFROR over the mine's 5 year life (fig. 114).

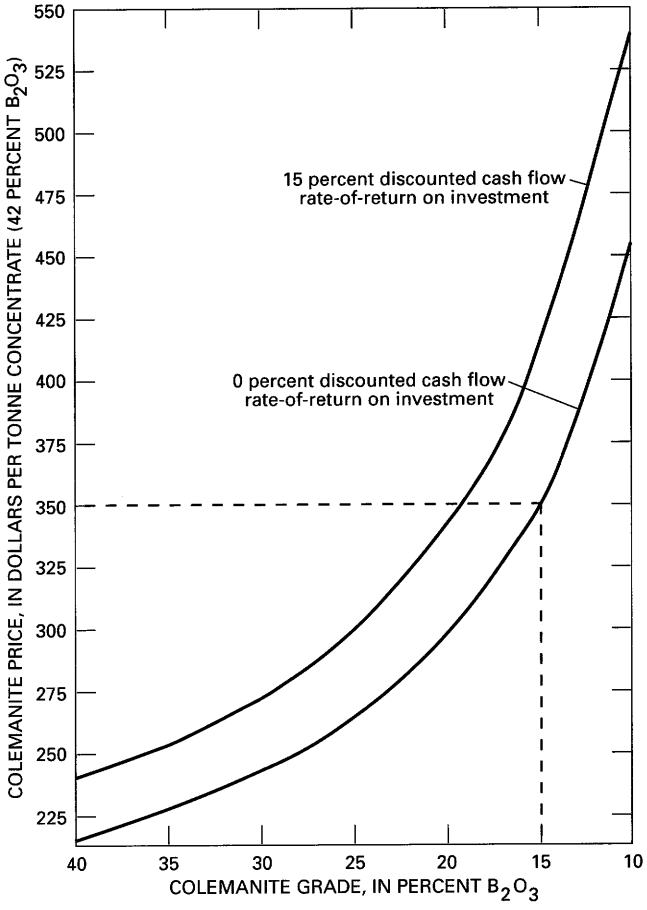


Figure 114. Sensitivity of colemanite grade and market price to attain specified discounted cash flow rate-of-return (DCFROR) for a hypothetical lacustrine borate deposit. Dashed line shows that ore grade would need to exceed approximately 15 percent B_2O_3 in order to achieve 0 percent DCFROR.

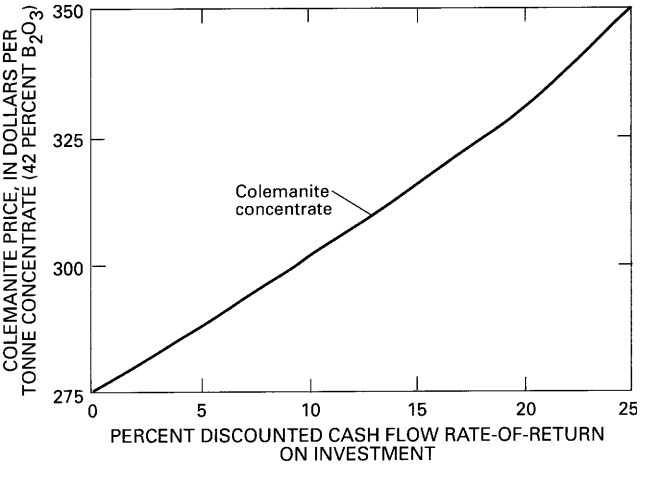


Figure 115. Impact of colemanite concentrate value on discounted cash flow rate-of-return for a hypothetical lacustrine borate deposit.

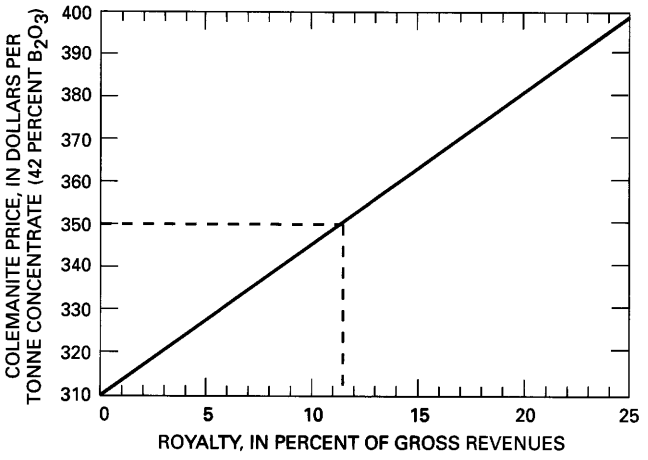


Figure 116. Sensitivity of royalties on discounted cash flow rate-of-return (DCFROR) for a hypothetical lacustrine borate deposit. Dashed line shows that using a market price of $350/t for colemanite concentrate and approximately 12 percent gross revenues, a 15 percent DCFROR (solid line) will be realized over the life of the project.

DCFROR analyses were performed at several different market values for the hypothetical colemanite concentrate in order to determine the potential impact on the profitability of the operation if the product did not meet the standards required by most buyers. Concentrates could have considerably lower values if market conditions are poor, or if they are considered to be of low grade, or if contaminants, such as chlorides are present. In order to remain profitable the hypothetical operation would need to receive prices exceeding approximately $275/t (fig. 115).

The potential impact of royalties on profitability compared with the market price required to receive 50 percent DCFROR was also analyzed. The current tax system requires that a royalty of 1.5 percent of gross revenues be paid on nonmetallic commodities. At a royalty of approximately 12 percent of gross revenues and a market price of $350/t of concentrate, a potential investor would receive a 15 percent DCFROR over the life of the project (fig. 116).

CONCLUSIONS

Development of a data base consisting of such information as actual and estimated costs for mining equipment, labor, electricity, fuel, transportation, the impact of tax policies, and availability of post-mill treatment facilities in Bolivia, permits explorationists, potential investors, and policy makers the opportunity to perform cash-flow analyses. The ability to develop sensitivity analyses by examining the effects of selected variables, such as feed grade and capacity, mining method, metallurgical recovery, selection of technologies, debt-equity relationships, market value of products, and impact of fiscal policies, provides an important tool in decision making for the development of an exploration program or investment decision. The results of these analyses may encourage the development of new government policies intended to attract investment by local and foreign corporations resulting in increased employment, development of new or improved infrastructure, additional foreign exchange, and higher tax revenues.

Methods of Resource Assessment

By Steve Ludington, G.J. Orris, *and* Dennis P. Cox

Introduction **218**
Delineation of permissive areas **218**
Grade and tonnage models **219**
Estimation of number of undiscovered deposits **219**

INTRODUCTION

An assessment of mineral resources can take many forms. The simplest might be a statement like, "Yes, this is a good place to look for minerals." Another type of assessment might consist of an exhaustive inventory of the location, nature, and amount of known resources, in principle, much like what a shepherd does in counting sheep. This would only be possible if the area were completely explored and no undiscovered deposits remained. Our goal in the present study has been a quantitative assessment of the undiscovered metallic and nonmetallic mineral resources on the Altiplano and in the Cordillera Occidental, Bolivia.

An assessment of undiscovered resources is different from simple enumeration. It cannot be verified within the lifetimes of the assessors. Only with the passage of time, and with exhaustive exploration, will the truth be known. Thus, it is clearly an estimate and not a precise measurement. Assessments of undiscovered resources are of use to strategic planners, who plan for a nation's economic and military security; to economic planners, who estimate current and future mineral supplies and plan development; to mineral production companies, that use it to guide and help plan exploration; to governmental planning agencies, that help make decisions between competing land uses; and to public agencies that lease, trade, or sell publicly owned mineral resources.

The three-part quantitative assessment method used in this study has been described in Menzie and Singer (1990), Singer and Cox (1988), and Singer and Ovenshine (1979). A particularly attractive feature of this form of assessment is that the individual parts can be done independently. For example, quantification of an assessment, using permissive areas defined independently years earlier, may become possible because of the subsequent preparation of a grade and tonnage model.

DELINEATION OF PERMISSIVE AREAS

The first part of the assessment process is to define areas that are permissive for the the occurrence of the deposit type being evaluated. This is different from delineating areas where deposits are most likely to occur, because, by definition, the permissive area will contain all undiscovered deposits that are postulated in the assessment process. In other words, the permissive area is the land that remains after the elimination of those areas where the deposit type could not possibly occur. In practice, this definition is not strictly adhered to. If it were, the maps of permissive areas would commonly be all-inclusive and therefore, of limited value. There are very few types of mineral deposits whose genesis we understand well enough that we can eliminate the last vestige of probability that they might occur in any particular place.

In this study, we have outlined within some of the permissive areas, subareas that are particularly favorable for the occurrence of deposits (pl. 7). These favorable areas were designated because of the coincidence of a large number of important features in the geologic environment that are characteristic of a particular deposit type, and we believe that the areal density of undiscovered deposits is higher than throughout the permissive area in general, although we have made no attempt to specify how much higher.

Boundaries of the permissive areas on plate 7 may not correspond exactly to the outcrops of permissive rocks on the geologic map (pl. 1). This is because we considered undiscovered deposits at some depth below the surface, and permissive areas may extend beneath the cover of younger rocks. This subsurface extension of permissive areas is entirely subjective because we lack detailed geophysical

information with which to estimate depths to basement rocks and because there is very little information about the depth of Quaternary basins on the Altiplano.

Some deposits, especially of some industrial minerals, may form only at limited depths (pl. 8). As an example, evaporation of saline lakes occurs only at the surface of the Earth and minerals that contain loosely bound water, such as natron or mirabilite, may not persist after burial. A particular feature of evaporite deposits is that, because of the short time represented by the lithologic record preserved at the surface, we may be predicting deposits that are yet to form, or forming today, in addition to those that already exist.

GRADE AND TONNAGE MODELS

Grade and tonnage models are used as part of the resource assessment to help classify the deposits, thus aiding in delineation, and to provide information about the potential value of undiscovered deposits. Combined with estimates of the number of undiscovered deposits, they are instrumental in translating geologic expertise into statements that economists can use.

Frequency distributions of tonnage and grade of well-explored deposits are available for 60 deposit types (Cox and Singer, 1986; Bliss, 1992; Orris and Bliss, 1991). For this study, we use some of those models, and have created some new ones.

ESTIMATION OF NUMBER OF UNDISCOVERED DEPOSITS

The method used to estimate the number of undiscovered mineral deposits in this study was subjective and used the expert judgment of a number of geologists familiar with the data. The assessment team gathered all the pertinent information about the various types of mineral deposits that might occur in the study area. After reviewing the geologic, geochemical, and geophysical information, and after delineating the boundaries of the permissive areas, each member of the assessment team made estimates of the number of undiscovered deposits at different probability levels. The estimates were shared among team members, and those with extreme estimates, both high and low, were asked to justify their responses. The estimates were discussed until consensus was attained.

Undiscovered Metallic Deposits

By Steve Ludington, Dennis P.Cox, Orlando André-Ramos, Angel Escobar-Diaz, Eduardo Soria-Escalante, W. Earl Brooks, B.M. Gamble, Keith R. Long, John W. Cady, *and* Daniel H. Knepper

Sediment-hosted copper deposits **220**
Permissive and favorable areas **220**
Grade and tonnage model **221**
Estimated number of undiscovered deposits **221**
Basaltic copper deposits **221**
Sandstone uranium deposits **222**
Sediment-hosted gold deposits **222**
Syntectonic antimony and related deposits **222**
Placer gold deposits **222**
Bolivian polymetallic veins **222**
Permissive and favorable areas **222**
Grade and tonnage model **223**
Estimated number of undiscovered deposits **223**
Distal disseminated silver deposits **223**
Porphyry and epithermal precious-metal deposits **223**
Volcanogenic uranium and rhyolite-hosted tin deposits **224**

FIGURES

117. Grade model for sediment-hosted copper deposits **221**
118. Tonnage model for sediment-hosted copper deposits **221**

SEDIMENT–HOSTED COPPER DEPOSITS

PERMISSIVE AND FAVORABLE AREAS

Sediment-hosted copper deposits are known to exist in all parts of the Tertiary sedimentary sequence in the study area, thus all rocks of this age are delineated as permissive for undiscovered sediment-hosted copper deposits (pl. 7). Cretaceous strata contain redbeds as well as evaporites and are also delineated as permissive, although no sediment-hosted copper deposits are known to occur in them. Because sediment-hosted copper deposits have been mined to a depth of more than 450 m in the Corocoro district, we delineated the permissive area and estimated the number of unknown deposits to a depth of 500 m below the surface.

Rocks of lower Tertiary age (pl. 1, Ts1) host the overwhelming majority of deposits in the northern part of the study area and we believe they are more favorable for the occurrence of sediment-hosted copper deposits than are younger rocks; because we are not certain if the same is true in the southern part of the study area, we did not delineate them separately on plate 7. Deposits in the Corocoro, Callapa, and Chacarilla areas are closely associated with diapirs of gypsum and gypsiferous shale and the largest deposits at Corocoro and Chacarilla are situated within 5 km of the flank of a major diapir. Massive halite was discovered by drilling in the Corocoro area (Avila-Salinas, 1990); this suggests that the gypsum observed in outcrop is a cap overlying a salt intrusion at depth. Brine springs are presently active along the flanks of diapirs between Corocoro and Callapa. We believe that diapirs introduced heat and copper-rich brines into sedimentary rocks along their flanks. These fluids mixed with reduced fluids in the

sedimentary strata and formed the copper deposits. Therefore, we delineated an area of Tertiary sedimentary rocks within 5 km of known diapirs as favorable for undiscovered deposits (pl. 7).

GRADE AND TONNAGE MODEL

The geologic factors discussed in the section on Mineral deposit models limit the thickness and extent of reductant traps for copper deposition; sediment-hosted copper deposits in Bolivia are small and consequently the grade and tonnage model of Mosier and others (1986) is not appropriate. An applicable grade and tonnage model was constructed from reserve and production data for 13 Bolivian deposits and districts in which the grade was apparently not raised by hand sorting (figs. 117, 118). Tonnages of these deposits have a high standard deviation; the median tonnage is only 70,000 tonnes, whereas the largest 10 percent are larger than 2,000,000 tonnes. The two largest deposits, Corocoro and Chacarilla, are well below the median tonnage for the distribution of Mosier and others (1986) for deposits worldwide. The range of grades is narrow; most deposits cluster around a median of 3.2 percent copper.

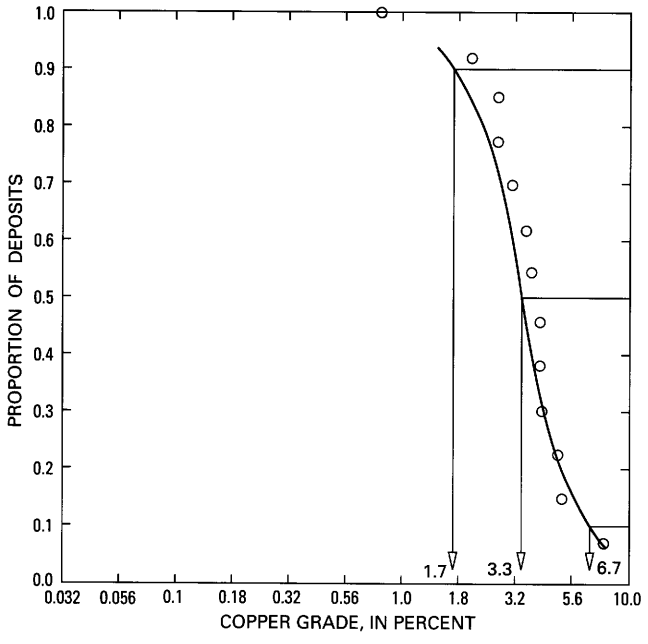


Figure 117. Grade model for 13 sediment-hosted copper deposits on the Altiplano and in the Cordillera Occidental, Bolivia. Each circle represents a single deposit, cumulated in ascending grade. Logarithmic scale used for grade. Smoothed curves are plotted through the mean and standard deviation of the log normal distribution that has the same mean and standard deviation as the deposit data. Fine lines with arrows are intercepts for the 90th, 50th, and 10th percentiles.

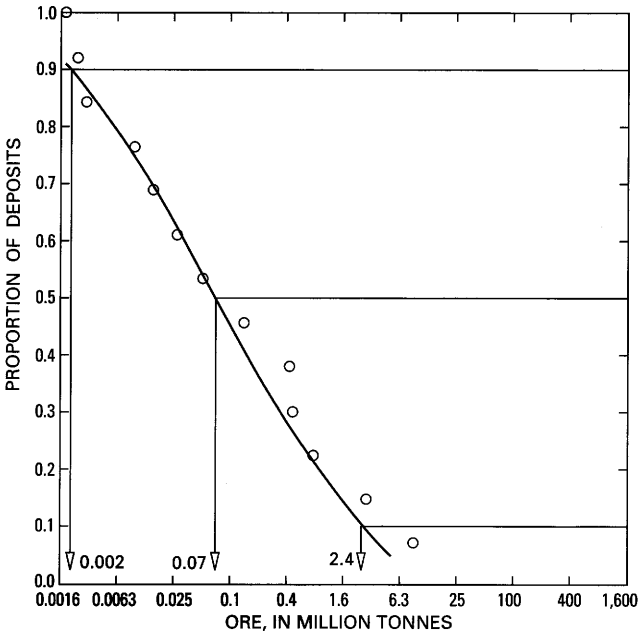


Figure 118. Tonnage model for 13 sediment-hosted copper deposits on the Altiplano and in the Cordillera Occidental, Bolivia. Each circle represents a single deposit, cumulated in ascending tonnage. Logarithmic scale used for tonnage. Smoothed curves are plotted through the mean and standard deviation of the log normal distribution that has the same mean and standard deviation as the deposit data. Fine lines with arrows are intercepts for the 90th, 50th, and 10th percentiles.

ESTIMATED NUMBER OF UNDISCOVERED DEPOSITS

The assessment team estimated that there is a 90 percent chance for the occurrence of 20 or more deposits, a 50 percent chance for the occurrence of 40 or more deposits, and a 10 percent chance for the occurrence of 70 or more deposits. For each of these estimates, half of the deposits are larger than 70,000 tonnes and half have a grade of greater than 3.2 percent copper.

BASALTIC COPPER DEPOSITS

The basaltic copper deposit type shares many characteristics with the sediment-hosted copper deposit type. A critical feature for the occurrence of basaltic copper is the presence of basalt in the sedimentary section. Because we lack sufficient information about the distribution of basalt and there is no separate grade and tonnage model for this deposit type, we include these deposits in the delineation and undiscovered deposit estimate for sediment-hosted copper. A favorable area for basaltic copper deposits that surrounds the known basalt horizon in the Azurita Formation is show on plate 7.

SANDSTONE URANIUM DEPOSITS

Part of the same area delineated as permissive for sediment-hosted copper is also permissive for a closely related deposit type, sandstone uranium. A critical feature for the occurrence of sandstone uranium deposits is the presence of uranium-rich source rocks, from which potential ore fluids may leach uranium. Because we lack data about the existence of suitable source rocks and because there is no grade and tonnage model for the deposit type, we do not delineate a permissive area or make a deposit estimate for sandstone uranium deposits.

SEDIMENT–HOSTED GOLD DEPOSITS

As discussed in the section on Mineral deposit models, reliable criteria for the occurrence of sediment-hosted gold deposits are controversial. In other parts of the world, such deposits are not found in young, poorly consolidated sedimentary rocks, and so we excluded the Tertiary sedimentary rocks on the Altiplano. We also excluded the Cretaceous sedimentary sequence near Sevaruyo, because deposits in other parts of the world have not been found in rift basin environments. The remaining Paleozoic outcrops on the Altiplano constitute the permissive area (pl. 7). Because of the low grades of these deposits (Mosier and others, 1992), all of the known deposits are mined by open-pit methods. Therefore, we have chosen to assess undiscovered deposits only to 500 m below the surface.

Deposits are more likely to occur where thrusting and crustal thickening during the Andean orogeny has deeply buried portions of the Paleozoic stratigraphic section. Although we know the location of a few of these thrust faults, our knowledge of the subsurface crustal structure of the study area is insufficient to specifically delineate a portion of the area as favorable. Because there are no known examples, there is insufficient information to make an estimate of the number of undiscovered deposits. A revised grade and tonnage model has been published by Mosier and others (1992).

SYNTECTONIC ANTIMONY AND RELATED DEPOSITS

The factors controlling the occurrence of syntectonic antimony and related deposit types are also poorly known. All the known syntectonic antimony and low-sulfide gold-quartz vein deposits in the Cordillera Oriental, Bolivia, are in Paleozoic sedimentary rocks, many of them affected by mild metamorphism. For this reason, we delineate the Paleozoic rocks on the Altiplano as a permissive area for both deposit types (pl. 7). Because the permissive area is very small, and because there are no known examples in the study area, there is insufficient information to make an estimate of the number of undiscovered deposits. Bliss (1986) has published a grade and tonnage model for low-sulfide gold-quartz deposits.

PLACER GOLD DEPOSITS

Placer gold deposits are formed by erosion of preexisting deposits that contain coarse gold. The most obvious deposit types that could yield placers in Bolivia are the low-sulfide gold-quartz veins and gold-bearing syntectonic antimony. On the Altiplano, placer gold deposits are most likely to be found in the surficial sediments that surround the Paleozoic uplifts. In addition, we know of at least one gold placer deposit that that may have its provenance in Bolivian polymetallic vein deposits. There is insufficient information to delineate a permissive area.

BOLIVIAN POLYMETALLIC VEINS

PERMISSIVE AND FAVORABLE AREAS

Bolivian polymetallic veins form in response to the intrusion of dacitic plutons, and do not appear to be favored by a particular age or lithology of host rock, or by a particular type of basement rock. We outlined in the section on Mineral deposit models the reasons why, in the study area, we believe these deposits are restricted in age to Miocene or younger. There is no evidence for any of these deposits having formed less than 5 m.y. ago, and no incontrovertible evidence for any having formed less than 8 m.y. ago. Consequently, we have eliminated what we consider to be post-mineralization cover rocks, the young volcanic units (pl. 1, QTv, QTig), as well as the youngest group of sedimentary rocks (pl. 1, QTs). The remaining area is permissive for the occurrence of Bolivian polymetallic vein deposits and is shown on plate 7. Although polymetallic vein deposits related to Paleozoic plutons similar to those east and north of La Paz, may exist in the study area, we expect that the majority of undiscovered deposits are Miocene. Because of their high potential value, and because the volume of altered and veined rock in some of these systems is very large (pl. 3, image E), we considered deposits to a depth of 1,000 m in delineating the permissive area, and in estimating the number of deposits.

The most favorable areas are those near dacitic intrusions, and the greatest concentration of these is the region of Sud Lípez, where nine of the twenty known polymetallic vein deposits in the study area are located.

GRADE AND TONNAGE MODEL

Normally, the presence of so many known deposits (table 8) would allow the construction of a reliable grade and tonnage model. In the case of Bolivia, however, several factors make this impossible. First, a large proportion of the production from these deposits occurred in the distant past, much of it before 1825, and, while there are records of the amount of silver produced, there are no records of the amount of material processed, so calculation of tonnage and grade is impossible from this information. Secondly, large amounts of lead, zinc, tin, and other metals were simply discarded in the early days. And thirdly, because most of these deposits have been mined by underground methods, there was virtually no determination of pre-mining size and grade by drilling for these deposits. Thus, with the single exception of Kori Kollo, which has been developed during the 1980's, we do not know with any degree of certainty the original size or grade of any Bolivian polymetallic vein deposit.

Nevertheless, in order to help conduct a meaningful resource assessment, we felt that it was important to give some indication of the size and grade of these deposits. Accordingly, we have constructed a subjective grade and tonnage model for these deposits that includes grades for the two historically most important metals, silver and tin. This subjective model was based on some modern information about grades of materials remaining on dumps, on grades of a few deposits mined during the 20th century, on knowledge of the lateral extent and width of veins in some districts, and on a few modern estimates for pre-mining grades and tonnages for some deposits (for example, Bernstein, 1989).

We estimate that Bolivian polymetallic vein deposits have a 90 percent chance of containing 500,000 tonnes or more, a 50 percent chance of containing 11,000,000 tonnes or more, and a 10 percent chance of containing 250,000,000 tonnes or more of ore. They have a 90 percent chance of a silver grade of 20 g/t or more, a 50 percent chance of a silver grade of 140 g/t or more, and a 10 percent chance of a silver grade of 1,000 g/t or more. In addition, they have a 90 percent chance of a tin grade of 0.1 percent or more, a 50 percent chance of a tin grade of 0.4 percent or more, and a 10 percent chance of a tin grade of 2 percent or more. We believe that all these figures are within a factor of 3 of being correct, and thus, they can lead to a useful resource estimation for the study area. We have used these size and grade figures to guide our estimate of the number of undiscovered deposits.

ESTIMATED NUMBER OF UNDISCOVERED DEPOSITS

Because known Bolivian polymetallic vein deposits are very large, it can be argued that large numbers of undiscovered deposits do not exist. Where they are exposed at productive levels, their associated hydrothermally altered area is many kilometers across and extremely distinctive; for example, the Chocaya district, seen on plate 3, image E. Deposits that crop out have therefore probably been discovered. The great vertical extent of alteration and mineralization, which probably reached to at least very near the paleosurface, means that most undiscovered deposits are those that are covered by younger rocks.

The assessment team estimated that there is a 90 percent chance for the occurrence of 3 or more deposits, a 50 percent chance for the occurrence of 6 or more deposits, and a 10 percent chance for the occurrence of 25 or more deposits. For each of these estimates, half of the deposits are larger than 11,000,000 tonnes; half have a grade of greater than 0.4 percent tin and half have 140 g/t or more silver. The amounts of lead, zinc, tungsten, bismuth, antimony, and gold will be highly variable, and we lack sufficient information to estimate them.

Although we estimate a modest number of undiscovered deposits, the amount of undiscovered resources in these deposits in the study area is very large. In fact, we believe the resource remaining in known deposits is considerably larger than that contained in undiscovered deposits. Few of the known deposits have been explored adequately by diamond drilling, and thus, their limits are poorly known. Because of the lack of information about gold grades, the potential value of gold in many districts is also high, and we believe that exploration in known districts may result in the discovery of resources of all the metals contained in the polymetallic vein deposits.

DISTAL DISSEMINATED SILVER DEPOSITS

Because their formation is so closely related to the polymetallic vein systems, distal disseminated silver deposits share the permissive area with Bolivian polymetallic veins. There is little indication that they exist in the study area, and we make no estimate of undiscovered deposits.

PORPHYRY AND EPITHERMAL PRECIOUS-METAL DEPOSITS

In the section on Mineral deposit models, we discussed the interrelationship of porphyry gold deposits, quartz-alunite vein deposits, quartz-adularia vein deposits, hot-spring deposits, and epithermal manganese deposits, and the fact that they tend to form as parts of systems in the same geologic environment. Therefore, only one area is delineated permissive for all these deposit types on plate 7.

In order to delineate the permissive area, we first excluded the map units on plate 1 composed exclusively of sedimentary rocks. Next, the older volcanic rocks (pl. 1, Tvnd, Tig) which are generally eroded below the level that would expose the family of mineral deposits considered here, with the possible exception of porphyry gold, were excluded. The resulting permissive area, which consists essentially of the map units QTev and QTig from plate 1, as well as the Salinas de Garci Mendoza district, the Carangas area, and the Laurani area, where field observations suggest exposures higher in the volcanic section, is shown on plate 7. This permissive area was delineated for a depth of 500 m.

Although there is a possibility that porphyry copper deposits might underlie some of the altered areas in very young volcanic rocks in the Cordillera Occidental, the deposits would be relatively deeply buried, probably deeper than 1 km. We believe the probability of encountering porphyry copper deposits in the study area is negligible, and they are not delineated on plate 7.

There is insufficient information to make an estimate of numbers of deposits. There are only a few well understood examples of these deposit types in the study area, and, at present erosional levels, the different types cannot be readily distinguished. A comparison of the location of young volcanic centers (pl. 1) and areas of visual hydrothermal alteration (pl. 2), does permit a minimum estimate of the number of exposed hydrothermal systems. Of some 380 volcanic centers, more than 130 appear to exhibit distinctive alteration patterns, many of which could be the upper expression of epithermal systems.

Grade and tonnage models for porphyry copper deposits, quartz-alunite veins, quartz-adularia veins, hot-spring deposits, and epithermal manganese deposits may be found in Cox and Singer (1986).

VOLCANOGENIC URANIUM AND RHYOLITE-HOSTED TIN DEPOSITS

Both volcanogenic uranium and rhyolite-hosted tin deposit types are restricted to evolved, high-silica volcanic rocks and are likely to be found only in the Los Frailes and Morococala volcanic fields. The result is a very small permissive area (pl. 7). The number of expected undiscovered deposits is very low and no estimate was made. A grade and tonnage model for rhyolite-hosted tin has been published by Singer and Mosier (1986).

Undiscovered Nonmetallic Deposits

By G.J. Orris, Sigrid Asher-Bolinder, Orlando André-Ramos, Angel Escobar-Diaz, Eduardo Soria-Escalante, John W. Cady, Daniel H. Knepper, Dennis P. Cox, Keith R. Long, *and* Steve Ludington

Introduction **225**
Lacustrine borates **226**
Permissive and favorable areas **226**
Grade and tonnage model **226**
Estimated number of undiscovered deposits **226**
Lithium, boron, sodium carbonate, sodium sulfate, and potash in brines **226**
Lacustrine bedded halite and potash **227**
Gypsum **227**
Sodium sulfate and carbonate **227**
Hectorite **227**
Sedimentary zeolites **227**
Lacustrine diatomite **228**
Permissive and favorable areas **228**
Grade and tonnage model **228**
Estimated number of undiscovered deposits **228**
Barite veins **228**
Dimension stone **228**
Fumarolic sulfur **228**

TABLE

41. Percentiles of grade and tonnage distribution for selected industrial mineral deposits **226**

INTRODUCTION

The rocks of the Altiplano and Cordillera Occidental, Bolivia have the potential to host a large variety of industrial mineral deposit types. Many of these deposit types are associated with alkaline-saline lakes and their sediments. We have attempted to evaluate the potential for lacustrine brines, zeolites, and hectorite, as well as the potential for lacustrine evaporites such as gypsum, borates, halite, and potash. Areas permissive for these deposit types and for lacustrine diatomite are overlapping and are considered to be the same for this study (pl. 8). In the Cenozoic rocks, the presence or possible presence of lacustrine sediments was the determining feature for delineation of permissive areas. The following map units from plate 1 may contain lacustrine sediments, and thus constitute the permissive area: Qsu, Qs, Ql, QTs, QTig, Ts2, Tvnd, Tig, Tdp, and Ts1. Older sedimentary units are largely marine in origin and do not contain lacustrine sediments.

The geology of the study area is varied enough that there is potential for a wide variety of nonmetallic deposits, not all of which are related to alkaline-saline lakes. There is enough information available to discuss the potential for barite veins, dimension stone, and fumarolic sulfur later in this section. Other nonmetallic deposit types such as halite and gypsum, marine diatomite, bedded barite in the Paleozoic rocks, construction materials, silica sand and sandstone, sedimentary kaolin and bentonite, hydrothermal bentonite, fluorite veins, and perlite may occur in the study area, but there is insufficient information to evaluate them.

LACUSTRINE BORATES

PERMISSIVE AND FAVORABLE AREAS

Lacustrine evaporites are known to occur throughout the Cenozoic sedimentary sequences in the study area. As described in the section on Mineral deposit models, significant boron contents are known to exist in the evaporites and alkaline lake deposits in the southern half of the study area and in the large basin east of Charaña in the northwest part of the study area. In a general sense, all of the Cenozoic lacustrine sedimentary sequences are permissive for borates. However, analyses of a limited number of Tertiary evaporites have shown no notable boron contents. In addition, borate minerals are not stable below certain depths of burial making borate mineralization unlikely in the lower parts of Tertiary sedimentary sequences. Known borate mineralization consists dominantly of ulexite deposits associated with Quaternary alkaline lakes and salars. Colemanite and borax have been identified with ulexite at scattered locations in the study area.

Ballivian and Risacher (1981) sampled many alkaline lakes and salars for their study, but fewer than 25 of the more than 200 alkaline and salars in the study area have been studied in more than a cursory way. Exploration drilling has largely been restricted to Salar de Uyuni, and to a lesser extent, Salars de Empexa and Coipasa, and no exploration drilling or sampling has occurred in sediments in basins that do not currently have a surface lake or salar. In some sense, much of the Altiplano is a single closed basin that has existed since the early Tertiary. But many levels of subbasins exist and, to conduct a more detailed evaluation would require information about age and composition of sediments that does not exist. In this report, basins, or permissive areas, are represented by the distribution of geologic map units that include or may include Cenozoic lacustrine sediments (pl. 8). In summary, although all of the Cenozoic lacustrine sedimentary sequences are considered permissive for boron mineralization, the identified presence of boron in the basins of the southern half of the study area and in the large basin east of Charaña make these areas more favorable for the occurrence of lacustrine ulexite-colemanite-(borax) mineralization, although they are not delineated separately on plate 8.

GRADE AND TONNAGE MODEL

Percentiles of grade and tonnage distributions for these borate deposits are shown in table 41. These models were constructed from a world data set of borate deposits meeting the criteria described in the section on Mineral deposit models. There is no significant correlation between grade and tonnage for this deposit type.

ESTIMATED NUMBER OF UNDISCOVERED DEPOSITS

An assessment team estimated that there is a 90 percent chance for the occurrence of 6 or more deposits, a 50 percent chance for the occurrence of 20 or more deposits, and a 10 percent chance for the occurrence of 50 or more deposits. Half of these deposits have a grade of less than 22 percent B_2O_3. Half of the deposits have a tonnage less than 0.9 million tonnes.

LITHIUM, BORON, SODIUM CARBONATE, SODIUM SULFATE, AND POTASH IN BRINES

Permissive areas for the occurrence of lacustrine brines include all the closed and semiclosed basins in the study area and geologic map units shown on plate 1 that may include Tertiary lacustrine sediments (pl. 8). Areas with existing alkaline and saline lakes and salars often have known brine resources. Additional resources are most likely below adjacent marsh or pampa areas and in the deltaic deposits of rivers feeding these lakes and salars. Lithium- and (or) boron-bearing brines are largely known in the lakes and salars of the southern half of the study area and in the large basin east of Charaña. Undiscovered resources of

Table 41. *Percentiles of grade and tonnage distributions for selected industrial mineral deposits, Altiplano and Cordillera Occidental, Bolivia*

[Number of deposits compiled for models: borate, 27; lacustrine diatomite, 17; barite veins, 30; fumarolic sulfur, 44]

Variable	Percentiles		
	90	50	10
Borate deposits			
Tonnes x 10^6	0.038	0.9	13.6
Grade (percent B_2O_3)	13.2	22.2	31.2
Lacustrine diatomite deposits			
Tonnes x 10^6	0.0025	0.09	2.2
Grade (percent diatomite)	65	89	97
Barite veins			
Tonnes x 10^6	0.0037	0.055	1.27
Grade (percent $BaSO_4$)	65.0	95.0	98.1
Fumarolic sulfur deposits			
Tonnes x 10^6	0.11	1.01	9.28
Grade (percent S)	16.5	41.1	65.7

lithium- and boron-enriched brines are considered to be most likely adjacent to the known brines and unlikely in most of the Tertiary evaporite sequences which do not have identified brines or elevated boron and lithium contents. Alkaline brines that might contain economic sodium carbonate are most likely to be found in the same environments as the lithium- and boron-enriched brines and peripheral to known alkaline lake systems in the southern part of the study area, the basinal areas east of Charaña, and Lago Poopó. Additional resources of sodium sulfate brine and potash-enriched brines are also most likely in the subsurface sediments of marshes, pampas, and river deltas peripheral to known surface brine occurrences.

LACUSTRINE BEDDED HALITE AND POTASH

Permissive areas for the occurrence of halite and potash consist of the geologic map units shown on plate 1 that may include Cenozoic lacustrine sedimentary sequences (pl. 8). Extensive resources of halite are available in surface deposits at Salars de Uyuni and Coipasa and are currently being mined (Ballivian and Risacher, 1981). Additional resources are likely in other sediments related to the evaporation of Lagos Minchin and Tauca. Massive halite is known to occur at depth in Tertiary sediments near Corocoro, and may occur in other Tertiary evaporite sequences. Sylvite is known to occur in very minor amounts in Quaternary salar deposits. The existence of economic potash deposits is considered to be unlikely, but they could occur in massive halite deposits in the Tertiary stratigraphic section. Because of the solubility of sylvite and other potassium minerals, it is unlikely that large deposits of potash exist in any great amounts in the sediments below the current lakes and salars.

GYPSUM

Occurrences of gypsum are known in many of the Cenozoic lacustrine sedimentary sequences on the Bolivian Altiplano and in the Cordillera Occidental. Permissive areas for undiscovered deposits are delineated on plate 8. Some areas and formations in the delineated permissive domain for lacustrine sediments are known to have gypsum occurrences and are therefore favorable for the discovery of additional lacustrine gypsum deposits. Although not delineated on plate 8, these favorable areas would include geologic map unit Tdp (pl. 1), which, in part, is composed of formations known to contain gypsum or gypsiferous sediments, including the Campaña, Umala, Chuquichambi, and Jalluma Formations. Gypsum is also known to be associated with many of the surficial saline-alkaline lakes and salars.

SODIUM SULFATE AND CARBONATE

As with most other evaporite minerals and brines, the permissive areas for undiscovered deposits of sodium carbonate and sodium sulfate consist of the Cenozoic lacustrine sedimentary rocks, especially those sequences containing evaporites (pl. 8). The occurrence of extensive deposits of trona, nahcolite, or other sodium-carbonate-bearing minerals in Bolivia, similar to the Green River deposits in Wyoming (Dyni, 1991) is not supported by the available data. There is a small possibility that such deposits exist in relatively unexplored parts of the Tertiary stratigraphic section; it cannot be proven that such deposits are not present. Small, localized deposits of sodium carbonate, as well as sodium sulfate, are considered more likely to occur. Preservation of these deposits is dependent upon enveloping clay units that provide an impermeable barrier to the destruction of the deposits by ground or surface waters. Undiscovered resources of this deposit type are most likely to occur in clay-rich sediments peripheral to known alkaline (sodium carbonate) or sulfate (sodium sulfate) lakes or salars.

HECTORITE

Permissive areas for the occurrence of hectorite include areas where volcanic glass might have come in contact with lithium-bearing fluids over some period of time and where lacustrine sediments enriched in calcium and magnesium formed in an arid climate (Asher-Bolinder, 1991a). Volcanic rocks and thermal springs are believed to be the source of most lithium. These circumstances would most likely occur in or peripheral to basins containing alkaline lakes in areas of roughly contemporaneous volcanism. Although smectite clays are not known to be widely distributed in the study area, we cannot eliminate the possibility for these deposits. In the study area, we believe that hectorite is most likely to have formed in, or immediately adjacent to, alkaline-saline lakes, and the areas delineated permissive for evaporites and other deposit types related to alkaline-saline lakes (pl. 8) are also permissive for hectorite. Although not delineated, the geology of the basins in the southern half of the study area is considered to be more favorable for the occurrence of these deposits, because of widespread and documented sources of lithium.

SEDIMENTARY ZEOLITES

Sedimentary zeolites have not been identified in the study area, however, little work has been done on the Quaternary and Late Tertiary lacustrine sedimentary units

and spatially associated tuffs. These deposits are believed to form from the reaction of vitric tuff with saline, alkaline pore water trapped during lacustrine sedimentation. Sedimentary zeolite deposits are commonly spatially associated with bedded lacustrine evaporites (halite, trona, borates), diatomite, and lacustrine carbonates and clays. As with the previously discussed deposit types, Cenozoic lacustrine sedimentary rocks with associated volcaniclastic rocks must be considered permissive for sedimentary zeolite deposits given the current level of geologic information (pl. 8). The basins of the southern part of the study area seem to have a larger amount of volcanic rocks in an environment more conducive to the development of alkaline lakes than the more northern part of the study area. The southern basins may therefore be more favorable for near-surface deposits, although they are not separately delineated on plate 8.

LACUSTRINE DIATOMITE

PERMISSIVE AND FAVORABLE AREAS

Lacustrine diatomite deposits commonly occur in sediments that were deposited in low-energy, extensive, and shallow basins that had an abundant supply of soluble silica and nutrients and an absence of toxic or growth-inhibiting constituents. These basins were thus capable of sustained high rates of diatom reproduction. In addition, minimal clastic, chemical, and organic contamination of the diatomite is necessary for relatively high grade material to form (Shenk, 1991). These conditions may have existed multiple times during the evolution of the study area. Lacustrine diatomite deposits are commonly associated with lacustrine evaporite deposits, especially gypsum and trona. For these reasons, permissive areas for lacustrine diatomite deposits were judged to be the same as the previously discussed deposit types (pl. 8). An arbitrary depth of 500 m was used to estimate the number of deposits.

GRADE AND TONNAGE MODEL

Percentiles of grade and tonnage distributions for lacustrine diatomite deposits are shown in table 41. These deposits have a median tonnage of approximately 90,000 tonnes and a median grade of approximately 89 percent diatomite. The grade-tonnage model was constructed from a small data set of these deposits and in part reflects the economic bias of selective mining of sedimentary intervals as thin as 20 cm in many parts of the world. The reader should also note that these models do not measure the type or variability of diatom species in the deposits and thus the models carry incomplete information on the marketability of the diatomite.

ESTIMATED NUMBER OF UNDISCOVERED DEPOSITS

The assessment team estimated that there is a 90 percent chance for the occurrence of one or more lacustrine diatomite deposits, a 50 percent chance for the occurrence of at least 5 deposits, and a 10 percent chance for the occurrence of 50 or more deposits.

BARITE VEINS

Permissive areas for barite vein deposits include the same areas as those that are permissive for Bolivian polymetallic vein deposits, sediment-hosted gold deposits, and epithermal precious-metal deposits (pl. 7). Barite vein deposits are commonly spatially associated with these deposit types. It should be noted that because of their low unit value, the barite vein deposits would not be economic to the depths estimated for the metallic deposits in these permissive areas. Grade and tonnage statistics of known barite vein deposits in the world are shown in table 41. The median tonnage is 55,000 tonnes and the median grade is 95 percent Ba_2SO_4.

DIMENSION STONE

It is difficult to consider all the possible sources of dimension stone; in a general sense any rock may find some use as a building or paving material. Local use of building stone is highly dependent on the availability of materials that are easier to shape and use and the level of need for durability. Material suitable for shipping any distance must exhibit a natural beauty as well as more measurable characteristics such as resistance to chemical and physical erosion. Without a doubt, Bolivia may have additional dimension stone resources, but the magnitude cannot be quantified and we do not delineate permissive areas.

FUMAROLIC SULFUR

The permissive area for undiscovered fumarolic sulfur deposits is limited to the immediate vicinity of young volcanic rocks (pl. 1, QTev), primarily in the Cordillera Occidental; it is coextensive with the area outlined for epithermal precious-metal deposits delineated on plate 7. An upper limit for the number of undiscovered fumarolic sulfur deposits can be calculated by subtracting the number

of known deposits (table 14) from the number of major and minor volcanic centers shown on plate 1. More than 130 of the volcanic centers appear to exhibit distinctive alteration patterns, and, although many of these could be the upper expression of epithermal precious-metal systems, many may also represent fumarolic sulfur deposits. Sulfur deposits may also be present beneath capping lavas and exhibit little or no surface alteration. The range of sizes and grades of known fumarolic sulfur deposits in the world is contained in table 41.

References

Acland, Sarah, 1989, Geology of northern Quimsa Chata and Serrania Chilla, south of Tiwanacu, Bolivia: Cambridge University, unpublished B.S. thesis, 72 p.

Ahlfeld, Friedrich, 1936, Die Zink- und Kadmiumlagerstätten von Berenguela, Bolivien: Metall und Erz, v. 33, no. 23, p. 613–615.

Ahlfeld, Friedrich, 1944, La geología del mineral de San Cristóbal de Lípez (Bolivia): Mineria Boliviana, v. 1, no. 8, p. 9–15.

Ahlfeld, Friedrich, 1954, Los yacimientos minerales de Bolivia: Bilbao, Imprenta Industria for Banco Minero de Bolivia and Corporación Minera de Bolivia, 277 p.

Ahlfeld, Friedrich, 1967, Metallogenic epochs and provinces of Bolivia; Part 1, The tin province; Part 2, The metallogenic provinces of the Altiplano: Mineralium Deposita, v. 2, p. 291–311.

Ahlfeld, F.E., and Schneider-Scherbina, A., 1964, Los yacimientos minerales y de hidrocarburos de Bolivia: Bolivia Departamento Nacional de Geología Boletín 5 (Especial), 388 p.

Alarcón, H., and Cadima, J., 1967, [Geologic map of the] Salinas de Garci Mendoza [quadrangle], Hoja 6035 [Bolivia]: Servicio Geológico de Bolivia, scale 1:100,000.

Alarcón, H., and Kitakaze, A., 1987, Especies minerales en los depósitos de estaño-wolfram y polimetálico en la provincia metalogénica Andina de Bolivia: La Paz, Universidad Mayor de San Andres, Instituto de Geología Económica, Publicación Especial no. 3, p. 3–16.

Alarcón B., H., and Villalpando B., A., 1988, Alteraciones hidrotermales y termometria del yacimiento "La Joya", Oruro, Bolivia, *in* Extended abstracts, Yacimientos epitermales en ambientes de volcanismo reciente: Seminario-Taller, La Paz, Bolivia, September 4–16, 1988, 2 p.

Alarcón B., H., and Villalpando B., A., 1991, Petrografia, alteraciónes, y termometria de los Cerros "La Joya" y Kori-Kollo, *in* Memoría del IV Coloquio del Instituto de Geología Economica: La Paz, Universidad Mayor de San Andres, p. 1–25.

Alarcón, H., Ponce, J., Cadima, J., Delgadillo, H., Sanjines, O., 1967, [Geologic map of the] Tagua [quadrangle], Hoja 6034 [Bolivia]: Servicio Geológico de Bolivia, scale 1:100,000.

Alfaro, M., 1989, Proyecto de metales preciosos Sud Lipez, Departamento de Potosí, Bolivia: La Paz, United Nations Development Program, Project BOL/87/012, unpublished report, 48 p.

Alvarez, A., and Noble, D.C., 1988, Sedimentary rock-hosted disseminated precious metal mineralization at Purísima Concepción, Yauricocha district, central Peru: Economic Geology, v. 83, p. 1368–1378.

Alvarez, A., and Salazar, J., 1969, Informe de asistencia técnica a la concesión minera sucesivas Corina: Servicio Geológico de Bolivia Informe GB–M–633, 18 p.

André R., Orlando, 1989a, Informe Mina Taricoya: La Paz, Empresa Minera Illimani, unpublished report, 4 p.

André R., Orlando, 1989b, Informe Mina Titiri: La Paz, Empresa Minera Illimani, unpublished report, 3 p.

Anzoleaga V., Oscar, 1988, The La Joya copper-gold-silver district, Bolivia, *in* Extended Abstracts, Yacimientos epitermales en ambientes de volcanismo reciente: Seminario-Taller, La Paz, Bolivia, September 4–16, 1988, 2 p.

Anzoleaga, O., Columba, M., and Alarcón, H., 1990, Resumen geológico del Cerro Kori Kollo-descripción geológica: Sociedad Geológica Boliviana, Seminario-Taller, September 12, 1990.

Arellano L., Jorge, Aspectos petrológicos y mineralógicos de la zona de San Cristobal (Prov. Nor Lípez, Dpto. de Potosí), *in* Memoría del IV Coloquio del Instituto de Geología Economica: La Paz, Universidad Mayor de San Andres, p. 113–127.

Argandoña C., José, 1989, Alteraciones y geotermometría de las rocas superficiales del yacimiento de San José (Oruro): La Paz, Universidad Mayor de San Andres, Facultad de Ciencias Geológicas, unpublished Tesis de Grado, 80 p.

Arinabar, O., and Martinez, E., 1990, Structural interpretation of the Altiplano, Bolivia, *in* Structure and evolution of the Atlas Mountain system in Morocco and structure and evolution of the Central Andes in northern Chile and southern Bolivia and northwestern Argentina: Abstract volume, Final workshop of the research group on mobility of active continental margins, Freie Universität Berlin, Technische Universität Berlin, Deutsche Forschungsgemeinschaft Bonn-Bad Godesberg, May 23–25, 1990, p. 47.

Ascarrunz, R., Claure, L., Revollo, R., Alarcón, J., Ponce, J., and Barrientos, M., 1967, [Geologic map of the] Corocoro [quadrangle], Hoja 5942 [Bolivia]: Servicio Geológico de Bolivia, 1:100,000

Asher-Bolinder, Sigrid, 1991a, Descriptive model of lithium-rich playa brine, *in* Orris, G.J., and Bliss, J.D., eds., Some industrial mineral deposit models—descriptive deposit models: U.S. Geological Survey Open-File Report 91–11A, p. 47–48.

Asher-Bolinder, Sigrid, 1991b, Descriptive model of lithium in smectites of closed basins, *in* Orris, G.J., and Bliss, J.D., eds., Some industrial mineral deposit models—descriptive deposit models: U.S. Geological Survey Open-File Report 91–11A, p. 9–10.

Avila-Salinas B., W.A., 1965, Geología del distrito minero de Carangas y sus alrededores: La Paz, Universidad Mayor de San Andres, Facultad de Ciencias Geológicas, unpublished Tesis de Grado, 150 p.

Avila-Salinas B., W. A., 1973, Sobre la genesís a la roca de Comanche, provincia Pacajes del departamento de La Paz: Sociedad Geológica Boliviana Boletín 20, p. 109–128.

Avila-Salinas, W.A., 1990, Origin of copper ores at Corocoro, Bolivia, *in* Fontboté, L., Amstutz, G.C., Cardozo, M., Cedillo, E., and Frutos, J., eds., Stratabound ore deposits in the Andes: Berlin [and] Heidelberg, Springer-Verlag, p. 660–670.

Avila-Salinas B., W.A., Ploskonka, E., and Arduz T., M., 1975, Estudio petrográfico de la mina Toldos, Departamento de Potosí: Servicio Geológico de Bolivia, unpublished report, 27 p.

Baby, P., Sempéré, T., Oller, J., Barrios, L., Hérail, G., and Marocco, R., 1990, Un bassin en compression d'âge oligo-miocène dans le sud de l'Altiplano bolivien: Académie des Sciences de France, Comptes-Rendus des Séances, série 2, v. 311, p. 341–347.

Baker, M.C.W., 1981, The nature and distribution of upper Cenozoic ignimbrite centers in the central Andes: Journal of Volcanology and Geothermal Research, v. 11, p. 293–315.

Baker, M. C. W. and Francis, P. W., 1978, Upper Cenozoic volcanism in the central Andes—ages and volumes: Earth and Planetary Science Letters, v. 41, p. 175–187.

Ballivian, M., and Barrios, J., 1969, Informe sobre orientación técnica minera Mina Susana sectores sucsesivas Susana y sucsesivas Nelson: Servicio Geológico de Bolivia Informe GB–M–639, 16 p.

Ballivian, M., and Cordero, G., 1969, Informe sobre orientación técnica azufrera Wilma: Servicio Geológico de Bolivia Informe GB–M–655, 7 p.

Ballivian, M., and Vargas, W., 1971, Informe sobre asistencia técnica Mina Plasmar: Servicio Geológico de Bolivia Informe GB–M–684, 10 p.

Ballivian, O., and Risacher, F., 1981, Los salares del altiplano boliviano; métodos de estudio y estimación económica: Paris and La Paz, l'Office de la Recherche Scientifique et Technique Outre-Mer and Universidad Mayor de San Andres, 246 p.

Ballón, R., and Vargas, W., 1968, Informe sobre prospección de yacimiento de azufre Mina Luz Marina: Servicio Geológico de Bolivia Informe GB–M–624, 26 p.

Barrios, J., and Prevost, X., 1970, Informe sobre orientación técnica mina cuprífera Corona de España: Servicio Geológico de Bolivia Informe GB–M–648, 5 p.

Bassi, H.G.L., 1980, Inspecciones mineras en dos yacimientos cupríferos estratiformes del suroeste de Bolivia: Congreso Geológico Argentino, 6th, Bahía Blanca, 1975, Actas, v. 3, p. 13–23.

Berger, B.R., 1986a, Descriptive model of hot-spring Au-Ag, *in* Cox, D.P., and Singer, D.A., eds., Mineral deposit models: U.S. Geological Survey Bulletin 1693, p. 143.

Berger, B.R., 1986b, Descriptive model of quartz-alunite Au, *in* Cox, D.P., and Singer, D.A., eds., Mineral deposit models: U.S. Geological Survey Bulletin 1693, p. 158.

Berger, B.R., 1986c, Descriptive model of low-sulfide Au-quartz veins, *in* Cox, D.P., and Singer, D.A., eds., Mineral deposit models: U.S. Geological Survey Bulletin 1693, p. 239.

Berger, B.R., and Bagby, W.C., 1991, The geology and origin of Carlin-type gold deposits, *in* Foster, R.P., ed., Gold metallogeny and exploration: Glasgow and London, Blackie and Sons, Ltd., p. 210–248.

Berger, B.R. and Henley, R.W., 1989, Advances in the understanding of epithermal gold-silver deposits, with special reference to the western United States, *in* Reid, P.K., Ramsay, W.R.H., and Groves, D.I., eds., The geology of gold deposits—the perspective in 1988: Economic Geology Monograph 6, p. 405–423.

Bernal, Ruben, 1979, Mineralización de cobre y petrografía de la región Corocoro norte, Provincia Pacajes, Departamento La Paz: La Paz, Universidad Mayor de San Andres, Facultad de Ciencias Geológicas, unpublished Tesis de Grado, 84 p.

Bernstein, Merwin, 1989, Cerro Rico, Potosí—expectations for bulk tonnage hard rock and alluvial ores: La Paz, United Nations Development Program, Project BOL/87/012, unpublished report, 17 p.

Berton, Adrien, 1937, The Corocoro copper district of Bolivia: American Institute of Mining Engineers Transactions, v. 126, p. 540–558.

Bliss, James D., 1986, Grade and tonnage model of low-sulfide Au-quartz veins, *in* Cox, D. P., and Singer, D. A., eds., Mineral deposit models: U.S. Geological Survey Bulletin 1693, p. 239–243.

Bliss, J. D., ed., 1992, Developments in mineral deposit modeling: U. S. Geological Survey Bulletin 2004.

Bonham, H.F., 1989, Bulk-mineable gold deposits in the western United States, *in* Reid, P.K., Ramsay, W.R.H., and Groves, D.I., eds., The geology of gold deposits—the perspective in 1988: Economic Geology Monograph 6, p. 193–207.

Borja, G., Espinoza, A., and Hinojosa, A., 1989, Geología y exploración preliminar del yacimiento argentífero Chocaya, Potosí-Bolivia: La Paz, United Nations Development Project, unpublished report, 22 p.

Boyle, R.W., 1979, The geochemistry of gold and its deposits: Geological Survey of Canada Bulletin 280, 584 p.

Branisa, L., 1965, Los fósiles guías de Bolivia: Servicio Geológico de Bolivia Boletín 6, 282 p.

Buerger, M.J., and Maury, J.L., 1927, Tin ores of Chocaya, Bolivia: Economic Geology, v. 22, p. 1–13.

Bustillos C., Oscar, 1966, Estudio geológico de la peninsula de Yonza: La Paz, Universidad Mayor de San Andres, Facultad de Ciencias Geológicas, unpublished Tesis de Grado.

Cadima V., J., and Lafuente G., F., 1969, Prospección general de algunas borateras particulares Río Grande y Llipi-Llipi: Servicio Geológico de Bolivia Informe GB–M–647, 36 p.

Cadima V., J., Flores C., O., Ballón A., R., and Vargas S., C., 1969, Estudio geológico y prospección estratégica del yacimiento de arenas siliceas de Uyuni: Servicio Geológico de Bolivia Informe V–014, 17 p.

Campbell, D.F., 1942, The Oruro silver-tin district, Bolivia: Economic Geology, v. 37, p. 87–115.

Camus, Francisco, 1990, The geology of hydrothermal gold deposits in Chile: Journal of Geochemical Exploration, v. 36, p. 197–232.

Cardona G., Reynaldo, 1974, Estudio geológico de la región de Quetena: La Paz, Universidad Mayor de San Andres, Facultad de Ciencias Geológicas, unpublished Tesis de Grado, 84 p.

Carmouze, J.P., Arze, C., Miranda, Y., and Quintanilla, J., 1978, Circulación de materia (agua-sales disueltas) a traves del sistema fluvio-lacustre del Altiplano; la regulación hídrica o hidroquímica de los lagos Titicaca y Poopo: L'Office de la Recherche Scientifique et Technique de Outre-Mer, Cahiers, Série Géologie, v. 10, p. 49–68.

Caro, E., 1964a, Informe sobre orientación técnica mina argento-estañifera Candelaria: Bolivia Departamento Nacional de Geología Informe DNG–M–358, 19 p.

Caro, E., 1964b, Informe sobre orientación técnica mina argento-plumbo-zinquífera Santa Rosa: Bolivia Departamento Nacional de Geología Informe DNG–M–359, 6 p.

Caro, E., and Vargas, F., 1963, Informe sobre orientación técnica mina cuprífera Palmira: Bolivia Departamento Nacional de Geología Informe DNG–M–316, 4 p.

Carrasco C., Raúl, 1962, Contribución al conocimiento geológico del Terciario Altiplánico, zona Comanche, Prov. Pacajes: La Paz, Universidad Mayor de San Andrés, Faculdad de Ciencias Geológicas, unpublished Tesis de Grado.

Carrasco, Raúl, 1977, Manifestaciones geotérmicas en Bolivia: Servicio Geológico de Bolivia Boletín, Serie A, v. 1, no. 1, p. 61–74.

Chace, F.M., 1948, Tin-silver veins of Oruro, Bolivia: Economic Geology, v. 43, p. 333–383, 435–470.

Clark, S., and Orris, G.J., 1991, Descriptive model of vein barite, *in* Orris, G.J., and Bliss, J.D., eds., Some industrial mineral deposit models—descriptive deposit models: U.S. Geological Survey Open-File Report 91–11A, p. 19–20.

Cobbing, E.J., 1985, The tectonic setting of the Peruvian Andes, *in* Pitcher, W.S., Atherton, M.P., Cobbing, E.J., and Beckinsale, R.D., eds., Magmatism at a plate edge—the Peruvian Andes: Glasgow and London, Blackie and Sons Ltd., p. 2–12.

Columba C., M., Ruiz G., L., Gonzáles C., A., Vargas A., W., Jiménez H., L., Arias A., F., and Vargas S., C., 1974, Proyecto Chuquichambi, Contrato GEOBOL–Aldo Motasi, Informe de Prospección Geológica, Zona Chuquichambi, Concesiones Celia y San Miguel: Servicio Geológico de Bolivia, Departamento de Geología Económica Informe GE–62, 150 p.

Cordero, G., 1966, Metalogénesis stock "Quimsa Chata": Servicio Geológico de Bolivia Informe LP–23, 20 p.

Cordero, G., and Ballivian, M., 1969, Prospección del yacimiento de azufre Bienvenida: Servicio Geológico de Bolivia Informe GB–M–654, 8 p.

Cordero, G., Jiménez, L., and Villa, P., 1968, Informe sobre prospección de yacimientos de azufre mina Rosario del Rey: Servicio Geológico de Bolivia Informe GB–M–585, 15 p.

Corporación Minera de Bolivia, 1990, San Antonio de Lipez placer: Oruro, Corporación Minera de Bolivia, prospectus, 4 p.

Cortez H., Luís, 1966, Estudio geológico de la región de Esmoraca, Provincia Sud Lípez, Departamento de Potosí: La Paz, Universidad Mayor de San Andres, Facultad de Ciencias Geológicas, unpublished Tesis de Grado, 79 p.

Cortez, L., and Kuronuma, H., 1969, Informe sobre orientación técnica minera Mina Esperanza y Segunda Esperanza: Servicio Geológico de Bolivia Informe GB–M–645, 9 p.

Cox, D.P., 1986a, Descriptive model of porphyry Cu, *in* Cox, D.P., and Singer, D.A., eds., Mineral deposit models: U.S. Geological Survey Bulletin 1693, p. 76.

Cox, D.P., 1986b, Descriptive model of volcanic-hosted Cu-As-Sb, *in* Cox, D.P., and Singer, D.A., eds., Mineral deposit models: U.S. Geological Survey Bulletin 1693, p. 123.

Cox, D.P., 1986c, Descriptive model of polymetallic veins, *in* Cox, D.P., and Singer, D.A., eds., Mineral deposit models: U.S. Geological Survey Bulletin 1693, p. 125.

Cox, D.P., 1986d, Descriptive model of basaltic Cu, in Cox, D.P., and Singer, D.A., eds., Mineral deposit models: U.S. Geological Survey Bulletin 1693, p. 130.

Cox, D.P., 1986e, Descriptive model of sediment-hosted Cu, *in* Cox, D.P., and Singer, D.A., eds., Mineral deposit models: U.S. Geological Survey Bulletin 1693, p. 205–206.

Cox, D.P., and Singer, D.A., eds., 1986, Mineral deposit models: U.S. Geological Survey Bulletin 1693, 379 p.

Cox, D.P., and Singer, D.A., 1990, Descriptive and grade-tonnage models for distal disseminated Ag-Au deposits: U. S. Geological Survey Open-File Report 90–282, 7 p.

Dávila, J., Olivares, C., Claure. M., and Solíz, N., 1963, [Geologic map of the] Río Mulatos [quadrangle], Hoja 6234 [Bolivia]: Bolivia Departamento Nacional de Geología, scale 1:100,000.

Davis, J.C., 1986, Statistics and data analysis in geology: New York, John Wiley, 646 p.

Davis, J.R., Howard, K.A., Rettig, S.L., Smith, R.L., Ericksen, G.E., Risacher, F., Alarcon, H., and Morales, R., 1982, Progress report on lithium-related geologic investigations in Bolivia: U.S. Geological Survey Open-File Report 82–782, 18 p.

de Silva, S.L., 1989, Altiplano-Puna volcanic complex of the central Andes: Geology, v. 17, p. 1102–1106.

del Carpio D., Edilber, 1972, Estudio geológico regional de Soniquera, Provincia Sud Lípez, Departamento Potosí: La Paz, Universidad Mayor de San Andres, Facultad de Ciencias Geológicas, unpublished Tesis de Grado.

Delgadillo, Edgar, 1967, Informe sobre prospección geofísica mina de plomo y plata Toldos: Servicio Geológico de Bolivia Informe GB–M–541, 8 p.

Delgado A., Johnny, 1962, Estudio de la mineralización del cobre en la zona Chacarilla, Departamento La Paz: La Paz, Universidad Mayor de San Andres, Facultad de Ciencias Geológicas, unpublished Tesis de Grado.

Dewey, J.F., and Bird, J.M., 1970, Mountain belts and the new global tectonics: Journal of Geophysical Research, v. 75, p. 2625–2647.

Dobrovony, E., 1962, Geología del Valle de La Paz: Bolivia Departamento Nacional de Geología Boletín 3, 153 p.

Donoso L., G., 1959, Viaje de orientación técnica concesión Granada: Bolivia Departamento Nacional de Geología Informe DYMM–38, 4 p.

Dyni, J.R., 1991, Descriptive model of sodium carbonate in bedded lacustrine evaporite; Deposit subtype—Green River, *in* Orris, G.J., and Bliss, J.D., eds., Some industrial mineral deposit models: descriptive deposit models: U.S. Geological Survey Open-File Report 91–11A, p. 40–44.

Echenique M., Antonio, 1972, Geología económica del yacimiento de azufre de San Pablo de Napa, Provincia Campos, Departamento Potosí: La Paz, Universidad Mayor de San Andres, Facultad de Ciencias Geológicas, unpublished Tesis de Grado.

Echenique M., A., Ballivian Ch., O., Risacher, F., and Mamani, A., 1978, Informe geológico—económico de la Laguna Collpa y de la Laguna Hedionda: La Paz, Universidad Mayor de San Andres and l'Office de la Recherche Scientifique et Technique Outre-Mer, unpublished report, 20 p.

Empresa Minera Illimani, 1989, Annual report: La Paz, Bolivia, Empresa Minera Illimani S.A.

Empresa Minera Illimani, 1990, Tomuyo: La Paz, Bolivia, Empresa Minera Illimani S.A., unpublished report, 29 p.

Entwistle, L.P., and Gouin, L.O., 1955, The chalcocite ore deposits of Corocoro, Bolivia: Economic Geology, v. 50, p. 555–570.

Ericksen, G.E., and Salas, R., 1989, Geology and resources of salars in the Central Andes, *in* Ericksen, G.E., Cañas P., M.T., and Reinemund, J.A., eds., Geology of the Andes and its relation to hydrocarbon and mineral resources: Houston, Texas, Circum-Pacific Council for Energy and Mineral Resources Series, v. 11, p. 151–164.

Ericksen, G.E., Vine, J.D., and Ballon, R., 1977, Lithium-rich brines at Salar de Uyuni and nearby salars in southwestern Bolivia: U.S. Geological Survey Open-File Report 77–615, 47 p.

Ericksen, G.E., Vine, J.D., and Ballon, R., 1978, Chemical composition and distribution of lithium-rich brines in Salar de Uyuni and nearby salars in southwestern Bolivia, *in* Penner, S.S., ed., Lithium needs and resources: Oxford, Pergamon Press, p. 355–363.

Evernden, J.F., Kriz, S.J., and Cherroni, M.C., 1977, Potassium-argon ages of some Bolivian rocks: Economic Geology, v. 72, p. 1042–1061.

Fernández C., A., Hörmann, P.K., Kussmaul, S., Meave, J., Pichler, H., and Subieta, T., 1973, First petrographic data on young volcanic rocks of SW–Bolivia: Tschermaks Mineralogische und Petrographische Mitteilungen, v. 19, p. 149–172.

Flint, S., 1986, Sedimentary and geologic controls on red-bed ore genesis—The Middle Tertiary San Bartolo copper deposit, Antofagasta Province, Chile: Economic Geology, v. 81, p. 761–778.

Flores A., Mario, 1988, Identificación y evaluación preliminar de yacimientos epitermales de metales preciosos de San Antonio de Lípez, Potosí, Bolivia: La Paz, United Nations Development Program, Project BOL/87/12, unpublished report, 24 p.

Flores C., Oscar, 1968, Informe sobre orientación técnica mina Corina: Servicio Geológico de Bolivia Informe GB–M–572, 7 p.

Flores-Balcazar, J., 1979, Relación geológica del yacimiento de San José: Sociedad Geológica Boliviana, Anales de la VI Convención Nacional de Geología, Oruro, Bolivia, v. 6, no. 1, p. 177–188.

Francis, P.W., Halls, C., and Baker, M.C.W., 1983, Relationships between mineralization and silicic volcanism in the Central Andes: Journal of Volcanology and Geothermal Research, v. 18, p. 165–190.

Francis, P.W., and Wells, G.L., 1988, Landsat thematic mapper observations of debris avalanche deposits in the central Andes: Bulletin of Volcanology, v. 50, p. 258–278.

Gamarra I., Reynaldo, 1968, Estudio geológico regional y especializado de la región de San Cristobal, Mina Toldos y Santa Barbara de Jayula: La Paz, Universidad Mayor de San Andres, Facultad de Ciencias Geológicas, unpublished Tesis de Grado.

Gamboa, C., 1982, Reservas actualizadas de la mina María Luisa: Oruro, Corporación Minera de Bolivia, unpublished report, 4 p.

Garzón M., Dionisio, 1991, Laurani, un yacimiento epitermal asociado al emplazamiento de un domo volcanico: Sociedad Geológica Boliviana Boletín, in press.

Georgi, H.M., 1958, Informe de asistencia técnica mina Carangas: Bolivia Departamento Nacional de Geología Informe DCMS–37, 4 p.

Gillespie, A.R., 1980, Digital techniques of image enhancement, *in* Siegal, B.S., and Gillespie, A.R., eds., Remote sensing in geology: New York, John Wiley, p. 139–226.

Goodell, P.C., 1985, Classification and model of uranium deposits in volcanic environments, *in* Uranium deposits in volcanic rocks: Vienna, International Atomic Energy Agency, p. 1–16.

Grant, J.N., Halls, C., Avila, W., and Avila, G., 1977, Igneous geology and the evolution of hydrothermal systems in the sub-volcanic tin deposits of Bolivia, *in* Volcanic processes in ore genesis: Geological Society of London Special Publication 7, p. 117–126.

Grant, J.N., Halls, C., Salinas, W.A., and Snelling, N.J., 1979, K-Ar ages of igneous rocks and mineralization in part of the Bolivian tin belt: Economic Geology, v. 74, p. 838–851.

Grant, J.N., Halls, C., Sheppard, S.M.F., and Avila, W., 1980, Evolution of the porphyry tin deposits of Bolivia, *in* Ishihara, S., and Takenouchi, S., eds., Granitic magmatism and related mineralization: The Society of Mining Geologists of Japan, Mining Geology Special Issue 8, p. 151–173.

Grimes, D.J., and Marranzino, A.P., 1968, Direct current arc and alternating current spark emission spectrographic field methods for the semiquantitative analysis of geologic materials: U.S. Geological Survey Circular 591, 6 p.

Guerra, M., and Ascarrunz K., R., 1964a, Informe sobre el estudio de yacimiento bentonítico mina La Encontrada: Bolivia Departamento Nacional de Geología Informe DNG–M–342, 97 p.

Guerra, M., and Ascarrunz K., R., 1964b, Informe sobre orientación técnica mina cuprífera Ana María: Bolivia Departamento Nacional de Geología Informe DNG–M–337, 6 p.

Guerra, M., and Ascarrunz K., R., 1964c, Informe sobre orientación técnica mina cuprífera La Encontrada: Bolivia Departamento Nacional de Geología Informe DNG–M–343, 7 p.

Guerra, M., and Ascarrunz K., R., 1964d, Informe sobre orientación técnica mina cuprífera San Silvestre: Bolivia Departamento Nacional de Geología Informe DNG–M–340, 7 p.

Guerra, M., and Ascarrunz K., R., 1964e, Informe sobre orientación técnica minas cupríferas del grupo minero Transvaal: Bolivia Departamento Nacional de Geología Informe DNG–M–341, 4 p.

Guerra, M., Uribe, H., and Otazo, N., 1965a, Informe sobre orientación técnica mina aurífera Iroco: Servicio Geológico de Bolivia Informe GB–M–459, 9 p.

Guerra, M., Uribe, H., and Otazo, N., 1965b, Informe sobre orientación técnica minera mina de plata Empresa Minera La Plata: Servicio Geológico de Bolivia Informe GB–M–463, 13 p.

Guerra, M., Uribe, H., and Otazo, N., 1965c, Informe sobre orientación técnica minera mina de plomo y plata Carangas: Servicio Geológico de Bolivia Informe GB–M–464, 9 p.

Guilbert, J.M., and Park, C.F., 1986, The geology of ore deposits: New York, Freeman and Co., 985 p.

Gutiérrez, G., 1975, Informe geológico en los alrededores de San Vicente: Oruro, Corporación Minera de Bolivia, unpublished report.

Hansen, R.O., and Pawlowski, R.S., 1989, Reduction to the pole at low latitudes by Wiener filtering: Geophysics, v. 54, p. 1607–1613.

Harben, P.W., and Bates, R.L., 1990, Industrial minerals—Geology and world deposits: London, Industrial Minerals Division of Metal Bulletin Plc., 312 p.

Harris, D.C., and Chen, T.T., 1975, Studies of type pavonite material: Canadian Mineralogist, v. 13, p. 408–410.

Heald, P., Foley, N.K., and Hayba, D.O., 1987, Comparative anatomy of volcanic-hosted epithermal deposits—acid sulphate and adularia-sericite types: Economic Geology, v. 82, p. 1–26.

Hofstra, A.H., Leventhal, J.S., Northrop, H.R., Landis, G.P., Rye, R.O., Birak, D.J., and Dahl, A.R., 1991, Genesis of sediment-hosted disseminated-gold deposits by fluid mixing and sulfidization—Chemical-reaction-path modeling of ore-depositional processes documented in the Jerritt Canyon district, Nevada: Geology, v. 19, p. 36–40.

Howarth, R.J., and Sinding-Larsen, R., 1983, Multivariate analysis, *in* Howarth, R.J., ed., Statistics and data analysis in geochemical prospecting: Amsterdam, Elsevier, Handbook of exploration geochemistry, v. 2, chap. 6, p. 207–289.

Ibáñez B., V., and Medina C., A., 1988, Características geológicas y evaluación del potencial mineral del yacimiento de metales preciosos Buena Vista, Potosí, Bolivia: La Paz, United Nations Development Program, Project BOL/87/12, unpublished report, 15 p.

Imai, H., Lee, M.S., Takenouchi, S., Fujiki, Y., Iida, K., Sakimoto, T., and Tsukagoshi, S., 1978, Geologic structure and mineralization of polymetallic xenothermal vein-type deposits in Japan, *in* Imai, Hideki, ed., Geological studies of mineral deposits in Japan and East Asia: Tokyo University Press, p. 86–122.

Instituto de Geología Económica, 1985, K-Ar ages of mineralization at the Caracoles, Siglo XX, Colquechaca, Colavi, Huari Huari, Unificada, Tasna, Inocentes and Buena Vista mines in Bolivia: La Paz, Universidad Mayor de San Andres de Bolivia, Instituto de Geología Económica, Publicación Especial no. 2, p. 270–281.

International Association of Geodesy, 1967, Geodetic Reference System 1967: International Association of Geodesy Special Publication 3, 116 p.

Isacks, B.L., 1988, Uplift of the central Andean plateau and bending of the Bolivian orocline: Journal of Geophysical Research, v. 93, p. 3211–3231.

Jacobson, H.S., Murillo, C., Ruíz, L., Tapia, O., Zapata, H., Alarcón, H., Delgadillo, E., and Velasco, C., 1969, Geology and mineral deposits of the San Cristobal district, Villa Martín province, Potosí, Bolivia: U.S. Geological Survey Bulletin 1273, 22 p.

James, D.E., 1971, Plate tectonic model for the evolution of the Central Andes: Geological Society of America Bulletin, v. 82, p. 3325–3346.

Japan International Cooperation Agency, 1977, Informe de investigación geológica en área San Vicente, República de Bolivia, Fase 1: Tokyo and La Paz, Japan International Cooperation Agency and Metal Mining Agency of Japan.

Japan International Cooperation Agency, 1978, Informe de investigación geológica en región a sur, República de Bolivia, Fase 2: Tokyo and La Paz, Japan International Cooperation Agency and Metal Mining Agency of Japan.

Japan International Cooperation Agency, 1979, Informe de investigación geológica en región a sur, República de Bolivia, Fase 3: Tokyo and La Paz, Japan International Cooperation Agency and Metal Mining Agency of Japan.

Japan International Cooperation Agency, 1988, Informe sobre la exploración cooperativa de mineral en el área Lipez, República de Bolivia, Fase 1: Tokyo and La Paz, Japan International Cooperation Agency and Metal Mining Agency of Japan, 91 p.

Japan International Cooperation Agency, 1989, Informe sobre la exploración cooperative de mineral en el área Lipez, Fase 2: Tokyo and La Paz, Japan International Cooperation Agency and Metal Mining Agency of Japan, 127 p.

Jiménez, Mario, 1971, Geología y posibilidades de mineral de las minas Buena Vista, Leoplan y Pulacayito: Oruro, Corporación Minera de Bolivia, unpublished report, 29 p.

Jiménez Ch., N., and Núñez A., G., 1988, Evaluación del potencial en metales preciosos de los Cerros Pucasalle y Puca Orkho, provincia Sud Lipez, Potosí, Bolivia: La Paz, United Nations Development Program, Project BOL/87/12, unpublished report, 36 p.

Jiménez Ch., N., Ibáñez V., V., and Medina C., A., 1988, Características geológicas y perspectivas económicas del área volcánica Pocosoni-La Joya, Oruro, Bolivia: La Paz, United Nations Development Program, Project BOL/87/12, unpublished report, 31 p.

Kelly, W.C., and Turneaure, F.S., 1970, Mineralogy, paragenesis and geothermometry of the tin and tungsten deposits of the eastern Andes, Bolivia: Economic Geology, v. 65, p. 609–680.

Kirkham, R.V., 1989, Distribution, settings, and genesis of sediment-hosted stratiform copper deposits, *in* Boyle, R.W., Brown, A.C., Jefferson, C.W., Jowett, E.C., and Kirkham, R.V., eds., Sediment-hosted stratiform copper deposits: Geological Association of Canada Special Paper 36, p. 3–38.

Knepper, D.H., Jr., 1982, Lineaments derived from analysis of linear features mapped from Landsat images of the Four Corners region of the southwestern United States: U.S. Geological Survey Open-File Report 82–849, 79 p.

Knepper, D.H., Jr., 1988, Mapping hydrothermal alteration with Landsat Thematic Mapper data, *in* Lee, Keenan, ed., Remote sensing in exploration geology—A combined short course and field trip: International Geological Congress, 28th, Washington, D.C., Guidebook T182, p. 13–21.

Koeberlin, F.R., 1926, Geologic features of Bolivian tin-bearing veins: Engineering and Mining Jounal, v. 121, p. 636–642.

Kohanowski, N.N., 1944, Geología de yacimientos cupríferos en Bolivia: Minería Boliviana, v. 1, no. 6, p. 9–21.

Kriz, S. J., 1963a, [Geologic map of the] Charaña [quadrangle], Hoja 5741 [Bolivia]: Bolivia Departamento Nacional de Geología, scale 1:100,000.

Kriz, S. J., 1963b, [Geologic map of the] Santiago de Machaca [quadrangle], Hoja 5742 [Bolivia]: Bolivia Departamento Nacional de Geología, scale 1:100,000.

Kruse, F.A., and Raines, G.L., 1984, A technique for enhancing digital color images by contrast stretching in Munsell color space, *in* Proceedings of the International Symposium on Remote Sensing of the Environment, Third Thematic Conference, Remote Sensing for Exploration Geology, April 16–19, 1984, Colorado Springs, Colorado: p. 755–760.

Kuronuma, H., 1971, Estudio preliminar sobre la precipitación del cobre nativo y la calcosina en depósitos de tipo manto en el altiplano Boliviano: Servicio Geológico de Bolivia Boletín 15, p. 57–64.

Kussmaul, S., Hormann, P.K., Ploskonka, E., and Subieta, T., 1977, Volcanism and structure of southwestern Bolivia: Journal of Volcanology and Geothermal Research, v. 2, p. 73–111.

Kussmaul, S., Jordan, L., and Ploskonka, E., 1975, Isotopic ages of Tertiary volcanic rocks of SW Bolivia: Bundesanstalt für Bodenforschung und geologischen Landesämter, Geologische Jahrbuch, Part B, v. 14, p. 111–120.

Lavenu, A., 1986, Etude tectonique et neótectonique de l'Altiplano et de la Cordillère orientale des Andes boliviennes: Paris, Université de Paris-Sud, Centre d'Orsay, unpublished Thèse de Doctorat des Sciences, 434 p.

Lavenu, Alain, Bonhomme, M.G., Vatin-Perignon, N., and de Pachtere, P., 1989, Neogene magmatism in the Bolivian Andes between 16°S and 18°S; stratigraphy and K/Ar geochronology: Journal of Latin American Earth Science, v. 2, p. 35–47.

Le Bas, M.J., Le Maitre, P.W., Streckeisen, A., and Zanettin, B., 1986, A chemical classification of volcanic rocks based on the total alkali-silica diagram: Journal of Petrology, v. 27, p. 745–750.

Lehmann, Berndt, 1978, A Precambrian core sample from the Altiplano, Bolivia: Geologische Rundschau, v. 67, p. 270–278.

Lehmann, B., Ishihara, S., Michel, H., Miller, J., Rapela, C., Sanchez, A., Tistl, M., and Winkelmann, L., 1990, The Bolivian tin province and regional tin distribution in the Central Andes—A reassessment: Economic Geology, v. 85, p. 1044–1058.

Lehmann, B., Petersen, U., Santiváñez, R., and Winkelmann, L., 1988, Distribución geoquímica de estaño y boro en la secuencia Paleozoica de la Cordillera Real de Bolivia: Boletín de la Sociedad Geológica del Perú, v. 77, p. 19–27.

Lehrberger, Gerhard, 1988, Gold-antimonite deposits in marine sediments of the eastern Cordillera of the Bolivian Andes, *in* Goode, A.D.T., Smyth, E.L., Birch, W.D., and Bosma, L.I., eds., Bicentennial gold 88; extended abstracts; poster programme: Geological Society of Australia Abstracts, v. 23, nos. 1–2, p. 319–321.

Leroy, J., George-Aniel, B., and Pardo-Leyton, E., 1985, Deposits and radioactive anomalies in the Sevaruyo region (Bolivia), *in* Uranium deposits in volcanic rocks: Vienna, International Atomic Energy Agency, p. 289–300.

Lezeca B., José, 1989, Geodinámica y distribución del oro en una cuenca altiplánica región Caracollo-Soledad-Oruro: La Paz, Universidad Mayor de San Andres, Facultad en Ciencias Geológicas, unpublished Tesis de Grado.

Lindgren, W., and Abbot, A.C., 1931, The silver-tin deposits of Oruro, Bolivia: Economic Geology, v. 26, p. 453–459.

Litherland, M., Annells, R.N., Darbyshire, D.P.F., Fletcher, C.J.N., Hawkins, M.P., Klinck, B.A., Mitchell, W.I., O'Connor, E.A., Pitfield, P.E.J., Power, G., and Webb, B.C., 1989, The Proterozoic of eastern Bolivia and its relation to the Andean Mobile belt: Precambrian Research, v. 43, p. 157–174.

Livo, K.E., 1990, REMAPP–PC—Remote sensing image processing software for MS–DOS personal computers: U.S. Geological Survey Open-File Report 90–88, 58 p.

Ljunggren, P., and Meyer, H.C., 1964, The copper mineralization in the Corocoro basin, Bolivia: Economic Geology, v. 59, p. 110–125.

Locardi, E., 1985, Uranium in acidic volcanic environments, *in* Uranium deposits in volcanic rocks: Vienna, International Atomic Energy Agency, p. 17–27.

Long, K.R., 1991, Descriptive model of fumarolic sulfur, *in* Orris, G.J., and Bliss, J.D., eds., Some industrial mineral deposit models—descriptive deposit models: U.S. Geological Survey Open-File Report 91–11A, p. 11–12.

López A., H., 1958, Informe de asistencia técnica mina Llanquera: Bolivia Departamento Nacional de Geología Informe DCMS–16, 2 p.

López A., H., and Murillo, C., 1963a, Informe de asistencia técnica mina cuprífera Porvenir: Bolivia Departamento Nacional de Geología Informe DNG–M–244, 5 p.

López A., H., and Murillo, C., 1963b, Informe sobre orientación técnica mina de cobre Victoria y Elena: Bolivia Departamento Nacional de Geología Informe DNG–M–225, 5 p.

López A., H., and Murillo V., J., 1963c, Informe sobre orientación técnica mina cuprífera Veta Verde: Bolivia Departamento Nacional de Geología Informe DNG–M–243, 13 p.

López M., R., and Pinto V., J., 1990, Consideración preliminar sobre los prospectos Machu Socavón y Nuevo Mundo, distrito minero de San Antonio de Lípez, Potosí: La Paz, United Nations Development Program, Project BOL/87/12, unpublished report, 10 p.

Ludington, Steve, 1986, Methods for comparing major-element chemistry of igneous rocks: Abstracts with Programs for the 14th Proceedings of the International Mineralogical Association, p. 160–161.

Ludington, Steve, Cox, D.P., Sherlock, M.G., Singer, D.A., Berger, B.R., and Tingley, J.V., 1991, Spatial and temporal analysis of precious-metal deposit models for a mineral resource assessment of Nevada: Ottawa, Inernational Association for the Genesis of Ore Deposits, in press.

Lyons, Wilfred A., 1957, Geología y resultados de las perforaciones en Cobrizos: Bolivia Departamento Nacional de Geología, unpublished report.

Madu, B.E., Nesbitt, B.E., and Muehlenbachs, Karlis, 1990, A mesothermal gold-stibnite-quartz vein occurrence in the Canadian cordillera: Economic Geology, v. 85, p. 1260–1268.

Maldonado, J., 1969, Informe geológico preliminar de yacimiento argentífero San Vicente-Monserrat: Oruro, Corporación Minera de Bolivia, unpublished report.

Mannion, L.E., 1975, Sodium carbonate deposits, *in* Lefond, S.J., ed., Industrial minerals and rocks (nonmetallics other than fuels), (4th edition): New York, American Institute of Mining, Metallurgical, and Petroleum Engineers, p. 1061–1079.

Markham, B.L., and Barker, J.L., 1985, Landsat MSS and TM post-calibration dynamic ranges, exoatmospheric reflectances, and at-satellite temperatures: Lanham, Maryland, Earth Observation Satellite Company, Technical Notes, p. 3–8.

Marsh, H.W., and Robinson, W.J., 1966, Report on geological and geophysical examination of the silver-copper-tin properties, San Vicente District: Oruro, Prospection, Ltd., unpublished report to Corporación Minera de Bolivia.

Martinez, C., 1980, Structure et évolution de la chaîne andine dans le nord de la Cordillère des Andes de Bolivie: L'Office de la Recherche Scientifique et Technique Outre-Mer Traveaûx et Documents 119, 352 p.

Matthews, P.F.P., 1991, Bolivian mining—signs of recovery: Mining Magazine, v. 164, no. 4, p. 226–230.

McAllister, J.F., 1944, Tin resources of the Oruro District, Bolivia: La Paz, U.S. Geological Survey, unpublished report, 87 p.

McBride, S.L., 1977, A K–Ar study of the Cordillera Real, Bolivia and its regional setting: Kingston, Ontario, Queen's University, unpublished Ph.D. dissertation, 101 p.

McNamee, James, 1985a, Cerro Chinchillaguay: La Paz, Compañía Minera del Sur S.A., unpublished report, 11 p.

McNamee, James, 1985b, Cerro Santaille: La Paz, Compañía Minera del Sur S.A., unpublished report, 2 p.

McNamee, James, ed., 1988, Todos Santos-Carangas, *in* Field guide, Yacimientos epitermales en ambientes de volcanismo reciente: Seminario-Taller, La Paz, Bolivia, Sept. 4–16, 1988, p. 37–40.

McVey, Hal, 1989, Republic of Bolivia nonmetallic minerals, market study and overview: La Paz, United Nations Development Program, Project BOL/87/012, unpublished report, 40 p.

Meave, Jaime, 1966, Estudio Geológico de la región de Tatasi, La Paz, Bolivia: La Paz, Universidad Mayor de San Andres, Facultad de Ciencias Geológicas, unpublished Tesis de Grado.

Meave, Jaime, 1972, Estratigrafía de Terciario en la región de los Lípez-Potosí: Sociedad Geológica Boliviana Boletín, v. 18, p. 76–83.

Medina C., A., and Ibáñez V., V., 1988a, Características geológicas y evaluación del potencial mineral del yacimiento de metales preciosos Lipeña-La Moza y Barrahuayco, Potosí, Bolivia: La Paz, United Nations Development Program, Project BOL/87/12, unpublished report, 24 p.

Medina C., A., and Ibáñez V., V., 1988b, Características geológicas y evaluación del potencial mineral del yacimiento de metales preciosos Mercedes, Potosí, Bolivia: La Paz, United Nations Development Program, Project BOL/87/12, unpublished report, 15 p.

Medina C., A., Jiménez Ch., N., and Ibáñez V., V., 1988, Características geológicas y evaluación del potencial mineral del yacimiento de metales preciosos Maria Luisa, Oruro, Bolivia: La Paz, United Nations Development Program, Proyecto BOL/87/12, unpublished report, 32 p.

Mendoza T., Eugenio, 1977, Bismuto y plata en Sud Lípez, Mina Bolivar, Cantón Santa Isabel, Departamento Potosí: La Paz, Universidad Mayor de San Andres, Facultad de Ciencias Geológicas, unpublished Tesis de Grado.

Menzie, W.D., and D.A. Singer, 1990, A course on mineral resource assessment: Proceedings of the International Symposium on Mineral Exploration—the case of artificial intelligence: Tokyo and Tsukuba, Japan, Mining and Materials Processing Institute of Japan, p. 177–188.

Merida A., Roberto, 1969, Estudio geológico y minero del distrito de Esmoraca: La Paz, Universidad Mayor de San Andres, Facultad de Ciencias Geológicas, unpublished Tesis de Grado.

Meyer, H.C., and Murillo, J.E., 1961, Investigaciones geológicas en la faja cuprífera altiplánica sobre la geología en las provincias Aroma, Pacajes y Carangas: Bolivia Departamento Nacional Geológico Boletín 1, 49 p.

Ministerio de Minas y Metalurgia, 1957, [Geologic map of the] Corocoro [quadrangle], Hoja 37 [Bolivia]: Bolivia Ministerio de Minas y Metalurgia, scale 1:250,000.

Mitchell, A.H., and Reading, H.G., 1969, Continental margins, geosynclines, and ocean floor spreading: Journal of Geology, v. 77, p. 629–646.

Mitchell A., Jorge, 1968, Estudio geológico de la región de Curahuara de Carangas-Crucero Totora, Provincia Sajama, Departamento Oruro y Provincia Pacajes, Departamento La Paz: La Paz, Universidad Mayor de San Andres, Facultad de Ciencias Geológicas, La Paz, Bolivia, unpublished Tesis de Grado, 58 p.

Montes de Oca, Ismael, 1982, Geografía y recursos naturales de Bolivia: La Paz, Imprenta Superel Ltda., 628 p.

Montes de Oca, I., and Vedia M., J., 1965, Informe sobre el estudio del yacimiento de caliza Cerro Calera: Servicio Geológico de Bolivia Informe GB–M–470, 6 p.

Montes de Oca, I., Sirvas, F., Torres, E., Murillo, H.C., Nuñez, R., and Gaspar, J., 1963, [Geologic map of the] Charaña [quadrangle], Hoja 5741 [Bolivia]: Bolivia Departamento Nacional de Geología, scale 1:100,000.

Morris, H.T., 1986, Descriptive model of polymetallic replacement deposits, *in* Cox, D.P., and Singer, D.A., eds., Mineral deposit models: U.S. Geological Survey Bulletin 1693, p. 99.

Mosier, D.L., 1986, Descriptive model of epithermal Mn, *in* Cox, D.P., and Singer, D.A., eds., Mineral deposit models: U.S. Geological Survey Bulletin 1693, p. 165.

Mosier, D.L., Menzie, W.D., and Kleinhampl, F.J., 1986, Geologic and grade-tonnage information on Tertiary epithermal precious- and base-metal vein districts associated with volcanic rocks: U.S. Geological Survey Bulletin 1666, 39 p.

Mosier, D.L., Singer, D.A., and Cox, D.P., 1986, Grade and tonnage model of sediment-hosted Cu, *in* Cox, D. P., and Singer, D. A., eds., Mineral deposit models: U.S. Geological Survey Bulletin 1693, p. 206–208.

Mosier, D. L., Singer, D. A., Bagby, W. C., and Menzie, W. D., 1992, Grade and tonnage model of sediment-hosted Au, *in* Mosier, D. L., ed., Developments in mineral deposit modeling, U. S. Geological Survey Bulletin 2004.

Motooka, J.M., 1988, An exploration geochemical technique for the determination of preconcentrated organometallic halides by ICP–AES: Applied Spectroscopy, v. 42, no. 7, p. 1293–1296.

Muriel, C., 1971, Informe geológico de Corocoro y zonas adyacentes: Oruro, Corporación Minera de Bolivia, Sub-Gerencia de Geología, Oruro, Bolivia, unpublished report.

Murillo, J.E., 1960, Informe sobre orientación técnica mina San Miguel: Bolivia Departamento Nacional de Geología Informe DYMM–70, 4 p.

Murillo, J., and Bustillos, O., 1968, Valuación de yacimientos no metálicos de sales de sodio, potasio, sulfatos y carbonatos de sodio, provincias Poopó-Abaroa, departamento de Oruro: Servicio Geológico de Bolivia Informe GB–M–591.

Murillo, C., Ruíz, L., Tapia, O., Zapata, H., Alarcón, H., Velasco, C., Delgadillo, E., and Mendoza, E., 1967, Estudio geológico y mineralógico del distrito de San Cristóbal: Servicio Geológico de Bolivia, unpublished report, 27 p.

Murillo, J.E., Kuronuma, H., Prevost, X., Revollo, R., and Juárez, L., 1969, Yacimientos de antimonio y cobre: Servicio Geológico de Bolivia Informe V–016, 55 p.

Nakamura, T., and Hunahashi, M., 1970, Ore veins of Neogene volcanic affinity in Japan, *in* Tatsumi, T., ed., Volcanism and ore genesis: Tokyo, University of Tokyo Press, p. 215–230.

Officer, H.G., 1917a, Combined report on the Escapa copper mine and the Cuidado silver mine: Andes Exploration Co., unpublished report; available from the Anaconda Geological Documents Collection, International Archive of Economic Geology, American Heritage Center, University of Wyoming, 5 p.

Officer, H.G., 1917b, Report on the Huancané mines: Andes Exploration Co., unpublished report; available from the Anaconda Geological Documents Collection, International Archive of Economic Geology, American Heritage Center, University of Wyoming, 15 p.

O'Leary, R.M., and Meier, A.L., 1984, Analytical methods used in geochemical exploration, 1984: U.S. Geological Survey Circular 948, 48 p.

Orris, G.J., 1991, Grade and tonnage model for lacustrine borates, *in* G.J. Orris and J.D. Bliss, eds., Some industrial mineral deposit models—grade-tonnage models: U.S. Geological Survey Open-File Report 91–11B.

Orris, G.J., and Bliss, J.D., 1991, Grade and tonnage models for industrial mineral deposits: U.S. Geological Survey Open-File Report 91–11B.

Pardo-Leyton, E., 1985, Uranio en rocas ígneas—Intrusivas subefusivas y piroclásticas del Orógeno Andino boliviano, *in* Uranium deposits in volcanic rocks: Vienna, International Atomic Energy Agency, p. 255–274.

Papke, K.G., 1976, Evaporites and brines in Nevada playas: Nevada Bureau of Mines and Geology Bulletin 87, 35 p.

Parra U., Fernando, 1968, Estudio petrográfico-geológico minero del área de Tapaquilena, parte nor-occidental de la Provincia Sud Lípez, Departamento Potosí: La Paz, Universidad Mayor de San Andres, Facultad de Ciencias Geológicas, unpublished Tesis de Grado.

Paton, Stuart, 1989, Geology of southern Quimsa Chata and Serranía Chilla, south of Tiwanacu, Bolivia: Cambridge University, unpublished B.S. thesis, 63 p.

Peacock, M.A., 1931, Classification of igneous rock series: Journal of Geology, v. 39, p. 54–67.

Pearton, T.N., and Viljoen, M.J., 1986, Antimony mineralization in the Murchison greenstone belt—an overview, *in* Anhaeusser, C.R., and Maske, S., eds., Mineral deposits of southern Africa: Johannesburg, Geological Society of South Africa, p. 283–320.

Peccerillo, A., and Taylor, S.R., 1976, Geochemistry of Eocene calkalkaline volcanic rocks from the Kastamonu area, northern Turkey: Contributions to Mineralogy and Petrology, v. 58, p. 63–81.

Pélissonier, Hubert, 1964, Structure géologique et genèse du gisement du cuivre de Corocoro (Bolivie): Société Geólogique Française Bulletin, 7e Série, v. 6, p. 502–514.

Pilger, R.H., 1984, Cenozoic plate kinematics, subduction and magmatism—South American Andes: Geological Society of London Journal, v. 141, p. 793–802.

Pinto V., José, 1988a, Modelo conceptual y evaluación del potenciál mineral del yacimiento de metáles preciosos Chocaya, Potosí-Bolivia: La Paz, United Nations Development Program, Project BOL/87/12, unpublished report, 44 p.

Pinto V., José, 1988b, Large volume, low grade epithermal precious metal deposits in the department Potosí, Bolivia, *in* Extended abstracts, Yacimientos epitermales en ambientes de volcánismo reciente: Seminario-Taller, La Paz, Bolivia, September 4–16, 1988, 2 p.

Pinto, José, 1988c, Muestro de reconocimiento para mineralización de metales preciosos en gran volumen, Pulacayo, El Asiento, Chocaya, Monserrat, San Vicente—Potosí, Bolivia: La Paz, United Nations Development Program, Project BOL/87/12, unpublished report, 12 p.

Pinto, José, 1988d, Modelo conceptual y evaluación del potenciál mineral del yacimiento de metáles preciosos Tatasi—Potosí, Bolivia: La Paz, United Nations Development Program, Project BOL/87/12, unpublished report, 12 p.

Pinto V., J., 1989a, Geología y exploración preliminar del prospecto antimonio-aurífero Mestizo, Sud Lípez, Bolivia: La Paz, United Nations Development Program, Project BOL/87/012, unpublished report, 31 p.

Pinto V., J., 1989b, Modelo conceptual y evaluación del potencial mineral del yacimiento de metales preciosos Monserrat, Potosi, Bolivia: La Paz, United Nations Development Program, Project BOL/87/012, unpublished report, 24 p.

Pinto V., J., 1989c, Modelo conceptual y evaluación del potencial mineral del yacimiento de metales preciosos San Vicente, Potosi, Bolivia: La Paz, United Nations Development Program, Project BOL/87/012, unpublished report, 29 p.

Pinto V., J., 1989d, Visita preliminar a los yacimientos de Choroma y Esmoraca, Potosi, Bolivia: La Paz, United Nations Development Program, Project BOL/87/012, unpublished report, 4 p.

Pinto, José, 1989e, Muestro de reconocimiento para mineralización de metales preciosos en gran volumen, San José—Oruro, Bolivia: La Paz, United Nations Development Program, Project BOL/87/12, unpublished report, 5 p.

Pitcher, W.S., and Cobbing, E.J., 1985, Phanerozoic plutonism in the Peruvian Andes, *in* Pitcher, W.S., Atherton, M.P., Cobbing, E.J., and Beckinsale, R.D., eds., Magmatism at a plate edge—the Peruvian Andes: Glasgow and London, Blackie and Sons, p. 19–25.

Ploskonka, E., 1975, Geología y petrografía del volcán Soniquera: Yacimientos Petrolíferos Fiscales Bolivianos Revista Técnica, v. 4, no. 3, p. 581–598.

Ponce V., José, 1967, Informe sobre orientación técnica minas Victoria y El Triunfo: Servicio Geológico de Bolivia Informe GB–M–547, 9 p.

Ponce V., J., and Avila, W., 1965a, [Geologic map of the] Carangas [quadrangle], Hoja 5837 [Bolivia]: Servicio Geológico de Bolivia, scale 1:100,000.

Ponce, J., and Avila, W., 1965b, [Geologic map of the] Sajama [quadrangle], Hoja 5839 [Bolivia]: Servicio Geológico de Bolivia, scale 1:100,000.

Ponce, J., Avila, W., and Delgadillo, J., 1967, [Geologic map of the] Todos Santos [quadrangle], Hoja 5836 [Bolivia]: Servicio Geológico de Bolivia, scale 1:100,000.

Radtke, A.S., 1985, Geology of the Carlin gold deposit, Nevada: U. S. Geological Survey Professional Paper 1267, 124 p.

Raines, G.L., 1977, Digital color analysis of color ratio composite Landsat scenes, *in* Proceedings, 11th International Symposium of Remote Sensing of the Environment, University of Michigan, Ann Arbor: p. 1463–1472.

Redwood, Stewart, 1987a, Metallogenic belts of the central Andes, *in* Pacific Rim Congress 87—[Proceedings]—An international congress on the geology, structure, mineralization, and economics of the Pacific Rim, 26–29 August, 1987: Parkville, Australia, Australasian Institute of Mining and Metallurgy, p. 899–907.

Redwood, Stewart D., 1987b, The Soledad Caldera, Bolivia—a Miocene caldera with associated epithermal Au-Ag-Cu-Pb-Zn mineralization: Geological Society of America Bulletin, v. 99, p. 395–404.

Redwood, S.D., and Macintyre, R.M., 1989, K-Ar dating of Miocene magmatism and related epithermal mineralization of the northeastern Altiplano of Bolivia: Economic Geology, v. 84, p. 618–630.

Reed, B.L., 1986a, Descriptive model of Sn veins, *in* Cox, D.P., and Singer, D.A., eds., Mineral deposit models: U.S. Geological Survey Bulletin 1693, p. 67–69.

Reed, B.L., 1986b, Descriptive model of porphyry Sn, *in* Cox, D.P., and Singer, D.A., eds., Mineral deposit models: U.S. Geological Survey Bulletin 1693, p. 108.

Reed, B.L., Duffield, W.A., Ludington, S.D., Maxwell, C.H., and Richter, D.H., 1986, Descriptive model of thyolite-hosted tin, *in* Cox, D.P., and Singer, D.A., eds., Mineral deposit models, U.S. Geological Survey Bulletin 1693, p. 168.

Requena, C., Saavedra, A., and Cortez, J., 1963, [Geologic map of the] Tiahuanacu [quadrangle], Hoja 5844 [Bolivia]: Bolivia Departamento Nacional de Geología, scale 1:100,000.

Requena M., Edgar, 1971, Estudio geológico y petrológico de la región Buena Vista, Mulato y Moroco: La Paz, Universidad Mayor de San Andres, Facultad de Ciencias Geológicas, unpublished Tesis de Grado.

Rettig, S.L., Jones, B.F., and Risacher, F., 1980, Geochemical evolution of brines in the Salar of Uyuni, Bolivia: Chemical Geology, v. 30, p. 57–79.

Reyes, J.M., Branisa, L., and Freile, A.J., 1962, Bibliografía geológica, mineralógica y paleontológica de Bolivia: Bolivia Departamento Nacional de Geología Boletín 4, 186 p.

Rico A., Rodolfo, 1978, Aplicación del método de polarización inducida a la busqueda de yacimientos de sulfuros diseminados dominio de frecuencia, San Vicente-Monserrat, Departamento Potosí: La Paz, Universidad Mayor de San Andres, Facultad de Ciencias Geológicas, unpublished Tesis de Grado.

Riera K., C.H., 1989, Mineralogía y geotermometría de los yacimientos de oro primario del área de Yani: La Paz, Universidad Mayor de San Andres, Facultad de Ciencias Geológicas, unpublished Tesis de Grado, 110 p.

Risacher, François, 1976, Reconocimiento de algunos salares del Altiplano Boliviano: La Paz, Universidad Mayor de San Andrés and l'Office de la Recherche Scientifique et Technique Outre-Mer, unpublished report, 10 p.

Risacher, François, 1978, Genèse d'une croûte de gypse dans un bassin de l'Altiplano Bolivien, *in* Evolution récente des hauts plateaux Andins en Bolivie: L'Office de la Recherche Scientifique et Technique de Outre-Mer, Cahiers, Série Géologie, v. 10, no. 1, p. 91–100.

Risacher, François, 1984, Origine des concentrations extrêmes en bore et en lithium dans les saumures de l'Altiplano bolivien: Académie des Sciences de France, Comptes-Rendus des Séances, série 2, v. 299, no. 11, p. 701–706.

Risacher, François, 1989, Estudio económico del Salar de Uyuni: Universidad Mayor de San Andrés and l'Office de la Recherche Scientifique et Technique de Outre-Mer, Informe, 67 p.

Risacher, F. and Fritz, B., 1991, Geochemistry of Bolivian salars, Lípez, southern Altiplano—Origin of solutes and brine evolution: Geochimica et Cosmochimica Acta, v. 55, p. 687–705.

Risacher, F., and Miranda, J., 1976, Indicios de interes económico en los salares del Sud Lípez: La Paz, Universidad Mayor de San Andres and l'Office de la Recherche Scientifique et Technique de Outre-Mer, unpublished report, 8 p.

Risacher, F., Samuel, J., and Krempp, G., 1984, Concentrations extrêmes en molybdène, tungstène et arsenic dans les saumure d'un lac de l'Altiplano de Bolivia; indication métallogènique: Académie des Sciences de France Comptes-Rendus des Séances, série 2, v. 299, no. 19, p. 1325–1328.

Rivas A., Edmundo, 1971, Estudio geológico del área Llanquera-Chuquichambi-Huayllamarca: La Paz, Universidad Mayor de San Andres, Facultad de Ciencias Geológicas, unpublished Tesis de Grado, 69 p.

Rivas, Salomón, 1968, Geología de la región norte del Lago Titicaca: Servicio Geológico de Bolivia Boletín 2, 88 p.

Rivas, Salomón, 1975, Geología de Tatasi: Yacimientos Petrolíferos Fiscales Bolivianos Revista Técnica, v. 4, p. 637–647.

Roberts, Malcom, 1899, Minerals found in the silver lodes of Tatasi and Portugalete, Bolivia: Institution of Mining and Metallurgy Transactions, v. 7, p. 91–93.

Rocha R., S., 1958, Informe sobre asistencia técnica Mina Bertha: Bolivia Departamento Nacional de Geología Informe DCMS–35, 3 p.

Rocha, S., and Balderrama, I., 1963, Informe sobre orientación técnica mina cuprífera Florida: Bolivia Departamento Nacional de Geología, unpublished report, 6 p.

Rodríguez E., R., Salazar L., J., Vargas S., C., Escobar M., G., Díaz J., A., Salinos A., H., del Perre, M.E., 1976, Yacimientos minerales de la cordillera occidental de los Andes: Consejo Nacional Maritimo/Comisión de Asesoría Maritima/Servicio Geológico de Bolivia, 41 p.

Rose, A.W., Hawkes, H.E., and Webb, J.S., 1979, Geochemistry in mineral exploration: London, Academic Press, 657 p.

Rowe, G., 1961, Pruebas flotación con minerales de la Mina Bolivar: Bolivia Departamento Nacional de Geología Informe DNG–M–74, 3 p.

Ruíz G., Lorgio, 1975, Algunas consideraciones sobre la génesis del yacimiento cuprífero de Chuquichambi: Yacimientos Petrolíferos Fiscales Bolivianos Revista Técnica, v. 4, no. 3, p. 459–470.

Rutland, R.W.R., 1966, An unconformity in the Corocoro basin, Bolivia, and its relation to the copper mineralization: Economic Geology, v.61, p. 962–964.

Rytuba, J.J., 1986, Descriptive model of hot-spring Hg, *in* Cox, D.P., and Singer, D.A., eds., Mineral deposit models: U.S. Geological Survey Bulletin 1693, p. 178.

Rytuba, J.J., and Cox, D.P., 1991, Porphyry gold—a supplement to U.S. Geological Survey Bulletin 1693: U. S. Geological Survey Open-File Report 91–116, 7 p.

Saavedra M., Antonio, and Shimada, Nobutaka, 1986, La mineralización en los cuerpos subvolcánicos de Bolivia, *in* Memoría del II Coloquio del Instituto de Geología Económica: La Paz, Universidad Mayor de San Andres, Instituto de Geología Económica, p. 168–177.

Sabins, F.F., Jr., 1987, Remote sensing principles and interpretation (2nd ed.): New York, W.H. Freeman, p. 235–277.

Sangster, D.F., 1984, Felsic intrusion-associated silver-lead-zinc veins, *in* Eckstrand, O. R., ed., Canadian mineral deposit types—a geological synopsis: Geological Survey of Canada, Economic Geology Report 36, p. 66.

Sanjinés V., Orlando, 1968a, Estudio geológico de la región de Tagua: La Paz, Universidad Mayor de San Andres, Facultad de Ciencias Geológicas, unpublished Tesis de Grado.

Sanjinés, R., 1968b, Informe de asistencia técnica minera a la propiedad de la Cooperative Minera Industrial "El Porvenir" Limitada, situada en el Cantón Huanaque, Provincia Daniel Campos (Nor Lípez), del Departamento de Potosí: Servicio Geológico de Bolivia, unpublished report, 14 p.

Sanjinés, R., Ballivian, M., and Antezana, G., 1968a, Informe de asistencia técnica a la propiedad minera El Portal-Cabaña: Servicio Geológico de Bolivia Informe GB–M–593, 13 p.

Sanjines, R., Ponce, J., and Hurtado, G., 1968b, Informe sobre el estudio geológico en los Cerros Tomasimil y Cabana: Servicio Geológico de Bolivia Informe GB–M–584, 10 p.

Santiesteban A., Carlos, 1972, Estudio geológico de la Serranía de Cañapa, Provincia Sud Lípez, Departamento Potosí: La Paz, Universidad Mayor de San Andres, Facultad de Ciencias Geológicas, unpublished Tesis de Grado.

Saravia A., Carlos F., 1971, Contribución al conocimiento de la génesis del yacimiento cuprífero Corocoro aspectos sobre su geología minera, Provincia Pacajes, Departamento La Paz: La Paz, Universidad Mayor de San Andres, Facultad de Ciencias Geológicas, unpublished Tesis de Grado, 140 p.

Sawatzky, D.L., 1985, Programmer's guide to REMAPP, REMote sensing Array Processing Procedures: U.S. Geological Survey Open-File Report 85–231, 21 p.

Schlatter, L.E., and Nederlof, M.H., 1966, Bosquejo de la geología y paleogeografía de Bolivia: Servicio Geológico de Bolivia Boletín 8, 49 p.

Schneider-Scherbina, A., 1961a, El yacimiento argentífero de cobre de Laurani, Sica Sica, Bolivia: La Paz, German Geological Mission to Bolivia Report MGA–15, 54 p.

Schneider-Scherbina, A., 1961b, Informe sobre las investigaciones preliminares de las ocurrencias de minerales polimetálicos argentíferos en el macizo de Quimsachata: La Paz, German Geological Mission to Bolivia Report MGA–20, 15 p.

Schneider-Scherbina, A., 1962a, Los yacimientos argentíferos del distrito de Carangas: La Paz, German Geological Mission to Bolivia Report MGA–29, 59 p.

Schneider-Scherbina, A., 1962b, Los yacimientos polimetálicos de Berenguela: La Paz, German Geological Mission to Bolivia Report MGA–39, 54 p.

Schneider-Scherbina, A., 1963, Los yacimientos de cobre del altiplano boliviano: La Paz, German Geological Mission to Bolivia Report MGA–44, 163 p.

Segurola, J.C., Yáñez, G., Calvetty, E., and Chunacero, J., 1987, Informe etapas B–C estudio de prefactibilidad, proyecto Candelaria: Bolivia Fondo Nacional de Exploración Minera Informe 165/81, 41 p.

Sébrier, M., Lavenu, A., Fornari, M., and Soulas, J.P., 1988, Tectonics and uplift in central Andes (Peru, Bolivia and northern Chile) from Eocene to present: Geodynamique, v. 3, p. 793–802.

Sempéré, Thierry, 1990, Cuadros estratigráficos de Bolivia- propuestas nuevas: Convenio l'Office de la Recherche Scientifique et Technique de Outre-Mer/Yacimientos Petrolíferos Fiscales Bolivianos Informe 20, 26 p.

Sempéré, T., Hérail, G., Oller, J., and Baby, P., 1989, Geologic structure and tectonic history of the Bolivian orocline: International Geological Congress, 28th, Washington, D.C., Abstracts, v. 3, p. 72–73.

Sempéré, T., Hérail, G., Oller, J., Baby, P., Barrios, L., and Marocco, R., 1990, The Altiplano—A province of intermontane foreland basins related to crustal shortening in the Bolivian orocline area, *in* Symposium International Geodynamique Andine, May 15–17, 1990, Grenoble: Paris, l'Office de la Recherche Scientifique et Technique de Outre-Mer, Séries Colloques et Seminaires, p. 167–170.

Sempéré, T., Hérial, G., Oller, J., and Bonhomme, M.G., 1990, Late Oligocene-early Miocene major tectonic crisis and related basins in Bolivia: Geology, v. 18, p. 946–949.

Servant-Vildary, Simone, 1978a, Les diatomées des sédiments superficiels d'un lac salé, chloruré, sulfaté sodique de l'Altiplano bolivien, le lac Poopó: L'Office de la Recherche Scientifique et Technique de Outre-Mer, Cahiers, Série Géologie, v. 10, no. 1, p. 79–89.

Servant-Vildary, Simone, 1978b, Les diatomées des dépots lacustres Quaternaires de l'Altiplano bolivien: L'Office de la Recherche Scientifique et Technique de Outre-Mer, Cahiers, Série Géologie, v. 10, no. 1, p. 25–35.

Servicio Geológico de Bolivia, 1969, Investigaciones de los yacimientos de cobre, provincias Nor y Sur Lipez, Potosí: Servicio Geológico de Bolivia, unpublished report, 23 p.

Servicio Geológico de Bolivia, 1971a, Mina 25 de Julio: Proyecto Lipez-COMIBOL–70 Informe GE–40, 14 p.

Servicio Geológico de Bolivia, 1971b, Mina Abaroa: Proyecto Lipez-COMIBOL–70 Informe GE–24, 91 p.

Servicio Geológico de Bolivia, 1971c, Mina Aguilar: Proyecto Lipez-COMIBOL–70 Informe GE–30, 14 p.

Servicio Geológico de Bolivia, 1971d, Mina Alianza: Proyecto Lipez-COMIBOL–70 Informe GE–31, 21 p.

Servicio Geológico de Bolivia, 1971e, Mina Antonia: Proyecto Lipez-COMIBOL–70 Informe GE–23, 8 p.
Servicio Geológico de Bolivia, 1971f, Mina Aviadora: Proyecto Lipez-COMIBOL–70 Informe GE–22, 7 p.
Servicio Geológico de Bolivia, 1971g, Mina Barrahuayco: Proyecto Lipez-COMIBOL–70 Informe GE–19, 3 p.
Servicio Geológico de Bolivia, 1971h, Mina Bartolo: Proyecto Lipez-COMIBOL–70 Informe GE–42, 16 p.
Servicio Geológico de Bolivia, 1971i, Mina Bolívar: Proyecto Lipez-COMIBOL–70 Informe GE–26, 27 p.
Servicio Geológico de Bolivia, 1971j, Mina Bonete: Proyecto Lipez-COMIBOL–70 Informe GE–01, 4 p.
Servicio Geológico de Bolivia, 1971k, Mina Buena Vista: Proyecto Lipez-COMIBOL–70 Informe GE–06, 18 p.
Servicio Geológico de Bolivia, 1971l, Mina Campanario: Proyecto Lipez-COMIBOL–70 Informe GE–21, 8 p.
Servicio Geológico de Bolivia, 1971m, Mina Caquilan: Proyecto Lipez-COMIBOL–70 Informe GE–37, 7 p.
Servicio Geológico de Bolivia, 1971n, Mina Cerro Colorado: Proyecto Lipez-COMIBOL–70 Informe GE–38, 10 p.
Servicio Geológico de Bolivia, 1971o, Mina Cobrizos: Proyecto Lipez-COMIBOL–70 Informe GE–35, 25 p.
Servicio Geológico de Bolivia, 1971p, Colorados de Bolivia: Proyecto Lipez-COMIBOL–70 Informe GE–15, 7 p.
Servicio Geológico de Bolivia, 1971q, Mina Copacabana: Proyecto Lipez-COMIBOL–70 Informe GE–41, 19 p.
Servicio Geológico de Bolivia, 1971r, Mina El Morro: Proyecto Lipez-COMIBOL–70 Informe GE–27, 12 p.
Servicio Geológico de Bolivia, 1971s, Mina Escala: Proyecto Lipez-COMIBOL–70 Informe GE–09, 32 p.
Servicio Geológico de Bolivia, 1971t, Mina Farellón: Proyecto Lipez-COMIBOL–70 Informe GE–36, 17 p.
Servicio Geológico de Bolivia, 1971u, Mina Himalaya: Proyecto Lipez-COMIBOL–70 Informe GE–03, 18 p.
Servicio Geológico de Bolivia, 1971v, Mina Hornillos: Proyecto Lipez-COMIBOL–70 Informe GE–17, 7 p.
Servicio Geológico de Bolivia, 1971w, Mina Ines: Proyecto Lipez-COMIBOL–70 Informe GE–33, 25 p.
Servicio Geológico de Bolivia, 1971x, Mina Jaquegua: Proyecto Lipez-COMIBOL–70 Informe GE–13, 23 p.
Servicio Geológico de Bolivia, 1971y, Mina Koholpani: Proyecto Lipez-COMIBOL–70 Informe GE–44, 10 p.
Servicio Geológico de Bolivia, 1971z, Mina La Moza: Proyecto Lipez-COMIBOL–70 Informe GE–18, 4 p.
Servicio Geológico de Bolivia, 1971aa, Mina Linares-Cerro Negro: Proyecto Lipez-COMIBOL–70 Informe GE–28/29, 21 p.
Servicio Geológico de Bolivia, 1971bb, Mina Lipeña: Proyecto Lipez-COMIBOL–70 Informe GE–07, 3 p.
Servicio Geológico de Bolivia, 1971cc, Mina Mallcu Cueva: Proyecto Lipez-COMIBOL–70 Informe GE–43, 7 p.
Servicio Geológico de Bolivia, 1971dd, Mina Mantos Blancos: Proyecto Lipez-COMIBOL–70 Informe GE–25, 32 p.
Servicio Geológico de Bolivia, 1971ee, Mina Martes: Proyecto Lipez-COMIBOL–70 Informe GE–20, 13 p.
Servicio Geológico de Bolivia, 1971ff, Mina Mercedes-Goya I: Proyecto Lipez-COMIBOL–70 Informe GE–05, 37 p.
Servicio Geológico de Bolivia, 1971gg, Mina Mesa Verde: Proyecto Lipez-COMIBOL–70 Informe GE–47, 12 p.
Servicio Geológico de Bolivia, 1971hh, Mina Mestizo: Proyecto Lipez-COMIBOL–70 Informe GE–11, 23 p.
Servicio Geológico de Bolivia, 1971ii, Mina Mulato: Proyecto Lipez-COMIBOL–70 Informe GE–04, 11 p.
Servicio Geológico de Bolivia, 1971jj, Mina Nuevo Mundo: Proyecto Lipez-COMIBOL–70 Informe GE–12, 40 p.
Servicio Geológico de Bolivia, 1971kk, Mina Pucasalle: Proyecto Lipez-COMIBOL–70 Informe GE–14, 7 p.
Servicio Geológico de Bolivia, 1971ll, Mina Puntillas: Proyecto Lípez-COMIBOL–70 Informe GE–34, 22 p.
Servicio Geológico de Bolivia, 1971mm, Mina Rosario: Proyecto Lipez-COMIBOL–70 Informe GE–48.
Servicio Geológico de Bolivia, 1971nn, Mina San Antonio: Proyecto Lipez-COMIBOL–70 Informe GE–10, 86 p.
Servicio Geológico de Bolivia, 1971oo, Mina San Francisco: Proyecto Lipez-COMIBOL–70 Informe GE–39, 13 p.
Servicio Geológico de Bolivia, 1971pp, Mina San Julián: Proyecto Lipez-COMIBOL–70 Informe GE–08, 4 p.
Servicio Geológico de Bolivia, 1971qq, Mina Santa Rosa: Proyecto Lipez-COMIBOL–70 Informe GE–02, 16 p.
Servicio Geológico de Bolivia, 1971rr, Mina Solución o Malil: Proyecto Lipez-COMIBOL–70 Informe GE–45, 9 p.
Servicio Geológico de Bolivia, 1971ss, Mina Sucre: Proyecto Lipez-COMIBOL–70 Informe GE–32, 10 p.
Servicio Geológico de Bolivia, 1971tt, Mina Ucrania: Proyecto Lipez-COMIBOL–70 Informe GE–46, 9 p.
Servicio Geológico de Bolivia, 1979, Mapa de lineamientos y cuerpos intrusivos de los Andes Bolivianos: Servicio Geológico de Bolivia, Programa ERTS–GEOBOL, scale 1:1,000,000.
Sheffels, B.M., 1988, Structural constraints on crustal shortening in the Bolivian Andes: Cambridge, Massachussetts Institute of Technology, unpublished Ph.D. dissertation, 170 p.
Sheffels, B.M., 1990, Lower bound on the amount of crustal shortening in the central Bolivian Andes: Geology, v. 18, p. 812–815.
Shenk, J.D., 1991, Lacustrine diatomite, *in* Orris, G.J., and Bliss, J.D., eds., Some industrial mineral deposit models—descriptive deposit models: U.S. Geological Survey Open-File Report 91–11A, p. 23–25.
Sheppard, R.A., 1991, Descriptive model of sedimentary zeolites; Deposit subtype—Zeolites in tuffs of saline, alkaline-lake deposits, *in* Orris, G.J., and Bliss, J.D., eds., Some industrial mineral deposit models—descriptive deposit models: U.S. Geological Survey Open-File Report 91–11A, p. 16–18.
Sheppard, R.A., Eyde, T.H., and Barclay, C.S.V., 1987, Geology, mineralogy, and mining of the Bowie zeolite deposit, Graham and Cochise Counties, Arizona, *in* Mumpton, F.A., ed., Zeo-Trip '87—an excursion to selected zeolite and clay deposits in southwestern New Mexico and eastern Arizona: Brockport, New York, International Committee on Natural Zeolites, p. 27–46.
Sillitoe, R.H., 1973, The tops and bottoms of porphyry copper deposits: Economic Geology, v. 68, p. 799–815.
Sillitoe, R.H., 1983, Enargite-bearing massive sulfide deposits, high in porphyry copper systems: Economic Geology, v. 78, p. 348–352.

Sillitoe, R.H., 1988, Appraisal of the bulk potential of selected precious-metal properties in Bolivia: La Paz, United Nations Development Program, Proyecto BOL/87/12, unpublished report, 25 p.

Sillitoe, R.H., 1991, Intrusion-related gold deposits, *in* Foster, R.P., ed., Gold metallogeny and exploration: Glasgow and London, Blackie and Sons, Ltd., p. 165–209.

Sillitoe, R.H., and Bonham, H.F., Jr., 1990, Sediment-hosted gold deposits—distal products of magmatic-hydrothermal systems: Geology, v. 18, p. 157–161.

Sillitoe, R.H., Halls, C., and Grant, J.N., 1975, Porphyry tin deposits in Bolivia: Economic Geology, v. 70, p. 913–927.

Singer, D.A., and Cox, D.P., 1988, Applications of mineral deposit models to resource assessments: U. S. Geological Survey Yearbook, Fiscal Year 1987, p. 55–57.

Singer, D.A., and Mosier, D.L., 1986, Grade and tonnage model of rhyolite-hosted Sn, *in* Cox, D.P., and Singer, D.A., eds., Mineral deposit models: U.S. Geological Survey Bulletin 1693, p. 169–171.

Singer, D. A., and Ovenshine, A.T., 1979, Assessing mineral resources in Alaska: American Scientist, v. 67, p. 582–589.

Singewald, J.T., Jr., and Berry, E.W., 1922, The geology of the Corocoro copper district of Bolivia: Baltimore, Maryland, Johns Hopkins Press, 117 p.

Sirvas C., J. F., 1964, Estudio geológico de la región Tambo-Mauri-Berenguela, Provincia Pacajes, Departamento La Paz: La Paz, Universidad Mayor de San Andres, Facultad de Ciencias Geológicas, unpublished Tesis de Grado, 86 p.

Soria-Escalante, E., Banks, N.G., and Stine, Cynthia, 1991, First assessment of recent volcanic activity and hazards in the western Andes of Bolivia [abs]: International Conference on Active Volcanoes and Risk Mitigation, 27 August-1 September, 1991, Naples, Italy.

Steinmann, Gustav, 1916, El origen de los yacimientos cupríferos de Corocoro y de otros semejantes en Bolivia: Revista Minera de Bolivia (Oruro), no. 1, 33 p.

Steven, T.A., and Ratté, J.C., 1960, Geology and ore deposits of the Summitville district, San Juan Mountains, Colorado: U.S. Geological Survey Professional Paper 487, 90 p.

Stoffregen, R.E., 1987, Genesis of acid-sulfate alteration and Cu-Au-Ag mineralization at Summitville, Colorado: Economic Geology, v. 82, p.1575–1591.

Sugaki, A., Kitakazi, A., and Hayashi, K., 1986, Study on the ore minerals from the Bolivian tin deposit (II); cassiterite and wolframite from the mines in the Potosí and Quechisla districts: Science Reports of the Tohaku University, Series 3, v. 16, no. 3, p. 353–365.

Sugaki, A., Kitakazi, A., and Sanjines, O., 1981, Study on the ore minerals from the Bolivian tin deposits (I), cassiterite and stannite from the mines of the Oruro district: Science Reports of the Tohaku University, Series 3, v. 15, no. 1, p. 65–77.

Sugaki, A., Ueno, H., Kitakaze, A., Hayashi, K., Kojima, S., Shima, N., Sanjines V., O., Velarde V., O. J., and Sanchez, A.C., 1985, Geological and mineralogical studies on the polymetallic hydrothermal ore deposits in [the] Andes area of Bolivia: Sendai, Japan, Report of Overseas Scientific Survey.

Sugaki, A., Ueno, H., Shimada, N., Kitakaze, A., Hayashi, K., Sanjines V., O., and Velarde V., O., 1986, Geological study on the ore deposits in the Sur Lípez district, Bolivia: Science Reports of the Tohoku University, Series 3, v. 16, no. 3, p. 327–352.

Sundt, F.A., 1915, Corocoro copper district of Bolivia: Engineering and Mining Journal, v. 99, p. 189–190.

Tavera V., Franz, 1972, Estudio geológico a semi-detalle de la región de San Antonio de Lípez (Zona Norte): La Paz, Universidad Mayor de San Andres, Facultad de Ciencias Geológicas, unpublished Tesis de Grado.

Terrazas R., Jaime, 1975, Geología y prospección minera del área de María Elena, Cantón Caquiaviri, Provincia Pacajes, Departamento La Paz: La Paz, Universidad Mayor de San Andres, Facultad de Ciencias Geológicas, unpublished Tesis de Grado, 90 p.

Thormann, W., 1960, Tectónica y mineralización del stock de cuarzo latita de San José; Oruro-Bolivia: La Paz, German Geological Mission to Bolivia Report MGA–5, 115 p.

Thormann, W., 1966, Investigaciones preliminares sobre la geotectonica y metalogénesis de la zona Challapata-Caxata, Bolivia: Servicio Geológico de Bolivia Boletín 7, 118 p.

Thorpe, R.S., Francis, P.W., Hammill, M., and Baker, M.C.W., 1982, The Andes, *in* Thorpe, R.S., ed., Andesites: New York, John Wiley and Sons, p. 187–205.

Tistl, M., and Schneider, H.J., 1986, The Variscan thermometamorphism and its relations to gold-quartz mineralizations in the NE Cordillera Real, Bolivia: Zentralblatt für Geologie und Paläontologie, Teil 1, Allgemeine, Angewandte, Regionale und Historische Geologie, Heft 9–10, p. 1579–1589.

Titley, S.R., and Beane, R.E., 1981, Porphyry copper deposits; Part I, Geologic settings, petrology, and tectogenesis: Economic Geology, 75th Anniversary Volume, p. 214–234.

Togashi, Yukio, 1986, Descriptive model of Sn-polymetallic veins, *in* Cox, D.P., and Singer, D.A., eds., Mineral deposit models: U.S. Geological Survey Bulletin 1693, p. 109.

Torrico B., H., 1966, Estudio geológico de la región de San Cristóbal: La Paz, Universidad Mayor de San Andrés, Facultad de Ciencias Geológicas, unpublished Tesis de Grado.

Turneaure, F.S., 1960a, A comparative study of major ore deposits in central Bolivia—Part I: Economic Geology, v. 55, p. 217–254.

Turneaure, F.S., 1960b, A comparative study of major ore deposits of central Bolivia—Part II: Economic Geology, v. 55, p. 574–606.

Turneaure, F.S., 1971, The Bolivian tin-silver province: Economic Geology, v. 66, p. 215–225.

Turner-Peterson, C.E., and Hodges, C.A., 1986, Descriptive model of sandstone U, *in* Cox, D.P., and Singer, D.A., eds., Mineral deposit models: U.S. Geological Survey Bulletin 1693, p. 209.

United Nations Development Project, 1989a, Folleto Tecnico Promocional-Monserrat-Yacimiento de oro y plata de baja ley y gran volumen, Potosí-Bolivia: La Paz, United Nations Development Program, Project BOL/87/012, unpublished report, 14 p.

United Nations Development Program, 1989b, Proyecto de metales preciosos, provincia Sud Lípez, Departamento Potosí, Bolivia: La Paz, United Nations Development Program, Project BOL/87/012, unpublished report.

Uribe S., Hernán, 1989, Yacimientos argentíferos-auríferos de Guadalupe y La Deseada: La Paz, Inti Illimani S.A., unpublished report.

U.S. Geological Survey and National Oceanic and Atmospheric Administration, 1982, Index to Landsat Worldwide Reference System (WRS), Landsats 1, 2, 3, and 4, Sheet 18: U.S. Geological Survey and National Oceanic and Atmospheric Administration in cooperation with the National Aeronautics and Space Administration, scale 1:10,000,000.

U.S. Office of Inter-American Affairs, 1944, Bolivia—Storehouse of metals: Washington, D.C., Government Printing Office, 12 p.

Valencia F., José, 1973, Estudio geológico de la región oriental del Cerro Bonete: La Paz, Universidad Mayor de San Andres, Facultad de Ciencias Geológicas, unpublished Tesis de Grado, 89 p.

Vargas, W., 1967, Valuación de yacimientos de cobre, primera parte, Corocoro-Guaqui: Servicio Geológico de Bolivia Informe LP–24, 36 p.

Vargas, W., 1968, Examen de recursos naturales y otros factores en las azufreras de la región Chacacomani-Huachacalla: Servicio Geológico de Bolivia Informe GB–M–587, 4 p.

Vargas, W., and Ballivian, M., 1972, Informe sobre asistencia técnica Mina Rondal: Servicio Geológico de Bolivia Infome GB–M–692, 7 p.

Vedia M., J., 1960a, Informe sobre orientación técnica minera Mina Los Colorados: Bolivia Departamento Nacional de Geología Informe TM–104, 4 p.

Vedia M., J., 1960b, Informe sobre orientación técnica minera Mina 10 de Diciembre: Bolivia Departamento Nacional de Geología Informe TM–105, 3 p.

Vedia M., J., and Ascarrunz K., R., 1970, Informe de asistencia técnica mina San Agustín: Servicio Geológico de Bolivia Informe GB–M–678, 11 p.

Vedia M., J., and Cortez A., G., 1966a, Informe sobre orientación técnica mina cuprífera Eduardo Abaroa: Servicio Geológico de Bolivia Informe GB–M–495.

Vedia M., J., and Cortez A., G., 1966b, Informe sobre orientación técnica mina de bismuto Salvadora: Servicio Geológico de Bolivia Informe GB–M–505, 4 p.

Vedia M., J., and Cortez A., G., 1966c, Informe sobre orientación técnica mina de hierro y plata Inca: Servicio Geológico de Bolivia Informe GB–M–497, 4 p.

Vedia M., J., and Cortez A., G., 1966d, Informe sobre orientación técnica mina plumbo-argentífera Animas: Servicio Geológico de Bolivia Informe GB–M–496, 5 p.

Vedia M., J. and Cortez A., G., 1966e, Informe sobre orientacion tecnica mina Bolivar: Servicio Geológico de Bolivia Informe GB–M–504, 10 p.

Vedia M., J., and Gonzales, A., 1970, Informe de asistencia técnica mina de cobre Santa María: Servicio Geológico de Bolivia Informe GB–M–658, 6 p.

Vedia M., J., and Llanos I., R., 1965, Informe sobre orientación técnica mina cuprífera La Incognita: Bolivia Departamento Nacional de Geología Informe DNG–M–445, 7 p.

Vedia M., J., Fernández, L., and Mendoza, E., 1971, Informe sobre asistencia técnica mina San Miguel: Servicio Geológico Geológico de Bolivia Informe GB–M–688, 7 p.

Velasco, C., and Barrientos, M., 1965, [Geologic map of the] Quechisla [quadrangle], Hoja 6331 [Bolivia]: Bolivia Departamento Nacional de Geología, scale 1:100,000.

Vergara, H., and Thomas, A., 1984, Carta geológica de Chile, Collacague, Hoja no. 59: Chile Servicio Nacional de Geología y Minería, scale 1:250,000.

Walthier, T.N., Sirvas, E., and Araneda, R., 1985, The El Indio gold, silver, copper deposit: Engineering and Mining Journal, v. 186, no. 10, p. 38–42.

Wenrich, K.J., 1985, Geochemical characteristics of uranium-enriched volcanic rocks, *in* Uranium deposits in volcanic rocks: Vienna, International Atomic Energy Agency, p. 29–51.

Wiseman, W.I., and Tandy, C.W., 1975, Sodium sulfate deposits, *in* Lefond, S.J., ed., Industrial minerals and rocks (nonmetallics other than fuels), (4th edition): New York, American Institute of Mining, Metallurgical, and Petroleum Engineers, p. 1081–1093.

Worner, G., Moorbath, S., and Harmon, R.S., 1990, Isotopic variations in central Andean lavas: International Volcanological Congress, Mainz, 3–8 September, 1990, International Association for Volcanology and Chemistry of the Earth's Interior, Abstract Volume.

Wright, A., 1983, The Ortiz gold deposit (Cunningham Hill)—Geology and exploration, *in* Papers given at the precious-metals symposium: Nevada Bureau of Mines and Geology Report 36, p. 42–51.

Yeend, W.E., 1986, Descriptive model of placer Au-PGE, *in* Cox, D.P., and Singer, D.A., eds., Mineral deposit models: U.S. Geological Survey Bulletin 1693, p. 261.

Zambrana B., René, 1971, Prospección geofísica en el distrito minero de San Antonio de Lípez: La Paz, Universidad Mayor de San Andres, Facultad de Ciencias Geológicas, unpublished Tesis de Grado, 39 p.

Zamora G., Carlos, 1989, El yacimiento de La Joya, Oruro (Geología, mineralogía, alteraciones y geotermometría): La Paz, Universidad Mayor de San Andres, Facultad de Ciencias Geológicas, unpublished Tesis de Grado, 76 p.

Zapata, H., 1987, Las concentraciones de cobre en la parte oriental del Terciario Altiplánico, *in* Memoría del III Coloquio del Instituto de Geología Económica: La Paz, Universidad Mayor de San Andres, Instituto de Geología Económica, p. 167–185.

Zapata, H., and Delgadillo, H., 1968, Valuación de yacimientos de cobre, segunda parte, Tiahuanacu-Jesus de Machaca-Corque-Turco: Servicio Geológico de Bolivia Informe LP–25, 26 p.

Zubrzycki, P.F., and Murillo, J.E., 1958a, Informe Mina "Himalaya": Corporación Minera de Bolivia, unpublished report, 4 p.

Zubrzycki, P.P. and Murillo, J. E., 1958b, El yacimiento polimetálico de Jaquegua: Oruro, Corporación Minera de Bolivia, unpublished report, 7 p.

APPENDIX A

MINES, PROSPECTS, AND MINERAL OCCURRENCES, ALTIPLANO AND CORDILLERA OCCIDENTAL, BOLIVIA

BY

KEITH R. LONG

Table A–1. *Mines, prospects, and occurrences on the Altiplano and in the Cordillera Occidental, Bolivia*

[Abbreviations used: °C, degrees Celsius; cm, centimeter; g/cm^3, grams per cubic centimeter; g/kg, grams per kilogram; g/L, grams per liter; g/t, grams per tonne; ha, hectare, km, kilometer; km^2, square kilometer, L/s, liters per second; m, meter; m^2, square meter; m^3, cubic meter; mm, millimeter; mg/kg, milligrams per kilogram; mg/L, milligrams per liter; m.y., million years; pH, hydrogen ion activity; ppm, parts per million; t, tonnes; TDS, total dissolved salts]

Map no.	Site name (Synonym)	Lat S., Long W. (deg, min, sec)	Deposit description and references
		Basaltic Copper Deposits	
106	Azurita mine	18 04 06, 68 09 22	Stratabound Cu-Ag mineralization hosted by a fluvial coarse-grained sandstone to conglomerate sandwiched between two basalt flows. Sedimentary rocks, including shale, exhibit stratibound cuprite-native copper mineralization and are cut by subvertical fractures filled by cuprite-tennantite-celestite. Native copper, partly oxidized to chrysocolla, replaces calcite cement in basalt. Alteration minerals in basalt are chlorite, kaolinite, and carbonate. Exposed mineralized zone is 1 km long and consists of five mantos, each as thick as 1.6 m. Production (1948-62) was 70,000 t at 3.5-4.0% Cu. Reserves in 1969 were 660,000 t at 2.2% Cu. (Schneider-Scherbina, 1963; Murillo and others, 1969)
116	Tambillo mine (Hislata)	19 24 37, 67 23 02	Native copper disseminated in basalt of the Totora Formation. (Ahlfeld and Schneider-Scherbina, 1964; Schneider-Scherbina, 1963)
118	Concepción prospect	19 34 34, 67 16 38	Stockwork of veinlets of native copper, cuprite, and malachite in a zone 1.5 m wide in plagioclase basalt of the Tambillo Formation. (Murillo and others, 1969)
429	Aviadora mine	21 50 --, 66 16 --	Chalcocite, native copper, cuprite, malachite, and calcite, filling fractures 0.1-3 m wide in plagioclase basalt of the Rondal Formation. (Servicio Geológico de Bolivia, 1971f)
430	Campanario mine	21 53 --, 66 16 --	Bornite, covellite, chalcocite, malachite, quartz, hematite, and calcite fill N. 44° W. and N. 81° W. trending fissures and open spaces in basalt and conglomerate of the Rondal Formation. (Servicio Geológico de Bolivia, 1971l)
		Bedded Salt Deposits	
67	Caquingora mine	17 14 39, 68 29 36	Brine springs fed by solutions passing through unexposed beds of Tertiary halite and gypsum. (Ahlfeld and Schneider-Scherbina, 1964)
69	Jayuma de Llallagua mine	17 17 46, 68 29 03	Brine springs fed by solutions passing through unexposed beds of Tertiary halite and gypsum. (Ahlfeld and Schneider-Scherbina, 1964)
119	Colchani mine	20 18 50, 66 58 43	Since the mid-1500's, site of mining of salt crust at eastern edge of Salar de Uyuni. Salt is about 95% halite; remainder is sodium sulfate, trona, and insoluble residues. (Ahlfeld and Schneider-Scherbina, 1964; Rettig and others, 1980)
186	Salar de Coipasa deposit	19 22 00, 68 08 00	A salar, 2,000 km^2 in extent, with a halite crust 0.5 m thick. Estimated tonnage is 1.7 million tonnes salt. (Ericksen and others, 1977, 1978; Rettig and others, 1980; Ballivian and Risacher, 1981)
211	Salar de Uyuni deposit	20 00 00, 68 00 00	A salar with halite (plus minor sylvite and gypsum) crust as thick as 15 m (minimum 50 cm, average 10 m) overlying a layer of impermeable mud. Additional salt layers are known to occur below the exposed salt crust from drilling. Estimated tonnage for exposed salt crust is 64 billion tonnes salt. (Ericksen and others, 1978; Ballivian and Risacher, 1981; Davis and others, 1982)
214	Salar de Empexa deposit	20 19 46, 68 28 33	Much of salar consists of salt crust about 400 km^2 in area, averaging 0.2 m thick. Estimated tonnage 100 million tonnes salt. (Ericksen and others, 1977, 1978; Ballivian and Risacher, 1981).
245	Salar de la Laguna deposit	20 50 17, 68 27 34	Salar has crust of halite, natron, and sodium sulfate. (Ballivian and Risacher, 1981)
250	Salar Laguani deposit	20 56 31, 68 18 10	Salar with halite crust. (Ballivian and Risacher, 1981)
252	Salar de Ollagüe deposit	21 10 30, 68 14 00	Salar with halite crust. (Ericksen and Salas, 1989)

Table A–1. *Mines, prospects, and occurrences on the Altiplano and in the Cordillera Occidental, Bolivia*—Continued

254	Salar de Chiguana deposit	21 08 00, 68 02 45	Salar with halite crust. (Ballivian and Risacher, 1981)
268	Laguna Chiar Kkota deposit	21 35 00, 68 04 00	Small crust of gypsum, halite, calcite, and sylvite. (Ballivian and Risacher, 1981)
352	Laguna Coruto deposit	22 25 45, 67 00 00	Extensive deposit of halite and gypsum on northwest part of lake basin. (This study)
		Bolivian Polymetallic Vein Deposits	
		Quimsa Chata Area	
14	Quimsa Chata district (Tiwanaku; includes Caracollo, Carmen, Granada, Nasa Poke, Omonima, San Bartolomé, San Carlos, Santa Rosa mines)	16 38 00, 68 39 30	Veins of galena, sphalerite, chalcopyrite, tetrahedrite, pyrite, barite, tourmaline, and quartz cut lower Tertiary Tiahuanaku Formation sandstone and conglomerate intruded by 11-13 m.y. Quimsa Chata dacite stock. Veins strike N. 20° E. and N. 50°-60° E., are 0.1-1 m wide, as much as 500 m long, and cover an area of 3 by 2.5 km. Host dacite is intensely sericitized and pyritized; other alteration includes silicification and kaolinization. Recent sampling yields values of Ag generally less than 2 g/t and Au less than 0.01 g/t. In 1961 some 20,000 t of dumps were found to contain as much as 4.4% Pb, 21% Zn, 6.7% Cu, and 2,160 g/t Ag. (Ahlfeld and Schneider-Scherbina, 1964; Schneider-Scherbina, 1961b; Cordero, 1966; Redwood and Macintyre, 1989; MINTEC, oral commun., 1990)
17	San Luís mine (María del Carmen Mercedes)	16 42 02, 68 47 10	Veins trending N. 30° E., 20-30 cm wide cut Devonian quartzite and shale. Veins contain galena and sphalerite. (Empresa Minera Illimani, 1989)
18	Montebello mine	16 43 45, 68 45 42	Veins trending N. 30° E., 20-30 cm wide cut Eocene Tiahuanacu sandstone. Veins have significant values in Cu, Pb, Zn, and Ag. (Empresa Minera Illimani, 1989)
		Cerro Surichata Area	
38	Chucuani mine (Colqencha, Cerro Koricahua)	16 59 39, 68 11 33	Miocene (16.6 m.y.) dacite cut by N. 80° W. trending, northwest dipping veins and some disseminated mineralization. Exposed mineralization consists of oxides of Pb, Ag, Zn, Au, Cu, As, and Sb. Systematic sampling found as much as 0.04 g/t Au, 70 ppm Cu, 2,000 ppm Pb, 1,000 ppm Zn, 20 g/t Ag, 300 ppm As, and 40 ppm Sb. (MINTEC, oral commun., 1990)
39	Nuestra Señora de La Paz prospect	16 58 42, 68 10 39	Argillic altered Miocene dacite hosts disseminated Pb-Ag mineralization. Samples contain as much as 109 g/t Ag, average 27 g/t Ag. (Empresa Minera Illimani, 1989)
		Cerro Lipiza Area	
43	Tomuyo deposit	17 10 30, 68 00 05	Intensely altered and fractured dacite intrudes quartzose sandstone of the Vila Vila Formation on the east flank of a regional anticline. Dacite is cut by veinlets of barite, limonite, jarosite, specularite, goethite, pyrite, and magnetite. Alteration consists of intense replacement of primary feldspars and micas by sericite, pyrite, chlorite, dickite, and halloysite. Native gold and silver occur with native mercury as disseminated grains and globules of amalgam as much as 0.25 mm in size in altered dacite. Recent drilling and sampling suggest a reserve potential of 23 million tonnes of oxide ore at about 0.7 g/t Au. Limited silver analyses suggest a silver-to-gold ratio greater than 100:1. (Empresa Minera Illimani, 1990)
44	Titiri deposit	17 10 05, 67 59 00	Altered dacite intrudes Paleozoic shale cut by an east-west fault. Argillic and sericitic alteration diminishes rapidly with depth. Visible mineralization consists of pyrite, galena, arsenopyrite, chalcopyrite, limonite, hematite, and goethite. Drilling (9 holes to depth of 40 m) intersected a mineralized zone averaging 6 m thick, 0.05 g/t Au and 8 g/t Ag. (André, 1989b).
45	Taricagua deposit (Taricoya)	17 11 40, 67 58 25	Altered and fractured dacite intrudes fractured Paleozoic shale and quartzose sandstone. Argillic and sericitic alteration is limited to northern 30% of the intrusive. Veinlets of jamesonite, pyrite, galena, limonite, jarosite, hematite, realgar, cervantite, and chalcopyrite fill fractures in altered dacite and adjacent wall rock. Drilling (21 holes to depth of 40 m) intersected a mineralized zone averaging 25 m thick, 0.21 g/t Au, and 5.8 g/t Ag. (Ahlfeld, 1954; André, 1989a)

Table A–1. *Mines, prospects, and occurrences on the Altiplano and in the Cordillera Occidental, Bolivia*—Continued

		La Joya District	
51	San Pablo and Carmen mines (Cerro La Joya)	17 46 50, 67 30 19	Veins of enargite, electrum, tennantite, covellite, chalcopyrite, chalcocite, bismuthinite, native bismuth, pyrite, arsenopyrite, tourmaline, and quartz cut Devonian shale and siltstone on southeast flank of Cerro La Joya. Sediments are intruded by propylitized granodiorite porphyry. (Ahlfeld and Schneider-Scherbina, 1964; Jiménez and others, 1988; Zamora, 1989; this study)
52	La Barca prospect (Cerro Quiriri)	17 46 05, 67 27 32	Northeast-trending mineralized fractures hosted by altered dacite and Devonian Catavi Formation clastic sediments. (This study)
53	San Andrés mine (Cerro Llallagua)	17 46 12, 67 27 27	Two parallel, N. 10°-20° E. trending veins cut altered Tertiary intrusive. Veins are as much as 500 m long, 1-2 m wide, and worked to 400 m depth. Mineralization consists of native gold, jamesonite, galena, sphalerite, wolframite, chalcopyrite, boulangerite, stibnite, pyrite, arsenopyrite, marcasite, pyrrhotite, ankerite, and quartz. Veins are oxidized to about 100 m depth. High grade ore shoot mined 1936-40 yielded about 5 t of 50 g/t ore in 1940. (Ahlfeld, 1954; this study)
54	Kori Kollu mine (Inti Raymi, Cerro Chuquina)	17 48 10, 67 27 00	Intensely altered dacite intrusive cut by closely spaced, parallel veins oriented N. 10°-20° E. dipping 75°-85° northwest. Alteration consists of intense sericitization with as much as 15 volume percent disseminated pyrite. Upper 35-50 m of orebody is oxidized and consists of jarosite and goethite which replace disseminated and vein pyrite. A sulfide zone of sphalerite, galena, tetrahedrite, chalcopyrite, stibnite, electrum, pyrite, and arsenopyrite veins occurs beneath a weak chalcocite enrichment blanket. Intrusion and mineralization are dated at 15 m.y. Reserves in 1990 were 58.7 million tonnes of sulfide ore at 2.3 g/t Au and 13.8 g/t Ag and 6 million tonnes of oxide ore at 1.9 g/t Au and 24.7 g/t Ag. (Redwood, 1987a; Alarcón and Villalpando, 1988; Anzoleaga, 1988; this study)
		Oruro District	
59	San José de Oruro mine	17 57 12, 67 08 00	More than 8 northeast-trending veins that dip 30°-70° northeast and southwest cut Tertiary intrusive rhyolite porphyry, Tertiary quartz monzonite porphyry, and Silurian shale. Best ore is in veins cutting rhyolite porphyry with pay zones about 1 m wide. Quartz monzonite porphyry and shales are poor hosts and are cut by narrow veins that pinch out rapidly downwards. Intrusives and associated intrusive breccias are pervasively sericitized. Veins consist of tetrahedrite, freiburgite, jamesonite, plumosite, andorite, galena, sphalerite, chalcopyrite, cassiterite, stannite, stibnite, enargite, sulfantimonides of Pb, tourmaline, pyrite, alunite, sericite, dickite, and quartz. Mineralized zone is 2,000 m long, 1,200 m wide, and is explored to 550 m depth with no decrease in grade. Veins grade 500 to 1,500 g/t Ag, 10% Pb with unknown values of Sn, Cu, Sb, and Zn. Silver to gold ratio is about 1,000:1. Reserves and past production are poorly known. (Lindgren and Abbott, 1931; Campbell, 1942; McAllister, 1944; Chace, 1948; Ahlfeld and Schneider-Scherbina, 1964; Sillitoe and others, 1975; Argandoña, 1989)
		Berenguela District	
126	Cerro Wila Kkollu occurrence	17 17 30, 69 23 50	Sericitically altered dacite with visible pyrite. Rhyolite domes to the east are sericitically altered and contain abundant fractures filled with pyrite. (This study)
127	Cerro Tatito Kkollu occurrence	17 18 20, 69 22 45	North-south fractures and hydrothermal breccias in silicified Mauri conglomerate, andesite, and volcanoclastics, all intruded by rhyolite. Values of Ag, Cu, As, Zn, Pb, and Sb reported. Mineralized zone is as much as a few hundred meters wide. (This study)

Table A–1. *Mines, prospects, and occurrences on the Altiplano and in the Cordillera Occidental, Bolivia*—Continued

131	San Luís mine (Mary-Mary, Heil Hitler, Viluiyo, Kairiri, Elisa)	17 16 10, 69 12 54	East-west veins, 10-30 cm wide, with ore shoots 10-35 m long and as wide as 3 m, cut Eocene Berenguela sandstone. Veins contain sphalerite, greenockite, galena, tennantite, and native copper and have kaolinite selvages. Abundant Cu found in oxidized zone, 5-10 m deep at east end of vein system. (Schneider-Scherbina, 1962b, Sirvas, 1964; this study)
133	San José de Berenguela mine (Elisa, Hucurani)	17 17 17, 69 13 57	East-west veins cut Eocene Berenguela sandstone in an area 2 by 0.4 km. Veins are composed of galena, sphalerite, tennantite, rhodocrosite, manganese oxides, and opal. (Schneider-Scherbina, 1962b; this study)
134	Lourdes Ines mine (Marimarini)	17 17 36, 69 14 17	N. 75° W. trending vein about 500 m long cuts Eocene Berenguela sandstone. Veins contain sphalerite, greenockite, galena, tennantite, stromeyerite, stephanite, and huachecornite. (Schneider-Scherbina, 1962b; this study)
135	Dos Amigos mine (Pacocagua)	17 19 06, 69 14 32	East-west vein about 350 m long in a fault that cuts Eocene Berenguela sandstone intruded by rhyolite. Veins are composed of sphalerite, galena, pearceite, pyrite, quartz, and barite. All rocks are altered to quartz and sericite. Workings encountered SiO_2 rich fluid and CO_2 gas. (Schneider-Scherbina, 1962b; this study)
136	Manco Kapac mine (Nelly)	17 17 52, 69 12 37	Veins oriented N. 75°-85° W. over a length of 1 km cut Eocene Berenguela sandstone. Upper 50 m of veins are oxidized with cerussite-chlorargyrite-manganese oxides that contain 190 g/t Ag. Unoxidized veins contain tennantite, galena, sphalerite, freieslebenite, greenockite, chalcopyrite, bornite, stephanite, stromeyerite, polybasite, miargyrite, argentite, covellite, kaolinite, and chalcedony. (Schneider-Scherbina, 1962b; Sirvas, 1964)
137	Anaconda, El Zorro, and Jokolluni mines (Yokohama)	17 18 26, 69 08 43	East-west vein, 600+ m long, 25 cm wide, with a 5 m wide alteration halo of pyrite-sericite-kaolinite, cuts middle Tertiary Mauri Formation sandstone, conglomerate, and andesite. Veins are composed of sphalerite, greenockite, chalcopyrite, tennantite, freieslebenite, galena, argentite, stromeyerite, chalcopyrite, stephanite, miargyrite, proustite, native silver, huachecornite, maucherite, calcite, and pyrite. (Ahlfeld, 1936; Schneider-Scherbina, 1962b; this study)
		Sonia-Susana Area	
164	Sonia prospect	18 47 00, 68 50 30	North end of a large alteration zone in an eroded stratovolcano complex. East-west veins and stockworks of Fe and manganese oxides in silicic, argillic and propylitic altered andesite and dacite. Altered zones have as much as 0.4 g/t Au and 16 g/t Ag. A sample of veinlet material had 2 g/t Au, 1,740 g/t Ag, 100 ppm As, and 110 ppm Sb. (MINTEC, oral commun., 1990; this study)
166	Paco Khaua prospect (Paco Cagua)	18 48 50, 68 49 00	Sericitized, argillized, and silicified rhyolite cut by veins and stockworks of cassiterite and Pb, Cu, and Ag minerals. Average grade of surface samples was 0.01 g/t Au and 5 g/t Ag. (Empresa Minera Illimani, 1989)
167	Susana prospect	18 51 45, 68 49 45	South end of a large alteration zone in an eroded stratovolcano complex. North-south veins of galena, Cu, Fe, and manganese oxides, and fluorite? in silicic, argillic, and propylitic altered andesite and dacite. Altered zones have as much as 0.4 g/t Au and 16 g/t Ag. (MINTEC, oral commun., 1990; this study)
		Todos Santos District	
168	Paco Kkollu prospect (Cerro Jankho Willkhi)	18 50 30, 68 39 00	Intensely altered rhyolite with disseminated silver mineralization. Values of 100-150 g/t Ag reported. (Pan Andean S.A., oral commun., 1990; this study)
169	Negrillos mine (La Plata)	18 50 26, 68 37 42	Propylitized and argillized tuff and andesite breccia host three veins; two veins are oriented N. 70° W., dip 85° northeast, are 300 m long and 1-40 cm wide, the other vein is oriented N. 50° E., dip 85° northwest to vertical, is 1 km long, and as wide as 1 m. Veins are composed of galena, sphalerite, tetrahedrite, pyrargyrite, polybasite, freibergite, chalcopyrite, quartz, pyrite, chalcedony, and rhodonite. Oxidized ore extends to 30 m depth and consists of masses and nodules of manganese oxides with cerussite. (Guerra and others, 1965b; Avila-Salinas, 1965; this study)

Table A–1. *Mines, prospects, and occurrences on the Altiplano and in the Cordillera Occidental, Bolivia*—Continued

171	Carangas mine (Orkho Thunko)	18 56 19, 68 37 42	Two mineralized zones in rhyolite porphyry and explosion breccia of the Tertiary Carangas volcanics. N. 65° W. trending veins extend 1.7 km at Cerro San Antonio. Veins at Cerro Espíritu Santo strike N. 65° W., are as wide as 12 cm, and occur in a 350 m wide zone. Veins contain cerargyrite, native silver, tennantite, proustite-pyrargyrite, sphalerite, galena, chalcopyrite, pyrite, chalcedony, opal, barite, Mn carbonate, siderite, sericite, and kaolinite. Host rhyolite is silicified, argillized, and pyritized. Past production is estimated at 1.5 million tonnes ore, leaving 10,000 t 35-50% Pb slag. Dump samples have as much as 20% Pb and 800 g/t Ag. (Schneider-Scherbina, 1962a; Guerra and others, 1965c; Avila-Salinas, 1965; this study)
175	Todos Santos mine	19 00 48, 68 43 19	Argillized and chloritized rhyolite dome cut by N. 10° E. and N. 80° W. trending veins. Mineralized zone is 4 by 1 km in area and as thick as 50 m. Veins contain tetrahedrite, proustite-pyrargryite, stephanite, cerargyrite, miargyrite, argentite, sphalerite, galena, pyrite, quartz, hematite, and manganese oxides. Reserves estimated in 1988 are 1 million tonnes at 70 g/t Ag and 0.07 g/t Au. (McNamee, 1988)
		Salinas de Garci Mendoza District	
188	Candelaria mine	19 37 50, 67 41 47	Vein of Ag oxides, trending N. 55° W. dip 60° north, 0.8 m wide, cuts vitric tuff. (Sanjinés, 1968b)
189	Canguro prospect (Natividad, Cerro Kancha)	19 38 30, 67 41 21	Silicified and brecciated andesite intruded by dacite and rhyolite dikes and cut by veins of galena, sphalerite, pyrite, siderite, quartz, and barite. At Cerro Kancha an extremely silicified, vuggy dacite is associated with zones of pervasive alunitic-advanced argillic and propylitic alteration. (MINTEC, oral commun., 1990; this study)
191	La Deseada mine	19 40 15, 67 42 12	Altered tuff, flows, and volcanic breccia cut by east-west veins, 600-1,000 m long, 1-2.5 m wide, that dip 80° north to vertical. Veins contain galena, sphalerite, malachite, azurite, quartz, barite, and pyrite. Alteration is zoned, top to bottom, from silicification, silicification-argillization, to propylitization. (Medina and others, 1988; Uribe, 1989)
192	Guadalupe mine	19 41 20, 67 42 28	Altered andesite cut by altered and mineralized dacite dikes oriented N. 70°-85° E., dip 80° north to vertical, 100 to 1,000 m long, and as wide as 15 m. Dikes have a pervasive silicic overprint on argillic alteration. Andesite is propylitized with local argillic zones. Dikes carry enargite, tetrahedrite, azurite, malachite, quartz, barite, pyrite, and iron oxides. Reserves estimated in 1990 are 2.5 million tonnes at 0.4 g/t Au and 280 g/t Ag. Dumps contain 20,000 t at 0.4 g/t Au and 400 g/t Ag. (Sanjinés, 1968a; Medina and others, 1988; Uribe, 1989; this study)
193	María Luisa mine	19 42 30, 67 42 51	Weakly silicified Tertiary pyroclastics, flows, and breccias are cut by N. 70°-80° W. trending dip 70° north to vertical vein systems as long as 3 km and generally 2 m wide. Veins have alteration halos of intense silicification and argillization that extend out 30 m. Altered wall rocks contain as much as 1% disseminated pyrite and unidentified dark sulfides. Veins contain sphalerite, galena, freibergite, argentite, stephanite, chalcopyrite, quartz, and pyrite. Oxidized ore consists of cerussite, covellite, cerargyrite, jarosite, limonite, and specularite. Reserves in 1982 were 304,500 t at 4.4% Zn, 4.0% Pb, and 267 g/t Ag. (Sanjinés, 1968a; Gamboa, 1982; Medina and others, 1988; Sillitoe, 1988; this study)
194	San Miguel and Margarita mines	19 43 54, 67 40 40	San Miguel and Margarita mines work the same vein system that trends N. 45°-75° W. or N. 80° E., dips 80° northeast to vertical. Veins are silicified and mineralized shear zones, range from 60 cm to 6 m wide, with ore shoots as long as 70 m. The ore shoots contain about 30% of the ore. Veins cut propylitized Tertiary pyroclastics and have argillic envelopes as wide as 2 m. Veins contain sphalerite, galena, chalcopyrite, quartz, pyrite, and ankerite. Reserves in 1967 were 253,000 t at 7% Pb and 84 g/t Ag. (Sanjinés, 1968a; Medina and others, 1988; this study)

Table A–1. *Mines, prospects, and occurrences on the Altiplano and in the Cordillera Occidental, Bolivia*—Continued

		San Cristóbal District	
236	Hedionda mine (Santa Bárbara de Jayula)	21 05 18, 67 12 19	Mineralized brecciated contact between intrusive dacite porphyry and Upper Quehua Formation agglomerate. Alteration is argillic and ore minerals are native silver, galena, sphalerite, and pyrite. Mine was difficult to work because of CO_2 gas. (Jacobson and others, 1969; Torrico, 1966)
237	Bertha, Colón, Tesorera, and Trapiche mines	21 06 00, 67 32 30	Veins of galena, argentite, sphalerite, pyrite, arsenopyrite, and siderite cut Upper Quehua Formation pyroclastics and dacite porphyry. Veins oriented north to northwest dip northeast, oriented northeast dip 40° northwest, and oriented N. 55° E. dip 85° southeast, and are all 10-50 cm wide. (Rocha, 1958; Torrico, 1966; Murillo and others, 1967; Jacobson and others, 1969)
238	Animas mine (Joukia)	21 06 21, 67 13 17	Mineralized breccia pipe cutting Eocene Potoco Formation sandstone and shale. Galena, sphalerite, and pyrite replace breccia matrix. Breccia pipe is 300 m long and 40 m wide, elongated N. 30° W. Breccia fragments and matrix are silicified and argillized. Reserves in 1966 were 131,250 t at 0.98% Pb and 1.0% Zn. (Vedia and Cortez, 1966d; Murillo and others, 1967; Torrico, 1966; Jacobson and others, 1969)
239	Inca and Toldos mines	21 06 40, 67 12 20	Argillized biotite-hornblende dacite porphyry intrudes Eocene Potoco sandstone. Inca mine developed on north to N. 30° W. trending, 10-40 cm wide veins, dipping steeply northeast along contact between intrusive and sandstone. Open pit mine at Toldos works a 440 by 350 m zone, about 100 m deep, of N. 35°-40° E. dip 55° northwest to vertical irregular branching veins in rhyodacite intrusive. Major veins exploited in colonial times were as wide as 1 m; veinlets worked today are 1-30 cm wide. Veins are composed of native silver, stromeyerite, galena, sphalerite, tetrahedrite, chalcopyrite, pyrargyrite, polybasite, pyrite, barite, siderite, hematite, quartz, magnetite, and calcite. Reserves in 1990 were 3 million tonnes at 120 g/t Ag. An additional 4 million tonnes were indicated. (Torrico, 1966; Vedia and Cortez, 1966c; Delgadillo, 1967; Gamarra, 1968; Jacobson and others, 1969; Avila-Salinas and others, 1975; this study)
		Comunidad Todos Santos Area	
367	Antonio mine (Antonia)	21 44 43, 67 12 59	An east-west alteration zone 2 km long hosting east-west trending 60°-70° north dipping, few centimeter wide, veins of stibnite, cervantite, galena, sphalerite, chalcopyrite, quartz, barite, and pyrite in bleached Eocene Potoco Formation sandstone intruded by biotite dacite. Altered zone also contains disseminated stibnite. (Servicio Geológico de Bolivia, 1971e; this study)
368	Almacén mine (Hornillos)	21 46 23, 67 08 36	Vein oriented N. 80° W. 30 cm wide and vein oriented N. 60° W. 40-90 cm wide of galena, sphalerite, quartz, pyrite, siderite, kaolinite, and manganese oxides cut altered dacite and andesite. Alteration minerals are hematite, sericite, calcite and pyrite. (Servicio Geológico de Bolivia, 1971v)
		San Antonio de Lípez District	
378	El Mestizo prospect	21 54 21, 66 57 11	Deposit consists of a 300 by 250 m stockwork zone, 100 m deep, and two peripheral mineralized shear zones: one 700 m long, 10 m wide, strikes N. 35° E., the other 900 m long, 20 m wide, strikes N. 75° E. Mineralized fractures in stockwork zone are oriented N. 30°-40° E. and N. 60°-80° E. and have a density of 5-30 per meter. Host rocks are Tertiary sandstone, mudstone, and carbonate intruded by Tertiary basalt and dacite. Alteration consists of a core zone of silicification with distal propylitic and argillic zones. Mineralization consists of stibnite, native gold and silver, sphalerite, covellite, bornite, quartz, pyrite, barite, and marcasite. Potential resources estimated in 1989 are 13 million tonnes ore in shear zones at 2 g/t Au and 40 to 75 million tonnes stockwork ore at 0.7 g/t Ag. (Pinto, 1989a; this study)
379	Nuevo Mundo mine	21 56 22, 66 54 00	Altered biotite dacite cut by N. 68°-80° E. vertical veins, as wide as 2 m, of chalcopyrite, tennantite, chalcocite, pyrite, calcite, barite, and quartz. Alteration minerals are sericite, kaolinite, chlorite, pyrite, and silica. Ore carries values in Pb, Zn, and Ag as well as Cu. (Servicio Geológico de Bolivia, 1971jj)

Table A–1. *Mines, prospects, and occurrences on the Altiplano and in the Cordillera Occidental, Bolivia*—Continued

380	Mesa de Plata mine (San Antonio, Blanca)	21 51 38, 6 51 53	Mesa de Plata mine develops four major east-west vein systems in a 3 km long zone of alteration and disseminated mineralization east of the town of San Antonio. Veins are as much as 650 m long, 10 m wide, and 170 m in vertical extent. Veins cut Tertiary pyroclastics and siltstones intruded by silicified and argillized biotite hornblende dacite. Veins have advanced argillic envelopes enclosed by jarosite-illitic mica-kaolinite and calcite-smectite-kaolinite zones. Intense sericitiztion found at depth. Veins are composed of cassiterite, galena, sphalerite, chalcopyrite, tetrahedrite, greenockite, aikinite, native silver, argentite, polybasite, pyrargyrite, stephanite, pyrite, arsenopyrite, magnetite, barite, quartz, rhodocrosite, marcasite, siderite, saponite, and ankerite. Potential resources estimated in 1988 are 1.58 million tonnes vein ore at 290 g/t Ag, 3.6% Pb, 3.7% Zn, and 0.3% Sn, and 14-30 million tonnes of disseminated ore of unknown grade. (Servicio Geológico de Bolivia, 1971nn; Rivas, 1971; Zambrana, 1971; Tavera, 1972; Sugaki and others, 1986; Flores, 1988; this study)
381	Machu Socavón mine	21 52 08, 66 49 55	Two vein systems and disseminated mineralization in altered Tertiary biotite-hornblende dacite. Alteration consists of a core of silicification flanked by inner sericite and outer argillic zones. Silicified zone is capped by opaline bodies within propylitized dacite. Veins are oriented N. 70° E. dip 80° northeast to vertical and N. 30° W., extend 170-200 m in length, and are 0.15-5 m wide. Disseminated ore consists of a stockwork of limonite-jarosite-alunite veinlets around bodies of opal in upper part of the deposit. Veins contain galena, sphalerite, barite, and quartz. Potential resources estimated in 1988 are 30-60 million tonnes of disseminated ore at less than 32 g/t Ag. (Servicio Geológico de Bolivia, 1971nn; Flores, 1988)
		Jaquegua Area	
382	Jaquegua mine	21 57 51, 66 45 18	East-west vertical veins, as wide as 1 m or more, cut silicified, kaolinized, and sericitized tuff of the Upper Quehua Formation intruded by Miocene biotite dacite over an area of more than 10 km^2. Veins contain galena, sphalerite, argentite, barite, and manganese oxides. (Servicio Geológico de Bolivia, 1971x; this study)
		Escala Area	
384	Escala mine (Crosca)	21 35 16, 66 51 57	Veins oriented N. 55°-70° W. and N. 70° E. cut an altered Miocene rhyolite porphyry stock 3.5 km in diameter. Veins are 10-50 cm wide and are found in two zones each as much as 4 m wide and 500 m long. Veins contain galena, sphalerite, chalcopyrite, chalcocite, tetrahedrite, jamesonite, semseyite, quartz, pyrite, marcasite, arsenopyrite, siderite, pyrrhotite, and chalcedony. Alteration consists of pervasive propylitization with silicification and kaolinization localized along a zone of fracturing and brecciation. (Servicio Geológico de Bolivia, 1971s; Sugaki and others, 1986; Alfaro, 1989; this study)
		Buena Vista Area	
392	Buena Vista mine (San Juan)	21 43 33, 66 37 50	Veins oriented N. 70°-75° W. dip 70°-75° northeast cut altered pyroclastics of the Upper Quehua Formation. Main vein is 700 m long and 10-80 cm wide, explored to 300 m depth. Unexposed altered dacite intersected in angled drill hole 190 m long. Alteration consists of sericitization and kaolinization with locally disseminated pyrite and Pb-Zn-Ag sulfides. Sericite has been dated at 11.1 m.y. Veins contain galena, sphalerite, chalcopyrite, electrum, argentite, pyrargyrite, jalpaite, famatinite, tetrahedrite-tennantite, bournonite, fizelyite, boulangerite, semseysite, stibnite, realgar, orpiment, miargyrite, pyrite, and quartz. Potential resources estimated in 1985 were 13 million tonnes at 1 g/t Au. (Requena, 1971; Servicio Geológico de Bolivia, 1971k; Sugaki and others, 1986; Ibañez and Medina, 1988; this study)
393	Leoplán mine	21 43 54, 66 37 58	N. 55°-60° W. vertical veins, 3-15 cm wide, cut lithic and lapilli tuff of the Eocene Potoco Formation. Veins contain galena, tetrahedrite, sphalerite, and stibnite. (Ibañez and Medina, 1988)

Table A–1. *Mines, prospects, and occurrences on the Altiplano and in the Cordillera Occidental, Bolivia*—Continued

394	Pulacayito mine	21 44 18, 66 36 19	Antimony-bearing vein in Upper Quehua Formation. (Ibañez and Medina, 1988)
		Cerro Morokho Area	
395	Mulato mine	21 49 20, 66 34 00	Altered east-west structures as wide as 30 m in Upper Quehua Formation cut by 1-3 cm wide veins oriented N. 60° W. dip 80° northeast and oriented N. 30° W. Vein systems are as long as 2 km. Alteration zones composed of kaolin and silica with disseminated pyrite-chalcopyrite-tetrahedrite. Veins are composed of galena, pyrargyrite, tetrahedrite, sphalerite, chalcopyrite, bismuthinite, pavonite, barite, pyrite, quartz, and marcasite. (Requena, 1971; Servicio Geológico de Bolivia, 1971ii)
396	Morokho mine (Himalaya)	21 50 34, 66 35 04	Silicified and kaolinized biotite dacite cut by 10-70 cm wide veins oriented N. 60° W. to east-west, dipping 70°-90° southwest, explored to 150 m depth. Veins contain galena, sphalerite, tetrahedrite, teallite, pyrargyrite, miargyrite, native silver, cassiterite, quartz, pyrite, marcasite, manganocalcite, and ankerite. Also, a sericitized zone, 4 km^2 in area, with 5-50 fractures per meter filled by goethite-jarosite veinlets. This stockwork zone carries values in Ag, As, Sb, and Sn. Potential resources estimated in 1989 were 48.25 million tonnes at an unknown grade. (Requena, 1971; Servicio Geológico de Bolivia, 1971u; Corporación Minera de Bolivia, 1990; this study)
		Santa Isabel Area	
398	Santa Isabel mine (Candelaria)	21 37 40, 66 30 07	Fracture fillings and veins cutting pervasively propylitized Tertiary rhyolite porphyry in a brecciated zone 800 m in diameter and 500 m deep. Argillic and sericitic alteration localized along zones of fracturing. Veins are 20-180 cm wide and contain galena, sphalerite, chalcopyrite, tetrahedrite-tennantite, bournonite, jamesonite, semseyite, pyrargyrite, cassiterite, stannite, franckeite, fizelyite, petzite, native gold, quartz, calcite, pyrite, marcasite, and arsenopyrite. Rhyolite is sericitized and chloritized and carries disseminated pyrite. At about 4,700 m altitude cassiterite-silver mineral-bearing oxide zone passes into pyrite-sphalerite-galena sulfide zone. Just south of Santa Isabel is a zone of intense argillic alteration with veins trending N. 80° W. dipping 70° south, 0.2 m wide, associated with disseminated pyrite, chalcopyrite, and chalcocite. Potential resources in 1987 estimated at 691,000 t ore at 155-494 g/t Ag, 1.8-6.7% Pb, as much as 4.6% Zn, 0.3-1.0% Sn, and about 3 g/t Au. (Caro, 1964a, 1964b; Sugaki and others, 1986; Segurola and others, 1987; this study)
400	Mercedes mine (Goya I, Santa Rosa)	21 38 41, 66 30 22	Altered dacite intrudes basalt of the Rondal Formation and is cut by veins as wide as 60 cm trending N. 40°-80° E. and N. 20°-80° W. Alteration consists of argillization in a central zone of intense fracturing and a shell of less fractured, chloritized rock, centered on a dacite intrusive. Veins contain galena, sphalerite, native silver, stibnite, Sn oxide, chalcocite, chalcopyrite, quartz, and pyrite. (Servicio Geológico de Bolivia, 1971ff; Valencia, 1973; Medina and Ibañez, 1988b; this study)
		Cerro Bonete District	
401	Barrahuayco mine (Huarrawaico)	21 43 12, 66 28 34	Altered Miocene dacite cut by 8-70 cm wide veins oriented N. 40°-70° W. dipping 70°-80° southwest and a stockwork zone 100 m wide, oriented N. 40°-60° W. and east-west with 8 fractures per square meter. Veins contain quartz, pyrite, galena, chalcopyrite, and probably sphalerite; stockwork fractures are filled by iron oxides. Silicification and argillization occur in the central, stockwork zone, and propylitization outside that zone. Potential resources estimated in 1988 at 10-16 million tonnes at an unknown grade. (Servicio Geológico de Bolivia, 1971g; Medina and Ibañez, 1988a)

Table A–1. *Mines, prospects, and occurrences on the Altiplano and in the Cordillera Occidental, Bolivia*—Continued

402	La Moza and Lipeña mines	21 44 05, 66 27 25	Two mines work veins along the same east-west structure cutting altered Miocene biotite dacite. Host rocks are sericitized and have a core zone of silicification that grades out into argillization and propylitization. A main N. 88° E. trending dip 63° south 110 cm wide structure controls a stockwork zone of veinlets as wide as 0.1 m oriented N. 35°-80° W. 40°-70° southwest dip with a fracture density of 10 per square meter. Larger, 1-20 cm wide, veins strike N. 11°-58° E. and N. 36°-49° W. Veinlets in stockwork zone contain quartz, barite, pyrite, galena, chalcopyrite, bismuthinite, and probably sphalerite and Sn-bearing minerals. Potential resources estimated in 1988 were 54-150 million tonnes at an unknown grade. (Servicio Geológico de Bolivia, 1971bb; Medina and Ibañez, 1988a; this study)
403	Bonete mine	21 45 13, 66 28 14	Veins oriented N. 23°-80° W. cut kaolinized Miocene dacite. Veins contain chalcopyrite, bismuthinite, galena, tennantite, bornite, quartz, and siderite. (Servicio Geológico de Bolivia, 1971j; Jiménez and Núñez, 1988)
404	Santa Rosa mine	21 47 23, 66 29 38	Brecciated and altered Miocene dacite cut by veins trending N. 55° W. dipping southwest 14 cm wide and veins trending N. 76° E. dipping 84° northwest 0.1-1.6 m wide. Alteration is sericitic and propylitic. Veins contain galena, spahlerite, tetrahedrite, malachite, quartz, barite, and pyrite. Estimated production was 8,800 t. Dumps contain 13,000-14,000 m^3 of as much as 250 g/t Ag, 0.8-7.2% Pb tailings. (Caro, 1964b; Servicio Geológico de Bolivia, 1971qq; Valencia, 1973; Sugaki and others, 1986; Jiménez and Núñez, 1988; this study)
405	Rosario II mine	21 49 00, 66 29 00	Quartz-galena veins cut silicified and propylitized Miocene dacite and rhyodacite. (Valencia, 1973; Jiménez and Núñez, 1988)
406	Pampa Guadalupe mine	21 49 00, 66 29 00	Silicified Miocene dacite to rhyodacite cut by veins of galena, chrysocolla, colloidal quartz, and siderite. (Valencia, 1973; Jiménez and Núñez, 1988)
407	Esperanza and Segunda Esperanza mines	21 48 42, 66 29 22	Two mines work two N. 50° W. trending veins, one (Esperanza) dips 80° W. and is 5-50 cm wide, the other (Segunda Esperanza) dips 88° E. and is 83 cm wide. Veins cut kaolinized Miocene dacite and contain galena (Esperanza) or iron oxides, limonite, and clay (Segunda Esperanza). (Cortez and Kuronuma, 1969).
408	Pucasalle mine (La Colorada)	21 48 41, 66 26 46	Altered Miocene biotite dacite to rhyodacite cut by a N. 78° E. trending 58°-85° northwest dipping vein 1 m wide. Vein contains galena, sphalerite, pyrite, and quartz. Host rock is silicified, chloritized, sericitized, and has disseminated pyrite. Estimated production is 7,000 t. (Servicio Geológico de Bolivia, 1971kk; Valencia, 1973; Jiménez and Núñez, 1988; this study)
409	Los Colorados de Bolivia mine (Rosario I)	21 49 06, 66 27 06	Altered Miocene dacite to rhyodacite cut by east-west veins dipping 70°-80° N., 0.01-1.42 m wide. Veins contain galena, sphalerite, benjaminite, bismuthinite, pyrite, and quartz. Propylitized host rock carries disseminated pyrite. (Vedia 1960a; Servicio Geológico de Bolivia, 1971p; Valencia, 1973; Jiménez and Núñez, 1988; this study)
410	La Salvadora mine	21 48 22, 66 26 43	Altered brecciated Miocene biotite dacite cut by N. 60°-80° E. and N. 50°-70° W. striking, 50° south to vertical dipping veins, 5-25 cm wide. Veins contain pavonite, aikenite, bismuthinite, chalcopyrite, galena, sphalerite, tetrahedrite, pyrargyrite, quartz, ankerite, and siderite. Alterations is propylitic, sericitic, and silicic. (Ahlfeld, 1954; Vedia and Cortez, 1966b; Valencia, 1973; Jiménez and Núñez, 1988)
411	Bolívar mine	21 47 47, 66 27 04	Propylitized and brecciated Miocene dacite cut by a vertical east-west veins 10-25 cm wide. Veins contain pavonite, aikinite, benjaminite, bismuthinite, chalcopyrite, quartz, ankerite, siderite, and pyrite. (Ahlfeld, 1954; Rowe, 1961; Valencia, 1973; Mendoza, 1977; Jiménez and Núñez, 1988; this study)
412	Dos Martillos and San José mines	21 47 05, 66 28 11	N. 70° W. (San José mine) and N. 40° W. (Dos Martillos mine) trending galena-bearing veins cut altered Miocene dacite. (Jiménez and Núñez, 1988)
413	Herrería mine (10 de Diciembre)	21 46 34, 66 28 08	Altered Miocene dacite porphyry cut by east-west 65°-75° south dipping veins. Alteration minerals are sericite, kaolinite, and carbonate. Veins contain galena, sphalerite, chalcopyrite, cassiterite, bismuthenite, and pyrite. (Vedia, 1960b; Jiménez and Núñez, 1988)

Table A–1. *Mines, prospects, and occurrences on the Altiplano and in the Cordillera Occidental, Bolivia*—Continued

414	San Julian mine	21 45 21, 66 26 27	East-west quartz-galena-iron oxide vein, 0.2-1.2 m wide, cuts silicified and sericitized Miocene biotite dacite. (Servicio Geológico de Bolivia, 1971pp; Jiménez and Núñez, 1988)
		Esmoraca Area	
420	Lipina mine	21 39 20, 66 19 50	Mine in altered Miocene dacite located on Pueblo Viejo (6328-III) 1:50,000 scale topographic map.
421	San Martín mine	21 40 46, 66 19 59	Bi mine in altered Miocene dacite located on La Cienaga (6328-IV) 1:50,000 scale topographic map.
422	Farellones mine (Khasayoj)	21 39 10, 66 17 10	Hematite-pyrite, Bi-Sn-W-bearing veins hosted by propylitized and sericitized Miocene dacite. (Pinto, 1989d)
423	Aguas Calientes, Conchita, and Germania mines	21 40 25, 66 17 15	Propylitized and sericitized Miocene dacite cut by east-west 70°-80° south dipping en echelon veins, each as much as 200 m long and 60 cm wide. Veins contain native gold, chalcopyrite, bismuthinite, chalcocite, bornite, enargite, bismutite, matildite, wolframite, and pyrite. (Cortez, 1966; Merida, 1969; Pinto, 1989d)
424	Central and Pueblo Viejo mines	21 40 10, 66 16 35	East-west veins, more than 100 m deep, in propylitized and sericitized Miocene dacite and underlying Tertiary sandstone of quartz, pyrite, tourmaline, hematite, wolframite, cassiterite, bismuthinite, specularite, chalcocite, bornite, enargite, sphalerite, and chalcopyrite. (Pinto, 1989d; this study)
425	Azulejos mine	21 40 41, 66 17 05	Two east-west veins, 15-30 cm wide, several hundred meters long, of pyrite, chalcopyrite, bismuthinite, and gold hosted by propylitized and sericitized Miocene dacite. (Pinto, 1989d)
		San Vicente District	
432	Monserrat mine	21 13 40, 66 18 57	Altered Tertiary conglomerate of the San Vicente Formation hosts major east-west vein structures intersected by smaller N. 80° E. trending 40°-70° northwest dipping and N. 60° W. 60° southwest dipping vein sets. Vein intersections control stockwork zones of veinlets oriented N. 80° E. 80°-90° north or south dipping, 1-3 cm wide, in densities of 5-10 per linear meter. Major veins are as much as 300 m long and 10-50 cm wide. Veins have alteration halos of silicification as wide as 2 m. Mineralized zone is 1.7 by 0.4 km in area and 300 m thick. Alteration is zoned from top to bottom from silicification to argillization to sericitization (encountered in drilling). Veins are composed of galena, pyrargyrite, tetrahedrite, boulangerite, sphalerite, chalcopyrite, cassiterite, stannite, bournonite, pyrite, marcasite, and quartz. Oxidized cap of jarosite, iron oxides, Pb, Ag, Bi, and Sb sulfosalts is found in the upper 40 m of the deposit. Deposit is zoned from central Sn to distal Pb-Ag. Potential resources in 1987 estimated at 17 million tonnes at about 0.3 g/t Au and 150 g/t Ag. (Marsh and Robinson, 1966; Maldonado, 1969; Japan International Cooperation Agency, 1977, 1978, 1979; Rico, 1978; Pinto, 1989b, United Nations Development Program, 1989b)
433	San Vicente mine (Tajos, San Francisco, Confianza)	21 16 17, 66 19 05	Tertiary conglomerate of the San Vicente Formation intruded by 13.4 m.y. dacite dikes along east-west fracture zones. East-west veins dipping south follow same fracture set in an area 4.6 by 2.8 km explored to 600 m depth. Veins are 100-200 m apart, 150-1,300 m long, and 0.1-1.5 m wide. Vein intersections have ore shoots as wide as 15 m. Silicification halos around veins extend out from 2 to 30 m, and are enveloped in turn by a pyrite-sericite zone that extends an additional 4-12 m. Veins contain galena, tetrahedrite, sphalerite, stromeyerite, galenobismuthinite, chalcocite, covellite, chalcopyrite, stannite, cassiterite, electrum, luzonite, roquesite, aikinite, pyrargyrite, bornite, jamesonite, freiburgite, quartz, pyrite, marcasite, barite, siderite, and phosphophyllite. Potential resources in 1988 were estimated at 20 million tonnes at an unknown grade. Measured reserves in 1989 were 995,000 t at 8.42% Zn and 397 g/t Ag plus 868,000 t low grade ore at 2.85% Zn and 156 g/t Ag. Ore also carries values in Pb (0.1-2%), Cu (0.1-0.8%), and Sn (0.01-1.4%). (Ahlfeld, 1954; Marsh and Robertson, 1966; Maldonado, 1969; Gutiérrez, 1975; Japan International Cooperation Agency, 1977, 1978, 1979, 1988, 1989; Rico, 1978; Pinto, 1989c; this study)

Table A–1. *Mines, prospects, and occurrences on the Altiplano and in the Cordillera Occidental, Bolivia*—Continued

		Borate Deposits	
162	Laguna Sacabaya deposit	18 38 40, 68 57 45	Ulexite, in the form of cottonballs, found in the southern part of the salar. (This study)
183	Salar de Coipasa deposit	19 05 23, 68 18 27	Ulexite occurs with clay and gypsum where ephemeral streams flow into the salar. (Ballivian and Risacher, 1981)
184	Salar de Coipasa deposit	19 12 22, 68 21 35	Ulexite occurs with clay and gypsum where ephemeral streams flow into the salar. (Ballivian and Risacher, 1981)
213	Laqueca deposit	20 14 23, 68 26 57	Borate deposit 1 km^2 in area and 30 cm thick. (Cadima and Lafuente, 1969; Ballivian and Risacher, 1981)
215	Istma deposit (Isma)	20 25 52, 68 38 29	Borate deposit 4 km^2 in area and 30-40 cm thick. (Cadima and Lafuente, 1969; Ballivian and Risacher, 1981)
228	Llipi Llipi deposit	20 46 13, 67 24 18	Lenses of ulexite in a fluvial-deltaic complex on southeast edge of Salar de Uyuni. Individual lenses are 50-300 m in diameter and 5-50 cm thick. Deposit is 0.7 km^2 in area, 30 cm thick. (Ballivian and Risacher, 1981)
230	Río Grande deposit	20 43 36, 67 15 01	Lenses of ulexite in a fluvial-deltaic complex on southeast edge of Salar de Uyuni. Individual lenses are 50-300 m in diameter and 5-50 cm thick. Deposit is as thisk as 60 cm. Potential resources estimated in 1969 were 3.7 million tonnes at 59% borax. (Cadima and Lafuente, 1969; Ballivian and Risacher, 1981)
249	Pajoncha deposit	20 52 33, 68 16 28	Ulexite deposit 5 km^2 in area with average thickness of 5 cm. Potential resources estimated in 1981 as 300,000 t of ulexite. (Cadima and Lafuente, 1969; Ballivian and Risacher, 1981)
253	La Carrillana deposit	21 08 43, 68 04 55	Deposit of ulexite 1 km^2 in area and 30 cm thick. (Ballivian and Risacher, 1981)
266	Laguna Hedionda Norte occurrence	21 33 40, 68 02 49	Ulexite occurrence. (Ballivian and Risacher, 1981)
267	Laguna Chiar Kkota occurrence	21 35 00, 68 04 00	Ulexite occurrence. (Ballivian and Risacher, 1981)
275	Laguna Hedionda Norte occurrence	21 37 00, 68 04 00	Ulexite occurrence. (Ballivian and Risacher, 1981)
281	Lagunas Pastos Grandes deposit	21 40 22, 67 47 12	Zone of ulexite in south-central part of a saline ephemeral lake. Potential resource estimated in 1981 at 1.2 million tonnes ulexite. (Ballivian and Risacher, 1981)
288	Laguna Capina Sur deposit	21 55 29, 67 34 19	Ulexite found in a clay and lime mud layer as thick as 60 cm. Estimated potential resources in 1981 were 900,000 t of ulexite. (Ballivian and Risacher, 1981; this study)
292	Laguna Colorada occurrence	22 13 00, 67 49 00	Large floes of ulexite 1-3 m thick near western shore of lake. (Ballivian and Risacher, 1981; this study)
305	Boratera de Challviri deposits	22 28 00, 67 35 00	Borax found in lenses of variable thickness in lake muds. Colemanite and ulexite reported. Potential resources estimated in 1981 at 3 million tonnes at 61% ulexite. (Ballivian and Risacher, 1981; this study)
307	Boratera de Challviri occurrence	22 29 00, 67 33 00	Ulexite occurrence. (Ballivian and Risacher, 1981)
309	Boratera de Challviri occurrence	22 32 30, 67 35 00	Ulexite and gypsum occurrence. (Ballivian and Risacher, 1981)
310	Boratera de Challviri occurrence	22 34 00, 67 34 00	Ulexite and gypsum occurrence. (Ballivian and Risacher, 1981)
311	Boratera de Challviri occurrence	22 34 30, 67 32 30	Ulexite and colemanite found 10-27 cm below surface of salt crust. (Ballivian and Risacher, 1981; this study)
348	Laguna Mama Khumu occurrence	22 16 30, 67 05 00	Ulexite and native sulfer in layers 30-80 cm thick below a 2 cm thick halite crust. (This study)
		Clay Deposits	
13	Santa Rosa mine in Quimsa Chata district	16 38 27, 68 38 47	Hydrothermal kaolinite in argillized Tiahuanacu sandstone xenoliths in Miocene dacite. (This study)
56	Caracollo deposit	17 39 53, 67 12 37	Lacustrine clays found in a 30 km northwest trending belt between Caracollo and Oruro. Clay consists of illite, is nonswelling, and is used for the manufacture of bricks. Estimated resources in 1982 were 2 million tonnes of clay. (Montes de Oca, 1982; this study)

Table A–1. *Mines, prospects, and occurrences on the Altiplano and in the Cordillera Occidental, Bolivia*—Continued

89	La Encontrada deposit	17 34 00, 68 14 00	Beds of bentonized Tertiary tuff on west flank of a northwest trending anticline near La Encontrada copper mine. Bentonite is 85-99% montmorillonite, remainder is quartz, biotite, and iron oxides. (Guerra and Ascarrunz, 1964a)
		Dimension Stone Deposits	
35	Comanche quarry	16 57 43, 68 25 12	Early Miocene (17.9 m.y.) Miriquiri andesite quarried as a decorative stone. (Ahlfeld and Schneider-Scherbina, 1964; Avila-Salinas, 1973; Redwood and MacIntyre, 1989; this study)
158	Volcán Quemado quarry	18 37 24, 68 45 45	Light-pinkish-gray welded tuff at western base of volcano has been quarried for dimension stone. Tuff breaks with a rough conchidal fracture and is deeply weathered. (This study)
		Epithermal Manganese Deposits	
209	Granada mine	20 07 22, 68 15 56	North-south vertical veins of psilomelane, pyrolusite, limonite, hematite, and chalcedony in manganese oxide cemented Tertiary rhyolite-rhyodacite breccia and Quaternary stromatolitic limestone. Breccia includes fragments of chalcedony and altered volcanics. Veins are 150 m long and 50-150 cm deep. (Donoso, 1959; this study)
251	Negra mine	21 02 27, 68 17 51	N. 55° W. trending veins, 2-90 cm wide, of Mn and iron oxides cut Pliocene vitric tuff. Values as high as 20 g/t Ag in vein samples. (Sanjinés, 1968a)
		Epithermal Quartz Alunite Vein Deposits	
48	Laurani mine	17 22 51, 67 46 30	Fractured, altered, and eroded stratovolcano cut by N. 15° E. trending 80° southeast dipping, N. 45° E. 70° northwest dipping, and N. 10° E. 75° northwest dipping vein sets. Host rocks are late Miocene (8.4 m.y.) andesite, dacite, rhyolite, and pyroclastics. Mineralized area is 2 by 1 km; individual veins are 0.3-1 m wide. Deposit is zoned to the northeast with a pyrite-Au-enargite core, enargite-tennantite middle zone, and sphalerite-galena-Ag outer zone. Alteration consists of intense propylitization, silicification and argillization. Veins are composed of enargite, tennantite-freibergite, luzonite, electrum, chalcopyrite, bornite, famatinite, stibnoluzonite, galena, sphalerite, jordanite, stephanite, polybasite, miargyrite, proustite-pyrargyrite, tetrahedrite, bournonite, chalcostibnite, argentite, cassiterite, stannite, patrinite, bismuthenite, matildite, rickardite, umangite, calaverite, barite, siderite, quartz, pyrite, sericite, and arsenopyrite. Reserves in 1990 were 2 million tonnes at 2.5 g/t Au, 220 g/t Ag, and 1.0% Cu. (Schneider-Scherbina, 1961a; Ahlfeld and Schneider-Scherbina, 1964; Redwood and MacIntyre, 1989; this study)
		Fumarolic Sulfur Deposits	
124	Cerro Huaricuna occurrence	17 14 30, 69 25 00	Occurrence of native sulfur. (Ahlfeld and Schneider-Scherbina, 1964)
129	Cerro Serkhe occurrence	17 21 13, 69 21 51	Occurrence of native sulfur. (Ahlfeld and Schneider-Scherbina, 1964)
145	Cerro Suni Khaua occurrence	17 50 02, 68 58 37	Occurrence of native sulfur. (McVey, 1989)
146	Cerro Anallajchi occurrence	17 55 22, 68 53 44	Occurrence of native sulfur. (Empresa Minera Illimani, 1989)
152	Nevados Payachata occurrence	18 08 34, 69 07 48	Occurrence of native sulfur. (McVey, 1989)
153	Cerro Parinacota occurrence	18 09 22, 69 08 01	Occurrence of native sulfur. (McVey, 1989)
156	Nevado Quimsa Chata deposit	18 23 30, 69 02 30	Deposit of native sulfur reported to contain 30 million tonnes at 36% S. (Rodríguez and others, 1976)
163	Cerro Poquentica occurrence	18 44 48, 68 58 54	Occurrence of native sulfur. (McVey, 1989)
172	Cerro Curumaya occurrence	19 00 30, 68 50 00	Occurrence of native sulfur. (McVey, 1989)

Table A–1. *Mines, prospects, and occurrences on the Altiplano and in the Cordillera Occidental, Bolivia*—Continued

176	Cerro Cumi occurrence	19 05 24, 68 46 03	Occurrence of native sulfur. (McVey, 1989)
178	10 de Noviembre mine (Cerro Cabaraya)	19 08 02, 68 41 45	Native sulfur disseminated in tuff and altered basalt; in tuff grade 30-40% S, in basalt 10% S. Total tonnage reported to be 50 million tonnes. (Vargas, 1968; Rodríguez and others, 1976)
179	Cerro Saca Sacani prospect	19 08 00, 68 37 45	Native sulfur disseminated in altered andesite. Alteration types are argillic, alunitic, and propylitic. (This study)
181	Victoria prospect	19 08 08, 68 31 35	Occurrence of native sulfur on Cerro Tata Sabaya, an altered stratvolcano. (McVey, 1989)
198	Cerro Tunupa deposit	19 49 28, 67 38 45	Native sulfur and gypsum occur as pockets and nodules in volcanic ash. Deposit is 400 m thick. Resources reported as 200 million tonnes at 46-83% S (Sanjinés, 1968a; Rodríguez and others, 1976)
199	Volcán Sillillica occurrence	19 43 26, 68 40 31	Occurrence of native sulfur. (McVey, 1989)
200	Nevado Candelaria occurrence	19 44 46, 68 40 45	Occurrence of native sulfur. (McVey, 1989)
201	Cordillera Sillajguay deposit	19 45 27, 68 40 16	Pockets and veinlets of native sulfur in volcanic ash. Potential resources of 1.2 million tonnes at 69.5% S. (Ahlfeld and Schneider-Scherbina, 1964)
202	Cerro Iru Putuncu occurrence	19 52 53, 68 32 19	Occurrence of native sulfur. (McVey, 1989)
206	Cerro Caltama occurrence	20 03 33, 68 19 04	Occurrence of native sulfur. (McVey, 1989)
208	Cerro Tankhani occurrence	20 07 19, 68 25 38	Occurrence of native sulfur. (McVey, 1989)
216	San Pablo de Napa mine	20 31 04, 68 35 45	Impregnations of native sulfur in Pliocene volcanic ash. Deposit is flat lying, 1.3 by 0.6 km in area and more than 0.6 m thick. Potential resources are 20 million tonnes at about 40% S. (Ahlfeld and Schneider-Scherbina, 1964; Echenique, 1972)
217	Victoria mine (Santa Victoria)	20 33 12, 68 31 54	Manto of disseminated native sulfur in Pliocene volcanic ash 3-5 m thick, capped by basalt. (Ahlfeld and Schneider-Scherbina, 1964)
218	Beatriz, Concepción, El Desierto, and María Eugenia mines (Cerro Cayte)	20 32 14, 68 31 46	Mines work the same manto of disseminated sulfur in Pliocene volcanic ash in an area of active fumaroles. Manto is 0.5-5 m thick and dips 15°-20° north. Concepción mine had a reserve of 320,000 t at 59% S and El Desierto had 235,000 t at 56% S. (Ahlfeld and Schneider-Scherbina, 1964)
221	Milluri mine (Volcán Ocaña)	20 37 01, 68 25 41	Manto of disseminated native sulfur in Pliocene volcanic ash capped by a lava flow. Manto is 500 m long, 150 m wide, and 6 m thick; reserves of 80,000 t at 60% S. (Ahlfeld and Schneider-Scherbina, 1964)
222	Cerro Cono occurrence	20 38 30, 68 25 30	Occurrence of native sulfur. (McVey, 1989)
241	Volcán Iru Putuncu occurrence	20 43 39, 68 32 58	Native sulfur deposits associated with active fumaroles. Most sulfur mineralization is on Chilean side of the border. (Ahlfeld and Schneider-Scherbina, 1964)
243	Salar de la Laguna deposit	20 51 15, 68 29 00	Native sulfur deposit reported to contain 200 million tonnes at 55% S. (Rodríguez and others, 1976)
248	Candelaria, Carlota and Tres Rayas mines (Volcán Olca)	20 56 27, 68 28 18	Native sulfur deposits associated with active fumaroles. Mineralized zone 25 by 75 m in area with 30-50% S disseminated in basaltic andesite capped by limonite-hematite-manganese oxide-bearing agglomerate. Potential resources estimated in 1964 at 200,000 t at 55% S. (Ahlfeld and Schneider-Scherbina, 1964; this study)
255	Cerro Chiguana occurrence	21 06 57, 67 51 32	Occurrence of native sulfur. (McVey, 1989)
256	Santa Rosa mine (Volcán Ollagüe)	21 18 09, 68 10 19	Deposits of native sulfur on southeast flank of Volcán Ollagüe. Most sulfur found on Chilean side of border where fumarolic activity is still underway. Resources estimated as 50 million tonnes ore. (Rodríguez and others, 1976)
258	Cerro Tomasamil occurrence	21 17 30, 67 57 20	Occurrence of native sulfur. (McVey, 1989)

Table A–1. *Mines, prospects, and occurrences on the Altiplano and in the Cordillera Occidental, Bolivia*—Continued

261	El Triunfo, Luz Marina and Victoria mines (Cerro Cañapa)	21 29 30, 68 05 42	El Triunfo and Victoria mines work impregnations, veinlets, and pockets of native sulfur as mantos in volcanic ash. Luz Marina mine works a hematite cemented breccia of blocks of native sulfur and native sulfur disseminated in talus. Tuffs are capped by andesite. Host rocks are altered with sericite-hematite-calcite. Reserves at Luz Marina in 1968 were 10.4 million tonnes at 30% S, and at Victoria in 1967, 232,000 t at 55-60% S. (Ponce, 1967; Ballón and Vargas, 1968; Santiesteban, 1972)
264	Cerro Caquella occurrence	21 28 27, 67 56 05	Disseminations, pockets, veinlets, and mantos of native sulfur and manganese oxides in volcanic ash. Deposit is 5 ha in area and at least 1 m thick. Resources estimated at 50 million tonnes at an unknown grade. (Rodríguez and others, 1976)
277	Cerro Ascotán Ramaditas occurrence	21 39 50, 68 07 01	Occurrence of native sulfur. (Rodríguez and others, 1976; McVey, 1989)
278	Corina mine (Cerro Tapaquillcha)	21 36 17, 67 57 30	Stockwork veinlets of native sulfur in fractured and altered biotite dacite and andesite. Mantos of impregnations of native sulfur and gypsum and native sulfur flows in volcanic ash. Alteration consists of chalcedony and illite. Reserves in 1967 were 4.4 million tonnes at 40% S. (Flores, 1968; Parra, 1968; Alvarez and Salazar, 1969)
282	Cerro Cachi Laguna occurrence	21 39 47, 67 53 32	Zone of argillized Pliocene biotite-hornblende dacite 6 km^2 in area with sparsely disseminated native sulfur. (Rodríguez and others, 1976; this study)
289	Cahuana mine (Cerro Cabaña or Cahuana, El Portal)	22 03 33, 67 57 39	Veinlets and impregnations of native sulfur in altered and fractured tuff capped by dacite or andesite flows. Reserves in 1968 were 4.8 million tonnes at 10.8% S. (Sanjinés and others, 1968a)
297	Cerro Pabellón occurrence	22 19 37, 67 45 33	Occurrence of native sulfur. (Rodríguez and others, 1976; McVey, 1989)
298	Rosario del Rey mine	22 15 00, 67 33 00	Altered vitric tuff with about 4% disseminated native sulfur. Local high grade zones contain as much as 90% S. Resources in 1968 were 5.1 million tonnes at 51% S. (Cordero and others, 1968)
299	Bienvenida mine	22 16 38, 67 33 10	Native sulfur disseminated in altered tuff and lava flows. (Cordero and Ballivian, 1969)
300	Cerro Tocor Puri occurrence	22 24 56, 67 53 46	Occurrence of native sulfur. (Rodríguez and others, 1976; McVey, 1989)
301	Cerro Michina occurrence	22 26 00, 67 53 30	Occurrence of native sulfur. (Rodríguez and others, 1976; McVey, 1989)
312	Carmen mine	22 35 14, 67 49 41	Native sulfur deposit. Carmén, Rosita, San Vicente, and Juanita mines reported to contain a total of 200 million tonnes ore. (Rodríguez and others, 1976; McVey, 1989)
313	Rosita mine	22 35 14, 67 49 11	Deposit of native sulfur. (Rodríguez and others, 1976; McVey, 1989)
314	San Vicente mine	22 35 51, 67 51 09	Deposit of native sulfur. (Rodríguez and others, 1976; McVey, 1989)
316	Juanita mine	22 36 04, 67 47 35	Deposit of native sulfur. (Rodríguez and others, 1976; McVey, 1989)
318	Cerro Sairecabur occurrence	22 42 20, 67 53 03	Occurrence of native sulfur. (Rodríguez and others, 1976; McVey, 1989)
319	Wilma and Nelly prospects	22 42 49, 67 44 17	Native sulfur disseminated in volcanic rock over an area of 185,000 m^2. Resources estimated at 50 million tonnes ore. (Ballivian and Cordero, 1969; Rodríguez and others, 1976)
323	Susana mine (Nelson, Pampa)	22 45 21, 67 34 23	Disseminated native sulfur and pockets of native sulfur in altered pyroclastics capped by a kaolinized dacite flow. Potential resources estimated in 1990 were 320 million tonnes at 18-54% S. (Ballivian and Barrios, 1969)
324	Volcán Llicancahur occurrence	22 49 49, 67 52 33	Occurrence of native sulfur. (Rodríguez and others, 1976; McVey, 1989)
325	Volcán Juriques occurrence	22 50 29, 67 49 12	Occurrence of native sulfur. (Rodríguez and others, 1976; McVey, 1989)
330	Cerro Zapaleri occurrence	22 48 10, 67 11 08	Occurrence of native sulfur. (Rodríguez and others, 1976; McVey, 1989)
339	Cerro Piedras Grandes occurrence	22 30 56, 67 02 33	Occurrence of native sulfur. (Rodríguez and others, 1976; McVey, 1989)

Table A–1. *Mines, prospects, and occurrences on the Altiplano and in the Cordillera Occidental, Bolivia*—Continued

340	Dulce Nombre mine	22 32 50, 67 01 49	Deposit of native sulfur. (Rodríguez and others, 1976)
345	Uturuncu mine	22 14 50, 67 10 53	Native sulfur and minor realgar disseminated in volcanic ash. Resources estimated at 50 million tonnes ore. (Ahlfeld and Schneider-Scherbina, 1964; Rodríguez and others, 1976)
354	Cerro Soniquera occurrence	22 00 08, 67 13 10	Occurrence of native sulfur. (del Carpio, 1972; Ploskonka, 1975)
		Gypsum Beds and Diapir Deposits	
40	Unknown	17 02 00, 68 15 20	Gypsum deposit. (McVey, 1989)
66	Unknown	17 12 21, 68 29 50	Gypsum deposit. (McVey, 1989)
97	Crucero mine	17 47 43, 68 16 35	Deposit of bedded gypsum in Tertiary Totora Formation 22 km long and 15 m thick. (Mitchell, 1968)
		Lacustrine Diatomite Deposits	
231	Vito occurrence	20 52 30, 67 00 00	Diatomite occurrence. (This study)
293	Laguna Colorada occurrence	22 14 15, 67 47 30	Diatomite occurrence. (This study)
295	Laguna Colorada occurrence	22 12 00, 67 43 00	Diatomite occurrence. (This study)
320	Laguna Verde occurrence	22 47 15, 67 48 45	Diatomite occurrence. (This study)
		Perlite Deposits	
174	Todos Santos deposit	19 00 48, 68 43 19	Obsidian vitrophyre margin to a Tertiary rhyolite dome. (Anonymous, 1988)
		Precious Metal Placer Deposits	
55	Aysa Kkollu placers	17 44 16, 67 16 30	Placer Au in Pleistocene glacial moraine. (Lezeca, 1989)
341	Peña Barrosa placers	22 12 04, 67 21 22	Au placers found on a tributary to Río Quetena. Gold may be derived from low sulfide Au-quartz veins that may occur in nearby Silurian clastics. (Rodríguez and others, 1976)
385	Río San Pablo placer	21 32 45, 66 50 15	Reported placer occurrence with gold as much as 2 mm in size. (This study)
387	Viladel placer (San Antonio)	21 45 23, 66 50 23	Placer gold found in ancient terraces in folded Ordovician quartzite and slate. Veinlets of quartz-jarosite found nearby. (United Nations Development Program, 1989b; Corporación Minera de Bolivia, 1990)
389	Marte placer	21 51 10, 66 43 49	Placer gold found in Recent fluvial channels. 95% of heavy mineral fraction is ilmenite, magnetite and hematite. Sphene, leuxocene, spinel, zircon, topaz, hornblende and goethite also found. Values as high as 1.3 g/m^3 Au reported. (Servicio Geológico de Bolivia, 1971ee)
399	Río Santa Isabel placer	21 37 00, 66 29 50	Placer gold and cassiterite in Recent alluvium. (Ahlfeld, 1954; this study)
		Pumice and Volcanic Ash Deposits	
159	Volcán Quemado occurrence	18 37 24, 68 45 45	Surface slopes near top of the volcano are covered with loose pumice and volcanic ash. (This study)
		Saline and Alkaline Lake Brine Deposits	
161	Laguna Sacabaya deposit	18 38 40, 68 57 45	Alkaline brine lake. Brines contain 27-41 ppm B, 6-11 ppm Li, 4 ppm Sr, and 10 ppb Cd. (This study)
186	Salar de Coipasa deposit	19 22 00, 68 08 00	Salt crust saturated with Li-K-B chloride brine. Analyses: 1.223-1.247 g/cm^3, pH 6.97-7.37, 251-524 mg/kg Li, 7.14-18.3 g/kg K, 497-1,300 mg/kg B, 8.99-21.8 g/kg Mg, 88-221 mg/kg Br, 14-18 mg/kg Sr, 19-30 mg/kg F. (Ericksen and others, 1978; Rettig and others, 1980; Ballivian and Risacher, 1981; this study)

Table A–1. *Mines, prospects, and occurrences on the Altiplano and in the Cordillera Occidental, Bolivia*—Continued

211	Salar de Uyuni deposit	20 00 00, 68 00 00	Saline Li-B-K brines saturate salt crust (excludes Río Grande area). Analysis: pH 7.25, 325 g/L TDS. Estimated resources in 1981 were 5.5 million tonnes Li, 110 million tonnes K, and 3.2 million tonnes B. (Ericksen and others, 1977, 1978; Rettig and others, 1980; Ballivian and Risacher, 1981; Davis and others, 1982)
214	Salar de Empexa deposit	20 19 46, 68 28 33	Saline Li-B-K brines saturate salt crust of salar. Analysis: 210-580 ppm Li, 0.77-2.0% K, 0.85-2.3% Mg. (Ericksen and others, 1977, 1978; Ballivian and Risacher, 1981; this study)
229	Río Grande deposit (Salar de Uyuni)	20 39 00, 67 19 00	In southeast portion of Salar de Uyuni. Saline B-Li-K brines saturate salt crust to 10 m depth over an area of 15 by 12 km. Analyses: density 1.000-1.279, pH 5.99-8.07, 3.1-1,090 mg/kg B, 3.1-2,060 mg/kg Li, 27-27,400 mg/kg K, 45-41,300 mg/kg Mg, 1-26 mg/kg F, as much as 291 mg/kg Br, 0.5-37 mg/kg Sr. Estimated resources in 1981 were 600,000 t Li, 4,500,000 t K, and 390,000 t B. (Ballivian and Risacher, 1981)
245	Salar de la Laguna deposit	20 50 17, 68 27 34	Saline brines saturate salt crust. (Ballivian and Risacher, 1981; this study)
250	Salar Laguani deposit	20 56 31, 68 18 10	Saline brines saturate salt crust. (Ballivian and Risacher, 1981)
263	Laguna Cañapa Norte deposit	21 30 00, 68 00 30	Saline B-Li-K brine lake 1.25 km^2 in area. Analysis: pH 8.34, 13 mg/L B, 19.5 mg/L Li, 212 mg/L K, 34 mg/L Mg. Estimated resources in 1981 were 1 t Li and 10 t of K. (Ballivian and Risacher, 1981)
268	Laguna Chiar Kkota deposit	21 35 00, 68 04 00	Saline B-Li-K brine lake 2 km^2 in area, 20 cm average depth, and volume of 400,000 m^3. Analysis: density 1.050, pH 8.28, 250 mg/L B, 176 mg/L Li, 2.5 g/L K, 1.14 g/L Mg, 25 g/L Na. (Ballivian and Risacher, 1981; this study)
270	Laguna Hedionda Norte deposit	21 34 00, 68 03 00	Saline B-Li-K brine lake 3.5 km^2 in area, average depth is 20 cm, and volume is 700,000 m^3. Brine analysis: density 1.006, pH 7.28, 20.5 mg/L B, 15 mg/L Li, 200 mg/L K, 114 mg/L Mg. Estimated resources in 1981 were 84 t of Li and 1,470 t K. (Ballivian and Risacher, 1981; this study)
272	Laguna Chulluncani deposit	21 32 45, 67 53 00	Saline Li-B-K brine lake 800,000 m^2 in area. Average depth is 15 cm and volume is 120,000 m^3. Brine analysis: pH 8.8, 22.5 mg/L Li, 960 mg/L B, 12 g/L K, 1.9 g/L Mg. Estimated resources in 1981 were 3 t Li, 100 t B, and 1,500 t K. (Ballivian and Risacher, 1981)
274	Laguna Honda Norte deposit	21 37 00, 68 04 00	Saline brine lake 0.4 km^2 in area. Average depth is 20 cm and volume is 80,000 m^3. (Ballivian and Risacher, 1981)
276	Laguna Ramaditas deposit	21 38 00, 68 05 00	Saline B-K-Li brine lake 2 km^2 in area (seasonally variable). Analysis: density 1.020, pH 8.15, 77 mg/L B, 11.7 mg/L Li, 1.03 g/L K, 325 mg/L Mg. Estimated resource in 1981 was 7 t Li. (Ballivian and Risacher, 1981)
280	Lagunas Pastos Grandes deposit	21 38 30, 67 47 40	Saline B-K-Li brine lake 4.65 million m^2 in area, with an average depth of 0.15 m and a volume of 700,000 m^3. Analysis: density 1.211, pH 7.20, 945 mg/L B, 14.2 g/L K, 1.64 g/L Li, 3.48 g/L Mg. Estimated resources in 1981 were 1,100 t Li, 9,800 t K, and 630 t B. (Ballivian and Risacher, 1981; this study)
283	Laguna Cachi deposit	21 43 45, 67 56 30	Alkaline B-Li-Mo-W brine lake. Portion of lake with brine is 1.5 km^2 in area with an average depth of 0.17 m. Analysis: temperature 21-25 °C, density 1.044-1.238, pH 10.05-10.60, 216-2,500 mg/L B, 177-848 mg/L Li, 25-50 mg/L Mo, 11-20 mg/L W, 438-2,300 mg/L As, 40-70 mg/L F, 0.4-2.9 mg/L Mg. (Ballivian and Risacher, 1981; Risacher and others, 1984; this study)
285	Laguna Khara deposit	21 53 50, 67 51 30	Alkaline brine lake 12 km^2 in area. Analysis: pH 9.40, 85 mg/L B, 208 mg/L K, 36 mg/L Li, 110 mg/L Mg. (Ballivian and Risacher, 1981)
287	Laguna Capina Sur deposit	21 55 30, 67 34 20	Saline B-Li-K brine lake 8 km^2 in area, average depth 20 cm, and volume 1.6 million m^3. Analysis: pH 8.6, 280 mg/L B, 193 mg/L Li, 1.46 g/L K, 260 mg/L Mg, 800 mg/L Ca. Estimated resources in 1981 were 450 t B, 300 t Li, and 2,300 t K. Li content of clays and borates exceeds that of brines. B content of evaporites and lacustrine sediments exceeds that of the brine by at least an order of magnitude. (Risacher and Miranda, 1976; Ballivian and Risacher, 1981; this study)

Table A–1. *Mines, prospects, and occurrences on the Altiplano and in the Cordillera Occidental, Bolivia*—Continued

290	Laguna Colorada deposit	22 11 20, 67 46 30	Saline brine lake with a pH of 5.0, 1,120 ppm TDS, 9.6 ppm B, 2.6 ppm Li, and 70 ppb V. (Ballivian and Risacher, 1981; this study)
321	Laguna Verde deposit	22 47 40, 67 48 20	Saline brine lake with estimated 20-40 g/L TDS, 20 ppm B, and 6 ppm Li. (Ballivian and Risacher, 1981; this study)
327	Laguna Honda Sur deposit	22 34 10, 67 27 00	Alkaline brine lake, 300,000 m^2, in area with an average depth of 0.1 m. Brine analysis: density 1.024, pH 9.88, 36.8 g/L TDS. (Ballivian and Risacher, 1981)
332	Laguna Kollpa deposit	22 28 20, 67 24 40	Alkaline brine lake 900,000 m^2 in area with an average depth of 1.5 m. Analysis: density 1.032-1.037, pH 10.8, 75-96 mg/L B, 1.05-1.27 g/L K, 0.5 mg/L Li, 3.1 mg/L Mg. (Ballivian and Risacher, 1981)
333	Laguna Hedionda Sur deposit	22 27 20, 67 23 00	Alkaline brine lake, 2.82 million sqaure meters in area, average depth 0.75 m, and volume 2.115 million cubic meters. Analysis: density 1.028, pH 10.46, 114 mg/L B, 0.5 mg/L Li, 1.65 g/L K, 2.8 mg/L Mg. Total dissoved salts are 33.5 g/L of which 32% are NaCl and KCl. (Ballivian and Risacher, 1981)
335	Laguna Catalcito deposit	22 35 00, 67 14 00	Slightly saline B-Li-K brine lake. Analysis: pH 5.5, 70 ppb Ni, 3.17 ppm Li, 6.6 ppm B, 32 ppm K, 5.8 ppm Mg, 390 ppb Sr. (This study)
336	Laguna Kalina (Laguna Busch) deposit	22 36 35, 67 12 45	Brine lake. Analysis: 500 ppm B, 200 ppm Li, 20 ppm Sr, 1,110 ppm K, 130 ppb Ti, 130 ppb Mo. (This study)
338	Laguna Loromayu deposit	22 24 27, 67 12 30	Saline brine lake. Analysis: pH 8.5, >500 ppm B, 608 ppm Li, 1,040 ppm Mg, and 29 ppm Sr. (Ballivian and Risacher,1981; this study)
346	Laguna Celeste deposit	22 12 33, 67 06 16	Alkaline brine lake. Analysis: pH 9.0, 24.4 ppm B, 7.7 ppm Li, 85.3 ppm Mg, 200 ppm K, 40 ppm Sr. (This study)
347	Laguna Mama Khumu deposit	22 15 42, 67 04 30	Saline brine lake. Analysis: 4.9 ppm B, 1.3 ppm Li, 8.5 ppm Mg. (This study)
349	Laguna Chojllas deposit	22 22 30, 67 05 36	Saline brine lake. Analysis: pH 6.5, 141 ppm B, 66 ppm Li, 210 ppb Ba, 355 ppm K, 179 ppm Mg, 20 ppm Sr. (This study)
352	Laguna Coruto deposit	22 24 45, 67 00 00	Alkaline brine lake. Analysis: pH 7.5, 3.4 ppm B, 1.16 ppm Li, 170 ppb Sr, 50 ppb Ba, 13 ppm K, 40 ppb Ni. (This study)
		Sediment-hosted Copper Deposits	
		San Silvestre Area	
1	Virgen de Copacabana prospect	16 35 45, 69 05 00	Manto of chalcocite, cuprite, malachite, and azurite in Tiahuanacu Formation. (This study)
2	EMUSA mine	16 36 37, 68 59 01	Stratabound Cu mineralization in Tiahuanacu Formation sandstone. (Requena and others, 1963)
3	Unknown	16 37 00, 68 56 35	Stratabound Cu mineralization in Tiahuanacu Formation sandstone. (Requena and others, 1963)
4	El Coreanito mine	16 38 42, 68 54 20	Manto of chalcocite, cuprite, malachite, tenorite, and azurite in Tiahuanacu Formation. (This study)
5	Ana María and Vatutin mines	16 36 30, 68 53 15	Chalcocite, malachite, and azurite replace organic matter in a manto as thick as 15 m of early Tertiary Huayllamarca Formation sandstone. (Guerra and Ascarrunz, 1964b; Vargas, 1967)
6	Santa Lucia mine	16 35 59, 68 54 01	Stratabound Cu mineralization in Tiahuanacu Formation sandstone. (Zapata and Delgadillo, 1968)
7	Santa Cruz mine	16 36 41, 68 51 46	Stratabound Cu mineralization in Tiahuanacu Formation sandstone. (Zapata and Delgadillo, 1968)
8	Palmira mine	16 36 00, 68 50 00	Chalcocite, malachite, azurite, and cuprite replace organic matter in mantos 0.5-0.8 m thick in Tiahuanacu Formation sandstone. (Caro and Vargas, 1963)
9	Aurora and Santa María mines	16 36 52, 68 48 59	Stratabound Cu mineralization in Tiahuanacu Formation sandstone. (Zapata and Delgadillo, 1968)
10	San Isidro mine	16 36 44, 68 49 06	Stratabound Cu mineralization in Tiahuanacu Formation sandstone. (Zapata and Delgadillo, 1968)
11	Jankho Kkollu mine	16 36 54, 68 47 51	Stratabound Cu mineralization in Tiahuanacu Formation sandstone. (Zapata and Delgadillo, 1968)

Table A–1. *Mines, prospects, and occurrences on the Altiplano and in the Cordillera Occidental, Bolivia*—Continued

12	La Incognita mine	16 37 03, 68 47 13	Cu minerals replace organic matter in Tiahuanacu Formation sandstone. (Vedia and Llanos, 1965)
15	Tres Amigos and Virgen de Fátima mines	16 37 31, 68 36 06	Chalcocite, azurite, and malachite replace organic matter in mantos 0.05-2 m thick and as long as 300 m in Tiahuanacu Formation sandstone and Huayllamarca Formation sandstone and conglomerate. Reserves in 1968 estimated as 39,600 t at an unknown grade. (Vargas, 1967; Zapata and Delgadillo, 1968)
19	Calluma and Cobre Chaca mines	16 44 00, 68 46 00	Stratabound Cu mineralization in Tiahuanacu Formation sandstone. (Zapata and Delgadillo, 1968)
20	Siempre Adelante mine	16 45 14, 68 44 16	Stratabound Cu mineralization in Tiahuanacu Formation sandstone. (Zapata and Delgadillo, 1968)
21	La Casualidad and San Francisco mines	16 45 15, 68 43 52	Chalcocite, covellite, malachite, and azurite replace organic matter in mantos in Tiahuanacu Formation sandstone. (Vargas, 1967)
22	María Elena mine	16 45 05, 68 41 45	Chalcocite, azurite, and malachite replace organic matter in seven mantos as long as 180 m in Huayllamarca Formation sandstone. (Vargas, 1967; Zapata and Delgadillo, 1968)
23	San Silvestre mine	16 46 57, 68 39 32	Chalcocite, azurite, and malachite replace organic matter in 10 mantos 120-150 m long and 0.3-1 m thick in Huayllamarca Formation sandstone. (Guerra and Ascarrunz, 1964d; Zapata and Delgadillo, 1968)
		Chacoma Area	
24	Lord de Senes mine	16 44 --, 68 27 --	Stratabound Cu mineralization in 5 mantos, 200 m long, 0.4-1.2 m thick, in Tiahuanacu Formation sandstone. (Zapata, 1987)
25	Cerro Tancaloma prospect	16 45 26, 68 27 19	Stratabound Cu mineralization in a manto 60 m long and 2 m thick in Tiahuanacu Formation sandstone. (Zapata, 1987)
26	Koniri mine	16 45 28, 68 24 08	Stratabound Cu mineralization in Coniri Formation sandstone. (Ahlfeld and Schneider-Scherbina, 1964)
27	Cerro Pusimujuna prospect	16 46 50, 68 27 34	Stratabound Cu mineralization in a manto 50 m long and 2 m thick in Tiahuanacu Formation sandstone. (Zapata, 1987)
28	Letanias mine	16 47 15, 68 26 00	Stratabound Cu mineralization in 4 mantos, 30-40 m long, and 70 cm thick in Tiahuanacu Formation sandstone. (Zapata, 1987)
29	Cutuna mine	16 46 --, 68 26 --	Stratabound Cu mineralization in 2 mantos over 200 m long and 0.8-1.4 m thick in Tiahuanacu Formation sandstone. (Zapata, 1987)
30	Chacoma prospect	16 48 02, 68 25 13	Stratabound Cu mineralization in 4 mantos, 60-450 m long, and 0.6 m thick in Upper Huayllamarca Formation sandstone and shale. (Zapata, 1987; this study)
32	Las Mercedes mine	16 51 06, 68 25 54	Stratabound Cu mineralization in Upper Huayllamarca Formation sandstone. (Meyer and Murillo, 1961)
33	Iquiri mine (San Simon II)	16 52 --, 68 23 --	Stratabound Cu mineralization in 4 mantos, 60 m long, and as thick as 20 cm in Tiahuanacu Formation sandstone. (Zapata, 1987)
34	San Simón I prospect	16 54 --, 68 22 --	Stratabound Cu mineralization in Tiahuanacu Formation sandstone. (Zapata, 1987)
		Corocoro Area	
37	Llallagua mine	17 00 06, 68 24 26	Chalcocite mineralization in Huayllamarca Formation sandstone. (Carrasco, 1962)
41	Cerro Wila Kkollu	17 07 20, 68 17 00	Stratabound Cu mineralization in Topohoco Formation conglomerate. (Ascarrunz and others, 1967)
60	María Elena mine (Elena, Victoria)	17 04 56, 68 40 45	Chalcocite, brochantite, cuprite, malachite, azurite, and chrysocolla occur in irregular lenses in medium-grained Totora Formation sandstone of 1.3 m average thickness in a zone 500 m long. Sandstone is cut by gypsum veinlets. Reserves in 1975 were 300,000 t of ore at an unknown grade. (López and Murillo, 1963b; Vargas, 1967; Terrazas, 1975)
61	Porvenir mine	17 01 30, 68 30 00	Chalcocite, covellite, and malachite replaces organic matter in mantos in Ballivian Formation sandstone. (López and Murillo, 1963a)

Table A–1. *Mines, prospects, and occurrences on the Altiplano and in the Cordillera Occidental, Bolivia*—Continued

62	Pisakheri mine (Anaconda, Pisaqueri, Violeta)	17 02 27, 68 29 21	Native copper, chalcocite, cuprite, malachite, and azurite replace clay matrix in Eocene Ballivian Formation litharenite. (Carrasco, 1962; Ljunggren and Meyer, 1964; Bernal, 1979)
63	Americas Unidas mine	17 07 32, 68 28 16	Chalcocite, covellite, cuprite, malachite, and azurite replace organic matter in nineteen mantos as much as 2.5 km long and 4 m thick in Eocene Ballivian Formation litharenite. (Bernal, 1979)
64	Transvaal mine (Consolidated, Libertad)	17 07 28, 68 27 16	Stratabound Cu mineralization in a manto 0.45 m thick in Eocene Ballivian Formation sandstone. (Guerra and Ascarrunz, 1964e)
65	Corocoro district (Buen Pastos, Capilla, Challcoma, Copacabana, Estrella, Guallatiri, Libertad, Malcocoya, Remedios, San Angel, San Agustín, San Geronimo, Santa Rita, Santa Rosa, Tancani, Viscachani, Yanabarra mines)	17 10 09, 68 27 04	Late Oligocene unconformity between Eocene Ballivian and Late Oligocene Caquiaviri Formations hosts significant Cu mineralization. Ore in weathered, gray sandstones and shales of the Ballivian Formation consists of native copper filling pores in sandstone, fractures in sandstone and shale, and replacement of organic matter and aragonite cement. Native copper ores were oxidized to 60 m depth to azurite, malachite, and cuprite. Ore in red sandstones of the Caquiaviri Formation consists of chalcocite and minor to trace galena and sphalerite that replace cement and organic matter. Concentrates of this ore contain significant to trace values of Ag, Pb, Zn, Sb, As, and Fe, but only Ag was recovered. Ore yielded about 15 g/t Ag per 1% Cu grade; Pb averages 2%. Mineralized zone is 4 km long, 15 m wide and is explored to 650 m depth. Mine produced about 500,000 t of Cu from 7 million tonnes ore until 1952 with remaining reserves of 427,000 t ore at 4.11% Cu and 157,000 t dump material at 0.9% Cu. Reserves in 1974 were 840,000 t at 3.75% Cu. (Singewald and Berry, 1922; Entwhistle and Gouin, 1955; Ljunggren and Meyer, 1964; Pélissioner, 1964; Rutland, 1966; Saravia, 1971; Muriel, 1971; Lawson Entwistle, oral commun., 1990)
68	Asunta mine	17 14 56, 68 27 46	Stratabound Cu mineralization in Eocene Ballivian Formation sandstone. (Ascarrunz and others, 1967)
70	Veta Verde mine	17 21 38, 68 24 05	Chalcocite, bornite, galena, native copper, cuprite, domeykite, malachite, and azurite replace anhydrite cement in four mantos which crop out over a length of 2.5 km in conglomerate and sandstone of the Tertiary Totora and Huayllamarca Formations. Galena occurs in lenses as thick as 0.5 m at south end of deposit. Past production (1921-62) yielded 769 t of concentrate at 15.2% Cu. Reserves in 1963 were 50,000 t at 0.5 to 6% Cu. (Meyer and Murillo, 1961; López and Murillo, 1963c; Schneider-Scherbina, 1963; Ljunggren and Meyer, 1964)
		Callapa Area	
71	San Agustín mine	17 24 57, 68 28 53	Cu minerals replace cement in fluvial sandstone of the Totora Formation in mantos 0.5-1.1 m thick. (Vedia and Ascarrunz, 1970)
72	Copacabana, El Hogar and Trinidad mines	17 24 00, 68 21 20	Stratabound Cu mineralization in Tertiary Totora and Huayllamarca Formation sandstones. (Meyer and Murillo, 1961)
73	Dinamita, Gran Poder and Pucara mines	17 24 20, 68 20 30	Stratabound Cu mineralization in Tertiary Totora Formation sandstone. (Meyer and Murillo, 1961)
74	San Francisco prospect	17 24 26, 68 19 22	Chalcocite, cuprite, and malachite mineralization in Totora Formation sandstone. (Meyer and Murillo, 1961)
75	Jayuma mine	17 22 28, 68 15 57	Stratabound Cu mineralization in Eocene Ballivian Formation sandstone. (Empresa Minera Illimani, 1989)
76	San Miguel mine	17 26 28, 68 20 55	Chalcocite and malachite mineralization in a manto of 40 cm average thickness in Late Tertiary Totora Formation sandstone. (Vedia and others, 1971; Columba and others, 1974; Empresa Minera Illimani, 1989)
77	Santiago mine	17 26 55, 68 21 48	Stratabound Cu mineralization in Late Tertiary Totora Formation sandstone. (Meyer and Murillo, 1961)
78	El Carmen and Exploradadora mines	17 26 30, 68 19 13	Stratabound Cu mineralization in Late Tertiary Totora Formation sandstone. (Meyer and Murillo, 1961)
79	16 de Julio mine	17 26 12, 68 18 46	Stratabound Cu mineralization in Late Tertiary Totora Formation sandstone. (Meyer and Murillo, 1961)

Table A–1. *Mines, prospects, and occurrences on the Altiplano and in the Cordillera Occidental, Bolivia*—Continued

80	Noé mine (La Explotada)	17 27 22, 68 17 53	Chalcocite, native copper, malachite, and azurite mineralization in five mantos hosted by late Tertiary Totora Formation sandstone. (Meyer and Murillo, 1961)
81	Esperanza mine	17 30 35, 68 19 37	Chalcocite, malachite, and azurite replaces organic matter in five mantos, each averaging 2 m thick, hosted by Late Tertiary Totora Formation sandstone. (Meyer and Murillo, 1961)
82	Chiguana mine	17 29 50, 68 16 45	Stratabound Cu mineralization in Late Tertiary Totora Formation sandstone. (Meyer and Murillo, 1961)
83	Copacabana mine	17 30 52, 68 16 12	Stratabound Cu mineralization in Late Tertiary Totora Formation sandstone. (Meyer and Murillo, 1961)
84	Micaya mine	17 31 22, 68 16 06	Stratabound Cu mineralization in Late Tertiary Totora Formation sandstone. (Meyer and Murillo, 1961)
85	Tolamarca mine	17 31 25, 68 15 05	Stratabound Cu mineralization in Late Tertiary Totora Formation sandstone. (Meyer and Murillo, 1961)
86	Copacabana mine	17 31 05, 68 15 14	Stratabound Cu mineralization in Late Tertiary Totora Formation sandstone. (Meyer and Murillo, 1961)
87	Ancojaira mine	17 31 08, 68 14 00	Stratabound Cu mineralization in Late Tertiary Totora Formation sandstone. (Meyer and Murillo, 1961)
88	Copacabana mine	17 33 38, 68 17 41	Stratabound Cu mineralization in late Tertiary Totora Formation sandstone. (Meyer and Murillo, 1961)
		Chacarilla Area	
90	La Encontrada mine	17 34 00, 68 14 00	Chalcocite, malachite, and azurite mineralization in mantos hosted by Tertiary sandstone. (Guerra and Ascarrunz, 1964c)
91	Chacarilla district (Amigo, Borda, Congreso, Esperanza, Eureka, Mizague, Porfía, San Fermín and Teviña mines)	17 35 00, 68 12 00	Chalcocite, native copper, lesser bornite, chalcopyrite, cuprite, tenorite, and malachite mineralization in mantos hosted by Early Tertiary Chuquichambi and Huayllamarca Formation sandstones. At least sixteen mantos as thick as 4 m are known in an area 8 km long. Pyrite, celestite, and gypsum are found in wall rocks. Past production was (1952-59) 4,865 t concentrates at 20.1% Cu and (1963-76) 1,457,000 t ore at 2.55% Cu. Reserves in 1976 were 813,000 t at 3.0% Cu. (Meyer and Murillo, 1961; Delgado, 1962; Ahlfeld and Schneider-Scherbina, 1964; this study)
92	Resguardo mine	17 35 56, 68 16 43	Stratabound Cu mineralization in late Tertiary Totora Formation sandstone. (Meyer and Murillo, 1961)
93	El Inca and La Codiciada mines	17 37 14, 68 15 44	Stratabound Cu mineralization in late Tertiary Totora Formation sandstone. (Meyer and Murillo, 1961)
		Chuquichambi Area	
94	Cerro Antaquira prospect	17 39 53, 68 07 56	Stratabound Cu mineralization in Tertiary Huayllamarca Formation sandstone. (Ministerio de Minas y Metalurgia, 1957)
95	Buena Esperanza mine	17 43 35, 68 05 35	Stratabound Cu-Pb-Ag mineralization in Tertiary Huayllamarca Formation sandstone. (This study)
96	Tangani prospect	17 45 47, 68 25 24	Stratabound Cu mineralization in mantos 10-30 cm thick hosted by Late Tertiary Totora Formation sandstone. (Mitchell, 1968)
98	Añahuani prospect	17 47 35, 67 57 45	Chalcocite, azurite, and malachite mineralization in Tertiary Umala Formation sandstone. (Ministerio de Minas y Metalurgia, 1957)
99	Huayllamarca mine (Santa María)	17 50 55, 67 56 51	Stratabound Cu mineralization in Tertiary Huayllamarca Formation sandstone. (Vedia and Gonzales, 1970; Rivas, 1971)
100	Chuquichambi deposit	17 54 17, 67 54 38	Chalcocite and lesser chalcopyrite, partly oxidized to azurite and malachite, replace calcite cement in preferred beds of Tertiary Huayllamarca Formation sandstone. (Ruíz, 1975)
101	Llanquera prospect (San Miguel)	17 59 19, 67 44 21	Chalcocite, malachite, and azurite mineralization in six lense-shaped mantos that crop out over an area 20 km long hosted by Late Tertiary Coniri sandstone. Reserves estimated in 1958 were 325,000 t at 5% Cu. (López, 1958; Murillo, 1960)

Table A–1. *Mines, prospects, and occurrences on the Altiplano and in the Cordillera Occidental, Bolivia*—Continued

		Turco Area	
105	Santa Clara mine (Clara)	18 02 26, 68 20 10	Chalcocite, malachite, azurite, and chrysocolla disseminated in bands 5-10 cm thick hosted by Miocene Turco Formation tuffaceous sandstone and crystal tuff. Reserves in 1969 estimated at 1,960 t at 5.6% Cu. (Murillo and others, 1969; Kuronuma, 1971)
108	Corona de España mine	18 07 30, 68 09 00	Small nodules, dendrites, and bands of native copper in about five mantos, each as much as 38 m long and 1 m thick hosted by Miocene Turco Formation sandstone. Ore is oxidized to cuprite, azurite, malachite, and chrysocolla to a depth of 30-50 m. Ore developed by workings in 1969 estimated at 4,230 t at 3.25% Cu. (Barrios and Prevost, 1970)
109	Cuprita mine	18 15 55, 68 03 52	Lenses of native copper, cuprite, and other copper oxides, 5-50 m in diameter, spaced 50-300 m apart in a belt 6.5 km long hosted by Miocene Azurita Formation conglomerate and sandstone. Copper oxides found as cement in conglomerate and native copper, partly oxidized, is found in sandstone. Reserves in 1958 estimated at 138,000 t at 2.0% Cu. (Georgi, 1958; Murillo and others, 1969)
		Sevaruyo Area	
117	Amistad mine (San Geronimo, Sevaruyo)	19 22 24, 66 55 08	Native copper, chalcocite, azurite, and malachite occur along fractures and bedding planes in mantos 250-450 m long, 0.7-2 m thick, hosted by Tertiary Chamorra Formation sandstone. Reserves in 1969 estimated at 3,500 t at 4.7% Cu. (Schneider-Scherbina, 1963; Murillo and others, 1969)
		Uyuni Area	
233	Cobrizos mine	20 59 37, 67 12 36	Veinlets of chalcocite, covellite, cuprite, malachite, and azurite, accompanied by veinlets of gypsum and carbonate, in fractures that follow or cut stratification in Eocene Potoco Formation sandstone. In places sandstone is cemented by calcite, azurite, and iron oxides and cut by calcite veinlets. Copper carbonates occur as mantos in Quaternary Minchin Formation limestone. Workings strongly contaminated by CO_2 gas. Reserves in 1957 estimated at 400,000 t at 0.6% Cu and 0.1 g/t Ag. (Lyons, 1957; Servicio Geológico de Bolivia, 1971o)
234	Puntillas mine	21 03 17, 67 26 18	Veins, 3-28 cm wide, and mantos, as much as 50 m long and 10 cm thick, of brochantite, malachite, tenorite, chrysocolla, chalcedony, and manganese oxide mineralization hosted by Miocene San Vicente Formation conglomerate. Reserves in 1971 estimated at 1,760 t at 7.7% Cu. (Servicio Geológico de Bolivia, 1971ll)
235	Inés mine	21 06 27, 67 27 10	Chalcocite, tenorite, malachite, azurite, and chrysocolla mineralization in a manto hosted by gypsiferous Eocene Potoco Formation sandstone. Reserves in 1970 estimated at 15,100 t at 3.6% Cu. (Servicio Geológico de Bolivia, 1971w)
240	Koholpani mine	21 11 30, 67 09 15	Chalcocite, malachite, and azurite mineralization in a manto 20-90 cm thick hosted by Oligocene Lower Quehua Formation calcareous conglomerate. (Servicio Geológico de Bolivia, 1971y)
		Serranía de las Minas Area	
357	Farellón mine	21 34 32, 67 25 00	Calcite, malachite, and azurite cement Eocene Potoco Formation arkosic sandstone cut by veins of chalcocite, azurite, malachite, tenorite, cuprite, hematite, and manganese oxides. (Servicio Geológico de Bolivia, 1971t)
359	Cerro Colorado mine (Negra)	21 37 15, 67 25 01	Mantos 2-36 cm thick and veins 2-20 cm wide of chalcocite, malachite, and chysocolla hosted by Late Tertiary San Vicente Formation sandstone. Cu minerals replace sericite-hematite cement in sandstone. Deposit of colluvium nearby contains 20-30 cm clasts of chalcocite-malachite mineralization in beds 1.5-2 m thick. (Servicio Geológico de Bolivia, 1971n)
361	Copacabana mine (Huallpa Coya)	21 41 30, 67 26 58	Mantos 0.1-1 m thick of veinlets of malachite and chrysocolla, and veins of chalcocite, bornite, malachite, and chrysocolla 0.05-0.15 m wide, hosted by late Tertiary San Vicente Formation sandy conglomerate. (Servicio Geológico de Bolivia, 1971q)

Table A–1. *Mines, prospects, and occurrences on the Altiplano and in the Cordillera Occidental, Bolivia*—Continued

362	25 de Julio mine (Peña Blanca)	21 42 49, 67 28 02	Three sets of veinlets 1-25 cm wide of chalcopyrite, native copper, cuprite, malachite, azurite, and chrysocolla occur in a tabular zone within fractured late Tertiary San Vicente Formation conglomerate. (Servicio Geológico de Bolivia, 1971a)
363	Bartola mine (San Bartolo)	21 42 57, 67 27 47	Chalcocite, malachite, chrysocolla, azurite, and covellite mineralization in mantos hosted by late Tertiary San Vicente Formation sandy conglomerate. Reserves in 1971 estimated at 2,400 t at 3.5% Cu. (Servicio Geológico de Bolivia, 1971h)
		Avaroa Area	
365	Estela mine	21 49 30, 67 19 40	Stratabound Cu mineralization hosted by Miocene Upper Quehua Formation. (Rodríguez and others, 1976)
369	Cerro Negro and Linares mines	21 37 42, 67 08 40	Bornite, malachite, and azurite mineralization in mantos hosted by Oligocene Lower Quehua Formation sandstone. Manto at Linares mine is 300 m long and 20 cm thick. (Servicio Geológico de Bolivia, 1971aa)
370	Aguilar mine	21 39 05, 67 09 04	Chalcocite, bornite, malachite, and chrysocolla mineralization in a manto capped by shale, 50 cm thick, hosted by Oligocene Lower Quehua Formation sandstone. (Servicio Geológico de Bolivia, 1971c)
371	Alianza mine	21 41 16, 67 09 06	Mantos of sandstone cemented by calcite, iron oxides, malachite, and chlorite cut by fractures filled by chalcocite, malachite, azurite, bornite, and chalcopyrite and gypsum veinlets. Mantos are 0.6-0.8 m wide and are hosted by Oligocene Lower Quehua sandstone. Reserves in 1971 were 2,000 t at 4.4% Cu. (Servicio Geológico de Bolivia, 1971d)
372	Sucre mine	21 44 19, 67 06 25	Mantos and veinlets of malachite and chrysocolla in Late Tertiary San Vicente Formation conglomerate and sandstone. Mantos in conglomerate are as thick as 50 cm, those in sandstone as thick as 15 cm. (Servicio Geológico de Bolivia, 1971ss)
373	El Morro mine	21 39 19, 67 07 04	Chalcocite, malachite, and azurite in mantos 0.1-0.45 m thick and veins 0.06-0.6 m wide hosted by Tertiary sandstone. Reserves in 1971 estimated as 3,000 t at 3.1% Cu. (Servicio Geológico de Bolivia, 1971r)
374	Bolívar mine (San Salvador, Cabrería)	21 38 05, 67 06 11	Chalcocite, chalcopyrite, malachite, and azurite replace organic matter in 3 mantos hosted by Oligocene Lower Quehua kaolinized sandstone. Reserves in 1971 estimated as 9,400 t at 2.7% Cu. (Servicio Geológico de Bolivia, 1971i)
375	Loa mine	21 39 44, 67 05 17	Stratabound copper mineralization hosted by Oligocene Lower Quehuea Formation. (Rodríguez and others, 1976)
376	Avaroa mine (Eduardo Abaroa; El Descuido)	21 36 27, 67 02 43	Six mantos of chalcocite, native copper, cuprite, azurite, malachite, tenorite, and chrysocolla 0.5-3 m long, 10-20 cm thick, and 50-80 cm wide. Fractures trending N. 30°-50° E. and dipping 65°-85° northwest filled by chalcocite and bornite. Mineralization hosted by Oligocene Lower Quehua sandstone capped by tuff. Reserves in 1972 estimated as 450,000 t at 5.0% Cu. (Vedia and Cortez, 1966a; Servicio Geológico de Bolivia, 1971b; Bassi, 1980)
377	Mantos Blancos mine	21 38 39, 67 03 13	Mantos 0.5 m thick of disseminated chalcocite and veins as long as 700 m of quartz, chalcocite, bornite, and chalcopyrite hosted by Oligocene Lower Quehua arkosic sandstone. Reserves in 1971 estimated as 23,000 t ore at 4.5% Cu plus 3,600 t dump material at 2.5% Cu. (Servicio Geológico de Bolivia, 1971dd)
		Esmeralda Area	
386	Ladislao Cabrera mine	27 37 10, 66 51 30	Chrysocolla and malachite mineralization in Eocene Potoco Formation sandstone and tuff. (Murillo and others, 1969)
391	Rosario prospect	21 32 00, 66 43 16	Hematite concretions cored by malachite and a 13 cm wide vein of chalcocite, all in a lense 150 m long, 25 m wide, and 2 m thick hosted by Eocene Potoco sandstone. (Servicio Geológico de Bolivia, 1971mm)
415	Esmeralda and San Pablo mines	21 23 30, 66 34 08	Chalcocite, cuprite, and tenorite mineralization in mantos 30-180 cm thick and as much as 140 m long and 20 m wide hosted by bleached Tertiary sandstone. (Bassi, 1980)
416	Don Piot and San Pedro mines	21 24 30, 66 34 15	Stratabound copper mineralization in Tertiary sandstone. (Servicio Geológico de Bolivia, 1969)

Table A–1. *Mines, prospects, and occurrences on the Altiplano and in the Cordillera Occidental, Bolivia*—Continued

417	Ucrania prospect	21 25 00, 66 32 19	Stratabound malachite, azurite, and chrysocolla mineralization hosted by Eocene Potoco Formation sandstone. (Servicio Geológico de Bolivia, 1971tt)
418	Huancané mine (La Reservada)	21 26 10, 66 32 44	Chalcocite, native copper, cuprite, tenorite, and copper carbonate mineralization in mantos as much as 30 m long and 15-20 m thick hosted by Eocene Potoco sandstone and Late Tertiary San Vicente conglomerate. (Officer, 1917b; Servicio Geológico de Bolivia, 1969)
419	Mesa Verde and San Pablito mines	21 22 17, 66 31 35	Stratabound native copper, chalcocite, and malachite mineralization hosted by Oligocene Lower Quehua Formation conglomerate. Nearby Tertiary basalt altered with pyrite and chlorite. (Servicio Geológico de Bolivia, 1971gg)
		Silica Sand Deposits	
120	Uyuni deposit	20 28 10, 66 49 40	Beds of Quaternary silica sand along railroad southwest of Uyuni. Sand averages 90.44% SiO_2 and 4.16% FeO. Resources estimated in 1969 were 8.9 million tonnes sand. (Cadima and others, 1969)
160	Volcán Quemado occurrence	18 37 24, 68 45 45	The west edge of the summit crater on the volcano is covered by dunes 300 m long and 100 m wide, perhaps 5-10 m deep, of sandy volcanic glass with minor quartz, feldspar, and mica. (This study)
197	Unknown	19 48 56, 67 46 31	Silica sand occurrence. (McVey, 1989)
		Sodium Sulfate Deposits	
244	Salar de la Laguna occurrence	20 50 17, 68 27 34	Salar with abundant sodium sulfate. One sample had 90% sodium sulfate. (Ballivian and Risacher, 1981)
262	Laguna Cañapa Norte occurrence	21 30 00, 68 00 30	Mirabilite and tenardite deposited on lake bed and dissolved in saline brine. Lake is 1.25 km^2 in area. Brine contain 5.07 g/L SO_4 and 3.59 g/L Na. Estimated resources in 1981 were 30,000 t mirabilite and 300 t sodium sulfate. (Ballivian and Risacher, 1981)
265	Laguna Hedionda Norte occurrence	21 34 00, 68 03 00	Mirabilite deposited on lake bed and dissolved in saline brine. Lake is 3.5 km^2 in area with average depth of 20 cm. Brine contains 455 mg/L SO_4 and 2.1 g/L Na. Estimated resources in 1981 were 19,000 t mirabilite (Ballivian and Risacher, 1981)
269	Laguna Chiar Kkota occurrence	21 35 00, 68 04 00	Saline brine lake, 2 km^2 in area, average depth 20 cm, with dissolved sodium sulfate. Brine has 4.08 g/L SO_4 and 25 g/L Na. (Ballivian and Risacher, 1981)
273	Laguna Chulluncani occurrence	21 32 45, 67 53 00	Saline brine lake 800,000 m^2 in area, average depth 15 cm, with dissolved sodium sulfate. Brine has 26 g/L SO_4 and 31 g/L Na. Estimated resources in 1981 were 4,800 t sodium sulfate. (Ballivian and Risacher, 1981).
274	Laguna Honda Norte occurrence	21 37 00, 68 94 00	Saline brine lake 0.4 km^2 in area, average depth 20 cm with dissolved sodium sulfate. Estimated resources in 1981 were 300 t sodium sulfate. (Ballivian and Risacher, 1981)
290	Laguna Colorada occurrence	22 11 20, 67 46 30	Mirabilite found on eastern shore of saline lake. (Ballivian and Risacher, 1981)
337	Laguna Loromayu occurrence	22 24 27, 67 01 49	Saline brine lake with dissolved sodium sulfate. (Ballivian and Risacher, 1981)
		Thermal Springs and Fumaroles	
149	Río Junthuma hot springs	18 05 --, 69 03 --	Hot springs (82 °C, 5-10 L/s) with silica sinter. (Carrasco, 1977)
150	Río Kasilla hot springs	18 04 39, 68 58 37	Hot springs (46 °C, pH 5.5, 1-5 L/s) with silica sinter in organic matter-bearing Quaternary ash. (Carrasco, 1977; this study)
157	Volcán Quemado thermal area	18 37 28, 68 45 04	Steaming vents and fumaroles on dome of nonperlitic welded tuff. (This study)
161	Laguna Sacabaya warm springs	18 38 40, 68 57 45	Warm springs (35 °C) emerging from basalt. Analysis: 23 ppm B, 87 ppm K, 5.6 ppm Li, 116 ppm Mg, 3.4 ppm Sr. (This study)
165	Estancia Viluyo hot springs (Río Paco Khaua)	18 47 16, 68 48 25	Hot springs (39 °C, 2 L/s) issuing from Recent colluvium. (Carrasco, 1977)

Table A–1. *Mines, prospects, and occurrences on the Altiplano and in the Cordillera Occidental, Bolivia*—Continued

184	Salar de Coipasa warm springs	19 14 36, 68 22 08	Warm springs (12 °C, pH 6.5) with iron oxide precipitates. Waters contain 1,590 ppm TDS and anomalous Mn, Ca, K, Mg, Na, and Co. (This study)
218	Mina Concepción thermal area	20 33 --, 68 31 --	Area of active fumaroles with deposition of native sulfur and extensive hydrothermal alteration. (Carrasco, 1977)
219	El Desierto thermal area	20 31 --, 68 34 --	Warm springs (31 °C, 1-5 L/s) feeding Salar de Empexa. Fumaroles actively sublimating native sulfur. (Carrasco, 1977; this study)
220	Towa hot springs	20 32 27, 68 26 22	Hot springs (78 °C, 1.8 L/s) and geysers with siliceous sinter. Analysis: pH 6.5, 7.2 g/L TDS, 32 ppm B, 11 ppm Li, and 100 ppb V. (Carrasco, 1977; this study)
246	Salar de la Laguna hot springs	20 52 --, 68 27 --	Hot springs (40 °C, 26 L/s) within lacustrine terrace deposits. Analysis: pH 6.0, 120 mg/L TDS, 3 ppm B, and 70 ppb V. (Carrasco, 1977; this study)
247	Volcán Olca thermal area	20 56 --, 68 29 --	Active fumaroles depositing native sulfur. (Carrasco, 1977)
279	Lagunas Pastos Grandes hot springs	21 38 --, 67 51 --	Hot springs (37 °C, 5.7-10 L/s) that issue from andesitic lava flows. (Carrasco, 1977)
294	Laguna Colorada warm springs	21 14 15, 67 44 30	Warm springs (21 °C). Analysis: pH 5, 300 mg/L TDS, anomalous B. (This study)
296	Río Huaylla Jara thermal area	21 17 30, 67 52 00	Hot springs (81 °C, 5-6 L/s) and geysers, active fumaroles and mut pots, associated with sinter and hydrothermal alteration. (Carrasco, 1977)
302	Cerro Michína thermal area	22 26 00, 67 53 30	Active fumaroles. (Carrasco, 1977)
303	Río Aguita Brava thermal area	22 26 47, 67 50 33	Hot springs (84 °C, 7-10 L/s) and geysers, active fumaroles and mud pots, associated with sinter and hydrothermal alteration. (Carrasco, 1977)
304	Sol de Mañana thermal area	22 25 35, 67 45 35	Hot springs (30 °C) and fumaroles (70 °C). Water analysis: pH 4.5, 3 g/L TDS. (This study)
306	Salar de Challviri thermal area	22 31 --, 67 39 --	Active fumaroles. (Carrasco, 1977)
308	Polkes hot springs	22 30 30, 67 38 20	Hot springs (37 °C, 10-20 L/s) that issue from fractured lava flows on the southeast flank of Cerro Polkes into Salar de Challviri. (Carrasco, 1977)
315	Campamento Mina Río Blanco warm springs	22 38 14, 67 48 32	Warm springs (32 °C, 5-10 L/s) that issue from Recent terrace gravels. Analysis: pH 6.3, 260 mg/L TDS, anomalous Al, Co, Cr, Fe, Mn, Ni, Sí, and Zn. (Carrasco, 1977; this study)
322	Campamento Mina Susana warm springs	22 44 --, 67 36 --	Warm springs (36 °C, 9.3 L/s) that issue from andesitic lava flows. (Carrasco, 1977)
326	Río de Aguas Calientes warm springs	22 49 30, 67 37 00	Warm springs (20 °C, 10-20 L/s) that issue from lava flows. (Carrasco, 1977)
342	Río Quetena Chico warm springs	22 11 00, 67 22 30	Warm springs (20 °C, 1.8 L/s) and geysers in alluvial terrace deposits associated with iron oxide alteration. (Carrasco, 1977)
344	Campamento Mina Uturuncu warm springs	22 12 --, 67 16 --	Warm springs (21 °C, 5-7 L/s) that issue from ignimbrites. (Carrasco, 1977)
350	Laguna Coruto warm springs	22 27 --, 67 02 --	Warm springs with anomalous B, Ba, Li, Ni, and Sr. (This study)
		Travertine Deposits	
16	Cerro Calera deposit	16 29 04, 68 35 45	Travertine deposited by thermal waters discharged from Coniri fault zone. Travertine is 75.8% $CaCO_3$ and is quarried as dimension stone. Contaminants include clay and marl. (Ahlfeld and Schneider-Scherbina, 1964; Montes de Oca and Vedia, 1965)
46	Lomitas quarry (Jantaña)	17 23 48, 67 49 35	Lensoid body of carbonate sinter in Tertiary volcanic breccia veined by calcite. (Ahlfeld and Schneider-Scherbina, 1964)
49	Huincu Tataya quarry	17 26 22, 67 47 45	Carbonate sinter mine located on Chijmini (6041-IV) 1:50,000 topographic map.

Table A–1. *Mines, prospects, and occurrences on the Altiplano and in the Cordillera Occidental, Bolivia*—Continued

132	Mirzapani quarry (Berenguela)	17 16 58, 69 13 02	About 8 beds of carbonate sinter, 1-3 m thick, separated by beds of porous silica sinter. Carbonate beds are 97.47% $CaCO_3$, 0.3% $MgCO_3$, 1.11% SO_3, 2.11% Fe_2O_3, 0.45% Al_2O_3, and 0.5% insoluble residue. Carbonate sinter is colloidal and sold as a "marble-onyx" dimension stone. (Ahlfeld and Schneider-Scherbina, 1964)
135	Dos Amigos deposit (Pacocagua)	17 19 06, 69 14 31	Apron of opaline sinter along fault that hosts Pacocagua (Dos Amigos) polymetallic vein deposit. Deposit is as thick as 12 m thick and contains 1,000 m^3 sinter. (Schneider-Scherbina, 1962b; this study)
366	Unknown	21 50 45, 67 19 20	Travertine quarry. (This study)
		Trona Deposits	
114	Lago Poopo occurrence	19 00 00, 67 00 00	Weak alkaline brine lake with minor dissolved natron. (Carmouze and others, 1978; Murillo and Bustillos, 1968; Ballivian and Risacher, 1981)
187	Salar de Coipasa occurrence (Salitrales Caballo Jihuata)	19 31 30, 67 57 30	Trona occurrence. (McVey, 1989)
284	Laguna Cachi occurrence	21 43 45, 67 56 30	Alkaline brine lake 1.5 km^2 in area, average depth of 0.17 m, with dissolved sodium carbonate. Lake freezes in the winter forming a crust of natron, thermonatrite, and halite. Brines contain 75-81 g/L CO_3 and 80-92 g/L Na. Soda crust contains 47.30% Na_2CO_3, 11.00% $NaHCO_3$, 11.05% Na_2SO_4, and 7.10% NaCl. Estimated resources in 1981 were 18,000 t trona. (Ahlfeld and Schneider-Scherbina, 1964; Ballivian and Risacher, 1981; this study)
286	Laguna Khara occurrence	21 53 50, 67 51 30	Alkaline brine lake 12 km^2 in area, average depth 3 m, with dissolved sodium carbonate. Brines contain 516 mg/L CO_3, 1.22 g/L HCO_3, and 2.5 g/L Na. Brines have 8.19 g/L TDS, 36.4% of which is trona. Estimated resource in 1981 was 96,000 t trona. (Ballivian and Risacher, 1981)
291	Laguna Colorada occurrence	22 11 20, 67 46 30	Saline brine lake with trona. (Ballivian and Risacher, 1981)
328	Laguna Honda Sur	22 34 10, 67 27 00	Alkaline brine lake 300,000 m^2 in area, average depth of 0.1 m, with dissolved sodium carbonate. Brine contains 2.29 g/L CO_3 and 409 mg/L HCO_3. Estimated resources in 1981 were 120 t trona. (Ballivian and Risacher, 1981)
332	Laguna Kollpa	22 28 58, 67 24 30	Saline lake with trona precipitates. (Rodríguez and others, 1976; this study)
334	Laguna Hedionda Sur	22 27 20, 67 23 00	Alkaline brine lake 2,820,000 m^2 in area, average depth of 0.75 m, with dissolved trona. Total dissolved salts are 33.5 g/L at 56% trona, 32% NaCl and KCl, and 12% sulfates. Brines contain 10.7 g/L CO_3, 336 mg/L HCO_3, and 12.5 g/L Na. Estimated resources in 1981 were 39,000 t trona. (Ballivian and Risacher, 1981)
		Unassigned Deposits	
31	Pandal prospect	16 44 50, 68 17 50	Prospect in Devonian clastic sediments cut by Tertiary dacite intrusives. (MINTEC, oral commun., 1990)
36	Pachekala prospect	16 59 45, 68 27 27	Au-bearing breccia bodies in Miocene (15-18 m.y.) dacite cemented by specularite or magnetite, with accessory apatite, barite and pyrite. Drilling to 100 m depth encountered values as much as 5 g/t Au, 200 ppm Cu, 2,000 ppm Pb, and some Zn. (Redwood and MacIntyre, 1989; MINTEC, oral commun., 1990; this study)
42	Mocal prospect	17 08 45, 68 02 29	Silurian Catavi Formation clastics cut by Tertiary intrusive. (MINTEC, oral commun., 1990)
47	María Concepción and Santa Rosa mines	17 23 52, 67 49 19	Adjacent mines work a mineralized calcite sinter deposit. Ore mineral is mimetite and ore grades about 3% Pb, 18 g/t Ag and 0.01 g/t Au. Deposit is very small. (Empresa Minera Illimani, 1989)
50	Kiska prospect	17 51 15, 67 32 35	Stockwork of Au-bearing quartz-jarosite-hematite-alunite veins in silicified Paleozoic sediments intruded by altered porphyry. Alunite dated at 13.6 m.y. (This study)

Table A–1. *Mines, prospects, and occurrences on the Altiplano and in the Cordillera Occidental, Bolivia*—Continued

57	Iroco mine	17 57 58, 67 09 18	Two vein sets, trending north-south dip 50° east or west and N. 45° W. dip 60° northeast cut Paleozoic argillaceous sandstone. Veins are a few centimeters to 1 m wide and contain native gold, chalcopyrite, quartz, opal, chalcedony, and pyrite. Veins are on the axis of a N. 20° E. trending anticline. Gold particles are about 30 microns in size. Reserves in 1990 were 250,000 troy oz Au. (Ahlfeld and Schneider-Scherbina, 1964; Guerra and others, 1965a; J. MacNamee, oral commun., 1990)
58	Florida mine	17 59 45, 67 08 40	Veins trending north-south dip 70° east, N. 50° W. dip 60° southwest, and N. 60° W. dip 70° southwest cut Paleozoic sandstone. Veins contain chalcocite and malachite and carry values in Ag. (Rocha and Balderrama, 1963)
102	Janko Vilique	18 00 25, 67 47 06	Cu mine in Tertiary Huayllamarca Formation sandstone located on Corque (SE-19) 1:250,000 topographic map.
103	Wara Wara prospect	18 13 30, 68 32 30	Altered, eroded Tertiary andesite-dacite stratovolcano. Alteration types include argillic, silicic, sericitic, and alunitic. Values as much as 0.04 g/t Au, 1 g/t Ag, 230 ppm As, and 18 ppm Sb measured. (MINTEC, oral commun., 1990; this study)
104	Turaquiri mine	18 08 17, 68 25 16	Pb-Ag veins in altered and eroded stratovolcano complex. (Ahlfeld, 1954)
107	Copajuyo prospect	18 05 25, 68 06 36	Argillized and silicified dacite flows and intrusive overly Tertiary sandstone. Disseminated chalcopyrite, pyrite, specularite, and magnetite found in sandstone. Values as much as 0.5 g/t Au and 15 g/t Ag measured in both dacite and sandstone. (MINTEC, oral commun., 1990)
110	Potosí prospect	18 51 21, 68 11 54	Altered volcanics. (MINTEC, oral commun., 1990)
111	Belén de Andamarca prospect	18 49 08, 67 38 54	Tertiary intrusive. (MINTEC, oral commun., 1990)
112	Ijualla mine	18 48 57, 67 30 55	Pb mine located on Andamarca (6037-I) 1:50,000 topographic map.
113	Tunavi prospect	19 00 16, 67 22 34	Tertiary rhyodacite. (MINTEC, oral commun., 1990)
115	Pampa Aullagas prospect	19 11 50, 67 02 34	Tertiary rhyodacite intrusive. (MINTEC. oral commun., 1990)
121	El Norteño prospect	17 07 31, 69 25 50	Argillized and silicified andesite with values as much as 0.2 g/t Au and 0.5 g/t Ag. (MINTEC, oral commun., 1990)
122	La Española prospect	17 13 13, 69 33 30	Argillized and silicified Abaroa Formation andesite and volcanoclastics intruded by propylitized and silicified dacite. Disseminated and stockwork sulfides and narrow veins (15 cm) of massive sulfides in zones of intense silicification and argillization. (ASARCO, oral commun., 1990; this study)
123	Golden Hill prospect	17 13 00, 69 25 00	Argillized and silicified andesite with values as much as 0.4 g/t Au and 30 g/t Ag. (MINTEC, oral commun., 1990)
125	Alfa prospect	17 17 00, 69 24 00	Argillized and silicified andesite intruded by dacite. As much as 0.3 g/t Au and 8 g/t Ag measured. (MINTEC, oral commun., 1990)
128	Serkhe prospect	17 20 46, 69 21 55	Argillized and silicified 6 m.y. Cerke andesite. A few samples anomalous in Au (as much as 0.1 g/t) and Ag (as much as 8 g/t) measured. (MINTEC, oral commun., 1990)
130	Choquepiña District (Kusima, Perseverancia, Atahuallpa, Titania mines)	17 12 28, 69 09 14	Veins with acicular chalcopyrite, chalcocite, covellite, neodigenite, and kaolinite, trend N. 65° E. dip 60° southeast, cut Tertiary Mauri Formation sandtone. (Schneider-Scherbina, 1962b; Ahlfeld and Schneider-Scherbina, 1964)
138	Las Vegas prospect	17 33 30, 69 14 30	Large N. 30° W. trending structure intruded by bleached and oxidized andesite cuts Tertiary sandstone. Sporadic values of as much as 0.2 g/t Au and 1 g/t Ag measured. (MINTEC, oral commun., 1990)
139	Cerro Tiquerani Norte occurrence	17 39 07, 69 11 56	Altered Tertiary intrusive. (Montes de Oca and others, 1963)
140	Cerro Tiquerani Sur occurrence	17 40 18, 69 11 40	Altered Tertiary intrusive. (Montes de Oca and others, 1963)
141	Cerro Canasita prospect (Khanasita)	17 47 51, 69 09 09	Altered Tertiary andesite. (MINTEC, oral commun., 1990)

Table A–1. *Mines, prospects, and occurrences on the Altiplano and in the Cordillera Occidental, Bolivia*—Continued

142	La Riviera propsect	17 49 29, 69 07 08	Western zone has propylitized andesite with tetrahedrite, native silver, cuprite, malachite, azurite, and chrysocolla mineralization with as much as 2% Cu and 50 g/t Ag. Eastern zone has argillic and silicic alteration with hypogene alunite and disseminated pyrite in andesite cut by veinlets of chalcedony, jarosite, and limonite with 0.1-0.3 g/t Au, and as much as 20 g/t Ag, 200 ppm As and 80 ppm Sb. Rhyolite dikes and sills intrude andesite. (MINTEC, oral commun., 1990)
143	La Montura prospect	17 57 00, 69 14 50	Argillized andesite with traces of Au, as much as 600 ppm As, and less than 1 g/t Ag. (MINTEC, oral commun., 1990)
144	La Escondida prospect (Wacan Kkollu)	17 47 56, 68 53 40	Argillized, silicified, and pyritized andesite covering an area of 250,000 km^2. Disseminated iron oxides, opal, pyrite, jarosite, and barite with 2-4 g/t Ag and 0.02-0.03 g/t Au. (Empresa Minera Illimani, 1989)
147	Mantos Negros mine	17 55 22, 68 53 44	Irregular deposit of manganese oxides in altered (argillic?) andesite. Nearby zone of hydrothermal breccia with about 2 g/t Ag and 0.02-0.03 g/t Au. (Empresa Minera Illimani, 1989)
148	Blanca Nieves prospect	18 03 08, 69 04 02	Altered stratovolcano. (MINTEC oral commun., 1990)
151	Nevado Sajama occurrence	18 06 34, 68 52 18	A reported fumarolic sulfur occurrence is disputed by Ahlfeld and Schneider-Scherbina (1964). Sb mineralization is also reported to occur.
154	Caupolicán prospect	18 14 20, 69 03 14	Altered stratovolcano. (MINTEC, oral commun., 1990)
155	Pacuni prospect	18 18 00, 68 49 00	Ag-Pb vein in altered dacite breccia and intrusive in eroded stratovolcano. (MINTEC, oral commun., 1990)
170	Mantos mine (Mantu)	18 53 19, 68 47 43	Cu mine in Carangas Formation located on 1:100,000 geologic map. Site visit found only green clay. (Ponce and Avila, 1965; this study)
173	Milenka prospect (Cerro Curumaya)	19 00 51, 68 49 47	Silicified, sericitized, and argillized hornblende-pyroxene andesite and biotite dacite in eroded core of a stratovolcano. Au values as much as 0.2 g/t and Ag less than 1 g/t found. Possible remnants of solfataric alteration and native sulfur mineralization. (MINTEC, oral commun., 1990; this study)
177	María Elena prospect (Cerro Culebra)	19 04 18, 68 42 14	Opalized subvolcanic dacite intrusive in core of a late Miocene argillized andesite stratovolcano. Northeast-trending silicic sills and dikes also cut andesite. Disseminated pyrite and jarosite mineralization with as much as 0.5 g/t Au and less than 1 g/t Ag. (MINTEC, oral commun., 1990; this study)
180	Anita prospect	19 08 27, 68 36 07	Argillized and silicified andesite and dacite cut by north-south and east-west trending fault veins. Values as much as 0.5 g/t Au found. (MINTEC, oral commun., 1990)
182	Casinquira mine	19 10 50, 68 27 18	Pb-Ag mine on southwest base of Cerro Pariani stratovolcano located on Villa Vitalina (5936-III) 1:50,000 topographic map.
185	Paola prospect	19 19 00, 68 17 45	Altered Quaternary stratovolcano. (MINTEC, oral commun., 1990)
190	Santa Catalina occurrence	19 39 55, 67 40 05	Iron oxide bearing hot spring deposits. (This study)
195	Iñexa prospect	19 43 16, 67 57 01	Intense siliceous and argillic alteration in brecciated hornblende dacite lava flows, with limonite boxwork gossan, intruded by hornblende dacite. (MINTEC, oral commun., 1990; this study)
196	Año Nuevo prospect	19 43 08, 67 49 07	Veins trending N. 30° E. and N. 45°-60° W. with silicified alteration envelopes cut propylitized and locally sericitized and argillized Tertiary? andesite and dacite. Veins contain galena and sphalerite and less than 0.05 g/t Au and as much as 87 g/t Ag. Prospect may occur in a window of older Tertiary volcanics and therefore may be a Bolivian polymetallic vein system similar to María Luisa to the east. (MINTEC, oral commun., 1990; this study)
203	Cerro Santaile prospect	19 54 51, 68 30 40	Silicified zone 10-30 m wide, 1.3 km long, cut by thick quartz-pyrite veins hosted by late Tertiary conglomerate and pyroclastics. Extensive sampling found 0.03-1.6 g/t Au and 0.2-3.5 g/t Ag. (McNamee, 1985b)

Table A–1. *Mines, prospects, and occurrences on the Altiplano and in the Cordillera Occidental, Bolivia*—Continued

204	Chinchilhuma (Cerro Chinchillahuay) district. (Aguilani, Baltazar, Condor, San Juan, San Salvador mines)	19 59 00, 68 21 00	Veins, trending N. 10° W. dip 75°-80° southwest and as wide as 20 cm, of pyrite, galena, sphalerite, jacobsite, cuprite, malachite, cassiterite, and specularite cut late Miocene hornblende dacite intruded by rhyolite. Mineralized zones are brecciated. Alteration consists of silicification and argillization. (Sanjinés, 1968b; McNamee, 1985a; this study)
205	Cerro Puquisa occurrence (Paco Kkollu)	20 04 15, 68 22 00	Limonite veinlets in silicified and argillized pyroclastics cored by a silicified breccia dome. (This study)
207	Cerro Panizo prospect	20 05 04, 68 29 43	Altered stratovolcano. (MINTEC, oral commun., 1990)
210	Cerro Pescado occurrence	20 09 00, 67 49 00	Chrysocolla and malachite fill vesicles in andesite in a zone 25 m wide. (This study)
212	Veta Kkollu mine	20 19 15, 67 55 34	Cu mine in Tertiary Yonza Formation located on Cerro Pabellón (6033-III) 1:50,000 topographic map.
223	Mac I prospect	20 38 34, 68 25 03	Altered Pliocene stratovolcano. (MINTEC, oral commun., 1990)
224	Cerro Colorado mine	20 33 57, 67 59 19	Veins less than 3 cm wide of malachite and azurite in fractured Tertiary Yonza Formation basalt. (Bustillos, 1966)
225	Cerro Pabellón deposit	20 37 44, 67 58 21	Stockwork of specularite veins in 800 m diameter zone in Tertiary sediments intruded by andesite. Veins carry trace amounts of Sn, Co, Cu, Ga, Mo, Ni, and V. (Bustillos, 1966)
226	Solución mine (Malil)	20 39 52, 67 45 01	A N. 10° W. vein, 20-30 cm wide, cuts dacite. Vein contains galena, sphalerite, limonite, and hematite. Reserves in 1971 estimated as 3,000 t at 1.4% Pb and 1.4% Zn. Values in Ag as much as 24 g/t. (Servicio Geológico de Bolivia, 1971rr)
227	Plasmar mine	20-38-58, 67 38 41	Rhyodacite cut by veins of galena, pyrite, and hematite. Workings exploit an ore shoot 1-3 m wide. (Ballivian and Vargas, 1971)
232	Cerro Pujíos mine	20 46 20, 66 55 00	North-trending quartz-chrysocolla veins cut Silurian Uncia Formation clastic rocks. Reported to have been worked for turquoise. (This study)
242	Millunu occurrence	20 51 45, 68 33 15	Large area of iron oxide bearing silicified andesite that extends accross the border from Chile. Samples taken on the Chilean side of the border have as much as 93 ppm Cu, 29 ppm Mo, 117 ppm Pb, 10 ppm Zn, 0.4 g/t Ag, and less than 20 ppb Au. (Vergara and Thomas, 1984)
257	Cerro Tomasamil prospect	21 17 00, 67 57 40	Veins trend east-west dip 80° north, as wide as 5 m, and trend N. 10° E., 10-20 cm wide, cut altered hornblende andesite. Veins contain iron oxides, sericite, hematite, and clay. A separate brecciated zone is cemented by magnetite, sphalerite, and specularite. Alteration minerals are sericite, hematite, limonite, and clay. (Sanjinés and others, 1968b)
259	Cuidado mine	21 15 30, 67 42 30	Vertical N. 45° W. trending breccia zones cut argillized, sericitized, and silicified dacite porphyry. Mineralized and altered zone is 12 km^2 in area. Breccia contains quartz, pyrite, and barite and has values of as much as 0.7% Sb and 150 g/t Ag. (Officer 1917a; this study)
260	Eskapa mine	21 13 35, 67 41 20	Vertical N. 10° W. trending veins cut brecciated biotite dacite porphyry dome. Veins contain tenorite, chrysocolla, malachite, and calcite with as much as 30 g/t Ag and 0.3% Pb. (Officer, 1917a; this study)
268	Laguna Chiar Kkota occurrence	21 35 00, 68 04 00	Native sulfur probably formed from the reduction of gypsiferous sediments by bacteria. (Ballivian and Risacher, 1981; this study)
271	Puca Mokho mine	21 33 35, 68 01 34	Disseminated native copper, cuprite, azurite, and malachite in sandstone. (Rodríguez and others, 1976)
282	Cerro Cachi Laguna alteration zone	21 39 47, 67 53 32	Argillized biotite-hornblende dacite with as much as 2 g/t Ag and 0.15% Pb. (This study)
317	Cerro Podorosa-Cerro Amarillo alteration zone	22 38 00, 67 46 00	Zone of argillized, sericitized, and silicified dacite porphyry bearing disseminated pyrite (oxidized to limonite) and as much as 2 g/t Ag, 0.05% Pb, 0.15% Cu, and 15 ppm Sn. (This study)
329	Río Vallecitos occurrence	22 44 30, 67 12 22	Reported occurrence of copper mineralization. (Rodríguez and others, 1976)
331	Cristóbal Colón mine	22 48 00, 67 12 00	Reported occurrence of manganese oxides and possible Cu mineralization. (Rodríguez and others, 1976)

Table A–1. *Mines, prospects, and occurrences on the Altiplano and in the Cordillera Occidental, Bolivia*—Continued

343	Quetena Grande district	22 11 08, 67 21 15	Veins of Cu and Ag. (Cardona, 1974)
351	Jaqueline mine	22 27 17, 67 00 21	Apparently small workings for evaporites on the south shore of Laguna Coruto. (Rodríguez and others, 1976; this study)
353	Sol de Mañana occurrence	22 06 30, 67 16 30	Mn occurrence. (Rodríguez and others, 1976)
355	Cerro Juvina occurrence	21 29 00, 67 32 00	Reported Zn mineralization. (Rodríguez and others, 1976)
356	San Francisco mine	21 26 42, 67 28 42	Veins in fractures of highly variable orientation as wide as 54 cm, but generally less than 10 cm wide, cut altered and brecciated biotite-hornblende Upper Quehua lithic tuff. Veins contain malachite, chrysocolla, hematite, and limonite and have Ag values. Alteration minerals are pyrite, chlorite, and hematite. (Servicio Geológico de Bolivia, 1971oo; this study)
358	Caquillán mine	21 36 03, 67 24 00	Chalcopyrite and malachite occur as weak impregnations and lenses in a fault zone 0.5-0.8 m wide that cuts Ordovician shale and sandstone. Veinlets of quartz and pyrite occur in the wall rock. (Servicio Geológico de Bolivia, 1971m)
360	12 de Octubre mine	21 40 15, 67 23 57	Sb mine hosted by Ordovician clastic sediments. (Rodríguez and others, 1976)
364	Mallcu Cueva mine	21 46 41, 67 28 48	Veinlets of hematite, with traces of Cu, trend N. 9°W. dip 50°-60° northeast, in fractures as wide as 0.5 m in Ordovician shale. (Servicio Geológico de Bolivia, 1971cc)
383	Rosario mine	21 33 00, 66 53 00	Irregular veins of chrysocolla, brochantite, jasper, and agate cut brecciated basaltic andesite. (This study)
388	Candelaria mine	21 46 15, 66 49 45	Veinlets of quartz, jarosite, and gold in Paleozoic clastic sediments. (United Nations Development Program, 1989)
390	Trapiche mine	21 53 26, 66 41 48	Sb mine in Upper Quehua Formation. (Rodríguez and others, 1976)
397	Pululus occurrence	21 30 08, 66 40 10	Reported U occurrence. Weakly disseminated copper oxides, chrysocolla, and malachite are found in Pleistocene conglomerate composed of Ordovician shale clasts in a tuffaceous matrix. (Murillo and others, 1969)
426	Roncal mine	21 47 18, 66 15 53	Cu mine located on La Cienaga (6328-IV) 1:50,000 topographic map. Appears to occur in Devonian clastics.
427	Rondal mine	21 48 52, 66 18 26	Veinlets trend east-west, N. 70° W., and N. 85° E. in a zone 100 m long of chalcocite, native copper, cuprite, malachite, azurite, and chrysocolla cut Tertiary lavas. (Vargas and Ballivian, 1972)
428	Thiutato mine	21 49 15, 66 14 10	Cu mine located on (6328-I) 1:50,000 topographic map.
431	Quillacas mine	21 56 18, 68 19 22	Copper and bismuth minerals of unknown type found in the Rondal Formation. (Ahlfeld and Schneider-Scherbina, 1964)

APPENDIX B

LOCATIONS, DESCRIPTIONS, AND ANALYSES OF SAMPLES COLLECTED AS PART OF THE STUDY OF THE ALTIPLANO AND CORDILLERA OCCIDENTAL, BOLIVIA

Appendix B - Locations, descriptions, and analyses of samples collected as part of the study of the Altiplano and Cordillera Occidental, Bolivia

INTRODUCTION

More than 35,000 chemical determinations of geologic materials were made in the course of this study. A variety of methods were used to collect, prepare, and analyze the samples; these methods are described below.

ANALYSTS

The following persons performed chemical analyses of geologic materials in the course of this study: B.M. Adrian, P.H. Briggs, J.H. Bullock, Jr., K.J. Curry, D.L. Fey, P.L. Hageman, R.H. Hill, R.T. Hopkins, Jr., A.H. Love, R.J. Knight, R.E. McGregor, J.B. McHugh, C.A. Motooka, J.M. Motooka, B.H. Roushey, D.F. Siems, E.P. Welsch, and D.M. Yannacito.

SAMPLE COLLECTION AND PREPARATION

Composite rock and ore samples were collected to most accurately reflect the composition of the materials. Sample sizes ranged from approximately 0.5 kg to as much as 5 kg. All rock samples were crushed, split, and pulverized to 0.15 mm with ceramic plates before analysis.

Water samples were collected in 0.5 L containers, and were filtered and acidified with 6N nitric acid after temperature and pH were recorded.

Sampling methods for the La Joya pilot geochemical study were somewhat different, are described in detail in that section of the report, and are summarized here. Each sediment, soil, and rock sample was a composite of 4-6 subsamples collected in an area no larger than 20 m in longest dimension, and is composed of approximately 0.5 kg of material. Rock samples were crushed and then pulverized preceding chemical analysis. Sediment samples were air dried at ambient temperature and then sieved to -0.25 mm and +0.25 mm fractions. Both fractions were subsequently pulverized to <0.15 mm prior to chemical analysis. Soil samples were oven-dried at 30° C, and then pulverized before chemical analysis.

ANALYTICAL METHODS

Direct-Current Arc Atomic Emission Spectrography (DC-ARC AES)

As many as 37 major, minor, and trace elements are simultaneously determined by this method. A 10-mg sample is mixed with 20 mg of pure graphite and is packed tightly into the cavity of a preformed graphite electrode. The sample is burned to completion in a direct-current arc at 12-15 amperes. The spectrum of the sample is recorded on photographic film and concentrations of the elements are determined by visual comparison with spectra of standards.

The precision of the method has been documented to generally be within one adjoining reporting interval on each side of the mean 83% of the time (except for results near the limits of determination), and within two reporting intervals on each side of the mean 96% of the time. Concentrations of the elements are reported in the intervals 1, 1.5, 2, 3, 5, 7, or orders of magnitude thereof between and including the lower and upper limits of determination.

Lower and upper limits of determination of the elements analyzed using this method include the following: Ca, 0.05-20%; Fe, 0.05-20%; Mg, 0.02-10%; Na, 0.2-5%; P, 0.2-10%; Ti, 0.002-1%; Ag, 0.5-5,000 ppm; As, 200-10,000 ppm;.Au, 10-500 ppm; Be, 1-1,000 ppm; B, 10-2,000 ppm; Ba, 20-5,000 ppm; Bi, 10-1,000 ppm; Cd, 20-500 ppm; Co, 10-2,000 ppm; Cr, 10-5,000 ppm; Cu, 5-20,000 ppm; Ga, 5-500 ppm; Ge, 10-100 ppm; La, 50-1,000 ppm; Mn, 10-5,000 ppm; Mo, 5-2,000 ppm; Nb, 20-2,000 ppm; Ni, 5-5,000 ppm; Pb, 10-20,000 ppm; Sb, 100-10,000 ppm; Sc, 5-100 ppm; Sn, 10-1,000 ppm; Sr, 100-5,000 ppm; Th, 100-2,000 ppm; V, 10-10,000 ppm; W, 20-10,000 ppm; Y, 10-2,000 ppm; Zn, 200-10,000 ppm; and Zr, 10-1,000 ppm.

Inductively Coupled Plasma-Atomic Emission Spectrometry (ICP-AES)

As many as 40 major, minor, and trace elements are determined by this method. An 0.200 g sample, to which 50 micrograms lutetium has been added as an internal standard, is digested to dryness with 3 mL HCl, 2 mL HNO_3, 1 mL $HClO_4$, and 2 mL HF at 110 °C. Additional $HClO_4$ and water are added to the residue and taken to dryness at 150 °C. One milliliter aqua regia is added and the sample is brought to 10.00 g with 1% HNO_3. The solution is heated at 95 °C for one hour, after which it is analysed by ICP-AES.

The precision is generally 5-10% relative standard deviation for most determinations with an optimal limit of of 1-2%. Niobium determinations are accurate to within 10-35% relative standard deviation.

Lower limits of determination of the elements analyzed using this method include the following: Al, 0.005%; Ca, 0.005%; Fe, 0.005%; K, 0.05%; Mg, 0.005%; Na, 0.005%; P, 0.005%; Ti, 0.005%; Ag, 2 ppm; As, 10 ppm;.Au, 8 ppm; Ba, 1 ppm; Be, 1 ppm; Bi, 10 ppm; Cd, 2 ppm; Ce, 4 ppm; Co, 1 ppm; Cr, 1 ppm; Cu, 1 ppm; Eu, 2 ppm; Ga, 4 ppm; Ho, 4 ppm; La, 2 ppm; Li, 2 ppm; Mn, 4 ppm; Mo, 2 ppm; Nb, 4 ppm; Nd, 4 ppm; Ni, 2 ppm; Pb, 4 ppm; Sc, 2 ppm; Sn, 10 ppm; Sr, 2 ppm; Ta, 40 ppm; Th, 4 ppm; U, 100 ppm; V, 2 ppm; Y, 2 ppm; Yb, 1 ppm; and Zn, 2 ppm.

Lower determination limits can be obtained using a 1.0 g sample which is treated with 5.0 mL HCl and 1.0 mL 30% hydrogen peroxide. After one hour, the digest is placed in a boiling water bath for 20 minutes. The digest is cooled and 4.0 mL of a solution of ascorbic acid-potassium iodide solution is added. The sample-reagent combination is mixed and allowed to stand for 20 minutes. Three milliliters of diisobutylketone containing a tertiary amine hydrochloride are added and the combined components are shaken for five minutes. The separated organic phase, separated in the centrifuge, is transferred to an autosampler from where it is drawn into the spectrometer and analyzed for 10 elements.

Based on replicate analyses of geochemical reference samples, the precision is generally better than 5% relative standard deviation. Accuracy is generally biased lower than actual values.

The upper limits of determination for elements using this method extend four orders of magnitude beyond the following lower limits of determination: Ag, 0.045 ppm; As, 0.600 ppm; Au, 0.150 ppm; Bi, 0.600 ppm; Cd, 0.050 ppm; Cu, 0.050 ppm; Mo, 0.090 ppm; Pb, 0.600 ppm; Sb, 0.600 ppm; and Zn, 0.050 ppm.

Flame or Graphite Furnace Atomic Absorption Spectrophotometry (AAS) for Gold

A 10 g sample is ignited in a muffle furnace at 700 °C for one hour, or until sulfides and organic matter are completely oxidized. The sample is digested on a hotplate with 10 mL HBr containing 0.5% Br_2. Ten milliliters of methylisobutylketone (MIBK) and 10 mL water are added to the cooled sample-acid mixture which is then shaken for 3 minutes; the organic phase is separated in the centriguge. The MIBK is washed with 40 mL 0.1M HBr and is introduced into the flame or graphite furnace of an atomic absorption spectrophotometer.

Heterogenous distribution of Au in samples makes it difficult to make a general statement about precision and accuracy, but the method is believed to be the best available.

The lower limit of determination is 0.05 ppm by flame AAS and 0.002 ppm by graphite furnace AAS. Concentrations of gold greater than 2 ppm can be determined by flame AAS following dilution. The upper limit for graphite furnace is 0.05 ppm, concentrations above which are determined by the flame method.

Flame Atomic Absorption Spectrophotometry (AAS) for Tellurium and Thallium

A 4.0 g sample is digested to dryness with 2 mL water, 5 mL HNO_3, 15 mL HCl, and 20 mL HF at 100°-110° C. Five milliliters of HBr are added and the sample is again taken to dryness at the same temperature. This residue is mixed with 0.22 mL of a HBr-10% Br_2 solution and 5 mL of water; this is warmed to dissolve the residue. The solution is brought to 20 mL with water. Four milliliters of MIBK are added and the combined organic and aqueous phases are shaken for five minutes. The phases are separated with the centrifuge, and Tl is determined in the MIBK by AAS. The remaining MIBK is removed and discarded and 10 mL HBr added to the aqueous phase. The solution is mixed, followed by addition of 2 or more g of ascorbic acid and mixing to reduce any ferric iron present to the ferrous form. Four milliliters of MIBK are added, followed by shaking, separation in the centrifuge, and determination of Te by AAS.

Based on replicate analyses of geochemical reference samples, the precision is generally 10-30% relative standard deviation. Accuracy is considered adequate.

The lower limit of determination for all three elements is 0.05 ppm. The upper limit of determination for each element can be extended beyond 20 ppm by dilution of the MIBK phase.

Continuous Flow-Cold Vapor Atomic Absorption Spectrophotometry (AAS) for Mercury

A 0.100 g sample is digested with 2.0 mL of HNO_3 and 0.5 mL of a 25% sodium dichromate aqueous solution for three hours at 110° C. The cooled digest is diluted to 12 mL with water and transferred to a continuous-flow manifold containing hydoxylamine hydrochloride and sodium chloride in 6M sulfuric acid. Mercury is reduced to its elemental state using stannous chloride. The mercury is introduced by airstream into the optical cell of an atomic absorption spectrophotometer wherein its concentration is determined.

Based on replicate analyses of geochemical reference samples, the precision is generally 5-15% relative standard deviation. Accuracy is considered adequate.

The lower limit of determination is 0.02 ppm. Samples containing greater than 3.4 ppm require dilution.

Continuous Flow-Hydride Generation Atomic Absorption Spectrophotometry (AAS) for Selenium and Arsenic

A 0.25 g sample is moistened with 1 mL 1% HNO_3, and then digested overnight or until the solution is reduced to 2 mL with 6 mL $HClO_4$, 9 mL HNO_3, and 10 mL HF at 105°-110° C. Twenty five mL of HCl are added and the solution is transferred to a 60 mL polyethylene bottle. The weight is adjusted to 54 g with distilled water. An aliquot of this solution is injected with an autosampler into the hydride generator of an atomic absorption spectrophotometer where As and Se are determined.

Based on replicate analyses of geochemical reference samples, the precision is generally 5-25% relative standard deviation. Accuracy is considered adequate.

The optimum concentration ranges for the elments are 0.2-2 ppm for Se and 0.2-40 ppm for As. Above these ranges, alternative techniques should be considered.

Wavelength Dispersive X-Ray Fluorescence Spectroscopy (WDXRF)

Ten major elements are determined as oxides by this method. A 0.800 g sample is ignited in a platinum crucible at 925° C for 45 minutes; the weight loss is reported as percent loss on ignition (LOI). An 8.000 g charge of lithium tetraborate is added to the sample and thoroughly mixed. A 0.250 mL aliquot of a 50% solution of lithium bromide is added as a nonwetting agent. The crucible is placed in a muffle furnace on an automatic fluxer, and the combined sample and flux is melted at 1120° C. The melt is maintained in the furnace at this temperature for 40 minutes while it is simultaneously homogenized through the rocking motion of the fluxer. The molten homogenous mixture is poured into a specially designed platinum mold. When cool, the resulting glass disk is inspected and introduced into the wavelength dispersive X-ray fluorescence spectrometer. The major element concentrations are determined by comparing the fluorescence intensities obtained from the sample to those obtained from standards.

With respect to precision, 49 short term replicate analyses of a basalt standard resulted in relative standard deviations (RSDs) of less than 1% for 6 of the 10 elements, ranging from 0.2% for SiO_2 to 0.6% for MgO. For the other elements, RSD for Na_2O at a concentration of 3.20% was 2.8%; for TiO_2 at a concentration of 0.88% was 1.1%; for P_2O_5 at a concentration of 0.60% was 1.7%; and for MnO at a concentration of 0.18% was 5.6%. Analyses of USGS standards generally gives results that are sufficiently accurate compared with other published values with the occasional exception of elements determined at concentrations close to the lower limit of determination.

Lower and upper limits of determination for elements determined by this method, reported as oxides, are as follows: SiO_2, 0.10-99.0%; Al_2O_3, 0.10-28.0%; Fe_2O_3, 0.04-28.0%; MgO, 0.10-60.0%; CaO, 0.02-60.0%; Na_2O, 0.15-30.0%; K_2O, 0.02-30.0%; TiO_2, 0.02-10.0%; P_2O_5, 0.05-50.0%; and MnO, 0.01-15.0%.

Delayed Neutron Counting Following Neutron Irradiation for Uranium and Thorium

A 2 dram poly vial (about 10 g of silicate rock) is filled with sample, and the sample weight is recorded. The vials are trimmed, sealed, and stacked into delayed neutron system magazines and transported to the reactor where the samples are briefly irradiated in a constant flux of neutrons. The samples are then introduced into the delayed neutron analysis system where delayed neutrons emanating from the sample are counted. The raw counting data is reduced to uranium and thorium concentration values.

The precision for the analysis of about 10 g of material is ±5% for U and ±15% for Th.

The lower limits of determination are about 0.1 ppm for U and about 1 ppm for Th.

Water methods

Water samples are analysed by ICP-AES.

Table B-1. *Locations and descriptions of samples collected as part of the study of metallic mineral deposits, Altiplano and Cordillera Occidental, Bolivia*

[Locations were digitized primarily from 1:50,000-scale quadrangles indicated. Alt., altered; bx, breccia; Co., Cerro; ppy, porphyry; qtz, quartz]

Sample no.	S. Lat	W. Long	Lithology	Locality	Quadrangle name and no.
90BAH006	21.1100	67.2133	Mineralized bx	Toldos Mine	San Cristobal (6130-I)
90BAH015a	21.2573	68.7158	Barite-rich alt. bx	Eskapa	Estancia Sora (6030-III)
90BAH015b	21.2573	68.7158	Barite-rich alt. bx	Eskapa	Estancia Sora (6030-III)
90BAH015c	21.2573	68.7158	Barite-rich alt. bx	Eskapa	Estancia Sora (6030-III)
90BAH015d	21.2573	68.7158	Barite-rich alt. bx	Eskapa	Estancia Sora (6030-III)
90BAH030	16.6422	68.6656	Argillized volcanic rock	Quimsa Chata	Sacacami (5843-I)
90BAH031	16.6443	68.6652	White kaolin	Quimsa Chata	Sacacami (5843-I)
90BAH032	16.6438	68.6553	Silica-pyrite rock	Quimsa Chata	Sacacami (5843-I)
90BAH033	16.6479	68.6517	Alt. Fe-staomed volcanic rock	Quimsa Chata	Sacacami (5843-I)
90BAH034	16.6413	68.6524	Coarse pyrite vein material	Quimsa Chata	Sacacami (5843-I)
90BAH035	16.6393	68.6596	Sericitically alt. volcanic rock	Quimsa Chata	Sacacami (5843-I)
90BAH037	16.6367	68.6628	Alt. vesicular lava with sulfides	Quimsa Chata	Sacacami (5843-I)
90BAH039	16.6347	68.6661	Alt. vesicular lava	Quimsa Chata	Sacacami (5843-I)
90BAH040	16.6347	68.6610	Clay alteration of volcanic rock	Quimsa Chata	Sacacami (5843-I)
90BBG001a	19.0680	68.5158	Red granite	North of Co. Tata Sabaya	Todos Santos (5836-I)
90BBG003	19.0105	68.7248	Dome vitrophyre	Todos Santos	Todos Santos (5836-I)
90BBG004	19.0105	68.7248	Rhyolite	Todos Santos	Todos Santos (5836-I)
90BBG005a	19.0105	68.7248	Argillized bx with sulfides	Todos Santos	Todos Santos (5836-I)
90BBG005b	19.0105	68.7248	Argillized bx with sulfides	Todos Santos	Todos Santos (5836-I)
90BBG006b	19.0105	68.7248	fault gouge	Todos Santos	Todos Santos (5836-I)
90BBG006c	19.0105	68.7248	Argillized bx with sulfides	Todos Santos	Todos Santos (5836-I)
90BBG007	19.0105	68.7248	Argillized bx with sulfides	Todos Santos	Todos Santos (5836-I)
90BBG008	19.0105	68.7248	Argillized bx with sulfides	Todos Santos	Todos Santos (5836-I)
90BBG009a	19.0105	68.7248	Bx clasts with sulfides	Todos Santos	Todos Santos (5836-I)
90BBG009b	19.0105	68.7248	Bx matrix with sulfides	Todos Santos	Todos Santos (5836-I)
90BBG010a	19.0105	68.7248	Specular hematite veinlet	Todos Santos	Todos Santos (5836-I)
90BBG010b	19.0105	68.7248	Argillized bx with sulfides	Todos Santos	Todos Santos (5836-I)
90BBG011a	18.8318	68.6181	Ore	Negrillos	Negrillos (5837-I)
90BBG011b	18.8318	68.6181	Ore	Negrillos	Negrillos (5837-I)
90BBG012	18.8255	68.6162	Ore	Negrillos	Negrillos (5837-I)
90BBG013c	19.1364	68.6379	Andesite	Saca Sacani	Todos Santos (5836-I)
90BBG014	19.0774	68.6956	Alt. dacite intrusion	Maria Elena	Todos Santos (5836-I)
90BBG015a	19.0774	68.6956	Argillized Fe-oxide intrusion	Maria Elena	Todos Santos (5836-I)
90BBG015b	19.0774	68.6956	Argillized intrusion	Maria Elena	Todos Santos (5836-I)
90BBG015c	19.0774	68.6956	Argillized intrusion	Maria Elena	Todos Santos (5836-I)
90BBG016a	19.0774	68.6956	Argillized intrusion	Maria Elena	Todos Santos (5836-I)
90BBG016b	19.0774	68.6956	Silicified dike(?)	Maria Elena	Todos Santos (5836-I)
90BBG018a	19.0127	68.8240	Argillized rock	Milenka	Parajaya (5836-IV)
90BBG018b	19.0127	68.8240	Silicified, Fe-stained rock	Milenka	Parajaya (5836-IV)
90BBG018c	19.0127	68.8240	Bx	Milenka	Parajaya (5836-IV)
90BBG018d	19.0127	68.8240	Argillized Fe-stained volcanic	Milenka	Parajaya (5836-IV)
90BBG018e	19.0127	68.8240	Alt. tuff	Milenka	Parajaya (5836-IV)
90BBG020	18.9387	68.6274	Argillized silicified tuff	Carangas	Carangas (5837-II)
90BBG021	18.9387	68.6274	Argillized tuff	Carangas	Carangas (5837-II)
90BBG022a	18.9387	68.6274	Bx pipe	Carangas	Carangas (5837-II)
90BBG022b	18.9387	68.6274	Bx clasts	Carangas	Carangas (5837-II)
90BBG023	18.9387	68.6274	Bx	Carangas	Carangas (5837-II)
90BBG024	18.9387	68.6274	Rhyolite intrusion	Carangas	Carangas (5837-II)
90BBG025a	18.9387	68.6274	Qtz vein in tuff	Carangas	Carangas (5837-II)
90BBG025b	18.9387	68.6274	Argillized tuff	Carangas	Carangas (5837-II)
90BBG025c	18.9387	68.6274	Mn-oxide + qtz vein in tuff	Carangas	Carangas (5837-II)
90BBG026	18.8882	68.6025	Silicified andesite bx	6 km NNE of Carangas	Carangas (5837-II)
90BBG029	18.8380	68.8322	Sheared andesite with pyrite	Sonia Susana	Julo (5837-IV)
90BBG030	18.8317	68.8262	Alt. andesite	Sonia Susana	Julo (5837-IV)
90BBG031	18.8289	68.8249	Alt. andesite	Sonia Susana	Julo (5837-IV)
90BBG032a	18.8231	68.8231	Alt. andesite	Sonia Susana	Julo (5837-IV)
90BBG032b	18.8231	68.8231	Alt. andesite with qtz vein	Sonia Susana	Julo (5837-IV)
90BBG032c	18.8231	68.8231	Alt. andesite with qtz vein	Sonia Susana	Julo (5837-IV)
90BBG033a	18.7893	68.8066	Alt. volcanic float	Sonia Susana	Julo (5837-IV)
90BBG033b	18.7893	68.8066	Alt. volcanic float	Sonia Susana	Julo (5837-IV)

Table B-1. *Locations and descriptions of samples collected as part of the study of metallic mineral deposits, Altiplano and Cordillera Occidental, Bolivia*–Continued

Sample no.	S. Lat	W. Long	Lithology	Locality	Quadrangle name and no.
90BBG034	18.8501	68.8389	Alt. andesite with pyrite, hematite	Sonia Susana	Cerro Capitan (5837-III)
90BBG040	18.2997	68.5546	Alt. volcanic float	Wara Wara	Cosapa (5839-II)
90BBG045	19.6269	67.7013	Argillized volcanic or intrusive	Salinas de Garci Mendoza	Salinas de Garci Mendoza (6035-II)
90BBG046a	19.6482	67.7481	Argillized silicified volcanic	Salinas de Garci Mendoza	Salinas de Garci Mendoza (6035-II)
90BBG046b	19.6482	67.7481	Argillized volcanic	Salinas de Garci Mendoza	Salinas de Garci Mendoza (6035-II)
90BBG047	19.7097	67.7147	Ore	Maria Luisa	Alianza (6034-I)
90BBG048a	19.7097	67.7147	Ore	Maria Luisa	Alianza (6034-I)
90BBG049	19.7097	67.7147	Ore	Maria Luisa	Alianza (6034-I)
90BBG050b	19.7028	67.7172	Rhyolite dome? with qtz veinlet	Maria Luisa	Alianza (6034-I)
90BBG051a	19.6873	67.7111	Ore	Guadalupe	Alianza (6034-I)
90BBG051b	19.6873	67.7111	Ore	Guadalupe	Alianza (6034-I)
90BBG052a	19.7351	67.6789	Ore	Margarita	Alianza (6034-I)
90BBG052b	19.7351	67.6789	Argillized volcanic wall rock	Margarita	Alianza (6034-I)
90BBG052d	19.7351	67.6789	Ore from dump	Margarita	Alianza (6034-I)
90BBG053a	19.7310	67.6801	Ore	San Miguel	Alianza (6034-I)
90BBG053b	19.7310	67.6801	Alt. volcanic wall rock	San Miguel	Alianza (6034-I)
90BBG054	19.7322	67.6771	Qtz vein	San Miguel	Alianza (6034-I)
90BBG055a	19.6809	67.7992	Silicified volcanic or intrsion	Co. Kaltami	Iñexa (6034-IV)
90BBG056a	19.6999	67.7986	Silicified dike	Estancia Iranuta	Iñexa (6034-IV)
90BBG056b	19.6999	67.7986	Argillized andesite	Estancia Iranuta	Iñexa (6034-IV)
90BBG057	19.6689	67.6716	Fe-oxide stained hot-spring sinter	Co. Santa Catalina	Alianza (6034-I)
90BBG058b	19.6873	67.7111	Silicified dike with sericite	Guadalupe	Alianza (6034-I)
90BBG058c	19.6873	67.7111	Propylitized andesite	Guadalupe	Alianza (6034-I)
90BBG059	19.6781	67.7099	Dacite dike	Co. Husachata	Alianza (6034-I)
90BBR003	19.0042	68.7163	andesite flow	Todos Santos dome	Todos Santos (5836-I)
90BBR004	19.0077	68.7097	Rhyolite block-and-ash flow	South of Río Todos Santos	Todos Santos (5836-I)
90BBR008	18.8318	68.6181	Andesite bx	Negrillos	Negrillos (5837-I)
90BBR010	18.8548	68.6103	Plagioclase-biotite ash-flow tuff	South of Negrillos	Carangas (5837-II)
90BBR015	19.0803	68.6932	Alt.rhyolite ppy	Maria Elena	Todos Santos (5836-I)
90BBR016	19.0803	68.6932	Alt. rhyolite dike	Maria Elena	Todos Santos (5836-I)
90BBR019	19.0185	68.8162	Porphyritic vitrophyre	Co. Curumaya	Parajaya (5836-IV)
90BBR020	19.0156	68.8186	Frothy dacite flow	Co. Curumaya	Parajaya (5836-IV)
90BBR021a	19.0156	68.8186	Frothy dacite flow	Co. Curumaya	Parajaya (5836-IV)
90BBR021b	19.0156	68.8186	Frothy dacite flow	Co. Curumaya	Parajaya (5836-IV)
90BBR021c	19.0156	68.8186	Frothy dacite flow	Co. Curumaya	Parajaya (5836-IV)
90BBR021d	19.0156	68.8186	Frothy dacite flow	Co. Curumaya	Parajaya (5836-IV)
90BBR022	18.9898	68.6367	Qtz-rich ash-flow tuff	North of La Rivera	Carangas (5837-II)
90BBR026	18.7657	68.6118	Flow-banded rhyolite	North of Negrillos	Negrillos (5837-I)
90BBR029	18.8501	68.8389	Alt float	Sonia-Susana	Cerro Capitan (5837-III)
90BBR031	18.7893	68.8066	Pink ash-flow tuff	Estancia Jarumani	Julo (5837-IV)
90BBR036a	18.2497	68.5370	Alt. andesite bx	Wara Wara	Agua Rica (5839-II)
90BBR036c	18.2497	68.5370	Alt. andesite bx	Wara Wara	Agua Rica (5839-II)
90BBR036d	18.2497	68.5370	Alt. andesite bx	Wara Wara	Agua Rica (5839-II)
90BBR036e	18.2497	68.5370	Alt. andesite bx	Wara Wara	Agua Rica (5839-II)
90BBR036g	18.2497	68.5370	Alt. andesite bx	Wara Wara	Agua Rica (5839-II)
90BBR036h	18.2497	68.5370	Alt. andesite bx	Wara Wara	Agua Rica (5839-II)
90BBR037	18.2753	68.2868	Ash-flow tuff	West of Turco	Estancia Anton Cura Huara (5939-III)
90BBR041	19.6252	67.7074	Porphyritic dacite intrusion	Salinas de Garci Mendoza	Salinas de Garci Mendoza (6035-II)
90BBR0440	19.6200	67.7019	Alt. dacite	Salinas de Garci Mendoza	Salinas de Garci Mendoza (6035-II)
90BBR044a	19.6200	67.7019	Alt. dacite	Salinas de Garci Mendoza	Salinas de Garci Mendoza (6035-II)
90BBR048a	19.6246	67.7214	Alt. rhyolite dike	Southeast of Rancho Alcaya	Salinas de Garci Mendoza (6035-II)
90BBR050	19.6494	67.6801	Silica rib	Estancia Marka Vinto	Salinas de Garci Mendoza (6035-II)
90BBR051	19.6453	67.6734	Silicified tuff	Estancia Marka Vinto	Salinas de Garci Mendoza (6035-II)
90BBR054a	19.6367	67.6934	Oxidized vuggy qtz. rock	Co. Kancha	Salinas de Garci Mendoza (6035-II)
90BBR055	19.6367	67.6934	Rhyolite dike	Co. Kancha	Salinas de Garci Mendoza (6035-II)
90BBR058c	19.6482	67.6898	Qtz.-alunite rock	Co. Kancha	Salinas de Garci Mendoza (6035-II)
90BBR063	19.6697	67.7019	Silicified Fe-oxide vein	Co. Kancha	Salinas de Garci Mendoza (6035-II)
90BCX002	16.9667	68.4250	Dacite porphyry	Comanche	Collana (5943-III)
90BCX003	17.1667	68.4500	Coarse sandstone	Corocoro district	Caquiaviri (5842-I)
90BCX004	17.1256	68.4711	Oxidized Cu ore in sandstone	Americas Unidas Mine	Caquiaviri (5842-I)

Table B-1. *Locations and descriptions of samples collected as part of the study of metallic mineral deposits, Altiplano and Cordillera Occidental, Bolivia*–Continued

Sample no.	S. Lat	W. Long	Lithology	Locality	Quadrangle name and no.
90BCX005	17.2750	68.5000	Water, brine spring near diapir	Caquingora	Calacoto (5842-II)
90BCX006	17.2917	68.4750	Water, brine spring near diapir	Jalluma	Pirapi (5942-III)
90BCX007	17.1708	68.4500	Chalcocite ore in sandstone	Corocoro district	Calacoto (5842-II)
90BCX008a	17.1750	68.4417	Red shale, mudstone	Corocoro district	Calacoto (5842-II)
90BCX008b	17.1750	68.4417	Tan sandstone	Corocoro district	Calacoto (5842-II)
90BCX009	17.1778	68.4417	Sandstone	Corocoro district	Calacoto (5842-II)
90BCX010	17.1778	68.4458	Conglomerate	Corocoro district	Calacoto (5842-II)
90BCX011	17.1692	68.4511	Water from Corocoro mine adit	Corocoro district	Calacoto (5842-II)
90BCX012	17.1750	68.4417	Bedded gypsum	Corocoro district	Calacoto (5842-II)
90BCX013a	17.0500	68.4917	FeOx-stained conglomerate	SW of Anaconda Mine	Caquiaviri (5842-I)
90BCX013b	17.0500	68.4917	Cu-stained ss	SW of Anaconda Mine	Caquiaviri (5842-I)
90BCX014	17.0408	68.4892	Chalcocite ore	Anaconda Mine	Caquiaviri (5842-I)
90BCX015	17.0500	68.4875	Iron-stained tuff	SW of Anaconda Mine	Caquiaviri (5842-I)
90BCX017	17.5694	68.2042	Chalcocite ore in conglomerate	Congreso Mine	San Pedro de Curahuara (5941-II)
90BCX018	17.5722	68.1931	Chalcocite ore in sandstone	Porfía Mine	San Pedro de Curahuara (5941-II)
90BCX019a	17.5736	68.1931	Chalcocite ore in sandstone	Porfía Mine	San Pedro de Curahuara (5941-II)
90BCX019b	17.5736	68.1931	Gypsum and mudstone from diapir	Chacarilla district	San Pedro de Curahuara (5941-II)
90BCX019c	17.5736	68.1931	Yellow alt. mudstone from diapir	Chacarilla district	San Pedro de Curahuara (5941-II)
90BCX020	17.5778	68.1958	Mudstone from diapir	Chacarilla district	San Pedro de Curahuara (5941-II)
90BCX021	17.1750	67.9667	Warm spring, public bath	Viscachani	Patacamaya (6042-III)
90BCX022a	18.0861	68.1583	Oxidized copper ore	Prospect SW of Azurita	Mina Azurita (5939-I)
90BCX022b	18.0861	68.1583	Tuff	Prospect SW of Azurita	Mina Azurita (5939-I)
90BCX023a	18.0750	68.1472	Native Cu-ore	Azurita mine	Mina Azurita (5939-I)
90BCX023b	18.0750	68.1472	Basalt	Azurita mine	Mina Azurita (5939-I)
90BCX023	18.0683	68.1561	Cuprite, native Cu ore	Azurita mine	Mina Azurita (5939-I)
90BCX024	18.1083	68.1556	Tuff	NE of Turco	Mina Azurita (5939-I)
90BCX025	18.1667	68.0333	Tuff	NE of Turco	Mina Azurita (5939-I)
90BCX026	18.2667	68.0569	Native copper ore	Cuprita Mine	Turco (5939-II)
90BCX027	21.5833	66.8667	Sphalerite-galena vein	Escala Mine	Mina Escala (6229-III)
90BCX028	21.5833	66.8833	Sericitic alteration of tuff	Escala Mine	Mina Escala (6229-III)
90BCX029	21.5833	66.8833	Sericitic alteration with Cu oxide	Escala Mine	Mina Escala (6229-III)
90BCX030a	21.6075	67.0453	Chalcocite ore in sandstone	Avaroa Mine	Río Quetena (6129-I)
90BCX030b	21.6075	67.0453	Chalcocite ore in sandstone	Avaroa Mine	Río Quetena (6129-I)
90BCX031	21.6878	67.1517	Oxidized copper ore in sandstone	Alianza Mine	Mina Avaroa (6129-II)
90BCX032	21.6514	67.1511	Oxidized sandstone Cu ore	Aguilar Mine	Río Quetena (6129-I)
90BDB001	17.1963	67.7270	Dacite ppy	Sica Sica	Sicasica (6042-II)
90BDB002	17.2004	67.7178	Dacite ppy	Sica Sica	Sicasica (6042-II)
90BDB003	17.1939	67.7180	Dacite ppy	Sica Sica	Sicasica (6042-II)
90BDB004	17.0297	67.8853	Dacite ppy	Viscachani	Patacamaya (6042-III)
90BDB005	17.1774	67.9806	Dacite ppy	Viscachani	Patacamaya (6042-III)
90BDB006	17.2272	67.9988	Dacite ppy	Viscachani	Patacamaya (6042-III)
90BDB007	17.1341	68.0668	Dacite ppy	Viscachani	Ayo Ayo (5942-I)
90BDB008	16.9689	68.2242	Dacite ppy	Colquencha	Calamarca (5943-II)
90BDB009	17.1427	68.1526	Dacite ppy	Viscachani	Ayo Ayo (5942-I)
90BDB010	17.0245	68.4602	Andesite	Miriquiri	Estación General Ballivian (5942-IV)
90BDB011	16.9631	68.4193	Dacite ppy	Comanche	Collana (5943-III)
90BDB012	16.7677	68.2839	Dacite ppy	Viacha	Letanías (5943-IV)
90BDB013	16.7326	68.2450	Dacite ppy	Viacha	Letanías (5943-IV)
90BDB014	21.7898	66.4938	Ore from dump	Santa Rosa	La Cienega (6328-IV)
90BDB015	21.7907	66.4947	Ore from dump	Santa Rosa	La Cienega (6328-IV)
90BDR001a	17.8029	67.4485	Dacite int.	Kori Kollo	Soledad (6140-IV)
90BDR001b	17.7828	67.4290	Dacite flow	Escatanque	Soledad (6140-IV)
90BDR005	19.3314	66.8404	Dacite dome	Co. Gordo	Santuario de Quillacas (6236-III)
90BDR006	19.5678	66.8446	Ash-flow tuff	Río Mulato	Coroma (6235-III)
90BDR007	21.1167	67.2000	Sulfide vein	Inca Mine	San Cristobal (6130-I)
90BDR008a	21.1167	67.2000	Dacite int.	Inca Mine	San Cristobal (6130-I)
90BDR008b	21.1167	67.2000	Sulfide vein	Inca Mine	San Cristobal (6130-I)
90BDR009	21.1100	67.2133	Run-of-mine ore	Toldos Mine	San Cristobal (6130-I)
90BDR010	21.1100	67.2133	Dacite int.	Toldos Mine	San Cristobal (6130-I)
90BDR012	21.3541	67.6469	Ash-flow tuff	Sora Puncu	Villa Alota (6029-I)

Table B-1. *Locations and descriptions of samples collected as part of the study of metallic mineral deposits, Altiplano and Cordillera Occidental, Bolivia*–Continued

Sample no.	S. Lat	W. Long	Lithology	Locality	Quadrangle name and no.
90BDR015	22.2985	67.7679	Ash-flow tuff	Co. Pabellón	Cerro Panizo (6027-II)
90BDR016	22.1678	67.5866	Ash-flow tuff	Co. Panizos	Cerro Panizo (6027-II)
90BDR0220	21.7275	66.6288	Dacite int.	Mesa de Plata	San Pablo de Lípez (6228-I)
90BDR0250	20.9364	66.2913	Ash-flow tuff	Chocaya	Gran Chocaya (6331-III)
90BDR029a	21.0895	67.2056	Alt. dacite	Hedionda Mine	San Cristobal (6130-I)
90BDR029	21.0895	67.2056	Sulfide vein	Hedionda Mine	San Cristobal (6130-I)
90BDR030	21.0929	67.2032	Dacite ppy	San Cristobal	San Cristobal (6130-I)
90BDR031	21.1100	67.2133	Andesite ppy	Toldos Mine	San Cristobal (6130-I)
90BDR033	21.2083	67.1317	diabase dike	Laguna Huaylla Khara	Estancia Charquini (6130-II)
90BDR0340	21.4433	67.4633	Ash-flow tuff	San Francisco mine	Estancia San Francisco (6129-IV)
90BDR034a	21.4433	67.4633	Chips of vein material	San Francisco mine	Estancia San Francisco (6129-IV)
90BDR034b	21.4433	67.4633	Dacite dike	San Francisco mine	Estancia San Francisco (6129-IV)
90BDR034c	21.4433	67.4633	Sulfide vein	San Francisco mine	Estancia San Francisco (6129-IV)
90BDR034d	21.4433	67.4633	Smelter slag	San Francisco mine	Estancia San Francisco (6129-IV)
90BDR0350	21.2317	67.6900	Dacite ppy	Mina Eskapa	Estancia Sora (6030-II)
90BDR035a	21.2317	67.6900	Sulfide vein	Mina Eskapa	Estancia Sora (6030-II)
90BDR037	21.4950	67.8633	Andesite flow	Co. Caquella	Cerro Inti Pasto (6029-IV)
90BDR038	21.6669	67.9077	Dacite dome	Co. Cachi Laguna	Cerro Cachi Laguna (6028-IV)
90BDR039	22.4300	67.8800	Andesite flow	Co. Apacheta	Cerro Michina (6026-IV)
90BDR0400	22.6083	67.7300	Alt. andesite	Co. Amarillo	Volcán Putana (6026-III)
90BDR040a	22.6083	67.7300	Alt. volcanic	Co. Amarillo	Cerro Boratera (6026-II)
90BDR040b	22.6083	67.7300	Silicified bx	Co. Amarillo	Cerro Boratera (6026-II)
90BDR040c	22.6163	67.7723	Alt. volcanic	Co. Amarillo	Volcán Putana (6026-III)
90BDR0410	22.6217	67.7300	Dacite flow	Co. Poderosa	Cerro Boratera (6026-II)
90BDR041a	22.6217	67.7300	Andesite flow	Co. Poderosa	Cerro Boratera (6026-II)
90BDR042	22.6450	67.6633	Ash-flow tuff	Río Chunchillerito	Cerro Boratera (6026-II)
90BDR043	22.3233	67.7367	Andesite flow	Co. Pabellón	Cerro Panizo (6027-II)
90BDR044	22.2217	67.7200	Ash-flow tuff	Laguna Colorada	Cerro Panizo (6027-II)
90BDR046	22.1717	67.6900	Ash-flow tuff	Co. Sanibria	Cerro Panizo (6027-II)
90BDR048	21.8404	67.3182	Travertine	Soniquera	Soniquera (6128-III)
90BDR051a	21.5839	66.8680	Argillized rhyolite	Mina Escala	Mina Escala (6229-III)
90BDR051b	21.5839	66.8680	Silicified vein	Mina Escala	Mina Escala (6229-III)
90BDR051c	21.5839	66.8680	Ore	Mina Escala	Mina Escala (6229-III)
90BDR052	21.5873	66.8680	Ore	Mina Escala	Mina Escala (6229-III)
90BDR053	21.5650	66.8550	Lava	Río Caneharito	Mina Escala (6229-III)
90BDR0540	21.5600	66.8667	Andesite	Mina Rosario	Mina Escala (6229-III)
90BDR054a	21.5600	66.8667	Ore	Mina Rosario	Mina Escala (6229-III)
90BDR055	21.5600	66.8667	Rhyolite ppy	Mina Escala	Mina Escala (6229-III)
90BDR057	21.7800	66.5600	Dacite ppy	Co. Aguilar	San Pablo de Lípez (6228-I)
90BDR0580	21.8100	66.4483	Ore	La Salvadora	La Cienega (6328-IV)
90BDR058b	21.8100	66.4483	Brecciated dacite	La Salvadora	La Cienega (6328-IV)
90BDR058c	21.8100	66.4483	Dacite	La Salvadora	La Cienega (6328-IV)
90BDR0600	21.8100	66.4983	Ore	Mina Bolívar	La Cienega (6328-IV)
90BDR060b	21.8100	66.4983	Dacite	Mina Bolívar	La Cienega (6328-IV)
90BDR0610	21.6290	66.5094	Ore	Candeleria	Cerro Santa Isabel (6229-II)
90BDR061a	21.6367	66.7100	Ore	Candeleria	La Cienega (6328-IV)
90BDR061b	21.6310	66.5138	Ore	Candeleria	Cerro Santa Isabel (6229-II)
90BDR061c	21.6368	66.5147	Rhyolite	Candeleria	Cerro Santa Isabel (6229-II)
90BDR062	21.6367	66.7100	Sedimentary rock	Río San Pablo	Cerro Santa Isabel (6229-II)
90BDR064	17.7828	67.4290	Dacite flow	Co. Escatanque	Soledad (6140-IV)
90BEB001	18.7384	66.8559	Fine-grained sandstone	16 km north of Challapata	Huancani (6237-IV)
90BEB002a	21.1100	67.2133	Barite vein with sulfosalts	San Cristobal	San Cristobal (6130-I)
90BEB002	21.1100	67.2133	Dacite	San Cristobal	San Cristobal (6130-I)
90BEB003a	21.6723	67.9009	Alt. dacite	Co. Cachi Laguna	Cerro Cachi Laguna (6028-IV)
90BEB003b	21.6723	67.9009	Alt. dacite	Co. Cachi Laguna	Cerro Cachi Laguna (6028-IV)
90BEB003d	21.6723	67.9009	Alt. dacite	Co. Cachi Laguna	Cerro Cachi Laguna (6028-IV)
90BEB005a	21.8243	66.4479	Dacite bx	Mina Colorados de Bolivia	La Cienega (6328-IV)
90BEB005b	21.8193	66.4532	Dacite bx	Mina Colorados de Bolivia	La Cienega (6328-IV)
90BEB005c	21.8188	66.4542	Fe-oxide vein	Mina Colorados de Bolivia	La Cienega (6328-IV)
90BEB005d	21.8204	66.4504	Dacite bx	Mina Colorados de Bolivia	La Cienega (6328-IV)

Table B-1. *Locations and descriptions of samples collected as part of the study of metallic mineral deposits, Altiplano and Cordillera Occidental, Bolivia*–Continued

Sample no.	S. Lat	W. Long	Lithology	Locality	Quadrangle name and no.
90BES001	17.1264	69.4328	Dacite lava	El Norteño	Antacahua (5742-IV)
90BES002	17.1214	69.4333	Alt. volcanic rock	El Norteño	Antacahua (5742-IV)
90BES003	17.1184	69.4342	Silicified lava	El Norteño	Antacahua (5742-IV)
90BES004	17.1147	69.4303	Argillically alt. rock	El Norteño	Antacahua (5742-IV)
90BES005	17.1158	69.4303	Silicified volcanic rock	El Norteño	Antacahua (5742-IV)
90BES006	17.2342	69.5108	Argillized dacite	La Española	Thola Kkollu (5642-II)
90BES007	17.2361	69.5102	Silicified dacite	La Española	Thola Kkollu (5642-II)
90BES008	17.2407	69.5091	Argillized dacite	La Española	Thola Kkollu (5642-II)
90BES009	17.2407	69.5091	Vein	La Española	Thola Kkollu (5642-II)
90BES010	17.2383	69.5243	Dacite	La Española	Thola Kkollu (5642-II)
90BES011	17.2512	69.5522	Dacitic ash-flow tuff	La Española	Thola Kkollu (5642-II)
90BES012	17.2527	69.5614	Andesite lava	La Española	Thola Kkollu (5642-II)
90BES013	17.2546	69.5594	Dacite lava	La Española	Thola Kkollu (5642-II)
90BES014	17.2178	69.4425	Dacite lava	Golden Hill	Sinejavi (5742-III)
90BES015	17.2208	69.4278	Silicified lava	Golden Hill	Sinejavi (5742-III)
90BES016	17.2197	69.4261	Silicified lava	Golden Hill	Sinejavi (5742-III)
90BES029	17.2252	69.5289	Argillically altered rock	La Española	Thola Kkollu (5642-II)
90BES030	17.2247	69.5275	Argillically altered rock	La Española	Thola Kkollu (5642-II)
90BES031	17.1881	69.5386	Dacite lava	La Española	Thola Kkollu (5642-II)
90BES032	17.2208	69.5244	Argillically altered rock	La Española	Thola Kkollu (5642-II)
90BES033	17.2675	69.4058	Dacite lava	Golden Hill	Sinejavi (5742-III)
90BES034	17.2856	69.4625	Pumice	Golden Hill	Sinejavi (5742-III)
90BES035	17.2200	69.4264	Dacite lava	Golden Hill	Sinejavi (5742-III)
90BES036	17.2683	69.4181	Dacite lava	Golden Hill	Sinejavi (5742-III)
90BES037	20.0650	68.3590	Silicified dacite	Paco Kkollu	Huanaque (5933-IV)
90BES039	20.0650	68.3522	Silicified volcanic rock	Paco Kkollu	Huanaque (5933-IV)
90BES040	20.0671	68.3518	Silicified bx	Paco Kkollu	Huanaque (5933-IV)
90BES041	20.0673	68.3504	Silicified bx	Paco Kkollu	Huanaque (5933-IV)
90BES042	20.0636	68.3526	Silicified volcanic rock	Paco Kkollu	Huanaque (5933-IV)
90BES043	20.0644	68.3546	Silicified volcanic rock	Paco Kkollu	Huanaque (5933-IV)
90BES044	20.0642	68.3600	Dacite ash-flow tuff	Paco Kkollu	Huanaque (5933-IV)
90BES045	20.1194	68.3492	Manganese vein	Siljshihua	Cahuana Chica (5934-III)
90BES046	19.8951	68.3585	Silicified bx	Chinchilhuma	Cahuana Chica (5934-III)
90BES047	19.8964	68.3659	Alt. ppy.	Chinchilhuma	Cahuana Chica (5934-III)
90BES048	19.8996	68.3687	Dacite	Chinchilhuma	Cahuana Chica (5934-III)
90BES049	19.9020	68.3603	Argillically altered rock	Chinchilhuma	Cahuana Chica (5934-III)
90BES050	19.9076	68.3586	Galena-qtz.-pyrite vein	Chinchilhuma	Cahuana Chica (5934-III)
90BES051	19.8975	68.3599	Silicified bx	Chinchilhuma	Cahuana Chica (5934-III)
90BES052	19.9096	68.3592	Argillically altered rock	Chinchilhuma	Cahuana Chica (5934-III)
90BES053	19.9047	68.3591	Ore from dump	Chinchilhuma	Cahuana Chica (5934-III)
90BES054	19.9047	68.3591	Ore from dump	Chinchilhuma	Cahuana Chica (5934-III)
90BES055	19.9667	68.3564	Smelter slag	Chinchilhuma	Cahuana Chica (5934-III)
90BES056	19.9336	68.3548	Argillically altered rock	Chinchilhuma	Cahuana Chica (5934-III)
90BES057	19.9425	68.3543	Argillically altered rock	Chinchilhuma	Cahuana Chica (5934-III)
90BES058	19.9372	68.3515	Iron-manganese vein	Chinchilhuma	Cahuana Chica (5934-III)
90BES059	19.7141	67.9503	Dacite	Iñexa	Iñexa (6034-IV)
90BES060	19.7208	67.9489	Silicified altered rock	Iñexa	Iñexa (6034-IV)
90BES061	19.7222	67.9491	Argillically altered rock	Iñexa	Iñexa (6034-IV)
90BES062	19.7212	67.9508	Argillically altered rock	Iñexa	Iñexa (6034-IV)
90BES063	19.7212	67.9464	Argillically altered rock	Iñexa	Iñexa (6034-IV)
90BES064	19.7193	67.9505	Silicified altered rock	Iñexa	Iñexa (6034-IV)
90BES065	19.7164	67.9524	Silicified altered rock	Iñexa	Iñexa (6034-IV)
90BES066	19.9006	68.3572	Dacite lava	Iñexa	Iñexa (6034-IV)
90BES067	19.7228	67.9464	Dacite lava	Iñexa	Iñexa (6034-IV)
90BES068	19.7228	67.9444	Dacite lava	Iñexa	Iñexa (6034-IV)
90BES069	19.7208	67.9425	Argillized mudflow	Iñexa	Iñexa (6034-IV)
90BSL001	17.8029	67.4485	Dacite	Kori Kollo	Soledad (6140-IV)
90BSL002	17.8030	67.4494	Dacite	Kori Kollo	Soledad (6140-IV)
90BSL003a	17.8004	67.4496	Dacite	Kori Kollo	Soledad (6140-IV)
90BSL004	17.7687	67.5047	Dacite	La Joya	Cerro La Joya (6040-I)

Table B-1. *Locations and descriptions of samples collected as part of the study of metallic mineral deposits, Altiplano and Cordillera Occidental, Bolivia*–Continued

Sample no.	S. Lat	W. Long	Lithology	Locality	Quadrangle name and no.
90BSL005	17.7674	67.5070	Aplite	La Joya	Cerro La Joya (6040-I)
90BSL006	17.7682	67.5134	Bx	La Joya	Cerro La Joya (6040-I)
90BSL007	17.7729	67.5139	Bx	La Joya	Cerro La Joya (6040-I)
90BSL008	17.9538	67.1192	Sulfide vein	San José	Oruro (6140-II)
90BSL009	17.9538	67.1192	Sulfide bx	San José	Oruro (6140-II)
90BSL010	17.9538	67.1192	Dacite intrusion	San José	Oruro (6140-II)
90BSL011	17.9433	67.1287	Sulfide bx	San José	Oruro (6140-II)
90BSL012	22.4538	67.7354	Alt. andesite	Sol de Mañana	Cerro Negro (6027-III)
90BSL013	21.7275	66.6288	Sulfide vein	Buena Vista	San Pablo de Lípez (6228-I)
90BSL014	21.7275	66.6288	Alt. ash-flow tuff	Buena Vista	San Pablo de Lípez (6228-I)
90BSL030	17.7670	67.4587	Tourmaline vein	La Barca	Soledad (6140-IV)
90BSL031	17.7673	67.4596	Dacite	La Barca	Soledad (6140-IV)
90BSL032	17.7691	67.4592	Jasperoid vein	La Barca	Soledad (6140-IV)
90BSL033	17.7568	67.4632	Dacite	La Barca	Soledad (6140-IV)
90BSL034	17.7568	67.4632	Mafic enclave	La Barca	Soledad (6140-IV)
90BSL035	17.7653	67.4561	Jasperoid vein	La Barca	Soledad (6140-IV)
90BSL036	17.8032	67.4476	Jasperoid vein	Kori Kollo	Soledad (6140-IV)
90BSL037	17.8015	67.4466	Dacite	Kori Kollo	Soledad (6140-IV)
90BSL038a	17.8049	67.4468	Sulfide vein	Kori Kollo	Soledad (6140-IV)
90BSL038b	17.8049	67.4468	Sulfide vein	Kori Kollo	Soledad (6140-IV)
90BSL039	17.8040	67.4491	Sulfide vein	Kori Kollo	Soledad (6140-IV)
90BSL040	17.7888	67.4539	Dacite	Llallagua	Soledad (6140-IV)
90BSL041a	17.7866	67.4572	Sulfide vein	Llallagua	Soledad (6140-IV)
90BSL041b	17.7866	67.4572	Sulfide vein	Llallagua	Soledad (6140-IV)
90BSL042	17.7833	67.4608	Oxidized vein	Llallagua	Soledad (6140-IV)
90BSL043	17.7851	67.4604	Dacite	Llallagua	Soledad (6140-IV)
90BSL044	17.7916	67.4586	Sedimentary rock	Llallagua	Soledad (6140-IV)
90BSL045	17.7877	67.4586	Silicified dacite	Llallagua	Soledad (6140-IV)
90BSL046	17.7577	67.4623	Dacite	Llallagua	Soledad (6140-IV)
90BSL047	17.7588	67.5069	Dacite	La Joya	Soledad (6140-IV)
90BSL048	17.7549	67.5090	Dacite	La Joya	Soledad (6140-IV)
90BSL049a	17.7726	67.5038	Sulfide vein	La Joya	Soledad (6140-IV)
90BSL049b	17.7726	67.5038	Sulfide vein	La Joya	Soledad (6140-IV)
90BSL050	17.7645	67.6300	Dacite	Co. Llallagua	Cerro La Joya (6040-I)
90BSL051	17.7889	67.6106	Dacite	Co. Quimsa Chata	Cerro La Joya (6040-I)
90BSL052a	17.8462	67.5460	Sedimentary rock	Kiska	Llanquera (6040-II)
90BSL052b	17.8462	67.5460	Sedimentary rock	Kiska	Llanquera (6040-II)
90BSL053	17.8467	67.5457	Dacite	Kiska	Llanquera (6040-II)
90BSL054	17.3788	67.7776	Dacite	Laurani	Chijmuni (6041-IV)
90BSL055	17.3813	67.7730	Sulfide vein	Laurani	Chijmuni (6041-IV)
90BSL056	17.3854	67.7823	Alt. dacite	Laurani	Chijmuni (6041-IV)
90BSL057	21.2240	67.2317	Granodiorite	Condor Huasi	Estancia Charquini (6130-II)
90BSL058	21.2991	67.2490	Sedimentary rock	Condor Huasi	Estancia Charquini (6130-II)
90BSL059a	21.2960	67.2522	Sedimentary rock	Condor Huasi	Estancia Vena (6130-III)
90BSL059b	21.2960	67.2522	Sedimentary rock	Condor Huasi	Estancia Vena (6130-III)
90BSL060	21.2707	67.2589	Andesite	Condor Huasi	Estancia Vena (6130-III)
90BSL061	21.5165	67.3587	Dacite	Co. Gordo	Estancia Casa Grande (6129-III)
90BSL062	21.5172	67.3580	Jasperoid	Co. Gordo	Estancia Casa Grande (6129-III)
90BSL063	21.6959	67.2250	Bx dike	Kharataka	Comunidad Todos Santos (6128-I)
90BSL064	21.6959	67.2250	Chalcedony vein	Kharataka	Comunidad Todos Santos (6128-I)
90BSL065	21.6950	67.2245	Red jasper	Kharataka	Comunidad Todos Santos (6128-I)
90BSL066	21.7422	67.2108	Stibnite vein	Todos Santos	Comunidad Todos Santos (6128-I)
90BSL067	21.7536	67.2218	Dacite	Todos Santos	Comunidad Todos Santos (6128-I)
90BSL068	21.7460	67.2210	Stibnite vein	Todos Santos	Comunidad Todos Santos (6128-I)
90BSL070	21.7553	67.1531	Sulfide vein	Todos Santos	Comunidad Todos Santos (6128-I)
90BSL071	21.7711	67.1570	Sulfide vein	Todos Santos	Comunidad Todos Santos (6128-I)
90BSL072	21.7651	67.1462	Oxidized vein	Todos Santos	Comunidad Todos Santos (6128-I)
90BSL073	21.7622	67.1441	Dacite	Todos Santos	Comunidad Todos Santos (6128-I)
90BSL074	21.8795	66.9410	Dacite	S.A. de Lipez	San Antonio de Lipez (6228-III)
90BSL075a	21.8593	66.8651	Sulfide vein	Mesa de Plata	San Antonio de Lipez (6228-III)

Table B-1. *Locations and descriptions of samples collected as part of the study of metallic mineral deposits, Altiplano and Cordillera Occidental, Bolivia*–Continued

Sample no.	S. Lat	W. Long	Lithology	Locality	Quadrangle name and no.
90BSL075b	21.8593	66.8651	Sulfide vein	Mesa de Plata	San Antonio de Lipez (6228-III)
90BSL075c	21.8593	66.8651	Sulfide vein	Mesa de Plata	San Antonio de Lipez (6228-III)
90BSL076	21.8669	66.8709	Alt. dacite	Mesa de Plata	San Antonio de Lipez (6228-III)
90BSL077	21.9469	66.7419	Barite vein	Jaquegua	San Antonio de Esmoruco (6228-II)
90BSL079	21.9504	66.7462	Ash-flow tuff	Jaquegua	San Antonio de Esmoruco (6228-II)
90BSL080	21.9605	66.7476	Ash-flow tuff	Jaquegua	San Antonio de Esmoruco (6228-II)
90BSL081	21.9601	66.7497	Barite vein	Jaquegua	San Antonio de Esmoruco (6228-II)
90BSL082	21.9631	66.7418	Barite vein	Jaquegua	San Antonio de Esmoruco (6228-II)
90BSL083	21.9414	66.7407	Dacite	Jaquegua	San Antonio de Esmoruco (6228-II)
90BSL084a	21.6740	66.2778	Sulfide vein	Esmoraca	La Cienega (6328-IV)
90BSL084b	21.6740	66.2778	Sulfide vein	Esmoraca	La Cienega (6328-IV)
90BSL084c	21.6740	66.2778	Sulfide vein	Esmoraca	La Cienega (6328-IV)
90BSL085	21.6740	66.2778	Dacite	Esmoraca	La Cienega (6328-IV)
90BSL086	21.6740	66.2778	Stockwork vein	Esmoraca	La Cienega (6328-IV)
90BSL087	21.6739	66.2778	Stockwork vein	Esmoraca	La Cienega (6328-IV)
90BSL088a	21.6685	66.2945	Sulfide vein	Esmoraca	La Cienega (6328-IV)
90BSL088b	21.6685	66.2945	Sulfide vein	Esmoraca	La Cienega (6328-IV)
90BSL088c	21.6685	66.2945	Sulfide vein	Esmoraca	La Cienega (6328-IV)
90BSL089	21.6706	66.2937	Dacite	Esmoraca	La Cienega (6328-IV)
90BSL090	21.6706	66.2923	Dacite	Esmoraca	La Cienega (6328-IV)
90BSL091	21.6707	66.2910	stockwork vein and bx	Esmoraca	La Cienega (6328-IV)
90BSL092a	21.6717	66.2829	Sulfide vein	Esmoraca	La Cienega (6328-IV)
90BSL092b	21.6717	66.2829	Sulfide vein	Esmoraca	La Cienega (6328-IV)
90BSL093	21.7451	66.2074	River gravel	Río Esmoraca	Esmoraca (6328-I)
90BSL094a	21.6240	66.1824	Sulfide vein	Mina Sucre	Khuchu (6329-II)
90BSL094b	21.6240	66.1824	High-grade sulfide vein	Mina Sucre	Khuchu (6329-II)
90BSL095	21.8430	66.5840	Sulfide vein	Morokho	San Antonio de Esmoruco (6228-II)
90BSL096	21.8392	66.5783	diorite	Morokho	San Antonio de Esmoruco (6228-II)
90BSL097	21.8474	66.5848	Dacite	Morokho	San Antonio de Esmoruco (6228-II)
90BSL098	21.8437	66.5789	Dacite	Morokho	San Antonio de Esmoruco (6228-II)
90BSL099	21.8461	66.5741	Dacite	Morokho	San Antonio de Esmoruco (6228-II)
90BSL100a	21.8488	66.5895	Dacite	Morokho	San Antonio de Esmoruco (6228-II)
90BSL100b	21.8488	66.5728	Dacite	Morokho	San Antonio de Esmoruco (6228-II)
90BSL101	21.8454	66.5836	Dacite bx	Morokho	San Antonio de Esmoruco (6228-II)
90BSL102	21.8372	66.5638	Dacite	Morokho	San Antonio de Esmoruco (6228-II)
90BSL103	21.8392	66.5367	Ash-flow tuff	Morokho	San Antonio de Esmoruco (6228-II)
90BSL104	21.9034	66.4549	Ash-flow tuff	Loma Grande	Pueblo Viejo (6328-III)
90BSL105	21.9034	66.4542	Ash-flow tuff	Loma Grande	Pueblo Viejo (6328-III)
90BSL106	21.9033	66.4533	Ash-flow tuff	Loma Grande	Pueblo Viejo (6328-III)
90BSL107	21.9033	66.4524	Ash-flow tuff	Loma Grande	Pueblo Viejo (6328-III)
90BSL108	21.9033	66.4513	Ash-flow tuff	Loma Grande	Pueblo Viejo (6328-III)
90BSL109	unk	unk	Alunite vein	Kiska	Llanquera (6040-II)
90BSL110	unk	unk	Alunite vein	Kori Kollo	Soledad (6140-IV)
90BSL115	21.8213	66.4913	Alt. dacite	Co. Colorado	La Cienega (6328-IV)
90BSL116	21.8219	66.4794	Alt. dacite	Co. Colorado	La Cienega (6328-IV)
90BSL117	21.8188	66.4600	Alt. dacite	Co. Colorado	La Cienega (6328-IV)
90BSL118	21.6016	66.5426	Alt. dacite	Co. Sta. Isabel	Cerro Santa Isabel (6229-II)
90BSL119	16.9823	68.4707	Bx with Fe-oxide matrix	Pachekala	Collana (5943-III)
90BSL120	16.9923	68.4627	Bx with Fe-oxide matrix	Pachekala	Collana (5943-III)
90BSL121	16.9923	68.4627	Bx with Fe-oxide matrix	Pachekala	Collana (5943-III)
PNZ001	unk	unk	Ash-flow tuff	Panizos Caldera	Cerro Chinci Jarán (6227-I)
PNZ002	unk	unk	Ash-flow tuff	Panizos Caldera	Cerro Chinci Jarán (6227-I)
PNZ003	unk	unk	Ash-flow tuff	Panizos Caldera	Cerro Chinci Jarán (6227-I)
PNZ004	unk	unk	Ash-flow tuff	Panizos Caldera	Cerro Chinci Jarán (6227-I)
PNZ005	unk	unk	Ash-flow tuff	Panizos Caldera	Cerro Chinci Jarán (6227-I)
PNZ006	21.9919	66.4735	Ash-flow tuff	Panizos Caldera	Pueblo Viejo (6328-III)
PNZ007	21.9919	66.4735	Ash-flow tuff	Panizos Caldera	Pueblo Viejo (6328-III)
PNZ008	17.0246	68.4602	Ash-flow tuff	Panizos Caldera	San Antonio de Esmoruco (6228-II)
PNZ009	17.0246	68.4602	Ash-flow tuff	Panizos Caldera	San Antonio de Esmoruco (6228-II)
PNZ010	17.0246	68.4602	Ash-flow tuff	Panizos Caldera	San Antonio de Esmoruco (6228-II

Table B-2. *Quantitative analyses of rock samples collected as part of the study of metallic mineral deposits, Altiplano and Cordillera Occidental, Bolivia*

[All values in ppm. [1]Au represents gold determined by flame or graphite furnace AAS. [2]Au, As, Bi, Cd, Sb, Zn, Cu, Pb, Ag, and Mo analyzed by peroxide dissolution ICP-AES. Leaders (--) indicate the sample was not analyzed for that element]

Sample No.	[1]Au	[2]Au	As	Bi	Cd	Sb	Zn	Cu	Pb	Ag	Mo
90BAH006	<0.002	<1.5	100	<6	6	440	4800	600	19000	560	2.3
90BAH015a	0.2	<1.5	790	160	0.41	7700	40	49	180	400	1.8
90BAH015b	0.002	<1.5	85	<6	0.37	310	25	<0.3	45	51	<0.9
90BAH015c	<0.004	<1.5	33	<6	<0.3	20	29	<0.3	<6	<0.45	<0.9
90BAH015d	<0.002	<1.5	210	<6	0.67	3800	36	4.1	3400	33	<0.9
90BAN030	0.15	<1.5	150	29	0.33	82	30	21	1500	2100	7.2
90BAN031	0.008	<0.15	49	110	1.2	160	160	15	370	9.7	1.3
90BAN032	0.02	<0.15	35	7.7	0.15	9.3	11	13	430	4.2	1.4
90BAN033	0.1	<0.15	450	4.6	1.4	100	450	1200	3800	35	12
90BAN034	0.1	<0.15	65	66	5.3	18	790	220	720	26	1.8
90BAN035	0.026	<0.15	100	4	0.19	3	46	42	770	7	8.4
90BAN037	0.7	<1.5	96	53	540	7000	3600	48	68000	400	4
90BAN039	0.004	<0.15	57	2.5	0.28	49	70	140	460	6.8	3.1
90BAN040	0.004	<0.15	14	<0.6	0.054	48	15	7.1	2800	3.7	<0.09
90BBG003	<0.002	--	--	--	--	--	--	--	--	--	--
90BBG004	<0.002	--	--	--	--	--	--	--	--	--	--
90BBG005a	<0.002	--	--	--	--	--	--	--	--	--	--
90BBG005b	<0.002	--	--	--	--	--	--	--	--	--	--
90BBG006b	<0.002	--	--	--	--	--	--	--	--	--	--
90BBG006c	<0.002	--	--	--	--	--	--	--	--	--	--
90BBG007	<0.002	--	--	--	--	--	--	--	--	--	--
90BBG008	<0.002	--	--	--	--	--	--	--	--	--	--
90BBG009a	<0.002	--	--	--	--	--	--	--	--	--	--
90BBG009b	<0.002	--	--	--	--	--	--	--	--	--	--
90BBG010a	<0.002	--	--	--	--	--	--	--	--	--	--
90BBG010b	<0.002	--	--	--	--	--	--	--	--	--	--
90BBG011a	0.008	--	--	--	--	--	--	--	--	--	--
90BBG011b	0.1	--	--	--	--	--	--	--	--	--	--
90BBG012	<0.002	--	--	--	--	--	--	--	--	--	--
90BBG014	<0.002	--	--	--	--	--	--	--	--	--	--
90BBG014	0.002	<0.15	13	1	0.093	0.63	17	13	35	0.17	3.7
90BBG015a	<0.002	--	--	--	--	--	--	--	--	--	--
90BBG015b	<0.002	--	--	--	--	--	--	--	--	--	--
90BBG015c	<0.002	--	--	--	--	--	--	--	--	--	--
90BBG016a	<0.002	--	--	--	--	--	--	--	--	--	--
90BBG016b	<0.002	--	--	--	--	--	--	--	--	--	--
90BBG018a	<0.002	--	--	--	--	--	--	--	--	--	--
90BBG018b	<0.002	--	--	--	--	--	--	--	--	--	--
90BBG018c	<0.002	--	--	--	--	--	--	--	--	--	--
90BBG018d	<0.002	--	--	--	--	--	--	--	--	--	--
90BBG018e	<0.002	<0.15	3.1	<0.6	0.13	<0.6	32	12	44	0.59	1.1
90BBG020	<0.002	--	--	--	--	--	--	--	--	--	--
90BBG021	<0.002	--	--	--	--	--	--	--	--	--	--
90BBG022a	<0.002	--	--	--	--	--	--	--	--	--	--
90BBG023	<0.002	--	--	--	--	--	--	--	--	--	--
90BBG025a	<0.002	--	--	--	--	--	--	--	--	--	--
90BBG025b	<0.002	--	--	--	--	--	--	--	--	--	--
90BBG025c	<0.002	--	--	--	--	--	--	--	--	--	--
90BBG026	<0.002	--	--	--	--	--	--	--	--	--	--
90BBG029	0.024	--	--	--	--	--	--	--	--	--	--
90BBG030	0.004	--	--	--	--	--	--	--	--	--	--
90BBG031	0.006	--	--	--	--	--	--	--	--	--	--
90BBG032a	0.004	--	--	--	--	--	--	--	--	--	--
90BBG032b	0.038	--	--	--	--	--	--	--	--	--	--
90BBG032c	0.018	--	--	--	--	--	--	--	--	--	--

Table B-2. *Quantitative analyses of rock samples collected as part of the study of metallic mineral deposits, Altiplano and Cordillera Occidental, Bolivia*--Continued

Sample No.	[1]Au	[2]Au	As	Bi	Cd	Sb	Zn	Cu	Pb	Ag	Mo
90BBG033a	<0.002	<0.15	2.9	<0.6	0.053	<0.6	5.6	0.68	5.1	<0.045	0.25
90BBG033b	<0.002	<0.15	<0.60	<0.6	<0.03	<0.6	0.96	0.82	<0.6	<0.045	0.3
90BBG034	0.004	<0.15	2.8	<0.6	0.18	0.69	180	310	27	0.32	0.38
90BBG040	<0.002	<0.15	3.7	<0.6	0.11	<0.6	36	9.3	24	0.16	1.2
90BBG045	<0.002	<0.15	19	<0.6	0.45	2.9	59	12	52	2.1	1.1
90BBG046a	<0.002	<0.15	2.9	<0.6	0.85	<0.6	160	25	61	0.19	0.25
90BBG046b	<0.002	<0.15	1.1	<0.6	0.65	<0.6	98	3.3	39	0.27	0.47
90BBG047	0.55	<0.15	91	9.6	28	23	>1700	360	6500	1000	4.5
90BBG048a	0.1	<0.15	120	<0.6	38	<0.6	>1700	330	1100	82	5.8
90BBG049	0.85	<1.5	140	<6	250	86	5800	1400	59000	1400	9.2
90BBG050b	0.004	<0.15	3.9	3.4	2	0.96	390	14	440	11	13
90BBG051a	0.65	<1.5	560	48	0.66	50	110	4500	320	86	<0.9
90BBG051b	0.9	<15	8100	<60	<3	640	47	30000	550	450	<9
90BBG052a	2.1	<1.5	8.3	<6	870	39	3300	130	98000	20	<0.9
90BBG052b	0.006	<0.15	19	<0.6	8.2	0.64	1100	18	310	1.4	0.53
90BBG052d	1.05	<1.5	<6	<6	300	46	500	2000	110000	1200	<0.9
90BBG053a	0.05	<1.5	20	<6	840	33	5000	6.3	85000	14	<0.9
90BBG053b	0.002	<0.15	<0.60	<0.6	2.1	<0.6	550	8	250	0.87	0.5
90BBG054	0.01	<0.15	<0.60	<0.6	14	<0.6	>1700	8.8	1900	<0.045	0.87
90BBG055a	<0.002	<0.15	330	1.6	0.47	13	38	91	87	0.32	1.9
90BBG056a	<0.002	<0.15	<0.60	<0.6	0.092	<0.6	29	4	38	0.18	0.34
90BBG056b	<0.002	<0.15	<0.60	<0.6	0.71	<0.6	110	15	9.3	0.059	0.45
90BBG057	<0.002	<0.15	32	<0.6	0.66	<0.6	>1700	1.1	530	<0.045	0.7
90BBG058b	0.1	<0.15	390	5.9	2.4	27	40	350	420	150	0.72
90BBG058c	0.002	<0.15	<0.60	<0.6	9.4	0.65	>1700	100	8.5	0.29	3.2
90BBG059	<0.002	<0.15	<0.60	<0.6	0.094	<0.6	69	17	8.2	0.18	0.36
90BBR003	<0.002	--	--	--	--	--	--	--	--	--	--
90BBR004	<0.002	--	--	--	--	--	--	--	--	--	--
90BBR015	<0.002	--	--	--	--	--	--	--	--	--	--
90BBR016	<0.002	--	--	--	--	--	--	--	--	--	--
90BBR021a	<0.002	--	--	--	--	--	--	--	--	--	--
90BBR021b	<0.002	--	--	--	--	--	--	--	--	--	--
90BBR021c	<0.002	--	--	--	--	--	--	--	--	--	--
90BBR021d	<0.002	--	--	--	--	--	--	--	--	--	--
90BBR026	<0.002	--	--	--	--	--	--	--	--	--	--
90BBR029	<0.002	--	--	--	--	--	--	--	--	--	--
90BBR036a	<0.002	--	--	--	--	--	--	--	--	--	--
90BBR036c	<0.002	--	--	--	--	--	--	--	--	--	--
90BBR036d	<0.002	--	--	--	--	--	--	--	--	--	--
90BBR036e	<0.002	--	--	--	--	--	--	--	--	--	--
90BBR036h	<0.002	--	--	--	--	--	--	--	--	--	--
90BBR041	<0.002	<0.15	<0.60	<0.6	0.036	<0.6	52	15	3	<0.045	0.5
90BBR048a	<0.002	<0.15	<0.60	<0.6	0.25	<0.6	15	25	5.4	0.55	1.1
90BBR050	<0.002	<0.15	12	0.8	<0.03	<0.6	9.3	3.8	15	0.34	0.77
90BBR051	<0.002	<0.15	3.7	<0.6	0.11	<0.6	8.5	3	4.9	<0.045	0.32
90BBR054a	<0.002	<0.15	3.8	<0.6	<0.03	<0.6	5.8	1.5	12	<0.045	1.8
90BBR055	<0.002	<0.15	12	<0.6	0.049	1.2	8	6.8	14	0.7	1.6
90BBR058c	<0.002	<0.15	2.1	<0.6	<0.03	<0.6	2.5	2.7	4.4	<0.045	6.6
90BBR063	0.074	<0.15	96	<0.6	0.48	14	190	120	6100	65	130
90BCX003	--	<0.15	19	<0.6	6.5	<0.6	620	250	180	0.33	3.1
90BCX004	--	<18	<72	<72	<3.6	<72	<3.6	62000	160	<5.4	<11
90BCX007	0.002	--	--	--	--	--	--	--	--	--	--
90BCX008a	--	<0.15	40	<0.6	0.058	0.66	86	69	33	<0.045	2.9
90BCX008b	--	<0.15	44	<0.6	0.35	0.73	34	260	140	<0.045	0.96
90BCX009	--	<0.15	3.2	<0.6	<0.03	<0.6	53	36	19	<0.045	0.59

Table B-2. *Quantitative analyses of rock samples collected as part of the study of metallic mineral deposits, Altiplano and Cordillera Occidental, Bolivia*--Continued

Sample No.	[1]Au	[2]Au	As	Bi	Cd	Sb	Zn	Cu	Pb	Ag	Mo
90BCX010	--	<0.15	6.3	<0.6	<0.03	<0.6	22	100	12	<0.045	0.88
90BCX012	--	<0.15	2.4	<0.6	0.21	<0.6	15	36	10	<0.045	19
90BCX013a	--	<0.15	3.8	<0.6	<0.03	0.7	21	920	60	<0.045	0.89
90BCX013b	--	<22	<86	<86	<4.3	<86	<4.3	55000	<86	<6.5	<13
90BCX014	0.012	--	--	--	--	--	--	--	--	--	--
90BCX015	<0.002	<0.15	17	<0.6	0.86	0.84	120	19	450	<0.045	21
90BCX017	<0.002	--	--	--	--	--	--	--	--	--	--
90BCX018	<0.002	--	--	--	--	--	--	--	--	--	--
90BCX019a	<0.002	--	--	--	--	--	--	--	--	--	--
90BCX019b	--	<0.15	<0.60	<0.6	0.11	<0.6	17	260	12	<0.045	0.16
90BCX019c	--	<0.15	8.5	<0.6	23	1	30	630	73	<0.045	5.8
90BCX020	--	<0.15	67	<0.6	0.28	<0.6	90	54	16	<0.045	4.7
90BCX022a	--	<25	<100	<100	<5.1	<100	<5.1	55000	<100	<7.6	<15
90BCX022b	<0.002	<0.15	<0.60	<0.6	0.081	<0.6	31	15	7.6	<0.045	0.23
90BCX023	<0.002	--	--	--	--	--	--	--	--	--	--
90BCX023b	<0.002	<0.15	2.5	<0.6	0.3	<0.6	31	49	14	<0.045	1.7
90BCX026	<0.002	--	--	--	--	--	--	--	--	--	--
90BCX027	0.04	<9.5	<38	<38	4600	1800	110	1100	70000	1200	<5.7
90BCX028	<0.002	<0.15	21	<0.6	1.2	1.4	51	7.5	120	0.14	0.55
90BCX029	<0.002	<28	<110	<110	<5.7	<110	18	97000	370	38	<17
90BCX030a	<0.002	--	--	--	--	--	--	--	--	--	--
90BCX030b	<0.002	--	--	--	--	--	--	--	--	--	--
90BCX031	--	<22	420	<86	120	<86	<4.3	48000	<86	20	<13
90BCX032	--	<22	<86	<86	<4.3	<86	<4.3	53000	<86	<6.5	<13
90BDB002	<0.002	<0.15	10	<0.6	<0.03	3.8	20	12	9.5	<0.045	0.58
90BDB008	--	<0.15	<0.6	3.5	<0.03	0.78	64	19	19	<0.045	0.41
90BDB009	--	<0.15	1.1	<0.6	<0.03	<0.6	24	11	2.7	<0.045	0.44
90BDB010	--	<0.15	1.3	<0.6	<0.03	<0.6	11	3.1	2.1	<0.045	0.6
90BDB011	--	<0.15	<0.60	<0.6	0.06	<0.6	34	8.1	1.8	<0.045	0.52
90BDB012	--	<0.15	0.79	<0.6	<0.03	0.66	22	24	1.5	<0.045	0.16
90BDB013	--	<0.15	0.78	<0.6	0.035	0.62	23	47	4.6	<0.045	0.91
90BDB014	<0.002	<0.15	330	14	6.5	92	480	130	12000	38	11
90BDB015	<0.002	<0.15	320	38	2	57	310	28	3300	11	3.5
90BDR001b	--	<0.15	<0.60	<0.6	0.043	1.6	20	9.9	21	0.18	0.19
90BDR001a	0.026	<0.15	74	1.6	0.59	28	12	9.1	110	9.9	0.73
90BDR005	--	<0.15	<0.60	<0.6	0.068	1.3	20	2.4	15	0.064	0.24
90BDR006	--	<0.15	<0.60	<0.6	0.072	1.2	60	1.6	15	0.087	0.11
90BDR007	<0.002	<0.15	260	16	0.52	47	550	57	14000	24	0.83
90BDR008a	<0.002	<0.15	4.1	<0.6	3.2	1	340	0.82	87	0.25	3.2
90BDR008b	<0.002	<0.15	6.7	<0.6	3.7	2.4	770	1.8	310	0.68	1.4
90BDR009	<0.002	<0.15	130	0.81	7.9	49	1300	85	4900	48	3.2
90BDR010	<0.002	<0.15	6.5	<0.6	1.6	13	520	21	790	14	1.4
90BDR012	--	<0.15	15	<0.6	0.26	0.68	39	8.5	5.5	<0.045	0.45
90BDR015	--	<0.15	3.8	<0.6	0.049	<0.6	16	4.2	7	<0.045	0.75
90BDR016	<0.002	<0.15	<0.60	<0.6	0.066	<0.6	12	3	6.3	<0.045	0.44
90BDR022	<0.002	<0.15	13	<0.6	0.66	21	25	4.5	3400	8.5	0.44
90BDR025	<0.002	<0.15	1.1	<0.6	1.7	1.5	270	3.7	72	0.23	0.35
90BDR029	0.014	<1.5	1100	<6	1300	1100	>17000	410	64000	2600	21
90BDR029a	<0.002	<1.5	480	9.3	30	6.1	7400	26	3100	30	2.8
90BDR030	<0.002	--	--	--	--	--	--	--	--	--	--
90BDR031	<0.002	--	--	--	--	--	--	--	--	--	--
90BDR034	<0.002	--	--	--	--	--	--	--	--	--	--
90BDR034a	<0.002	<1.5	150	<6	77	34	8000	120	1500	580	6.3
90BDR034c	0.022	<1.5	5200	<6	0.49	2100	340	71	360000	83	<0.9
90BDR034d	<0.002	<7.5	300	120	3.3	150	920	88000	410	24	4.6

Table B-2. *Quantitative analyses of rock samples collected as part of the study of metallic mineral deposits, Altiplano and Cordillera Occidental, Bolivia*--Continued

Sample No.	[1]Au	[2]Au	As	Bi	Cd	Sb	Zn	Cu	Pb	Ag	Mo
90BDR035	<0.002	--	--	--	--	--	--	--	--	--	--
90BDR035a	<0.002	<7.5	<30	180	<1.5	190	140	160000	1200	30	<4.5
90BDR037	<0.002	--	--	--	--	--	--	--	--	--	--
90BDR038	<0.002	--	--	--	--	--	--	--	--	--	--
90BDR039	<0.002	--	--	--	--	--	--	--	--	--	--
90BDR040a	<0.002	<1.5	75	9.2	0.44	11	54	2000	270	1.7	<0.9
90BDR040b	<0.002	<1.5	15	<6	0.42	<6	25	61	130	<0.45	<0.9
90BDR040c	<0.002	<1.5	15	<6	0.53	<6	25	<0.3	56	<0.45	<0.9
90BDR041	<0.002	--	--	--	--	--	--	--	--	--	--
90BDR041a	<0.002	--	--	--	--	--	--	--	--	--	--
90BDR042	<0.002	--	--	--	--	--	--	--	--	--	--
90BDR043	<0.002	--	--	--	--	--	--	--	--	--	--
90BDR044	<0.002	--	--	--	--	--	--	--	--	--	--
90BDR046	<0.002	--	--	--	--	--	--	--	--	--	--
90BDR051a	0.014	<1.5	20	<6	1.3	<6	64	<0.3	400	8.7	<0.9
90BDR051b	0.002	<1.5	66	<6	1.2	6.7	39	<0.3	140	1.4	<0.9
90BDR051c	0.016	<1.5	160	<6	2200	370	>17000	1900	140000	410	14
90BDR052	0.046	<1.5	500	<6	1800	2800	35000	2500	360000	950	7.5
90BDR053	<0.002	--	--	--	--	--	--	--	--	--	--
90BDR054	<0.002	--	--	--	--	--	--	--	--	--	--
90BDR054a	<0.002	<7.5	<30	87	16	120	940	78000	2600	92	<4.5
90BDR055	<0.002	--	--	--	--	--	--	--	--	--	--
90BDR057	<0.002	--	--	--	--	--	--	--	--	--	--
90BDR058	<0.002	<1.5	380	190	1.5	650	380	370	510	70	<0.9
90BDR058b	0.6	<1.5	140	120000	38	190	4200	15000	58000	15000	<0.9
90BDR058c	<0.002	--	--	--	--	--	--	--	--	--	--
90BDR060	0.012	<1.5	970	26000	7.7	160	1000	24000	5200	490	18
90BDR060b	<0.002	--	--	--	--	--	--	--	--	--	--
90BDR061	0.55	<1.5	5200	110	490	46	>17000	550	950	30	16
90BDR061a	0.028	<1.5	8400	<6	2900	1500	>17000	390	150000	1200	16
90BDR061b	0.038	<1.5	1500	58	620	60	>17000	120	4700	29	7.3
90BDR061c	<0.002	--	--	--	--	--	--	--	--	--	--
90BDR062	0.002	<1.5	140	17	4.1	<6	330	19	170	2.9	<0.9
90BEB001	44	<1.5	14	<6	0.42	<6	84	12	<6	<0.45	<0.9
90BEB002a	<0.002	<1.5	620	<6	3.9	84	750	110	3900	1000	2.4
90BEB003a	<0.002	<1.5	390	<6	0.34	<6	25	4.2	790	1.4	<0.9
90BEB003b	<0.002	<1.5	72	<6	0.35	<6	23	3.4	120	0.64	1.2
90BEB003d	<0.002	<1.5	900	<6	0.41	6.7	41	3.6	340	<0.45	<0.9
90BEB005a	<0.002	<1.5	720	140	19	770	3400	1100	9100	330	9.3
90BEB005b	<0.002	<1.5	580	61	1.8	120	200	140	1600	62	2.3
90BEB005c	<0.002	<1.5	570	180	2.5	89	260	190	1000	41	1.7
90BEB005d	<0.002	<1.5	210	68	1.4	64	640	100	4900	46	1.4
90BES001	<0.002	--	--	--	--	--	--	--	--	--	--
90BES002	0.014	--	--	--	--	--	--	--	--	--	--
90BES003	<0.002	--	--	--	--	--	--	--	--	--	--
90BES004	<0.002	--	--	--	--	--	--	--	--	--	--
90BES005	<0.002	--	--	--	--	--	--	--	--	--	--
90BES006	<0.002	<0.15	2.3	<0.6	0.12	<0.6	12	25	220	3.1	0.61
90BES007	<0.002	<0.15	1.2	<0.6	0.039	<0.6	18	40	20	2.8	1.5
90BES008	0.066	<0.15	17	2.2	0.34	<0.6	44	3.9	55	13	0.68
90BES009	0.25	<0.15	<0.60	<0.6	0.19	<0.6	14	37	54	390	0.51
90BES010	<0.002	<0.15	<0.60	<0.6	0.31	<0.6	230	20	55	2.1	0.56
90BES011	--	<0.15	0.85	<0.6	0.094	<0.6	32	25	7.6	<0.045	0.35
90BES012	--	<0.15	<0.60	<0.6	<0.03	<0.6	22	31	6.9	<0.045	0.18
90BES013	--	<0.15	<0.60	<0.6	<0.03	<0.6	24	24	4.6	<0.045	0.28

Table B-2. *Quantitative analyses of rock samples collected as part of the study of metallic mineral deposits, Altiplano and Cordillera Occidental, Bolivia*--Continued

Sample No.	[1]Au	[2]Au	As	Bi	Cd	Sb	Zn	Cu	Pb	Ag	Mo
90BES014	<0.002	--	--	--	--	--	--	--	--	--	--
90BES015	<0.004	--	--	--	--	--	--	--	--	--	--
90BES016	<0.002	--	--	--	--	--	--	--	--	--	--
90BES029	<0.002	<0.15	20	2.3	<0.03	<0.6	2	18	3.8	0.42	0.62
90BES030	<0.002	<0.15	8.9	1.1	<0.03	<0.6	3.3	5.2	32	0.24	0.17
90BES031	<0.002	<0.15	<0.60	<0.6	<0.03	<0.6	35	17	2.9	0.059	0.16
90BES032	0.008	<0.15	<0.60	<0.6	0.032	<0.6	7.1	31	26	0.28	3.5
90BES033	<0.002	--	--	--	--	--	--	--	--	--	--
90BES034	<0.002	--	--	--	--	--	--	--	--	--	--
90BES035	<0.002	--	--	--	--	--	--	--	--	--	--
90BES036	<0.002	--	--	--	--	--	--	--	--	--	--
90BES037	<0.002	<0.15	1	<0.6	0.049	<0.6	26	7.8	3.6	<0.045	0.79
90BES039	<0.002	<0.15	<0.60	<0.6	<0.03	<0.6	<0.03	<0.03	1	<0.045	<0.09
90BES040	<0.002	<0.15	<0.60	<0.6	<0.03	<0.6	<0.03	<0.03	1.1	<0.045	<0.09
90BES041	<0.002	<0.15	1.1	<0.6	<0.03	<0.6	1.6	0.71	1.8	<0.045	0.25
90BES042	<0.002	<0.15	<0.60	<0.6	<0.03	<0.6	1.1	0.25	1.2	<0.045	<0.09
90BES043	<0.002	<0.15	0.7	<0.6	<0.03	<0.6	1.6	0.058	1.4	<0.045	0.29
90BES044	<0.002	<0.15	4.6	<0.6	0.11	<0.6	15	2.3	5.1	<0.045	0.77
90BES045	0.004	<0.15	240	<0.6	15	1.4	320	4.5	1.5	<0.045	8.1
90BES046	0.006	<0.15	<0.60	<0.6	<0.03	<0.6	0.79	0.19	20	2.9	0.11
90BES047	<0.002	<0.15	2.5	<0.6	<0.03	0.94	18	2.1	110	1.2	0.62
90BES048	<0.002	<0.15	0.79	<0.6	0.59	<0.6	85	11	2.2	<0.045	0.58
90BES049	<0.004	<0.15	4.6	<0.6	0.39	1.6	160	0.89	7.6	<0.045	<0.09
90BES050	0.2	<0.15	53	<0.6	100	13	>1300	260	7100	25	3.8
90BES051	0.028	<0.15	28	<0.6	0.097	62	28	18	280	150	6.3
90BES052	0.3	<0.15	130	1.1	0.08	18	36	190	3300	14	1.9
90BES053	1.2	<1.5	17	<6	160	12	9300	990	7200	22	3.9
90BES054	0.4	<1.5	35	14	48	12	4900	6900	980	67	2.8
90BES055	0.008	<1.5	8.1	<6	<0.3	180	170	25	51000	7.5	<0.9
90BES056	0.006	<0.15	27	<0.6	1.7	4.5	330	140	2200	4.3	17
90BES057	<0.002	<0.15	17	<0.6	1.6	0.98	300	2.7	550	0.66	0.32
90BES058	0.016	<0.15	7.3	<0.6	96	<0.6	>1300	22	260	0.14	11
90BES059	0.002	<0.15	1.4	<0.6	<0.03	<0.6	67	16	5	<0.045	1.1
90BES060	<0.002	<0.15	<0.60	<0.6	0.044	<0.6	5.1	0.9	3.3	<0.045	0.17
90BES061	<0.002	<0.15	1.8	<0.6	0.084	<0.6	10	0.92	8.7	<0.045	0.36
90BES062	<0.002	<0.15	<0.60	<0.6	<0.03	<0.6	3.6	0.18	3.1	<0.045	0.34
90BES063	<0.002	<0.15	0.91	<0.6	<0.03	<0.6	4.9	1.8	8	0.07	0.54
90BES064	<0.002	<0.15	<0.60	<0.6	0.046	<0.6	6.2	0.36	3.1	<0.045	0.14
90BES065	<0.002	<0.15	<0.60	<0.6	<0.03	<0.6	3.7	0.057	2.9	<0.045	0.18
90BES066	<0.002	<0.15	1.1	<0.6	0.08	<0.6	32	5.4	1.7	<0.045	0.2
90BES067	<0.002	<0.15	0.81	<0.6	<0.03	<0.6	22	7.5	1.6	<0.045	0.26
90BES069	<0.002	<0.15	<0.60	<0.6	0.033	<0.6	4.4	0.22	4.7	<0.045	<0.09
90BSL001	2.8	2.1	940	27	<0.03	100	2.8	8.8	780	11	0.54
90BSL002	1.8	1.2	17	3	0.095	11	13	10	50	12	0.34
90BSL003	0.1	0.16	11	0.76	0.035	12	1.4	1.8	9.9	6.7	0.51
90BSL004	--	<0.15	2.2	<0.6	0.038	0.77	40	1.1	3.9	<0.045	0.3
90BSL005	--	<0.15	110	51	<0.03	44	<0.03	10	19	3.2	9.6
90BSL006	0.022	0.2	46	5.2	<0.03	2.2	<0.03	8	14	0.15	0.9
90BSL007	0.02	<0.15	200	15	<0.03	6.2	1.5	14	14	0.54	0.92
90BSL009	0.026	<0.15	420	2.7	0.49	73	15	19	94	16	0.13
90BSL010	0.012	<0.15	110	1.4	0.15	68	5.7	6.1	75	0.84	0.36
90BSL012	<0.002	<0.15	1.5	<0.6	0.041	1.2	4.7	2.2	19	0.055	0.2
90BSL013	9	--	--	--	--	--	--	--	--	--	--
90BSL014	0.02	<0.15	110	<0.6	3.5	65	280	39	1100	9.2	0.2
90BSL030	0.012	<0.15	80	7.4	0.097	4.5	16	5.6	400	2.8	1.4

Table B-2. *Quantitative analyses of rock samples collected as part of the study of metallic mineral deposits, Altiplano and Cordillera Occidental, Bolivia*--Continued

Sample No.	[1]Au	[2]Au	As	Bi	Cd	Sb	Zn	Cu	Pb	Ag	Mo
90BSL031	0.034	<0.17	320	1.8	0.17	21	26	19	1700	8.8	2
90BSL032	2.8	1.7	490	<6	<0.3	4300	1.3	15	37000	35	<0.9
90BSL033	--	--	--	--	--	--	--	--	--	--	--
90BSL034	--	--	--	--	--	--	--	--	--	--	--
90BSL035	1.55	1.5	800	3.1	<0.03n	190	1.1	42	1100	12	1.6
90BSL036	4.7	3.4	710	19	0.28	57	26	11	5200	46	0.92
90BSL037	0.012	<0.15	34	1.5	1.4	7.4	16	7.8	33	0.5	0.69
90BSL038a	0.35	<1.5	390	<6	2.4	71	120	57	260	7.7	4.7
90BSL039	12	<1.5	3200	6200	2.6	13000	200	8300	11000	86	<0.9
90BSL040	--	--	--	--	--	--	--	--	--	--	--
90BSL041a	36	10	4200	<6	720	61000	>14000	4300	170000	180	1.5
90BSL042	0.1	<0.15	660	3.1	16	29	1200	20	200	2.7	0.97
90BSL043	0.002	<0.15	35	<0.6	4	3.9	790	9.6	730	1.3	0.65
90BSL044	<0.002	<0.15	14	2	3.2	47	430	42	29	1.3	3.4
90BSL045	0.004	<0.15	54	<0.6	9.2	12	1300	4.2	80	0.48	0.78
90BSL046	--	--	--	--	--	--	--	--	--	--	--
90BSL047	--	--	--	--	--	--	--	--	--	--	--
90BSL048	--	--	--	--	--	--	--	--	--	--	--
90BSL049a	3.1	<1.5	1500	6400	1.1	8900	75	3300	1900	2100	<0.9
90BSL049b	0.75	<15	5900	2300	12	14000	1300	27000	620	2100	<9
90BSL050	--	--	--	--	--	--	--	--	--	--	--
90BSL051	--	--	--	--	--	--	--	--	--	--	--
90BSL052a	0.044	<0.15	61	9.5	0.084	13	4.8	11	33	1.1	17
90BSL053	0.016	<0.15	46	8.1	0.032	1.7	1.7	23	20	0.14	4.9
90BSL054	--	--	--	--	--	--	--	--	--	--	--
90BSL055	1.2	<15	890	<60	3.3	1100	130	22000	520	38	<9
90BSL056	0.004	<0.15	91	0.83	<0.03	8.8	7.1	98	16	0.37	0.41
90BSL057	--	<0.15	17	<0.6	0.16	<0.6	32	8.2	1.7	<0.045	0.24
90BSL058	<0.002	<0.15	780	1.2	0.43	3.1	13	68	150	0.59	7.6
90BSL059b	<0.002	<0.15	2700	1.2	1.9	21	270	52	18	<0.045	8.5
90BSL059a	0.002	<0.15	810	1.4	0.078	12	180	52	25	<0.045	2.6
90BSL060	--	<0.15	7.3	<0.6	0.056	<0.6	540	28	2.5	0.059	2.6
90BSL061	<0.002	<0.15	52	<0.6	0.6	<0.6	120	14	9.3	<0.045	2.7
90BSL062	<0.002	<0.15	110	<0.6	1.3	<0.6	27	9.1	10	<0.045	12
90BSL063	<0.002	<0.15	86	0.69	0.94	9.9	30	15	25	<0.045	0.56
90BSL064	<0.002	<0.15	13	<0.6	0.43	<0.6	3.7	1.4	2.6	<0.045	0.22
90BSL065	<0.002	<0.15	32	<0.6	<0.03	<0.6	4.2	5.8	1.5	<0.045	0.67
90BSL066	0.05	<0.15	2500	<0.6	5.3	840	850	48	1100	13	660
90BSL067	--	<0.15	1.5	<0.6	0.12	<0.6	52	1.2	2.8	<0.045	0.32
90BSL068	3.3	<1.5	<6	<6	<0.3	86000	<0.3	180	1100	32	<0.9
90BSL070	0.01	<1.5	14	<6	1600	380	8800	440	49000	39	8.5
90BSL071	<0.002	<1.5	<6	<6	5900	110	300	250	100000	390	<0.9
90BSL072	0.004	<0.15	130	<0.6	150	43	>1600	82	920	59	3
90BSL073	--	<0.15	2.7	<0.6	<0.03	<0.6	77	33	3.7	0.048	0.81
90BSL074	--	<0.15	3.8	0.96	0.95	<0.6	140	22	21	0.097	0.27
90BSL076	<0.002	<0.15	240	<0.6	3.9	170	160	3.4	1400	0.9	1.8
90BSL077	<0.002	<0.15	30	1.6	3.8	26	430	9	3400	150	0.45
90BSL079	--	<0.15	23	1.1	0.11	0.98	53	10	27	0.051	0.45
90BSL080	<0.002	<0.15	280	<0.6	0.71	96	>1600	38	11000	11	5.3
90BSL081	<0.002	<1.5	300	<6	36	230	2300	65	37000	340	1.1
90BSL082	0.014	<1.5	<6	<6	6.4	800	<0.3	<0.3	130000	390	<0.9
90BSL083	--	<0.15	6.3	<0.6	0.11	50	13	3.9	55	0.29	0.45
90BSL084a	1.2	<1.5	160	24000	1.2	120	320	8400	2500	5.9	7.3
90BSL084b	1.5	<1.5	540	61000	<0.3	290	140	5200	2800	4.6	5.2
90BSL084c	0.1	<1.5	74	530	<0.3	44	130	6300	70	4.7	25

Table B-2. *Quantitative analyses of rock samples collected as part of the study of metallic mineral deposits, Altiplano and Cordillera Occidental, Bolivia*--Continued

Sample No.	[1]Au	[2]Au	As	Bi	Cd	Sb	Zn	Cu	Pb	Ag	Mo
90BSL085	<0.002	<0.15	20	20	0.3	7.5	130	44	50	0.27	1
90BSL086	0.15	<0.15	140	1000	0.26	32	180	350	770	13	3.1
90BSL087	.0200N	<0.15	35	12	0.25	14	96	41	49	0.1	2.2
90BSL088a	0.004	<0.15	15	22	<0.03	3.8	2.7	3.3	20	2.3	0.73
90BSL088b	0.004	<0.15	43	6.3	0.091	8.2	6.1	12	85	0.63	6.1
90BSL088c	2.1	<6	120	9000	<1.2	37	23	12000	100	22	4.6
90BSL089	0.002	<0.15	<0.60	<0.6	<0.03	<0.6	3.6	3.9	2.8	0.08	<0.09
90BSL090	--	<0.15	1.5	<0.6	0.33	0.75	250	34	2.8	0.09	0.15
90BSL091	<0.002	<0.15	63	35	<0.03	4.6	11	29	17	0.43	0.66
90BSL092a	15	20	60	88	<0.3	37	75	6400	69	14	50
90BSL094a	100	75	<6	<6	<0.3	91000	<0.3	27	75	0.75	<0.9
90BSL094b	3.5	<15	<60	<60	3.8	250000	1100	<3	970	<4.5	<9
90BSL095	0.028	<1.5	1300	<6	350	9100	>16000	88	21000	320	14
90BSL097	0.004	<0.15	760	1.3	0.25	180	37	5.6	26	2.4	0.74
90BSL098	0.002	<0.15	920	<0.6	0.3	110	57	9.5	52	0.58	0.6
90BSL099	<0.002	<0.15	18	1.3	0.11	49	26	10	23	<0.045	0.25
90BSL100?	<0.002	<0.15	18	0.71	0.061	30	9.2	2.1	25	0.1	0.24
90BSL100a	<0.002	<1.5	53	<6	<0.3	9	2.3	10	36	<0.45	<0.9
90BSL100b	<0.002	<1.5	87	<6	<0.3	<6	3.5	4.9	35	<0.45	<0.9
90BSL101	<0.002	<0.15	17	0.73	0.17	19	64	10	17	0.054	0.17
90BSL102	--	<0.15	2.4	<0.6	0.18	1.3	100	15	370	0.51	0.21
90BSL104	--	<0.15	1.1	<0.6	0.047	<0.6	30	7.9	9.4	<0.045	0.14
90BSL105	--	<0.15	1.3	<0.6	0.039	<0.6	27	9.6	1.9	<0.045	0.14
90BSL106	--	<0.15	2.1	<0.6	<0.03	<0.6	35	9.8	11	0.054	0.15
90BSL107	--	<0.15	4.4	0.63	0.038	0.66	48	12	13	0.059	0.29
90BSL115	<0.002	<0.15	85	<0.6	0.56	68	55	6.3	53	0.56	0.37
90BSL116	<0.002	<0.15	29	<0.6	0.21	35	44	4.9	330	0.74	0.67
90BSL117	<0.002	<0.15	58	5.4	0.14	19	22	4	26	6.6	0.49
90BSL118	<0.002	<0.15	280	<0.6	0.14	110	17	3.8	14	<0.045	0.38
90BSL119	<0.002	<0.15	2.3	<0.6	<0.03	0.91	33	24	2.2	<0.045	0.54
90BSL120	0.6	0.66	4.7	<0.6	0.051	<0.6	3	17	11	0.048	1.6
PNZ001	--	<0.15	1.4	<0.6	0.13	<0.6	13	5.4	2.6	<0.045	0.64
PNZ002	<0.002	<0.15	19	<0.6	<0.03	0.95	3.9	12	6.7	0.097	2.7
PNZ003	--	<0.15	1.3	<0.6	0.093	<0.6	20	7.2	3.7	<0.045	0.23
PNZ005	--	<0.15	1.2	<0.6	0.1	<0.6	19	7.2	3.9	<0.045	0.13
PNZ006	--	<0.15	1.9	<0.6	0.079	<0.6	19	6.6	3.6	<0.045	0.42
PNZ007	--	<0.15	1.6	<0.6	0.075	<0.6	31	4.6	4.5	<0.045	0.44
PNZ010	--	<0.15	2.6	0.62	0.17	11	44	9.3	12	0.2	0.56

Table B-3. *Semiquantitative spectrographic analyses of rock samples collected as part of the study of metallic mineral deposits, Altiplano and Cordillera Occidental, Bolivia*

[All determinations by DC-ARC AES. Elements with asterisks (*) are reported in percent; all other elements are reported in ppm. N, the element was present below the lower limit of determination]

Sample no.	Ba	Fe*	Mg*	Ca*	Ti*	Mn	Ag	As	B	Au
90BBG001a	1500	5	1	0.7	0.7	1500	<0.5	N	50	N
90BBG003	1000	0.7	0.2	1	0.15	300	<0.5	N	30	N
90BBG003	1000	0.7	0.5	0.7	0.1	500	<0.5	<200	30	N
90BBG004	1500	0.5	0.15	0.3	0.15	100	0.5	N	50	N
90BBG004	1500	0.5	0.5	0.5	0.15	200	<0.5	N	50	N
90BBG005a	1000	1.5	0.3	<0.05	0.3	1500	50	N	50	N
90BBG005b	1000	3	0.15	<0.05	0.2	500	7	N	30	N
90BBG006b	200	5	1	0.07	0.3	3000	30	N	200	N
90BBG006c	2000	5	0.3	0.07	0.5	2000	50	N	100	N
90BBG007	2000	3	0.2	<0.05	0.5	1000	5	N	50	N
90BBG008	700	3	0.5	<0.05	0.3	1500	200	N	200	N
90BBG009a	2000	5	0.3	0.2	1	>5000	5	N	50	N
90BBG009b	1000	2	0.5	0.1	0.2	>5000	2	N	100	N
90BBG010a	1000	3	0.2	<0.05	0.3	500	200	N	50	N
90BBG010b	1500	2	0.3	<0.05	0.2	700	20	N	50	N
90BBG011a	100	3	0.3	0.5	0.3	>5000	300	200	100	N
90BBG011b	30	1.5	0.05	0.2	0.07	>5000	1000	300	30	N
90BBG012	50	0.7	0.2	0.7	0.005	>5000	700	<200	30	N
90BBG013c	1500	5	3	5	1	1000	<0.5	N	30	N
90BBG014	1000	7	1	0.3	0.5	200	<0.5	N	100	N
90BBG014	1500	5	0.5	1	0.5	700	2	N	50	N
90BBG015a	1000	2	0.03	0.1	0.3	70	0.7	N	150	N
90BBG015b	700	0.2	<0.02	<0.05	0.2	20	<0.5	N	30	N
90BBG015c	1000	0.5	0.05	0.1	0.5	70	<0.5	N	150	N
90BBG016a	1000	1	0.05	0.3	0.3	50	<0.5	N	30	N
90BBG016b	500	0.15	<0.02	<0.05	0.07	<10	N	N	N	N
90BBG018a	2000	3	0.1	0.7	0.7	50	<0.5	N	100	N
90BBG018b	2000	2	0.5	1.5	1	200	10	N	15	N
90BBG018c	3000	7	1	1	1	200	<0.5	N	20	N
90BBG018d	2000	2	0.2	0.7	0.7	50	<0.5	N	30	N
90BBG018e	2000	5	0.7	1	0.7	500	0.7	N	50	N
90BBG020	1000	0.7	0.03	0.07	0.1	2000	1	<200	50	N
90BBG021	1000	1.5	0.3	0.07	0.5	200	50	N	100	N
90BBG022a	1500	1.5	0.05	0.07	0.3	70	300	<200	50	N
90BBG022b	1500	1.5	0.02	0.07	0.2	50	100	<200	30	N
90BBG023	1500	1	0.03	0.05	0.2	50	50	<200	30	N
90BBG024	1500	0.3	0.05	0.07	0.1	70	<0.5	N	20	N
90BBG025a	700	1	0.3	0.1	0.3	100	200	<200	100	N
90BBG025b	2000	2	0.7	0.2	0.3	150	10	N	150	N
90BBG025c	3000	1.5	0.2	0.05	0.3	100	700	<200	150	N
90BBG026	2000	5	0.7	3	1	500	7	N	10	N
90BBG029	500	10	0.7	0.05	0.3	1000	3	N	15	N
90BBG030	2000	7	3	2	0.5	5000	2	N	10	N
90BBG031	1500	5	0.5	<0.05	0.2	200	10	N	30	N
90BBG032a	3000	2	0.5	0.05	0.3	300	5	N	50	N
90BBG032b	700	5	0.2	<0.05	0.2	100	5	<200	15	N
90BBG032c	500	10	0.1	<0.05	0.03	100	1	300	20	N
90BBG033a	150	0.1	0.5	0.7	0.005	300	N	<200	30	N
90BBG033b	100	0.07	<0.02	0.2	0.002	70	N	<200	30	N
90BBG034	700	15	3	1	0.5	5000	N	N	20	N

Table B-3. *Semiquantitative spectrographic analyses of rock samples collected as part of the study of metallic mineral deposits, Altiplano and Cordillera Occidental, Bolivia*--Continued

Sample no.	Ba	Fe*	Mg*	Ca*	Ti*	Mn	Ag	As	B	Au
90BBG040	1500	5	0.02	0.05	0.7	20	<0.5	N	10	N
90BBG045	1000	2	0.7	0.1	0.7	50	1	N	30	N
90BBG046a	700	5	5	5	0.15	5000	<0.5	N	50	N
90BBG046b	2000	3	1	2	0.3	1500	<0.5	N	50	N
90BBG047	700	7	0.05	0.05	0.02	3000	1500	200	10	N
90BBG048a	200	3	0.02	0.05	0.005	3000	200	200	15	N
90BBG049	100	2	0.02	<0.05	0.005	2000	2000	500	10	N
90BBG050b	1500	1	0.5	<0.05	0.2	3000	30	N	30	N
90BBG051a	200	20	<0.02	<0.05	0.3	500	200	700	10	N
90BBG051b	50	>20	<0.02	<0.05	0.15	50	1000	>10000	<10	N
90BBG052a	70	3	0.2	0.5	<.002	5000	70	<200	20	N
90BBG052b	2000	3	1	0.7	0.3	>5000	3	N	30	N
90BBG052d	1000	7	0.5	1.5	0.02	>5000	1500	<200	15	N
90BBG053a	150	3	0.15	0.1	0.03	3000	20	N	10	N
90BBG053b	2000	3	1.5	0.2	0.5	3000	0.7	N	20	N
90BBG054	2000	3	0.5	0.05	0.15	>5000	0.7	N	20	N
90BBG055a	300	3	<0.02	<0.05	0.2	70	2	300	20	N
90BBG056a	1000	0.7	0.2	<0.05	0.07	100	0.5	N	50	N
90BBG056b	2000	5	1.5	5	1	2000	N	N	70	N
90BBG057	200	5	0.2	>20	0.002	2000	N	N	70	N
90BBG058b	1000	1	0.02	0.07	0.5	50	200	300	10	N
90BBG058c	1500	5	2	2	1	2000	0.7	N	10	N
90BBG059	2000	5	3	2	0.7	1500	<0.5	N	20	N
90BBG059	2000	5	3	3	0.7	1500	<0.5	N	20	N
90BBR003	2000	7	0.03	<0.05	0.5	500	1000	300	30	N
90BBR004	2000	3	1	1	0.3	1500	0.5	N	50	N
90BBR008	1500	7	1.5	5	0.7	1000	N	N	20	N
90BBR010	1500	2	1	0.7	0.3	2000	N	N	150	N
90BBR015	1000	0.7	<0.02	0.07	0.2	70	<0.5	N	50	N
90BBR016	700	0.7	0.02	<0.05	0.3	30	<0.5	N	10	N
90BBR019	3000	7	5	3	1	1500	N	N	10	N
90BBR020	2000	3	3	3	0.5	1500	N	N	30	N
90BBR021a	1500	3	0.05	0.5	0.5	200	<0.5	N	30	N
90BBR021b	1000	5	0.05	0.2	0.3	200	<0.5	N	30	N
90BBR021c	3000	5	1.5	2	1	1000	N	N	30	N
90BBR021d	2000	5	0.5	1	0.7	500	0.7	N	50	N
90BBR022	1000	1.5	0.3	0.7	0.2	200	<0.5	N	20	N
90BBR026	2000	1	0.15	0.2	0.2	700	N	N	20	N
90BBR029	300	1	0.3	0.05	0.2	50	<0.5	N	30	N
90BBR031	700	1	0.7	0.2	0.15	500	<0.5	N	30	N
90BBR036a	1500	5	0.03	0.07	0.3	50	N	N	<10	N
90BBR036c	1500	2	<0.02	0.05	0.7	30	N	N	10	N
90BBR036d	2000	1	0.03	0.07	0.5	50	<0.5	N	<10	N
90BBR036e	1000	0.7	0.02	0.05	0.3	30	N	N	<10	N
90BBR036g	3000	5	1.5	1.5	1	500	<0.5	N	10	N
90BBR036h	1500	3	0.05	0.2	0.5	70	N	N	15	N
90BBR037	2000	3	1.5	1	0.7	1000	N	N	15	N
90BBR041	2000	5	5	3	1	1500	N	N	10	N
90BBR041	2000	5	3	2	1	1000	N	N	10	N
90BBR044	2000	5	3	2	1	700	N	N	15	N

Table B-3. *Semiquantitative spectrographic analyses of rock samples collected as part of the study of metallic mineral deposits, Altiplano and Cordillera Occidental, Bolivia*--Continued

Sample no.	Ba	Fe*	Mg*	Ca*	Ti*	Mn	Ag	As	B	Au
90BBR044a	2000	3	2	1	0.7	500	N	N	10	N
90BBR048a	1000	3	0.2	0.05	0.5	50	1	N	50	N
90BBR050	1000	5	0.02	0.05	1	50	0.7	N	15	N
90BBR051	1000	0.2	0.03	0.1	>1	70	<0.5	N	20	N
90BBR054a	1500	2	<0.02	<0.05	0.3	50	<0.5	N	<10	N
90BBR055	2000	2	<0.02	0.1	0.3	70	2	N	20	N
90BBR058c	2000	0.05	<0.02	0.05	0.7	30	N	N	10	N
90BBR063	300	5	0.05	<0.05	0.15	100	100	<200	30	N
90BCX003	1500	3	0.3	0.5	0.7	5000	2	N	50	N
90BCX004	1500	3	0.5	0.3	0.3	150	10	N	50	N
90BCX007	2000	3	0.3	0.7	0.2	>5000	7	N	50	N
90BCX008a	700	7	2	2	0.5	1500	N	N	70	N
90BCX008b	150	2	1	2	0.5	700	<0.5	N	30	N
90BCX009	150	3	1.5	0.7	0.7	1500	N	N	30	N
90BCX010	1500	3	0.7	0.7	0.5	500	N	N	50	N
90BCX012	150	1	0.7	20	0.15	1000	N	N	30	N
90BCX013a	1000	5	0.3	1.5	0.5	>5000	N	N	30	N
90BCX013b	700	3	0.15	0.7	0.3	200	15	N	20	N
90BCX014	1000	0.7	0.3	1.5	0.3	1000	50	N	30	N
90BCX015	300	1.5	1	1.5	0.15	1000	N	N	15	N
90BCX017	500	5	0.2	0.7	0.2	200	15	N	50	N
90BCX018	200	0.7	0.2	3	0.15	700	3	N	30	N
90BCX019a	500	1	0.7	3	0.5	1500	15	N	30	N
90BCX019b	1000	0.7	0.5	10	0.15	1500	N	N	30	N
90BCX019c	500	5	0.7	3	0.3	700	N	N	30	N
90BCX020	300	5	0.5	5	0.3	300	N	N	100	N
90BCX022	700	2	0.15	0.3	0.15	150	5	N	20	N
90BCX022b	200	1	0.3	0.7	0.1	1500	N	N	15	N
90BCX023	>5000	3	0.5	1	>1	200	150	N	30	N
90BCX023a	500	7	3	15	1	1000	N	N	15	N
90BCX026	700	1.5	0.2	0.7	0.5	150	20	N	20	N
90BCX027	300	15	0.1	0.1	0.1	700	500	7000	15	N
90BCX028	200	0.7	0.2	0.1	0.07	500	7	N	50	N
90BCX029	200	5	0.3	3	0.2	1000	20	N	150	N
90BCX030a	300	5	0.7	1	0.3	1000	20	N	50	N
90BCX030b	300	5	1.5	3	0.2	1500	15	200	50	N
90BCX031	500	3	0.7	1.5	0.2	500	30	700	30	N
90BCX032	200	5	0.7	0.3	0.2	150	5	N	70	N
90BDB001	700	2	1	0.7	0.3	200	3	N	20	N
90BDB002	1000	1	0.7	0.3	0.5	30	1.5	N	50	N
90BDB003	1000	3	1.5	1.5	0.3	700	0.7	N	20	N
90BDB004	1000	3	1	1	0.3	300	1	N	10	N
90BDB005	1000	3	1	2	0.3	700	N	N	<10	N
90BDB006	700	3	1.5	1.5	0.3	700	N	N	15	N
90BDB007	700	2	0.7	0.7	0.3	700	N	N	10	N
90BDB008	1000	2	0.7	2	0.3	300	<0.5	N	15	N
90BDB009	1500	3	0.7	5	0.3	500	<0.5	N	10	N
90BDB010	1500	3	0.7	3	0.3	500	N	N	20	N
90BDB011	1500	3	1	3	0.3	1000	N	N	N	N
90BDB012	1000	2	0.7	0.7	0.3	200	N	N	15	N

Table B-3. *Semiquantitative spectrographic analyses of rock samples collected as part of the study of metallic mineral deposits, Altiplano and Cordillera Occidental, Bolivia*--Continued

Sample no.	Ba	Fe*	Mg*	Ca*	Ti*	Mn	Ag	As	B	Au
90BDB013	1500	3	1	1	0.3	300	<0.5	N	15	N
90BDB014	1500	3	0.15	0.07	0.2	150	20	<200	20	N
90BDB015	200	5	0.03	0.1	0.3	30	15	<200	<10	N
90BDR001a	300	1	0.3	<0.05	0.7	100	15	N	15	N
90BDR001b	700	5	1	1.5	0.7	500	1	N	20	N
90BDR005	1000	3	1.5	2	0.7	500	<0.5	N	<10	N
90BDR006	1000	3	1	7	1	500	N	N	30	N
90BDR007	>5000	20	0.02	0.07	0.003	300	20	200	N	N
90BDR008a	1500	2	0.7	0.2	0.3	1000	<0.5	N	30	N
90BDR008b	3000	3	0.5	0.15	0.3	500	2	N	30	N
90BDR009	>5000	10	0.3	0.15	0.3	1500	70	N	50	N
90BDR010	3000	3	0.7	0.3	0.3	1000	100	N	15	N
90BDR012	700	3	1	10	0.7	500	N	N	50	N
90BDR015	300	5	1.5	3	0.3	700	N	N	10	N
90BDR016	500	5	1	3	0.7	700	N	N	20	N
90BDR022	700	3	0.5	0.05	0.5	300	30	N	30	N
90BDR025	500	3	1	1.5	0.7	1000	N	N	30	N
90BDR030	1500	2	0.5	1.5	0.5	150	<0.5	N	15	N
90BDR031	1500	3	0.5	0.7	0.7	700	3	N	30	N
90BDR034	500	3	0.7	1.5	0.3	700	70	N	30	N
90BDR035	1000	3	1	2	0.3	700	3	N	20	N
90BDR037	700	3	1.5	2	0.5	700	<0.5	N	10	N
90BDR038	700	3	1.5	3	0.3	700	N	N	15	N
90BDR039	700	3	1.5	3	0.3	700	N	N	15	N
90BDR041	700	3	1.5	7	0.3	700	N	N	15	N
90BDR041a	700	5	1.5	1.5	0.3	500	N	N	10	N
90BDR042	300	3	1	1.5	0.3	500	N	N	10	N
90BDR043	700	3	1.5	2	0.3	700	N	N	<10	N
90BDR044	500	3	0.7	1.5	0.3	500	N	N	15	N
90BDR046	500	3	1	2	0.3	500	N	N	15	N
90BDR053	1000	3	1.5	5	0.5	700	N	N	15	N
90BDR054	300	3	1.5	3	0.3	700	N	N	<10	N
90BDR055	500	0.7	0.2	0.7	0.07	700	2	N	20	N
90BDR057	1000	3	1	7	0.3	700	<0.5	N	20	N
90BDR058c	500	5	0.7	0.3	0.3	>5000	N	N	70	N
90BDR060b	1000	3	1.5	3	0.3	1000	N	N	20	N
90BDR061c	1000	1.5	0.5	0.15	0.3	150	N	N	20	N
90BES001	1000	3	1.5	1.5	0.3	700	N	N	<10	N
90BES002	1500	5	0.5	0.1	0.3	30	N	N	30	N
90BES003	1500	3	0.7	0.3	0.3	30	N	N	<10	N
90BES004	1000	2	0.03	0.15	0.3	<10	N	N	10	N
90BES005	1500	5	0.5	0.15	0.7	30	N	N	20	N
90BES006	3000	1.5	0.3	0.05	0.5	200	5	N	15	N
90BES007	2000	2	0.15	0.07	0.2	50	3	N	15	N
90BES008	200	3	0.3	<0.05	0.5	30	15	N	70	N
90BES009	50	20	<0.02	N	0.3	20	300	N	N	N
90BES010	1500	3	1	2	0.3	1500	20	N	15	N
90BES011	1500	3	0.7	1	0.5	700	N	N	10	N
90BES012	1500	5	1	1.5	0.7	500	<0.5	N	15	N

Table B-3. *Semiquantitative spectrographic analyses of rock samples collected as part of the study of metallic mineral deposits, Altiplano and Cordillera Occidental, Bolivia*--Continued

Sample no.	Ba	Fe*	Mg*	Ca*	Ti*	Mn	Ag	As	B	Au
90BES014	1500	5	1.5	7	0.3	700	N	N	<10	N
90BES015	700	0.3	0.02	0.05	0.15	<10	<0.5	N	20	N
90BES016	1000	2	0.15	<0.05	0.3	<10	N	N	50	N
90BES029	300	3	0.3	0.15	0.7	50	5	N	500	N
90BES030	500	1.5	0.7	0.07	1	50	1	N	10	N
90BES031	1000	5	1.5	3	0.7	500	1.5	N	10	N
90BES032	2000	7	0.3	0.05	0.5	30	1.5	N	30	N
90BES033	1000	3	0.7	1.5	0.3	500	N	N	15	N
90BES034	500	0.7	0.3	0.3	0.07	700	N	N	15	N
90BES035	700	3	0.7	1	0.3	500	N	N	10	N
90BES036	1500	3	1	2	0.3	700	N	N	<10	N
90BES037	1500	3	0.7	0.7	0.5	700	N	N	15	N
90BES039	1000	0.7	0.05	0.07	0.15	100	<0.5	N	20	N
90BES040	700	0.3	0.02	0.15	0.07	200	0.5	N	20	N
90BES041	1000	0.7	0.03	0.2	0.07	500	<0.5	N	15	N
90BES042	1000	1	0.05	0.3	0.3	150	0.5	<200	30	N
90BES043	700	0.5	<0.02	<0.05	0.07	20	0.5	N	<10	N
90BES044	700	2	0.3	0.5	0.3	1000	N	N	20	N
90BES045	1500	3	0.3	0.7	0.02	>5000	N	1500	30	N
90BES046	300	0.7	0.07	<0.05	0.15	700	10	<200	70	N
90BES047	700	0.7	0.15	<0.05	0.1	30	3	N	50	N
90BES048	1000	3	0.7	1.5	0.5	500	<0.5	N	15	N
90BES049	1500	3	0.3	0.7	0.3	>5000	<0.5	N	100	N
90BES050	70	3	0.07	<0.05	0.05	>5000	300	700	10	N
90BES051	1500	1.5	0.07	<0.05	0.07	700	700	300	30	N
90BES052	300	7	0.15	<0.05	0.2	500	150	1500	30	N
90BES053	20	3	<0.02	<0.05	0.005	1500	200	300	<10	N
90BES054	50	15	0.05	<0.05	0.07	700	500	700	N	N
90BES055	1500	3	0.5	3	0.15	>5000	200	300	100	N
90BES056	150	1.5	0.3	0.15	0.3	500	7	N	70	N
90BES057	1500	2	0.15	0.07	0.3	1500	10	200	20	N
90BES058	300	2	0.3	0.5	0.007	>5000	1.5	<200	150	N
90BES059	1500	3	0.5	1.5	0.5	300	0.5	N	10	N
90BES060	1500	1.5	0.07	0.2	0.3	200	0.5	<200	30	N
90BES061	1000	3	0.1	0.15	0.15	200	<0.5	N	30	N
90BES062	700	1.5	0.03	0.07	0.2	50	0.5	<200	30	N
90BES063	1000	1.5	0.15	0.15	1	70	<0.5	N	70	N
90BES064	1000	1.5	0.3	0.3	0.3	200	1	N	30	N
90BES065	1000	1	0.03	0.15	0.3	30	<0.5	N	15	N
90BES066	1500	3	1.5	2	0.5	1000	N	N	10	N
90BES067	1500	3	0.3	1.5	0.7	200	N	N	15	N
90BES069	700	0.7	0.1	0.1	0.3	150	<0.5	N	30	N
90BSL001	500	15	0.02	<0.05	2	20	15	1000	N	N
90BSL002	300	5	0.5	<0.05	0.5	100	15	N	15	N
90BSL003a	150	0.7	0.2	0.07	0.7	50	15	N	30	N
90BSL004	1000	3	1.5	3	0.7	700	N	N	15	N
90BSL005	700	7	0.7	0.1	0.7	30	7	N	1000	N
90BSL006	300	3	0.7	0.07	0.5	50	N	N	2000	N
90BSL007	500	3	1.5	0.1	0.7	30	2	200	>2000	N
90BSL009	<20	>20	0.3	<0.05	0.07	20	20	1000	2000	N

Table B-3. *Semiquantitative spectrographic analyses of rock samples collected as part of the study of metallic mineral deposits, Altiplano and Cordillera Occidental, Bolivia*--Continued

Sample no.	Ba	Fe*	Mg*	Ca*	Ti*	Mn	Ag	As	B	Au
90BSL010	300	7	0.3	<0.05	0.3	150	1.5	<200	1500	N
90BSL012	1500	0.2	<0.02	0.1	0.7	<10	N	N	10	N
90BSL013	N	10	0.03	<0.05	0.003	>5000	700	1000	N	N
90BSL014	500	2	0.7	<0.05	0.7	500	15	N	150	N
90BSL030	700	3	1	0.3	0.3	200	5	N	>2000	N
90BSL031	700	5	0.3	0.15	0.5	150	7	<200	30	N
90BSL032	500	15	<0.02	<0.05	0.015	30	15	1000	N	N
90BSL034	700	3	1	3	0.3	700	N	N	15	N
90BSL035	300	7	0.03	<0.05	0.03	20	5	200	N	N
90BSL036	300	7	0.15	<0.05	0.07	100	30	500	15	N
90BSL037	1500	1.5	0.3	<0.05	0.3	150	1.5	N	30	N
90BSL038a	150	7	0.3	<0.05	0.1	70	7	700	1000	N
90BSL039	100	15	0.15	<0.05	0.07	50	70	5000	20	N
90BSL040	1500	3	1	1.5	0.3	700	<0.5	N	15	N
90BSL041	N	15	<0.02	N	0.003	70	150	>10000	N	N
90BSL042	200	15	0.15	0.3	0.15	200	3	700	70	N
90BSL043	1500	2	0.15	0.1	0.2	1500	10	N	15	N
90BSL044	700	5	0.5	0.3	0.3	5000	N	N	70	N
90BSL045	1500	3	0.7	0.3	0.3	2000	2	N	30	N
90BSL046	700	2	0.7	1.5	0.2	500	N	N	20	N
90BSL047	1000	2	1	0.7	0.3	1500	N	N	10	N
90BSL048	1500	3	1.5	1.5	0.3	1500	<0.5	N	20	N
90BSL049a	300	20	0.07	<0.05	0.07	100	700	5000	70	N
90BSL049b	70	20	<0.02	<0.05	0.015	100	2000	7000	N	N
90BSL050	1000	1	0.3	1.5	0.3	150	N	N	20	N
90BSL051	1000	1.5	0.7	1.5	0.2	500	N	N	20	N
90BSL052	500	3	0.05	0.1	0.15	20	10	N	100	N
90BSL053	700	2	0.1	0.3	0.3	50	3	N	150	N
90BSL054	700	2	1	1	0.3	500	N	N	30	N
90BSL055	2000	7	0.03	0.05	0.3	20	30	7000	30	N
90BSL056	1000	1.5	0.3	<0.05	0.3	20	3	N	30	N
90BSL057	700	2	0.7	0.7	0.2	500	N	N	<10	N
90BSL058	500	5	0.05	<0.05	0.2	30	1	700	30	N
90BSL059a	300	10	0.15	0.1	0.15	70	N	300	30	N
90BSL059b	2000	20	0.1	0.1	0.1	700	N	5000	30	N
90BSL060	1000	2	0.3	3	0.3	500	0.5	N	<10	N
90BSL061	1500	5	0.5	1.5	0.3	700	N	N	20	N
90BSL062	700	3	0.02	<0.05	0.002	500	N	<200	50	N
90BSL063	500	1.5	0.7	15	0.07	>5000	N	N	50	N
90BSL064	30	0.7	0.3	15	0.002	>5000	N	N	30	N
90BSL065	30	0.5	0.03	0.05	<.002	30	<0.5	N	70	N
90BSL066	300	3	0.7	1.5	0.15	700	10	7000	100	N
90BSL067	700	1.5	0.7	1	0.3	150	N	N	15	N
90BSL068	>5000	2	0.15	1.5	0.07	100	20	1500	50	N
90BSL070	500	3	0.15	5	0.07	1000	50	<200	20	N
90BSL071	1500	7	0.3	3	0.015	700	200	<200	N	N
90BSL072	1500	5	0.7	15	0.07	5000	70	<200	30	N
90BSL073	700	3	1.5	7	0.3	500	N	N	10	N
90BSL074	700	3	1.5	1.5	0.3	700	N	N	15	N
90BSL076	1000	3	0.02	0.1	0.3	70	3	<200	<10	N

Table B-3. *Semiquantitative spectrographic analyses of rock samples collected as part of the study of metallic mineral deposits, Altiplano and Cordillera Occidental, Bolivia*--Continued

Sample no.	Ba	Fe*	Mg*	Ca*	Ti*	Mn	Ag	As	B	Au
90BSL077	>5000	3	0.03	0.07	0.003	>5000	150	N	15	N
90BSL079	700	3	1.5	5	0.3	500	N	N	30	N
90BSL080	3000	10	0.03	<0.05	0.07	700	10	<200	20	N
90BSL081	>5000	7	0.15	0.7	0.03	>5000	150	200	15	N
90BSL082	>5000	7	0.02	<0.05	0.015	>5000	200	N	N	N
90BSL083	1000	2	0.7	0.7	0.3	700	0.7	N	30	N
90BSL084a	700	15	0.2	0.07	0.03	1000	7	N	20	N
90BSL084b	300	>20	0.3	0.05	0.015	700	10	300	N	N
90BSL084c	200	20	0.5	0.07	0.07	500	5	N	20	N
90BSL085	100	5	0.5	0.15	0.15	1000	<0.5	N	150	N
90BSL086	700	7	0.15	0.05	0.15	5000	15	<200	100	N
90BSL087	1000	7	0.3	0.15	0.3	1500	N	N	70	N
90BSL088a	50	20	0.02	<0.05	0.015	150	5	N	50	N
90BSL088b	70	3	1	0.07	0.15	100	1.5	N	>2000	N
90BSL088c	50	20	0.03	N	0.015	70	15	500	50	N
90BSL089	700	3	0.7	0.07	0.5	1500	0.5	N	70	N
90BSL090	1500	3	0.7	0.5	0.3	700	N	N	10	N
90BSL091	1000	5	0.7	0.05	0.3	150	1.5	N	>2000	N
90BSL092a	N	>20	0.07	<0.05	0.002	2000	70	<200	N	N
90BSL094a	70	0.15	0.05	0.07	0.015	150	5	N	30	N
90BSL094b	200	0.1	0.05	0.07	0.01	100	1.5	<200	15	N
90BSL095	300	3	1	3	0.07	>5000	150	700	30	N
90BSL097	1000	2	0.5	0.1	0.3	700	7	500	30	N
90BSL098	500	3	0.3	0.07	0.15	150	2	700	50	N
90BSL099	700	2	0.5	0.7	0.3	150	<0.5	N	30	N
90BSL100a	700	1.5	0.5	<0.05	0.7	150	10	N	150	N
90BSL100b	1000	2	0.5	<0.05	0.7	150	30	<200	70	N
90BSL101	1000	2	0.7	3	0.3	700	<0.5	N	70	N
90BSL102	1000	3	1	3	0.3	500	2	N	20	N
90BSL104	700	3	1	1.5	0.3	200	N	N	<10	N
90BSL105	700	3	1	3	0.3	300	N	N	<10	N
90BSL106	700	3	1	2	0.3	300	0.7	N	<10	N
90BSL107	1000	3	1.5	3	0.3	500	N	N	15	N
90BSL115	1000	1.5	1	0.2	0.5	150	1.5	N	50	N
90BSL116	1000	0.3	0.15	0.05	0.07	150	5	N	30	N
90BSL117	200	1	0.3	<0.05	0.2	10	5	<200	30	N
90BSL118	1500	2	1	0.7	0.3	300	0.5	N	50	N
90BSL119	500	15	0.7	0.3	0.2	300	N	N	N	N
90BSL120	1500	10	0.03	0.15	0.2	70	N	N	N	N
PNZ001	700	3	1	1.5	0.3	500	N	N	20	N
PNZ002	700	3	0.15	0.07	0.3	20	N	N	20	N
PNZ003	700	3	1	1.5	0.3	500	N	N	15	N
PNZ005	700	3	1	1.5	0.3	500	N	N	10	N
PNZ006	700	3	1	1.5	0.3	300	N	N	15	N
PNZ007	700	3	1	3	0.5	500	N	N	20	N
PNZ010	1500	1.5	0.7	0.2	0.3	150	2	N	50	N

Table B-3. *Semiquantitative spectrographic analyses of rock samples collected as part of the study of metallic mineral deposits, Altiplano and Cordillera Occidental, Bolivia*--Continued

Sample no.	Ni	Be	Bi	Cd	Co	Cr	Cu	La	Mo	Nb
90BBG001a	5	1	N	N	15	10	30	100	N	<20
90BBG003	<5	2	N	N	N	N	5	70	<5	<20
90BBG003	<5	2	N	N	N	N	5	70	N	N
90BBG004	<5	1	N	N	N	N	5	100	N	<20
90BBG004	5	1.5	N	N	N	N	5	100	N	20
90BBG005a	10	1	N	100	50	<10	20	70	N	<20
90BBG005b	5	1	N	500	10	<10	30	70	N	N
90BBG006b	7	2	N	30	20	<10	150	70	<5	<20
90BBG006c	5	1.5	N	30	15	<10	50	50	N	20
90BBG007	5	<1	N	70	10	<10	50	70	5	<20
90BBG008	7	1.5	N	150	20	<10	50	50	5	<20
90BBG009a	10	2	N	N	30	<10	70	50	N	20
90BBG009b	5	2	N	N	10	<10	15	70	N	<20
90BBG010a	15	1.5	N	20	20	<10	100	70	N	N
90BBG010b	10	1	N	N	30	N	70	70	N	N
90BBG011a	15	1.5	N	50	20	<10	3000	70	<5	N
90BBG011b	5	<1	N	>500	15	<10	7000	N	5	N
90BBG012	5	1	N	300	<10	<10	1500	N	<5	N
90BBG013c	20	2	N	N	30	30	50	150	5	<20
90BBG014	5	1	N	N	<10	10	30	100	10	<20
90BBG014	5	1.5	N	N	<10	10	30	70	15	<20
90BBG015a	<5	1.5	N	N	N	<10	20	70	<5	N
90BBG015b	5	<1	N	N	N	20	7	<50	N	N
90BBG015c	5	1.5	N	N	N	N	10	50	N	<20
90BBG016a	5	1.5	N	N	N	15	30	50	N	<20
90BBG016b	5	N	N	N	N	50	5	50	N	N
90BBG018a	<5	1.5	N	N	N	<10	15	100	<5	20
90BBG018b	5	1	N	N	<10	<10	15	100	<5	20
90BBG018c	7	1	N	N	<10	70	50	100	<5	<20
90BBG018d	<5	1.5	N	N	<10	<10	10	70	<5	20
90BBG018e	7	1.5	N	N	10	20	30	100	5	<20
90BBG020	<5	1	N	N	<10	<10	10	50	N	<20
90BBG021	7	1.5	N	N	<10	10	15	70	<5	20
90BBG022a	<5	1.5	N	N	<10	<10	100	70	5	20
90BBG022b	<5	1.5	N	N	N	N	100	100	<5	20
90BBG023	<5	1.5	N	N	N	N	30	70	<5	20
90BBG024	<5	1.5	N	N	N	N	7	100	N	<20
90BBG025a	5	2	N	N	N	<10	50	70	<5	20
90BBG025b	7	2	N	N	15	10	20	100	5	20
90BBG025c	5	2	N	N	<10	<10	100	70	<5	20
90BBG026	5	1	N	N	20	<10	15	70	N	20
90BBG029	20	2	N	N	15	70	200	N	50	N
90BBG030	30	1	<10	N	15	30	50	50	N	N
90BBG031	5	1	<10	N	<10	15	100	200	20	<20
90BBG032a	<5	1	N	N	N	50	100	N	10	<20
90BBG032b	5	2	N	N	N	100	150	N	50	N
90BBG032c	5	1.5	N	N	N	15	150	N	N	N
90BBG033a	<5	<1	N	N	N	<10	7	<50	N	N
90BBG033b	5	<1	N	N	N	N	<5	<50	N	N
90BBG034	7	2	N	N	20	15	500	N	N	N

Table B-3. *Semiquantitative spectrographic analyses of rock samples collected as part of the study of metallic mineral deposits, Altiplano and Cordillera Occidental, Bolivia*--Continued

Sample no.	Ni	Be	Bi	Cd	Co	Cr	Cu	La	Mo	Nb
90BBG040	7	1.5	N	N	N	100	30	70	<5	N
90BBG045	7	1	N	N	N	150	20	50	<5	<20
90BBG046a	10	1.5	N	N	20	10	50	<50	N	<20
90BBG046b	7	1.5	N	N	<10	20	10	50	N	30
90BBG047	10	5	20	100	<10	10	700	N	10	N
90BBG048a	5	5	<10	100	<10	<10	500	N	10	N
90BBG049	5	5	N	500	10	<10	3000	N	30	N
90BBG050b	<5	1.5	10	N	<10	<10	50	70	30	30
90BBG051a	50	<1	50	N	30	15	7000	N	N	N
90BBG051b	50	N	70	N	50	<10	>20000	N	N	N
90BBG052a	5	1.5	<10	>500	30	<10	500	N	N	N
90BBG052b	<5	2	N	<20	<10	10	70	50	N	30
90BBG052d	5	2	<10	>500	30	10	5000	N	<5	N
90BBG053a	5	2	N	>500	20	<10	50	N	N	N
90BBG053b	15	1.5	N	N	30	10	20	50	N	20
90BBG054	5	2	N	<20	15	10	20	50	N	<20
90BBG055a	5	<1	<10	N	N	10	100	100	<5	20
90BBG056a	<5	1	N	N	N	<10	10	50	N	20
90BBG056b	15	<1	N	N	30	30	20	70	N	<20
90BBG057	7	50	N	N	N	10	5	N	N	N
90BBG058b	<5	1	10	N	N	20	500	50	N	<20
90BBG058c	15	1.5	N	<20	30	20	150	70	5	30
90BBG059	10	1.5	N	N	20	20	30	100	N	20
90BBG059	7	1	N	N	20	15	30	100	<5	20
90BBR003	<5	1	N	N	N	10	50	50	7	<20
90BBR004	<5	1.5	N	N	<10	10	10	100	5	<20
90BBR008	10	1.5	N	N	20	20	50	100	N	<20
90BBR010	5	1	N	N	<10	<10	7	100	N	<20
90BBR015	5	1	N	N	N	N	10	50	N	<20
90BBR016	5	N	N	N	N	15	15	50	N	N
90BBR019	30	1	N	N	20	50	30	100	<5	20
90BBR020	10	1.5	N	N	15	15	20	100	<5	<20
90BBR021a	5	2	N	N	10	<10	30	70	5	<20
90BBR021b	<5	1.5	N	N	N	<10	20	50	5	N
90BBR021c	20	1	N	N	50	10	50	100	5	20
90BBR021d	<5	1.5	N	N	10	10	30	100	5	<20
90BBR022	5	1.5	N	N	<10	10	7	150	N	<20
90BBR026	<5	1.5	N	N	N	N	5	150	N	30
90BBR029	<5	1.5	N	N	N	<10	10	100	7	30
90BBR031	<5	2	N	N	N	<10	5	100	N	20
90BBR036a	5	1	N	N	N	30	20	70	<5	N
90BBR036c	5	1	N	N	N	150	30	200	<5	N
90BBR036d	5	1.5	N	N	N	50	50	150	N	N
90BBR036e	5	1	N	N	N	70	20	100	N	N
90BBR036g	20	2	N	N	20	70	70	200	5	20
90BBR036h	5	1.5	N	N	N	50	30	150	7	20
90BBR037	15	1.5	N	N	15	50	20	100	N	20
90BBR041	20	1.5	N	N	30	50	30	100	N	30
90BBR041	20	1.5	N	N	20	30	30	100	<5	30
90BBR044	15	1.5	N	N	20	30	30	100	N	<20

Table B-3. *Semiquantitative spectrographic analyses of rock samples collected as part of the study of metallic mineral deposits, Altiplano and Cordillera Occidental, Bolivia*--Continued

Sample no.	Ni	Be	Bi	Cd	Co	Cr	Cu	La	Mo	Nb
90BBR044a	15	2	N	N	15	30	20	100	N	<20
90BBR048a	<5	1	N	N	N	<10	50	<50	<5	20
90BBR050	5	<1	N	N	N	50	20	70	N	20
90BBR051	5	1	N	N	N	10	7	N	N	30
90BBR054a	5	1.5	N	N	N	10	7	200	<5	<20
90BBR055	5	<1	N	N	N	<10	20	100	<5	<20
90BBR058c	5	1.5	N	N	N	<10	10	N	7	50
90BBR063	5	1	N	N	N	15	150	N	200	N
90BCX003	5	<1	N	N	10	10	700	<50	N	<20
90BCX004	7	1.5	N	N	<10	20	>20000	<50	N	<20
90BCX007	N	<1	N	N	<10	10	>20000	N	N	N
90BCX008a	30	2	N	N	20	100	3000	50	N	<20
90BCX008b	15	<1	N	N	10	50	3000	<50	N	<20
90BCX009	20	<1	N	N	15	50	50	<50	N	<20
90BCX010	15	<1	N	N	10	30	100	<50	N	<20
90BCX012	<5	1	N	N	N	<10	30	N	30	N
90BCX013a	<5	<1	N	N	N	<10	700	N	N	20
90BCX013b	<5	1	N	N	N	<10	>20000	N	N	<20
90BCX014	<5	<1	N	N	N	<10	>20000	<50	N	N
90BCX015	<5	2	N	N	N	<10	30	50	50	<20
90BCX017	<5	<1	N	N	<10	<10	>20000	N	30	N
90BCX018	<5	1	N	N	N	<10	>20000	N	N	N
90BCX019a	<5	<1	N	N	N	30	>20000	N	50	N
90BCX019b	<5	1	N	N	N	10	300	N	N	N
90BCX019c	10	<1	N	N	15	50	700	<50	<5	<20
90BCX020	10	1	N	N	10	10	30	<50	N	<20
90BCX022	<5	<1	N	N	N	<10	20000	N	N	N
90BCX022b	<5	3	N	N	N	N	15	<50	N	70
90BCX023	20	<1	N	N	<10	100	>20000	N	10	20
90BCX023a	70	<1	N	N	50	500	30	N	N	N
90BCX026	70	1.5	N	N	<10	10	>20000	<50	N	20
90BCX027	7	<1	N	>500	15	N	1500	N	20	N
90BCX028	<5	3	N	N	N	N	20	N	N	30
90BCX029	10	1.5	N	N	20	10	>20000	N	N	<20
90BCX030a	10	<1	N	N	20	<10	>20000	N	N	<20
90BCX030b	7	<1	N	N	20	10	>20000	N	N	N
90BCX031	7	1	N	70	<10	20	>20000	<50	N	N
90BCX032	10	1	N	N	<10	30	>20000	N	N	N
90BDB001	30	2	N	N	20	70	20	50	N	<20
90BDB002	15	2	N	N	10	50	30	70	<5	20
90BDB003	30	1.5	N	N	30	100	30	70	N	<20
90BDB004	10	1.5	N	N	20	10	20	70	N	20
90BDB005	5	1.5	N	N	15	15	15	70	N	20
90BDB006	20	1.5	N	N	20	100	30	70	N	20
90BDB007	5	2	N	N	15	<10	<5	50	N	20
90BDB008	20	1.5	<10	N	15	30	20	100	N	<20
90BDB009	<5	1	N	N	10	30	15	70	N	20
90BDB010	N	1	N	N	N	N	<5	70	<5	20
90BDB011	<5	1.5	N	N	10	N	15	70	<5	<20
90BDB012	30	1.5	N	N	15	50	30	70	N	N

Table B-3. *Semiquantitative spectrographic analyses of rock samples collected as part of the study of metallic mineral deposits, Altiplano and Cordillera Occidental, Bolivia*--Continued

Sample no.	Ni	Be	Bi	Cd	Co	Cr	Cu	La	Mo	Nb
90BDB013	50	1.5	N	N	20	100	30	100	N	<20
90BDB014	<5	1.5	15	N	N	20	50	50	10	<20
90BDB015	<5	1.5	30	N	N	50	30	70	<5	<20
90BDR001a	<5	1	N	N	N	<10	30	50	N	<20
90BDR001b	30	1	N	N	20	100	30	50	N	N
90BDR005	N	<1	N	N	<10	30	10	70	N	<20
90BDR006	N	5	N	N	<10	10	5	100	N	20
90BDR007	20	5	15	N	50	N	50	N	N	N
90BDR008a	<5	1	N	N	<10	N	<5	<50	7	<20
90BDR008b	<5	<1	N	N	<10	N	<5	<50	N	<20
90BDR009	20	1.5	N	N	70	30	50	N	<5	<20
90BDR010	<5	1	N	N	20	N	50	<50	5	<20
90BDR012	7	<1	N	N	15	100	15	<50	<5	<20
90BDR015	7	1	N	N	20	50	10	<50	<5	<20
90BDR016	5	<1	N	N	20	15	7	<50	N	<20
90BDR022	<5	1	N	N	<10	10	10	<50	N	N
90BDR025	7	1.5	N	N	15	15	7	<50	N	<20
90BDR030	<5	<1	N	N	<10	10	N	50	N	<20
90BDR031	<5	<1	N	N	<10	<10	7	70	N	<20
90BDR034	15	1.5	N	N	15	50	30	50	N	<20
90BDR035	5	1.5	N	N	15	<10	500	70	N	<20
90BDR037	10	1	N	N	20	70	20	50	N	<20
90BDR038	15	1.5	N	N	20	50	20	70	<5	<20
90BDR039	10	1	N	N	20	100	10	70	<5	<20
90BDR041	5	1	N	N	15	70	7	70	<5	<20
90BDR041a	15	1.5	N	N	20	50	10	50	<5	<20
90BDR042	5	1.5	N	N	15	10	7	50	N	<20
90BDR043	<5	1	N	N	15	30	7	50	<5	<20
90BDR044	5	1.5	N	N	15	15	7	50	<5	<20
90BDR046	<5	1.5	N	N	15	15	7	50	<5	<20
90BDR053	7	1	N	N	20	30	20	50	<5	20
90BDR054	7	<1	N	N	30	15	10	<50	N	<20
90BDR055	<5	2	N	N	N	<10	<5	<50	N	30
90BDR057	15	2	N	N	15	70	15	70	N	<20
90BDR058c	7	2	<10	N	10	30	30	70	N	<20
90BDR060b	10	1.5	N	N	15	70	<5	70	<5	20
90BDR061c	<5	1.5	N	N	N	<10	<5	70	N	<20
90BES001	30	1.5	N	N	15	50	20	70	N	<20
90BES002	<5	<1	N	N	N	70	30	70	20	<20
90BES003	<5	1	N	N	<10	70	20	70	5	<20
90BES004	<5	<1	N	N	N	50	10	100	<5	<20
90BES005	20	<1	N	N	20	100	30	100	N	<20
90BES006	<5	1.5	N	N	N	20	50	50	<5	20
90BES007	<5	1	N	N	<10	<10	50	50	5	20
90BES008	20	1	10	N	20	30	20	50	N	20
90BES009	20	N	N	N	15	20	700	N	N	30
90BES010	10	1.5	N	N	15	15	20	50	N	<20
90BES011	20	1	N	N	30	30	50	50	N	<20
90BES012	50	1	N	N	30	50	50	70	5	<20
90BES013	30	1.5	N	N	20	50	50	70	7	<20

Table B-3. *Semiquantitative spectrographic analyses of rock samples collected as part of the study of metallic mineral deposits, Altiplano and Cordillera Occidental, Bolivia*--Continued

Sample no.	Ni	Be	Bi	Cd	Co	Cr	Cu	La	Mo	Nb
90BES014	20	1	N	N	30	30	30	100	N	<20
90BES015	<5	<1	N	N	N	<10	5	<50	N	N
90BES016	<5	1	N	N	N	<10	10	70	N	<20
90BES029	<5	1.5	<10	N	<10	50	50	50	N	<20
90BES030	<5	1.5	<10	N	N	30	30	50	N	<20
90BES031	15	1.5	N	N	30	30	50	<50	N	<20
90BES032	<5	<1	N	N	<10	30	20	50	5	<20
90BES033	7	1	N	N	20	<10	30	70	N	<20
90BES034	<5	2	N	N	N	<10	<5	<50	<5	20
90BES035	15	1.5	N	N	20	<10	20	50	<5	<20
90BES036	20	1.5	N	N	20	30	30	70	<5	<20
90BES037	7	1	N	N	<10	10	15	50	5	<20
90BES039	<5	1	N	N	N	<10	7	50	7	<20
90BES040	N	1.5	N	N	N	<10	5	<50	<5	<20
90BES041	<5	2	N	N	N	<10	5	50	7	20
90BES042	<5	2	N	N	N	<10	10	50	7	20
90BES043	N	2	N	N	N	<10	7	<50	7	<20
90BES044	<5	3	N	N	<10	<10	10	50	<5	20
90BES045	150	2	N	100	700	300	50	N	100	N
90BES046	<5	1	N	N	N	<10	15	<50	N	<20
90BES047	<5	1.5	N	N	N	N	5	<50	<5	<20
90BES048	5	1.5	N	N	10	<10	15	<50	N	<20
90BES049	20	1	N	N	50	<10	20	<50	N	<20
90BES050	<5	1.5	N	>500	<10	<10	3000	N	20	N
90BES051	5	1.5	N	20	N	10	200	<50	70	<20
90BES052	<5	1	20	<20	N	<10	1500	N	30	<20
90BES053	<5	<1	<10	>500	<10	<10	10000	N	10	N
90BES054	5	<1	100	500	<10	<10	>20000	N	15	N
90BES055	5	1.5	N	20	20	<10	1000	<50	10	<20
90BES056	<5	1.5	N	N	N	10	150	50	20	<20
90BES057	<5	1	N	50	<10	15	100	<50	5	20
90BES058	30	1	N	>500	50	<10	300	50	100	N
90BES059	15	1	N	N	15	30	20	50	<5	30
90BES060	5	1.5	N	N	N	<10	15	70	7	20
90BES061	<5	1.5	N	N	N	<10	15	70	10	20
90BES062	<5	1	N	N	N	<10	15	70	10	20
90BES063	<5	1	N	N	N	70	15	70	7	30
90BES064	<5	2	N	N	N	<10	20	70	<5	30
90BES065	<5	1.5	N	N	N	<10	7	70	7	20
90BES066	15	1.5	N	N	15	50	20	50	N	20
90BES067	15	1	N	N	15	30	20	50	<5	<20
90BES069	<5	2	N	30	N	10	10	50	<5	<20
90BSL001	N	N	20	N	N	<10	20	<50	N	N
90BSL002	<5	<1	<10	N	N	30	20	50	N	<20
90BSL003a	<5	1	N	N	N	10	<5	50	N	<20
90BSL004	15	<1	N	N	15	100	N	50	N	<20
90BSL005	<5	1	70	N	N	100	20	100	20	<20
90BSL006	<5	1.5	<10	N	N	70	15	50	N	<20
90BSL007	<5	3	30	N	N	100	20	50	N	20
90BSL009	30	1	<10	N	10	15	30	N	N	N

Table B-3. *Semiquantitative spectrographic analyses of rock samples collected as part of the study of metallic mineral deposits, Altiplano and Cordillera Occidental, Bolivia*--Continued

Sample no.	Ni	Be	Bi	Cd	Co	Cr	Cu	La	Mo	Nb
90BSL010	15	1.5	N	N	10	70	20	<50	N	<20
90BSL012	<5	1.5	N	N	N	N	<5	<50	N	20
90BSL013	N	<1	N	500	15	N	3000	N	15	N
90BSL014	5	1.5	N	N	<10	50	50	<50	N	<20
90BSL030	<5	1.5	10	N	N	30	7	50	<5	20
90BSL031	<5	<1	N	N	N	70	30	70	<5	<20
90BSL032	N	<1	10	N	N	<10	30	N	N	N
90BSL034	7	1	N	N	20	30	15	50	N	<20
90BSL035	N	<1	N	N	N	10	20	N	N	N
90BSL036	N	1.5	20	N	N	15	20	N	N	<20
90BSL037	15	2	N	N	30	30	10	50	5	<20
90BSL038a	7	1.5	15	N	10	<10	50	<50	7	<20
90BSL039	<5	<1	>1000	N	10	30	7000	<50	N	N
90BSL040	30	1.5	N	N	20	70	20	50	N	<20
90BSL041	<5	<1	30	300	N	N	3000	<50	N	N
90BSL042	20	1.5	N	N	<10	15	20	<50	N	<20
90BSL043	7	1	N	N	<10	30	10	50	N	<20
90BSL044	70	2	N	N	100	100	30	70	5	20
90BSL045	15	1.5	N	N	15	70	7	100	<5	<20
90BSL046	10	1.5	N	N	15	10	7	50	N	<20
90BSL047	30	1.5	N	N	20	100	10	50	N	<20
90BSL048	30	1.5	N	N	20	100	20	70	N	<20
90BSL049a	15	<1	1000	N	30	15	3000	N	N	N
90BSL049b	5	<1	1000	20	30	10	>20000	<50	N	N
90BSL050	7	1.5	N	N	<10	70	10	70	N	<20
90BSL051	7	2	N	N	10	30	7	50	N	<20
90BSL052	<5	<1	70	N	N	20	30	N	20	<20
90BSL053	<5	<1	15	N	N	30	30	100	10	20
90BSL054	30	2	N	N	20	70	15	70	N	<20
90BSL055	30	<1	20	N	20	100	15000	70	N	20
90BSL056	7	1.5	N	N	N	100	200	70	N	<20
90BSL057	5	1	N	N	10	N	7	50	N	N
90BSL058	<5	<1	N	N	<10	<10	30	<50	7	<20
90BSL059a	<5	1	N	N	N	15	30	N	N	N
90BSL059b	30	5	N	N	30	10	30	N	N	N
90BSL060	<5	1	N	N	<10	N	20	70	7	<20
90BSL061	5	1	N	N	30	<10	20	70	5	20
90BSL062	7	<1	N	N	<10	<10	7	N	15	N
90BSL063	<5	<1	N	N	<10	<10	15	N	N	N
90BSL064	N	1	N	N	N	N	<5	N	N	N
90BSL065	<5	1.5	N	N	N	N	N	N	N	N
90BSL066	30	1	N	N	20	20	30	N	500	N
90BSL067	<5	2	N	N	N	N	<5	50	N	N
90BSL068	<5	<1	N	N	N	<10	300	70	50	<20
90BSL070	7	1	N	500	30	<10	700	N	10	N
90BSL071	20	<1	N	>500	30	N	1000	N	N	N
90BSL072	20	1.5	N	150	50	15	50	N	N	N
90BSL073	20	<1	N	N	20	30	30	50	N	<20
90BSL074	50	1.5	N	N	20	150	30	70	N	<20
90BSL076	<5	1.5	N	N	N	15	7	<50	<5	<20

Table B-3. *Semiquantitative spectrographic analyses of rock samples collected as part of the study of metallic mineral deposits, Altiplano and Cordillera Occidental, Bolivia*--Continued

Sample no.	Ni	Be	Bi	Cd	Co	Cr	Cu	La	Mo	Nb
90BSL077	7	10	<10	N	N	N	30	N	N	N
90BSL079	15	1.5	N	N	20	70	15	70	N	<20
90BSL080	5	3	N	N	N	<10	30	N	N	N
90BSL081	10	7	N	50	20	N	50	<50	N	N
90BSL082	5	2	15	N	15	N	30	<50	N	N
90BSL083	15	1.5	N	N	10	70	7	70	N	<20
90BSL084a	N	2	>1000	N	N	N	5000	200	10	N
90BSL084b	N	3	>1000	N	N	<10	3000	500	7	N
90BSL084c	10	2	150	N	N	15	5000	500	20	N
90BSL085	7	3	70	N	<10	30	50	50	N	<20
90BSL086	7	3	700	N	10	30	300	50	5	<20
90BSL087	15	2	30	N	15	70	30	70	N	<20
90BSL088a	300	<1	15	N	700	<10	20	N	N	N
90BSL088b	7	7	15	N	20	20	20	N	15	<20
90BSL088c	30	<1	>1000	N	200	<10	15000	N	<5	N
90BSL089	10	1.5	N	N	N	30	50	50	N	<20
90BSL090	7	2	N	N	10	20	30	50	N	<20
90BSL091	<5	3	100	N	<10	20	100	<50	N	<20
90BSL092a	100	1	30	N	300	<10	10000	<50	50	N
90BSL094a	<5	<1	30	N	N	N	70	<50	N	N
90BSL094b	<5	<1	15	N	N	<10	30	<50	N	N
90BSL095	<5	3	10	200	N	N	50	<50	N	N
90BSL097	<5	1.5	10	N	N	70	15	50	N	<20
90BSL098	<5	1.5	<10	N	N	20	15	<50	N	<20
90BSL099	10	3	<10	N	10	50	20	50	N	<20
90BSL100a	5	1.5	30	N	10	70	150	70	5	<20
90BSL100b	<5	1.5	10	N	N	70	50	50	N	20
90BSL101	10	2	<10	N	10	50	15	<50	N	<20
90BSL102	20	2	N	N	15	100	30	100	<5	20
90BSL104	15	2	N	N	15	70	10	70	N	<20
90BSL105	15	2	N	N	15	100	50	100	N	<20
90BSL106	20	1.5	N	N	15	100	15	50	N	<20
90BSL107	20	2	N	N	20	100	20	100	N	<20
90BSL115	<5	1.5	<10	N	N	100	10	50	N	<20
90BSL116	<5	2	<10	N	N	N	7	<50	N	20
90BSL117	<5	1.5	<10	N	N	30	7	<50	N	<20
90BSL118	15	2	N	N	10	100	<5	70	<5	<20
90BSL119	30	<1	N	N	50	<10	30	N	N	N
90BSL120	N	<1	N	N	N	N	20	N	10	<20
PNZ001	<5	1.5	N	N	15	20	7	70	5	<20
PNZ002	<5	<1	N	N	N	20	20	70	7	20
PNZ003	5	1.5	N	N	15	20	7	50	<5	<20
PNZ005	5	1.5	N	N	10	15	7	50	N	<20
PNZ006	7	1.5	N	N	15	15	7	50	N	<20
PNZ007	5	1.5	N	N	15	20	7	70	N	<20
PNZ010	5	2	N	N	<10	20	10	50	N	<20

Table B-3. *Semiquantitative spectrographic analyses of rock samples collected as part of the study of metallic mineral deposits, Altiplano and Cordillera Occidental, Bolivia*--Continued

Sample no.	V	Pb	Sb	Sc	Sn	Sr	W	V	Zn	Zr
90BBG001a	100	70	N	15	<10	200	N	50	N	500
90BBG003	15	50	N	5	N	300	N	15	N	70
90BBG003	10	30	N	<5	N	300	N	15	N	70
90BBG004	<10	50	N	<5	N	150	N	15	N	100
90BBG004	<10	50	N	<5	N	200	N	20	N	150
90BBG005a	100	7000	N	7	N	100	N	20	10000	150
90BBG005b	70	3000	N	5	N	100	N	20	2000	100
90BBG006b	70	10000	N	7	N	N	N	20	3000	150
90BBG006c	70	3000	N	10	N	100	N	20	3000	150
90BBG007	70	1000	N	10	N	<100	N	15	200	150
90BBG008	70	15000	<100	7	N	N	N	15	10000	100
90BBG009a	100	100	N	15	N	200	N	30	700	200
90BBG009b	70	50	N	5	N	<100	N	15	700	100
90BBG010a	50	1000	N	10	N	<100	20	20	2000	70
90BBG010b	50	5000	N	7	N	100	N	20	2000	70
90BBG011a	150	20000	300	10	N	<100	N	20	5000	100
90BBG011b	50	>20000	1000	<5	N	N	N	<10	>10000	30
90BBG012	20	>20000	1000	N	N	<100	N	<10	>10000	<10
90BBG013c	200	30	N	10	N	1500	N	50	N	300
90BBG014	150	200	N	15	20	500	N	15	N	300
90BBG014	70	200	N	7	N	700	N	20	<200	200
90BBG015a	70	100	N	5	N	700	N	10	N	150
90BBG015b	150	30	N	N	N	500	N	<10	N	70
90BBG015c	20	30	N	<5	N	100	N	10	N	300
90BBG016a	100	50	N	7	N	500	N	10	N	150
90BBG016b	300	30	N	<5	<10	700	N	<10	N	20
90BBG018a	100	50	N	7	N	1000	N	20	N	300
90BBG018b	100	50	N	5	N	700	N	20	N	300
90BBG018c	200	30	N	10	N	1000	N	15	N	300
90BBG018d	100	30	N	7	N	1000	N	20	N	500
90BBG018e	150	100	N	10	N	1500	N	20	N	500
90BBG020	30	150	<100	5	N	100	N	10	200	100
90BBG021	70	5000	<100	10	N	100	N	20	500	200
90BBG022a	50	7000	<100	7	N	200	N	30	700	300
90BBG022b	15	7000	<100	5	N	100	N	30	300	200
90BBG023	20	3000	<100	5	N	<100	N	30	N	300
90BBG024	<10	50	N	<5	N	100	N	20	N	200
90BBG025a	50	5000	100	7	N	<100	N	20	500	200
90BBG025b	70	1000	N	10	N	300	N	30	700	150
90BBG025c	70	7000	200	7	N	<100	N	20	500	200
90BBG026	100	50	N	10	N	700	N	30	N	300
90BBG029	150	50	N	10	15	150	<20	15	2000	100
90BBG030	200	100	N	15	N	1000	N	20	300	200
90BBG031	20	1500	N	5	10	150	20	50	200	300
90BBG032a	100	1000	N	10	N	300	N	10	N	150
90BBG032b	100	50	N	10	20	100	N	<10	<200	70
90BBG032c	100	100	N	7	N	200	N	10	<200	50
90BBG033a	10	N	N	N	N	N	N	<10	N	10
90BBG033b	<10	N	N	N	N	<100	N	<10	N	<10
90BBG034	150	30	N	15	N	100	20	30	200	150

Table B-3. *Semiquantitative spectrographic analyses of rock samples collected as part of the study of metallic mineral deposits, Altiplano and Cordillera Occidental, Bolivia*--Continued

Sample no.	V	Pb	Sb	Sc	Sn	Sr	W	V	Zn	Zr
90BBG040	100	70	N	7	N	5000	N	10	<200	300
90BBG045	150	30	N	10	N	200	N	15	N	150
90BBG046a	50	100	N	5	N	200	N	20	300	100
90BBG046b	70	100	N	7	N	200	N	30	<200	200
90BBG047	30	7000	<100	<5	N	N	N	<10	10000	15
90BBG048a	20	1000	<100	<5	N	N	N	<10	10000	<10
90BBG049	20	>20000	100	N	N	N	N	<10	>10000	<10
90BBG050b	20	1500	N	<5	N	<100	N	15	1000	200
90BBG051a	30	200	<100	5	15	300	N	10	500	100
90BBG051b	10	300	1000	<5	700	200	N	N	500	50
90BBG052a	20	>20000	N	N	N	N	N	N	>10000	N
90BBG052b	30	700	N	5	N	200	N	20	3000	300
90BBG052d	30	>20000	N	N	N	100	50	<10	>10000	30
90BBG053a	20	>20000	N	<5	N	N	N	N	>10000	30
90BBG053b	70	200	N	15	N	300	N	30	1000	150
90BBG054	30	2000	N	<5	N	100	N	15	5000	150
90BBG055a	50	70	N	<5	50	1000	<20	15	N	200
90BBG056a	10	50	N	<5	N	N	N	10	N	100
90BBG056b	200	50	N	20	N	1000	N	50	<200	200
90BBG057	<10	1000	N	<5	N	>5000	N	15	1000	N
90BBG058b	50	3000	<100	7	15	1000	N	15	N	150
90BBG058c	200	30	N	20	N	1000	N	50	2000	500
90BBG059	200	30	N	10	N	1000	N	30	N	300
90BBG059	150	30	N	15	N	1000	N	50	N	500
90BBR003	150	10000	<100	10	N	150	N	20	700	300
90BBR004	30	100	N	5	N	500	N	20	N	200
90BBR008	200	30	N	10	N	1000	N	30	N	200
90BBR010	30	30	N	5	N	200	N	30	N	300
90BBR015	20	30	N	<5	N	300	N	15	N	300
90BBR016	100	50	N	N	N	1000	N	10	N	70
90BBR019	150	30	N	10	N	2000	N	20	N	300
90BBR020	100	50	N	7	N	1000	N	20	N	200
90BBR021a	70	30	N	<5	N	500	N	10	N	150
90BBR021b	50	30	N	<5	N	500	N	10	N	200
90BBR021c	200	50	N	15	N	1500	N	50	<200	300
90BBR021d	70	50	N	5	N	1000	N	10	N	300
90BBR022	20	50	N	<5	N	300	N	15	N	150
90BBR026	10	30	N	<5	N	200	N	20	N	200
90BBR029	<10	10	N	5	N	200	N	20	N	200
90BBR031	15	30	N	5	N	100	N	30	N	200
90BBR036a	70	30	N	10	N	3000	N	10	N	200
90BBR036c	70	50	N	5	<10	3000	N	<10	N	200
90BBR036d	70	50	N	7	N	3000	N	10	N	200
90BBR036e	70	30	N	<5	N	2000	N	<10	N	200
90BBR036g	150	30	N	10	N	2000	N	30	200	500
90BBR036h	100	30	N	5	N	1000	N	15	N	300
90BBR037	70	50	N	5	N	1000	N	15	N	100
90BBR041	150	20	N	15	N	2000	N	20	N	500
90BBR041	150	20	N	15	N	2000	N	20	N	300
90BBR044	100	30	N	7	N	2000	N	15	N	200

Table B-3. *Semiquantitative spectrographic analyses of rock samples collected as part of the study of metallic mineral deposits, Altiplano and Cordillera Occidental, Bolivia*--Continued

Sample no.	V	Pb	Sb	Sc	Sn	Sr	W	V	Zn	Zr
90BBR044a	100	20	N	7	N	2000	N	15	N	150
90BBR048a	20	20	N	<5	N	100	N	10	N	300
90BBR050	70	20	N	10	N	3000	N	20	N	500
90BBR051	50	<10	N	10	N	150	N	20	N	500
90BBR054a	70	30	N	5	N	>5000	N	15	N	200
90BBR055	70	50	N	10	N	1500	N	20	N	200
90BBR058c	15	N	N	5	N	N	N	10	N	500
90BBR063	70	3000	N	5	N	1000	N	10	500	100
90BCX003	150	100	N	5	N	300	N	15	700	300
90BCX004	100	100	N	7	N	300	N	30	N	500
90BCX007	70	150	N	<5	N	2000	N	15	N	150
90BCX008a	200	70	N	20	N	300	N	30	N	150
90BCX008b	150	200	N	15	70	200	N	20	N	200
90BCX009	150	30	N	15	N	100	N	20	N	300
90BCX010	150	20	N	10	N	300	N	30	N	500
90BCX012	50	20	N	5	N	1500	N	15	N	30
90BCX013a	70	70	N	5	N	1000	N	20	N	300
90BCX013b	70	1500	N	5	N	1500	N	10	N	500
90BCX014	100	30	N	<5	N	300	N	15	N	700
90BCX015	30	700	N	5	N	5000	N	30	<200	70
90BCX017	100	70	N	<5	N	300	N	20	N	200
90BCX018	50	30	N	N	N	500	N	15	N	150
90BCX019a	150	30	N	7	N	700	N	20	N	500
90BCX019b	30	15	N	<5	N	300	N	15	N	30
90BCX019c	100	70	N	7	N	700	N	50	N	200
90BCX020	70	20	N	7	N	1500	N	30	N	200
90BCX022	70	15	N	5	N	150	N	15	N	150
90BCX022b	15	150	N	7	N	150	N	50	N	100
90BCX023	200	30	N	10	N	1000	N	20	N	70
90BCX023a	200	30	N	30	N	1000	N	30	<200	100
90BCX026	100	30	N	<5	N	500	N	15	N	300
90BCX027	70	>20000	1500	7	100	<100	N	30	>10000	50
90BCX028	10	5000	N	<5	N	N	N	20	1000	100
90BCX029	100	200	N	15	N	500	N	30	N	150
90BCX030a	150	50	N	10	N	500	N	20	200	150
90BCX030b	150	150	N	10	N	500	N	20	700	70
90BCX031	200	70	N	15	N	700	N	50	N	150
90BCX032	150	20	N	10	N	300	N	20	N	150
90BDB001	70	30	N	7	N	500	N	15	N	150
90BDB002	70	50	N	10	N	500	N	20	N	200
90BDB003	100	30	N	10	N	500	N	20	N	150
90BDB004	100	30	N	7	N	500	N	20	N	150
90BDB005	100	30	N	10	N	700	N	30	N	150
90BDB006	150	30	N	15	N	700	N	30	N	150
90BDB007	70	50	N	7	N	500	N	20	N	150
90BDB008	70	70	N	7	N	1000	N	15	N	300
90BDB009	70	50	N	10	N	1000	N	30	N	200
90BDB010	50	30	N	10	N	1500	N	30	N	200
90BDB011	70	20	N	10	N	1000	N	30	N	150
90BDB012	70	30	N	7	N	700	N	10	N	150

Table B-3. *Semiquantitative spectrographic analyses of rock samples collected as part of the study of metallic mineral deposits, Altiplano and Cordillera Occidental, Bolivia*--Continued

Sample no.	V	Pb	Sb	Sc	Sn	Sr	W	V	Zn	Zr
90BDB013	100	30	N	15	N	700	N	20	N	150
90BDB014	100	5000	150	10	N	500	N	20	500	100
90BDB015	150	2000	100	15	N	1500	N	20	300	150
90BDR001a	70	150	100	7	30	N	N	15	N	150
90BDR001b	100	150	N	10	N	500	N	20	N	150
90BDR005	100	70	N	10	N	700	N	20	N	200
90BDR006	150	100	N	15	<10	1000	N	30	N	200
90BDR007	10	2000	200	N	N	1500	N	70	1000	N
90BDR008a	70	150	N	7	<10	150	N	20	300	200
90BDR008b	70	300	N	5	<10	300	N	15	500	150
90BDR009	100	3000	150	10	N	500	N	20	1000	200
90BDR010	70	500	N	5	N	300	N	20	500	200
90BDR012	150	50	N	20	N	700	N	30	N	150
90BDR015	150	30	N	15	N	500	N	20	N	100
90BDR016	150	30	N	15	N	500	N	20	N	150
90BDR022	150	5000	N	7	N	100	N	10	N	100
90BDR025	150	70	N	7	N	300	N	15	200	150
90BDR030	100	50	N	10	N	1000	N	20	<200	150
90BDR031	150	300	N	15	N	300	N	30	300	200
90BDR034	150	150	N	15	N	500	N	30	1000	70
90BDR035	100	50	N	10	N	700	N	30	N	150
90BDR037	150	30	N	15	N	500	N	20	N	150
90BDR038	150	50	N	15	N	700	N	20	N	150
90BDR039	150	50	N	15	N	500	N	30	N	150
90BDR041	150	50	N	20	N	700	N	50	N	150
90BDR041a	150	30	N	20	N	500	N	30	N	150
90BDR042	150	30	N	15	N	500	N	20	N	100
90BDR043	150	30	N	20	N	500	N	30	N	150
90BDR044	100	50	N	15	N	300	N	30	N	100
90BDR046	150	30	N	15	N	300	N	30	N	150
90BDR053	150	50	N	20	N	700	N	50	N	150
90BDR054	200	20	N	30	N	500	N	30	<200	100
90BDR055	10	70	N	5	N	200	N	50	N	70
90BDR057	150	50	N	15	<10	700	N	30	N	150
90BDR058c	150	300	<100	15	N	N	N	30	300	150
90BDR060b	150	200	N	20	N	700	N	50	500	200
90BDR061c	70	70	<100	7	<10	150	N	50	N	150
90BES001	100	30	N	15	N	700	N	20	<200	150
90BES002	150	50	N	10	N	700	N	15	N	150
90BES003	150	30	N	15	N	700	N	15	N	150
90BES004	150	30	N	15	N	700	N	15	N	200
90BES005	150	100	N	15	N	1500	N	30	N	200
90BES006	70	500	N	7	<10	200	N	10	<200	150
90BES007	20	100	N	<5	N	300	N	<10	N	200
90BES008	150	150	N	10	N	N	N	20	N	200
90BES009	30	70	N	7	N	N	N	15	N	300
90BES010	70	150	N	7	N	300	N	15	300	150
90BES011	100	30	N	7	N	500	N	15	N	150
90BES012	150	70	N	10	N	500	N	20	<200	200
90BES013	150	70	N	7	N	500	N	15	<200	200

Table B-3. *Semiquantitative spectrographic analyses of rock samples collected as part of the study of metallic mineral deposits, Altiplano and Cordillera Occidental, Bolivia*--Continued

Sample no.	V	Pb	Sb	Sc	Sn	Sr	W	V	Zn	Zr
90BES014	150	30	N	15	N	1000	N	20	N	150
90BES015	150	50	N	7	N	700	N	<10	N	70
90BES016	150	50	N	15	N	700	N	<10	N	150
90BES029	150	15	N	7	10	150	N	15	N	200
90BES030	150	70	N	10	N	200	N	15	N	200
90BES031	150	30	N	7	N	500	N	15	N	150
90BES032	200	150	N	20	30	300	N	15	N	100
90BES033	100	30	N	10	N	700	N	20	N	150
90BES034	<10	70	N	7	N	150	N	10	N	100
90BES035	70	50	N	7	N	700	N	15	N	100
90BES036	100	50	N	15	N	1000	N	20	N	150
90BES037	70	30	N	7	N	500	N	30	N	150
90BES039	20	30	N	<5	N	200	N	10	N	100
90BES040	20	30	N	N	N	150	N	<10	<200	50
90BES041	<10	50	N	<5	N	150	N	10	N	70
90BES042	20	50	N	<5	N	200	N	15	N	200
90BES043	20	50	N	<5	N	150	N	<10	N	50
90BES044	50	50	N	7	N	200	N	20	N	150
90BES045	150	150	N	7	N	700	50	15	1500	30
90BES046	30	150	150	<5	N	N	N	15	N	200
90BES047	15	200	100	<5	N	N	N	15	300	100
90BES048	70	30	N	7	N	500	N	15	<200	150
90BES049	150	100	N	10	N	300	N	20	1500	100
90BES050	30	>20000	300	<5	N	N	N	<10	>10000	20
90BES051	50	2000	1000	<5	N	N	N	<10	3000	70
90BES052	100	15000	300	5	N	N	N	10	1500	70
90BES053	10	>20000	300	N	30	N	N	<10	>10000	<10
90BES054	30	5000	150	<5	70	N	N	<10	>10000	20
90BES055	50	>20000	2000	7	50	500	N	15	3000	70
90BES056	50	3000	N	7	N	N	N	10	700	100
90BES057	100	7000	<100	7	N	150	N	15	3000	100
90BES058	50	3000	N	N	N	300	N	70	>10000	N
90BES059	100	70	N	10	N	500	N	20	<200	200
90BES060	15	100	N	<5	N	300	N	15	<200	200
90BES061	20	150	N	5	N	500	N	15	200	300
90BES062	15	100	N	<5	N	500	N	15	N	300
90BES063	150	50	N	10	N	500	N	20	<200	300
90BES064	15	70	N	<5	N	300	N	15	N	200
90BES065	15	70	N	<5	N	150	N	15	N	200
90BES066	70	30	N	10	N	500	N	20	<200	200
90BES067	150	30	N	10	N	300	N	20	<200	200
90BES069	50	50	N	5	N	200	N	15	N	150
90BSL001	50	700	500	<5	20	<100	N	20	N	150
90BSL002	100	50	100	10	50	N	30	30	N	200
90BSL003a	70	20	150	7	70	N	N	30	N	150
90BSL004	100	30	N	15	N	700	N	20	N	200
90BSL005	150	150	150	20	15	1500	<20	20	N	300
90BSL006	150	150	N	15	<10	200	N	20	N	200
90BSL007	150	500	N	20	30	500	<20	30	N	200
90BSL009	50	70	150	7	30	N	N	15	N	15

Table B-3. *Semiquantitative spectrographic analyses of rock samples collected as part of the study of metallic mineral deposits, Altiplano and Cordillera Occidental, Bolivia*--Continued

Sample no.	V	Pb	Sb	Sc	Sn	Sr	W	V	Zn	Zr
90BSL010	70	50	100	10	50	100	N	20	N	150
90BSL012	30	<10	N	N	N	300	N	<10	N	200
90BSL013	<10	>20000	10000	N	N	N	N	N	>10000	N
90BSL014	100	2000	150	10	<10	N	N	15	700	150
90BSL030	150	500	N	15	50	200	<20	30	N	150
90BSL031	150	1500	N	15	30	300	N	30	N	150
90BSL032	30	15000	3000	N	150	500	N	<10	N	N
90BSL034	150	30	N	15	N	500	N	20	N	150
90BSL035	70	300	150	N	N	300	N	<10	N	15
90BSL036	70	3000	150	5	70	N	N	10	N	30
90BSL037	70	150	N	7	N	100	N	15	N	100
90BSL038a	70	300	150	7	30	N	N	30	<200	100
90BSL039	70	15000	10000	10	50	N	N	15	300	30
90BSL040	100	150	N	10	N	500	N	20	<200	150
90BSL041	<10	>20000	>10000	N	100	N	30	N	>10000	N
90BSL042	70	200	<100	10	15	150	N	20	1000	150
90BSL043	70	700	N	7	N	200	N	15	500	70
90BSL044	100	70	100	20	<10	200	N	50	300	200
90BSL045	100	150	<100	15	N	200	N	20	700	200
90BSL046	70	30	N	7	N	500	N	15	N	100
90BSL047	70	200	N	10	N	300	N	15	300	100
90BSL048	100	200	N	10	N	700	N	20	300	100
90BSL049a	30	1500	3000	10	100	700	150	30	<200	50
90BSL049b	<10	700	>10000	<5	150	200	200	15	1500	N
90BSL050	100	50	N	10	N	700	N	<10	N	150
90BSL051	70	50	N	7	N	500	N	10	N	150
90BSL052	50	200	150	<5	20	300	<20	10	N	150
90BSL053	70	100	N	<5	20	500	N	30	N	200
90BSL054	70	30	N	7	N	500	N	15	N	100
90BSL055	70	300	1500	7	100	2000	30	15	300	100
90BSL056	70	70	<100	7	N	500	N	15	N	150
90BSL057	70	10	N	7	N	300	N	20	N	150
90BSL058	70	50	N	5	N	150	N	20	N	150
90BSL059a	70	30	N	10	N	150	N	<10	200	50
90BSL059b	50	30	N	15	N	200	N	20	300	50
90BSL060	50	30	N	7	N	500	N	30	500	150
90BSL061	100	30	N	10	N	700	N	30	<200	150
90BSL062	100	<10	N	N	N	N	N	N	N	N
90BSL063	70	70	N	10	N	500	N	20	N	100
90BSL064	10	15	N	5	N	200	N	15	N	<10
90BSL065	10	N	N	N	N	N	N	N	N	30
90BSL066	70	1000	1000	7	N	<100	N	20	700	70
90BSL067	50	50	N	<5	N	200	N	15	N	150
90BSL068	30	2000	>10000	7	N	500	N	70	<200	150
90BSL070	30	20000	1500	7	N	200	N	15	>10000	20
90BSL071	30	>20000	500	<5	N	150	N	10	>10000	15
90BSL072	100	2000	150	20	N	500	N	50	7000	30
90BSL073	150	30	N	20	N	700	N	20	N	100
90BSL074	100	30	N	15	N	500	N	30	<200	150
90BSL076	70	1500	150	<5	N	<100	N	10	300	100

Table B-3. *Semiquantitative spectrographic analyses of rock samples collected as part of the study of metallic mineral deposits, Altiplano and Cordillera Occidental, Bolivia*--Continued

Sample no.	V	Pb	Sb	Sc	Sn	Sr	W	V	Zn	Zr
90BSL077	50	500	500	7	N	>5000	N	10	500	N
90BSL079	150	50	N	15	N	700	N	30	N	150
90BSL080	50	700	300	5	N	N	N	10	1000	50
90BSL081	70	15000	500	5	N	200	N	30	1500	15
90BSL082	70	>20000	1000	5	N	5000	N	30	1000	15
90BSL083	100	70	200	15	N	500	N	20	N	150
90BSL084a	30	1000	150	5	700	N	700	70	300	50
90BSL084b	30	700	300	7	700	N	500	200	200	N
90BSL084c	50	100	150	7	700	N	500	70	<200	50
90BSL085	70	100	<100	7	70	N	50	20	<200	100
90BSL086	70	700	150	10	30	200	100	20	300	70
90BSL087	100	100	<100	15	<10	<100	N	30	<200	100
90BSL088a	<10	30	N	N	30	N	100	30	N	<10
90BSL088b	100	70	N	7	100	<100	70	20	N	100
90BSL088c	<10	50	N	<5	30	N	150	<10	N	N
90BSL089	70	200	N	10	15	<100	N	15	700	300
90BSL090	70	30	N	10	N	300	N	30	300	150
90BSL091	100	50	N	15	15	200	<20	15	N	100
90BSL092a	30	70	500	5	1000	N	3000	150	300	N
90BSL094a	<10	300	>10000	N	N	N	N	N	500	15
90BSL094b	<10	500	>10000	N	N	N	N	N	700	<10
90BSL095	30	15000	7000	<5	>1000	150	N	15	>10000	20
90BSL097	100	200	300	10	50	300	N	15	300	100
90BSL098	70	100	200	7	20	150	N	15	<200	70
90BSL099	70	30	100	7	N	300	N	20	N	100
90BSL100a	100	150	150	10	150	<100	500	10	N	200
90BSL100b	100	150	<100	10	30	100	150	<10	N	200
90BSL101	100	30	<100	10	N	300	N	20	N	100
90BSL102	150	500	N	15	N	700	N	30	<200	150
90BSL104	100	30	N	10	N	700	N	20	<200	70
90BSL105	100	30	N	15	N	700	N	30	N	100
90BSL106	100	30	N	15	N	700	N	30	N	150
90BSL107	150	50	N	20	N	1000	N	30	N	150
90BSL115	150	70	100	15	10	200	N	30	<200	200
90BSL116	15	300	100	7	<10	200	N	30	N	70
90BSL117	70	50	<100	10	<10	300	N	20	N	100
90BSL118	150	50	150	20	N	200	<20	30	N	150
90BSL119	700	10	N	7	N	N	N	15	N	70
90BSL120	70	20	N	7	N	300	20	20	N	150
PNZ001	150	30	N	20	N	500	N	30	N	200
PNZ002	150	30	N	15	N	300	N	20	N	150
PNZ003	150	30	N	20	N	500	N	30	N	200
PNZ005	150	30	N	15	N	500	N	30	N	150
PNZ006	100	30	N	15	N	300	N	20	N	100
PNZ007	150	50	N	15	N	500	N	30	N	150
PNZ010	70	30	<100	7	N	N	N	15	N	100

Table B-4 - *Quantitative analyses of selected rock samples collected as part of the study of metallic mineral deposits, Altiplano and Cordillera Occidental, Bolivia*

[All elements reported in ppm. As and Se determined by continuous flow-hydride generation AAS; Te and Tl determined by flame AAS; and Hg determined by continuous flow-cold vapor AAS. Leaders (--) indicate sample not analyzed for that element]

Sample no.	As	Hg	Se	Te	Tl
90BAH006	--	--	--	<0.05	1.40
90BAH015a	--	--	--	44	0.25
90BAH015b	--	<0.2	--	10.2	<0.05
90BAH015c	--	0.2	--	0.40	0.80
90BAH015d	--	4.6	--	17.0	0.85
90BAN030	330	--	0.6	8.15	0.50
90BAN031	56	--	1.1	1.00	1.20
90BAN032	20	--	1.0	3.10	0.10
90BAN033	490	--	1.2	0.15	1.35
90BAN034	100	--	30	18.5	0.20
90BAN035	94	--	0.4	1.30	1.55
90BAN037	680	--	1.7	31	0.05
90BAN039	54	--	<0.1	0.25	1.85
90BAN040	16	--	<0.1	0.10	0.70
90BBG014	28	0.0	3.0	--	--
90BBG018e	6.2	<0.2	2.0	--	--
90BBG033a	7.5	0.0	<0.1	--	--
90BBG033b	0.2	<0.2	<0.1	--	--
90BBG034	5.5	0.0	<0.1	--	--
90BBG040	3.9	<0.2	2.5	--	--
90BBG045	24	0.4	0.1	--	--
90BBG046a	3.3	0.0	<0.1	--	--
90BBG046b	1.7	<0.2	<0.1	--	--
90BBG047	87	0.5	1.3	--	--
90BBG048a	40	0.0	0.7	--	--
90BBG049	98	0.5	0.3	--	--
90BBG050b	5.5	0.0	0.1	--	--
90BBG051a	430	1.3	0.8	--	--
90BBG051b	11,000	0.1	--	--	--
90BBG052a	58	<0.2	0.3	--	--
90BBG052b	6.7	<0.2	<0.1	--	--
90BBG052d	37	0.8	0.4	--	--
90BBG053a	8.9	<0.2	2.1	--	--
90BBG053b	16	0.0	0.1	--	--
90BBG054	5.4	0.0	<0.1	--	--
90BBG055a	420	<0.2	0.7	--	--
90BBG056a	7.6	<0.2	0.1	--	--
90BBG056b	35	<0.2	<0.1	--	--
90BBG057	97	0.0	<0.1	--	--
90BBG058b	490	0.6	0.9	--	--
90BBG058c	4.1	<0.2	<0.1	--	--
90BBG059	3.0	<0.2	<0.1	--	--
90BBR003	410	0.4	1.8	--	--
90BBR004	4.7	0.0	<0.1	--	--
90BBR015	11	<0.2	0.1	--	--
90BBR016	4.4	<0.2	0.1	--	--
90BBR021a	11	0.1	0.2	--	--
90BBR021b	5.9	0.1	0.1	--	--
90BBR021c	5.1	0.1	0.2	--	--
90BBR021d	3.8	0.0	<0.1	--	--

Table B-4 - *Quantitative analyses of selected rock samples collected as part of the study of metallic mineral deposits, Altiplano and Cordillera Occidental, Bolivia*--Continued

Sample no.	As	Hg	Se	Te	Tl
90BBR026	2.1	0.0	<0.1	--	--
90BBR029	16	<0.2	0.6	--	--
90BBR036a	2.6	<0.2	<0.1	--	--
90BBR036c	30	0.0	0.5	--	--
90BBR036d	2.2	0.0	0.4	--	--
90BBR036e	3.2	0.0	1.0	--	--
90BBR036h	3.0	<0.2	<0.1	--	--
90BBR041	0.8	<0.2	<0.1	--	--
90BBR048a	5.6	0.1	0.3	--	--
90BBR050	20	<0.2	8.1	--	--
90BBR051	9.6	0.1	0.4	--	--
90BBR054a	10	0.0	2.5	--	--
90BBR055	21	<0.2	2.7	--	--
90BBR058c	2.3	0.3	2.8	--	--
90BBR063	100	0.0	1.4	--	--
90BDB008	1.1	--	<0.2	--	--
90BDB009	3.2	--	<0.2	--	--
90BDB010	2.7	--	<0.2	--	--
90BDB011	0.7	--	<0.2	--	--
90BDB012	2.4	--	<0.2	--	--
90BDB013	2.5	--	<0.2	--	--
90BDB014	350	--	--	--	--
90BDB015	320	--	--	--	--
90BDR001	--	<0.2	--	<0.05	1.20
90BDR007	--	<0.2	--	<0.05	<0.05
90BDR008a	--	<0.2	--	<0.05	2.10
90BDR008b	--	0.0	--	<0.05	1.50
90BDR009	--	0.4	--	0.05	1.15
90BDR010	--	--	--	<0.25	1.30
90BDR015	--	--	--	--	--
90BDR016	--	<0.2	--	<0.05	0.75
90BDR022	--	<0.2	--	<0.05	5.90
90BDR025	--	<0.2	--	<0.05	2.20
90BDR029	--	--	--	0.25	1.80
90BDR029a	--	<0.2	--	0.60	2.50
90BDR034a	--	--	--	<0.05	30
90BDR034c	--	--	--	<0.05	0.20
90BDR034d	--	10	--	<0.05	51
90BDR035a	--	0.2	--	<0.05	0.35
90BDR040a	--	0.1	--	0.50	0.80
90BDR040b	--	0.1	--	0.15	0.20
90BDR040c	--	<0.2	--	0.20	2.80
90BDR051a	--	0.4	--	0.15	1.60
90BDR051b	--	<0.2	--	0.40	0.05
90BDR051c	--	--	--	1.00	0.40
90BDR052	--	--	--	0.25	1.30
90BDR054a	--	--	--	<0.05	0.20
90BDR058	--	--	--	<0.05	4.50
90BDR058b	--	0.6	--	<0.05	0.30
90BDR060	--	--	--	<0.05	0.70
90BDR061	--	<0.2	--	<0.05	1.75
90BDR061a	--	--	--	0.20	0.60
90BDR061b	--	0.4	--	0.15	15
90BDR062	--	0.0	--	<0.05	0.90
90BEB001	--	0.1	--	<0.05	0.30

Table B-4 - *Quantitative analyses of selected rock samples collected as part of the study of metallic mineral deposits, Altiplano and Cordillera Occidental, Bolivia*--Continued

Sample no.	As	Hg	Se	Te	Tl
90BEB002a	--	--	--	<0.05	<0.05
90BEB003a	--	<0.2	--	<0.05	3.50
90BEB003b	--	0.4	--	<0.05	2.15
90BEB003d	--	0.0	--	0.05	4.25
90BEB005a	--	0.4	--	<0.05	0.85
90BEB005b	--	0.2	--	3.00	0.50
90BEB005c	--	0.1	--	2.80	0.60
90BEB005d	--	<0.2	--	1.40	1.50
90BES001	--	<0.2	--	0.05	0.40
90BES002	--	<0.2	--	--	--
90BES003	--	0.0	--	1.05	0.70
90BES004	--	0.1	--	6.00	0.25
90BES005	--	0.0	--	--	--
90BES006	--	0.1	--	0.40	2.80
90BES007	--	0.1	--	0.50	1.30
90BES008	--	0.0	--	1.10	1.40
90BES009	--	0.1	--	3.90	0.10
90BES010	--	<0.2	--	<0.05	0.75
90BES011	--	0.0	--	--	--
90BES012	--	<0.2	--	--	--
90BES013	--	<0.2	--	--	--
90BES014	--	0.0	--	<0.05	0.20
90BES015	--	0.6	--	1.05	<0.05
90BES016	--	0.1	--	0.50	0.20
90BES029	--	<0.2	--	1.00	1.00
90BES030	--	<0.2	--	0.45	0.40
90BES031	--	<0.2	--	<0.05	0.25
90BES032	--	<0.2	--	0.20	1.70
90BES033	--	<0.2	--	<0.05	0.15
90BES034	--	0.0	--	<0.05	0.60
90BES035	--	0.0	--	<0.05	0.35
90BES036	--	<0.2	--	<0.05	0.20
90BES037	--	0.0	--	<0.05	0.45
90BES039	--	0.3	--	<0.05	0.40
90BES040	--	0.1	--	<0.05	0.60
90BES041	--	0.0	--	<0.05	0.75
90BES042	--	0.0	--	<0.05	0.50
90BES043	--	0.2	--	<0.05	0.20
90BES044	--	<0.2	--	<0.05	0.50
90BES045	--	0.0	--	<0.05	47
90BES046	--	0.2	--	<0.05	0.50
90BES047	--	0.0	--	<0.05	2.10
90BES048	--	<0.2	--	<0.05	0.40
90BES049	--	0.0	--	<0.05	2.00
90BES050	--	0.6	--	0.25	0.10
90BES051	--	--	--	28	0.90
90BES052	--	0.4	--	0.70	1.30
90BES053	--	0.4	--	0.15	<0.05
90BES054	--	0.2	--	0.20	0.20
90BES055	--	0.0	--	<0.05	0.15
90BES056	--	<0.2	--	<0.05	2.20

Table B-4 - *Quantitative analyses of selected rock samples collected as part of the study of metallic mineral deposits, Altiplano and Cordillera Occidental, Bolivia*--Continued

Sample no.	As	Hg	Se	Te	Tl
90BES057	--	0.0	--	<0.05	4.50
90BES058	--	<0.2	--	<0.05	0.40
90BES059	--	<0.2	--	<0.05	0.50
90BES060	--	<0.2	--	0.10	0.35
90BES061	--	0.0	--	0.15	0.35
90BES062	--	<0.2	--	0.30	0.35
90BES063	--	0.3	--	0.25	0.55
90BES064	--	<0.2	--	0.15	0.90
90BES065	--	0.0	--	0.10	0.60
90BES066	--	<0.2	--	<0.05	0.10
90BES067	--	<0.2	--	<0.05	0.30
90BES069	--	<0.2	--	0.35	0.55
90BSL001	--	<0.2	--	<0.05	1.20
90BSL002	--	0.2	--	<0.05	1.15
90BSL003	--	<0.2	--	<0.15	0.75
90BSL006	--	0.1	--	0.10	1.70
90BSL007	--	0.0	--	1.40	1.10
90BSL009	--	<0.2	--	0.10	0.15
90BSL010	--	0.0	--	<0.05	2.40
90BSL012	--	5.6	--	<0.05	0.20
90BSL013	--	--	--	<0.05	3.30
90BSL014	--	<0.2	--	<0.05	4.00
90BSL057	19	--	0.2	--	--
90BSL058	750	--	--	--	--
90BSL059	540	--	--	--	--
90BSL059	5,500	--	--	--	--
90BSL060	7.9	--	0.2	--	--
90BSL061	51	--	--	--	--
90BSL062	97	--	--	--	--
90BSL063	75	--	--	--	--
90BSL064	13	--	<0.1	--	--
90BSL065	31	--	--	--	--
90BSL066	4,400	--	--	--	--
90BSL067	3.3	--	<0.2	--	--
90BSL068	1,600	--	--	--	--
90BSL070	270	--	--	--	--
90BSL071	200	--	--	--	--
90BSL072	150	--	--	--	--
90BSL073	2.7	--	<0.2	--	--
90BSL074	4.5	--	<0.2	--	--
90BSL076	210	--	--	--	--
90BSL077	46	--	--	--	--
90BSL079	25	--	<0.2	--	--
90BSL080	330	--	--	--	--
90BSL081	330	--	--	--	--
90BSL082	59	--	--	--	--
90BSL083	11	--	<0.2	--	--
90BSL084a	17	--	--	--	--
90BSL084b	99	--	--	--	--
90BSL084c	51	--	--	--	--

Table B-4 - *Quantitative analyses of selected rock samples collected as part of the study of metallic mineral deposits, Altiplano and Cordillera Occidental, Bolivia*--Continued

Sample no.	As	Hg	Se	Te	Tl
90BSL085	16	--	--	--	--
90BSL086	140	--	--	--	--
90BSL087	38	--	--	--	--
90BSL088a	81	--	--	--	--
90BSL088b	74	--	--	--	--
90BSL088c	800	--	--	--	--
90BSL089	--	<0.2	--	<0.05	0.90
90BSL090	1.9	--	<0.2	--	--
90BSL091	54	--	--	--	--
90BSL095	890	--	--	--	--
90BSL097	590	--	--	--	--
90BSL098	780	--	--	--	--
90BSL099	18	--	--	--	--
90BSL100a	17	--	--	--	--
90BSL101	19	--	--	--	--
90BSL102	1.8	--	<0.2	--	--
90BSL104	1.4	--	<0.2	--	--

Table B-4 - *Quantitative analyses of selected rock samples collected as part of the study of metallic mineral deposits, Altiplano and Cordillera Occidental, Bolivia*--Continued

Sample no.	As	Hg	Se	Te	Tl
90BSL105	1.9	--	<0.2	--	--
90BSL106	2.8	--	<0.2	--	--
90BSL107	5.2	--	<0.2	--	--
90BSL115	72	--	--	--	--
90BSL116	26	--	--	--	--
90BSL117	52	--	--	--	--
90BSL118	270	--	<0.1	--	--
90BSL119	2.7	--	<0.1	--	--
90BSL120	4.3	--	<0.1	--	--
PNZ001	2.2	--	<0.2	--	--
PNZ002	19	--	<0.1	--	--
PNZ003	1.4	--	<0.2	--	--
PNZ005	1.1	--	<0.2	--	--
PNZ006	2.1	--	<0.2	--	--
PNZ007	4.9	--	<0.2	--	--
PNZ010	5.3	--	<0.2	--	--

Table B-5. *Major-element analyses of rock samples collected as part of the study of metallic mineral deposits, Altiplano and Cordillera Occidental, Bolivia*

[All elements reported in weight percent. All elements determined by WDXRF. Leaders (--) indicate element was not detected]

Sample no.	SiO_2	Al_2O_3	$FeTO_3$	MgO	CaO	Na_2O	K_2O	TiO_2	P_2O_5	MnO	LOI	sum
90BDR001	83.8	8.07	1.19	0.36	0.03	--	2.48	0.66	0.06	--	2.75	99.40
90BDR001	62.9	15.1	4.83	2.15	3.31	3.15	4.07	0.83	0.29	0.06	2.90	99.59
90BDR005	62.1	16.2	4.53	2.23	4.62	2.64	4.11	1.07	0.38	0.06	1.45	99.39
90BDR006	64.0	16.6	3.47	1.31	3.4	2.48	4.65	0.83	0.5	0.04	2.41	99.69
90BDR008	66.9	16.2	1.98	0.63	0.38	2	8.73	0.46	0.22	0.13	1.89	99.52
90BDR008	64.3	15.5	4.26	0.59	0.34	1.48	9.23	0.43	0.21	0.07	1.79	98.2
90BDR010	61.5	15.1	6.67	0.88	0.61	1.04	9.04	0.43	0.21	0.24	2.83	98.55
90BDR012	63.3	16.2	5.02	1.15	4.85	3.14	3.11	0.73	0.28	0.06	1.74	99.58
90BDR015	59.9	17.6	5.87	2.77	5.54	2.90	2.36	0.81	0.13	0.08	1.53	99.49
90BDR016	63.7	16.2	5.26	2.25	4.87	2.75	3.16	0.77	0.17	0.07	0.37	99.57
90BDR025	61.5	15.3	4.48	1.74	3.56	2.62	4.22	0.83	0.25	0.15	4.33	98.98
90BDR030	62.6	17.9	2.91	0.47	1.86	2.59	8.54	0.61	0.28	--	1.10	98.86
90BDR031	59.4	18.1	4.16	0.51	0.86	1.02	10.0	0.87	0.40	0.09	3.77	99.18
90BDR034	63.7	16.3	4.62	0.96	3.95	2.88	3.44	0.70	0.18	0.07	2.08	98.88
90BDR035	62.0	17.3	4.79	1.63	3.99	3.56	3.14	0.64	0.30	0.08	1.7	99.13
90BDR037	60.4	17	5.75	2.93	5.36	3.21	3.24	0.93	0.26	0.07	1.1	100.25
90BDR038	62.5	16.3	5.38	2.57	4.07	3.15	3.18	0.83	0.17	0.07	1.17	99.39
90BDR039	61.4	15.9	5.76	2.75	5.03	2.36	3.68	0.85	0.18	0.07	1.51	99.49
90BDR041	63.6	15.9	4.71	2.15	4.44	2.98	3.07	0.67	0.18	0.07	1.94	99.71
90BDR041a	60.7	16.4	6.38	2.91	5.18	2.70	2.63	0.94	0.23	0.09	1.74	99.90
90BDR042	65.3	16.1	4.74	1.80	4.48	3.18	3.17	0.66	0.15	0.06	0.42	100.06
90BDR043	62.3	16.5	4.99	2.39	5.16	2.85	3.06	0.72	0.18	0.07	1.34	99.56
90BDR044	64.7	15.5	4.83	2.06	4.49	2.71	3.57	0.75	0.18	0.07	0.31	99.17
90BDR046	62.9	16.4	5.68	2.47	4.87	2.79	3.08	0.83	0.19	0.08	0.35	99.64
90BDR053	61.7	16.2	5.88	2.16	4.68	3.11	2.88	0.74	0.24	0.11	1.76	99.46
90BDR054	51.4	17.8	9.47	3.46	9.87	2.81	1.78	1.39	0.33	0.15	1.41	99.87
90BDR055	74.8	13.2	0.70	0.19	1.09	3.25	4.8	0.06	0.07	0.06	0.40	98.62
90BDR057	62.5	15.0	4.05	1.49	4.29	2.02	4.12	0.66	0.26	0.03	4.56	98.98
90BDR058c	59.8	14.4	10.3	1.01	0.54	0.32	5.47	0.67	0.26	1.20	5.07	99.04
90BDR060b	63.2	15.8	4.8	2.69	3.22	2.41	3.46	0.72	0.28	0.12	2.46	99.16

Table B-5. *Major-element analyses of rock samples collected as part of the study of metallic mineral deposits, Altiplano and Cordillera Occidental, Bolivia*--Continued

Sample no.	SiO_2	Al_2O_3	$FeTO_3$	MgO	CaO	Na_2O	K_2O	TiO_2	P_2O_5	MnO	LOI	sum
90BDR061c	65.6	15.7	2.62	0.49	0.40	0.72	10.8	0.48	0.24	--	1.69	98.74
90BG001a	69.4	14.3	3.46	0.61	1.19	3.80	4.78	0.51	0.12	0.07	0.75	98.99
90BG003	70.7	12.7	0.76	0.24	1.78	1.98	4.86	0.14	--	--	5.89	99.05
90BG004	75.2	13.3	0.40	0.17	0.72	3.22	4.63	0.11	--	--	0.9	98.65
90BG013c	59.5	16.3	4.92	1.77	4.54	3.56	3.09	0.91	0.39	0.05	3.3	98.33
90BG022b	72.7	12.7	1.37	--	0.11	1.16	8.55	0.19	0.06	--	1.46	98.3
90BG024	78.0	11.6	0.32	0.1	0.17	1.6	4.55	0.13	--	--	1.71	98.18
90BG059	59.3	16.8	5.51	2.18	4.06	4.34	3.67	0.87	0.39	0.11	1.94	99.17
90BR008	57.8	17.9	6.97	0.92	6.34	4.04	2.47	0.79	0.38	0.07	1.67	99.35
90BR010	69.2	14.1	2.08	0.88	1.19	1.95	5.97	0.30	--	0.08	3.30	99.05
90BR020	64.2	15.8	3.84	1.43	3.26	4.27	3.56	0.68	0.27	0.07	1.90	99.28
90BR022	74.0	13.3	1.24	0.25	0.95	3.62	4.95	0.18	--	--	0.38	98.87
90BR031	73.5	13.1	1.25	0.60	0.66	2.58	5.11	0.17	--	0.03	2.14	99.14
90BR036g	63.1	17.1	3.9	0.90	2.89	4.19	4.01	1.03	0.36	--	1.22	98.7
90BR037	69.6	14.2	2.78	1.08	1.99	3.80	3.83	0.50	0.18	0.05	0.82	98.83
90BR041	46.1	13.9	14.2	6.97	11.2	2.48	0.12	2.19	0.24	0.22	0.71	98.33
90BR044	64.0	15.3	4.40	1.46	2.55	4.15	3.67	0.83	0.44	0.04	1.96	98.8
90BR044a	64.1	15.0	4.11	1.63	2.19	3.51	3.53	0.78	0.41	0.03	3.64	98.93
90BR019	59.6	16.2	6.33	2.85	5.07	4.27	3.16	1.17	0.57	0.09	0.14	99.45
PNZ01	64.1	16.2	5.20	1.94	3.98	1.98	4.05	1.00	0.31	0.06	0.90	99.72
PNZ03	63.4	15.7	5.47	1.97	3.95	1.71	3.71	0.97	0.27	0.06	2.65	99.86
PNZ05	63.3	15.6	5.44	1.97	4.08	1.74	3.69	0.96	0.27	0.05	2.62	99.72
PNZ06	63.6	15.4	5.56	1.82	3.5	1.70	3.77	0.99	0.26	0.06	3.22	99.88
PNZ07	63.4	16.9	4.71	1.72	4.14	2.03	3.98	0.88	0.3	0.05	1.35	99.46
PNZ10	68.1	14.9	2.72	1.31	0.41	0.17	8.50	0.42	0.18	--	2.67	99.38
90BSL002	74.0	11.4	4.94	0.35	--	--	3.34	0.57	--	--	4.71	99.31
90BSL003	85.0	6.35	0.85	0.26	0.04	--	1.86	0.61	0.05	--	3.89	98.91
90BSL004	64.3	14.7	4.03	2.08	1.70	4.33	3.69	0.66	0.25	0.04	2.10	97.88
90BSL005	64.0	11.8	7.36	0.80	0.18	0.17	3.82	1.01	0.43	--	8.59	98.16
90BSL010	63.8	13.8	9.76	0.50	0.04	--	2.77	0.65	0.15	--	7.19	98.66
90BSL034	58.3	15.7	5.64	2.38	5.75	3.48	3.03	0.8	0.24	0.11	4.19	99.62
90BSL040	60.8	14.6	5.10	2.58	3.74	3.60	4.15	0.76	0.34	0.12	3.39	99.18
90BSL046	63.0	15.3	4.27	1.46	4.40	3.29	3.35	0.62	0.20	0.06	3.56	99.51
90BSL047	61.7	14.4	5.14	2.66	2.67	3.63	4.74	0.77	0.27	0.28	2.85	99.11
90BSL048	63.6	14.9	4.73	2.65	2.78	3.69	3.93	0.69	0.25	0.21	1.71	99.14
90BSL050	69.6	15.6	1.23	0.41	1.75	3.77	3.82	0.51	0.12	--	2.16	98.97
90BSL051	67.9	14.2	2.82	1.21	2.50	3.70	3.98	0.44	0.19	0.05	1.80	98.79
90BSL054	62.1	14.3	4.17	2.15	3.77	2.99	4.07	0.72	0.28	0.07	4.55	99.17
90BSL057	60.5	16.6	6.04	2.00	2.63	7.02	2.37	0.75	0.42	0.1	1.01	99.44
90BSL060	62.6	16.8	3.71	0.45	5.85	3.15	3.39	0.59	0.31	0.05	2.31	99.21
90BSL067	68.0	15.3	2.71	1.06	3.11	2.46	4.64	0.7	0.23		1.14	99.35
90BSL073	56.4	18.1	6.01	2.63	7.72	2.97	2.06	0.48	0.22	0.07	3.00	99.66
90BSL074	61.0	15.5	5.62	3.41	4.65	2.51	3.26	0.81	0.27	0.13	2.25	99.41
90BSL079	63.5	14.9	3.92	1.47	5.38	2.58	2.71	0.57	0.18	0.04	4.18	99.43
90BSL083	63.8	15.9	4.68	0.87	1.69	1.58	8.00	0.74	0.28	0.06	1.61	99.21
90BSL090	65.3	15.3	3.55	1.58	1.26	1.97	7.49	0.57	0.22	0.12	2.08	99.44
90BSL102	65.5	14.4	3.92	1.98	3.49	2.29	4.56	0.64	0.26	0.04	2.01	99.09
90BSL104	64.1	14.2	3.69	2.02	4.05	1.91	2.87	0.56	0.22	0.02	5.68	99.32
90BSL105	63.5	16.0	4.27	1.91	3.74	2.39	5.13	0.65	0.27	0.04	1.33	99.23
90BSL106	60.9	15.9	4.61	2.41	4.52	2.60	3.07	0.69	0.28	0.03	4.44	99.45
90BSL107	61.8	15.7	4.52	2.29	3.89	2.81	3.70	0.67	0.28	0.04	3.61	99.31
90BDB001	64.5	15.2	4.49	1.77	2.68	3.31	4.06	0.86	0.29	0.03	2.04	99.23
90BDB003	63	14.7	4.66	2.25	3.58	2.99	3.63	0.85	0.29	0.12	3.28	99.35
90BDB004	63.2	15.7	4.98	1.83	3.52	3.33	3.92	0.87	0.46	0.05	1.41	99.27
90BDB005	60.7	15.2	5.03	2.14	4.51	3.02	3.6	0.71	0.35	0.10	4.08	99.44

Table B-5. *Major-element analyses of rock samples collected as part of the study of metallic mineral deposits, Altiplano and Cordillera Occidental, Bolivia*--Continued

Sample no.	SiO_2	Al_2O_3	$FeTO_3$	MgO	CaO	Na_2O	K_2O	TiO_2	P_2O_5	MnO	LOI	sum
90BDB006	59.9	15.9	6.67	2.63	5.42	3.20	3.38	0.98	0.45	0.12	0.76	99.41
90BDB007	65.8	15.8	4.52	1.35	2.34	3.00	3.84	0.6	0.53	0.09	1.50	99.37
90BDB008	64.2	14.2	3.54	0.72	3.56	3.34	4.3	0.72	0.35	0.02	4.28	99.23
90BDB009	65.6	15.8	4.45	1.10	3.24	3.45	3.21	0.59	0.43	0.04	1.57	99.48
90BDB010	63.5	17.6	4.82	0.64	3.40	2.67	4.66	0.47	0.21	0.04	1.51	99.52
90BDB011	60.6	17.5	5.59	1.52	5.60	4.07	2.75	0.67	0.36	0.18	0.46	99.30
90BDB012	67.1	15.1	3.32	1.32	2.64	4.00	4.01	0.64	0.27	--	0.85	99.25
90BDB013	60.8	14.6	6.32	2.71	4.17	3.38	3.81	1.16	0.48	0.06	1.93	99.42
90BES002	60.9	16.4	7.46	0.81	0.29	1.75	3.91	0.92	0.27	<0.02	6.48	99.19
90BES003	63.3	16.0	4.63	0.94	1.47	2.89	3.36	0.95	0.09	<0.02	5.28	98.91
90BES005	61.5	16.9	5.89	0.48	0.12	1.08	3.55	0.93	0.39	<0.02	8.16	99.00
90BES011	61.6	16.3	5.59	1.53	4.14	4.15	3.54	0.88	0.30	0.10	0.94	99.07
90BES012	60.6	16.8	4.86	2.17	4.12	4.16	3.38	0.81	0.31	0.06	2.08	99.35
90BES013	63.1	15.8	4.33	1.90	3.74	4.32	3.72	0.74	0.28	0.05	1.45	99.43
90BES016	67.2	15.7	2.56	0.32	0.10	0.71	4.41	0.79	0.22	<0.02	7.24	99.25
90BES031	59.7	16.8	6.15	2.31	5.45	3.75	2.83	0.98	0.33	0.08	1.56	99.94
90BES033	63.1	16.2	5.12	1.92	4.19	3.87	3.51	0.72	0.29	0.07	0.36	99.35
90BES035	62.2	15.5	5.01	2.04	4.19	3.67	3.63	0.68	0.31	0.08	1.31	98.62
90BES036	61.2	16.5	5.74	2.15	4.56	3.94	3.56	0.86	0.37	0.09	0.43	99.40
90BES037	68.1	15.1	3.14	0.88	2.32	4.15	3.79	0.46	0.17	0.08	0.84	99.03
90BES041	71.6	13.3	0.68	0.15	0.67	1.29	4.38	0.11	<0.05	0.05	6.93	99.16
90BES044	72.3	13.4	2.07	0.57	1.61	3.43	4.05	0.29	0.09	0.11	1.06	98.98
90BES047	80.1	11.4	0.60	0.31	<0.02	0.18	4.67	0.12	<0.05	<0.02	1.79	99.17
90BES048	62.5	16.6	4.72	1.13	4.57	4.03	2.80	0.73	0.37	0.08	1.69	99.22
90BES059	63.7	16.8	4.64	0.80	3.64	4.22	3.39	0.73	0.26	0.04	1.18	99.40
90BES063	68.2	16.4	1.33	0.27	0.23	0.79	2.97	1.00	0.34	<0.02	7.69	99.22
90BES066	61.8	16.5	5.07	1.94	4.39	3.82	2.90	0.66	0.31	0.09	1.94	99.42
90BES067	61.6	18.6	4.05	0.59	3.70	3.86	3.26	0.88	0.36	0.03	2.26	99.19

Table B-6. *Uranium and thorium analyses of rock samples collected as part of the study of sedimentary uranium deposits, Altiplano and Cordillera Occidental, Bolivia*

[All elements reported in ppm. All elements determined by delayed neutron counting]

Sample no.	Th	U
90BCX003	6.52	2.18
90BCX004	7.80	7.02
90BCX007	3.91	1.45
90BCX008a	15.4	4.11
90BCX008b	17.2	8.34
90BCX009	9.28	2.41
90BCX010	7.71	2.15
90BCX012	4.10	1.00
90BCX013a	5.53	1.45
90BCX013b	8.47	1.04
90BCX014	8.21	4.13
90BCX017	5.21	1.58
90BCX018	3.50	7.94
90BCX019a	4.42	1.84
90BCX019b	4.40	1.34
90BCX019c	7.35	2.66
90BCX020	11.0	15.0
90BCX022	4.00	2.09
90BCX023	4.50	7.37
90BCX026	8.47	1.46
90BCX030a	4.50	3.68
90BCX030b	4.60	6.82
90BCX031	5.70	9.56
90BCX032	7.80	8.48

Table B-7. Analyses of surface waters collected as part of the study of sediment-hosted copper deposits, Altiplano and Cordillera Occidental, Bolivia

[All elements reported in parts per billion (ppb), except those followed by an asterisk (*), which are reported in ppm (Ca, K, Mg, Na, Si, Sr)]

Element	90BCX005	90BCX006	90BCX011	90BCX021
Ca*	1,020	789	281	6.9
K*	<200	<200	<20	30
Mg*	100	77	40	14.8
Na*	34,600	35,400	1,030	586
Si*	3	3	7.6	21.4
Sr*	24,600	18,400	5,650	390
B	3,000	4,300	1,400	3,600
Ba	<400	<400	<40	80
Li	2200	1900	280	1670
Mn	2000	1000	<20	<20
Mo	<2,000	<2,000	<200	<200
Ni	<1,000	<1,000	<100	<100
Pb	<2,000	<2,000	<200	<200
Sn	<1,200	<1,200	<100	<100
Ti	300	300	80	<20
V	<1,200	<1,200	<100	<100
Zn	<600	<600	<60	<60

Table B-8. *Analyses of water samples collected as part of the study of alkaline, saline waters, Altiplano and Cordillera Occidental, Bolivia*

[All elements reported in parts per billion (ppb), except those followed by an asterisk (*), which are reported in ppm (Ca, K, Mg, Na, Si). Temperature and pH measured in the field. All elements determined by ICP-AES. Leaders (--) indicate no data available]

Sample no.	Locality name	Lat S	Long W	Total dissoved solids	Temp. ° C.	pH	Ca*	K*	Mg*
RF01	Kasilla Hot Spring	18.0775	69.1433	--	46	8.0	46.1	83	29.5
RF02	Laguna Sacabaya (spring)	18.6400	68.9525	--	--	7.5	172	87	116
RF03	Laguna Sacabaya (spring)	18.0761	68.9750	--	35	7.7	258	164	191
RF04	Laguna Sacabaya	18.6561	68.9392	--	--	7.6	268	171	198
RU03	Laguna Sacabaya (spring)	18.0761	68.9758	--	35	7.7	199	94	147
RU04	Laguna Sacabaya	18.5061	68.9431	--	--	7.7	223	105	165
RU05	Laguna Verde	22.8183	67.7711	--	--	7.8	94	37	44.9
RU06	Sol de Mañana (spring)	22.4297	67.7542	3,000	32	7.7	134	63	30.6
RU07	Mina Juanita (spring)	22.6369	67.8089	260	32	2.6	86.7	7	37.6
RU08	Challviri	22.4819	67.5592	230	30	7.7	23.4	<4	1
RU09	Laguna Cachi	21.7308	67.9533	230	14	--	1.9	12	0.8
RU10	Pastos Grandes (influx)	21.7053	67.7811	85	5	7.7	41	6	14.5
RU11	Pastos Grandes (spring)	22.5878	67.8344	160	10	7.1	9.5	7	4.4
RU12	Laguna Chojllas (spring)	22.3717	67.0928	125	11	7.0	6.7	4	1.2
RU13	Laguna Coruto (spring)	22.4414	67.0225	230	18	7.7	107	29	18.6
RU13S	Busch o Kalina (spring)	22.6056	67.1806	--	4	7.5	40.8	15	5.7
RU14	Laguna Coruto	22.4369	67.0119	--	--	8.5	11.7	13	1
RU15	Laguna Chojllas	22.3558	67.0844	1,000	2	8.1	714	355	179
RU15S	Busch o Kalina	22.6103	67.1778	--	--	7.9	526	1,110	155
RU16	Laguna Mama Khumu	22.2600	67.0844	280	8	7.3	26.8	15	8.5
RU17	Laguna Celeste	22.2161	67.1047	1,650	0	9.0	8.2	200	85.3
RU17S	Laguna Catalcito	22.4803	67.4056	--	--	7.6	31.3	32	5.8
RU18	Laguna Colorado	22.1897	67.8133	1,120	0	7.7	29.8	61	16.9
RU19	Laguna Colorado (spring)	22.1686	67.8072	300	21	7.5	12.5	16	6.8
RU19S	Laguna Totoral	22.5428	67.2853	--	--	8.1	20.3	<4	1.4
RU21	Volcán Olca (spring)	20.8661	68.4389	120	40	7.9	117	73	68.7
RU21S	Laguna Loromayu	20.3936	67.2064	--	--	8.3	422	12,300	1040
RU22	Empexa (spring)	20.5408	68.4725	7,200	78	8.3	6.6	125	6.2
RU23	Río Khoto Tributary	19.0842	67.9797	--	--	8.2	82.9	35	45.5
RU24	S.alarde Coipasa	19.2233	68.3847	--	--	6.9	1,610	3,500	1730
RU25	Río Laugo	19.0561	68.1589	--	--	8.0	88.7	44	63.2
RU26	Salar de Coipasa (spring)	19.2433	68.3689	1,590	12	7.2	818	478	470
RU28	Pisiga Sucre (well)	19.2583	68.5681	900	11	7.6	138	32	42.1
RU30	Río Sabaya	19.1197	68.3003	--	11	7.5	686	2,560	1360
RU32	Río Lauca Jahuira	19.2111	67.8056	--	--	7.8	152	50	75.6

Table B-8 - *Analyses of water samples collected as part of the study of alkaline, saline waters, Altiplano and Cordillera Occidental, Bolivia*–Continued

Sample no.	Na*	Si*	Sr	Ni	Ba	B	Li	Mn	Mo	Ti	V	Zn
RF01	430	102	960	30	<40	9,600	2,370	<20	<20	<20	<60	<20
RF02	1,010	48.8	3,390	60	40	23,200	5,590	<20	20	<20	<60	<20
RF03	1,750	52.7	4,210	<20	<40	39,600	11,100	<20	<20	<20	<60	<20
RF04	1,820	54.7	4,380	30	<40	41,200	11,500	<20	<20	40	<60	<20
RU03	1,100	50	3,200	<20	<40	24,300	6,210	<20	<20	<20	<60	<20
RU04	1,240	56.1	3,590	60	<40	27,300	6,990	<20	<20	<20	<60	<20
RU05	651	50.4	1,840	<20	<40	20,800	6,350	<20	<20	<20	70	<20
RU06	169	83	380	30	<40	1,200	340	<20	<20	<20	<60	<20
RU07	55	163	120	60	<40	22,300	60	1,690	<20	<20	<60	1,580
RU08	82	44.7	40	40	<40	900	100	<20	<20	<20	60	<20
RU09	115	25	20	90	<40	1,400	790	<20	<20	<20	<60	<20
RU10	18	42.8	190	130	<40	600	80	<20	<20	<20	<60	<20
RU11	69	27.1	150	<20	<40	1,100	780	<20	<20	<20	<60	<20
RU12	68	21.5	60	30	<40	1,600	1,010	<20	<20	<20	<60	<20
RU13	458	35.1	2,100	30	50	8,900	5,040	<20	<20	<20	<60	<20
RU13S	121	52.3	410	30	<40	2,300	880	<20	<20	<20	<60	<20
RU14	95	55.1	170	40	<40	3,400	1,160	<20	<20	<20	<60	<20
RU15	3,260	30.4	20,500	<20	210	141,000	65,800	<20	<20	<20	<60	<20
RU15S	2,780	53.2	20,000	<20	130	>500,000	200,000	<20	130	120	<60	<20
RU16	248	39.8	410	<20	<40	4,900	1,290	<20	<20	<20	<60	<20
RU17	985	12.6	40	<20	<40	24,400	7,700	<20	<20	<20	<60	<20
RU17S	307	30.5	390	70	<40	6,600	3,170	<20	<20	<20	<60	<20
RU18	569	55.8	430	<20	<40	9,600	2,560	<20	<20	<20	70	<20
RU19	112	42.2	140	30	<40	1,900	460	<20	<20.	<20	<60	<20
RU19S	114	49.9	130	<20	<40	1,900	330	<20	<20	<20	<60	<20
RU21	236	85.6	650	<20	<40	3,200	190	<20	<20.	<20	70	<20
RU21S	2,550	37.7	29,600	40	220	>500,000	608,000	<20	<20	<20	<60	<20
RU22	1580	142	2600	30	60	32,200	11,400	120	20	<20	100	<20
RU23	257	40.7	990	<20	60	5,500	1,130	<20	<20	<20	<60	<20
RU24	861	23.4	21,500	<20	290	88,200	105,000	670	<20	<20	<60	<20
RU25	800	41.2	1000	<20	60	5,000	1010	<20	<20	30	<60	<20
RU26	2500	16.1	3690	<20	40	30,700	9420	5,050	<20	<20	<60	<20
RU28	274	31.8	660	20	<40	1,600	400	30	<20	<20	<60	<20
RU30	1,990	42.9	24,300	<20	190	244,000	105,000	<20	<20	<20	<60	<20
RU32	976	12.7	2370	50	110	5700	2230	<20	<20	20	<60	<20

Table B-9. *Analyses of samples collected as part of the study of nonmetallic mineral deposits, Altiplano and Cordillera Occidental, Bolivia*

[All determinations by ICP-AES. Elements with asterisks (*) reported in percent; all other elements reported in ppm. Leaders (--) indicate no data available.]

Sample no.	Locality/lithology	Lat S.	Long W.	Al*	Ca*	Fe*	K*	Mg*
B01	Kaolinite	16.6408	68.6128	5.4	0.06	0.75	2.4	0.21
B02	Altered dacite	16.6408	68.6461	2.9	0.04	5.1	1.3	0.18
B03	Polymetallic vein ore	16.6408	68.6461	0.38	0.41	12	0.11	0.36
B06	Mudstone	16.8117	68.4139	6.2	1.9	1.1	1.1	0.74
B10	Volcanic ash	17.5814	69.3528	5.5	4.4	3.1	1.4	1.7
B11	Altered ash	17.5814	69.3528	5.3	1	2.8	2.8	0.36
B12	Volcanic ash	17.6058	69.3450	7	0.83	1	4.1	0.19
B13	Spring precipitate	17.5847	69.3681	6.7	2.5	2.6	2.6	0.82
B14	Peat	17.8644	69.1656	0.88	1.5	5.7	0.54	0.48
B15	Evaporite crust	18.0775	68.9767	0.02	0.12	0.06	0.88	0.55
B15a	Hot spring sinter	18.0775	68.9767	0.66	0.86	0.51	0.32	0.29
B16	Laguna Sacabaya ulexite ore	18.6567	68.9397	0.05	7.4	0.04	0.71	1.4
B17	Laguna Sacabaya mud	18.6517	68.9400	2.8	15	1.2	1.2	1
B18	Volcanic ash	18.6233	68.7625	8.2	1.1	0.65	3.3	0.08
B19	Vent sediments	18.6244	68.7511	17	0.33	1.2	0.85	0.04
B20	CORDEOR clay	17.6644	67.2075	11	0.26	5.1	3.4	1.1
B20a	Tuff	18.6197	67.7533	7.6	0.72	0.82	3.4	0.12
B21a	Mina Susana ore	22.7558	67.5731	0.05	<0.01	<0.01	<0.1	<0.01
B22	Mina Susana clay	22.7558	67.5731	1.1	0.06	0.24	0.14	0.12
B23	Laguna Verde ash	22.8189	67.7706	1.5	6.8	1.1	0.58	1.4
B24	Laguna Verde limestone	22.8189	67.7706	0.41	35	0.35	0.21	0.74
B25	Sol de Mañana mud	22.4297	67.7544	9.4	0.34	3	1.1	0.15
B26	Laguna Challviri ulexite ore	22.5625	67.5853	0.89	8.1	0.37	0.4	0.57
B27	Laguna Challviri crust	22.5625	67.5853	0.03	4.2	<0.01	0.6	0.64
B28	Laguna Cachi ore (trona)	21.7308	67.9533	0.02	0.06	<0.01	2.9	0.02
B29	Laguna Cachi crust	21.7308	67.9533	6.4	3.6	2.3	2.6	1.7
B30	Laguna Pastos Grandes crust	21.6869	67.7964	3.7	3.5	2	1.8	1.4
B32	Laguna Hedionda Norte crust	21.5642	68.0358	0.03	1.1	0.02	0.45	0.48
B33	Laguna Hedionda Norte mud	21.5642	68.0358	<0.01	11	0.11	1	2.6
B35	Laguna Coruto crust	22.4200	67.0275	3.5	8.1	1.7	1.4	1.1
B36	Laguna Mama Khumu crust	22.2522	67.0725	0.12	18	0.13	0.53	1.6
B37	Laguna Mama Khumu ore	22.2022	67.0725	0.03	17	<0.01	0.58	0.78
B38	Laguna Colorada ulexite	22.1897	67.8136	0.12	7.7	0.09	1.1	0.45
B38a	Laguna Colorada thenardite	22.1897	67.8136	<0.01	0.41	0.01	<0.1	0.1
B40	Isla Pescado limestone	20.1464	67.8150	0.67	37	0.39	0.2	1
B41	Mina Olca Mn cap	20.9403	68.4500	8.7	4.5	5.4	1.5	1.8
B43	Salar de la Laguna crust	20.8656	68.4386	<0.01	6.7	0.07	4.5	4.6

Table B-9. *Analyses of samples collected as part of the study of nonmetallic mineral deposits, Altiplano and Cordillera Occidental, Bolivia*--Continued

Sample no.	Na*	P*	Si*	Ti*	Mn	Ag	As	B	Ba	Be
B01	0.05	0.06	--	0.26	49	<4	22	--	540	<2
B02	0.13	0.09	--	0.14	83	160	550	--	2000	<2
B03	<0.01	0.06	--	<0.01	83000	430	1100	--	2700	<2
B06	2.1	0.19	--	0.26	1100	34	<20	--	1300	<2
B10	1.2	0.99	--	0.31	25000	<4	92	--	3300	<2
B11	1	0.05	--	0.23	600	<4	<20	--	380	4
B12	2.1	0.02	--	0.14	550	<4	<20	--	1100	2
B13	2.2	0.07	--	0.32	57000	<4	140	--	1800	2
B14	0.62	0.1	--	0.1	1200	<4	290	--	270	<2
B15	27	<0.01	--	<0.01	130	<4	390	--	11	<2
B15a	0.61	0.02	44	0.06	12000	<4	160	190	440	<2
B16	14	<0.01	1.2	<0.01	110	<4	78	78000	30	<2
B17	2	0.08	18	0.1	450	<4	130	600	330	<2
B18	3.3	0.01	--	0.08	470	<4	<20	--	1300	2
B19	0.86	0.01	--	0.21	680	<4	<20	--	950	4
B20	0.54	0.08	--	0.44	550	<4	38	--	490	4
B20a	3	0.02	--	0.1	550	<4	<20	--	1300	2
B21a	0.02	<0.01	--	<0.01	<8	<4	<20	--	9	<2
B22	0.2	0.01	--	0.86	59	<4	<20	--	500	<2
B23	1.5	0.03	--	0.11	890	<4	97	--	140	<2
B24	0.47	0.07	--	0.04	3700	<4	350	--	160	<2
B25	0.18	0.07	--	0.53	57	<4	<20	--	610	<2
B26	9.8	<0.01	3.9	0.05	63	<4	31	100000	87	<2
B27	22	<0.01	0.26	<0.01	<8	<4	<20	49000	9	<2
B28	26	0.05	0.42	<0.01	<8	<4	2500	2500	2	<2
B29	5.8	0.08	26	0.27	380	<4	830	1000	450	<2
B30	15	0.04	17	0.21	380	<4	310	1200	300	<2
B32	25	<0.01	0.8	<0.01	<8	<4	880	680	7	<2
B33	7.3	0.02	9.6	<0.01	25	<4	6400	13000	50	<2
B35	3.1	0.06	25	0.19	580	<4	320	2100	250	<2
B36	7	0.01	2.9	0.02	94	<4	1500	13000	83	<2
B37	7.1	<0.01	0.78	<0.01	31	<4	170	29000	12	<2
B38	15	<0.01	1.1	<0.01	78	<4	10000	83000	61	<2
B38a	26	<0.01	0.45	<0.01	12	<4	160	700	2	<2
B40	0.6	0.09	--	0.04	700	<4	100	--	220	<2
B41	2.7	0.15	--	0.77	730	<4	<20	--	810	<2
B43	10	<0.01	0.97	<0.01	24	<4	84	1300	15	<2

Table B-9. *Analyses of samples collected as part of the study of nonmetallic mineral deposits, Altiplano and Cordillera Occidental, Bolivia*--Continued

Sample no.	Cd	Ce	Co	Cr	Cu	Ga	La	Li	Mo	Nb
B01	<4	41	<2	33	35	9	20	27	<4	<8
B02	<4	36	2	18	610	<8	21	94	<4	<8
B03	170	<8	7	<2	25000	<8	<4	12	6	<8
B06	<4	34	11	28	66000	14	18	31	<4	14
B10	<4	58	100	28	560	20	33	63	<4	<8
B11	4	56	12	120	65	15	31	34	<4	<8
B12	<4	81	3	2	24	16	44	36	<4	8
B13	<4	44	550	44	30	18	27	26	28	15
B14	<4	21	11	8	9	<8	11	14	5	<8
B15	<4	<8	<2	8	25	<8	<4	620	<4	<8
B15a	<4	<8	6	<2	20	<8	4	35	6	<8
B16	<4	<8	2	<2	8	<8	5	300	<4	<8
B17	5	20	8	5	20	<8	15	150	6	<8
B18	<4	63	<2	4	17	21	34	26	<4	10
B19	<4	110	<2	<2	4	39	59	68	<4	36
B20	<4	97	19	92	18	25	49	120	<4	11
B20a	<4	70	<2	<2	6	18	38	27	<4	11
B21a	<4	<8	<2	<2	5	<8	<4	<4	<4	<8
B22	<4	9	<2	5	<2	<8	4	7	4	16
B23	<4	12	6	8	13	<8	10	190	<4	<8
B24	<4	<8	4	4	8	<8	8	76	<4	<8
B25	<4	68	3	54	9	23	35	<4	<4	9
B26	<4	10	3	11	9	<8	7	620	<4	<8
B27	<4	<8	<2	<2	4	<8	<4	2300	<4	<8
B28	<4	<8	<2	<2	<2	<8	<4	720	38	<8
B29	<4	36	10	28	15	16	21	330	4	<8
B30	<4	29	8	32	13	8	17	750	<4	<8
B32	<4	<8	<2	<2	12	<8	<4	410	<4	<8
B33	<4	<8	4	<2	6	<8	6	840	<4	<8
B35	<20	32	5	14	21	10	19	300	<4	<8
B36	<4	<8	3	<2	<2	<8	6	430	<4	<8
B37	<4	<8	2	<2	<2	<8	5	440	<4	<8
B38	<4	<8	<2	<2	11	<8	4	2200	<4	<8
B38a	<4	<8	<2	5	<2	<8	<4	21	<4	<8
B40	<4	<8	6	2	<2	<8	9	46	<4	<8
B41	<4	59	19	14	49	22	31	14	<4	8
B43	<4	<8	<2	5	18	<8	<4	140	30	<8

Table B-9. *Analyses of samples collected as part of the study of nonmetallic mineral deposits, Altiplano and Cordillera Occidental, Bolivia*--Continued

Sample no.	Nd	Ni	Pb	Sc	Sr	Th	V	Y	Zn	U
B01	22	7	3700	6	670	<8	69	8	64	--
B02	18	<4	179000	4	1200	<8	44	7	270	--
B03	<8	<4	7900	<4	1000	27	<4	9	24000	--
B06	17	<4	230	8	230	<8	85	12	250	--
B10	28	64	120	10	580	18	110	12	150	--
B11	20	55	67	8	220	14	250	14	77	--
B12	30	<4	45	<4	180	11	23	14	47	--
B13	24	110	43	10	950	25	200	15	79	--
B14	11	6	9	<4	320	5.4	250	<4	20	3.9
B15	<8	<4	<8	<4	58	<8	<4	<4	5	--
B15a	<8	9	<8	<4	220	<8	13	<4	8	--
B16	<8	<4	<8	<4	2200	<8	4	<4	5	--
B17	14	13	23	<4	1500	<8	50	4	91	--
B18	26	<4	56	<4	470	10	4	11	42	--
B19	44	<4	140	4	150	29	<4	21	97	--
B20	49	49	20	19	210	20	130	21	85	--
B20a	29	4	43	<4	290	12	6	12	47	--
B21a	<8	<4	<8	<4	<4	<8	<4	<4	<4	--
B22	9	6	12	<4	16	<8	14	<4	6	--
B23	10	12	13	<4	610	<8	120	<4	75	--
B24	18	<4	<8	<4	2700	<8	81	<4	8	--
B25	33	<4	21	12	360	20	140	5	20	--
B26	<8	7	21	<4	4300	<8	16	<4	8	--
B27	<8	<4	<8	<4	460	<8	<4	<4	<4	--
B28	<8	<4	<8	<4	10	<8	<4	9	<4	--
B29	18	45	35	7	490	12	85	9	58	--
B30	14	7	10	8	530	9	68	9	40	--
B32	<8	<4	<8	<4	180	<8	4	<4	<4	--
B33	<8	5	<8	<4	1300	<8	50	<4	<4	--
B35	20	10	13	5	700	<8	95	6	64	--
B36	11	<4	<8	<4	720	<8	27	<4	<4	--
B37	<8	<4	<8	<4	580	<8	<4	<4	<4	--
B38	<8	<4	<8	<4	410	<8	<4	<4	<4	--
B38a	<8	<4	<8	<4	42	<8	<4	<4	<4	--
B40	24	12	<8	<4	1900	<8	10	<4	11	--
B41	37	11	<8	13	710	8	170	17	110	--
B43	<8	<4	<8	<4	460	<8	5	<4	4	--

Table B-10. *Locations of samples collected in the geochemical study of the La Joya district, Bolivia*

[Locations are given in decimal south latitude and west longitude. Locations digitized from 1:25,000-scale map]

Sample no.	Lat S.	Long W.
CH001	17.7261	67.6651
CH002	17.7250	67.6656
CS001	17.8028	67.4687
CS002	17.7985	67.4757
CS003	17.7963	67.4793
CS004	17.7945	67.4791
CS005	17.7858	67.4848
CS006	17.7920	67.4843
CS007	17.7728	67.4830
CS008	17.7662	67.4881
CS009	17.7659	67.4756
CS010	17.7746	67.4718
CS011	17.7772	67.4644
CS012	17.7816	67.4645
CS013	17.7743	67.4636
CS014	17.7959	67.4627
CS015	17.7906	67.4631
CS016	17.7879	67.4646
EQ001	17.8124	67.4113
EQ002	17.8257	67.4065
EQ003	17.8389	67.3877
EQ004	17.8374	67.3813
EQ005	17.8423	67.3759
EQ006	17.8475	67.3692
EQ007	17.8534	67.3643
EQ008	17.8543	67.3541
EQ009	17.8528	67.3508
EQ010	17.8429	67.3432
EQ011	17.8478	67.3407
EQ012	17.8505	67.3401
EQ013	17.8599	67.3356
EQ014	17.8630	67.3287
EQ015	17.8628	67.3125
EQ016	17.8588	67.2984
EQ017	17.8528	67.3002
EQ018	17.8330	67.2943
EQ019	17.8324	67.3002
EQ020	17.8316	67.3014
EQ021	17.8294	67.3001
EQ022	17.8073	67.4053
EQ023	17.8111	67.4078
EQ024	17.8049	67.4011
EQ025	17.8028	67.3983
EQ026	17.8006	67.3952
EQ027	17.7977	67.3901
EQ028	17.8001	67.3820
EQ029	17.8070	67.3718
EQ030	17.8107	67.3682
EQ031	17.8040	67.3489
EQ032	17.8366	67.3680

Table B-10. *Locations of samples collected in the geochemical study of the La Joya district, Bolivia*--Continued

Sample no.	Lat S.	Long W.
EQ033	17.8323	67.3619
EQ034	17.8264	67.3702
EQ035	17.8228	67.3648
EQ036	17.8247	67.3562
EQ037	17.8147	67.3633
EQ038	17.8048	67.3446
EQ039	17.8040	67.3425
EQ040	17.7983	67.3357
EQ041	17.7934	67.3311
EQ042	17.7914	67.3250
EQ043	17.7937	67.3161
EQ044	17.8233	67.2971
EQ045	17.8185	67.2989
EQ046	17.8197	67.3003
EQ047	17.8138	67.2931
EQ048	17.8117	67.2853
EQ049	17.8047	67.2829
EQ050	17.7965	67.2855
EQ051	17.7947	67.2888
EQ052	17.7943	67.2903
EQ053	17.8054	67.3128
EQ054	17.8183	67.3186
EQ055	17.8185	67.3170
EQ056	17.8126	67.3135
EQ057	17.8170	67.3023
EQ058	17.8130	67.3019
EQ059	17.8156	67.3028
EQ060	17.8018	67.3074
EQ061	17.7967	67.3075
EQ062	17.8002	67.2987
EQ063	17.7990	67.2973
KK001	17.8020	67.4467
KK002	17.8000	67.4460
KK003	17.7972	67.4480
KK004	17.7973	67.4508
KK005	17.7989	67.4527
KK006	17.8006	67.4527
KK007	17.8022	67.4514
KK008	17.8030	67.4486
KS001	17.8494	67.5445
KS002	17.8471	67.5444
KS003	17.8445	67.5451
KS004	17.8469	67.5465
KS005	17.8478	67.5467
KS006	17.8342	67.5471
LB001	17.7531	67.4615
LB002	17.7508	67.4618
LB003	17.7612	67.4602
LB004	17.7589	67.4634
LB005	17.7556	67.4623

Table B-10. *Locations of samples collected in the geochemical study of the La Joya district, Bolivia--* Continued

Sample no.	Lat S.	Long W.
LB006	17.7582	67.4606
LB007	17.7606	67.4581
LB008	17.7650	67.4559
LB009	17.7696	67.4562
LJ001	17.7705	67.5032
LJ002	17.7626	67.5048
LJ003	17.7601	67.5044
LJ004	17.7637	67.5107
LJ005	17.7648	67.5171
LJ006	17.7697	67.5222
LJ007	17.7734	67.5216
LJ008	17.7768	67.5192
LJ009	17.7786	67.5172
LJ010	17.7764	67.5109
LJ011	17.7754	67.5055
LJ012	17.7675	67.5042
LL001	17.7896	67.4494
LL002	17.7878	67.4335
LL003	17.7850	67.4357
LL004	17.7812	67.4583
LL005	17.7813	67.4615
LL006	17.7832	67.4619
LL007	17.7853	67.4625
LL008	17.7870	67.4620
LL009	17.7903	67.4586
LL010	17.7911	67.4538
NL001	17.7640	67.6300
NL002	17.7610	67.6270
NL003	17.7571	67.6309
NL004	17.7615	67.6325
QT001	17.7937	67.6134
QT002	17.7910	67.6140
QT003	17.7854	67.6139
QT004	17.7884	67.6105
QT005	17.7929	67.6085
QT006	17.7946	67.6101
QT007	17.7971	67.6070
QT008	17.7950	67.6075
QT009	17.7968	67.6032
QT010	17.8025	67.6012
QT011	17.8052	67.5992
QT012	17.7985	67.5986

Table B-11. *Analyses of rock samples collected in the geochemical study of the La Joya district, Bolivia*

[First 35 elements (Ba through Th) analyzed by DC-ARC AES. Elements with asterisks (*) are reported in percent; all other elements are reported in ppm. Hg analyzed by continuous flow-cold vapor AAS. Se analyzed by continuous flow-hydride generation AAS. Te analyzed by flame AAS. [1]Au analyzed by Flame or Graphite Furnace AAS. [2]Au, As, Bi, Cd, Sb, Zn, Cu, Pb, Ag, and Mo analyzed by peroxide dissolution ICP-AES. N, the element was present below the lower limit of determination]

Sample no.	Ba	Fe*	Mg*	Ca*	Ti*	Mn	Ag	As	Au	B
CH001	500	0.7	0.15	0.5	0.2	100	N	N	N	10
CH002	300	0.5	0.2	0.5	0.2	100	N	N	N	<10
CS001	100	2	0.3	<0.05	0.5	70	N	N	N	50
CS008	150	3	0.1	<0.05	0.5	300	N	N	N	100
CS013	150	1	0.15	<0.05	0.5	70	N	N	N	50
CS015	200	3	0.3	0.05	0.5	70	N	N	N	70
EQ001	500	2	0.7	1	0.5	200	<0.5	N	N	30
EQ002-1	500	3	1	1	0.7	200	N	N	N	30
EQ002-2	500	2	0.7	1	0.5	200	N	N	N	15
EQ003-1	700	3	1	1.5	0.7	200	N	N	N	30
EQ003-2	700	5	1	1	1	200	N	N	N	20
EQ004-1	500	3	0.7	1	0.7	200	N	N	N	30
EQ004-2	700	3	1.5	1.5	1	200	1	N	N	20
EQ005	700	3	0.5	1	0.7	200	<0.5	N	N	50
EQ006	700	3	1.5	1	0.5	200	<0.5	N	N	30
EQ007-1	700	5	1	1.5	0.7	200	N	N	N	30
EQ007-2	700	2	1	1	0.5	300	N	N	N	30
EQ008	700	3	1	1	0.7	200	N	N	N	30
EQ009	700	3	1	1.5	0.7	300	N	N	N	30
EQ010-1	700	3	0.7	0.1	0.5	150	N	N	N	50
EQ010-2	700	3	1.5	1	0.7	300	N	N	N	30
EQ011-1	500	2	0.15	0.5	0.5	100	N	N	N	50
EQ011-2	500	0.2	0.02	0.15	1	100	N	N	N	20
EQ012	700	2	0.7	1.5	0.7	200	N	N	N	20
EQ013	700	3	0.7	1	0.7	150	N	N	N	50
EQ014	700	3	1	1.5	0.5	200	N	N	N	30
EQ015	700	3	0.7	1	0.7	150	N	N	N	30
EQ016	700	3	1	1.5	0.7	200	N	N	N	30
EQ017	700	2	0.3	1	0.7	150	N	N	N	30
EQ018	700	3	1	1.5	0.5	300	N	N	N	50
EQ019	700	3	1	1	0.5	300	N	N	N	30
EQ022	700	5	1	1	0.7	700	N	N	N	20
EQ024	700	5	1.5	1.5	0.7	300	N	N	N	30
EQ026	700	5	1	1	0.7	300	N	N	N	50
EQ029	1000	5	1.5	1	0.3	200	1	N	N	50
EQ031	500	3	0.7	1	0.5	200	N	N	N	30
EQ032	1000	3	0.5	1	0.7	300	N	N	N	30
EQ033	700	5	1	1	0.5	200	N	N	N	30
EQ034	1000	5	1	1	1	200	<0.5	N	N	30
EQ035	1000	3	1	1.5	0.7	200	N	N	N	30
EQ036	500	2	0.5	1	0.5	200	N	N	N	20
EQ037	700	2	0.7	1	0.7	200	0.7	N	N	30
EQ038	1000	3	1	1.5	0.7	200	N	N	N	30
EQ039	500	2	0.3	1	0.5	150	N	N	N	30
EQ040	700	2	0.7	1	0.5	150	1	N	N	30
EQ041	700	3	0.7	1	0.7	200	N	N	N	50
EQ042	700	3	0.5	1	0.7	200	N	N	N	30
EQ044	700	3	0.7	1	1	200	N	N	N	30
EQ045	700	0.7	0.05	0.1	>1,000	70	N	N	N	30
EQ047	700	3	0.7	1	0.5	3000	N	N	N	50

Table B11. *Analyses of rock samples collected in the geochemical study of the La Joya district, Bolivia* - Continued

Sample no.	Ni	Be	Bi	Cd	Co	Cr	Cu	La	Mo	Nb
CH001	N	1	N	N	N	70	<5	70	10	N
CH002	N	1	N	N	N	100	7	70	N	N
CS001	30	<1	N	N	10	30	15	<50	N	N
CS008	50	1	N	N	15	70	20	50	N	N
CS013	20	1	N	N	<10	20	10	<50	N	N
CS015	50	1	N	N	10	50	20	50	10	N
EQ001	10	1	<10	N	10	100	50	50	<5	N
EQ002-1	15	<1	N	N	10	100	20	70	<5	N
EQ002-2	20	1	N	N	15	70	50	<50	<5	N
EQ003-1	10	2	N	N	10	200	15	70	15	N
EQ003-2	30	1.5	N	N	15	100	20	70	<5	N
EQ004-1	10	1.5	N	N	10	150	15	70	10	N
EQ004-2	30	1.5	N	N	10	100	20	70	N	N
EQ005	30	1.5	N	N	10	100	15	70	N	N
EQ006	15	1	N	N	10	150	50	70	<5	N
EQ007-1	30	1	N	N	15	100	20	70	<5	N
EQ007-2	20	1.5	N	N	10	200	15	70	7	N
EQ008	15	1.5	N	N	10	70	15	70	<5	N
EQ009	10	1.5	N	N	10	150	15	70	7	N
EQ010-1	15	<1	N	N	10	100	30	70	<5	N
EQ010-2	10	1	N	N	10	150	20	70	<5	N
EQ011-1	5	1	N	N	N	50	30	50	N	N
EQ011-2	N	1	N	N	N	10	10	50	N	N
EQ012	15	1.5	N	N	10	70	15	100	5	N
EQ013	15	1.5	N	N	10	100	15	50	5	N
EQ014	10	1.5	N	N	10	150	15	70	N	N
EQ015	15	1.5	N	N	10	70	15	50	N	N
EQ016	7	1.5	N	N	<10	70	10	50	N	N
EQ017	10	2	N	N	<10	30	15	50	N	N
EQ018	10	2	N	N	10	50	15	70	N	N
EQ019	15	1.5	N	N	10	50	10	70	N	N
EQ022	70	1.5	N	N	20	100	30	70	N	N
EQ024	30	1.5	N	N	15	150	20	70	N	N
EQ026	20	1.5	N	N	10	100	15	70	5	N
EQ029	20	1	N	N	15	300	20	100	10	N
EQ031	5	1.5	N	N	<10	50	5	70	N	N
EQ032	20	1.5	N	N	15	200	30	100	10	N
EQ033	15	1	N	N	15	150	20	70	<5	N
EQ034	20	1	N	N	15	100	15	100	<5	N
EQ035	20	1	N	N	15	100	15	100	<5	N
EQ036	15	1.5	N	N	20	50	10	70	N	N
EQ037	30	2	N	N	15	150	20	70	5	N
EQ038	15	1.5	N	N	15	100	30	70	<5	N
EQ039	7	2	N	N	10	50	10	70	N	N
EQ040	5	1.5	N	N	<10	30	7	70	N	N
EQ041	20	1.5	N	N	15	100	20	70	7	N
EQ042	7	1.5	N	N	10	50	7	50	<5	N
EQ044	15	1.5	N	N	10	100	15	70	10	N
EQ045	<5	<1	N	N	N	50	20	70	N	N
EQ047	30	1	N	N	30	70	20	50	7	N

Table B11. *Analyses of rock samples collected in the geochemical study of the La Joya district, Bolivia* - Continued

Sample no.	V	Pb	Sb	Sc	Sn	Sr	W	Y	Zn	Zr
CH001	20	<10	N	N	N	200	N	N	N	150
CH002	15	10	N	N	N	200	N	N	N	50
CS001	70	N	N	5	N	N	N	15	N	150
CS008	70	<10	N	7	N	N	N	20	N	300
CS013	50	<10	N	<5	N	N	N	10	N	150
CS015	100	<10	N	7	N	N	N	20	N	200
EQ001	50	10	N	<5	N	200	N	<10	N	100
EQ002-1	50	20	N	5	N	300	N	<10	N	150
EQ002-2	50	10	N	N	N	300	N	<10	N	100
EQ003-1	70	15	N	<5	N	300	N	10	N	300
EQ003-2	70	15	N	<5	N	300	N	10	N	700
EQ004-1	70	15	N	5	N	300	N	10	N	500
EQ004-2	100	10	N	5	N	300	N	10	N	500
EQ005	50	20	N	5	N	300	N	15	N	300
EQ006	70	20	N	5	N	300	N	10	N	200
EQ007-1	100	20	N	5	N	300	N	10	N	300
EQ007-2	70	15	N	5	N	300	N	15	N	150
EQ008	70	15	N	5	N	300	N	10	N	200
EQ009	70	20	N	5	N	300	N	15	N	200
EQ010-1	70	15	N	7	N	300	N	<10	N	300
EQ010-2	70	20	N	5	N	300	N	10	N	200
EQ011-1	100	15	N	5	N	700	N	<10	N	200
EQ011-2	20	N	N	N	N	N	N	<10	N	300
EQ012	70	15	N	<5	N	200	N	10	N	300
EQ013	50	10	N	<5	N	200	N	10	N	300
EQ014	50	20	N	<5	N	300	N	10	N	200
EQ015	50	10	N	<5	N	200	N	10	N	500
EQ016	50	20	N	5	N	300	N	10	N	200
EQ017	50	10	N	<5	N	200	N	10	N	300
EQ018	70	20	N	<5	N	500	N	15	N	200
EQ019	50	20	N	5	N	300	N	10	N	150
EQ022	100	15	N	7	N	300	N	15	N	300
EQ024	100	15	N	5	N	500	N	10	N	150
EQ026	70	15	N	5	N	500	N	15	N	200
EQ029	70	30	N	5	N	300	N	10	N	100
EQ031	70	15	N	5	N	300	N	10	N	150
EQ032	70	20	N	5	N	300	N	20	N	200
EQ033	70	30	N	5	N	300	N	10	N	150
EQ034	70	20	N	7	N	300	N	15	N	200
EQ035	100	20	N	5	N	500	N	15	N	200
EQ036	70	15	N	<5	N	200	N	10	N	300
EQ037	70	15	N	5	N	300	N	10	N	300
EQ038	70	20	N	5	N	300	N	15	N	200
EQ039	30	15	N	<5	N	300	N	<10	N	300
EQ040	70	20	N	<5	N	300	N	10	N	150
EQ041	70	15	N	5	N	300	N	10	N	300
EQ042	70	15	N	5	N	300	N	10	N	300
EQ044	70	20	N	7	N	300	N	15	N	200
EQ045	50	10	N	<5	N	300	N	N	N	500
EQ047	70	20	N	<5	N	300	N	<10	N	200

Table B11. *Analyses of rock samples collected in the geochemical study of the La Joya district, Bolivia* - Continued

Sample no.	Na	P	Ga	Ge	Th	Hg	Se	Te	[1]Au	[2]Au
CH001	1	N	15	N	N	<0.02	<0.1	<0.05	<0.002	<0.15
CH002	2	N	30	N	N	0.1	<0.1	<0.05	0.006	<0.15
CS001	0.7	N	15	N	N	0.02	<0.1	0.1	0.006	<0.15
CS008	1	N	20	N	N	0.02	0.1	<0.05	0.008	<0.15
CS013	0.5	N	5	N	N	0.02	<0.1	<0.05	0.008	<0.15
CS015	0.5	N	10	N	N	0.02	<0.1	<0.05	0.008	<0.15
EQ001	1	N	20	N	N	<0.02	0.1	0.1	0.026	<0.15
EQ002-1	1.5	N	50	N	N	<0.02	<0.1	<0.05	<0.002	<0.15
EQ002-2	1.5	N	20	N	N	<0.02	<0.1	0.1	0.004	<0.15
EQ003-1	1.5	N	30	N	N	0.02	<0.1	<0.05	<0.002	<0.15
EQ003-2	1.5	N	30	N	N	<0.02	<0.1	<0.05	<0.002	<0.15
EQ004-1	1.5	N	20	N	N	<0.02	<0.1	<0.05	<0.002	<0.15
EQ004-2	1	N	30	N	N	<0.02	<0.1	<0.05	<0.002	<0.15
EQ005	1.5	<0.2	30	N	N	<0.02	<0.1	0.1	<0.002	<0.15
EQ006	2	N	50	N	N	<0.02	<0.1	0.05	0.006	<0.15
EQ007-1	2	<0.2	50	N	N	<0.02	<0.1	<0.05	<0.002	<0.15
EQ007-2	1.5	<0.2	50	N	N	<0.02	<0.1	<0.05	<0.002	<0.15
EQ008	1.5	<0.2	50	N	N	<0.02	<0.1	<0.05	<0.002	<0.15
EQ009	2	<0.2	50	N	N	<0.02	<0.1	<0.05	<0.002	<0.15
EQ010-1	0.7	N	30	N	N	<0.02	<0.1	<0.05	<0.002	<0.15
EQ010-2	2	N	50	N	N	<0.02	<0.1	<0.05	<0.002	<0.15
EQ011-1	1	N	50	N	N	0.1	<0.1	<0.05	<0.002	<0.15
EQ011-2	0.5	N	5	N	N	<0.02	0.1	<0.05	<0.002	<0.15
EQ012	1	<0.2	30	N	N	0.02	<0.1	<0.05	<0.002	<0.15
EQ013	1	0.2	20	N	N	<0.02	<0.1	<0.05	<0.002	<0.15
EQ014	1.5	<0.2	30	N	N	<0.02	<0.1	<0.05	<0.002	<0.15
EQ015	1	N	20	N	N	<0.02	<0.1	<0.05	<0.002	<0.15
EQ016	2	N	50	N	N	<0.02	<0.1	<0.05	<0.002	<0.15
EQ017	1.5	N	30	N	N	<0.02	<0.1	<0.05	<0.002	<0.15
EQ018	1.5	N	30	N	N	<0.02	<0.1	<0.05	<0.002	<0.15
EQ019	1.5	N	50	N	N	<0.02	<0.1	<0.05	<0.002	<0.15
EQ022	1	<0.2	30	N	N	<0.02	<0.1	<0.05	<0.002	<0.15
EQ024	1.5	N	30	N	N	<0.02	0.1	<0.05	<0.002	<0.15
EQ026	1.5	N	30	N	N	<0.02	<0.1	<0.05	<0.002	<0.15
EQ029	2	N	50	N	N	<0.02	<0.1	<0.05	0.002	<0.15
EQ031	1.5	N	30	N	N	<0.02	<0.1	<0.05	<0.002	<0.15
EQ032	2	N	50	N	N	<0.02	<0.1	<0.05	<0.002	<0.15
EQ033	2	N	70	N	N	<0.02	<0.1	<0.05	<0.002	<0.15
EQ034	2	<0.2	50	N	N	<0.02	<0.1	<0.05	<0.002	<0.15
EQ035	2	N	50	N	N	<0.02	<0.1	<0.05	<0.002	<0.15
EQ036	1.5	N	30	N	N	<0.02	<0.1	<0.05	0.004	<0.15
EQ037	2	N	30	N	N	<0.02	<0.1	<0.05	<0.002	<0.15
EQ038	2	N	50	N	N	<0.02	<0.1	<0.05	<0.002	<0.15
EQ039	1.5	N	30	N	N	<0.02	<0.1	<0.05	<0.002	<0.15
EQ040	2	N	30	N	N	<0.02	<0.1	<0.05	<0.002	<0.15
EQ041	1.5	<0.2	30	N	N	<0.02	<0.1	<0.05	<0.002	<0.15
EQ042	1.5	N	30	N	N	<0.02	<0.1	<0.05	<0.002	<0.15
EQ044	2	N	50	N	N	<0.02	<0.1	<0.05	<0.002	<0.15
EQ045	0.3	N	15	N	N	0.1	0.1	<0.05	<0.002	<0.15
EQ047	1	N	30	N	N	0.04	<0.1	<0.05	<0.002	<0.15

Table B11. *Analyses of rock samples collected in the geochemical study of the La Joya district, Bolivia* - Continued

Sample no.	As	Bi	Cd	Sb	Zn	Cu	Pb	Ag	Mo
CH001	4.7	0.76	<0.03	2.7	45	5.4	7.4	0.12	11
CH002	9.7	0.68	0.035	3.8	46	7.7	5.7	0.16	15
CS001	12	2.6	<0.03	8.8	39	20	7.8	0.32	2.5
CS008	9.6	1.1	0.041	2.6	90	23	16	0.068	2.8
CS013	12	0.8	0.039	3.2	53	17	27	0.19	3
CS015	19	1.2	0.099	8.2	87	34	27	0.17	7.4
EQ001	17	2.3	0.062	17	53	70	5	0.42	5.2
EQ002-1	3.2	1.1	0.11	1.5	53	16	10	<0.045	3.1
EQ002-2	8.1	0.66	0.046	5.4	39	52	3.9	0.27	3.8
EQ003-1	3.7	<0.6	0.19	1.6	59	13	8	0.082	6.5
EQ003-2	2.8	<0.6	0.051	0.79	21	11	2.6	0.046	2.7
EQ004-1	6	<0.6	0.25	0.89	57	13	5.8	<0.045	4.6
EQ004-2	0.69	<0.6	0.036	<0.6	42	18	1.2	<0.045	2.2
EQ005	7.9	<0.6	0.054	1.3	16	7.6	5.7	0.055	3
EQ006	6.7	0.68	0.031	5.6	40	40	0.78	0.21	4.1
EQ007-1	1.9	<0.6	<0.03	<0.6	42	16	0.78	<0.045	2.3
EQ007-2	3.5	<0.6	0.033	0.91	47	9.8	3.8	<0.045	4.4
EQ008	<0.6	<0.6	0.042	<0.6	35	8.3	2.1	<0.045	2.1
EQ009	<0.6	<0.6	0.032	<0.6	43	9.5	2.3	<0.045	3.1
EQ010-1	9.5	<0.6	0.056	4.1	36	13	11	<0.045	2.6
EQ010-2	<0.6	<0.6	0.032	0.82	44	14	2.5	<0.045	2.5
EQ011-1	1.4	<0.6	0.034	0.73	26	9.9	9.7	<0.045	1.2
EQ011-2	<0.6	<0.6	0.063	<0.6	1.7	5.5	3	<0.045	1.5
EQ012	2.5	0.87	0.079	1.5	37	8.1	5	0.11	2.4
EQ013	5.3	<0.6	0.037	1.1	36	9.7	3	<0.045	2.6
EQ014	3.1	<0.6	0.042	1.2	43	11	2	0.06	2.3
EQ015	<0.6	<0.6	<0.03	<0.6	29	7.5	1.3	<0.045	1.7
EQ016	<0.6	<0.6	<0.03	<0.6	41	4.1	0.87	<0.045	1.5
EQ017	2.4	<0.6	0.031	<0.6	31	9.9	2.3	0.049	1.9
EQ018	<0.6	<0.6	<0.03	<0.6	40	10	0.74	<0.045	2
EQ019	<0.6	<0.6	0.061	<0.6	38	6.6	3.1	<0.045	1.2
EQ022	0.72	<0.6	0.088	<0.6	27	18	<0.6	<0.045	1.7
EQ024	2	<0.6	0.057	<0.6	34	16	2.5	<0.045	2.3
EQ026	3.4	<0.6	<0.03	<0.6	50	14	0.79	<0.045	2.9
EQ029	7.9	<0.6	0.15	1.8	64	17	13	0.096	5.9
EQ031	<0.6	<0.6	<0.03	<0.6	45	8.7	<0.6	<0.045	2.4
EQ032	9.8	<0.6	0.14	<0.6	24	25	2.6	0.067	5
EQ033	4	<0.6	0.035	<0.6	35	15	1.1	<0.045	2.1
EQ034	1.9	<0.6	0.035	<0.6	39	12	3.4	0.047	2
EQ035	1.5	<0.6	<0.03	<0.6	39	11	2.3	<0.045	2.5
EQ036	<0.6	<0.6	0.066	<0.6	47	15	1	<0.045	2.5
EQ037	0.89	<0.6	0.041	<0.6	34	20	2.8	0.045	4.4
EQ038	<0.6	<0.6	0.054	<0.6	44	21	1.2	<0.045	2.3
EQ039	1.4	<0.6	<0.03	<0.6	30	11	0.71	<0.045	2.7
EQ040	<0.6	<0.6	<0.03	<0.6	48	6.7	1.5	<0.045	1.8
EQ041	2.8	<0.6	0.058	<0.6	25	17	0.71	<0.045	3.1
EQ042	<0.6	<0.6	0.035	<0.6	45	7.9	<0.6	<0.045	2
EQ044	0.85	<0.6	0.031	1	46	8.8	1.6	<0.045	4.9
EQ045	6.5	<0.6	<0.03	0.87	4.4	4.2	11	0.075	2.4
EQ047	10	<0.6	0.48	2.1	48	21	14	0.19	6.5

Table B11. *Analyses of rock samples collected in the geochemical study of the La Joya district, Bolivia* - Continued

Sample no.	Ba	Fe*	Mg*	Ca*	Ti*	Mn	Ag	As	Au	B
EQ048	700	2	0.5	1	0.5	150	0.7	N	N	30
EQ050	500	3	0.7	0.7	0.5	150	N	N	N	30
EQ053	700	3	1	1	0.5	150	N	N	N	30
EQ054	300	0.7	<0.02	0.05	0.3	50	N	N	N	<10
EQ055	300	0.7	N	<0.05	0.3	20	<0.5	N	N	<10
EQ056	500	2	0.5	1	0.5	150	N	N	N	20
EQ057	700	3	0.7	1.5	0.7	200	N	N	N	30
EQ059	700	5	1	1.5	1	200	N	N	N	20
KK001	150	2	0.15	<0.05	0.3	100	2	N	N	100
KK002	500	2	0.3	0.1	0.5	150	<0.5	N	N	20
KK003	300	2	0.1	<0.05	0.2	100	N	N	N	70
KK004	100	5	0.07	<0.05	0.3	50	10	N	N	30
KK005	300	3	0.2	<0.05	0.3	150	2	N	N	70
KK006	150	7	0.07	N	0.3	100	30	200	N	15
KK007	100	5	0.03	<0.05	0.3	50	7	1500	N	30
KK008-1	100	2	0.2	<0.05	0.5	100	10	N	N	50
KK008-2	100	5	<0.02	<0.05	0.2	10	10	200	N	20
KS001-1	300	3	<0.02	0.2	>1,000	10	N	N	N	30
KS001-2	300	0.7	0.1	<0.05	0.5	20	N	N	N	1000
KS002	200	1.5	0.1	<0.05	0.3	50	N	N	N	700
KS003-1	200	1	0.1	0.07	1	100	N	N	N	1000
KS003-2	150	15	N	0.05	0.1	20	N	N	N	<10
KS004	100	0.7	0.15	0.1	1	20	N	N	N	50
KS005	200	2	0.05	0.07	0.5	100	N	N	N	300
KS006	150	1	0.02	0.05	0.7	50	N	N	N	300
LB001	300	2	0.3	0.1	0.3	1500	2	N	N	30
LB002	500	2	0.7	1	0.3	500	N	N	N	15
LB003	500	2	0.5	0.2	0.3	3000	2	N	N	50
LB004	300	2	0.7	1.5	0.3	300	N	N	N	15
LB005	300	2	0.5	1.5	0.3	200	N	N	N	30
LB006	500	2	0.5	1.5	0.3	200	30	N	N	20
LB007-1	150	5	0.1	<0.05	0.2	700	15	200	N	50
LB007-2	300	1.5	0.5	1	0.3	150	1.5	N	N	N
LB008	150	1	0.15	<0.05	0.7	70	1.5	N	N	70
LB009	200	1.5	0.2	<0.05	0.5	100	3	N	N	70
LJ001	100	3	0.2	0.05	0.5	100	0.5	N	N	50
LJ002	100	0.5	0.1	<0.05	0.5	50	0.7	N	N	70
LJ004	500	3	0.7	1	0.5	1000	N	N	N	15
LJ005	500	1	0.1	<0.05	0.5	100	0.7	N	N	30
LJ006	200	1.5	0.2	<0.05	0.3	50	N	N	N	200
LJ007	300	0.1	0.07	<0.05	0.2	100	0.7	N	N	50
LJ008-1	150	1.5	0.1	<0.05	0.7	30	N	N	N	150
LJ008-2	100	5	0.05	0.05	1	30	N	N	N	70
LJ009	100	0.5	0.1	0.05	0.5	50	N	N	N	100
LJ011	150	1.5	0.15	<0.05	0.5	50	N	N	N	100
LL001	300	1.5	0.5	1	0.3	1000	0.5	N	N	10
LL002	500	3	0.7	1	0.5	700	N	N	N	20
LL003	100	1	0.02	0.05	0.7	50	7	N	N	30
LL005	100	5	0.1	<0.05	0.7	200	7	N	N	70
LL008	70	3	0.15	0.05	0.3	100	7	N	N	50

Table B11. *Analyses of rock samples collected in the geochemical study of the La Joya district, Bolivia* - Continued

Sample no.	Ni	Be	Bi	Cd	Co	Cr	Cu	La	Mo	Nb
EQ048	15	<1	N	N	<10	150	15	50	10	N
EQ050	50	1	N	N	15	200	20	70	20	N
EQ053	15	<1	N	N	10	200	20	70	7	N
EQ054	N	<1	N	N	N	100	15	70	N	N
EQ055	N	<1	N	N	N	100	10	50	<5	N
EQ056	20	1	N	N	20	100	15	70	5	N
EQ057	15	1	N	N	10	100	15	50	5	N
EQ059	20	<1	N	N	20	150	20	70	<5	N
KK001	N	<1	<10	N	N	70	5	50	<5	N
KK002	10	1	N	N	<10	70	10	50	<5	N
KK003	N	1	N	N	N	50	5	<50	<5	N
KK004	N	<1	N	N	N	70	<5	50	N	N
KK005	N	1	N	N	N	50	50	<50	<5	N
KK006	N	<1	N	N	N	30	50	<50	N	N
KK007	N	N	N	N	N	70	30	70	N	N
KK008-1	N	<1	<10	N	N	100	50	50	N	N
KK008-2	N	N	20	N	N	30	<5	70	N	N
KS001-1	N	N	N	N	N	70	10	<50	N	N
KS001-2	10	<1	N	N	N	100	5	<50	5	N
KS002	<5	N	30	N	N	100	20	50	5	N
KS003-1	10	<1	N	N	N	150	15	<50	10	N
KS003-2	N	N	<10	N	N	50	30	N	N	N
KS004	5	N	N	N	N	150	10	50	30	N
KS005	5	N	N	N	N	150	15	<50	20	N
KS006	5	N	N	N	N	150	10	<50	20	N
LB001	10	<1	N	N	10	50	30	<50	N	N
LB002	10	<1	N	N	10	70	N	<50	N	N
LB003	15	<1	N	N	15	70	5	<50	N	N
LB004	15	<1	N	N	10	150	15	50	7	N
LB005	15	<1	N	N	10	70	15	50	<5	N
LB006	20	<1	10	N	10	100	50	50	5	N
LB007-1	N	<1	15	N	N	30	300	50	N	N
LB007-2	10	<1	10	N	<10	50	20	<50	N	N
LB008	N	<1	N	N	N	70	<5	50	N	N
LB009	N	<1	N	N	N	70	10	50	N	N
LJ001	30	<1	N	N	<10	50	30	<50	N	N
LJ002	20	<1	N	N	N	30	70	50	N	N
LJ004	30	<1	N	N	15	200	15	50	5	N
LJ005	N	<1	N	N	N	150	10	50	N	N
LJ006	N	<1	N	N	N	30	15	50	N	N
LJ007	N	<1	N	N	N	20	<5	N	N	N
LJ008-1	<5	<1	N	N	N	50	20	<50	N	N
LJ008-2	<5	N	N	N	N	100	10	100	7	N
LJ009	70	<1	N	N	N	50	70	<50	N	N
LJ011	7	1.5	N	N	N	30	15	50	N	N
LL001	10	N	N	N	<10	50	10	<50	N	N
LL002	15	<1	N	N	15	100	5	50	N	N
LL003	N	<1	N	N	N	70	<5	50	7	N
LL005	70	1	N	N	20	70	30	<50	<5	N
LL008	7	<1	N	N	N	30	30	<50	N	N

Table B11. *Analyses of rock samples collected in the geochemical study of the La Joya district, Bolivia* - Continued

Sample no.	V	Pb	Sb	Sc	Sn	Sr	W	Y	Zn	Zr
EQ048	50	15	N	<5	N	300	N	<10	N	200
EQ050	70	20	N	<5	N	300	N	10	N	300
EQ053	70	20	N	<5	N	300	N	10	N	100
EQ054	200	<10	N	7	N	700	N	<10	N	70
EQ055	70	30	N	N	N	300	N	N	N	70
EQ056	50	15	N	<5	N	300	N	10	N	150
EQ057	50	15	N	<5	N	300	N	10	N	150
EQ059	100	15	N	<5	N	300	N	10	N	150
KK001	30	200	<100	N	50	N	N	<10	N	70
KK002	50	<10	N	<5	N	200	N	70	1000	70
KK003	20	30	N	N	N	150	N	<10	N	70
KK004	20	300	100	N	30	100	N	<10	N	50
KK005	50	150	N	5	N	N	N	N	N	50
KK006	30	200	150	<5	30	100	N	<10	N	30
KK007	30	700	500	<5	50	150	N	<10	N	50
KK008-1	30	300	100	<5	50	<100	N	10	N	100
KK008-2	<10	200	100	N	10	N	N	10	N	70
KS001-1	100	30	N	5	15	200	N	N	N	300
KS001-2	70	20	N	5	N	100	N	20	N	300
KS002	70	15	N	<5	10	100	N	N	N	100
KS003-1	70	30	N	<5	<10	150	N	<10	<200	300
KS003-2	20	30	N	N	<10	200	N	N	N	50
KS004	70	10	N	<5	<10	100	20	10	N	300
KS005	50	50	N	N	N	300	N	<10	N	200
KS006	30	30	N	N	<10	200	N	20	N	500
LB001	70	1500	N	<5	N	100	N	<10	1000	70
LB002	50	10	N	<5	N	200	N	10	N	70
LB003	70	200	N	<5	N	<100	N	<10	1500	70
LB004	70	20	N	<5	N	300	N	<10	N	70
LB005	70	20	N	5	N	200	N	<10	N	70
LB006	100	20	N	<5	N	300	N	<10	N	70
LB007-1	50	7000	150	N	50	150	N	<10	N	30
LB007-2	50	10	<100	<5	N	300	N	N	N	70
LB008	30	50	N	<5	N	N	N	<10	N	200
LB009	70	500	<100	<5	20	N	N	<10	N	200
LJ001	50	<10	N	5	N	N	N	20	N	300
LJ002	50	<10	N	5	N	100	N	15	N	150
LJ004	70	150	N	<5	N	200	N	<10	700	100
LJ005	30	150	N	<5	N	100	N	<10	N	100
LJ006	20	20	N	<5	N	100	N	10	N	150
LJ007	20	200	N	<5	N	N	N	N	N	70
LJ008-1	70	N	N	<5	N	100	N	10	N	150
LJ008-2	50	20	N	<5	N	200	20	<10	N	500
LJ009	50	70	N	5	N	100	N	10	N	500
LJ011	100	15	N	7	N	N	N	20	N	200
LL001	50	300	N	5	N	200	N	<10	300	70
LL002	50	N	N	5	N	200	N	10	N	70
LL003	20	30	<100	N	<10	N	N	10	N	200
LL005	50	200	N	7	N	N	N	20	2000	200
LL008	30	2000	N	<5	N	N	N	<10	1000	100

Table B11. *Analyses of rock samples collected in the geochemical study of the La Joya district, Bolivia* - Continued

Sample no.	Na	P	Ga	Ge	Th	Hg	Se	Te	[1]Au	[2]Au
EQ048	1.5	N	30	N	N	0.02	<0.1	<0.05	<0.002	<0.15
EQ050	1	N	50	N	N	<0.02	<0.1	<0.05	<0.002	<0.15
EQ053	2	N	50	N	N	<0.02	<0.1	<0.05	<0.002	<0.15
EQ054	0.3	<0.2	70	N	N	0.3	<0.1	<0.05	<0.002	<0.15
EQ055	0.2	N	50	N	N	0.02	<0.1	<0.05	0.2	<0.15
EQ056	1	N	20	N	N	0.02	<0.1	<0.05	<0.002	<0.15
EQ057	1	N	20	N	N	0.02	<0.1	<0.05	0.01	<0.15
EQ059	1	N	20	N	N	0.02	0.2	<0.05	<0.004	<0.15
KK001	0.2	N	15	N	N	0.04	0.6	<0.05	0.074	0.18
KK002	2	N	20	N	N	0.02	<0.1	<0.05	0.014	<0.15
KK003	N	N	15	N	N	0.04	5	0.9	0.01	<0.15
KK004	N	N	20	N	N	0.02	<0.1	<0.05	0.03	<0.15
KK005	<0.2	N	20	N	N	0.02	<0.1	<0.05	0.054	<0.15
KK006	N	N	30	N	N	0.02	0.1	<0.05	0.1	0.27
KK007	N	N	30	N	N	0.04	<0.1	0.1	1.35	1.6
KK008-1	N	N	50	N	N	0.02	0.2	<0.05	0.1	1.9
KK008-2	N	N	N	N	N	0.04	0.2	<0.05	4.3	5
KS001-1	N	N	5	N	N	<0.02	1.2	0.45	0.02	<0.15
KS001-2	N	N	7	N	N	<0.02	0.5	0.3	0.034	<0.15
KS002	<0.2	N	10	N	N	<0.02	1.7	0.4	0.1	0.2
KS003-1	N	N	7	N	N	0.04	2.2	0.35	0.02	<0.15
KS003-2	0.5	N	10	N	N	0.02	13	0.2	0.1	<0.15
KS004	<0.2	N	<5	N	N	<0.02	1.4	0.35	0.014	<0.15
KS005	N	N	7	N	N	0.46	2.3	0.3	0.022	<0.15
KS006	N	N	N	N	N	<0.02	1.2	<0.05	0.012	<0.15
LB001	1	N	10	N	N	0.04	<0.1	<0.05	0.006	<0.15
LB002	1	N	10	N	N	<0.02	<0.1	<0.05	0.004	<0.15
LB003	0.7	N	20	N	N	0.02	<0.1	<0.05	0.046	<0.15
LB004	1.5	N	20	N	N	<0.02	<0.1	<0.05	0.01	<0.15
LB005	1	N	20	N	N	0.02	<0.1	<0.05	<0.002	<0.15
LB006	1.5	N	20	N	N	<0.02	<0.1	0.2	0.014	<0.15
LB007-1	0.5	N	20	N	N	8.1	2.3	2.6	0.45	0.64
LB007-2	1	N	10	N	N	0.02	<0.1	0.3	0.028	<0.15
LB008	N	N	7	N	N	0.04	0.1	0.4	0.042	<0.15
LB009	N	N	15	N	N	3.8	0.1	0.15	0.018	<0.15
LJ001	0.2	N	10	N	N	<0.02	<0.1	<0.05	0.012	<0.15
LJ002	N	N	10	N	N	0.02	0.3	<0.05	0.01	<0.15
LJ004	1.5	N	20	N	N	0.02	<0.1	<0.05	0.004	<0.15
LJ005	1	N	10	N	N	0.02	0.6	0.3	0.004	<0.15
LJ006	N	N	15	N	N	<0.02	1.8	0.3	0.058	<0.15
LJ007	N	N	5	N	N	<0.02	<0.1	<0.25	0.008	<0.15
LJ008-1	N	N	15	N	N	0.02	0.8	0.35	0.012	<0.15
LJ008-2	N	N	<5	N	N	0.04	1.1	0.45	0.85	0.71
LJ009	<0.2	N	7	N	N	<0.02	0.3	<0.05	0.006	<0.15
LJ011	0.3	N	20	N	N	<0.02	0.3	0.1	0.002	<0.15
LL001	1.5	N	10	N	N	0.02	<0.1	<0.05	0.004	<0.15
LL002	2	N	20	N	N	0.02	0.1	<0.05	0.012	<0.15
LL003	N	N	N	N	N	0.02	<0.1	<0.05	0.024	<0.15
LL005	0.2	N	10	N	N	0.42	0.1	0.15	0.006	<0.15
LL008	N	N	10	N	N	3	<0.1	<0.05	0.008	<0.15

Table B11. *Analyses of rock samples collected in the geochemical study of the La Joya district, Bolivia* - Continued

Sample no.	As	Bi	Cd	Sb	Zn	Cu	Pb	Ag	Mo
EQ048	7.1	0.64	0.13	2.9	50	13	9.7	0.23	9.2
EQ050	11	<0.6	0.1	3.2	54	16	15	0.34	12
EQ053	9.2	0.63	0.051	2.4	46	17	8.6	0.18	4.7
EQ054	8.5	<0.6	<0.03	1.5	5.1	6	5.9	0.072	3.1
EQ055	140	1.8	<0.03	7.5	3.6	3	35	0.43	5.9
EQ056	4	<0.6	0.074	0.68	42	13	11	0.06	5.5
EQ057	8	<0.6	0.095	1.2	42	9.4	7.7	0.11	4.4
EQ059	7.4	0.63	0.1	0.99	47	13	5.9	0.067	4.2
KK001	88	4.9	0.19	69	9.8	9.6	520	4	6.4
KK002	16	<0.6	0.33	9.2	710	16	7.3	0.22	5.5
KK003	44	1.5	0.04	3.1	4.8	7.9	64	0.47	7.7
KK004	290	4.1	0.053	120	8.1	5.8	680	14	6.6
KK005	150	<0.6	0.16	41	92	57	210	1	6.8
KK006	880	0.79	0.17	130	4.7	29	490	29	4.9
KK007	1000	6.2	1	260	12	35	1800	10	6.1
KK008-1	240	5.7	0.41	90	11	24	510	13	6.8
KK008-2	1000	28	<0.03	44	5	2.8	750	19	5.7
KS001-1	10	0.97	0.034	1.9	3.3	7.6	11	0.15	4.7
KS001-2	7.9	0.75	<0.03	2.1	3.3	4.1	11	0.16	6.6
KS002	270	34	0.12	6.9	6.3	37	24	0.22	6.6
KS003-1	37	1.1	0.67	3.7	180	12	83	0.26	9.1
KS003-2	89	2	0.059	3.4	11	37	34	0.17	9.4
KS004	22	0.68	0.036	2.5	4.2	7.7	7.4	0.093	13
KS005	32	1.6	0.096	5.6	8	13	26	0.87	18
KS006	31	0.96	0.12	5.9	6.3	14	21	0.22	17
LB001	47	<0.6	1.9	18	1100	39	2100	1.1	3.9
LB002	9.2	<0.6	0.19	6	55	3.2	7.3	0.16	4.3
LB003	63	<0.6	9.6	5	1200	12	440	1.4	4.2
LB004	11	<0.6	0.086	4.1	49	18	25	0.54	7.6
LB005	3.9	0.64	0.19	5.8	65	34	30	0.1	6.6
LB006	18	8.2	0.041	75	36	47	12	3.7	6.1
LB007-1	950	5.6	6.7	270	69	280	4000	17	6
LB007-2	30	13	0.047	120	48	29	21	6.2	6
LB008	22	6.5	0.039	10	6.8	4.3	83	2.9	8.1
LB009	100	0.98	0.2	39	26	16	1300	6.3	5.2
LJ001	9	0.71	0.058	2.1	46	38	12	0.45	2.7
LJ002	12	1.2	<0.03	2	4.6	73	17	0.49	2.1
LJ004	9.1	0.84	1.9	7	460	15	170	0.27	9.4
LJ005	8.2	1.5	0.15	2.9	14	16	270	1.1	6.2
LJ006	7.2	1.1	0.062	3.7	4.5	14	23	0.12	5.1
LJ007	12	0.62	0.051	16	18	4.1	410	1.8	5.9
LJ008-1	18	1.2	<0.03	2.5	2	22	5	0.074	2
LJ008-2	69	2.2	<0.03	11	6.8	11	14	0.17	8.8
LJ009	14	0.67	0.04	1.8	6.7	52	77	0.79	3.5
LJ011	25	0.79	0.18	4.2	27	17	32	0.15	1.4
LL001	17	<0.6	0.53	4.1	310	17	760	0.75	4.7
LL002	<0.6	<0.6	0.06	5.9	88	9	7	0.19	3.7
LL003	100	2.6	2.3	40	7.6	3.4	87	9.7	8.7
LL005	260	1.1	7.9	11	1400	30	620	1.4	3.4
LL008	74	<0.6	1.9	22	660	32	2800	3.3	2.9

Table B11. *Analyses of rock samples collected in the geochemical study of the La Joya district, Bolivia* - Continued

Sample no.	Ba	Fe*	Mg*	Ca*	Ti*	Mn	Ag	As	Au	B
LL009	700	2	0.15	0.7	0.3	>5,000	3	N	N	30
LL010	150	2	0.1	<0.05	0.7	100	<0.5	N	N	100
NL001	300	1	0.15	0.5	0.3	100	N	N	N	20
NL002	300	0.7	<0.02	0.2	0.3	30	N	N	N	50
NL003	300	2	0.2	0.5	0.3	100	N	N	N	20
NL004	300	2	0.3	0.7	0.3	150	0.5	N	N	20
QT001	300	1.5	0.5	0.7	0.3	150	N	N	N	20
QT002	300	1	0.3	0.7	0.2	150	N	N	N	50
QT003	500	1.5	0.7	0.7	0.3	150	N	N	N	20
QT004	300	1	0.5	0.7	0.3	150	N	N	N	30
QT005	300	1.5	0.5	0.7	0.3	150	N	N	N	20
QT006	300	1	0.5	0.7	0.3	150	N	N	N	15
QT007	500	1.5	0.7	1	0.3	150	N	N	N	20
QT008	500	1.5	0.5	0.7	0.3	150	N	N	N	20
QT009	300	1.5	0.3	0.7	0.3	150	N	N	N	20
QT010	300	1	0.2	0.5	0.3	100	N	N	N	30
QT011	500	2	0.5	0.7	0.3	150	N	N	N	20
QT012	300	1.5	0.3	0.7	0.3	150	N	N	N	20

Sample no.	Ni	Be	Bi	Cd	Co	Cr	Cu	La	Mo	Nb
LL009	15	<1	N	N	15	100	50	<50	N	N
LL010	20	<1	N	N	N	50	30	<50	N	N
NL001	10	1	N	N	N	100	5	<50	7	N
NL002	<5	1	N	N	N	100	15	<50	<5	N
NL003	30	1	N	N	10	100	10	50	<5	N
NL004	10	1	N	N	<10	150	10	50	10	N
QT001	15	1	N	N	10	200	10	50	<5	N
QT002	15	1	N	N	<10	70	7	50	N	N
QT003	15	<1	N	N	10	150	7	50	N	N
QT004	10	<1	N	N	<10	100	7	<50	7	N
QT005	15	1.5	N	N	10	100	7	<50	N	N
QT006	15	1	N	N	<10	100	10	<50	N	N
QT007	15	1	N	N	10	150	10	<50	<5	N
QT008	15	1.5	N	N	10	150	7	<50	N	N
QT009	15	1.5	N	N	10	70	7	70	<5	N
QT010	10	1	N	N	<10	70	5	<50	<5	N
QT011	15	1	N	N	10	100	7	50	<5	N
QT012	20	1	<10	N	10	70	15	<50	<5	N

Sample no.	V	Pb	Sb	Sc	Sn	Sr	W	Y	Zn	Zr
LL009	50	30	N	<5	N	N	N	10	1000	70
LL010	70	<10	N	7	N	<100	N	20	1000	150
NL001	30	10	N	N	N	200	N	N	N	100
NL002	50	<10	N	N	N	200	N	N	N	100
NL003	100	10	N	N	N	200	N	N	N	150
NL004	50	10	N	N	N	200	N	N	N	100
QT001	30	15	N	N	N	300	N	N	N	100
QT002	20	20	N	N	N	200	N	<10	N	100
QT003	30	15	N	N	N	200	N	<10	N	100
QT004	50	15	N	N	N	200	N	<10	N	150
QT005	50	30	N	N	N	200	N	<10	N	200
QT006	30	10	N	N	N	200	N	<10	N	100
QT007	50	15	N	N	N	200	N	<10	N	200
QT008	50	10	N	N	N	200	N	<10	N	150
QT009	30	10	N	N	N	200	N	<10	N	150
QT010	20	10	N	N	N	200	N	<10	N	100
QT011	50	15	N	N	N	300	N	<10	N	100
QT012	30	15	N	N	N	200	N	<10	N	150

Table B11. *Analyses of rock samples collected in the geochemical study of the La Joya district, Bolivia* - Continued

Sample no.	Na	P	Ga	Ge	Th	Hg	Se	Te	[1]Au	[2]Au
LL009	0.2	N	15	N	N	0.46	<0.1	<0.05	0.004	<0.15
LL010	0.2	N	15	N	N	0.02	<0.1	<0.05	0.004	<0.15
NL001	1.5	N	20	N	N	0.36	<0.1	<0.05	<0.002	<0.15
NL002	1	N	20	N	N	>34	0.2	0.1	<0.002	<0.15
NL003	1	N	20	N	N	0.12	<0.1	<0.05	<0.002	<0.15
NL004	1.5	N	20	N	N	0.72	<0.1	<0.05	<0.002	<0.15
QT001	1.5	N	30	N	N	<0.02	<0.1	<0.05	<0.002	<0.15
QT002	1	N	20	N	N	<0.02	<0.1	<0.05	0.004	<0.15
QT003	2	N	20	N	N	<0.02	<0.1	<0.05	<0.002	<0.15
QT004	1.5	N	20	N	N	<0.02	0.2	<0.05	<0.002	<0.15
QT005	1.5	N	20	N	N	<0.02	<0.1	<0.05	<0.002	<0.15
QT006	1.5	N	20	N	N	<0.02	<0.1	<0.05	<0.002	<0.15
QT007	1.5	N	20	N	N	0.04	<0.1	<0.05	<0.002	<0.15
QT008	1.5	N	20	N	N	<0.02	<0.1	<0.05	<0.002	<0.15
QT009	1.5	N	20	N	N	<0.02	<0.1	<0.05	<0.002	<0.15
QT010	1	N	15	N	N	<0.02	<0.1	<0.05	<0.002	<0.15
QT011	1.5	N	30	N	N	0.02	<0.1	<0.05	<0.002	<0.15
QT012	1.5	N	20	N	N	<0.02	<0.1	0.05	0.008	<0.15

Sample no.	As	Bi	Cd	Sb	Zn	Cu	Pb	Ag	Mo
LL009	32	<0.6	25	13	1200	58	50	1.8	3.6
LL010	28	<0.6	0.071	19	790	37	8.8	0.15	2.6
NL001	14	0.65	0.045	3.8	35	9.3	4.8	0.19	10
NL002	82	<0.6	0.055	3.4	9.4	8.5	6.3	0.16	9.2
NL003	11	<0.6	0.04	4.7	49	9.4	4	0.066	5.1
NL004	10	<0.6	0.033	1.6	49	11	2.8	<0.045	8
QT001	4.5	0.66	0.048	1.5	32	8.5	8.3	<0.045	6.5
QT002	15	<0.6	0.036	4	25	8.6	21	1.3	5.9
QT003	5.1	<0.6	0.11	0.85	36	7.1	15	<0.045	4.7
QT004	3.9	<0.6	0.054	1.4	40	7.9	5.3	<0.045	7.1
QT005	12	<0.6	0.06	0.96	37	8.9	33	0.14	4.5
QT006	2.4	<0.6	0.044	0.65	36	9.7	8.7	<0.045	4.7
QT007	9.6	0.65	0.16	2	47	8.4	8.5	0.097	4.7
QT008	3.4	<0.6	0.089	1.7	75	9.5	7.8	<0.045	6.7
QT009	2.9	<0.6	0.071	0.99	30	5.6	4	<0.045	4.1
QT010	8.9	<0.6	<0.03	1.3	23	7.1	6.8	<0.045	6.5
QT011	1.7	<0.6	<0.03	0.72	37	6.6	3.5	<0.045	4.5
QT012	46	6.9	0.11	3.6	26	16	20	0.099	5.1

Table B-12. *Analyses of soil samples collected in the geochemical study of the La Joya district, Bolivia*

[First 35 elements (Ba through Th) analyzed by DC-ARC AES. Elements with asterisks (*) are reported in percent; all other elements are reported in ppm. [1]Au represents gold determined by flame or graphite furnace AAS. [2]Au, As, Bi, Cd, Sb, Zn, Cu, Pb, Ag, and Mo analyzed by peroxide dissolution ICP-AES. Leaders (--) indicate no data available. N, the element was present below the lower limit of determination]

Sample no.	Ba	Fe*	Mg*	Ca*	Ti*	Mn	Ag	As	Au	B
CH001	300	2	0.3	0.5	0.5	150	N	N	N	70
CH002	300	1	0.3	0.5	0.3	150	N	N	N	70
CS13S1	200	2	0.5	0.7	0.3	150	N	N	N	50
KK001-1	300	5	1	0.2	0.3	150	2	500	N	100
KK001-2	300	3	0.15	0.15	0.3	100	5	N	N	70
KK002-1	300	2	0.5	0.3	0.3	200	5	N	N	70
KK002-2	300	3	0.15	0.15	0.3	100	2	N	N	50
KK003	200	1.5	0.5	0.3	0.3	200	0.5	N	N	70
KK004-2	300	3	1	0.2	0.5	500	<0.5	N	N	100
KK005-1	500	1.5	0.3	0.5	0.3	300	2	N	N	50
KK005-2	300	2	0.15	0.15	0.3	500	2	N	N	50
KK006	300	3	1	0.5	0.7	300	0.7	N	N	100
KK007-1	300	2	0.7	0.7	0.5	100	<0.5	N	N	100
KK007-2	200	3	0.2	0.5	0.3	150	5	<200	N	70
KK008-1	300	1.5	0.3	0.5	0.3	200	N	N	N	50
KK008-2	200	3	0.2	5	0.2	200	30	700	N	70
KS001	300	1.5	0.15	0.5	0.5	150	N	N	N	70
KS002	200	2	0.2	0.5	0.5	100	N	N	N	70
KS003	300	2	0.3	0.7	0.5	150	N	N	N	70
KS004	300	2	0.2	0.5	0.5	150	1	N	N	70
KS005	300	2	0.2	0.5	0.5	200	1.5	N	N	50
KS006	300	2	0.2	0.3	0.3	150	<0.5	N	N	70
LB001	300	5	0.7	0.5	0.5	200	1.5	N	N	100
LB002	300	1.5	0.3	1	0.5	100	<0.5	N	N	50
LB003	700	3	0.7	0.5	0.7	1500	1	N	N	20
LB004	500	2	0.3	0.5	0.7	300	0.5	N	N	30
LB005	500	5	0.5	0.7	0.5	200	N	N	N	50
LB006	500	2	0.3	0.5	0.5	200	<0.5	N	N	50
LB007	700	5	0.3	0.5	0.3	3000	2	N	N	30
LB008	500	2	0.3	1	0.3	200	1	N	N	50
LB009	500	3	0.5	1.5	0.5	150	2	N	N	70
LL008	1000	2	0.2	0.2	0.5	300	3	N	N	50
LL009	500	3	0.2	0.3	0.7	700	1.5	N	N	50
LL010	700	7	0.2	0.2	0.7	1500	1	N	N	70
NL001-1	500	3	0.5	1	0.5	300	N	N	N	70
NL001-2	500	1.5	0.15	1.5	0.3	70	N	N	N	50
NL002	300	2	0.3	0.5	0.5	150	N	N	N	70
NL003	500	1.5	0.3	0.7	0.3	150	N	N	N	50
NL004	200	1.5	0.2	0.5	0.5	150	N	N	N	50
QT002	500	2	0.7	1	0.3	300	N	N	N	50
QT003	500	2	0.5	0.7	0.5	200	N	N	N	50
QT004	300	2	0.5	0.7	0.5	300	N	N	N	50
QT005	300	2	0.5	0.7	0.5	150	0.5	N	N	50
QT006	300	2	0.3	1	0.3	200	N	N	N	70
QT007	300	1.5	0.7	10	0.2	200	N	N	N	30
QT008	300	1.5	0.5	3	0.3	200	N	N	N	70
QT009	500	1.5	0.5	10	0.3	300	N	N	N	30
QT010	300	1.5	0.5	5	0.3	100	N	N	N	50
QT011	300	1	0.3	2	0.2	100	N	N	N	30
QT012	300	2	0.3	1	0.5	300	N	N	N	50

Table B-12. *Analyses of soil samples collected in the geochemical study of the La Joya district, Bolivia* - Continued

Sample no.	Ni	Be	Bi	Cd	Co	Cr	Cu	La	Mo
CH001	15	<1	N	N	10	15	20	50	N
CH002	10	1	N	N	10	20	15	<50	N
CS13S1	15	1.5	N	N	10	15	20	<50	N
KK001-1	30	1.5	30	N	10	70	300	50	N
KK001-2	<5	1	30	N	N	15	20	50	N
KK002-1	15	1	70	N	<10	20	30	<50	N
KK002-2	7	1.5	N	N	N	15	20	<50	N
KK003	15	1	N	N	10	15	30	<50	N
KK004-2	20	1.5	N	N	15	30	50	50	N
KK005-1	7	1	N	N	<10	15	20	50	N
KK005-2	20	1.5	N	N	<10	15	15	<50	N
KK006	30	2	N	N	15	30	50	50	N
KK007-1	N	1	N	N	10	20	50	<50	N
KK007-2	10	1	15	N	N	15	30	50	N
KK008-1	10	1	N	N	10	15	30	<50	N
KK008-2	<5	1	70	N	N	10	30	<50	N
KS001	10	<1	N	N	10	10	15	<50	N
KS002	15	<1	N	N	10	10	10	<50	N
KS003	20	<1	N	N	10	20	30	<50	N
KS004	15	<1	N	N	10	10	15	<50	N
KS005	15	<1	N	N	10	15	15	<50	N
KS006	15	<1	N	N	10	15	20	<50	N
LB001	10	1	N	N	10	30	30	<50	N
LB002	10	1	N	N	<10	15	15	<50	N
LB003	15	1.5	N	N	15	20	20	<50	N
LB004	10	1	N	N	10	15	15	<50	N
LB005	15	<1	N	N	10	20	30	70	N
LB006	15	1	N	N	10	15	20	<50	N
LB007	15	1	<10	N	10	15	50	50	N
LB008	10	1	N	N	10	15	15	<50	N
LB009	10	1	N	N	<10	15	30	70	N
LL008	10	1	N	N	<10	20	20	70	N
LL009	15	1.5	N	N	<10	20	30	<50	N
LL010	30	1.5	N	N	10	50	30	50	N
NL001-1	20	1.5	N	N	15	30	50	50	N
NL001-2	7	1	N	N	<10	20	20	<50	N
NL002	20	1	N	N	15	15	20	<50	N
NL003	15	1	N	N	10	15	15	50	N
NL004	15	1	N	N	10	10	15	50	N
QT002	20	1.5	N	N	10	20	30	<50	N
QT003	15	1.5	N	N	10	20	20	50	N
QT004	15	1.5	N	N	10	20	20	50	N
QT005	15	1.5	N	N	10	20	15	50	N
QT006	20	1.5	N	N	10	20	20	<50	N
QT007	15	<1	N	N	10	30	20	<50	N
QT008	15	1.5	N	N	10	15	20	<50	N
QT009	15	1	N	N	10	15	10	<50	N
QT010	10	1	N	N	10	15	20	70	N
QT011	10	2	N	N	<10	15	10	50	N
QT012	15	1.5	N	N	10	10	15	50	N

Table B-12. *Analyses of soil samples collected in the geochemical study of the La Joya district, Bolivia* - Continued

Sample no.	Nb	V	Pb	Sb	Sc	Sn	Sr	W	Y
CH001	N	70	20	N	<5	N	200	N	10
CH002	N	30	15	N	<5	N	200	N	<10
CS13S1	N	50	15	N	<5	N	150	N	10
KK001-1	N	100	70	<100	10	N	100	N	20
KK001-2	N	50	700	150	<5	30	150	N	10
KK002-1	N	50	500	200	<5	<10	150	N	10
KK002-2	N	70	500	N	5	15	150	N	10
KK003	N	50	30	N	<5	N	200	N	10
KK004-2	N	70	100	N	7	N	150	N	30
KK005-1	N	70	200	N	<5	N	150	N	30
KK005-2	N	70	300	<100	5	N	100	N	<10
KK006	N	100	70	N	10	N	150	N	20
KK007-1	N	70	20	N	7	N	150	N	15
KK007-2	N	50	150	150	5	30	100	N	15
KK008-1	N	50	15	N	<5	N	150	N	10
KK008-2	N	50	300	300	<5	30	200	N	10
KS001	N	50	10	N	<5	N	200	N	<10
KS002	N	50	<10	N	<5	N	200	N	20
KS003	N	50	15	N	<5	N	200	N	10
KS004	N	50	<10	N	<5	N	200	N	<10
KS005	N	70	15	N	<5	N	200	N	20
KS006	N	50	15	N	<5	N	200	N	15
LB001	N	70	150	N	5	N	<100	N	15
LB002	N	50	30	N	<5	N	200	N	10
LB003	N	70	50	N	5	N	150	N	10
LB004	N	70	15	N	5	N	150	N	10
LB005	N	70	20	N	5	N	300	N	15
LB006	N	70	15	N	<5	N	200	N	10
LB007	N	100	500	100	5	N	150	N	15
LB008	N	70	150	N	<5	N	200	N	10
LB009	N	100	300	<100	5	N	150	N	15
LL008	N	70	300	N	5	N	150	N	15
LL009	N	70	200	N	5	N	150	N	15
LL010	N	70	100	N	10	N	100	N	20
NL001-1	N	70	30	N	7	N	200	N	10
NL001-2	N	50	20	N	<5	N	300	N	<10
NL002	N	70	15	N	<5	N	300	N	10
NL003	N	70	<10	N	<5	N	300	N	<10
NL004	N	50	10	N	<5	N	300	N	<10
QT002	N	50	20	N	<5	N	200	N	10
QT003	N	50	15	N	<5	N	200	N	10
QT004	N	50	20	N	<5	N	200	N	15
QT005	N	70	20	N	5	N	200	N	10
QT006	N	50	20	N	<5	N	200	N	10
QT007	N	30	30	N	<5	N	300	N	10
QT008	N	30	15	N	<5	N	200	N	<10
QT009	N	30	15	N	<5	N	500	N	<10
QT010	N	50	10	N	<5	N	300	N	<10
QT011	N	20	10	N	<5	N	200	N	<10
QT012	N	50	15	N	<5	N	200	N	10

Table B-12. *Analyses of soil samples collected in the geochemical study of the La Joya district, Bolivia* - Continued

Sample no.	Zn	Zr	Na	P	Ga	Ge	Th	[1]Au	[2]Au
CH001	N	500	1	N	20	N	N	<0.002	<0.15
CH002	N	300	1	N	10	N	N	<0.002	<0.15
CS13S1	N	100	1.5	N	10	N	N	<0.002	<0.15
KK001-1	N	100	1	N	50	N	N	0.25	--
KK001-2	N	700	0.7	<0.2	30	N	N	0.15	<0.15
KK002-1	N	500	1	N	15	N	N	0.15	<0.15
KK002-2	200	300	0.5	<0.2	15	N	N	0.04	<0.15
KK003	N	300	0.7	N	10	N	N	0.01	<0.15
KK004-2	N	500	1	N	20	N	N	0.008	<0.15
KK005-1	N	700	1	N	20	N	N	0.06	<0.15
KK005-2	<200	500	0.5	N	15	N	N	0.15	<0.15
KK006	N	300	1	N	30	N	N	0.01	<0.15
KK007-1	N	300	1	N	15	N	N	0.008	<0.15
KK007-2	N	>1,000	0.3	N	20	N	N	1.1	0.27
KK008-1	N	500	1	N	7	N	N	<0.002	<0.15
KK008-2	N	200	0.5	<0.2	30	N	N	1.35	1
KS001	N	150	1	N	10	N	N	0.002	<0.15
KS002	N	500	0.7	N	<5	N	N	<0.002	<0.15
KS003	N	300	1	0.3	10	N	N	0.004	<0.15
KS004	N	300	1	N	7	N	N	<0.002	<0.15
KS005	N	500	1	N	7	N	N	<0.004	<0.15
KS006	N	300	1	0.2	10	N	N	0.006	<0.15
LB001	N	1000	1	N	20	N	N	0.022	<0.15
LB002	N	500	1	N	15	N	N	0.002	<0.15
LB003	<200	500	1.5	N	30	N	N	0.012	<0.15
LB004	N	200	1	N	20	N	N	<0.002	<0.15
LB005	N	200	1.5	N	20	N	N	<0.002	<0.15
LB006	N	200	1	N	15	N	N	<0.002	<0.15
LB007	1000	150	1	<0.2	20	N	N	0.032	<0.15
LB008	<200	200	0.7	N	15	N	N	0.008	<0.15
LB009	N	200	0.7	N	15	N	N	0.02	<0.15
LL008	200	70	1	<0.2	20	N	N	0.002	<0.15
LL009	500	700	1	N	15	N	N	0.006	<0.15
LL010	1000	300	0.7	N	20	N	N	<0.002	<0.15
NL001-1	N	150	1.5	0.7	30	N	N	<0.002	<0.15
NL001-2	N	150	1.5	0.2	30	N	N	<0.002	<0.15
NL002	N	100	1	N	20	N	N	<0.004	<0.15
NL003	N	500	1	N	10	N	N	<0.002	<0.15
NL004	N	150	1	N	10	N	N	<0.004	<0.15
QT002	N	100	1	0.2	30	N	N	<0.002	<0.15
QT003	N	300	1	<0.2	15	N	N	<0.002	<0.15
QT004	N	300	1.5	<0.2	20	N	N	<0.002	<0.15
QT005	N	300	1	<0.2	20	N	N	<0.002	<0.15
QT006	N	100	1.5	0.2	15	N	N	<0.002	<0.15
QT007	N	70	1	0.2	15	N	N	<0.002	<0.15
QT008	N	150	1.5	N	15	N	N	<0.002	<0.15
QT009	N	100	1	<0.2	10	N	N	<0.002	<0.15
QT010	N	150	1	0.2	15	N	N	<0.002	<0.15
QT011	N	150	1.5	N	20	N	N	0.006	<0.15
QT012	N	150	1	<0.2	30	N	N	<0.002	<0.15

Table B-12. *Analyses of soil samples collected in the geochemical study of the La Joya district, Bolivia* - Continued

Sample no.	As	Bi	Cd	Sb	Zn	Cu	Pb	Ag	Mo
CH001	11	<0.6	0.13	1.2	43	11	18	0.053	0.76
CH002	10	<0.6	0.13	1	38	10	15	0.087	0.69
CS13S1	16	<0.6	0.12	1.3	42	16	19	0.059	0.47
KK001-1	--	--	--	--	--	--	--	--	--
KK001-2	180	17	0.25	100	18	11	710	5.2	1.3
KK002-1	150	20	0.3	57	84	29	490	3.6	1.9
KK002-2	180	3	0.32	25	150	16	610	2.9	0.92
KK003	69	1	0.48	4.5	59	38	54	0.42	0.72
KK004-2	34	0.77	1.4	4.1	130	69	84	0.4	0.97
KK005-1	77	0.95	0.66	22	110	14	240	1.6	0.75
KK005-2	130	<0.6	0.7	32	190	12	430	1.6	0.85
KK006	36	1	0.55	6.9	91	54	82	0.38	1
KK007-1	22	0.99	0.31	2.6	59	48	29	0.12	0.82
KK007-2	280	7.8	0.33	90	23	27	260	3.3	0.79
KK008-1	34	<0.6	0.12	1.6	35	24	18	0.067	0.77
KK008-2	1200	22	0.1	140	16	22	410	13	0.92
KS001	9.6	<0.6	0.11	0.94	36	9.2	11	<0.045	0.81
KS002	15	<0.6	0.11	0.75	42	13	13	<0.045	0.71
KS003	20	<0.6	0.12	1.3	41	16	14	0.069	0.93
KS004	15	<0.6	0.087	1.2	34	12	14	0.057	0.84
KS005	19	<0.6	0.11	1.6	38	12	16	0.078	0.74
KS006	20	<0.6	0.085	1.5	27	13	12	0.13	0.93
LB001	73	1.4	0.25	8.8	48	21	170	0.65	0.74
LB002	20	<0.6	0.12	3.9	35	9.9	63	0.15	0.49
LB003	30	<0.6	1.3	7.2	230	18	83	0.22	1.2
LB004	14	<0.6	0.13	1.3	46	13	13	0.09	0.73
LB005	38	<0.6	0.14	1.5	51	14	21	0.062	0.73
LB006	34	<0.6	0.15	2.3	60	16	15	0.067	0.67
LB007	98	3.8	3.3	48	580	26	600	1.4	1.3
LB008	45	0.77	0.31	13	160	13	180	0.43	0.58
LB009	110	0.85	0.94	21	150	24	400	1.7	0.74
LL008	50	<0.6	1.2	5.3	260	17	380	0.89	0.42
LL009	120	<0.6	1.3	19	350	25	310	0.51	0.62
LL010	46	<0.6	1.1	15	650	21	150	0.21	0.77
NL001-1	50	<0.6	0.24	0.85	43	21	18	0.054	1.9
NL001-2	50	<0.6	0.045	<0.6	11	7.1	6.8	<0.045	0.57
NL002	27	<0.6	0.089	1.6	39	13	14	0.077	0.66
NL003	55	<0.6	0.28	1.1	36	15	10	<0.045	0.34
NL004	26	<0.6	0.12	0.91	40	11	11	<0.045	0.58
QT002	19	<0.6	0.14	1.1	37	20	13	0.059	0.43
QT003	10	<0.6	0.1	1	28	10	12	0.061	0.46
QT004	13	<0.6	0.095	0.94	32	12	14	0.047	0.64
QT005	11	<0.6	0.076	1.3	31	11	12	<0.045	0.37
QT006	25	<0.6	0.13	1.1	31	14	13	<0.045	0.34
QT007	29	<0.6	0.14	0.95	28	12	8.1	<0.045	0.23
QT008	21	<0.6	0.18	1.2	35	13	13	0.07	0.46
QT009	26	<0.6	0.092	<0.6	21	7.8	4.7	<0.045	0.32
QT010	43	<0.6	0.11	<0.6	29	11	8.4	<0.045	0.85
QT011	16	<0.6	0.042	<0.6	18	13	8.4	<0.045	0.11
QT012	8.1	<0.6	0.11	<0.6	28	10	9.1	<0.045	0.59

Table B-13. *Analyses of -0.25 mm sediment samples collected in the geochemical study of the La Joya district, Bolivia*

[First 35 elements (Ba through Th) analyzed by DC-ARC AES. Elements with asterisks (*) are reported in percent; all other elements are reported in ppm. [2]Au, As, Bi, Cd, Sb, Zn, Cu, Pb, Ag, and Mo analyzed by peroxide dissolution ICP-AES. N, the element was present below the lower limit of determination]

Sample no.	Ba	Fe*	Mg*	Ca*	Ti*	Mn	Ag	As	Au	B
CS001	300	1.5	0.3	0.7	0.5	200	1	N	N	70
CS002	300	2	0.3	0.7	0.5	200	<0.5	N	N	70
CS003	300	2	0.3	0.5	0.5	200	N	N	N	50
CS004	300	3	0.5	1	0.7	200	N	N	N	70
CS005	300	1.5	0.3	1	0.3	150	N	N	N	50
CS006	300	1.5	0.2	1	0.3	150	0.5	N	N	50
CS007	300	2	0.3	1	0.7	200	N	N	N	70
CS008	300	1.5	0.2	1	0.3	150	1.5	N	N	70
CS009	300	1.5	0.3	1.5	0.3	200	N	N	N	50
CS010	300	1.5	0.2	1	0.5	200	N	N	N	70
CS011	300	2	0.3	0.7	0.5	200	N	N	N	70
CS012	300	3	0.3	0.7	0.7	200	0.5	N	N	70
CS014	300	2	0.3	0.7	0.5	200	N	N	N	70
CS016	200	1.5	0.2	0.7	0.7	200	N	N	N	50
EQ001	700	5	1	1.5	0.7	300	N	N	N	50
EQ002	700	3	1	1.5	0.7	200	N	N	N	50
EQ003	500	2	0.7	1	0.7	150	N	N	N	50
EQ004	500	2	0.5	1	0.7	150	<0.5	N	N	50
EQ005	700	3	0.7	1	0.5	200	N	N	N	50
EQ006	300	2	0.5	0.7	0.5	200	N	N	N	50
EQ007	300	2	0.5	0.7	0.5	150	N	N	N	50
EQ008	300	2	0.5	0.7	0.5	150	0.7	N	N	50
EQ009	200	1.5	0.3	0.5	0.3	100	N	N	N	30
EQ010	200	2	0.5	0.7	0.5	150	N	N	N	50
EQ011	300	2	0.5	0.5	0.5	100	N	N	N	50
EQ012	500	2	0.5	1	0.5	150	0.5	N	N	50
EQ013	200	1.5	0.3	0.5	0.3	150	N	N	N	30
EQ014	500	2	0.5	0.7	0.5	200	N	N	N	70
EQ015	300	1.5	0.3	0.7	0.3	150	N	N	N	50
EQ017	500	2	0.7	0.7	0.5	200	N	N	N	50
EQ018	300	1.5	0.5	0.5	0.3	150	N	N	N	50
EQ020	500	2	0.5	0.7	0.5	150	<0.5	N	N	50
EQ021	500	2	0.5	0.7	0.5	150	N	N	N	70
EQ022	500	2	0.5	0.7	0.7	200	N	N	N	70
EQ025	300	3	0.7	0.7	0.5	150	0.5	N	N	50
EQ026	500	3	0.7	1	0.5	150	<0.5	N	N	50
EQ027	300	3	0.7	1	0.7	200	<0.5	N	N	70
EQ028	500	3	0.7	1	0.5	200	N	N	N	70
EQ029	500	3	1	1	0.5	200	N	N	N	50
EQ030	300	2	0.5	0.7	0.3	200	N	N	N	50
EQ032	500	2	0.7	1	0.5	200	N	N	N	50
EQ033	300	2	0.5	0.7	0.5	200	0.5	N	N	70
EQ034	300	2	0.7	1	0.7	200	<0.5	N	N	50
EQ035	300	2	0.5	0.7	0.5	200	N	N	N	50
EQ036	500	2	0.7	0.7	0.3	200	N	N	N	50
EQ037	300	3	0.5	0.7	0.5	150	N	N	N	50
EQ038	700	3	0.7	1	0.7	200	2	N	N	50
EQ039	500	3	0.7	1	0.5	200	N	N	N	50
EQ040	700	3	0.7	0.7	0.5	200	<0.5	N	N	50
EQ041	500	3	0.7	0.7	0.5	200	0.5	N	N	70

Table B-13. *Analyses of -0.25 mm sediment samples collected in the geochemical study of the La Joya district, Bolivia*--Continued

Sample no.	Ni	Be	Bi	Cd	Co	Cr	Cu	La	Mo	Nb
CS001	10	1.5	N	N	10	20	20	<50	N	N
CS002	15	1.5	N	N	15	30	20	<50	N	N
CS003	10	1.5	N	N	10	15	20	<50	N	N
CS004	15	1	N	N	10	30	20	<50	N	N
CS005	5	1.5	N	N	<10	15	15	N	N	N
CS006	7	1	N	N	<10	15	15	N	N	N
CS007	10	1	N	N	<10	20	15	<50	N	N
CS008	7	1.5	N	N	<10	15	15	<50	N	N
CS009	7	1	N	N	<10	15	20	N	N	N
CS010	15	1	N	N	10	15	15	<50	N	N
CS011	15	1	N	N	10	30	20	<50	N	N
CS012	15	1	N	N	10	20	20	<50	N	N
CS014	15	1	N	N	10	15	20	<50	N	N
CS016	7	1	N	N	10	15	10	<50	N	N
EQ001	30	1.5	N	N	15	50	20	200	N	N
EQ002	15	1.5	N	N	10	30	20	70	N	N
EQ003	10	1.5	N	N	10	20	15	50	N	N
EQ004	10	1.5	N	N	10	100	15	100	N	N
EQ005	10	1.5	N	N	10	50	20	50	N	N
EQ006	7	1	N	N	<10	10	15	<50	N	N
EQ007	7	1.5	N	N	<10	15	15	70	N	N
EQ008	7	1.5	N	N	<10	10	10	50	N	N
EQ009	7	1.5	N	N	<10	<10	10	<50	N	N
EQ010	7	1	N	N	<10	15	15	50	N	N
EQ011	7	1	N	N	<10	20	20	50	N	N
EQ012	7	1	N	N	<10	15	15	70	N	N
EQ013	7	1	N	N	<10	10	15	50	N	N
EQ014	15	1	N	N	10	20	15	100	N	N
EQ015	10	1	N	N	<10	10	10	70	N	N
EQ017	15	1.5	N	N	10	30	20	100	N	N
EQ018	10	1	N	N	10	15	15	50	N	N
EQ020	10	1	N	N	<10	30	20	100	N	N
EQ021	10	1.5	N	N	10	20	20	50	N	N
EQ022	15	1.5	N	N	10	30	20	50	N	N
EQ025	15	1.5	N	N	10	30	20	50	N	N
EQ026	10	1	N	N	10	30	20	150	N	N
EQ027	20	1	N	N	15	30	20	50	N	N
EQ028	15	1.5	N	N	10	20	15	70	N	N
EQ029	20	1	N	N	15	20	20	50	N	N
EQ030	15	1	N	N	10	15	20	50	N	N
EQ032	10	1.5	N	N	10	15	20	50	N	N
EQ033	10	1.5	N	N	10	15	20	70	N	N
EQ034	15	2	N	N	10	30	15	50	N	20
EQ035	10	1	N	N	<10	20	15	<50	N	N
EQ036	10	1	N	N	10	15	20	50	N	N
EQ037	15	1.5	N	N	10	20	15	50	N	N
EQ038	15	1.5	N	N	15	20	20	70	N	N
EQ039	15	1.5	N	N	10	20	15	100	N	N
EQ040	15	1	N	N	15	20	20	70	N	N
EQ041	10	1	N	N	10	15	20	50	N	N

Table B-13. *Analyses of -0.25 mm sediment samples collected in the geochemical study of the La Joya district, Bolivia*--Continued

Sample no.	V	Pb	Sb	Sc	Sn	Sr	W	Y	Zn	Zr
CS001	50	10	N	5	N	150	N	10	N	700
CS002	50	15	N	5	N	150	N	15	N	500
CS003	70	10	N	5	N	200	N	15	N	700
CS004	70	10	N	5	N	200	N	15	N	700
CS005	50	N	N	5	N	200	N	10	N	500
CS006	30	<10	N	<5	N	200	N	<10	N	100
CS007	70	10	N	5	N	200	N	10	N	1000
CS008	30	<10	N	<5	N	200	N	10	N	500
CS009	50	10	N	5	N	300	N	10	N	300
CS010	50	10	N	<5	N	200	N	10	N	200
CS011	70	15	N	<5	N	200	N	10	N	700
CS012	70	50	N	5	N	200	N	10	N	700
CS014	50	20	N	5	N	150	N	10	N	700
CS016	70	<10	N	<5	N	150	N	10	N	1000
EQ001	70	20	N	7	N	300	N	15	N	500
EQ002	100	20	N	5	N	300	N	10	N	300
EQ003	70	15	N	5	N	200	N	30	N	500
EQ004	70	20	N	5	N	200	N	15	N	700
EQ005	70	20	N	5	N	200	N	10	N	500
EQ006	30	10	N	<5	N	200	N	10	N	200
EQ007	50	10	N	<5	N	200	N	10	N	200
EQ008	50	10	N	<5	N	300	N	15	N	200
EQ009	30	10	N	<5	N	150	N	10	N	150
EQ010	50	10	N	<5	N	200	N	<10	N	300
EQ011	70	20	N	<5	N	200	N	10	N	200
EQ012	50	20	N	<5	N	300	N	<10	N	200
EQ013	30	10	N	<5	N	200	N	10	N	300
EQ014	50	15	N	<5	N	300	N	10	N	300
EQ015	50	10	N	<5	N	200	N	10	N	500
EQ017	50	20	N	5	15	200	N	15	N	300
EQ018	50	10	N	<5	N	200	N	10	N	300
EQ020	50	20	N	5	N	200	N	10	N	300
EQ021	50	15	N	<5	N	200	N	10	N	500
EQ022	50	20	N	5	N	200	N	15	N	300
EQ025	50	15	N	5	50	200	N	10	N	500
EQ026	50	15	N	5	N	200	N	10	N	300
EQ027	50	15	N	7	N	200	N	15	N	500
EQ028	70	15	N	7	N	300	N	10	N	700
EQ029	50	20	N	10	N	200	N	10	N	200
EQ030	50	15	N	7	N	200	N	<10	N	200
EQ032	50	15	N	7	N	200	N	15	N	300
EQ033	30	15	N	5	N	200	N	10	N	500
EQ034	70	15	N	7	N	300	N	<10	N	200
EQ035	50	10	N	5	N	200	N	<10	N	500
EQ036	30	20	N	5	N	200	N	10	N	300
EQ037	50	15	N	7	N	200	N	10	N	300
EQ038	50	30	N	10	N	300	N	10	N	500
EQ039	30	20	N	7	N	300	N	10	N	200
EQ040	30	20	N	7	N	200	N	15	N	200
EQ041	50	20	N	7	N	200	N	15	N	300

Table B-13. *Analyses of -0.25 mm sediment samples collected in the geochemical study of the La Joya district, Bolivia*--Continued

Sample no.	Na	P	Ga	Ge	Th	^{2}Au	As	Bi	Cd	Sb
CS001	1	N	10	N	N	<0.15	14	<0.6	0.11	1.9
CS002	1	<0.2	20	N	N	<0.15	18	<0.6	0.086	2.1
CS003	1	N	10	N	N	<0.15	11	<0.6	0.083	1.8
CS004	1	0.2	15	N	N	<0.15	20	<0.6	0.1	1.4
CS005	0.7	N	7	N	N	<0.15	12	<0.6	0.073	1.1
CS006	1	N	7	N	N	<0.15	19	1.9	0.072	7.1
CS007	1	N	10	N	N	<0.15	12	0.64	0.09	1.6
CS008	0.7	N	5	N	N	<0.15	11	<0.6	0.079	1.1
CS009	1	N	15	N	N	<0.15	18	<0.6	0.13	1.4
CS010	1	N	10	N	N	<0.15	16	<0.6	0.1	2
CS011	1	N	10	N	N	<0.15	19	<0.6	0.09	2.2
CS012	1	N	10	N	N	<0.15	16	<0.6	0.14	5.6
CS014	1	N	10	N	N	<0.15	16	<0.6	0.097	3.7
CS016	0.7	N	10	N	N	<0.15	12	1.1	0.092	3.1
EQ001	1.5	N	30	N	N	<0.15	8.7	<0.6	0.069	1.3
EQ002	1.5	<0.2	20	N	N	<0.15	9.1	<0.6	0.095	1.8
EQ003	1	<0.2	20	N	N	<0.15	12	<0.6	0.071	1
EQ004	1.5	<0.2	30	N	N	<0.15	9.9	<0.6	0.069	1.1
EQ005	2	<0.2	20	N	N	<0.15	9.7	<0.6	0.1	1.3
EQ006	1.5	N	20	N	N	<0.15	9.1	<0.6	0.079	0.97
EQ007	1	<0.2	20	N	N	<0.15	7.4	<0.6	0.096	1.5
EQ008	1	N	20	N	N	<0.15	6.1	<0.6	0.062	0.95
EQ009	0.5	N	15	N	N	<0.15	9.5	<0.6	0.11	1.3
EQ010	1	N	15	N	N	<0.15	8.2	<0.6	0.066	1.2
EQ011	1	N	20	N	N	<0.15	11	0.61	0.073	1.4
EQ012	1	N	30	N	N	<0.15	8.6	<0.6	0.073	1.4
EQ013	0.7	N	15	N	N	<0.15	11	<0.6	0.11	1.7
EQ014	1.5	N	20	N	N	<0.15	7.5	0.63	0.074	1.1
EQ015	1	N	15	N	N	<0.15	7.9	<0.6	0.089	1
EQ017	1	N	30	N	N	<0.15	10	0.62	0.13	2.3
EQ018	0.7	N	15	N	N	<0.15	8.6	<0.6	0.092	1.2
EQ020	2	N	50	N	N	<0.15	11	0.63	0.09	1.5
EQ021	1.5	N	30	N	N	<0.15	11	0.8	0.12	2
EQ022	1	N	20	N	N	<0.15	17	0.85	0.13	2.3
EQ025	1	N	30	N	N	<0.15	12	0.67	0.1	1.8
EQ026	1.5	N	30	N	N	<0.15	11	0.65	0.11	1.6
EQ027	1	N	20	N	N	<0.15	11	0.64	0.088	1.4
EQ028	1	N	50	N	N	<0.15	9.3	0.63	0.13	1.6
EQ029	2	N	30	N	N	<0.15	10	0.79	0.19	2.2
EQ030	1	N	50	N	N	<0.15	11	0.69	0.11	1.7
EQ032	1	N	30	N	N	<0.15	11	0.95	0.11	1.6
EQ033	1	N	30	N	N	<0.15	11	0.71	0.11	1.7
EQ034	1	N	30	N	N	<0.15	8	<0.6	0.072	1.1
EQ035	0.7	N	30	N	N	<0.15	9.3	0.67	0.071	1.3
EQ036	1.5	N	15	N	N	<0.15	11	0.67	0.11	1.6
EQ037	1	N	50	N	N	<0.15	8.5	0.62	0.11	1.5
EQ038	1.5	N	30	N	N	<0.15	8.8	<0.6	0.1	1.3
EQ039	1	N	50	N	N	<0.15	6.9	0.61	0.065	1.1
EQ040	1	N	30	N	N	<0.15	8.5	0.63	0.078	1.1
EQ041	1	N	30	N	N	<0.15	9.9	0.74	0.12	1.5

Table B-13. *Analyses of -0.25 mm sediment samples collected in the geochemical study of the La Joya district, Bolivia*--Continued

Sample no.	Zn	Cu	Pb	Ag	Mo
CS001	64	13	16	<0.045	0.45
CS002	45	15	19	<0.045	0.52
CS003	36	12	15	<0.045	0.43
CS004	37	13	15	0.08	0.64
CS005	24	12	11	<0.045	0.37
CS006	20	21	11	0.31	0.35
CS007	30	9.5	13	<0.045	0.43
CS008	26	10	11	<0.045	0.33
CS009	29	11	12	<0.045	0.53
CS010	31	12	15	<0.045	0.42
CS011	35	12	16	<0.045	0.42
CS012	39	13	180	4.7	0.44
CS014	38	15	21	0.2	0.48
CS016	33	10	17	0.11	0.43
EQ001	48	15	11	<0.045	1.1
EQ002	47	12	14	0.16	0.57
EQ003	39	11	9.9	<0.045	0.36
EQ004	38	9.8	12	0.075	0.48
EQ005	38	11	11	<0.045	0.47
EQ006	30	8.7	11	0.068	0.36
EQ007	43	12	11	0.097	0.45
EQ008	31	9.4	8.5	0.063	0.43
EQ009	37	11	12	0.098	0.51
EQ010	27	7.6	9.2	0.058	0.43
EQ011	28	9	13	0.15	0.53
EQ012	39	9.5	12	0.089	0.43
EQ013	38	11	14	0.1	0.54
EQ014	33	8.3	10	<0.045	0.45
EQ015	30	8.6	10	<0.045	0.38
EQ017	47	13	16	0.085	0.52
EQ018	31	9.5	11	<0.045	0.38
EQ020	32	11	14	<0.045	0.63
EQ021	40	12	16	0.078	0.62
EQ022	37	16	18	0.089	0.51
EQ025	34	13	14	0.068	0.46
EQ026	36	13	14	0.06	0.48
EQ027	33	13	13	0.056	0.39
EQ028	49	13	13	0.057	0.48
EQ029	59	15	14	0.074	0.55
EQ030	37	12	14	0.056	0.43
EQ032	38	12	14	0.063	0.5
EQ033	34	9.5	13	0.055	0.46
EQ034	32	8.5	9.9	<0.045	0.42
EQ035	33	9.3	11	<0.045	0.39
EQ036	31	8.8	13	0.047	0.47
EQ037	41	11	12	<0.045	0.46
EQ038	39	10	12	0.048	0.48
EQ039	34	8.4	8.8	<0.045	0.48
EQ040	35	9.4	12	<0.045	0.52
EQ041	38	11	14	0.049	0.48

Table B-13. *Analyses of -0.25 mm sediment samples collected in the geochemical study of the La Joya district, Bolivia*--Continued

Sample no.	Ba	Fe*	Mg*	Ca*	Ti*	Mn	Ag	As	Au	B
EQ042	500	2	0.7	0.7	0.5	200	N	N	N	50
EQ043	500	3	0.7	1	0.7	200	<0.5	N	N	70
EQ044	300	2	0.5	0.7	0.3	200	<0.5	N	N	50
EQ045	500	3	0.7	0.7	0.5	300	N	N	N	70
EQ046	300	1.5	0.5	0.7	0.3	200	N	N	N	50
EQ047	500	3	0.7	1	0.5	200	0.5	N	N	50
EQ048	300	2	0.5	1	0.7	150	N	N	N	50
EQ049	500	2	0.5	1	0.5	150	N	N	N	50
EQ050	300	2	0.5	0.7	0.7	150	N	N	N	30
EQ051	300	2	0.5	1	0.5	150	N	N	N	30
EQ052	200	1.5	0.2	0.5	0.5	100	N	N	N	30
EQ053	500	2	0.7	1	0.5	150	N	N	N	50
EQ054	500	3	0.5	0.3	0.7	100	N	N	N	20
EQ055	300	2	0.2	1	0.5	100	N	N	N	50
EQ056	500	3	0.3	1	0.7	150	<0.5	N	N	30
EQ057	300	2	0.5	0.7	0.5	150	N	N	N	50
EQ058	500	3	0.7	0.7	0.5	150	N	N	N	30
EQ059	300	2	0.3	0.5	0.5	100	N	N	N	50
EQ060	300	2	0.3	0.7	0.5	200	N	N	N	30
EQ061	300	2	0.3	0.7	0.5	150	N	N	N	30
EQ062	300	2	0.2	0.5	0.5	150	N	N	N	50
EQ063	300	2	0.3	0.7	0.5	150	N	N	N	50
LB001	300	2	0.5	0.7	0.5	200	1	N	N	70
LB002	300	1.5	0.3	0.7	0.3	200	0.7	N	N	50
LB003	300	2	0.3	0.5	0.5	1000	1	N	N	70
LB008	300	1.5	0.3	2	0.3	150	2	N	N	70
LJ001	300	2	0.3	0.7	0.5	150	1.5	N	N	100
LJ002	500	3	0.2	0.5	0.7	300	<0.5	N	N	100
LJ003	300	3	0.3	0.5	0.5	500	0.7	N	N	50
LJ004	300	3	0.3	0.5	0.7	200	0.7	N	N	100
LJ005	300	1.5	0.15	0.5	0.5	150	0.5	N	N	70
LJ006	300	2	0.2	0.5	0.5	150	1	N	N	70
LJ007	300	1.5	0.2	0.5	0.5	150	N	N	N	70
LJ008	300	1.5	0.2	0.5	0.5	100	N	N	N	100
LJ009	300	2	0.2	0.7	0.5	150	N	N	N	100
LJ010	300	1.5	0.2	0.3	0.5	150	<0.5	N	N	100
LJ011	300	3	0.3	0.5	0.5	150	20	N	N	500
LJ012	500	1.5	0.2	0.5	0.5	200	<0.5	N	N	100
LL004	300	1.5	0.5	3	0.3	300	1	N	N	70
LL006	300	2	0.3	1.5	0.5	700	1.5	N	N	70
LL009	300	2	0.3	0.7	0.5	500	1	N	N	50

Table B-13. *Analyses of -0.25 mm sediment samples collected in the geochemical study of the La Joya district, Bolivia*--Continued

Sample no.	Ni	Be	Bi	Cd	Co	Cr	Cu	La	Mo	Nb
EQ042	15	1	N	N	10	20	20	50	N	N
EQ043	20	1	N	N	10	20	20	70	N	N
EQ044	15	1	N	N	10	20	20	50	N	N
EQ045	20	1	N	N	15	20	30	50	N	N
EQ046	7	1	N	N	<10	15	20	<50	N	N
EQ047	15	1	N	N	10	15	20	50	N	N
EQ048	15	1	N	N	10	20	15	100	N	N
EQ049	15	1	N	N	10	30	15	70	N	N
EQ050	15	<1	N	N	10	30	15	100	N	N
EQ051	15	<1	N	N	10	20	15	70	N	N
EQ052	10	1	N	N	<10	10	10	50	N	N
EQ053	20	1.5	N	N	10	30	20	70	N	N
EQ054	10	<1	N	N	<10	20	20	70	N	N
EQ055	15	1	N	N	<10	20	20	50	N	N
EQ056	15	<1	N	N	<10	20	20	100	N	N
EQ057	20	1	N	N	10	20	30	70	N	N
EQ058	20	<1	N	N	10	30	20	70	N	N
EQ059	15	<1	N	N	10	20	20	50	N	N
EQ060	15	1	N	N	10	15	20	70	N	N
EQ061	10	1	N	N	10	15	15	70	N	N
EQ062	15	<1	N	N	10	30	15	50	N	N
EQ063	15	1	N	N	10	15	20	50	N	N
LB001	10	1.5	N	N	10	15	30	<50	N	N
LB002	10	1	N	N	<10	15	20	<50	N	N
LB003	10	1.5	N	N	10	20	30	50	N	N
LB008	10	1	N	N	10	15	20	<50	N	N
LJ001	10	1.5	10	N	10	20	30	<50	N	N
LJ002	15	1.5	<10	N	15	30	20	70	N	N
LJ003	15	1.5	N	N	10	20	20	<50	N	N
LJ004	15	1.5	N	N	10	70	30	50	N	N
LJ005	7	1.5	N	N	<10	15	20	<50	N	N
LJ006	7	1.5	N	N	<10	20	50	<50	N	N
LJ007	5	1.5	N	N	<10	20	15	<50	N	N
LJ008	5	1.5	N	N	<10	15	10	50	N	N
LJ009	7	1.5	N	N	<10	20	20	50	N	N
LJ010	7	1.5	N	N	<10	15	15	<50	N	N
LJ011	7	1.5	150	N	<10	20	300	50	N	N
LJ012	10	1.5	N	N	<10	20	50	<50	N	N
LL004	7	1	N	N	<10	15	15	<50	N	N
LL006	15	1	N	N	10	30	20	50	N	N
LL009	10	1	N	N	10	20	15	<50	N	N

Table B-13. *Analyses of -0.25 mm sediment samples collected in the geochemical study of the La Joya district, Bolivia*--Continued

Sample no.	V	Pb	Sb	Sc	Sn	Sr	W	Y	Zn	Zr
EQ042	50	20	N	5	N	200	N	10	N	200
EQ043	50	20	N	10	N	200	N	10	N	300
EQ044	30	20	N	5	N	200	N	15	N	150
EQ045	50	30	N	15	N	200	N	15	N	200
EQ046	30	15	N	7	N	200	N	20	N	500
EQ047	50	20	N	10	N	200	N	10	N	300
EQ048	70	15	N	<5	N	300	N	10	N	200
EQ049	70	10	N	<5	N	200	N	10	N	200
EQ050	70	15	N	5	N	200	N	10	N	300
EQ051	70	15	N	<5	N	200	N	10	N	200
EQ052	50	<10	N	<5	N	150	N	<10	N	500
EQ053	70	20	N	<5	N	200	N	10	N	150
EQ054	70	15	N	<5	N	150	N	<10	N	300
EQ055	70	15	N	<5	N	200	N	10	N	500
EQ056	100	15	N	<5	50	200	N	15	N	500
EQ057	70	20	N	<5	N	200	N	10	N	300
EQ058	100	20	N	5	N	200	N	10	N	200
EQ059	70	15	N	<5	N	150	N	15	N	200
EQ060	70	10	N	<5	N	200	N	10	N	300
EQ061	70	10	N	<5	N	200	N	10	N	700
EQ062	50	10	N	<5	N	200	N	10	N	300
EQ063	70	15	N	<5	N	200	N	10	N	300
LB001	50	50	N	5	N	150	N	10	N	300
LB002	30	30	N	5	N	200	N	10	N	300
LB003	70	200	N	5	N	150	N	20	300	700
LB008	50	70	N	5	N	200	N	20	N	300
LJ001	100	15	N	5	N	150	N	10	N	500
LJ002	70	30	N	5	N	200	N	10	N	1000
LJ003	70	30	N	5	N	200	N	10	N	500
LJ004	70	50	N	5	N	150	N	15	N	200
LJ005	70	20	N	<5	N	150	N	<10	N	300
LJ006	70	20	N	<5	N	200	N	10	N	300
LJ007	70	15	N	<5	N	150	N	<10	N	1000
LJ008	70	15	N	5	N	200	N	10	N	1000
LJ009	70	20	N	5	N	200	N	20	N	300
LJ010	70	15	N	5	N	150	N	10	N	500
LJ011	70	70	N	7	N	150	100	20	N	500
LJ012	70	20	500	5	N	150	N	15	N	500
LL004	50	50	N	5	N	200	N	<10	N	70
LL006	70	200	N	5	N	200	N	10	N	500
LL009	70	100	N	<5	N	150	N	30	N	500

Table B-13. *Analyses of -0.25 mm sediment samples collected in the geochemical study of the La Joya district, Bolivia*--Continued

Sample no.	Na	P	Ga	Ge	Th	Au(2)	As	Bi	Cd	Sb
EQ042	1	N	30	N	N	<0.15	10	<0.6	0.097	1.3
EQ043	1	N	20	N	N	<0.15	11	0.72	0.12	1.5
EQ044	1	N	30	N	N	<0.15	10	0.69	0.12	1.8
EQ045	1	N	30	N	N	<0.15	13	<0.6	0.14	1.7
EQ046	1.5	N	30	N	N	<0.15	11	<0.6	0.14	2
EQ047	1	N	30	N	N	<0.15	13	<0.6	0.14	1.8
EQ048	1	N	20	N	N	<0.15	10	0.81	0.14	1.5
EQ049	1	N	20	N	N	<0.15	9.7	<0.6	0.14	1.3
EQ050	1	N	20	N	N	<0.15	7.3	0.62	0.13	1.1
EQ051	1	N	20	N	N	<0.15	9.7	<0.6	0.13	1.2
EQ052	0.7	N	7	N	N	<0.15	8.2	<0.6	0.1	0.71
EQ053	1.5	N	30	N	N	<0.15	12	<0.6	0.15	1.5
EQ054	1	N	20	N	N	<0.15	13	<0.6	0.085	1.6
EQ055	1	N	20	N	N	<0.15	15	0.62	0.086	1.6
EQ056	1	N	20	N	N	<0.15	13	0.98	0.08	1.4
EQ057	1	N	20	N	N	<0.15	12	0.7	0.15	1.8
EQ058	1.5	N	30	N	N	<0.15	12	<0.6	0.11	1.7
EQ059	1	N	20	N	N	<0.15	12	0.66	0.11	1.5
EQ060	0.7	N	15	N	N	<0.15	12	<0.6	0.14	0.91
EQ061	1	N	15	N	N	<0.15	9.6	<0.6	0.11	0.98
EQ062	1	N	10	N	N	<0.15	11	<0.6	0.095	0.92
EQ063	1	N	15	N	N	<0.15	13	<0.6	0.12	1.3
LB001	1	N	20	N	N	<0.15	24	0.71	0.21	4.7
LB002	1	N	15	N	N	<0.15	24	<0.6	0.2	5.6
LB003	1	N	20	N	N	<0.15	38	0.68	1.8	9.7
LB008	1	<0.2	15	N	N	<0.15	36	<0.6	0.28	7.6
LJ001	0.7	N	15	N	N	<0.15	28	11	0.077	18
LJ002	0.7	N	15	N	N	<0.15	36	3	0.22	12
LJ003	1	N	20	N	N	<0.15	18	1.3	0.12	4.1
LJ004	1	<0.2	20	N	N	<0.15	34	1.8	0.12	6.1
LJ005	0.7	<0.2	15	N	N	<0.15	19	0.98	0.096	2.7
LJ006	1	N	20	N	N	<0.15	19	0.94	0.1	2
LJ007	0.7	N	10	N	N	<0.15	21	<0.6	0.083	2.6
LJ008	0.7	N	15	N	N	<0.15	24	0.66	0.065	2.2
LJ009	1	N	15	N	N	<0.15	24	0.84	0.055	2.8
LJ010	0.7	N	15	N	N	<0.15	25	0.81	0.054	3.6
LJ011	0.7	<0.2	15	N	N	2.5	190	93	0.073	310
LJ012	0.7	<0.2	15	N	N	<0.15	31	2	0.21	9.3
LL004	1	N	15	N	N	<0.15	77	1.1	0.37	7.7
LL006	1	N	15	N	N	<0.15	110	1.3	1.4	12
LL009	1	N	10	N	N	<0.15	32	<0.6	0.51	5.7

Table B-13. *Analyses of -0.25 mm sediment samples collected in the geochemical study of the La Joya district, Bolivia*--Continued

Sample no.	Zn	Cu	Pb	Ag	Mo
EQ042	36	10	13	0.046	0.45
EQ043	44	13	14	0.059	0.49
EQ044	37	12	15	0.11	0.67
EQ045	40	15	17	0.14	0.66
EQ046	38	12	16	0.12	0.67
EQ047	42	14	15	0.11	0.65
EQ048	47	11	12	0.094	0.59
EQ049	51	11	12	0.06	0.66
EQ050	47	9.7	11	0.046	0.51
EQ051	41	10	12	0.072	0.55
EQ052	31	8.3	10	0.052	0.46
EQ053	55	19	24	0.094	0.81
EQ054	29	13	17	0.068	1
EQ055	30	12	16	0.077	0.68
EQ056	30	13	17	0.068	0.83
EQ057	45	15	20	0.13	0.76
EQ058	39	12	16	0.095	0.64
EQ059	37	13	16	0.087	0.63
EQ060	34	11	15	<0.045	0.63
EQ061	37	10	14	0.046	0.48
EQ062	29	10	13	<0.045	0.46
EQ063	37	13	15	0.065	0.57
LB001	47	14	69	0.33	0.44
LB002	49	12	63	0.28	0.51
LB003	300	23	240	0.47	1.1
LB008	76	15	83	0.43	1
LJ001	24	24	17	1.6	0.4
LJ002	69	20	28	0.28	0.71
LJ003	54	16	30	0.19	0.54
LJ004	39	22	37	0.26	0.57
LJ005	33	24	26	0.11	0.8
LJ006	31	33	18	<0.045	0.61
LJ007	29	13	14	<0.045	0.54
LJ008	21	9.4	11	<0.045	0.44
LJ009	23	13	15	0.1	0.43
LJ010	24	12	14	0.048	0.42
LJ011	24	180	120	39	0.43
LJ012	40	63	23	0.19	0.43
LL004	65	16	90	0.5	0.69
LL006	210	23	330	0.91	0.73
LL009	140	12	130	0.39	0.48

Table B-14. *Analyses of +0.25 mm sediment samples collected in the geochemical study of the La Joya district, Bolivia*

[First 35 elements (Ba through Th) analyzed by DC-ARC AES. Elements with asterisks (*) are reported in percent; all other elements are reported in ppm. [2]Au, As, Bi, Cd, Sb, Zn, Cu, Pb, Ag, and Mo analyzed by peroxide dissolution ICP-AES. N, the element was present below the lower limit of determination]

Sample no.	Ba	Fe*	Mg*	Ca*	Ti*	Mn	Ag	As	Au	B
CS001	300	3	0.5	0.5	0.3	700	N	N	N	70
CS002	500	3	0.5	0.7	0.7	300	N	N	N	50
CS003	300	3	0.5	0.5	0.5	300	N	N	N	50
CS004	300	5	0.5	1.5	0.5	500	N	N	N	70
CS005	300	1	0.2	1.5	0.7	150	N	N	N	30
CS006	300	1	0.15	1	0.2	100	0.7	N	N	50
CS007	300	1	0.2	1	0.2	150	N	N	N	30
CS008	300	1.5	0.5	1.5	0.2	200	N	N	N	50
CS009	300	1	0.2	1.5	0.3	150	1.5	N	N	30
CS010	300	3	0.3	1	0.2	500	N	N	N	70
CS011	300	2	0.5	1	0.5	300	N	N	N	50
CS012	300	3	0.3	0.7	0.7	700	20	N	N	70
CS014	300	3	0.2	0.5	0.7	500	0.5	N	N	70
CS015	300	3	0.5	0.3	0.7	500	N	N	N	70
CS016	300	3	0.3	0.5	0.7	1500	N	N	N	50
EQ001	500	3	1	1.5	0.7	150	N	N	N	10
EQ002	500	2	0.7	1.5	0.5	100	N	N	N	20
EQ003	500	3	1	1	0.7	200	N	N	N	30
EQ004	300	2	0.5	1.5	0.5	100	0.7	N	N	20
EQ005	300	1.5	0.5	1	0.3	100	N	N	N	30
EQ006	300	3	0.7	1	0.5	100	N	N	N	20
EQ007	500	2	0.7	1	0.5	150	N	N	N	30
EQ008	500	2	0.5	1	0.5	150	N	N	N	30
EQ009	500	3	1	1	0.7	200	N	N	N	30
EQ010	300	2	0.5	0.7	0.5	150	N	N	N	20
EQ011	500	2	0.5	0.7	0.5	100	N	N	N	30
EQ012	700	2	0.5	1	0.5	150	N	N	N	30
EQ013	500	3	0.7	1	0.5	150	N	N	N	50
EQ014	700	3	0.7	1	0.7	150	N	N	N	30
EQ015	500	2	0.5	1	0.5	150	N	N	N	30
EQ016	500	3	0.7	1	0.7	200	N	N	N	50
EQ017	500	2	0.7	1	0.5	150	N	N	N	50
EQ018	300	2	0.7	1	0.5	200	N	N	N	50
EQ021	500	3	0.7	0.7	0.5	150	N	N	N	50
EQ022	300	2	0.5	0.7	0.5	200	N	N	N	70
EQ023	300	2	0.7	1	0.5	150	N	N	N	50
EQ025	300	2	0.7	1	0.5	150	N	N	N	30
EQ027	300	3	0.7	1	0.5	150	N	N	N	50
EQ028	700	3	0.7	1.5	0.5	200	N	N	N	30
EQ029	1000	2	0.7	1	0.7	200	N	N	N	30
EQ030	500	3	1	1	0.7	200	N	N	N	20
EQ032	500	3	0.7	0.7	0.7	200	N	N	N	30
EQ033	500	3	0.7	1	0.5	150	N	N	N	30
EQ034	700	3	0.7	1.5	0.5	500	N	N	N	20
EQ035	500	3	1	0.7	0.5	200	N	N	N	20
EQ036	500	3	0.7	0.7	0.5	150	N	N	N	30
EQ037	500	3	1	1	0.5	200	N	N	N	30
EQ038	500	3	1	1	0.5	150	N	N	N	20
EQ039	500	3	0.7	1	0.5	100	N	N	N	20
EQ040	500	3	1	1	0.5	200	N	N	N	50

Table B-14. *Analyses of +0.25 mm sediment samples collected in the geochemical study of the La Joya district, Bolivia*--Continued

Sample no.	Ni	Be	Bi	Cd	Co	Cr	Cu	La	Mo	Nb
CS001	50	1.5	N	N	20	50	<50	<50	N	N
CS002	50	1.5	N	N	15	50	20	50	N	N
CS003	50	1	N	N	15	30	30	50	N	N
CS004	50	1	N	N	20	30	30	50	N	N
CS005	10	1	N	N	<10	15	<50	<50	N	N
CS006	10	1	N	N	<10	10	<50	<50	N	N
CS007	10	1	N	N	10	15	10	<50	N	N
CS008	15	1	N	N	10	15	<50	<50	N	N
CS009	7	1	N	N	<10	10	<50	<50	N	N
CS010	30	1	N	N	15	30	<50	<50	N	N
CS011	20	1	N	N	10	20	<50	<50	N	N
CS012	50	1.5	N	N	20	30	<50	<50	N	N
CS014	30	1.5	N	N	15	30	<50	<50	N	N
CS015	70	1.5	N	N	15	30	<50	<50	N	N
CS016	50	1.5	N	N	20	30	20	50	N	N
EQ001	50	<1	N	N	15	70	15	500	N	N
EQ002	20	1	N	N	15	50	15	70	N	N
EQ003	20	<1	N	N	20	70	20	70	N	N
EQ004	15	1	N	N	10	20	10	100	N	N
EQ005	10	1	N	N	<10	20	<50	<50	N	N
EQ006	10	1	N	N	10	30	20	70	N	N
EQ007	15	1	N	N	10	20	15	70	N	N
EQ008	15	1	N	N	10	20	15	50	N	N
EQ009	20	<1	N	N	10	30	20	70	N	N
EQ010	15	1	N	N	10	20	<50	<50	N	N
EQ011	10	1	N	N	10	30	20	70	N	N
EQ012	15	1	N	N	10	20	15	70	N	N
EQ013	30	1	N	N	15	20	15	100	N	N
EQ014	20	<1	N	N	15	50	15	150	N	N
EQ015	15	1	N	N	10	20	15	70	N	N
EQ016	20	1	N	N	10	20	15	70	N	N
EQ017	20	1	N	N	10	30	15	100	N	N
EQ018	30	1	N	N	15	20	15	70	N	N
EQ021	20	1	N	N	15	30	20	70	N	N
EQ022	30	1	N	N	15	30	20	70	N	N
EQ023	30	1	N	N	15	50	20	50	N	N
EQ025	30	1	N	N	15	50	20	70	N	N
EQ027	50	1	N	N	15	70	30	70	N	N
EQ028	20	<1	N	N	15	50	20	150	N	N
EQ029	20	<1	N	N	10	30	30	50	N	N
EQ030	20	1	N	N	10	70	20	70	N	N
EQ032	15	1	N	N	10	30	15	50	N	N
EQ033	15	1	N	N	10	30	15	50	N	N
EQ034	50	1	N	N	15	70	30	50	N	150
EQ035	20	1	N	N	10	50	15	50	N	N
EQ036	15	1	N	N	10	50	20	70	N	N
EQ037	15	1	N	N	10	50	20	70	N	N
EQ038	15	1	N	N	15	50	20	50	N	N
EQ039	15	1	N	N	10	30	15	50	N	N
EQ040	20	1	N	N	15	30	30	50	N	<20

Table B-14. *Analyses of +0.25 mm sediment samples collected in the geochemical study of the La Joya district, Bolivia--Continued*

Sample no.	V	Pb	Sb	Sc	Sn	Sr	W	Y	Zn	Zr
CS001	70	30	N	10	N	150	N	20	N	200
CS002	70	20	N	7	N	100	N	20	N	300
CS003	50	20	N	7	N	100	N	20	N	150
CS004	70	20	N	7	N	150	N	20	N	300
CS005	20	15	N	<5	N	300	N	<10	N	100
CS006	20	10	N	N	N	300	N	<10	N	70
CS007	30	10	N	<5	N	200	N	<10	N	100
CS008	50	15	N	<5	N	300	N	<10	N	200
CS009	20	10	N	<5	N	200	N	<10	N	70
CS010	70	15	N	5	N	200	N	10	N	200
CS011	50	15	N	5	N	200	N	10	N	100
CS012	70	500	N	7	N	150	N	20	N	200
CS014	70	20	N	7	N	100	N	15	N	300
CS015	70	30	N	7	N	100	N	20	N	300
CS016	70	20	N	5	N	100	N	20	N	200
EQ001	70	10	N	7	N	500	N	20	N	100
EQ002	50	15	N	<5	N	500	N	<10	N	100
EQ003	70	15	N	<5	N	200	N	10	N	100
EQ004	50	<10	N	<5	N	500	N	<10	N	70
EQ005	50	10	N	<5	N	200	N	<10	N	100
EQ006	50	15	N	<5	N	200	N	<10	N	100
EQ007	50	20	N	<5	N	300	N	10	N	100
EQ008	50	20	N	<5	N	500	N	10	N	150
EQ009	100	30	N	5	N	500	N	10	N	150
EQ010	70	15	N	<5	N	300	N	<10	N	200
EQ011	70	20	N	<5	N	300	N	<10	N	100
EQ012	70	20	N	<5	N	500	N	<10	N	100
EQ013	70	20	N	5	N	300	N	10	N	100
EQ014	70	20	N	5	N	500	N	10	N	70
EQ015	70	20	N	<5	N	300	N	<10	N	100
EQ016	70	20	N	5	N	300	N	10	N	100
EQ017	50	20	N	5	N	300	N	15	N	100
EQ018	70	20	N	5	N	300	N	10	N	150
EQ021	70	20	N	5	N	300	N	10	N	150
EQ022	70	20	N	5	N	200	N	15	N	200
EQ023	70	20	N	5	N	300	N	10	N	200
EQ025	70	15	N	5	N	300	N	10	N	200
EQ027	70	20	N	5	N	300	N	10	N	150
EQ028	70	20	N	5	N	300	N	10	N	100
EQ029	70	15	N	<5	N	300	N	10	N	300
EQ030	70	20	N	<5	N	300	N	10	N	150
EQ032	70	20	N	<5	N	200	N	10	N	150
EQ033	70	20	N	<5	N	200	N	10	N	300
EQ034	70	30	N	<5	15	300	30	15	N	300
EQ035	100	10	N	<5	N	300	N	<10	N	100
EQ036	70	20	N	<5	N	200	N	10	N	200
EQ037	50	20	N	<5	N	300	N	<10	N	100
EQ038	70	15	N	<5	N	200	N	<10	N	70
EQ039	70	15	N	<5	N	300	N	<10	N	100
EQ040	70	20	N	<5	N	200	N	15	N	150

Table B-14. *Analyses of +0.25 mm sediment samples collected in the geochemical study of the La Joya district, Bolivia*--Continued

Sample no.	Na	P	Ga	Ge	Th	[2]Au	As	Bi	Cd	Sb
CS001	0.7	N	30	N	N	<0.15	37	<0.6	0.25	6.2
CS002	0.5	N	30	N	N	<0.15	32	0.64	0.15	2.2
CS003	1	N	30	N	N	<0.15	22	<0.6	0.18	2.2
CS004	0.7	N	30	N	N	--	--	--	--	--
CS005	1	N	15	N	N	<0.15	14	<0.6	0.084	0.61
CS006	1	N	10	N	N	<0.15	21	1.8	0.085	5.9
CS007	1	N	15	N	N	<0.15	13	<0.6	0.071	0.74
CS008	1.5	N	20	N	N	<0.15	17	<0.6	0.12	0.84
CS009	1	N	10	N	N	<0.15	16	<0.6	0.095	<0.60
CS010	1	N	20	N	N	<0.15	31	<0.6	0.15	2.5
CS011	1	N	20	N	N	<0.15	31	<0.6	0.13	2.4
CS012	0.7	N	20	N	N	<0.15	44	1.2	0.45	28
CS014	1	N	30	N	N	<0.15	25	<0.6	0.18	6.8
CS015	0.5	N	20	N	N	<0.15	36	<0.6	0.21	15
CS016	0.7	N	20	N	N	<0.15	36	3.3	0.31	12
EQ001	2	N	20	N	N	<0.15	4.3	<0.6	0.058	<0.60
EQ002	1.5	N	20	N	N	<0.15	4.1	<0.6	0.07	0.72
EQ003	1.5	N	30	N	N	<0.15	19	<0.6	0.098	<0.60
EQ004	1.5	N	15	N	N	<0.15	8.7	<0.6	0.059	0.64
EQ005	1.5	N	20	N	N	<0.15	6.6	<0.6	0.054	<0.60
EQ006	2	N	30	N	N	<0.15	8	<0.6	0.073	0.84
EQ007	1.5	N	50	N	N	<0.15	4.4	<0.6	0.063	0.7
EQ008	1.5	N	30	N	N	<0.15	5	<0.6	0.052	0.62
EQ009	1.5	N	50	N	N	<0.15	5.6	<0.6	0.072	0.61
EQ010	1	N	20	N	N	<0.15	9	<0.6	0.065	1.3
EQ011	1.5	N	30	N	N	<0.15	13	<0.6	0.07	0.94
EQ012	1.5	N	30	N	N	<0.15	6.8	<0.6	0.063	1.1
EQ013	2	N	30	N	N	<0.15	8.8	<0.6	0.095	1.5
EQ014	2	N	50	N	N	<0.15	5.4	<0.6	0.058	0.63
EQ015	1.5	N	30	N	N	<0.15	7	<0.6	0.074	0.65
EQ016	1.5	N	20	N	N	<0.15	7.5	<0.6	0.08	1.4
EQ017	2	N	30	N	N	<0.15	8.7	<0.6	0.1	1.8
EQ018	1.5	N	20	N	N	<0.15	8.9	<0.6	0.1	1.1
EQ021	2	N	30	N	N	<0.15	9.7	0.73	0.14	1.7
EQ022	1.5	N	30	N	N	<0.15	0.65	<0.6	<0.03	<0.60
EQ023	1.5	N	30	N	N	<0.15	11	<0.6	0.071	0.74
EQ025	1	N	15	N	N	<0.15	11	<0.6	0.067	<0.60
EQ027	2	N	30	N	N	<0.15	12	<0.6	0.066	<0.60
EQ028	2	N	30	N	N	<0.15	5.9	<0.6	0.069	<0.60
EQ029	2	N	20	N	N	--	--	--	--	--
EQ030	2	N	50	N	N	<0.15	7.7	<0.6	0.06	<0.60
EQ032	1.5	N	30	N	N	<0.15	8.5	<0.6	0.053	<0.60
EQ033	2	N	30	N	N	<0.15	8.4	<0.6	0.059	<0.60
EQ034	2	N	50	N	N	--	--	--	--	--
EQ035	1.5	N	20	N	N	<0.15	6.6	<0.6	<0.03	<0.60
EQ036	2	N	30	N	N	<0.15	9.3	<0.6	0.067	<0.60
EQ037	2	N	50	N	N	<0.15	5.7	<0.6	0.055	<0.60
EQ038	2	N	30	N	N	<0.15	4.4	<0.6	<0.03	<0.60
EQ039	2	N	30	N	N	<0.15	4.3	<0.6	<0.03	<0.60
EQ040	1.5	N	30	N	N	<0.15	<0.6	<0.6	<0.03	<0.60

Table B-14. *Analyses of +0.25 mm sediment samples collected in the geochemical study of the La Joya district, Bolivia*--Continued

Sample no.	Zn	Cu	Pb	Ag	Mo
CS001	72	28	33	<0.045	0.67
CS002	80	27	28	<0.045	0.72
CS003	67	25	26	<0.045	0.64
CS004	--	--	--	--	--
CS005	21	9.4	10	<0.045	0.49
CS006	21	18	11	0.28	0.45
CS007	20	8.7	9.5	<0.045	0.41
CS008	29	14	14	<0.045	0.55
CS009	23	10	9.2	<0.045	0.54
CS010	51	20	22	<0.045	0.54
CS011	43	18	20	<0.045	0.52
CS012	85	26	1300	16	0.62
CS014	59	25	30	0.059	0.7
CS015	88	31	35	<0.045	0.7
CS016	73	27	46	0.3	0.83
EQ001	54	16	6.7	<0.045	1.5
EQ002	59	12	9.4	<0.045	0.46
EQ003	84	16	12	<0.045	0.48
EQ004	56	12	9	<0.045	0.55
EQ005	45	12	8.5	<0.045	0.48
EQ006	52	14	11	<0.045	0.63
EQ007	46	10	7.1	<0.045	0.41
EQ008	36	10	7.8	<0.045	0.45
EQ009	44	11	8.2	0.047	0.65
EQ010	37	9.7	12	<0.045	0.56
EQ011	34	12	16	0.072	0.72
EQ012	54	10	12	<0.045	0.38
EQ013	50	11	13	0.06	0.67
EQ014	53	9.1	8.3	0.11	0.59
EQ015	43	9.8	11	<0.045	0.4
EQ016	50	12	13	0.082	0.36
EQ017	52	13	14	0.084	0.52
EQ018	47	11	13	0.057	0.47
EQ021	48	14	16	0.089	0.71
EQ022	21	9.7	7.7	<0.045	<0.09
EQ023	38	17	15	<0.045	0.4
EQ025	41	19	14	<0.045	0.51
EQ027	46	22	16	<0.045	0.57
EQ028	65	13	9.9	<0.045	0.52
EQ029	--	--	--	--	--
EQ030	50	15	12	<0.045	0.52
EQ032	49	14	12	<0.045	0.61
EQ033	40	11	11	<0.045	0.58
EQ034	--	--	--	--	--
EQ035	46	11	9	<0.045	0.46
EQ036	40	12	12	<0.045	0.6
EQ037	52	13	10	<0.045	0.51
EQ038	57	13	9.2	<0.045	0.57
EQ039	45	10	7.4	<0.045	0.53
EQ040	0.39	<0.03	<0.6	<0.045	<0.09

Table B-14. *Analyses of +0.25 mm sediment samples collected in the geochemical study of the La Joya district, Bolivia--Continued*

Sample no.	Ba	Fe*	Mg*	Ca*	Ti*	Mn	Ag	As	Au	B
EQ041	500	3	0.7	0.7	0.5	150	N	N	N	30
EQ042	500	3	0.5	0.7	0.5	200	N	N	N	50
EQ043	500	3	0.7	1	0.5	200	N	N	N	30
EQ044	500	3	0.5	0.5	0.5	150	N	N	N	50
EQ045	300	3	0.5	0.5	0.5	150	N	N	N	50
EQ046	300	3	0.3	0.5	0.5	150	N	N	N	50
EQ047	300	3	0.7	1	0.5	150	N	N	N	30
EQ048	300	3	0.7	1.5	0.5	200	N	N	N	30
EQ049	300	3	1	1.5	0.7	150	N	N	N	30
EQ050	300	3	1	1.5	0.5	200	N	N	N	30
EQ051	300	3	0.7	1	0.5	200	N	N	N	30
EQ052	300	2	0.7	1.5	0.3	150	N	N	N	20
EQ053	300	3	1	1	0.5	200	N	N	N	50
EQ054	300	2	0.3	0.3	0.5	100	N	N	N	20
EQ055	300	2	0.3	0.3	0.5	100	N	N	N	30
EQ056	500	2	0.5	0.3	0.7	150	N	N	N	20
EQ057	300	2	0.7	0.7	0.5	150	N	N	N	50
EQ058	300	2	0.5	0.7	0.5	150	N	N	N	50
EQ059	300	3	0.5	0.7	0.5	150	N	N	N	50
EQ060	500	2	0.5	1	0.5	300	N	N	N	30
EQ061	500	2	0.7	1	0.5	200	<0.5	N	N	30
EQ062	200	2	0.3	0.7	0.3	200	N	N	N	50
EQ063	300	2	0.5	1	0.5	300	N	N	N	70
LB001	500	3	0.2	1	0.3	200	1	N	N	30
LB002	300	2	0.5	1	0.3	200	<0.5	N	N	50
LB003	500	5	0.3	0.7	0.3	2000	1.5	N	N	50
LB008	500	2	0.7	2	0.5	200	1	N	N	70
LJ001	700	3	0.5	0.7	0.7	300	3	N	N	500
LJ002	500	5	0.3	0.3	0.5	500	1.5	N	N	200
LJ003	300	3	0.5	0.7	0.3	500	1	N	N	70
LJ004	700	5	0.7	0.7	0.7	500	1.5	N	N	200
LJ005	300	2	0.2	0.5	0.5	200	0.7	N	N	150
LJ006	700	2	0.2	0.2	0.5	100	0.5	N	N	100
LJ007	500	3	0.5	0.5	0.5	150	<0.5	N	N	200
LJ008	500	3	0.3	0.3	0.5	100	0.5	N	N	200
LJ009	300	3	0.3	0.3	0.5	150	1	N	N	150
LJ010	300	3	0.5	0.2	0.5	200	N	N	N	150
LJ011	200	3	0.2	0.15	0.5	100	50	200	N	2000
LJ012	700	3	0.3	0.2	0.7	300	1	N	N	100
LL004	500	2	0.5	5	0.7	500	1	N	N	50
LL006	300	3	0.5	3	0.2	1000	2	N	N	50
LL009	500	2	0.5	0.7	0.3	700	1.5	N	N	30

Table B-14. *Analyses of +0.25 mm sediment samples collected in the geochemical study of the La Joya district, Bolivia*--Continued

Sample no.	Ni	Be	Bi	Cd	Co	Cr	Cu	La	Mo	Nb
EQ041	10	1	N	N	10	30	10	50	N	N
EQ042	15	1	N	N	10	20	15	70	N	N
EQ043	15	<1	N	N	10	30	10	50	N	N
EQ044	15	1	N	N	10	30	20	70	N	N
EQ045	20	1	N	N	10	20	<50	<50	N	N
EQ046	15	<1	N	N	<10	20	<50	<50	N	N
EQ047	15	<1	N	N	10	30	30	100	N	N
EQ048	20	1	N	N	15	30	20	70	N	N
EQ049	20	1	N	N	15	50	20	70	N	N
EQ050	20	1	N	N	15	50	50	150	N	N
EQ051	20	<1	N	N	10	30	15	70	N	N
EQ052	20	<1	N	N	10	20	10	50	N	N
EQ053	50	1	N	N	15	50	50	50	N	N
EQ054	10	<1	N	N	<10	20	20	70	N	N
EQ055	15	1	N	N	10	30	30	50	N	N
EQ056	10	1	N	N	10	30	20	50	N	N
EQ057	30	1.5	N	N	15	20	20	70	N	N
EQ058	30	1	N	N	15	30	20	50	N	N
EQ059	20	1	N	N	15	30	20	50	N	N
EQ060	20	1	N	N	20	20	15	50	N	N
EQ061	15	1	N	N	15	30	15	70	N	N
EQ062	20	1	N	N	10	15	15	70	N	N
EQ063	20	1.5	N	N	20	20	<50	<50	N	N
LB001	10	<1	N	N	N	10	<50	<50	N	N
LB002	10	1	N	N	<10	10	<50	<50	N	N
LB003	15	1.5	N	N	15	20	30	70	N	N
LB008	10	1	N	N	<10	15	<50	<50	N	N
LJ001	15	1	30	N	10	50	100	70	N	N
LJ002	70	1.5	10	N	15	70	70	70	N	N
LJ003	20	1	N	N	10	30	30	50	N	N
LJ004	20	1	<10	N	10	70	70	50	N	N
LJ005	7	1	N	N	N	50	<50	<50	N	N
LJ006	10	1.5	N	N	<10	50	150	50	N	N
LJ007	10	1.5	N	N	10	30	50	70	N	N
LJ008	5	1	<10	N	<10	70	50	100	N	N
LJ009	7	1	<10	N	<10	30	50	50	N	N
LJ010	10	1	N	N	10	30	50	50	N	N
LJ011	5	1	150	N	N	30	500	70	N	N
LJ012	50	1.5	N	N	20	30	300	50	N	N
LL004	15	<1	N	N	<10	20	<50	<50	N	N
LL006	15	1	N	N	10	30	30	50	N	N
LL009	10	1	N	N	<10	20	<50	<50	N	N

Table B-14. *Analyses of +0.25 mm sediment samples collected in the geochemical study of the La Joya district, Bolivia--Continued*

Sample no.	V	Pb	Sb	Sc	Sn	Sr	W	Y	Zn	Zr
EQ041	70	15	N	<5	N	200	N	<10	N	150
EQ042	70	30	N	<5	N	200	N	10	N	150
EQ043	70	20	N	5	N	300	N	10	N	100
EQ044	70	20	N	<5	N	200	N	15	N	300
EQ045	70	20	N	<5	<10	150	N	10	N	200
EQ046	70	30	N	<5	N	150	N	15	N	300
EQ047	70	20	N	<5	N	300	N	15	N	200
EQ048	70	20	N	5	N	300	N	10	N	100
EQ049	70	30	N	5	N	300	N	15	N	200
EQ050	70	100	N	<5	150	300	N	10	N	150
EQ051	70	20	N	<5	N	300	N	10	N	200
EQ052	50	20	N	<5	N	300	N	10	N	100
EQ053	70	30	N	<5	N	300	N	10	N	100
EQ054	70	15	N	<5	N	200	N	<10	N	200
EQ055	70	20	N	<5	N	300	N	<10	N	200
EQ056	70	20	N	<5	N	300	N	<10	N	100
EQ057	70	20	N	<5	N	300	N	10	N	200
EQ058	70	30	N	<5	N	300	N	10	N	500
EQ059	70	15	N	<5	N	300	N	10	N	300
EQ060	70	15	N	<5	N	500	N	<10	N	100
EQ061	70	20	N	<5	N	500	N	10	N	100
EQ062	50	15	N	<5	N	300	N	10	N	150
EQ063	70	20	N	<5	N	500	N	10	N	150
LB001	30	100	N	<5	N	300	N	<10	N	50
LB002	50	50	N	5	N	300	N	10	N	300
LB003	70	500	N	7	N	200	N	10	500	100
LB008	50	150	N	5	N	300	N	10	N	100
LJ001	70	50	N	7	N	200	N	20	N	200
LJ002	70	100	N	5	N	200	N	10	<200	150
LJ003	70	50	N	<5	N	200	N	<10	N	50
LJ004	100	150	N	7	N	200	N	15	N	100
LJ005	70	70	N	<5	N	200	N	10	N	100
LJ006	70	30	N	5	N	200	N	10	N	100
LJ007	70	50	N	5	N	300	N	10	N	150
LJ008	50	70	N	5	N	300	N	10	N	200
LJ009	70	50	N	5	N	200	N	20	N	300
LJ010	70	20	N	5	N	150	N	20	N	300
LJ011	70	200	700	5	15	100	100	30	N	150
LJ012	70	30	N	7	N	100	N	20	N	500
LL004	30	100	N	<5	N	500	N	10	N	70
LL006	50	700	N	5	N	200	N	10	300	100
LL009	50	150	N	<5	N	300	N	10	300	100

Table B-14. *Analyses of +0.25 mm sediment samples collected in the geochemical study of the La Joya district, Bolivia*--Continued

Sample no.	Na	P	Ga	Ge	Th	^{2}Au	As	Bi	Cd	Sb
EQ041	1.5	N	30	N	N	<0.15	6.7	<0.6	0.065	<0.60
EQ042	1.5	N	30	N	N	<0.15	7.3	<0.6	0.049	<0.60
EQ043	1.5	N	30	N	N	<0.15	7.2	<0.6	0.043	<0.60
EQ044	1.5	N	30	N	N	<0.15	12	<0.6	0.11	1.6
EQ045	1	N	20	N	N	<0.15	15	<0.6	0.14	1.2
EQ046	1	N	30	N	N	<0.15	12	<0.6	0.097	1.2
EQ047	1.5	N	30	N	N	--	--	--	--	--
EQ048	1	N	20	N	N	--	--	--	--	--
EQ049	2	N	50	N	N	--	--	--	--	--
EQ050	2	N	50	N	N	--	--	--	--	--
EQ051	1.5	N	30	N	N	<1.5	<6	<6.0	<0.3	<6.0
EQ052	1.5	N	50	N	N	<1.5	<6	<6.0	<0.3	<6.0
EQ053	1	N	50	N	N	<1.5	<6	<6.0	<0.3	<6.0
EQ054	0.7	N	30	N	N	<1.5	<6	<6.0	<0.3	<6.0
EQ055	1.5	N	30	N	N	<1.5	18	<6.0	<0.3	<6.0
EQ056	1	N	30	N	N	<1.5	<6	9.1	<0.3	<6.0
EQ057	1.5	N	50	N	N	<1.5	<6	<6.0	<0.3	<6.0
EQ058	1.5	N	30	N	N	<1.5	<6	<6.0	<0.3	<6.0
EQ059	1.5	N	30	N	N	<1.5	6.5	<6.0	<0.3	<6.0
EQ060	1.5	N	30	N	N	<1.5	<6	<6.0	<0.3	<6.0
EQ061	1.5	N	50	N	N	<1.5	<6	<6.0	<0.3	<6.0
EQ062	1	N	20	N	N	<1.5	<6	<6.0	<0.3	<6.0
EQ063	1.5	N	30	N	N	<1.5	6.9	<6.0	<0.3	<6.0
LB001	1	N	20	N	N	<0.15	41	0.69	0.3	6.1
LB002	0.7	N	10	N	N	<0.15	36	<0.6	0.3	8.5
LB003	1.5	N	50	N	N	<0.15	74	0.84	4.5	20
LB008	1	N	20	N	N	<0.15	72	1.3	0.47	15
LJ001	0.7	N	30	N	N	<0.15	85	19	0.19	35
LJ002	1	N	20	N	N	<0.15	100	6.3	0.77	20
LJ003	1	N	15	N	N	<0.15	29	2.1	0.21	5.2
LJ004	1.5	N	50	N	N	<0.15	69	3.1	0.28	15
LJ005	1	N	30	N	N	<0.15	47	2.2	0.2	5.2
LJ006	2	N	30	N	N	<0.15	41	2.1	0.22	1.9
LJ007	1	N	30	N	N	<0.15	61	1.6	0.15	5.1
LJ008	1.5	N	30	N	N	<0.15	83	2.3	0.13	6.4
LJ009	0.7	N	20	N	N	<0.15	88	2.9	0.12	8.3
LJ010	0.7	N	15	N	N	<0.15	51	1.7	0.079	7.8
LJ011	0.5	N	30	N	N	2	570	190	0.12	650
LJ012	0.5	N	20	N	N	<0.15	76	3.3	0.46	21
LL004	1	N	20	N	N	<0.15	120	<0.6	0.57	9.2
LL006	1.5	N	50	N	N	<0.15	220	0.95	2.8	19
LL009	1	N	20	N	N	<0.15	66	<0.6	1.2	10

Table B-14. *Analyses of +0.25 mm sediment samples collected in the geochemical study of the La Joya district, Bolivia*--Continued

Sample no.	Zn	Cu	Pb	Ag	Mo
EQ041	43	13	11	<0.045	0.55
EQ042	40	12	11	<0.045	0.52
EQ043	49	13	10	<0.045	0.56
EQ044	48	19	19	<0.045	0.79
EQ045	51	22	21	<0.045	0.66
EQ046	41	16	18	<0.045	0.69
EQ047	--	--	--	--	--
EQ048	--	--	--	--	--
EQ049	--	--	--	--	--
EQ050	--	--	--	--	--
EQ051	72	13	16	<0.45	1.4
EQ052	57	9.1	11	<0.45	1.5
EQ053	68	22	23	<0.45	1.9
EQ054	30	13	17	<0.45	2.1
EQ055	40	16	31	<0.45	1.7
EQ056	34	14	17	1.2	1.7
EQ057	57	16	20	<0.45	1.6
EQ058	52	15	23	<0.45	1.4
EQ059	57	15	19	<0.45	1.4
EQ060	47	12	18	<0.45	1.5
EQ061	61	12	24	<0.45	1.1
EQ062	41	12	19	<0.45	1.1
EQ063	51	16	20	<0.45	1.4
LB001	58	16	120	0.48	0.4
LB002	71	16	99	0.4	0.56
LB003	670	38	530	0.8	1.8
LB008	93	24	190	0.71	1.7
LJ001	29	51	38	2.6	0.62
LJ002	190	46	59	0.62	1.3
LJ003	96	26	52	0.32	0.81
LJ004	80	45	94	0.62	1.2
LJ005	40	64	49	0.37	2.3
LJ006	39	89	36	0.16	1
LJ007	29	28	27	0.18	0.89
LJ008	19	20	25	0.25	0.81
LJ009	17	25	30	0.67	0.58
LJ010	34	22	24	0.15	0.63
LJ011	19	330	270	67	0.52
LJ012	72	170	50	0.34	0.5
LL004	93	22	130	0.48	0.95
LL006	480	36	730	1.3	0.98
LL009	270	18	270	0.51	0.5

APPENDIX C

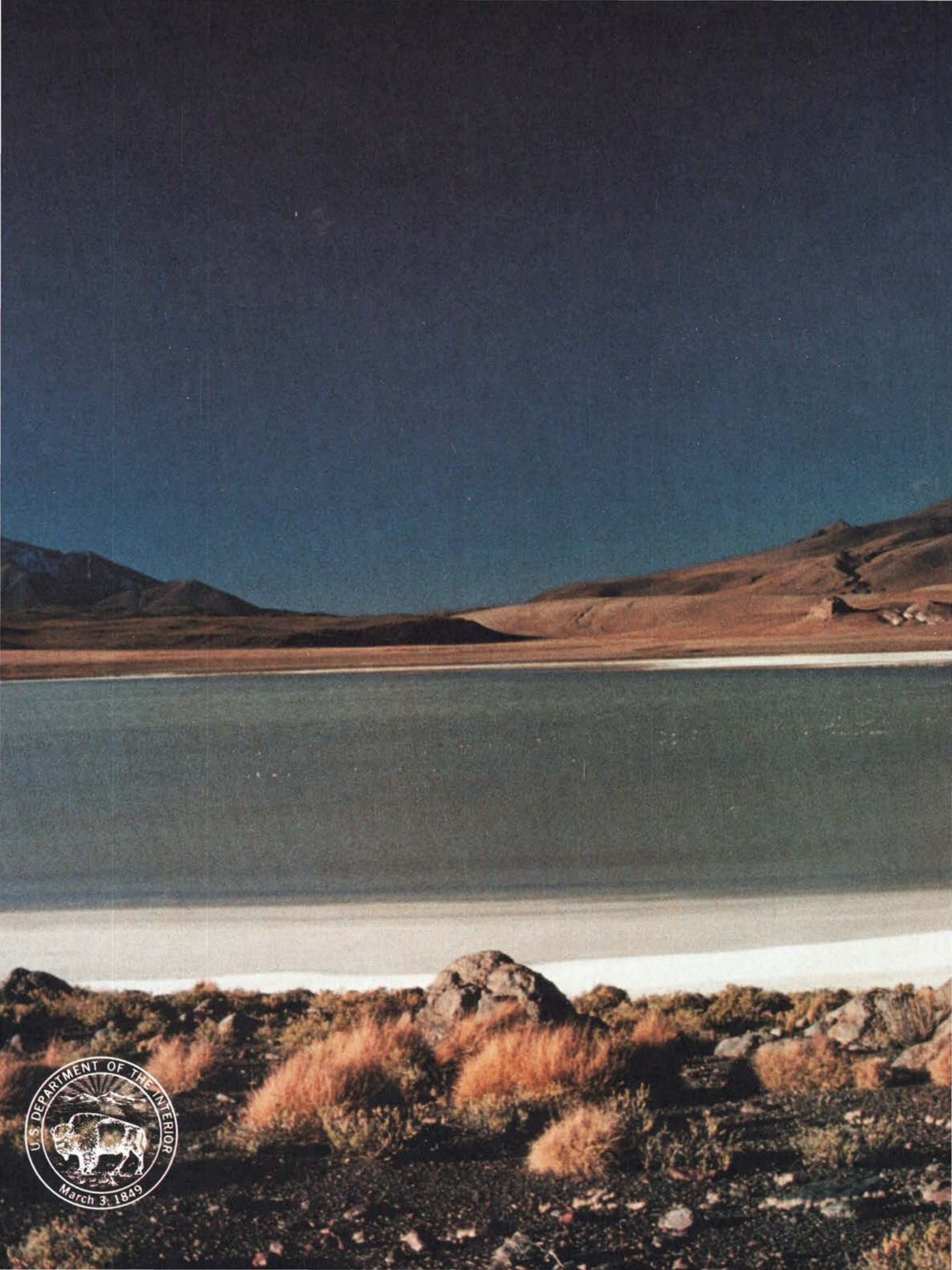
DATA FOR GEOCHRONOLOGY SAMPLES COLLECTED AS PART OF THE STUDY OF THE ALTIPLANO AND CORDILLERA OCCIDENTAL, BOLIVIA

Table C-1. *Data for geochronology samples collected as part of the study of the Altiplano and Cordillera Occidental, Bolivia*

[Constants used were $^{40}K/K = 1.167 \times 10^{-4}$ mol/mol; $\lambda_\beta = 4.962 \times 10^{-1}$/yr; $\lambda_\varepsilon + \lambda_{\varepsilon'} = 0.581 \times 10^{-1}$/yr. Samples 90BSL014, 109, 110, 90BDR010, 90BBR004a, 10, 14, and 90BBG024 were analyzed by E.H. McKee. Samples 90BDR030, 35, 53, and 55 were analyzed in duplicate for argon by Nora Shew, yielding a single age. Potassium measurements by S.T. Pribble. Mass spectrometry by J.Y. Saburomaru, J.C. Von Essen. rad, radiogenic]

Sample no.	Locality	Type of rock	Mineral analyzed	K_2O weight percent	$^{40}Ar_{rad}$ mol/g ($\times 10^{-11}$)	$^{40}Ar_{rad}$ percent of total	Age in Ma
90BSL014	Buena Vista	Vein wallrock	Sericite	4.57	7.306	55	11.1±0.3
90BDR010	Toldos	Dacite in pit	Biotite	7.47	9.136	54	8.5+0.3
90BSL109	Kiska	Late vein	Alunite	8.19	16.08	36	13.6±0.5
90BSL110	Kori Kollo	Late vein	Alunite	9.59	6.555	50	4.7±0.2
90BBR004a	Todos Santos	Dacite	Biotite	5.42	4.739	17	6.1±0.2
90BBR010	Negrillos	Carangas ash-flow tuff	Biotite	8.46	26.61	75	21.7±0.7
90BBR014	María Elena	Andesite dike	Hornblende	.783	.7091	17	6.3±0.2
90BBG024	Carangas	Rhyolite dike	Biotite	8.12	18.03	59	15.4±0.5
90BDR030	San Cristobal	Dacite stock	Biotite	8.90 8.91	10.32 10.34	49 56	8.0±0.1
90BDR035	Eskapa	Dacite flow	Biotite	8.46 8.51	7.696 7.727	37 44	6.3±0.1
90BDR053	Lower Quehua	Dacite flow	Biotite	8.08 8.09	21.43 21.07	60 53	18.2±0.3
90BDR055	Mina Escala	Rhyolite stock	Biotite	9.02 9.04	23.43 23.62	60 73	18.0±0.2




U.S. DEPARTMENT OF THE INTERIOR
March 3, 1849